NAS 1.9/4:35/13

VOLUME 25 / NUMBER 13
JULY 8, 1987
ACC. NOS. N87-20171 TO N87-20953

U. S. DOCUMENT
DEPOSITORY SHIPMENT
JUN 30 1987
SHAFER LIBRARY

STAR

AN ABSTRACT JOURNAL

Scientific and Technical Aerospace Reports

PRODUCED BY THE
SCIENTIFIC AND TECHNICAL
INFORMATION
OFFICE

NASA

NATIONAL AERONAUTICS AND SPACE ADMINISTRATION

WHAT YOU CAN DO FOR *STAR*

All users of this abstract service are urged to forward reports to be considered for announcement in *STAR*. This will aid NASA in its efforts to provide the fullest possible coverage of all scientific and technical publications that might support aeronautics and space research and development. If you have prepared relevant reports (other than those that you will transmit to NASA, DoD, or DOE through the usual contract- or grant-reporting channels), please send them for consideration to the NASA Scientific and Technical Information Facility, P.O. Box 8757, B.W.I. Airport, Maryland 21240.

Reprints of journal articles, book chapters, and conference papers are also welcome. These will be considered for announcement in *STAR*'s companion journal, *International Aerospace Abstracts*.

You may specify a particular source to be included in a report announcement if you wish; otherwise the report will be placed on public sale at the National Technical Information Service. Copyrighted publications will be announced but not distributed or sold.

PURCHASE OF *STAR*

The semimonthly issues are available for sale by the Superintendent of Documents, U.S. Government Printing Office, Washington, D.C. 20402.

PUBLISHED BY:

UNITED STATES GOVERNMENT
NATIONAL AERONAUTICS AND SPACE ADMINISTRATION
SCIENTIFIC AND TECHNICAL INFORMATION BRANCH
Scientific and Technical Aerospace Reports, Volume 25, is prepared by the NASA Scientific and Technical Information Facility operated for the National Aeronautics and Space Administration by RMS Associates.

The Administrator of the National Aeronautics and Space Administration has determined that the publication of this periodical is necessary in the transaction of the public business required by law of this Agency. Use of funds for printing this periodical has been approved by the Director of the Office of Management and Budget through March 22, 1988.

US ISSN 0036-8741

INTRODUCTION

Scientific and Technical Aerospace Reports (STAR) is a major component of a comprehensive National Aeronautics and Space Administration information system covering aeronautics, space, and supporting disciplines. *STAR* is issued on the 8th and 23rd of each month and announces current publications of the following types:

- NASA, NASA contractor, and NASA grantee reports
- Reports issued by other U.S. Government Agencies, domestic and foreign institutions, universities, and private firms
- Translations in report form
- NASA-owned patents and patent applications
- Dissertations and theses

Journal, book, and conference literature, cover-to-cover journal translations, and certain foreign dissertations are announced in a companion journal, *International Aerospace Abstracts (IAA)*, available on subscription from the American Institute of Aeronautics and Astronautics, Technical Information Service, 555 West 57th Street, 12th Floor, New York, New York 10019.

SUBJECT SCOPE

Subject scope of *STAR*, and *IAA* includes all aspects of aeronautics and space research and development, supporting basic and applied research, and applications. Aerospace aspects of earth resources, energy development, conservation, oceanography, environmental protection, urban transportation, and other topics of high national priority are also covered.

OTHER NASA PUBLICATIONS

Other NASA publications and information services are described in the publication, *The NASA Scientific and Technical Information System ... and How to Use It*, available without charge from the NASA Scientific and Technical Information Facility, P.O. Box 8757, B.W.I. Airport, Maryland 21240.

HOW TO USE *STAR* SUBJECT CATEGORIES

STAR is categorized by 10 major subject divisions divided into 76 specific subject categories and one general category/division. The major subject divisions are listed in the Table of Contents, together with a note for each that defines its scope and provides any cross-references. For example:

AERONAUTICS

Includes aeronautics (general); aerodynamics; air transportation and safety; aircraft communications and navigation; aircraft design, testing and performance; aircraft instrumentation; aircraft propulsion and power; aircraft stability and control; and research and support facilities (air).

For related information see also *Astronautics*.

Each major division is further divided into as many as nine specific categories, which are identified by category numbers.

Abstracts in *STAR* are grouped by specific category, the categories appearing in sequential order. Category breaks in the abstract section are identified by the category number and title, and a scope note. Cross-references to other categories are provided as appropriate. For example:

02 AERODYNAMICS

Includes aerodynamics of bodies, combinations, wings, rotors, and control surfaces; and internal flow in ducts and turbomachinery.

For related information see also *34 Fluid Mechanics and Heat Transfer.*

CROSS-REFERENCES

Individual *STAR* abstracts are not ordinarily cross-referenced, except for certain conference reports or book translations that have had separate abstracts written for their component papers or chapters. Citations and abstracts of the components follow immediately after those of the parent document. When the subject content of a component differs sufficiently from the general content of the parent, a cross-reference citation also is printed at the end of the category to which it normally would have been assigned if it were independent.

DOCUMENTS ON MICROFICHE

Documents on microfiche(1) are designated by a pound sign (#) following the accession number. The pound sign is used without regard to the source or quality of the microfiche.

AVAILABILITIES

One or more sources from which a document announced in *STAR* is available to the public is given in each citation. The most commonly indicated sources and their acronyms or abbreviations are listed below. If the publication is available from a source other than those listed, the publisher and his address will be displayed on the availability line or in combination with the corporate source line.

Avail: NTIS. Sold by the National Technical Information Service. Prices for hard copy (HC) and microfiche (MF) are indicated by a price code following the letters HC or MF in the *STAR* citation. Current values for the price codes are given in the tables on page vii.

Initially distributed microfiche under the NTIS SRIM (Selected Research in Microfiche) is available at greatly reduced unit prices. For this service and for information concerning subscription to NASA printed reports, consult the NTIS Subscription Section, Springfield, Va. 22161.

NOTE ON ORDERING DOCUMENTS: When ordering NASA publications (those followed by the * symbol), use the N accession number. NASA patent applications (only the specifications are offered) should be ordered by the US-Patent-Appl-SN number. Non-NASA publications (no asterisk) should be ordered by the AD, PB, or other *report* number shown on the last line of the citation, not by the N accession number. It is also advisable to cite the title and other bibliographic identification.

Avail: SOD (or GPO). Sold by the Superintendent of Documents, U.S. Government Printing Office, in hard copy. The current price and order number are given following the availability line. (NTIS will fill microfiche requests, as indicated above, for those documents identified by a # symbol.)

(1) A microfiche is a transparent sheet of film, 105 by 148 mm in size, containing as many as 60 to 98 pages of information reduced to micro images (not to exceed 26:1 reduction).

Avail: BLL (formerly NLL): British Library Lending Division, Boston Spa, Wetherby, Yorkshire, England. Photocopies available from this organization at the price shown. (If none is given, inquiry should be addressed to the BLL.)

Avail: DOE Depository Libraries. Organizations in U.S. cities and abroad that maintain collections of Department of Energy reports, usually in microfiche form, are listed in *Energy Research Abstracts*. Services available from the DOE and its depositories are described in a booklet, *DOE Technical Information Center - Its Functions and Services* (TID-4660), which may be obtained without charge from the DOE Technical Information Center.

Avail: ESDU. Pricing information on specific data, computer programs, and details on ESDU topic categories can be obtained from ESDU International Ltd. Requesters in North America should use the Virginia address while all other requesters should use the London address, both of which are on page vi.

Avail: Fachinformationszentrum, Karlsruhe. Sold by the Fachinformationszentrum Energie, Physik, Mathematik GMBH, Eggenstein Leopoldshafen, Federal Republic of Germany, at the price shown in deutschmarks (DM).

Avail: HMSO. Publications of Her Majesty's Stationery Office are sold in the U.S. by Pendragon House, Inc. (PHI), Redwood City, California. The U.S. price (including a service and mailing charge) is given, or a conversion table may be obtained from PHI.

Avail: NASA Public Document Rooms. Documents so indicated may be examined at or purchased from the National Aeronautics and Space Administration, Public Documents Room (Room 126), 600 Independence Ave., S.W., Washington, D.C. 20546, or public document rooms located at each of the NASA research centers, the NASA Space Technology Laboratories, and the NASA Pasadena Office at the Jet Propulsion Laboratory.

Avail: Univ. Microfilms. Documents so indicated are dissertations selected from *Dissertation Abstracts* and are sold by University Microfilms as xerographic copy (HC) and microfilm. All requests should cite the author and the Order Number as they appear in the citation.

Avail: US Patent and Trademark Office. Sold by Commissioner of Patents and Trademarks, U.S. Patent and Trademark Office, at the standard price of $1.50 each, postage free. (See discussion of NASA patents and patent applications below.)

Avail: (US Sales Only). These foreign documents are available to users within the United States from the National Technical Information Service (NTIS). They are available to users outside the United States through the International Nuclear Information Service (INIS) representative in their country, or by applying directly to the issuing organization.

Avail: USGS. Originals of many reports from the U.S. Geological Survey, which may contain color illustrations, or otherwise may not have the quality of illustrations preserved in the microfiche or facsimile reproduction, may be examined by the public at the libraries of the USGS field offices whose addresses are listed in this Introduction. The libraries may be queried concerning the availability of specific documents and the possible utilization of local copying services, such as color reproduction.

Avail: Issuing Activity, or Corporate Author, or no indication of availability. Inquiries as to the availability of these documents should be addressed to the organization shown in the citation as the corporate author of the document.

NASA PATENTS AND PATENT APPLICATIONS

Patents and patent applications owned by NASA are announced in *STAR* under appropriate subject categories and are referenced in the *STAR* indexes. In the Report/Accession Number Index, patents are indexed by the NASA Case Number (which appears in lieu of the report number in other indexes), the U.S. Patent Number, the U.S. Patent Application Serial Number, and the U.S. Patent Class. Patent applications for which patents have not yet been issued are indexed by the NASA Case Number and the U.S. Patent Application Serial Number.

NASA *patent application specifications* are sold in paper copy by the National Technical Information Service at price code A02. Microfiche are sold at price code A01. The US-Patent-Appl-SN- number should be used in ordering either paper copy or microfiche from NTIS. Printed copies of *patents* (which are not microfiched) are available for purchase at $1.50 per copy from:

Commissioner of Patents and Trademarks
U.S. Patent and Trademark Office
Washington, D.C. 20231

When ordering patents, the U.S. Patent Number should be used, and payment must be remitted in advance, preferably by money order or check payable to the Commissioner of Patents and Trademarks. Prepaid purchase coupons for ordering are also available from the Patent and Trademark Office. The patents and patent applications announced in *STAR* are owned by NASA and are available for royalty-free licensing. Requests for licensing terms and further information should be addressed to:

Assistant General Counsel for Patent Matters/Code GP
National Aeronautics and Space Administration
Washington, D.C. 20546

ELIGIBILITY AND REGISTRATION FOR NASA INFORMATION PRODUCTS AND SERVICES

A variety of services is available to organizations of the following types that have registered with NASA to receive specific services or products:

1. NASA offices, research centers, contractors, subcontractors, grantees, and consultants;
2. Other U.S. Government agencies and their contractors;
3. Libraries in the United States that have arrangements with NASA to maintain collections of NASA documents for public reference;
4. Other organizations in the United States having a need for NASA documents in work related to aeronautics and space research;
5. Organizations abroad that have established reciprocal document exchange arrangements with NASA.

Only the central service points or central points of document acquisition and control within qualified organizations are eligible to register for NASA products and services. Domestic organizations that may be eligible to receive various classes of NASA publications and services should address their requests for registration or for further information to:

NASA Scientific and Technical Information Facility
ATTN: Registration Activity
P.O. Box 8757
B.W.I. Airport, Maryland 21240

Organizations abroad should direct requests to the same address, but to the attention of: International Exchange Program.

AVAILABILITY OF *STAR* ABSTRACTS ON MICROFICHE

Microfiche of the abstract sections of this issue and other issues of *STAR* are available on annual subscription from NTIS, Attn: Subscriptions, 5285 Port Royal Road, Springfield, Virginia 22161. Annual subscription rates are $70.00 North America; $140.00 foreign. Abstract sections for previous years retroactive to 1964 are available at the current rates. Microfiche for individual *STAR* issue abstract sections are not available.

PUBLIC COLLECTIONS OF NASA DOCUMENTS

DOMESTIC: NASA and NASA-sponsored documents and a large number of aerospace publications are available to the public for reference purposes at the library maintained by the American Institute of Aeronautics and Astronautics, Technical Information Service, 555 West 57th Street, 12th Floor, New York, New York 10019

EUROPEAN: An extensive collection of NASA and NASA-sponsored publications is maintained by the British Library Lending Division, Boston Spa, Wetherby, Yorkshire, England for public access. The British Library Lending Division also has available many of the non-NASA publications cited in *STAR*. European requesters may purchase facsimile copy or microfiche of NASA and NASA-sponsored documents, those identified by both the symbols # and * from ESA - Information Retrieval Service European Space Agency, 8-10 rue Mario-Nikis, 75738 Paris CEDEX 15, France.

FEDERAL DEPOSITORY LIBRARY PROGRAM

In order to provide the general public with greater access to U.S. Government publications, Congress established the Federal Depository Library Program under the Government Printing Office (GPO), with 50 regional depositories responsible for permanent retention of material, inter-library loan, and reference services. At least one copy of nearly every NASA and NASA-sponsored publication, either in printed or microfiche format, is received and retained by the 50 regional depositories. A list of the regional GPO libraries, arranged alphabetically by state, appears on the inside back cover. These libraries are *not* sales outlets. A local library can contact a Regional Depository to help locate specific reports, or direct contact may be made by an individual.

ADDRESSES OF ORGANIZATIONS

American Institute of Aeronautics and Astronautics
Technical Information Service
555 West 57th Street, 12th Floor
New York, New York 10019

British Library Lending Division,
Boston Spa, Wetherby, Yorkshire,
England

Commissioner of Patents and Trademarks
U.S. Patent and Trademark Office
Washington, D.C. 20231

Department of Energy
Technical Information Center
P.O. Box 62
Oak Ridge, Tennessee 37830

ESA-Information Retrieval Service
ESRIN
Via Galileo Galilei
00044 Frascati (Rome) Italy

ESDU International, Ltd.
1495 Chain Bridge Road
McLean, Virginia 22101

ESDU International, Ltd.
251-259 Regent Street
London, W1R 7AD, England

Fachinformationszentrum Energie, Physik, Mathematik GMBH
7514 Eggenstein Leopoldshafen
Federal Republic of Germany

Her Majesty's Stationery Office
P.O. Box 569, S.E. 1
London, England

NASA Scientific and Technical Information Facility
P.O. Box 8757
B.W.I. Airport, Maryland 21240

National Aeronautics and Space Administration
Scientific and Technical Information Office (NTT-1)
Washington, D.C. 20546

National Technical Information Service
5285 Port Royal Road
Springfield, Virginia 22161

Pendragon House, Inc.
899 Broadway Avenue
Redwood City, California 94063

Superintendent of Documents
U.S. Government Printing Office
Washington, D.C. 20402

University Microfilms
A Xerox Company
300 North Zeeb Road
Ann Arbor, Michigan 48106

University Microfilms, Ltd.
Tylers Green
London, England

U.S. Geological Survey Library
National Center - MS 950
12201 Sunrise Valley Drive
Reston, Virginia 22092

U.S. Geological Survey Library
2255 North Gemini Drive
Flagstaff, Arizona 86001

U.S. Geological Survey
345 Middlefield Road
Menlo Park, California 94025

U.S. Geological Survey Library
Box 25046
Denver Federal Center, MS914
Denver, Colorado 80225

NTIS PRICE SCHEDULES

(Effective January 1, 1987)

Schedule A
STANDARD PRICE DOCUMENTS AND MICROFICHE

PRICE CODE	PAGE RANGE	NORTH AMERICAN PRICE	FOREIGN PRICE
A01	Microfiche	$ 6.50	$13.00
A02	001-025	9.95	19.90
A03	026-050	11.95	23.90
A04-A05	051-100	13.95	27.90
A06-A09	101-200	18.95	37.90
A10-A13	201-300	24.95	49.90
A14-A17	301-400	30.95	61.90
A18-A21	401-500	36.95	73.90
A22-A25	501-600	42.95	85.90
A99	601-up	*	*
NO1		45.00	80.00
NO2		48.00	80.00

Schedule E
EXCEPTION PRICE DOCUMENTS AND MICROFICHE

PRICE CODE	NORTH AMERICAN PRICE	FOREIGN PRICE
E01	$ 7.50	15.00
E02	10.00	20.00
E03	11.00	22.00
E04	13.50	27.00
E05	15.50	31.00
E06	18.00	36.00
E07	20.50	41.00
E08	23.00	46.00
E09	25.50	51.00
E10	28.00	56.00
E11	30.50	61.00
E12	33.00	66.00
E13	35.50	71.00
E14	38.50	77.00
E15	42.00	84.00
E16	46.00	92.00
E17	50.00	100.00
E18	54.00	108.00
E19	60.00	120.00
E20	70.00	140.00
E99	*	*

*Contact NTIS for price quote.

IMPORTANT NOTICE

NTIS Shipping and Handling Charges
U.S., Canada, Mexico — ADD $3.00 per TOTAL ORDER
All Other Countries — ADD $4.00 per TOTAL ORDER

Exceptions — Does NOT apply to:
ORDERS REQUESTING NTIS RUSH HANDLING
ORDERS FOR SUBSCRIPTION OR STANDING ORDER PRODUCTS *ONLY*

NOTE: Each additional delivery address on an order requires a separate shipping and handling charge.

VOLUME 25 NUMBER 13 / JULY 8, 1987

TABLE OF CONTENTS

AERONAUTICS

Includes aeronautics (general); aerodynamics; air transportation and safety; aircraft communications and navigation; aircraft design, testing and performance; aircraft instrumentation; aircraft propulsion and power; aircraft stability and control; and research and support facilities (air).

For related information see also *Astronautics.*

01 AERONAUTICS (GENERAL) 1709

02 AERODYNAMICS 1712

Includes aerodynamics of bodies, combinations, wings, rotors, and control surfaces; and internal flow in ducts and turbomachinery.

For related information see also *34 Fluid Mechanics and Heat Transfer*

03 AIR TRANSPORTATION AND SAFETY 1722

Includes passenger and cargo air transport operations; and aircraft accidents.

For related information see also *16 Space Transportation* and *85 Urban Technology and Transportation.*

04 AIRCRAFT COMMUNICATIONS AND NAVIGATION 1723

Includes digital and voice communication with aircraft; air navigation systems (satellite and ground based); and air traffic control.

For related information see also *17 Space Communications, Spacecraft Communications, Command and Tracking* and *32 Communications and Radar.*

05 AIRCRAFT DESIGN, TESTING AND PERFORMANCE 1724

Includes aircraft simulation technology.

For related information see also *18 Spacecraft Design, Testing and Performance* and *39 Structural Mechanics.* For land transportation vehicles see *85 Urban Technology and Transportation.*

06 AIRCRAFT INSTRUMENTATION 1725

Includes cockpit and cabin display devices; and flight instruments.

For related information see also *19 Spacecraft Instrumentation* and *35 Instrumentation and Photography.*

07 AIRCRAFT PROPULSION AND POWER 1725

Includes prime propulsion systems and systems components, e.g., gas turbine engines and compressors; and onboard auxiliary power plants for aircraft.

For related information see also *20 Spacecraft Propulsion and Power, 28 Propellants and Fuels,* and *44 Energy Production and Conversion.*

08 AIRCRAFT STABILITY AND CONTROL 1729

Includes aircraft handling qualities; piloting; flight controls; and autopilots.

For related information see also *05 Aircraft Design, Testing and Performance.*

09 RESEARCH AND SUPPORT FACILITIES (AIR) 1730

Includes airports, hangars and runways; aircraft repair and overhaul facilities; wind tunnels; shock tubes; and aircraft engine test stands.

For related information see also *14 Ground Support Systems and Facilities (Space).*

ASTRONAUTICS

Includes astronautics (general); astrodynamics; ground support systems and facilities (space); launch vehicles and space vehicles; space transportation; space communications, spacecraft communications, command and tracking; spacecraft design, testing and performance; spacecraft instrumentation; and spacecraft propulsion and power.

For related information see also *Aeronautics*

12 ASTRONAUTICS (GENERAL) 1731

For extraterrestrial exploration see *91 Lunar and Planetary Exploration.*

13 ASTRODYNAMICS 1736

Includes powered and free-flight trajectories; and orbital and launching dynamics.

14 GROUND SUPPORT SYSTEMS AND FACILITIES (SPACE) 1737

Includes launch complexes, research and production facilities; ground support equipment, e.g., mobile transporters; and simulators.

For related information see also *09 Research and Support Facilities (Air).*

15 LAUNCH VEHICLES AND SPACE VEHICLES 1737

Includes boosters; operating problems of launch/space vehicle systems; and reusable vehicles.

For related information see also *20 Spacecraft Propulsion and Power.*

16 SPACE TRANSPORTATION 1738

Includes passenger and cargo space transportation, e.g., shuttle operations; and space rescue techniques.

For related information see also *03 Air Transportation and Safety* and *18 Spacecraft Design, Testing and Performance.* For space suits see *54 Man/System Technology and Life Support.*

17 SPACE COMMUNICATIONS, SPACECRAFT COMMUNICATIONS, COMMAND AND TRACKING 1739

Includes telemetry; space communications networks; astronavigation and guidance; and radio blackout.

For related information see also *04 Aircraft Communications and Navigation* and *32 Communications and Radar.*

18 SPACECRAFT DESIGN, TESTING AND PERFORMANCE 1739

Includes satellites; space platforms; space stations; spacecraft systems and components such as thermal and environmental controls; and attitude controls.

For life support systems see *54 Man/System Technology and Life Support.* For related information see also *05 Aircraft Design, Testing and Performance, 39 Structural Mechanics,* and *16 Space Transportation.*

19 SPACECRAFT INSTRUMENTATION N.A.

For related information see also *06 Aircraft Instrumentation* and *35 Instrumentation and Photography.*

20 SPACECRAFT PROPULSION AND POWER 1745

Includes main propulsion systems and components, e.g. rocket engines; and spacecraft auxiliary power sources.

For related information see also *07 Aircraft Propulsion and Power, 28 Propellants and Fuels, 44 Energy Production and Conversion,* and *15 Launch Vehicles and Space Vehicles.*

CHEMISTRY AND MATERIALS

Includes chemistry and materials (general); composite materials; inorganic and physical chemistry; metallic materials; nonmetallic materials; propellants and fuels; and materials processing.

23 CHEMISTRY AND MATERIALS (GENERAL) N.A.

24 COMPOSITE MATERIALS 1747

Includes physical, chemical, and mechanical properties of laminates and other composite materials.

For ceramic materials see *27 Nonmetallic Materials.*

25 INORGANIC AND PHYSICAL CHEMISTRY 1749

Includes chemical analysis, e.g., chromatography; combustion theory; electrochemistry; and photochemistry.

For related information see also *77 Thermodynamics and Statistical Physics.*

26 METALLIC MATERIALS 1750

Includes physical, chemical, and mechanical properties of metals, e.g., corrosion; and metallurgy.

27 NONMETALLIC MATERIALS 1753

Includes physical, chemical, and mechanical properties of plastics, elastomers, lubricants, polymers, textiles, adhesives, and ceramic materials.

For composite materials see *24 Composite Materials.*

28 PROPELLANTS AND FUELS 1754

Includes rocket propellants, igniters and oxidizers; their storage and handling procedures; and aircraft fuels.

For related information see also *07 Aircraft Propulsion and Power, 20 Spacecraft Propulsion and Power,* and *44 Energy Production and Conversion.*

29 MATERIALS PROCESSING 1755

Includes space-based development of products and processes for commercial application.

For biological materials see *55 Space Biology.*

ENGINEERING

Includes engineering (general); communications and radar; electronics and electrical engineering; fluid mechanics and heat transfer; instrumentation and photography; lasers and masers; mechanical engineering; quality assurance and reliability; and structural mechanics.

For related information see also *Physics.*

31 ENGINEERING (GENERAL) 1755

Includes vacuum technology; control engineering; display engineering; cryogenics; and fire prevention.

32 COMMUNICATIONS AND RADAR 1757

Includes radar; land and global communications; communications theory; and optical communications.

For related information see also *04 Aircraft Communications and Navigation* and *17 Space Communications, Spacecraft Communications, Command and Tracking.* For search and rescue see *03 Air Transportation and Safety,* and *16 Space Transportation.*

33 ELECTRONICS AND ELECTRICAL ENGINEERING 1760

Includes test equipment and maintainability; components, e.g., tunnel diodes and transistors; microminiaturization; and integrated circuitry.

For related information see also *60 Computer Operations and Hardware* and *76 Solid-State Physics.*

34 FLUID MECHANICS AND HEAT TRANSFER 1765

Includes boundary layers; hydrodynamics; fluidics; mass transfer and ablation cooling.

For related information see also *02 Aerodynamics* and *77 Thermodynamics and Statistical Physics.*

35 INSTRUMENTATION AND PHOTOGRAPHY 1769

Includes remote sensors; measuring instruments and gages; detectors; cameras and photographic supplies; and holography.

For aerial photography see *43 Earth Resources and Remote Sensing.* For related information see also *06 Aircraft Instrumentation* and *19 Spacecraft Instrumentation.*

36 LASERS AND MASERS 1770

Includes parametric amplifiers.

For related information see also *76 Solid-State Physics.*

37 MECHANICAL ENGINEERING 1775

Includes auxiliary systems (nonpower); machine elements and processes; and mechanical equipment.

38 QUALITY ASSURANCE AND RELIABILITY 1777

Includes product sampling procedures and techniques; and quality control.

39 STRUCTURAL MECHANICS 1778

Includes structural element design and weight analysis; fatigue; and thermal stress.

For applications see *05 Aircraft Design, Testing and Performance* and *18 Spacecraft Design, Testing and Performance.*

GEOSCIENCES

Includes geosciences (general); earth resources and remote sensing; energy production and conversion; environment pollution; geophysics; meteorology and climatology; and oceanography.

For related information see also *Space Sciences.*

42 GEOSCIENCES (GENERAL) **N.A.**

43 EARTH RESOURCES AND REMOTE SENSING **1786**

Includes remote sensing of earth resources by aircraft and spacecraft; photogrammetry; and aerial photography.

For instrumentation see *35 Instrumentation and Photography.*

44 ENERGY PRODUCTION AND CONVERSION **1789**

Includes specific energy conversion systems, e.g., fuel cells; global sources of energy; geophysical conversion; and windpower.

For related information see also *07 Aircraft Propulsion and Power, 20 Spacecraft Propulsion and Power,* and *28 Propellants and Fuels.*

45 ENVIRONMENT POLLUTION **1792**

Includes atmospheric, noise, thermal, and water pollution.

46 GEOPHYSICS **1792**

Includes aeronomy; upper and lower atmosphere studies; ionospheric and magnetospheric physics; and geomagnetism.

For space radiation see *93 Space Radiation.*

47 METEOROLOGY AND CLIMATOLOGY **1798**

Includes weather forecasting and modification.

48 OCEANOGRAPHY **1800**

Includes biological, dynamic, and physical oceanography; and marine resources.

For related information see also *43 Earth Resources and Remote Sensing.*

LIFE SCIENCES

Includes life sciences (general); aerospace medicine; behavioral sciences; man/system technology and life support; and space biology.

51 LIFE SCIENCES (GENERAL) **1803**

52 AEROSPACE MEDICINE **1804**

Includes physiological factors; biological effects of radiation; and effects of weightlessness on man and animals.

53 BEHAVIORAL SCIENCES **1806**

Includes psychological factors; individual and group behavior; crew training and evaluation; and psychiatric research.

54 MAN/SYSTEM TECHNOLOGY AND LIFE SUPPORT **1807**

Includes human engineering; biotechnology; and space suits and protective clothing.

For related information see also *16 Space Transportation.*

55 SPACE BIOLOGY **N.A.**

Includes exobiology; planetary biology; and extraterrestrial life.

MATHEMATICAL AND COMPUTER SCIENCES

Includes mathematical and computer sciences (general); computer operations and hardware; computer programming and software; computer systems; cybernetics; numerical analysis; statistics and probability; systems analysis; and theoretical mathematics.

59 MATHEMATICAL AND COMPUTER SCIENCES (GENERAL) **1808**

60 COMPUTER OPERATIONS AND HARDWARE **1808**

Includes hardware for computer graphics, firmware, and data processing.

For components see *33 Electronics and Electrical Engineering.*

61 COMPUTER PROGRAMMING AND SOFTWARE **1809**

Includes computer programs, routines, algorithms, and specific applications, e.g., CAD/CAM.

62 COMPUTER SYSTEMS **1810**

Includes computer networks and special application computer systems.

63 CYBERNETICS **1811**

Includes feedback and control theory, artificial intelligence, robotics and expert systems.

For related information see also *54 Man/System Technology and Life Support.*

64 NUMERICAL ANALYSIS **1812**

Includes iteration, difference equations, and numerical approximation.

65 STATISTICS AND PROBABILITY **1813**

Includes data sampling and smoothing; Monte Carlo method; and stochastic processes.

66 SYSTEMS ANALYSIS **1813**

Includes mathematical modeling; network analysis; and operations research.

67 THEORETICAL MATHEMATICS **1814**

Includes topology and number theory.

PHYSICS

Includes physics (general); acoustics; atomic and molecular physics; nuclear and high-energy physics; optics; plasma physics; solid-state physics; and thermodynamics and statistical physics.

For related information see also *Engineering.*

70 PHYSICS (GENERAL) **1814**

For precision time and time interval (PTTI) see *35 Instrumentation and Photography;* for geophysics, astrophysics or solar physics see *46 Geophysics, 90 Astrophysics,* or *92 Solar Physics.*

71 ACOUSTICS 1814
Includes sound generation, transmission, and attenuation.
For noise pollution see *45 Environment Pollution.*

72 ATOMIC AND MOLECULAR PHYSICS 1816
Includes atomic structure, electron properties, and molecular spectra.

73 NUCLEAR AND HIGH-ENERGY PHYSICS 1817
Includes elementary and nuclear particles; and reactor theory.
For space radiation see *93 Space Radiation.*

74 OPTICS 1818
Includes light phenomena and optical devices.
For lasers see *36 Lasers and Masers.*

75 PLASMA PHYSICS 1818
Includes magnetohydrodynamics and plasma fusion.
For ionospheric plasmas see *46 Geophysics.* For space plasmas see *90 Astrophysics.*

76 SOLID-STATE PHYSICS 1818
Includes superconductivity.
For related information see also *33 Electronics and Electrical Engineering* and *36 Lasers and Masers.*

77 THERMODYNAMICS AND STATISTICAL PHYSICS 1820
Includes quantum mechanics; theoretical physics; and Bose and Fermi statistics.
For related information see also *25 Inorganic and Physical Chemistry* and *34 Fluid Mechanics and Heat Transfer.*

SOCIAL SCIENCES

Includes social sciences (general); administration and management; documentation and information science; economics and cost analysis; law, political science, and space policy; and urban technology and transportation.

80 SOCIAL SCIENCES (GENERAL) N.A.
Includes educational matters.

81 ADMINISTRATION AND MANAGEMENT 1821
Includes management planning and research.

82 DOCUMENTATION AND INFORMATION SCIENCE 1821
Includes information management; information storage and retrieval technology; technical writing; graphic arts; and micrography.
For computer documentation see *61 Computer Programming and Software.*

83 ECONOMICS AND COST ANALYSIS N.A.
Includes cost effectiveness studies.

84 LAW, POLITICAL SCIENCE AND SPACE POLICY 1822
Includes NASA appropriation hearings; aviation law; space law and policy; international law; international cooperation; and patent policy.

85 URBAN TECHNOLOGY AND TRANSPORTATION N.A.
Includes applications of space technology to urban problems; technology transfer; technology assessment; and surface and mass transportation.
For related information see *03 Air Transportation and Safety, 16 Space Transportation,* and *44 Energy Production and Conversion.*

SPACE SCIENCES

Includes space sciences (general); astronomy; astrophysics; lunar and planetary exploration; solar physics; and space radiation.
For related information see also *Geosciences.*

88 SPACE SCIENCES (GENERAL) N.A.

89 ASTRONOMY 1822
Includes radio, gamma-ray, and infrared astronomy; and astrometry.

90 ASTROPHYSICS 1823
Includes cosmology; celestial mechanics; space plasmas; and interstellar and interplanetary gases and dust.
For related information see also *75 Plasma Physics.*

91 LUNAR AND PLANETARY EXPLORATION 1827
Includes planetology; and manned and unmanned flights.
For spacecraft design or space stations see *18 Spacecraft Design, Testing and Performance.*

92 SOLAR PHYSICS 1828
Includes solar activity, solar flares, solar radiation and sunspots.
For related information see *93 Space Radiation.*

93 SPACE RADIATION 1840
Includes cosmic radiation; and inner and outer earth's radiation belts.
For biological effects of radiation see *52 Aerospace Medicine.* For theory see *73 Nuclear and High-Energy Physics.*

GENERAL

Includes aeronautical, astronautical, and space science related histories, biographies, and pertinent reports too broad for categorization; histories or broad overviews of NASA programs.

99 GENERAL N.A.

Note: N.A. means that no abstracts were assigned to this category for this issue.

SUBJECT INDEX I-1
PERSONAL AUTHOR INDEX I-45
CORPORATE SOURCE INDEX I-51
CONTRACT NUMBER INDEX I-61
REPORT/ACCESSION NUMBER INDEX I-63

TYPICAL CITATION AND ABSTRACT

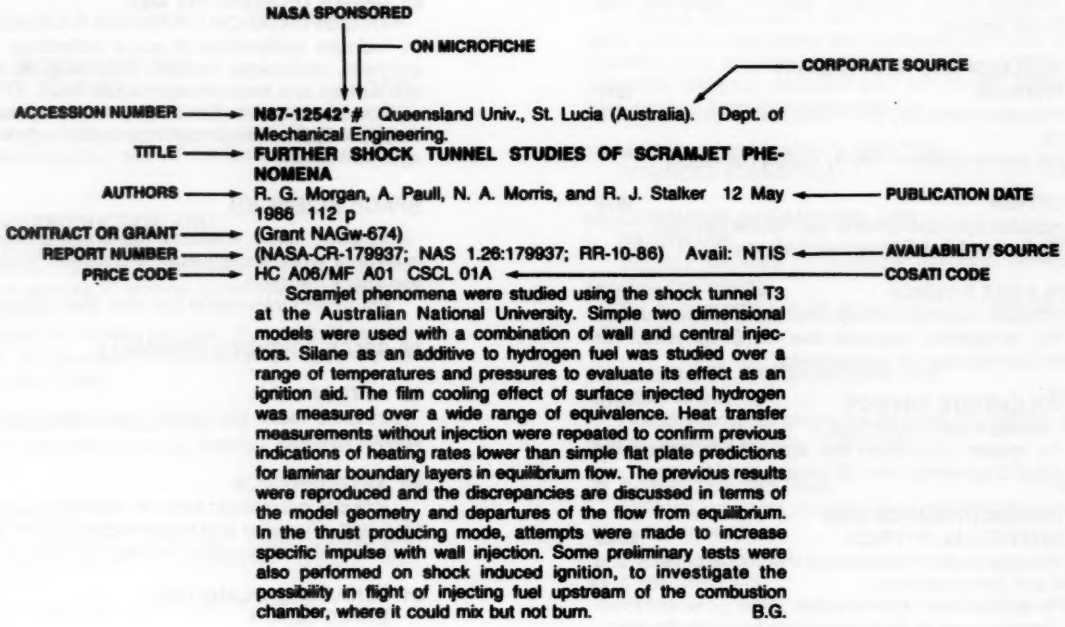
NASA SPONSORED
ON MICROFICHE
CORPORATE SOURCE
ACCESSION NUMBER
N87-12542*# Queensland Univ., St. Lucia (Australia). Dept. of Mechanical Engineering.
TITLE
FURTHER SHOCK TUNNEL STUDIES OF SCRAMJET PHENOMENA
AUTHORS
R. G. Morgan, A. Paull, N. A. Morris, and R. J. Stalker 12 May 1986 112 p
PUBLICATION DATE
CONTRACT OR GRANT
(Grant NAGw-674)
REPORT NUMBER
(NASA-CR-179937; NAS 1.26:179937; RR-10-86) Avail: NTIS
AVAILABILITY SOURCE
PRICE CODE
HC A06/MF A01 CSCL 01A
COSATI CODE
Scramjet phenomena were studied using the shock tunnel T3 at the Australian National University. Simple two dimensional models were used with a combination of wall and central injectors. Silane as an additive to hydrogen fuel was studied over a range of temperatures and pressures to evaluate its effect as an ignition aid. The film cooling effect of surface injected hydrogen was measured over a wide range of equivalence. Heat transfer measurements without injection were repeated to confirm previous indications of heating rates lower than simple flat plate predictions for laminar boundary layers in equilibrium flow. The previous results were reproduced and the discrepancies are discussed in terms of the model geometry and departures of the flow from equilibrium. In the thrust producing mode, attempts were made to increase specific impulse with wall injection. Some preliminary tests were also performed on shock induced ignition, to investigate the possibility in flight of injecting fuel upstream of the combustion chamber, where it could mix but not burn. B.G.

VOLUME 25 NUMBER 13 / JULY 8, 1987

Scientific and Technical Aerospace Reports

A Semimonthly Publication of the National Aeronautics and Space Administration

01 AERONAUTICS (GENERAL)

N87-20171*# National Aeronautics and Space Administration. Lewis Research Center, Cleveland, Ohio.
NUMERICAL CALCULATIONS OF TURBULENT REACTING FLOW IN A GAS-TURBINE COMBUSTOR
Chin-Shun Lin Apr. 1987 21 p
(NASA Order C-99066-G)
(NASA-TM-89842; E-3501; ICOMP-87-2; NAS 1.15:89842) Avail: NTIS HC A02/MF A01 CSCL 20D

A numerical study for confined, axisymmetrical, turbulent diffusion flames is presented. Local mean gas properties are predicted by solving the appropriate conservation equations in the finite difference form with the corresponding boundary conditions. The k-epsilon two-equation turbulence model is employed to describe the turbulent nature of the flow. A two-step kinetic model is assumed to govern the reaction mechanism. The finite reaction rate is the smaller of an Arrhenius type of reaction rate and a modified version of eddy-breakup model. Reasonable agreement is observed between calculations and measurements, but to obtain better agreement, more work is needed on improvements of the above mathematical models. However, the present numerical study offers an improvement in the analysis and design of the gas turbine combustors. B.G.

N87-20172* National Aeronautics and Space Administration, Washington, D.C.
AERONAUTICAL ENGINEERING: A CONTINUING BIBLIOGRAPHY WITH INDEXES (SUPPLEMENT 212)
Apr. 1987 134 p
(NASA-SP-7037(212); NAS 1.21:7037(212)) Avail: NTIS Avail: NTIS HC A07 CSCL 01A

This bibliography lists 493 reports, articles and other documents introduced into the NASA scientific and technical information system in March, 1987. E.R.

N87-20173# Office of Naval Research, London (England).
A SURVEY OF MILITARY AEROSPACE SYSTEMS TECHNOLOGY DEVELOPMENTS IN WESTERN EUROPE AND THE MIDDLE EAST
L. L. Coburn 17 Oct. 1986 48 p
(AD-A175635; ONRL-R-6-86) Avail: NTIS HC A03/MF A01 CSCL 01/3

Military aerospace system developments and defense aerospace research/development manufacturing are discussed in this report. The military aerospace systems include fighter aircraft, large aircraft, helicopters, air weapons, and space system. GRA

N87-20174# Advisory Group for Aerospace Research and Development, Neuilly-Sur-Seine (France). Structures and Materials Panel.
THE REPAIR OF AIRCRAFT STRUCTURES INVOLVING COMPOSITE MATERIALS
Loughton, England Oct. 1986 240 p In ENGLISH and FRENCH Meeting held in Oslo, Norway, 14-16 Apr. 1986
(AGARD-CP-402; ISBN-92-835-0400-3) Avail: NTIS HC A11/MF A01

Modern combat aircraft are making increasing use of composite materials in both primary and secondary structures, and the need for repair schemes which involve a mixture of composite and metallic materials is no longer exceptional. At its sixty-second meeting, the Structures and Materials Panel held a conference of Specialists, the aim of which was to share experiences of repairs involving composites and structures now in service. A further aim was to highlight the demand for the development of innovative times and increase repair capabilities under all conditions of service but also make for greater standardization. For individual titles, see N87-20175 through N87-20192.

N87-20175# Dornier-Werke G.m.b.H., Friedrichshafen (West Germany).
REPAIR PROCEDURES FOR COMPOSITE PARTS ON THE ALPHA JET
Th. Thiele *In* AGARD The Repair of Aircraft Structures Involving Composite Materials Oct. 1986 7 p (For primary document see N87-20174 13-01)
Avail: NTIS HC A11/MF A01

A survey is given of activities to develop repair procedures for the composite parts of the alpha jet. The complete program was divided into two parts: the first part covered the repair and test of specimen; the second part the repair and test of a full scale speed brake. Author

N87-20176# Messerschmitt-Boelkow-Blohm G.m.b.H., Munich (West Germany). Helicopter Div.
DESIGN FOR REPAIRABILITY OF HELICOPTER COMPOSITE BLADES c05
M. Hahn *In* AGARD The Repair of Aircraft Structures Involving Composite Materials Oct. 1986 15 p (For primary document see N87-20174 13-01)
Avail: NTIS HC A11/MF A01

First a careful definition is made of the specific kinds of damages where repairability is aimed for. The criteria of repairability are described using the example of the main rotor blade. Then some repair procedures are detailed, starting with the criteria to be used to decide on repair level, showing components in particular and the aspects of design to repairability. Comparison of early and later design is used to demonstrate how improvement with respect to repairability was achieved. The concluding chapter describes service experience with the main and tail rotor blades, gained e.g., out of more than one mio. flight hours of BO 105-fleet. Author

N87-20177# Lockheed-California Co., Burbank.
DEVELOPMENT OF FIELD LEVEL REPAIRS FOR COMPOSITE STRUCTURES
Robert H. Stone *In* AGARD The Repair of Aircraft Structures Involving Composite Materials Oct. 1986 12 p (For primary document see N87-20174 13-01)

Avail: NTIS HC A11/MF A01

Bolted and bonded field-level repairs have been developed, fabricated and tested at Lockheed-California Company for several recent contract and independent research programs. Bolted repairs are particularly well adapted to field repair situations. Bolted aluminum repair concepts have been developed and verified under a NASA sponsored program for an L-1011 composite inboard aileron, which is now in flight-service evaluation. Special drilling, machining, fastener installation and sealing procedures were developed for these repairs. Bolted repairs were also developed and validated under a Naval Air Development Center (NADC) sponsored program. These included various configurations of aluminum and titanium patches using blind fasteners, with drilling and installation procedures representative of field conditions including lack of back-side access. Repair specimens were tested in tension and compression, and the patches restored design strength levels to the damaged composite. Bonded field repairs require adhesives with room temperature storability in addition to the other structural/environmental requirements. Screening tests were run on various film and two-part adhesives. A two-part adhesive, developed by NADC and now commercially available, had the best combination of properties for field repairs. Other tests related to bonded field repairs determined that 177 C (350 F) curing film adhesives have several months' storability at room temperature, and verified prebond storability of titanium surface treatments for use in bonded repair kits. Author

N87-20178# Societe Nationale Industrielle Aerospatiale, Toulouse (France). Composite Structure Design Dept.

A.T.R. 42 CARBON FIBRE FLAP REPAIR DESIGN AND INSPECTION **c24**

Guy Hellard *In* AGARD The Repair of Aircraft Structures Involving Composite Materials Oct. 1986 9 p (For primary document see N87-20174 13-01)

Avail: NTIS HC A11/MF A01

The new commuter aircraft known as ATR.42 developed jointly by Aerospatiale and Aeritalia is the first aircraft of its category to be equipped with carbon fabric flaps. All the airlines which have placed orders for this aircraft are not equipped with the heavy installations required for working on the composite materials. Repair schemes using a simple technology have therefore to be developed. Partial or complete tests have shown that a perfect understanding of the structural ability to withstand the different types of damage was required beforehand. Repair methods using in situ pre-impregnation of dry fabrics have been developed with the relevant method. The mechanical strength of the various repairs and the effects of inadequate damage repairs have been investigated through tests. Author

N87-20179# Societe Nationale Industrielle Aerospatiale, Marignane (France). Advanced Engineering Dept.

REPAIR OF HELICOPTER COMPOSITE STRUCTURE TECHNIQUES AND SUBSTANTIATIONS

Manuel Torres and Bernard Plissonneau *In* AGARD The Repair of Aircraft Structures Involving Composite Materials Oct. 1986 21 p (For primary document see N87-20174 13-01)

Avail: NTIS HC A11/MF A01

The advantages of composite materials are now well known and have been widely demonstrated. Lighter weight, lower cost, shorter manufacturing cycles, damage tolerance, etc. are some of the advantages. As a result, composite materials are increasingly used in helicopters. Helicopter designs have made extensive use of composites for over twenty years. Composite rotor blades date from 1970. More recently, major programs have been undertaken to produce the future generation of helicopters with a totally composite fuselage. The increasing number of composite items in the aircraft structure raises the problem of damage and repair. This concern is further justified by the relatively high damage probability of a helicopter that may be operated in severe environmental conditions. The repair philosophy engages the responsibility of the aircraft manufacturer as well as the operator. The manufacturer must develop and substantiate repair methods that are as simple as possible. The operator must be equipped with suitable inspection and repair facilities. These repairs must ensure an adequate safety level for the remaining helicopter's service life. They must be suitable for the nature of the damage and the type of part involved. They must be as easy as possible to implement and require minimal special tools and expertise, and the repair cost must remain well below the price of new replacement parts. Author

N87-20180# Norges Tekniske Hoegskole, Trondheim. Dept. of Physics.

TV-HOLOGRAPHY: A PROMISING INSPECTION TOOL FOR ANALYSIS OF COMPOSITE MATERIALS **c35**

Ole J. Lokberg, Jan T. Malmo, and Arvid Strand (Conspectum A/S, Trondheim, Norway.) *In* AGARD The Repair of Aircraft Structures Involving Composite Materials Oct. 1986 7 p (For primary document see N87-20174 13-01)

Avail: NTIS HC A11/MF A01

Holographic measuring techniques combined with the speed and convenience of video recording and display, provide a real-time system which can be used to reveal extremely small movements. By various excitation-like heating, pressure and vibrations, we detect object defects and structural weaknesses. The system's construction and its modes of operation are discussed. Finally some examples are given of the applications of the system. Author

N87-20181# Messerschmitt-Boelkow-Blohm G.m.b.H., Munich (West Germany). Stress Office.

COMPOSITE REPAIR OF COCURED J-STIFFENED PANELS: DESIGN AND TEST VERIFICATION

Georg Guenther and Ludwig Lemmer *In* AGARD The Repair of Aircraft Structures Involving Composite Materials Oct. 1986 19 p (For primary document see N87-20174 13-01)

Avail: NTIS HC A11/MF A01

An increasing percentage of military aircraft fuselage and wing structures are being replaced by cocured integrated carbon fiber composite (CFC) structures. The probability of damage in day-to-day operation is increased, since most of the structure is located on the aircraft surface. The most common field of application for cocured stiffeners are thin panels critical to buckling under shear and/or compression loading and fuselage frames subject to bending. Bonded repair methods for two maintenance levels (depot and field) have been developed and tested using representative components. For the stiffened panels both repair methods (field and depot) fulfilled structural requirements and proved their durability in the fatigue tests. Test results of the stiffened skin elements showed that cocured fuselage structures with complex geometries are repairable without reduction in strength and stiffness. Tests performed after artificial ageing of the repaired structure proved their reliability in the environment. Author

N87-20182# Royal Aircraft Establishment, Farnborough (England).

EFFECT OF ADHESIVE BONDING VARIABLES ON THE PERFORMANCE OF BONDED CFRP PATCH REPAIRS OF METALLIC STRUCTURES

P. Poole, M. H. Stone, G. R. Sutton, and R. N. Wilson *In* AGARD The Repair of Aircraft Structures Involving Composite Materials Oct. 1986 21 p (For primary document see N87-20174 13-01)

Avail: NTIS HC A11/MF A01

The literature is briefly reviewed and limitations of the existing experimental data on the performance of bonded carbon fiber reinforced plastics (CFRP) patches are indicated. Earlier work from the Royal Aircraft Establishment is summarized, showing the importance of patch size and crack growth conditions prior to patching. Fatigue data for center-cracked, patched aluminum alloy thin sheets (7075-T76) are then presented. These show that: adhesive layer stiffness had only a moderate effect; differential contraction stresses had much less effect than predicted; and neither variations in surface treatment of the aluminum alloy before bonding nor exposure of the patched sheet to warm/moist conditions had any substantial effect on crack rates. Bond durability wedge and peel tests did show marked effects of alloy pretreatments. Explanations are advanced for the lack of effect of moisture

and alloy pretreatment on the alloy-adhesive bonds of the patched sheets. Author

N87-20183# Air Force Wright Aeronautical Labs., Wright-Patterson AFB, Ohio. Aeronautical Systems Div.
COMPOSITE REPAIR OF CRACKED ALUMINUM STRUCTURE
Larry G. Kelly *In* AGARD The Repair of Aircraft Structures Involving Composite Materials Oct. 1986 6 p (For primary document see N87-20174 13-01)
Avail: NTIS HC A11/MF A01

The use of bonded composite patches for repair of a wide range of typical fatigue cracked and otherwise damaged aluminum structural panels is discussed. Experimental data on stress intensity and crack growth characteristics were obtained to evaluate the advantages of such repairs. A range of metal thickness and patch parameters (thickness, orientation, bonding temperature) were tested. Edge cracked 4 inch by 18 inch 2024T3 aluminum panels were patched and fatigue behavior evaluated under constant amplitude and the Falstaff flight spectrum loading. The results showed panel thickness and fatigue test load spectrum to be important parameters. Present repair procedures for cracked aluminum aircraft structures call for bolted on metal patches. Advanced composite material bonded to such damaged structures offers the advantage of increased fatigue life. To quantify this advantage a test program was conducted with boron/epoxy patches on cracked aluminum panels. The panels were subjected to both constant amplitude and flight spectrum loads. The objective was to establish the reduction in stress intensity and thus reduced crack growth rate achieved through the use of room temperature and 250 F cured adhesive bonded patches. The pertinent parameters evaluated were aluminum thickness, patch area, and ply orientation. Dramatic improvements in fatigue life were achieved up to 20 times extended lifetimes for 1/16 inch repaired aluminum panels having an initial .34 inch induced crack. Author

N87-20184# Avions Marcel Dassault-Breguet Aviation, Saint-Cloud (France).
DAMAGE REPAIR OF IN-SERVICE COMPOSITE STRUCTURES: APPLICATION TO THE MIRAGE 2000 [REPARATION DE DOMMAGES EN SERVICE DES STRUCTURES COMPOSITES. APPLICATION AU MIRAGE 2000]
Daniel Chaumette and Francoise Henriot *In* AGARD The Repair of Aircraft Structures Involving Composite Materials Oct. 1986 10 p In FRENCH; ENGLISH summary (For primary document see N87-20174 13-01)
Avail: NTIS HC A11/MF A01

A summary is given of the 15 years experience AMD/BA has had in the field of composite structures repair, and the application to the case of the Mirage 2000. AMD/BA has developed repairs using a boron fiber dry fabric impregnated and bonded in situ on aluminum structures. These repairs have been the subject of tests, and of such practical applications as local reinforcements on the Mercure airliner. Since 1978 a large number of carbon fiber ailerons have been put in service on the fighter aircraft Mirage F1 and on the Falcon 50 business jet. Repair procedures have been developed for these elements. These elements have been troublefree up to now. Author

N87-20185# Societe de Construction des Avions Hurel-Dubois, Paris (France).
COMPOSITE STRUCTURE REPAIRS CARRIED OUT ACCORDING TO AERONAUTICAL TECHNIQUES [REPARATIONS DE STRUCTURES COMPOSITES REALISEES SELON LES TECHNIQUES AERONAUTIQUES]
Jean-Alain Jouan *In* AGARD The Repair of Aircraft Structures Involving Composite Materials Oct. 1986 13 p In FRENCH (For primary document see N87-20174 13-01)
Avail: NTIS HC A11/MF A01

Advanced composite materials (aramide, carbon, honeycomb) initially utilized in aircraft structures are seeing their domain of application extended to other sectors. The experiences of Hurel-Dubois with two specific composite material applications, frames for the Formula 1 racing car and structures for transoceanic racing catamarans, are discussed with reference to damage repair and the restoration of structural integrity. The various types of in-service damage are outlined and the materials and procedures for repair are described. Author

N87-20186# Messerschmitt-Boelkow-Blohm G.m.b.H., Munich (West Germany).
COMPOSITE REPAIR TECHNIQUES FOR J-STIFFENED COMPOSITE FUSELAGE STRUCTURES
K. Ledwa *In* AGARD The Repair of Aircraft Structures Involving Composite Materials Oct. 1986 11 p (For primary document see N87-20174 13-01)
Avail: NTIS HC A11/MF A01

The next generation of lightweight military aircraft will feature an essentially increased application of carbon fiber reinforced plastics (CFRP) to primary structure including fuselage side skins. Mainly for cost and weight reasons they will be large size integrally stiffened components cocured in a single shot operation. In order to avoid a costly replacement of the entire side skin in case of damage, adjusted repair techniques are required. Basic repair philosophies for field and depot level repairs using composite materials were defined and proved by two different types of test specimen. Specially designed flat panels with a 50 mm diameter hole penetrating skin and stiffener were followed by single curved side skin elements damaged by a destructive qualification test. Both types were repaired using different methods and finally destructive tested. The test results showed that the restoration of part stiffness and sufficient strength after repair can successfully be realized. Manufacturing problems were recognized concerning material choice and cure cycles at elevated temperatures and regarding the nondestructive inspection of applied repair patches. Author

N87-20187# Aeronautical Research Labs., Melbourne (Australia).
FIBRE COMPOSITE REPAIR OF CRACKED METALLIC AIRCRAFT COMPONENTS: PRACTICAL AND BASIC ASPECTS
A. A. Baker *In* AGARD The Repair of Aircraft Structures Involving Composite Materials Oct. 1986 21 p (For primary document see N87-20174 13-01)
Avail: NTIS HC A11/MF A01

Crack patching, the use of advanced fiber composite patches (such as boron/epoxy or graphite/epoxy) bonded with structural film adhesives to repair cracks in metallic aircraft components, is a significant development in aircraft maintenance technology, offering many advantages over conventional repair procedures based on metallic patches and mechanical fasteners. Selected theoretical and experimental aspects of Australian work on this topic are previewed. A preliminary design approach for estimating the minimum thickness patch that could be employed in a given repair situation is described. Finally, the case study on the repair to the wing skin of Mirage 3 aircraft is given. Aspects discussed include evaluation of minimum cure and surface-treatment conditions for adhesive bonding in repair situations; potential thermal and residual stress problems resulting from patching; studies on overlap joints representing repairs and crack propagation behavior in patched panels. Author

N87-20188# Naval Air Development Center, Warminster, Pa.
COMPOSITE REPAIR MATERIAL AND DESIGN DEVELOPMENT EFFORTS
R. C. Cochran, T. M. Donnellan, E. L. Rosenzweig, and R. E. Trabocco *In* AGARD The Repair of Aircraft Structures Involving Composite Materials Oct. 1986 13 p (For primary document see N87-20174 13-01)
Avail: NTIS HC A11/MF A01

Recent developments in the area of bonded and bolted composite repair are discussed. An ideal resin or adhesive for field repair would have the following characteristics: ambient storage, low temperature cure, short time cure, elevated temperature and moisture resistance, and vacuum processing. Two approaches were used to achieve resin formulations for repair patches which will meet these requirements. The first method

utilizes chemically hindred diamines as curing agents for epoxy resins. The second method involves isolation of the curing agents from the epoxy resin by phase separation. In the area of adhesives for field repair of composites, a two-part paste adhesive has been developed. The adhesive meets all of the program requirements and can be used with various repair materials. The design of bolted repairs for composite structures is discussed. A simplified design has been established which uses standard plate thicknesses, bolt sizes and spacing. Several patch shapes have been tested and found to restore design ultimate strains. Author

N87-20189# McDonnell Aircraft Co., St. Louis, Mo.
BATTLE DAMAGE REPAIR OF COMPOSITE STRUCTURES
Thomas V. Hinkle, Jack VanEs, and Charles L. Ramsey (Air Force Wright Aeronautical Labs., Wright-Patterson AFB, Ohio.) *In* AGARD The Repair of Aircraft Structures Involving Composite Materials Oct. 1986 11 p (For primary document see N87-20174 13-01)
Avail: NTIS HC A11/MF A01

Concepts and procedures for the rapid repair of battle-damaged composite structures are discussed. The damage consists of elongated or concentrated penetrations of solid wing skins and of honeycomb empennage. The size of the damage, in conjunction with the strength-critical nature of these structures, requires structural repairs in order to restore a strength capability commensurate with the maximum expected flight loads and service temperatures. Guidelines for these repairs are based on the USAF concept of operation for aircraft battle damage repair. Structural tests are being conducted to validate repair designs. Damage simulation, repair design, damage cleanup, repair fabrication, and available test results are reported. Author

N87-20190# Army Materials Technology Lab., Watertown, Mass.
UNCONVENTIONAL APPROACHES TO FIELD REPAIR
Stanley E. Wentworth, Michael S. Sennett, and John W. Gibson (Southern Research Inst., Birmingham, Ala.) *In* AGARD The Repair of Aircraft Structures Involving Composite Materials Oct. 1986 8 p (For primary document see N87-20174 13-01)
Avail: NTIS HC A11/MF A01

Field repair of composites presents special problems for the Army where the repair might literally be performed in a field or other remote location. In such a situation, access to electric power both for refrigeration to preserve reactive resin systems and for heating to cure the patch, is severely limited. In order to circumvent these problems, we have investigated some novel approaches to the packaging and curing of composite patches. One approach involves a self-contained kit in which all of the patch components including the reinforcement are separate from one another until the patch is needed, at which time they are combined in the proper ratio by means of a simple operation. Shelf-life for such a system, even without refrigeration is thus indefinite. Another approach makes use of optical fibers to carry light energy into the interior of an otherwise opaque graphite fiber-reinforced patch thereby permitting the use of a photochemically curable matrix resin. Initial efforts to implement these approaches, some of the difficulties encountered, and current attempts to circumvent them are discussed. Some new approaches are also outlined. Author

N87-20191# Advisory Group for Aerospace Research and Development, Neuilly-Sur-Seine (France).
PATCH REPAIR OF CORRODED AIRCRAFT SKIN AREAS
W. G. J. tHart and R. J. H. Wanhill *In* AGARD The Repair of Aircraft Structures Involving Composite Materials Oct. 1986 8 p Sponsored by the Royal Netherlands Air Force (For primary document see N87-20174 13-01)
Avail: NTIS HC A11/MF A01

Environmental conditions in Europe are conducive to corrosion attack of aircraft structures. In military aircraft, corrosion problems occur especially at countersunk fastener holes. The corrosion is generally removed by grinding. A limited amount of material removal is specified by the aircraft manufacturers, but it is sometimes necessary to exceed these limits. When this happens a repair is necessary to allow continued operation. An investigation of the effectiveness of bonded patch repairs was carried out. The patch materials were aluminum alloy sheet and aramid fiber reinforced composite prepreg. A cold curing acrylic based adhesive was used for bonding. Specimens with simulated patch repairs were subjected to both constant amplitude and flight simulation fatigue testing under various environmental conditions. The results indicated that bonded patches are potentially very good repairs for areas weakened by corrosion and its removal. Author

N87-20192# British Airways, Middlesex (England).
BRITISH AIRWAYS EXPERIENCE WITH COMPOSITE REPAIRS
K. B. Armstrong *In* AGARD The Repair of Aircraft Structures Involving Composite Materials Oct. 1986 12 p (For primary document see N87-20174 13-01)
Avail: NTIS HC A11/MF A01

British Airways experience with composite repairs since 1970 is discussed. The use of composite materials to repair metal structures such as Concorde wing leading edges is discussed. Repair of composite parts from Radomes starting in 1970, through B.747 body fairing and floor panels, to the repair of carbon fiber composite control surfaces and access doors on the B.757 is covered. Most of the repairs have used cold-setting resins (with heat lamp assisted curing) but some hot-setting adhesives and pre-pregs have been used. Effort is being made to develop techniques to facilitate the use of hot-setting adhesives. More information will be sought on diffusion and solubility coefficients of all types of adhesives to aid selection and improve the durability of repairs. Author

02 AERODYNAMICS

Includes aerodynamics of bodies, combinations, wings, rotors, and control surfaces; and internal flow in ducts and turbomachinery.

For related information see also *34 Fluid Mechanics and Heat Transfer.*

N87-20193# Maryland Univ., College Park.
OPTIMIZATION OF HYPERSONIC WAVERIDERS DERIVED FROM CONE FLOWS INCLUDING VISCOUS EFFECTS Ph.D. Thesis
Kevin Gerald Bowcutt 1986 256 p
Avail: Univ. Microfilms Order No. DA8628966

Over the past two years, interest in all aspects of hypersonic flight has grown explosively, driven by new vehicle concepts such as the aerospace plane, aero-assisted orbital transfer vehicles, and hypersonic cruise vehicles, to name a few. High lift-to-drag ratio (L/D) is important for one reason or another to almost all of the hypersonic vehicle concepts currently under investigation, yet it is well known that high values of L/D are very difficult to obtain at hypersonic speeds, due to the presence of strong shock waves (hence high wave drag) and massive viscous effects. In fact, there is a general empirical correlation by Kuchemann based on actual flight data for (L/D)max as a function of Mach number, given by (L/D)max = M sub infinity + 3 M sub infinity which represents a type of L/D barrier, which most real flight vehicles are unable to break. It is proposed to develop a new class of hypersonic vehicles which will overcome this L/D barrier. The vehicles are waveriders with windward surfaces derived from conical flows and optimized for maximum L/D. Included in the waverider analysis are upper surfaces derived from axisymmetric expansion flows, blunted leading edges to satisfy aerodynamic heating requirements, and most importantly, detailed viscous effects (including boundary layer transition). It is the inclusion of detailed viscous effects within the optimization process that makes the present work unique. Optimization is performed using a numerical non-linear minimization algorithm. Dissert. Abstr.

N87-20194 Colorado Univ., Boulder.
COMPUTATION OF TRANSONIC FLOW OVER POROUS AIRFOILS Ph.D. Thesis
Chung-Lung Chen 1986 116 p

Avail: Univ. Microfilms Order No. DA8700342

A numerical tool is constructed to examine the effects of a porous surface on transonic airfoil performance and to help understand the flow structure of passive shockwave/boundary layer interactions. The porous region is located near the shock with a cavity underneath it. This study is composed of two parts. Solved in the first part, with an inviscid-flow approach, is the transonic full-potential equation associated with transpiration boundary conditions obtained from porosity modeling. The numerical results of this part indicate that a porous airfoil has a wave drag lower than that of a solid airfoil. The observed lambda-shock structure in wind-tunnel tests can be predicted. Furthermore, the lift could be increased with an appropriate porosity distribution. In the second part, the modified version of either an interactive boundary layer (IBL) algorithm or a thin-layer Navier Stokes (TLNS) algorithm is used to study the outer flow, while a stream-function formulation is used to model the inner flow in the shallow cavity. The coupling procedure at the porous surface is based on Darcy's law and the assumption of a constant total pressure in the cavity. In addition, a modified Baldwin-Lomax turbulence model is used todescribe the transpired turbulent boundary layer in the TLNS approach, while the Cebeci turbulence model is used in the IBL approach. According to the present analysis, a porous surface can reduce the wave drag appreciably, but can also increase the viscous losses. As has been observed experimentally, the numerical results indicate that the total drag is reduced at higher Mach numbers and increased at lower Mach numbers when the angles of attack are small. Furthermore, the streamline patterns of passive shock/boundary layer interaction are revealed in this study.

Dissert. Abstr.

N87-20195 Virginia Polytechnic Inst. and State Univ., Blacksburg.
EXPERIMENTAL AND FINITE-ELEMENT INVESTIGATION OF FLOW PAST SINGLE AND MULTIPLE CYLINDERS Ph.D. Thesis

Manoranjan Dhaubhadel 1986 274 p

Avail: Univ. Microfilms Order No. DA8700097

Fluid flows past single and multiple cylinders in different configurations are investigated both experimentally and numerically. Three and five in-line cylinders and in-line and staggered bundles of cylinders with different pitch-to-diameter ratios are considered. Experimental work is comprised of laser Doppler velocimetry and flow visualization obtained in a water tunnel and skin friction, pressure, lift, drag and hot-wire measurements obtained in a wind tunnel. Both steady and pulsed flows are considered. Numerical work consists of finite element analysis of Navier-Stokes and energy equations governing viscous fluid flow past single and multiple cylinders. Measurements of the fluid dynamic quantities for flow past cylinders reveal that flow pulsation at frequencies which induce lock-on increases the organization of the flow in gaps between cylinders. A new pattern of flow field is found for flow past a triad and a pentad of cylinders with a pitch-to-diameter ratio of 1.8. The numerical analysis generates important integral characteristics like flow resistance and heat transfer. A staggered square arrangement of finite bundle of cylinders is found to have better heat transfer characteristics. Dissert. Abstr.

N87-20196 Stanford Univ., Calif.
A RATIONAL APPROACH TO LIFTING SURFACE THEORY WITH APPLICATION TO LARGE ANGLES OF ATTACK Ph. D. Thesis

Becker vanNiekerk 1986 165 p

Avail: Univ. Microfilms Order No. DA8700832

The acceleration potential formulation is advocated as an alternative to the velocity potential methods currently used to find the time accurate lift distributions on thin wings in unsteady subsonic flow. Advantages offered by the use of the acceleration potential are that compressibility can be accounted for and that no wake discretization is necessary. A classical variational statement is used to derive special properties of a weighted residual method. It is shown that some weighted integral of the sought solution can be obtained to second order accuracy in the solution to the original and adjoint problems. For aerodynamics, it is assumed that the reverse flow is adjoint to the original problem. In numerical solutions, the characteristic double pole singular integrals which arise in subsonic wing theory are integrated numerically with a new Gauss-type quadrature rule. This substantially simplifies the algebra involved in the use of kernel function methods. A detailed discussion of the possibility of using acceleration potential methods to do free wake analyses around slender wings is presented. Dissert. Abstr.

N87-20197 Georgia Inst. of Tech., Atlanta.
A NUMERICAL STUDY OF THE WEIS-FOGH MECHANISM Ph.D. Thesis

Myonghan Sohn 1986 190 p

Avail: Univ. Microfilms Order No. DA8628367

A numerical scheme is developed and utilized to study the time-dependent viscous flows about two-dimensional Weis-Fogh wings. The scheme uses the vorticity and the stream function as dependent variables. An integral representation is utilized to determine the surface vorticity and to calculate stream function values at the outer boundary of the computation field. Finite difference methods are used to solve the vorticity transport equation and the Poisson's equation for the stream function inside the computational domain. The present numerical scheme removes several restrictions encountered by previous investigators such as the inviscid flow assumption, flow Reynolds number limitation and the type of wing motion that may be treated. Two different types of wing motion, the fling and the fling followed by the moving apart of the wings, are treated for flow Reynolds numbers of 32 and 13000. The development of the flows around the wings are analyzed through the streamlines and equi-vorticity contours. Aerodynamic analyses are carried out through computed distributions of surface vorticity and surface pressure. The results confirm several experimental observations and successfully provide a physical interpretation of these observations. Several additional features of the aerodynamic load generation are revealed by the present study. The aerodynamic loads are found to be mainly a consequence of large suction pressure on the leeward surface caused by the strong separation vortex. The wings pump energy into the fluid at a high rate in the initial phase of fling. The Weis-Fogh wings obtain a significant gain in overall lift output through unsteady mechanisms. Dissert. Abstr.

N87-20198 Georgia Inst. of Tech., Atlanta.
NUMERICAL SOLUTIONS OF UNSTEADY FLOW PAST ROTOR SECTIONS Ph.D. Thesis

Wei Tang 1986 220 p

Avail: Univ. Microfilms Order No. DA8628368

An implicit finite-difference procedure was developed for the solution of the two-dimensional unsteady compressible Euler and Navier-Stokes equations in strong conservation form. An alternating-direction-implicit method is employed as the time marching algorithm. A body-fitted C-grid system that provides cluster in the direction normal to the body surface is used. The computer program resulting from this procedure can be used to calculate both the steady and unsteady flows, inviscid and viscous flows, laminar and turbulent flows. The turbulent shear stresses are simulated by a two layer algebraic eddy-viscosity model. The numerical procedure has been validated through comparisons of several inviscid and viscous flow solutions with other reliable numerical and experimental data. A vortex modeling method was also developed to study complex vortex-airfoil interaction problems. This model allows the solution scheme to capture and convect vortices without excessive numerical diffusion. This model is not restricted only to applications in weak blade-vortex interaction problems, in which the vortex core does not change shape. It can also be applied to strong vortex-airfoil interaction and vortex-airfoil collisions. Some weak vortex-airfoil interaction solutions have been compared with available numerical results from other researchers. Good agreement is observed. Using the present numerical scheme and the vortex modeling method, two categories of blade-vortex interaction problems, namely the weak interaction and the strong interaction with collision have been studied. Dissert. Abstr.

N87-20199# Advisory Group for Aerospace Research and Development, Neuilly-Sur-Seine (France). Fluid Dynamics Panel.
APPLICATIONS OF COMPUTATIONAL FLUID DYNAMICS IN AERONAUTICS
Loughton, England Nov. 1986 428 p In ENGLISH and FRENCH Symposium held in Aix-en-Provence, France, 7-10 Apr. 1986
(AGARD-CP-412; ISBN-92-835-0402-X) Avail: NTIS HC A19/MF A01

The goal of the symposium was to provide a balanced, if not exhaustive, assessment of the status of computational fluid dynamics in aerodynamic design and analysis, where CFD is making an increasingly major impact. The rapid progress in computer capability, the general availability of large scale computers and parallel achievements in numerical analysis, algorithm development and user experience were evidenced by the presentations. The sessions were divided into subject areas of: grid generation, inviscid flow, viscous-inviscid interactions, and Navier-Stokes solutions. For individual titles, see N87-20200 through N87-20231.

N87-20200# National Aerospace Lab., Amsterdam (Netherlands).
FLEXIBLE GRID GENERATION FOR COMPLEX GEOMETRIES IN TWO SPACE DIMENSIONS BASED ON VARIATIONAL PRINCIPLES **c61**
B. Oskam and G. H. Huising *In* AGARD Application of Computational Fluid Dynamics in Aeronautics Nov. 1986 14 p Sponsored by Netherlands Agency for Aerospace Programs (For primary document see N87-20199 13-02)
Avail: NTIS HC A19/MF A01

A method is described that is suitable for the numerical generation of boundary-conforming curvi-linear coordinate systems. The method is based on the decomposition of a multiply connected domain into a number of simply connected zones. In each zone the grid is computed by solving a system of Euler equations that minimizes a functional of the unknown transformation functions. This system of equations and the natural boundary conditions of the minimization problem are discussed. A first illustration of this technique is given for the case of a three-element airfoil. Author

N87-20201# Aircraft Research Association Ltd., Bedford (England).
A DISCUSSION ON A MESH GENERATION TECHNIQUE APPLICABLE TO COMPLEX GEOMETRIES **c61**
N. P. Weatherill, J. A. Shaw, C. R. Forsey, and K. E. Rose *In* AGARD Applications of Computational Fluid Dynamics in Aeronautics Nov. 1986 12 p Sponsored by Ministry of Defence and British Aerospace (For primary document see N87-20199 13-02)
Avail: NTIS HC A19/MF A01

A general three-dimensional block structured grid generation technique is described. It was coupled with an Euler algorithm to simulate the flow around complicated aerodynamic configurations. The flow field is subdivided into a set of non-overlapping blocks and grids are generated simultaneously in all of the blocks using an elliptic grid generation method. Appropriate boundary conditions applied on the face of the blocks ensure that grid lines pass smoothly between blocks leaving the grid globally smooth. Details of the surface and field grid generation are given and techniques to control the position of grid points are highlighted. Grid topologies for complicated civil and military configurations are discussed. Examples are given of grids for complicated configurations and some results of flow calculations on block structured grids are shown. Author

N87-20202# Dornier-Werke G.m.b.H., Friedrichshafen (West Germany). Theoretical Aerodynamic Group.
NUMERICAL GRID GENERATION AROUND COMPLETE AIRCRAFT CONFIGURATIONS **c61**
Willy Fritz *In* AGARD Applications of Computational Fluid Dynamics in Aeronautics Nov. 1986 8 p (For primary document see N87-20199 13-02)
Avail: NTIS HC A19/MF A01

A method for accurately generating boundary conforming, three-dimensional computational grids applicable to realistic aircraft configurations is presented. Configurations with an arbitrarily shaped and positioned wing, a horizontal tail (or canard) and a vertical tail attached to an arbitrarily shaped fuselage can be treated. The grid generation technique divides the computational domain into multiple rectangular blocks whose structure follow the natural lines of the configuration. For each of these contiguous sub-regions the grids are generated separately and then patched together to cover the entire physical region. The grids for the sub-regions are generated by the solution of elliptical partial differential equations (PDE). The method is an automated procedure but with interactive control and optimization possibilities which enable the user to produce coordinate lines with sufficient continuity across the block boundaries. Due to the block structure and the data organization of the method very fine grids (up to several millions of grid points) for complete aircraft configurations can be generated. Author

N87-20203*# National Aeronautics and Space Administration. Ames Research Center, Moffett Field, Calif.
GEOMETRY DEFINITION AND GRID GENERATION FOR A COMPLETE FIGHTER AIRCRAFT **c61**
Thomas A. Edwards *In* AGARD Applications of Computational Fluid Dynamics in Aeronautics Nov. 1986 12 p Previously announced as N86-28050 (For primary document see N87-20199 13-02)
Avail: NTIS HC A19/MF A01 CSCL 09B

Recent advances in computing power and numerical solution procedures have enabled computational fluid dynamicists to attempt increasingly difficult problems. In particular, efforts are focusing on computations of complex three-dimensional flow fields about realistic aerodynamic bodies. To perform such computations, a very accurate and detailed description of the surface geometry must be provided, and a three-dimensional grid must be generated in the space around the body. The geometry must be supplied in a format compatible with the grid generation requirements, and must be verified to be free of inconsistencies. A procedure for performing the geometry definition of a fighter aircraft that makes use of a commercial computer-aided design/computer-aided manufacturing system is presented. Furthermore, visual representations of the geometry are generated using a computer graphics system for verification of the body definition. Finally, the three-dimensional grids for fighter-like aircraft are generated by means of an efficient new parabolic grid generation method. This method exhibits good control of grid quality. Author

N87-20204# Royal Aircraft Establishment, Farnborough (England). Aerodynamics Dept.
AN ASSESSMENT OF THE USE OF LOW-ORDER PANEL METHODS FOR THE CALCULATION OF SUPERSONIC FLOWS **c61**
J. S. Smith and D. S. Woodward *In* AGARD Applications of Computational Fluid Dynamics in Aeronautics Nov. 1986 8 p (For primary document see N87-20199 13-02)
Avail: NTIS HC A19/MF A01

Three low-order panel methods developed for the analysis of supersonic flows were used to make calculations for a number of test configurations, with the aim of establishing the range of problems for which this class of computational method yields adequate solutions. The programs investigated were the Woodward USSAERO/C program, the related NLRAERO program, and the British Aerospace Warton supersonic panel program. Results obtained using these programs were evaluated against theoretical and experimental data for a number of test cases covering wing-alone, body-alone and wing-body geometries. It is concluded that low-order panel methods can provide adequate solutions for supersonic flows about wings, bodies and wing-body combinations, provided the assumptions implicit in the linearised potential flow model are not violated. Examples show that the prediction of lift and pitching moment curve slopes for quite complex configurations may be acceptable, but that the detailed pressure distributions are not always predicted satisfactorily. In particular, serious problems are encountered in calculating the flow about wings with

rounded supersonic leading edges due to the linearised flow model which is used. Author

N87-20205# Office National d'Etudes et de Recherches Aerospatiales, Paris (France).
NEW NUMERICAL TECHNIQUES IN THE METHOD OF SINGULARITIES FOR APPLICATION TO COMPLEX THREE-DIMENSIONAL CONFIGURATIONS [TECHNIQUES NUMERIQUES NOUVELLES DANS LES METHODES DE SINGULARITES POUR L'APPLICATION A DES CONFIGURATIONS TRIDIMENSIONNELLES COMPLEXES] **c64**
T. H. Le, Y. Morchoisne, and J. Ryan *In* AGARD Applications of Computational Fluid Dynamics in Aeronautics Nov. 1986 22 p In FRENCH Original language document was announced in IAA as A87-21085 (For primary document see N87-20199 13-02)
Avail: NTIS HC A19/MF A01

A singularity method for the analysis of steady irrotational inviscid incompressible flows around complex three-dimensional bodies is developed and demonstrated. The technique is based on numerical integration and a steepest-descent solution procedure and employs a simple lumping scheme to improve the accuracy while providing significantly lower computation times than conventional methods. Results for sample problems involving a helicopter fuselage and a wing are presented in tables and graphs. E.R.

N87-20206*# National Aeronautics and Space Administration. Ames Research Center, Moffett Field, Calif.
THE PREDICTION OF TRANSONIC LOADING ON ADVANCING HELICOPTER ROTORS
R. C. Strawn and C. Tung *In* AGARD Applications of Computational Fluid Dynamics in Aeronautics Nov. 1986 14 p (For primary document see N87-20199 13-02)
Avail: NTIS HC A19/MF A01

Two different schemes are presented for including the effect of rotor wakes on the finie-difference prediction of rotor loads. The first formulation includes wake effects by means of a blade-surface inflow specification. This approach is sufficiently simple to permit coupling of a full-potential finite-difference rotor code to a comprehensive integral model for the rotor wake and blade motion. The coupling involves a transfer of appropriate loads and inflow data between the two computer codes. Results are compared with experimental data for two advancing rotor cases. The second rotor-wake modeling scheme is a split potential formulation for computing unsteady blade-vortex interactions. Discrete vortex fields are introduced into a three-dimensional, conservative, full-potential rotor code. Computer predictions are compared with two experimental blade-vortex interaction cases. Author

N87-20207# Canadair Ltd., Montreal (Quebec).
PREDICTION OF WING-BODY-STORE AERODYNAMICS USING A SMALL PERTURBATION METHOD AND A GRID EMBEDDING TECHNIQUE
Fassi Kafyeke *In* AGARD Applications of Computational Fluid Dynamics in Aeronautics Nov. 1986 13 p Sponsored by Department of National Defence of Canada (For primary document see N87-20199 13-02)
Avail: NTIS HC A19/MF A01

A computer program providing accurate and cost effective predictions of transonic flow fields about three dimensional configurations has been developed at Canadair. The computation scheme uses the Small Perturbation Equation and a grid embedding technique. The flow field is solved iteratively, using successive line overrelaxation. The comparisons between computed results and experiment for a wing-body and a generic wing-body-pylon-store configuration show that a good level of accuracy can be obtained with this approach. The program was written with the overall emphasis on lowering the computation time and is considered as a stepping stone towards a full aircraft-store aerodynamic simulation. The potential of the method for analyzing complex three dimensional configurations is discussed, showing that the code is a very practical tool for the design office, for parametric studies or as a lead program for more sophisticated investigations using Euler or Navier-Stokes solvers. Author

N87-20208# National Aerospace Lab., Amsterdam (Netherlands). Information Div.
MATRICS, TRANSONIC POTENTIAL FLOW CALCULATIONS ABOUT TRANSPORT AIRCRAFT
J. vanderVooren, A. J. vanderWees, and J. H. Meelker *In* AGARD Applications of Computational Fluid Dynamics in Aeronautics Nov. 1986 14 p Sponsored in part by Netherlands Agency for Aerospace Programs (NIVR) (For primary document see N87-20199 13-02)
Avail: NTIS HC A19/MF A01

MATRICS is a system under development for the calculation of transonic (potential) flow about transport aircraft. The motivation for this development is discussed, as well as the basic concepts of the system. Details of the full potential flow solver, involving the newly developed Implicit Lower Upper decomposition/ Strongly Implicit Procedures (ILU/SIP) relaxation scheme, are given. A discussion on computer power required and some informatics aspects are also presented. Results of computations are presented and discussed. Author

N87-20209# British Aerospace Aircraft Group, Warton (England). Fluid Dynamics Section.
APPLICATIONS AND DEVELOPMENTS OF COMPUTATIONAL METHODS FOR THE AERODYNAMIC PROBLEMS OF COMPLEX CONFIGURATIONS
J. A. H. Petrie and P. M. Sinclair *In* AGARD Applications of Computational Fluid Dynamics in Aeronautics Nov. 1986 14 p (For primary document see N87-20199 13-02)
Avail: NTIS HC A19/MF A01

Problems encountered by the Aerodynamicist at a military design site are characterised by complex geometry and complex flow conditions. Because of the limitations of current Computational Fluid Dynamics (CFD) technology, its use represents a compromise in one or both of these areas. The way in which sensible use of the current generation of CFD codes can generate useful aerodynamic design data is illustrated by three particular examples; wing design, installed store loading and the prediction of store release trajectories. Although these examples will show that data can be generated by such techniques, they are by no means ideal. As an alternative to the methods being widely developed which require a body fitted grid, BAe Brough is developing an integral method which uses a rectangular grid passing through the configuration surface(s). The theory behind this method will be presented together with some results which show the technique to have great promise. Author

N87-20210# British Aerospace Aircraft Group, Warton (England). Aerodynamics Dept.
THE INTEGRATION OF COMPUTATIONAL FLUID DYNAMICS INTO THE MILITARY AIRCRAFT DESIGN PROCESS **c05**
W. R. Marchbank *In* AGARD Applications of Computational Fluid Dynamics in Aeronautics Nov. 1986 13 p (For primary document see N87-20199 13-02)
Avail: NTIS HC A19/MF A01

The rapid analysis and subsequent iterative refinement of aircraft shape is demonstrated by a number of applications of integrated CFD procedures, aimed at achieving specified supersonic performance. Without any reduction in transonic performance, the following complimentary benefits in the supersonic flight regime were established: (1) 5% reduction in drag through fuselage shaping; (2) 3% reduction in drag by decambering the wing through use of flaps; (3) 6% reduction in drag through a reduction in trim drag; (4) 15% increase in Thrust minus Drag through optimization of the intake flow field. Thus CFD based Project Procedures, used early in configuration design to refine the 3D lines, were used to increase supersonic turn rate by approximately 20%, for a fixed engine thrust, allowing supersonic design requirements to be met without penalizing transonic performance. Author

N87-20211# Naval Surface Weapons Center, Silver Spring, Md. Applied Mathematics Branch.

A SECOND ORDER GODUNOV METHOD FOR TACTICAL MISSILES **c64**

A. B. Wardlaw, Jr. and S. F. Davis *In* AGARD Applications of Computational Fluid Dynamics in Aeronautics Nov. 1986 10 p (For primary document see N87-20199 13-02)

Avail: NTIS HC A19/MF A01

A second order Godunov scheme is described for steady supersonic flow. This scheme, which marches the solution in space, is cast in a finite volume formulation and uses a mesh generated by a multiple zone procedure. Second order accuracy is obtained by computing local slopes and adding a predictor step. The bow shock is fit using the information contained within the Riemann problem. The scheme is applied to body-alone and finned configurations for which measurements are available. Reasonable agreement is obtained between experiment and calculation without the use of artificial viscosity or special procedures. Author

N87-20212# MATRA Service Aerodynamique, Velizy-Villacoublay (France).

SIMULATION OF A JET DEFLECTION SYSTEM WITH THE AID OF THE EULER EQUATIONS [SIMULATION D'UN SYSTEME DE DEVIATION DE JAT A L'AIDE DES EQUATIONS D'EULER] **c34**

M. Bredif, J. J. Chattot, C. Koeck, and P. Werle *In* AGARD Applications of Computational Fluid Dynamics in Aeronautics Nov. 1986 11 p In FRENCH (For primary document see N87-20199 13-02)

Avail: NTIS HC A19/MF A01

The solution method for the Euler equations is applied to the calculation of nozzle flow in missiles fitted with jet control surfaces. The approach utilized, an explicit finite volume method with convergence acceleration through the multigrid technique, is briefly described. The numerical results obtained are analyzed in detail and the interaction between the control surface and the nozzle wall is examined. Comparisons with experimental results are carried out. It is shown that the numerical simulation of the flow through the nozzle system with the jet control surface permits the accurate prediction of the thrust vector deviation due to control surface deflection, whereas the axial thrust loss is estimated low. Author

N87-20213# Dornier-Werke G.m.b.H., Friedrichshafen (West Germany). Theoretical Aerodynamic Group.

NUMERICAL SIMULATION OF INTERNAL AND EXTERNAL INVISCID AND VISCOUS 3-D FLOW FIELDS **c34**

Stefan Leicher *In* AGARD Applications of Computational Fluid Dynamics in Aeronautics Nov. 1986 27 p (For primary document see N87-20199 13-02)

Avail: NTIS HC A19/MF A01

A numerical method for solving the 3-D Euler equations in geometrical complex domains was developed. The approach divides the computational space into multiple blocks whose structure follows the natural lines of the configuration. A systematic, multi-block grid generation scheme is used to produce the grid. The flow solutions are obtained by solving the Euler equations by a finite volume discretization and a Runge-Kutta time stepping scheme. The main advantage of this method is the applicability to complex geometries, for example complete aircraft configurations including wing, fuselage, canard and tail. The coupling with a 3-D boundary layer method allows to account for viscous effects. Another application for the method was the simulation of flows in the presence of a propeller. Author

N87-20214*# Massachusetts Inst. of Tech., Cambridge. CFD Lab.

APPLICATIONS OF EULER EQUATIONS TO SHARP EDGE DELTA WINGS WITH LEADING EDGE VORTICES

Earll M. Murman and Arthur Rizzi (Aeronautical Research Inst. of Sweden, Bromma.) *In* AGARD Applications of Computational Fluid Dynamics in Aeronautics Nov. 1986 13 p (For primary document see N87-20199 13-02)

(Grant NAG1-358)

Avail: NTIS HC A19/MF A01

Studies on the solution of discrete Euler equations past swept delta wing configurations with sharp leading edges are presented. Freestream Mach numbers range from zero to supersonic, although the Mach number normal to the leading edge is subsonic for all cases discussed. A few examples are given to show the application of the numerical methods to representative problems. The major dicussion is directed at the application of Computational Fluid Dynamics to the understanding of the fundamental fluid mechanic mechanisms of this class of flows. Author

N87-20215# Avions Marcel Dassault, Saint-Cloud (France). Dept. d'Aerodynamique Theorique.

UTILIZATION OF EULER CODES IN NONLINEAR AERODYNAMICS [UTILISATION DES CODES EULER EN AERODYNAMIQUE NON LINEAIRE]

Pierre Perrier *In* AGARD Applications of Computational Fluid Dynamics in Aeronautics Nov. 1986 8 p In FRENCH (For primary document see N87-20199 13-02)

Avail: NTIS HC A19/MF A01

Principal solution techniques for Euler problems are reviewed including the finite difference and finite volume methods, the finite element method, perturbation techniques for potential non-rotational solutions, and methods covering rotational zones. Specific examples of Euler code computations are discussed, namely, air intake, nonstationary, and hypersonic calculations. Finally, the use of Euler codes as approximations of Navier-Stokes codes is examined. M.G.

N87-20216# Messerschmitt-Boelkow-Blohm G.m.b.H., Munich (West Germany). Helicopter and Military Aircraft Group.

EULER SOLUTION FOR A COMPLETE FIGHTER AIRCRAFT AT SUB- AND SUPERSONIC SPEED **c05**

Albrecht Eberle and Kent Misegades (Cray Research, Inc., Mendota Heights, Minn.) *In* AGARD Applications of Computational Fluid Dynamics in Aeronautics Nov. 1986 12 p (For primary document see N87-20199 13-02)

Avail: NTIS HC A19/MF A01

A survey is given on the construction of a novel high resolution Euler code which is applied for airflow calculations past a fighter type aircraft. The principle feature of the flow solver is a Godunov type averaging procedure based on the eigenvalue analysis of the Euler equations by means of which the fluxes are evaluated at the finite volume faces which separate constant sets of flow variables on either side. The procedure is third order accurate and locally monotonicity preserving thus avoiding the drawbacks of global TVD-schemes. The grid generation for complex configurations is performed from solutions of linear biharmonic equations with only one parameter prescribed by the program user. Vector computer performance of the explicit and implicit program versions are considered. Author

N87-20217# General Dynamics Corp., Fort Worth, Tex.

ANALYSIS OF THE F-16 FLOW FIELD BY A BLOCK GRID EULER APPROACH

Steve L. Karman, Jr., John P. Steinbrenner, and Keith M. Kisielewski *In* AGARD Applications of Computational Fluid Dynamics in Aeronautics Nov. 1986 14 p (For primary document see N87-20199 13-02)

Avail: NTIS HC A19/MF A01

A grid generation procedure was developed to create complex block grid systems, beginning with the generation of block surfaces, up to the generation of the full block volume grids. Parallel to this, a multiple block Euler equation solver was developed using a hybrid flux vector split and split MacCormack scheme, written to allow very general boundary conditions specification. The two codes are utilized herein to generate an inviscid analysis of an entire F-16 transonic flowfield. Preliminary results are presented and are seen to compare well with experimental data. Even better correlation with experimental data is expected once a fully converged solution is obtained. Author

N87-20218# Imperial Coll. of Science and Technology, London (England). Dept. of Mechanical Engineering.
COMPARISON OF FINITE DIFFERENCE CALCULATIONS OF A LARGE REGION OF RECIRCULATING FLOW NEAR AN AIRFOIL TRAILING EDGE
L. Reis and B. E. Thompson (Waterloo Univ., Ontario.) *In* AGARD Applications of Computational Fluid Dynamics in Aeronautics Nov. 1986 21 p Sponsored by British Ministry of Defense, Institute National de Investigacao Cientifica of Portugal and the National Science and Engineering Council of Canada (For primary document see N87-20199 13-02)
Avail: NTIS HC A19/MF A01

Calculations are presented for a turbulent boundary layer which separates upstream of a sharp trailing edge and results in a large region of recirculating flow and a curved downstream wake. The solutions obtained from two precedures that solve finite-difference equations formulated with hybrid combinations of upwind-central and bounded skew-upwind-central difference approximations for convective terms, are compared. Numerical error was smaller, and accordingly less false diffusion was apparent, in the bounded-skew calculations although there was no significant improvement in the agreement with experiment. Agreement between measured and calculated values of the lift coefficient was within 3% and required representation of momentum transport and pressure gradient normal to the surface, but the measured drag coefficient was less than 80% of that obtained in both calculations. Deficiencies are attributable, in part, to turbulence-model assumptions which do not represent the effects of stabilizing and destabilizing streamline curvature and the complex interaction of the backflow, pressure-side and curved suction-side boundary layers in the vicinity of the rear stagnation point downstream of the trailing edge. Author

N87-20219# Messerschmitt-Boelkow-Blohm G.m.b.H., Munich (West Germany).
ZONAL SOLUTIONS FOR AIRFOILS USING EULER BOUNDARY-LAYER AND NAVIER-STOKES EQUATIONS
M. A. Schmatz and E. H. Hirschel *In* AGARD Applications of Computational Fluid Dynamics in Aeronautics Nov. 1986 13 p (For primary document see N87-20199 13-02)
Avail: NTIS HC A19/MF A01

A method is presented to simulate steady viscous flows by a zonal concept, where local solutions of the Navier-Stokes equations are coupled with solutions of the Euler and the boundary-layer equations. The basic idea is to solve the Navier-Stokes equations only in those zones of the flowfield where strong interaction occurs. The overall goal is to reduce the computation costs. The governing equations and the coupling procedures are presented for general three dimensional viscous flows. Results are given from two dimensional applications obtained with an alternating coupling scheme. Then a close coupling scheme is introduced. For this purpose a new relaxation approach for the implicit unfactored Euler and Navier-Stokes equations was implemented. The computed results demonstrate good capability for the close approach. Author

N87-20220# Istanbul Univ. (Turkey). Faculty of Aeronautics and Astronautics.
NUMERICAL INVESTIGATION OF THE LAMINAR BOUNDARY LAYER ON A 3-D BODY STARTED IMPULSIVELY FROM REST
U. Gulcat *In* AGARD Applications of Computational Fluid dynamics in Aeronautics Nov. 1986 6 p (For primary document see N87-20199 13-02)
Avail: NTIS HC A19/MF A01

Unsteady flow of viscous incompressible fluid external to three dimensional bodies is considered. Based on the boundary layer concept the simplified version of the equations of motion are expressed in non-orthogonal coordinates which fits to body surface. The differential form of the equations are discretised with finite differencing to give a solution procedure which does not require any iteration while marching in space and in time. The procedure developed first tested for the flow past a circular cylinder. The results obtained are compared with the experimental and the results of the previous numerical works available. Finally three dimensional impulsive flow past an oblate spheroid is considered. The metric coefficients and all the necessary geometrical features obtained analytically are used in the governing equations. The numerical solution is carried until the time of flow reversal that occurs at the rear stagnation point of the spheroid. Author

N87-20221# Societe Nationale Industrielle Aerospatiale, Marignane (France). Div. Helicopteres.
THEORETICAL ANALYSIS OF FLOWS AROUND HELICOPTER FUSELAGES: APPLICATION TO DESIGN AND DEVELOPMENT
A. Cler *In* AGARD Applications of Computational Fluid Dynamics in Aeronautics Nov. 1986 8 p (For primary document see N87-20199 13-02)
Avail: NTIS HC A19/MF A01

Three dimensional aerodynamic calculations as applied to fuselage design are described. Three levels of complexity may be distinguished in the calculation programs: (1) a singularities method describing the potential flow around a fuselage, (2) an integral three dimensional boundary layer method for predicting three dimensional separations, and (3) a point vortex wake model. The first two methods are routinely used with very short response times, either on complete fuselages or for specific aircraft sections. Close agreement is obtained with the available experimental results. Various examples are given of applications to project or development work. Operational calculations cannot yet be performed with the wake model, as the method is still under development. In the current state of the art, aerodynamic calculations provide undeniable services but can by no means replace wind tunnel tests for determining complete aircraft drag. Author

N87-20222*# National Aeronautics and Space Administration. Ames Research Center, Moffett Field, Calif.
USING THE BOUNDARY-LAYER EQUATIONS IN THREE-DIMENSIONAL VISCOUS FLOW SIMULATION c34
William R. VanDalsem and Joseph L. Steger *In* AGARD Applications of Computational Fluid Dynamics in Aeronautics Nov. 1986 12 p Previously announced as N86-28061 (For primary document see N87-20199 13-02)
Avail: NTIS HC A19/MF A01

A simple and computationally efficient algorithm for solving the unsteady three dimensional boundary layer equations in a time accurate or relaxation mode is presented. The algorithm is used to compute the separated flow over a 6:1 ellipsoid at angle of attack and the transonic flow over a finite wing with shock induced separation. These results are compared to available experimental data. A method of using the boundary layer algorithm to accelerate a Navier-Stokes computation is also presented. Example computations indicate that a boundary layer algorithm can be used to improve both the accuracy and efficiency of a Navier-Stokes algorithm. Author

N87-20223# Office National d'Etudes et de Recherches Aeronautiques, Paris (France).
COMPUTATION OF THREE-DIMENSIONAL FLOWS BY VISCOUS-INVISCID INTERATION USING THE MZM METHOD c34
M. Lazareff and J. C. LeBalleur *In* AGARD Applications of Computational Fluid Dynamics in Aeronautics Nov. 1986 15 p In FRENCH; ENGLISH summary (For primary document see N87-20199 13-02)
Avail: NTIS HC A19/MF A01

The MZM numerical method (Multi-Zonal-Marching) previously suggested for solving the hyperbolic set of equations of the viscous layers, and the three dimensional turbulent mean velocity profiles modelling suggested for computing separated flows over infinite swept wings, have lead to the development of a very general three dimensional boundary layer method, fit for use on complex geometries, with any prescribed structured mesh, in view of a viscous-inviscid interaction analysis. The method was used successfully for computing transonic wings without separation, with solution of the coupling and rigorous integration of the boundary layer equations starting from the stagnation point. New results are here presented, without coupling, for configurations of ellipsoids of revolution, or flattened ellipsoids, at 30 deg or 60 deg of incidence, and for a geometry of the slender lifting-body type at

30 deg of incidence and 10 deg of yaw angle, with a quasi-total accessibility of the computation domain. These boundary-layer-alone calculations display a flow structure which exhibits a strong analog with accumulations lines, the numerical solution giving access to both sides of these lines. Author

N87-20224# Royal Aircraft Establishment, Farnborough (England). Aerodynamics Dept.
APPLICATIONS OF RAE VISCOUS FLOW METHODS NEAR SEPARATION BOUNDARIES FOR THREE-DIMENSIONAL WINGS IN TRANSONIC FLOW
M. C. P. Firmin *In* AGARD Applications of Computational Fluid Dynamics in Aeronautics Nov. 1986 14 p (For primary document see N87-20199 13-02)
Avail: NTIS HC A19/MF A01

Three applications of computational fluid dynamics (CFD) at high subsonic speeds, with transonic flow, are presented. Two of these relate to the prediction of the pressure distribution over swept wings at conditions close to the separation boundary and one to the design of a swept wing for a wind-tunnel model. The methods involved are a potential flow treatment of the inviscid flow coupled with a three dimensional, integral treatment of the turbulent boundary layer. The coupling between the viscous and inviscid flow codes is direct, through a transpiration condition at the wing surface and on a surface downstream of the wing. Author

N87-20225# Air Force Wright Aeronautical Labs., Wright-Patterson AFB, Ohio.
APPLICATION OF THE NAVIER-STOKES EQUATIONS TO SOLVE AERODYNAMIC PROBLEMS
J. S. Shang and W. L. Hankey (Wright State Univ., Dayton, Ohio.) *In* AGARD Applications of Computational Fluid Dynamics in Aeronautics Nov. 1986 12 p (For primary document see N87-20199 13-02)
Avail: NTIS HC A19/MF A01

An area presently evolving is Interdisciplinary Computational Fluid Dynamics (ICFD) in which the Navier-Stokes equations are coupled to another set of equations to solve interacting problems. The large computers approaching will permit elaborate solutions to these ICFD problems. Therefore, research on generic systems of equations by the CFD community is required to assist engineers to solve their coupled problems. Already some of the necessary research has been accomplished to solve ICFD problems. Advantage is taken of the present numerical algorithms and grid generation. The conservation form for the governing equations can be utilized and the field data to exploit vector processors can be arranged. However, new technology must be developed to model complex interface boundary conditions and to incorporate a variety of constitutive relationships for the state variables and transport processors. Also, it will become necessary to model many physical processes that are below subgrid scale. Examples of subgrid scale modeling phenomenon are turbulence, evaporation, atomization, devolatization, nucleation, chemical reactions, surface tension and surface roughness. This modeling can only be achieved after a series of numerical computations are combined with validation experiments. It also appears necessary that new numerical damping factors must be developed for ICFD in order to account for the new physics added to the problem with the attendant mathematical stiffness difficulties. Author

N87-20226# Boeing Military Airplane Development, Seattle, Wash.
CALCULATIONS FOR A GENERIC FIGHTER AT SUPERSONIC HIGH-LIFT CONDITIONS **c05**
J. C. Wai, G. Blom, and H. Yoshihara *In* AGARD Applications of Computational Fluid Dynamics in Aeronautics Nov. 1986 8 p (For primary document see N87-20199 13-02)
Avail: NTIS HC A19/MF A01

The parabolized Navier/Stokes method was used to calculate the flow over a generic fighter configuration with a canard and underwing nacelles at supersonic high lift conditions. The calculated pressure distributions agreed closely with experiments, but the pitot pressure profile predictions for the boundary layer were less satisfactory largely due to an inadequate mesh in the viscous sublayer. Author

N87-20227*# National Aeronautics and Space Administration. Ames Research Center, Moffett Field, Calif.
HIGH SPEED VISCOUS FLOW CALCULATIONS ABOUT COMPLEX CONFIGURATIONS
Denny S. Chaussee *In* AGARD Applications of Computational Fluid Dynamics in Aeronautics Nov. 1986 18 p (For primary document see N87-20199 13-02)
Avail: NTIS HC A19/MF A01 CSCL 01A

A review of past parabolized Navier-Stokes applications is presented. The equations, boundary conditions, the numerical method and the grid generation are all discussed. Results ranging from the low supersonic regime to the hypersonic regime are included. Author

N87-20228*# National Aeronautics and Space Administration. Ames Research Center, Moffett Field, Calif.
TRANSONIC NAVIER-STOKES WING SOLUTION USING A ZONAL APPROACH. PART 1: SOLUTION METHODOLOGY AND CODE VALIDATION
J. Flores, T. L. Holst, Unver Kaynak (Sterling Software, Palo Alto, Calif.), K. Gundy, and S. D. Thomas *In* AGARD Applications of Computational Fluid Dynamics in Aeronautics Nov. 1986 12 p Previously announced as N86-29765 (For primary document see N87-20199 13-02)
Avail: NTIS HC A19/MF A01 CSCL 01A

A fast diagonalized Beam-Warming algorithm is coupled with a zonal approach to solve the three dimensional Euler/Navier-Stokes equations. The computer code, called Transonic Navier-Stokes (TNS), uses a total of four zones for wing configurations (or can be extended to complete aircraft configurations by adding zones). In the inner blocks near the wing surface, the thin-layer Navier-Stokes equations are solved, while in the outer two blocks the Euler equations are solved. The diagonal algorithm yields a speedup of as much as a factor of 40 over the original algorithm/zonal method code. The TNS code, in addition, has the capability to model wind tunnel walls. Transonic viscous solutions are obtained on a 150,000-point mesh for a NACA 0012 wing. A three-order-of-magnitude drop in the L2-norm of the residual requires approximately 500 iterations, which takes about 45 min of CPU time on a Cray-XMP processor. Simulations are also conducted for a different geometrical wing called WING C. All cases show good agreement with experimental data. Author

N87-20229*# National Aeronautics and Space Administration. Ames Research Center, Moffett Field, Calif.
TRANSONIC NAVIER-STOKES WING SOLUTIONS USING A ZONAL APPROACH. PART 2: HIGH ANGLE-OF-ATTACK SIMULATION
Neal M. Chaderjian *In* AGARD Applications of Computational Fluid Dynamics in Aeronautics Nov. 1986 9 p Previously announced as N86-32392 (For primary document see N87-20199 13-02)
Avail: NTIS HC A19/MF A01 CSCL 01A

A computer code is under development whereby the thin-layer Reynolds-averaged Navier-Stokes equations are to be applied to realistic fighter aircraft configurations. This transonic Navier-Stokes code (TNS) utilizes a zonal approach in order to treat complex geometries and satisfy in-core computer memory constraints. The zonal approach was applied to isolate wing geometries in order to facilitate code development. The TNS finite difference algorithm, zonal methodology, and code validation with experimental data is addressed. Also addressed are some numerical issues such as code robustness, efficiency, and accuracy at high angles of attack. Special free-stream-preserving metrics proved an effective way to treat H-mesh singularities over a large range of severe flow conditions, including strong leading edge flow gradients, massive shock induced separation, and stall. Furthermore, lift and drag coefficients were computed for a wing up through Climax. Numerical oil flow patterns and particle trajectories are presented both for subcritical and transonic flow. These flow simulations are

rich with complex separated flow physics and demonstrate the efficiency and robustness of the zonal approach. Author

N87-20230# Deutsche Forschungs- und Versuchsanstalt fuer Luft- und Raumfahrt, Goettingen (West Germany). Inst. for Theoretical Fluid Mechanics.

SIMULATION OF THREE-DIMENSIONAL TRANSONIC FLOW WITH SEPARATION PAST A HEMISPHERE CYLINDER CONFIGURATION

W. Kordulla, H. Vollmers, and U. Dallmann *In* AGARD Applications of Computational Fluid Dynamics in Aeronautics Nov. 1986 15 p (For primary document see N87-20199 13-02)
(Grant DA-183/1-1/2)
Avail: NTIS HC A19/MF A01

The numerical simulation of the transonic laminar flow past a hemisphere cylinder at an angle of incidence of 0 deg and 19 deg is presented. In both cases the computations suggest unsteady flow behavior which requires further investigations, in particular because other applications by similar methods in two and three dimensions do allow the simulation of symmetric transonic and steady supersonic flows. One instantaneous flow result for the 19 deg case is used as an example to analyze the topology of a flow with separation. The analysis shows that the numerical simulation yields results consistent with possible topological structures, and can be used further to investigate steady state flows with separation. Author

N87-20231*# Air Force Wright Aeronautical Labs., Wright-Patterson AFB, Ohio.

NUMERICAL SIMULATION OF THE FLOW FIELD AROUND A COMPLETE AIRCRAFT

J. S. Shang and S. J. Scherr *In* AGARD Applications of Computational Fluid Dynamics in Aeronautics Nov. 1986 11 p Sponsored by NASA (For primary document see N87-20199 13-02)
Avail: NTIS HC A19/MF A01

The present effort represents a first attempt of numerical simulation of the flow field around a complete aircraft-like, lifting configuration utilizing the Reynolds averaged Navier-Stokes equations. The numerical solution generated for the experimental aircraft concept X24C-10D at a Mach number of 5.95 not only exhibited accurate prediction of detailed flow properties but also of the integrated aerodynamic coefficients. In addition, the present analysis demonstrated that a page structure of data collected into cyclic blocks is an efficient and viable means for processing the Navier-Stokes equations on the CRAY XMP-22 computer with external memory device. Author

N87-20232*# Titan Systems, Inc., Princeton, N.J.

THE EFFECT OF HEAVY RAIN ON AN AIRFOIL AT HIGH LIFT

Coleman DuP. Donaldson and Roger D. Sullivan Mar. 1987 36 p
(Contract NAS1-18088)
(NASA-CR-178248; NAS 1.26:178248; ARAP-597) Avail: NTIS HC A03/MF A01 CSCL 01A

No serious studies of the relationship of heavy rain to aircraft safety were made until 1981 when it was suggested that the torrential rain which often occurs at the time of severe wind shear might substantially increase the danger to aircraft operating at slow speeds and high lift in the vicinity of airports. While these data were not published until early 1983, appropriate measures were taken by NASA to study the effect of heavy rain on the lift of wings typical of commercial aircraft. One of the aspects of these tests that seemed confirmed by the data was the existence of a velocity effect on the lift data. The data seemed to indicate that when all the normal non-dimensional aerodynamic parameters were used to sort out the data, the effect of velocity was not accounted for, as it usually is, by the effect of dynamic pressure. Indeed, the measured lift coefficients at high lift indicated a dropoff in lift coefficient for the same free-stream water content as velocity was increased. indicated a drop-off in lift coefficient for the same free-stream water content as velocity was increased. Author

N87-20233*# National Aeronautics and Space Administration. Langley Research Center, Hampton, Va.

INVESTIGATION OF LEADING-EDGE FLAP PERFORMANCE ON DELTA AND DOUBLE-DELTA WINGS AT SUPERSONIC SPEEDS

Peter F. Covell, Richard M. Wood, and David S. Miller Apr. 1987 125 p
(NASA-TP-2656; L-16143; NAS 1.60:2656) Avail: NTIS HC A06/MF A01 CSCL 01A

An investigation of the aerodynamic performance of leading-edge flaps on three clipped delta and three clipped double-delta wing planforms with aspect ratios of 1.75, 2.11, and 2.50 was conducted in the Langley Unitary Plan Wind Tunnel at Mach numbers of 1.60, 1.90, and 2.16. A primary set of fullspan leading-edge flaps with similar root and tip chords were investigated on each wing, and several alternate flap planforms were investigated on the aspect-ratio-1.75 wings. All leading-edge flap geometries were effective in reducing the drag at lifting conditions over the range of wing aspect ratios and Mach numbers tested. Application of a primary flap resulted in better flap performance with the double-delta planform than with the delta planform. The primary flap geometry generally yielded better performance than the alternate flap geometries tested. Trim drag due to flap-induced pitching moments was found to reduce the leading-edge flap performance more for the delta planform than for the double-delta planform. Flow-visualization techniques showed that leading-edge flap deflection reduces crossflow shock-induced separation effects. Finally, it was found that modified linear theory consistently predicts only the effects of leading-edge flap deflection as related to pitching moment and lift trends. Author

N87-20234*# National Aeronautics and Space Administration. Langley Research Center, Hampton, Va.

UNSTEADY TRANSONIC FLOW CALCULATIONS FOR REALISTIC AIRCRAFT CONFIGURATIONS

John T. Batina, David A. Seidel, Samuel R. Bland, and Robert M. Bennett Mar. 1987 22 p Presented at the AIAA/ASME/ASCE/AHS 28th Structures, Structural Dynamics and Materials Conference, Monterey, Calif., 6-8 Apr. 1987
(NASA-TM-89120; NAS 1.15:89120; AIAA-87-0850) Avail: NTIS HC A02/MF A01 CSCL 01A

A transonic unsteady aerodynamic and aeroelasticity code has been developed for application to realistic aircraft configurations. The new code is called CAP-TSD which is an acronym for Computational Aeroelasticity Program - Transonic Small Disturbance. The CAP-TSD code uses a time-accurate approximate factorization (AF) algorithm for solution of the unsteady transonic small-disturbance equation. The AF algorithm is very efficient for solution of steady and unsteady transonic flow problems. It can provide accurate solutions in only several hundred time steps yielding a significant computational cost savings when compared to alternative methods. The new code can treat complete aircraft geometries with multiple lifting surfaces and bodies including canard, wing, tail, control surfaces, launchers, pylons, fuselage, stores, and nacelles. Applications are presented for a series of five configurations of increasing complexity to demonstrate the wide range of geometrical applicability of CAP-TSD. These results are in good agreement with available experimental steady and unsteady pressure data. Calculations for the General Dynamics one-ninth scale F-16C aircraft model are presented to demonstrate application to a realistic configuration. Unsteady results for the entire F-16C aircraft undergoing a rigid pitching motion illustrated the capability required to perform transonic unsteady aerodynamic and aeroelastic analyses for such configurations. Author

N87-20235*# National Aeronautics and Space Administration. Lewis Research Center, Cleveland, Ohio.

COMPOSITE GRID AND FINITE-VOLUME LU IMPLICIT SCHEME FOR TURBINE FLOW ANALYSIS

Yung K. Choo, Seokkwan Yoon (Sverdrup Technology, Inc., Cleveland, Ohio.), and Kestutis C. Civinskas (Army Aviation Research and Development Command, Cleveland, Ohio.) 1987 12 p Prepared for presentation at the 8th Computational Fluid

Dynamics Conference, Honolulu, Hawaii, 8-10 Jun. 1987; sponsored by AIAA
(NASA-TM-89828; E-3477; NAS 1.15:89828; USAAVSCOM-TR-87-C-5) Avail: NTIS HC A02/MF A01 CSCL 01A

A composite grid was generated in an attempt to improve grid quality for a typical turbine blade with large camber in terms of mesh control, smoothness, and orthogonality. This composite grid consists of the C grid (or O grid) in the immediate vicinity of the blade and the H grid in the upstream region and in the middle of the blade passage between the C grids. It provides a good boundary layer resolution around the leading edge region for viscous calculation, has orthogonality at the blade surface and slope continuity at the C-H (or O-H) interface, and has flexibility in controlling the mesh distribution in the upstream region without using excessive grid points. This composite grid eliminates the undesirable qualities of a single grid when generated for a typical turbine geometry. A finite-volume lower-upper (LU) implicit scheme can be used in solving for the turbine flows on the composite grid. This grid has a special grid node that is connected to more than four neighboring nodes in two dimensions and to more than six nodes in three dimensions. But the finite-volume approach poses no problem at the special point because each interior cell has only four neighboring cells in two dimensions and only six cells in three dimensions. The finite-volume LU implicit scheme was demonstrated to be robust and efficient for both external and internal flows in a broad flow regime. Author

N87-20236*# National Aeronautics and Space Administration. Langley Research Center, Hampton, Va.
INVESTIGATION OF TRANSONIC REGION OF HIGH DYNAMIC RESPONSE ENCOUNTERED ON AN ELASTIC SUPERCRITICAL WING
David A. Seidel, Clinton V. Eckstrom, and Maynard C. Sandford Mar. 1987 13 p Presented at the AIAA/ASME/ASCE/AHS 28th Structures, Structural Dynamics and Materials Conference, Monterey, Calif., 6-8 Apr. 1987
(NASA-TM-89121; NAS 1.15:89121; AIAA-87-0735-CP) Avail: NTIS HC A02/MF A01 CSCL 01A

Unsteady aerodynamic data were measured on an aspect ratio 10.3 elastic supercritical wing while undergoing high dynamic response above a Mach number of 0.90. These tests were conducted in the NASA Langley Transonic Dynamics Tunnel. A previous test of this wing predicted an unusual instability boundary based on subcritical response data. During the present test no instability was found, but an angle of attack dependent narrow Mach number region of high dynamic wing response was observed over a wide range of dynamic pressures. The effect on dynamic wing response of wing angle of attack, static outbound control surface deflection and a lower surface spanwise fence located near the 60 percent local chordline was investigated. The driving mechanism of the dynamic wing response appears to be related to chordwise shock movement in conjunction with flow separation and reattachment on both the upper and lower surfaces. Author

N87-20237# Colorado Univ., Boulder.
MULTIGRID CALCULATION OF BOUNDARY-FITTED ORTHOGONAL COORDINATES WITH APPLICATIONS TO UNSTEADY FLOWS Ph.D. Thesis
Robert R. Leben 1986 366 p
Avail: Univ. Microfilms Order No. DA8700366

The development and application of a numerical method for the investigation of two dimensional unsteady flows past an airfoil are studied. The method relies on a robust numerical algorithm for the generation of boundary-fitted orthogonal coordinates for airfoil shapes. The numerical technique employed is multigrid, an efficient method for solving the elliptic partial differential equations defining orthogonal mappings. Flow fields past airfoils are calculated using the multigrid generated coordinates in combination with a numerical method for the solution of the full unsteady Navier-Stokes equations in the stream function vorticity formulation. Multigrid is employed as the solution method for the stream function equation, which is identical to the grid generation equations, resulting in added efficiency in the flow solver. The complete numerical method is used to calculate the unsteady flow field produced by an airfoil in an accelerating flow. The calculations show good qualitative agreement with the experiments. This is the first numerical study of this flowfield and geometry, and provides important insight into the dynamics of unsteady separating flow. Author

N87-20238*# National Aeronautics and Space Administration. Lewis Research Center, Cleveland, Ohio.
LEWIS INVERSE DESIGN CODE (LINDES): USERS MANUAL
Jose M. Sanz Mar. 1987 67 p
(NASA-TP-2676; E-3221; NAS 1.60:2676) Avail: NTIS HC A04/MF A01 CSCL 01A

The method of complex characteristics and hodograph transformation for the design of shockless airfoils was introduced by Bauer, Garabedian, and Korn and has been extended by the author to design subcritical and supercritical cascades with high solidities and large inlet angles. This new capability was achieved by introducing a new conformal mapping of the hodograph domain onto an ellipse and expanding the solution in terms of Chebyshev polynomials. A new computer code, the NASA Lewis inverse design code, was developed based on this idea. This new design code is an efficient method for the design of airfoils in cascade. In particular, the design of subcritical cascades of airfoils is a very fast, robust, and versatile process. The inverse design code can be made to interact with a turbulent boundary layer calculation to obtain airfoils with no separated flows at the design condition. This report is intended to serve as a users manual for this design code. Material previously reported by the author is included here for completeness and quick access to the user. The manual contains a description of the method followed by a discussion of the design procedure and examples. The input parameters necessary to run the code are then described and their default values given. Output listings corresponding to six different blade shapes designed with the code are given, as well as the necessary input data to reproduce the computer runs. The examples have been chosen to show that a wide range of applications can be covered with the code, ranging from supercritical propeller sections to wind tunnel turning vanes that can operate with a large inlet flow angle range. Author

N87-20239*# General Electric Co., Cincinnati, Ohio. Aircraft Engine Business Group.
DEVELOPMENT OF A ROTOR WAKE/VORTEX MODEL. VOLUME 2: USER'S MANUAL FOR COMPUTER PROGRAM Final Report
R. K. Majjigi and P. R. Gliebe Jun. 1984 86 p
(Contract NAS3-23681)
(NASA-CR-174850-Vol-2; NAS 1.26:174850-Vol-2) Avail: NTIS HC A05/MF A01 CSCL 01A

The principal objective was to establish a verified rotor wake/vortex model for specific application to fan and compressor rotor-stator interaction and resulting noise generation. A description and flow chart of the Rotor Wake/Vortex Model computer program, a listing of the program, definitions of the input/output parameters, a sample input/output case, and input files for Rotor 55, the JT15D rotor, and Rotor 67, Stage 1 are provided. Author

N87-20240*# National Aeronautics and Space Administration. Langley Research Center, Hampton, Va.
SPIN-TUNNEL INVESTIGATION OF A 1/15-SCALE MODEL OF AN AUSTRALIAN TRAINER AIRPLANE
James S. Bowman, Jr., Raymond D. Whipple, and William L. White May 1987 40 p
(NASA-TM-89049; L-16191; NAS 1.15:89049) Avail: NTIS HC A03/MF A01 CSCL 01A

An investigation was conducted in the Langley Spin Tunnel of the spin and spin-recovery characteristics of a 1/15-scale model of an Australian trainer airplane. The invesigation included erect and inverted spins; configuration variables such as a long tail, fuselage strakes, 20 deg. elevator cutouts, and rudder modifications; and determination of the parachute size for emergency spin recovery. Also included in the investigation were wing leading-edge

modifications to evaluate Reynolds number effects. Results indicate that the basic configuration will spin erect at an angle of attack of about 63 deg. at about 2 to 2.3 seconds per turn. Recovery from this spin was unsatisfactory by rudder reversal or by rudder reversal and ailerons deflected to full with the spin. The elevators had a pronounced effect on the recovery characteristics. The elevators-down position was very adverse to recoveries, whereas the elevators-up position provided favorable recovery effects. Moving the vertical tail aft (producing a long tail configuration) improved the spin characteristics, but the recoveries were still considered marginal. An extension to the basic rudder chord and length made a significant improvement in the spin and recovery characteristics. Satisfactory recoveries were obtained by deflecting the rudder to full against the spin and the elevators and ailerons to neutral. Author

N87-20241*# National Aeronautics and Space Administration, Washington, D.C.
INTEGRAL METHOD OF WALL INTERFERENCE CORRECTION IN LOW-SPEED WIND TUNNELS
Changhai Zhou Apr. 1987 17 p Transl. into ENGLISH from Kongqi Lixue Xuebao (China), no. 2, Jun. 1985 p 1-8 Previously announced in IAA as A85-38962 Transl. by Kanner (Leo) Associates, Redwood City, Calif. Original document was prepared by Shenyang Aeronautics and Aerodynamics Research Inst., Ministry of Aeronautical Industry, China
(Contract NASw-4005)
(NASA-TT-20055; NAS 1.77:20055) Avail: NTIS HC A02/MF A01 CSCL 01A

The analytical solution of Poisson's equation, derived form the definition of vortex, was applied to the calculation of interference velocities due to the presence of wind tunnel walls. This approach, called the Integral Method, allows an accurate evaluation of wall interference for separated or more complicated flows without the need for considering any features of the model. All the information necessary for obtaining the wall correction is contained in wall pressure measurements. The correction is not sensitive to normal data-scatter, and the computations are fast enough for on-line data processing. Author

N87-20242*# National Aeronautics and Space Administration. Ames Research Center, Moffett Field, Calif.
SIMULATION OF TRANSONIC VISCOUS WING AND WING-FUSELAGE FLOWS USING ZONAL METHODS
Jolen Flores Mar. 1987 69 p
(NASA-TM-89421; A-87066; NAS 1.15:89421) Avail: NTIS HC A04/MF A01 CSCL 01A

The thin-layer Navier-Stokes equations are coupled with a zonal scheme (or domain-decomposition method) to develop the Transonic Navier-Stokes (TNS) wing-alone code. The TNS has a total of 4 zones and is extended to a total of 16 zones for the wing-fuselage version of the code. Results are compared on the Cray X-MP-48 and compared with experimental data. Author

N87-20243*# Sverdrup Technology, Inc., Cleveland, Ohio.
A NAVIER-STOKES SOLVER USING THE LU-SSOR TVD ALGORITHM Final Contractor Report
Seokkwan Yoon Mar. 1987 13 p
(Contract NAS3-24105)
(NASA-CR-179608; E-3499; NAS 1.26:179608) Avail: NTIS HC A02/MF A01 CSCL 20D

A new Navier-Stokes solver is developed by combining the efficiency of the LU-SSOR scheme and the accuracy of the flux-limited dissipation scheme. Application to laminar and turbulent flows and hypersonic flows proves the reliability of the new algorithm. Author

N87-20244# Naval Surface Weapons Center, Silver Spring, Md.
A MULTIPLE ZONE METHOD FOR SUPERSONIC TACTICAL MISSILES Final Report
A. B. Wardlaw, F. J. Priolo, and J. M. Solomon Jun. 1986 68 p
(AD-A175938; NSWC/TR-85-484) Avail: NTIS HC A04/MF A01 CSCL 20/4

A practical means of predicting the inviscid flow field about a supersonic missile is to numerically solve the steady, three-dimensional Euler equations. A major problem encountered in steady, supersonic calculations is the treatment of complex cross-sectional geometries which arise in conjunction with configurations featuring fins, inlets and tails. An alternative approach for treating complex missile and aircraft configurations is a multiple zone strategy. A multiple zone computational method applicable to finned bodies is supersonic flight is described. At each cross-section, the computational domain is broken into a number of zones, each of which can be described using a simple mapping. The zones are chosen to ensure that the bow shock, fin and body surfaces coincide with zone edges. At zone interfaces, the mesh may be discontinuous in a direction normal to the edge. Along zone edges, surfaces are allowed to form or disappear during the computation. The surface edges which form at points where surfaces appear or disappear are treated using a local analysis. The resulting algorith m is applicable to a wide range of configurations including interior as well as exterior supersonic flow fields. Calculations are compared to experiment for several different missile shapes. GRA

N87-20245# Naval Surface Weapons Center, Silver Spring, Md.
SURFACE PRESSURE MEASUREMENTS ON A DOUBLE DELTA WING/BODY CONFIGURATION AT MACH 2 AND MACH 3 (WTR 1396) Wind Tunnel Data Report, 25 Feb. - 1 Mar. 1984
Donald W. Ausherman Jun. 1986 102 p
(AD-A175951; NSWC/MP/86-240) Avail: NTIS HC A06/MF A01 CSCL 20/4

The surface pressures on a clipped double-delta wing/body configuration were measured at Mach 2 and Mach 3 in the Naval Surface Weapons Center (NSWC) Supersonic Tunnel Number Two at angles-of-attack up to 20 deg. The winged-body model configuration has a 2-inch diameter body consisting of a 3-caliber tangent-ogive nose and and a 7-caliber cylindrical afterbody. The wing was a clipped double-delta configuration. The body had 91 pressure taps located at various axial and circumferential locations, and the wing had 47. Surface pressures were measured at several angles-of-attack for various model roll positions at both Mach 2 and Mach 3. GRA

N87-20246# Air Force Systems Command, Wright-Patterson AFB, Ohio. Foreign Technology Div.
ACTA MECHANICA SINICA (SELECTED ARTICLES)
Lin Bingqiu and Gao Zhi 6 Jan. 1987 42 p Transl. into ENGLISH from Lixue Xuebao (China), v. 18, no. 8, May 1986 p 200-207; 215-225
(AD-A176240; FTD-ID(RS)T-1152-86) Avail: NTIS HC A03/MF A01 CSCL 20/4

Based on the Navier Stokes equations, the compressible viscous vortex equation for decribing the separated vortex of an aircraft is derived and a numerical method suitable for subsonic, transonic and supersonic flows is given which can compute the characteristics of separated vortex or trailing vortex. The break-down condition of the compressible separated vortex is derived and used to compute the break-down point. The principle of flow velocity and flow pattern measurements using Doppler-frequency shifted absorption (or emission) spectral lines as well as Doppler frequency shifted and deformational nonsaturated spectral line shapes is discussed. For the case of gas flow with simultaneously inhomogeneously and homogeneously broadened line, the general expressions of non-saturation spectral line-shaped and Doppler-frequency shifted spectral line are presented. GRA

N87-20247# Bristol Univ. (England). Dept. of Aeronautical Engineering.
INVESTIGATION OF FLOW UNDER THE FUSELAGE OF A POWERED LIGHT AIRCRAFT MODEL B.S. Thesis
S. A. Smith and R. J. Williams Jun. 1986 57 p
(BU-351; ETN-87-99212) Avail: NTIS HC A04/MF A01

The airflow under the fuselage of a scale model of the ARV Super 2 light aircraft was investigated to model the flow development in the slipstream of a propeller, particularly flow characteristics

at the position of the aircraft's radiator duct. Results at simulated conditions of cruise, climb, and ground run were produced to explain cooling problems experienced in flight testing of the full size aircraft. A significant increase of static pressure across the duct is shown to occur in flight conditions, this being a probable cause of cooling inefficiency. Measurement of velocity profiles shows no evidence of effects on cooling. Flow visualization indicates propeller swirl which may also affect cooling flow by interaction with external fittings on the fuselage. The model was used to verify the choice of position for the aircraft static holes. ESA

N87-20248# Royal Air Force Coll., Cranwell (England). Dept. of Transport Technology.
THE AERODYNAMIC EFFECTS OF A SERRATED STRIP NEAR THE LEADING EDGE OF AN AIRFOIL M.S. Thesis
R. A. Barker 1986 139 p
(ETN-87-99480) Avail: NTIS HC A07/MF A01

The aerodynamic effects of fixing a serrated strip near the leading edge, forward of the stagnation point at high incidence, was investigated using 2 airfoil models, both of 254 mm chord, but of different sections. The aerodynamic force and moment coefficients were determined for the basic and modified airfoils. The devices tested improve the maximum lift of a NACA 65(1)-212 section by up to 16% without drag penalties. However, they degrade the performance of an NLF(1)-0416 section. All leading-edge devices tested generate vortices which stream around the airfoil leading edge and over the suction surface. On the NACA airfoil only, these vortices reduce the extent of local separation near the leading edge and re-energize the turbulent boundary layer, thus delaying the onset of trailing edge separation. ESA

N87-20249# Office National d'Etudes et de Recherches Aerospatiales, Paris (France). Direction Scientifique de l'Aerodynamique.
STUDY OF THE UNSTEADY PRESSURE FIELD ON THE RA1-6SC1 PROFILE IN VIBRATING CONDITION [ETUDE DU CHAMP DE PRESSION INSTATIONNAIRE SUR LE PROFIL RA16SC1 EN REGIME DE TREMBLEMENT A S3MA]
B. Benoit Jun. 1986 48 p In FRENCH
(Contract STPA-85-95-009)
(ONERA-RTS-17/3423-AY; ETN-87-99385) Avail: NTIS HC A03/MF A01

Transonic flow wind tunnel tests were carried out to test two bidimensional flow characteristics of a supercritical profile. Results show that after the onset of separation the flow becomes unstable. A coupling between the shock wave and the separation is formed. Severe pressure fluctuations are measured. Their frequency for a given Mach number increases with the incidence. The analysis indicates that the reconstitution of unsteady forces from measurements of pressure fields is feasible. ESA

N87-20250# Office National d'Etudes et de Recherches Aerospatiales, Paris (France). Direction Scientifique de l'Aerodynamique.
WING-NACELLE INTERACTIONS. PROGRAM 1985. PART TWO: DEVELOPMENT OF A FINITE ELEMENT CODE FOR AN ISOLATED NACELLE [INTERACTION NACELLE-VOILURE. TRAVAUX 85. PARTIE 2: MISE AU POINT D'UN CODE D'ELEMENTS FINIS POUR UNE NACELLE ISOLEE]
J. Marechal Jul. 1986 60 p In FRENCH
(Contract STPA-85-95-009)
(ONERA-RTS-21/3271-AY; ETN-87-99386) Avail: NTIS HC A04/MF A01

The computation of three dimensional unsteady transonic flow around an isolated nacelle is studied. A finite element code was used to solve the complete potential equation in its conservative form. The potential equation is discretized using an H mesh and the linearization is made using a fixed point method. A gradient algorithm coupled to Cholesky factorization solves the problem accelerating the convergence. The results of three complete flow computations are included. ESA

N87-20251# Centre d'Etudes Aerodynamiques et Thermiques, Poitiers (France). Lab. d'Etudes Thermodynamiques.
STUDY OF COMPRESSIBILITY EFFECTS ON SUPERSONIC FREE FLOW Final Report [ETUDE DES EFFETS DE COMPRESSIBILITE SUR LES ECOULEMENTS LIBRES SUPERSONIQUES]
J. P. Bonnet Jun. 1986 35 p In FRENCH
(Contract DRET-84-057)
(ETN-87-99392) Avail: NTIS HC A03/MF A01

Following a study characterizing flow and wake at Mach 2, the supersonic effects at Mach 3 are studied. Wind tunnel tests were carried out and the space distribution of the axial velocity variations were determined. The calibrating methods are described. The results of the turbulence measurements, as well as numerical simulation results are presented. The average velocities evolve towards a classical asymptotic state associated to an evolution of the virtual origin which increases with the Mach number. ESA

03 AIR TRANSPORTATION AND SAFETY

Includes passenger and cargo air transport operations; and aircraft accidents.

For related information see also *16 Space Transportation* and *85 Urban Technology and Transportation.*

N87-20252*# Mesoscale Environmental Simulations, Inc., Hampton, Va.
THE TERMINAL AREA SIMULATION SYSTEM. VOLUME 2: VERIFICATION CASES
F. H. Proctor Washington NASA Apr. 1987 112 p
(Contract NAS1-17409)
(NASA-CR-4047-Vol-2; NAS 1.26:4047-Vol-2;
DOT/FAA/PM-86/50-Vol-2) Avail: NTIS HC A06/MF A01 CSCL 01C

The numerical simulation of five case studies are presented and are compared with available data in order to verify the three-dimensional version of the Terminal Area Simulation System (TASS). A spectrum of convective storm types are selected for the case studies. Included are: a High-Plains supercell hailstorm, a small and relatively short-lived High-Plains cumulonimbus, a convective storm which produced the 2 August 1985 DFW microburst, a South Florida convective complex, and a tornadic Oklahoma thunderstorm. For each of the cases the model results compared reasonably well with observed data. In the simulations of the supercell storms many of their characteristic features were modeled, such as the hook echo, BWER, mesocyclone, gust fronts, giant persistent updraft, wall cloud, flanking-line towers, anvil and radar reflectivity overhang, and rightward veering in the storm propagation. In the simulation of the tornadic storm a horseshoe-shaped updraft configuration and cyclic changes in storm intensity and structure were noted. The simulation of the DFW microburst agreed remarkably well with sparse observed data. The simulated outflow rapidly expanded in a nearly symmetrical pattern and was associated with a ringvortex. A South Florida convective complex was simulated and contained updrafts and downdrafts in the form of discrete bubbles. The numerical simulations, in all cases, always remained stable and bounded with no anomalous trends. Author

N87-20253*# Analytical Mechanics Associates, Inc., Mountain View, Calif.
DESIGN AND ANALYSIS OF ADVANCED FLIGHT PLANNING CONCEPTS Final Report
John A. Sorensen Washington NASA Mar. 1987 153 p
(Contract NAS1-17345)
(NASA-CR-4063; NAS 1.26:4063; AMA-85-09) Avail: NTIS HC A08/MF A01 CSCL 01C

The objectives of this continuing effort are to develop and evaluate new algorithms and advanced concepts for flight management and flight planning. This includes the minimization of fuel or direct operating costs, the integration of the airborne flight management and ground-based flight planning processes, and the enhancement of future traffic management systems design. Flight management (FMS) concepts are for on-board profile computation

and steering of transport aircraft in the vertical plane between a city pair and along a given horizontal path. Flight planning (FPS) concepts are for the pre-flight ground based computation of the three-dimensional reference trajectory that connects the city pair and specifies the horizontal path, fuel load, and weather profiles for initializing the FMS. As part of these objectives, a new computer program called EFPLAN has been developed and utilized to study advanced flight planning concepts. EFPLAN represents an experimental version of an FPS. It has been developed to generate reference flight plans compatible as input to an FMS and to provide various options for flight planning research. This report describes EFPLAN and the associated research conducted in its development. Author

N87-20254*# National Aeronautics and Space Administration. Langley Research Center, Hampton, Va.
TRAFFIC SCENARIO GENERATION TECHNIQUE FOR PILOTED SIMULATION STUDIES
David H. Williams and Douglas C. Wells (Embry-Riddle Aeronautical Univ., Daytona Beach, Fla.) Apr. 1985 46 p
(NASA-TM-86397; NAS 1.15:86397) Avail: NTIS HC A03/MF A01 CSCL 01C

Piloted simulation studies of cockpit traffic display concepts require the development of representative traffic scenarios. With the exception of specific aircraft interaction issues, most research questions can be addressed using traffic scenarios consisting of prerecorded aircraft movements merged together to form a desired traffic pattern. Prerecorded traffic scenarios have distinct research advantages, allowing control of traffic encounters with repeatability of scenarios between different test subjects. A technique is described for generation of prerecorded jet transport traffic scenarios suitable for use in piloted simulation studies. Individual flight profiles for the aircraft in the scenario are created interactively with a computer program designed specifically for this purpose. The profiles are then time-correlated and merged into a complete scenario. This technique was used to create traffic scenarios for the Denver, Colorado area with operations centered at Stapleton International Airport. Traffic scenarios for other areas may also be created using this technique, with appropriate modifications made to the navigation fix locations contained in the flight profile generation program. Author

N87-20255*# Mesoscale Environmental Simulations, Inc., Hampton, Va.
THE TERMINAL AREA SIMULATION SYSTEM. VOLUME 1: THEORETICAL FORMULATION
F. H. Proctor Washington NASA Apr. 1987 168 p Prepared in cooperation with SASC Technologies, Inc., Hampton, Va.
(Contract NAS1-17409)
(NASA-CR-4046-Vol-1; NAS 1.26:4046-Vol-1;
DOT/FAA-PM-86/50-Vol-1) Avail: NTIS HC A08/MF A01 CSCL 01C

A three-dimensional numerical cloud model was developed for the general purpose of studying convective phenomena. The model utilizes a time splitting integration procedure in the numerical solution of the compressible nonhydrostatic primitive equations. Turbulence closure is achieved by a conventional first-order diagnostic approximation. Open lateral boundaries are incorporated which minimize wave reflection and which do not induce domain-wide mass trends. Microphysical processes are governed by prognostic equations for potential temperature water vapor, cloud droplets, ice crystals, rain, snow, and hail. Microphysical interactions are computed by numerous Orville-type parameterizations. A diagnostic surface boundary layer is parameterized assuming Monin-Obukhov similarity theory. The governing equation set is approximated on a staggered three-dimensional grid with quadratic-conservative central space differencing. Time differencing is approximated by the second-order Adams-Bashforth method. The vertical grid spacing may be either linear or stretched. The model domain may translate along with a convective cell, even at variable speeds. Author

N87-20256# Bristol Univ. (England). Dept. of Aeronautical Engineering.
A PRELIMINARY STUDY INTO THE CONSTANT DRAG PARACHUTE FOR AIRCREW ESCAPE SYSTEMS B.S. Thesis
P. D. Marshall and R. B. Mustarde Jun. 1986 61 p
(BU-345; ETN-87-99207) Avail: NTIS HC A04/MF A01

Parachute geometries for use in high velocity, low altitude ejections, to maximize the survivability of such situations by creating a system which maintains a high level of deceleration were studied in a low speed wind tunnel, the forces in the streamwise direction during and after initial inflation being recorded for each test. The limitations of such testing were also noted. Variable geometry parachutes, possibly of the reefed type, are shown to have potential to be highly efficient at maintaining drag levels. The ideal system would employ a parachute of this type, coupled with an energy absorbing mechanism, parachute expansion being controlled via a force sensor built into the seat. ESA

04 AIRCRAFT COMMUNICATIONS AND NAVIGATION

Includes digital and voice communication with aircraft; air navigation systems (satellite and ground based); and air traffic control.

For related information see also *17 Space Communications, Spacecraft Communications, Command and Tracking* and *32 Communications and Radar.*

N87-20257*# National Aeronautics and Space Administration. Ames Research Center, Moffett Field, Calif.
RANGE FILTERING FOR SEQUENTIAL GPS RECEIVERS WITH EXTERNAL SENSOR AUGMENTATION
Russell Paielli Apr. 1987 22 p
(NASA-TM-89418; A-87050; NAS 1.15:89418) Avail: NTIS HC A02/MF A01 CSCL 17G

The filtering of the satellite range and range-rate measurements from single channel sequential Global Positioning System receivers is usually done with an extended Kalman filter which has state variables defined in terms of an orthogonal navigation reference frame. An attractive suboptimal alternative is range-domain filtering, in which the individual satellite measurements are filtered separately before they are combined for the navigation solution. The main advantages of range-domain filtering are decreased processing and storage requirements and simplified tuning. Several range filter mechanization alternatives are presented, along with an innovative approach for combining the filtered range-domain quantities to determine the navigation state estimate. In addition, a method is outlined for incorporating measurements from auxiliary sensors such as altimeters into the navigation state estimation scheme similarly to the satellite measurements. A method is also described for incorporating inertial measurements into the navigation state estimator as a process driver. Author

N87-20258# Naval Aerospace Medical Research Lab., Pensacola, Fla.
THE RETINAL IMAGE OF THE FRESNEL LENS OPTICAL LANDING SYSTEM Interim Report
Leonard A. Temme and William A. Monaco 19 Sep. 1986 37 p
(AD-A176090; NAMRL-1323) Avail: NTIS HC A03/MF A01 CSCL 06/16

The theory and geometry by which the Fresnel Lens Optical Landing System (FLOLS) provides glideslope information to the pilot attempting a carrier landing is described. From the theory, geometry, and the linear spatial dimensions of the FLOLS, the image it generates on the retina of the pilot is calculated. Since the dimensions of the retinal image are a function of the distance of the eye from the FLOLS, dimensions are calculated for distances of 1.0, 0.5, 0.25, and 0.125 nautical miles from the carrier ramp and at the ramp itself. These dimensions are also considered as a functions of time in seconds to the ramp, assuming an aircraft airspeed of 125 knots. The dimensions of the retinal image of the

FLOLS vary with the FLOLS position on the carrier. Calculations are reported for the USS LEXINGTON (AVT-16) and the USS KITTY HAWK (CV-63). The retinal image of the FLOLS is discussed as a visual stimulus for acuity discriminations and compared to acuity measured in the laboratory. The impact of the addition of the rate descent arrows, AVCARS, on FLOLS visibility is discussed in terms of the calculated dimensions of the retinal image and known neurophysiology. A modification of the current FLOLS display is suggested, which would increase its visibility, gain, and usable range. GRA

05 AIRCRAFT DESIGN, TESTING AND PERFORMANCE

Includes aircraft simulation technology.

For related information see also *18 Spacecraft Design, Testing and Performance* and *39 Structural Mechanics.* For land transportation vehicles see *85 Urban Technology and Transportation.*

N87-20259 Civil Aviation Authority, London (England).
HELICOPTER EXTERNAL LOAD OPERATIONS
Jul. 1986 18 p
(CAP-426; ISBN-0-86039-287-2; ETN-87-99496) Copyright. Avail: Issuing Activity

Advice on various aspects of helicopter external load operations for the benefit of operators, pilots, and persons supervising the securing and detaching of loads is given. Airworthiness; route planning; lifting and dropping site; safety of site personnel; safety of third parties at lifting and dropping sites; hand signals; loading procedures; load oscillation; accidental release/snagged loads; weather and altitude; and electrical static charges are covered. ESA

N87-20260 Maryland Univ., College Park.
AEROELASTIC STABILITY OF BEARINGLESS ROTORS IN FORWARD FLIGHT Ph.D. Thesis
Andrew Lynne Dull 1986 113 p
Avail: Univ. Microfilms Order No. DA8628975

Aeroelastic stability characteristics for selected bearingless rotor configurations are calculated and correlated to experimental data. The rotor blade is analyzed by a finite element formulation based on Hamilton's principle. The element model has fifteen degrees of freedom in axial, bending and torsion deflections. Quasi-steady strip theory is used for the aerodynamic calculations while non-circulatory forces and dynamic inflow are included to approximate the unsteady effects. The analysis consists of three stages; trim solution, blade steady response, and stability calculations. The trim solution is calculated for a simple rigid articulated blade for either wind tunnel or propulsive trim as the control input to the response calculations. The periodic response is calculated by a time finite element method after the nonlinear finite element in space equations are transformed to normal mode equations using the first few vacuum rotating modes. Then the stability is calculated from the perturbation equations of motion linearized about the steady response solution. These equations are transformed with the first few coupled rotating modes and solved for stability of Floquet transition matrix theory. The bearingless rotor analysis is correlated to hover lag mode stability data for a simple three-bladed rotor tested in three different pitch link configurations. A second more complicated bearingless configuration which includes precone, blade twist, blade sweep, and a lag shear restraint is then analyzed. Dissert. Abstr.

N87-20261*# National Aeronautics and Space Administration, Washington, D.C.
THE DESIGN OF COMPOSITE STRUCTURES: AIRCRAFT DESIGN
G. Hellard Apr. 1987 24 p Transl. into ENGLISH of "La Conception des Structures Composites" Rept. SNIAS-861-111-103 SNIAS, Toulouse, France, 13 Feb. 1986 p 1-22 Original language document was announced as N86-28082 Transl. by Kanner (Leo) Associates, Redwood City, Calif.
(Contract NASw-4005)
(NASA-TT-20011; NAS 1.77:20011; SNIAS-861-111-103; GCO/GH/CL-442.026/85) Avail: NTIS HC A02/MF A01 CSCL 01C

The principles of aircraft element design using composite materials are outlined. Glass carbon and Kevlar composites are discussed. Sandwich and monolothic structures are described and application criteria are detailed. Drawings detailing the composite elements of the A-310 to A-330 and ATR-42 aircrafts and the particular design of those elements are presented. Author

N87-20262# Royal Aircraft Establishment, Farnborough (England).
WSUH-1D: REVIEW OF DAMAGE FOLLOWING LIGHTNING STRIKE 30 NOVEMBER 1981
T. A. Gobl Sep. 1986 39 p Transl. into ENGLISH of "WSUH-1D: Schadensuebersicht nach Blitzschlag" Rept. TIR-29/81-BWB-ML German Air Force, Erding, West Germany, 1981
(RAE-Trans-2103; BR101809; TIR-29/81-BWB-ML) Avail: NTIS HC A03/MF A01

This report describes an investigation into the effects of a lightning strike to a BELL UH-1D helicopter operated by the German Air Force. The investigation was made by the Aircraft System Investigation Section of the Air Force Service Regiment, at Erding. Lightning attachments occurred to one main rotor blade, one tail rotor blade and to one undercarriage skid. It was found that arcing had occurred within the aluminum honeycomb core of the main rotor blade sufficient to initiate fatigue cracks in the trailing-edge extrusion. Arcing had also occurred within bearings and between moving parts of the rotor head mechanism. The damage to the rotor head was revealed during routine maintenance and rectification of leaking hydraulic actuators rather than by post-strike inspection. Some of the internal damage to the rotor blade only became evident when the blade was dismantled and was not detectable by NDT methods. Voltage surges induced into the helicopter electrical system caused failure of certain equipment. Author

N87-20263# Bristol Univ. (England). Dept. of Aeronautical Engineering.
MATERIALS SELECTION AND DESIGN STUDY OF A COMPOSITE MICROLIGHT WING STRUCTURE B.S. Thesis
A. J. Murphy and D. C. Murray Jun. 1985 98 p
(BU-335; ETN-87-99198) Avail: NTIS HC A05/MF A01

A design study of a composite wing to replace the built up wing on the MW5 microlight aircraft is presented. Material tests were performed on a wide range of glass fiber reinforced plastics, and from these an optimum skin configuration was found using a computerized analysis of mathematical models of both the structure and the loading. Styrofoam was chosen as the core material to resist skin buckling, and the resulting wing affords a weight saving of 27% over the built up wing, while giving a reserve factor of 2.8. A method of wing construction was devised, and schemes for the wing fittings were also drafted. The requirement for experimental verification of the wing design was appreciated, and an investigation into the feasibility of using scale models for part of the test program was assessed. ESA

N87-20176# Messerschmitt-Boelkow-Blohm G.m.b.H., Munich (West Germany). Helicopter Div.
DESIGN FOR REPAIRABILITY OF HELICOPTER COMPOSITE BLADES
M. Hahn *In* AGARD The Repair of Aircraft Structures Involving Composite Materials Oct. 1986 15 p (For primary document see N87-20174 13-01)
Avail: NTIS HC A11/MF A01

N87-20210# British Aerospace Aircraft Group, Warton (England). Aerodynamics Dept.
THE INTEGRATION OF COMPUTATIONAL FLUID DYNAMICS INTO THE MILITARY AIRCRAFT DESIGN PROCESS
W. R. Marchbank *In* AGARD Applications of Computational Fluid

Dynamics in Aeronautics Nov. 1986 13 p (For primary document see N87-20199 13-02)
Avail: NTIS HC A19/MF A01

N87-20216# Messerschmitt-Boelkow-Blohm G.m.b.H., Munich (West Germany). Helicopter and Military Aircraft Group.
EULER SOLUTION FOR A COMPLETE FIGHTER AIRCRAFT AT SUB- AND SUPERSONIC SPEED
Albrecht Eberle and Kent Misegades (Cray Research, Inc., Mendota Heights, Minn.) *In* AGARD Applications of Computational Fluid Dynamics in Aeronautics Nov. 1986 12 p (For primary document see N87-20199 13-02)
Avail: NTIS HC A19/MF A01

N87-20226# Boeing Military Airplane Development, Seattle, Wash.
CALCULATIONS FOR A GENERIC FIGHTER AT SUPERSONIC HIGH-LIFT CONDITIONS
J. C. Wai, G. Blom, and H. Yoshihara *In* AGARD Applications of Computational Fluid Dynamics in Aeronautics Nov. 1986 8 p (For primary document see N87-20199 13-02)
Avail: NTIS HC A19/MF A01

N87-20599# Spar Aerospace Ltd., Ste-Anne-de-Bellevue (Quebec).
OPTIMIZATION OF AEROSPACE STRUCTURES SUBJECTED TO RANDOM VIBRATION AND FATIGUE CONSTRAINTS
V. K. Jha, T. S. Sankar (Concordia Univ., Montreal, Quebec.), and R. B. Bhat *In* Shock and Vibration Information Center The Shock and Vibration Bulletin. Part 2: Modal Test and Analysis, Testing Techniques, Machinery Dynamics, Isolation and Damping, Structural Dynamics Aug. 1986 p 193-200 (For primary document see N87-20580 13-39)
Avail: NTIS HC A10/MF A01 CSCL 20/11

06 AIRCRAFT INSTRUMENTATION

Includes cockpit and cabin display devices; and flight instruments.

For related information see also *19 Spacecraft Instrumentation* and *35 Instrumentation and Photography.*

N87-20264*# Kansas Univ. Center for Research, Inc., Lawrence.
DEVELOPMENT OF A TAKEOFF PERFORMANCE MONITORING SYSTEM Ph.D. Thesis. Contractor Report, Jan. 1984 - Jun. 1985
Raghavachari Srivatsan and David R. Downing Mar. 1987 208 p (Contract NCC1-79)
(NASA-CR-178255; NAS 1.26:178255; KU-FRL-629-1) Avail: NTIS HC A10/MF A01 CSCL 01D

Discussed are the development and testing of a real-time takeoff performance monitoring algorithm. The algorithm is made up of two segments: a pretakeoff segment and a real-time segment. One-time imputs of ambient conditions and airplane configuration information are used in the pretakeoff segment to generate scheduled performance data for that takeoff. The real-time segment uses the scheduled performance data generated in the pretakeoff segment, runway length data, and measured parameters to monitor the performance of the airplane throughout the takeoff roll. Airplane and engine performance deficiencies are detected and annunciated. An important feature of this algorithm is the one-time estimation of the runway rolling friction coefficient. The algorithm was tested using a six-degree-of-freedom airplane model in a computer simulation. Results from a series of sensitivity analyses are also included. Author

N87-20265*# National Aeronautics and Space Administration. Langley Research Center, Hampton, Va.
INTEGRATION OF ALTITUDE AND AIRSPEED INFORMATION INTO A PRIMARY FLIGHT DISPLAY VIA MOVING-TAPE FORMATS
Terence S. Abbott and George G. Steinmetz Apr. 1987 29 p
(NASA-TM-89064; L-16221; NAS 1.15:89064) Avail: NTIS HC A03/MF A01 CSCL 01D

A ground-based aircraft simulation study was conducted to determine the effect on pilot performance of replacing the electromechanical altimeter and airspeed indicators with electronically generated representations integrated into the primary flight display via moving-tape (linear moving scale) formats. Several key factors relating to moving-tape formats were examined during the study: tape centering, secondary (trend) information, and tape orientation. The factor of centering refers to whether the tape was centered about the actual airspeed or altitude or about some defined reference value. Tape orientation refers to whether the values represented are arranged in either descending or ascending order. Six pilots participated in this study, with each subject performing 18 runs along a single, known flight profile. Subjective results indicated that the moving-tape formats were generally better than that of the conventional instruments. They also indicated that an actual-centered fixed pointer was preferred to a reference-centered pointer. Performance data for a visual secondary task showed that formats not containing trend information produced better performance; however, no difference was noted in airspeed tracking or altitude tracking performance. Regarding tape orientation, subjective comments indicated that there was lower work load and better performance when the airspeed tape had the high numbers at the top. Author

N87-20266 Department of the Navy, Washington, D. C.
AIRSPEED SENSING PRESSURE VALVE SYSTEM Patent
Peter Ayoub, inventor (to Navy) Issued 5 Aug. 1986 8 p Supersedes N85-18987, AD-D011472 (23 - 10, p 1425)
(AD-D012569; US-Patent-4,603,823; US-Patent-Appl-SN-627-307; US-Patent-Class-244-122) Avail: US Patent and Trademark Office CSCL 13/11

The present invention relates generally to a system for deploying a parachute during ejection of an occupant from a disabled aircraft, and more particularly to a fail-safe means of sensing airspeed in such a system. It is a general purpose and object of the present invention to provide a simple, yet effective airspeed sensor, used in a system for deploying a parachute during ejection of an occupant from a disabled aircraft, which stores peak dynamic pressure in order to selectively delay parachute deployment as a function of airspeed and altitude at ejection.
GRA

N87-20761# Selenia Industrie Elettroniche Associate S.p.A., Pomezia (Italy). Engineering Support Dept.
ON MODERN AVIONIC AND DEFENSE SYSTEMS LOGISTIC SUPPORT STANDARDIZATION AND COST EFFECTIVENESS
Vincenzo Buontempo *In its* Rivista Tecnica Selenia, Volume 10, Number 1 1986 p 11-24 Original contains color illustrations (For primary document see N87-20759 13-61)
Avail: NTIS HC A04/MF A01

07 AIRCRAFT PROPULSION AND POWER

Includes prime propulsion systems and systems components, e.g., gas turbine engines and compressors; and onboard auxiliary power plants for aircraft.

For related information see also *20 Spacecraft Propulsion and Power, 28 Propellants and Fuels,* and *44 Energy Production and Conversion.*

N87-20267*# National Aeronautics and Space Administration. Lewis Research Center, Cleveland, Ohio.
NASA-CHINESE AERONAUTICAL ESTABLISHMENT (CAE) SYMPOSIUM
1986 230 p Symposium held in Cleveland, Ohio, 23-27 Sep. 1985
(NASA-CP-2433; E-3033; NAS 1.55:2433) Avail: NTIS HC A01/MF A01 CSCL 21E

Several topics relative to combustion research are discussed.

A numerical study of combustion processes in afterburners; the modeling of turbulent, reactive flow; gas turbine research; modeling of dilution jet flow fields; and chemical shock tubes as tools for studying high-temperature chemical kinetics are among the topics covered. For individual titles, see N87-20268 through N87-20279.

N87-20268*# National Aeronautics and Space Administration. Lewis Research Center, Cleveland, Ohio.
COMBUSTION RESEARCH IN THE INTERNAL FLUID MECHANICS DIVISION **c25**
Edward J. Mularz *In its* NASA-Chinese Aeronautical Establishment (CAE) Symposium 1986 p 1-6 (For primary document see N87-20267 13-07)
Avail: NTIS HC A01/MF A01 CSCL 21B

The goal of this research is to bring computational fluid dynamics to a state of practical application for the aircraft engine industry. The approach is to have a strongly integrated computational and experimental program for all the disciplines associated with the gas turbine and other aeropropulsion systems by advancing the understanding of flow physics, heat transfer, and combustion processes. The computational and experimental research is integrated in the following way: the experiments that are performed provide an empirical data set so that physical models can be formulated to describe the processes that are occurring - for example, turbulence or chemical reaction. These experiments also form a data base for those who are doing code development by providing experimental data against which the codes can be verified and assesed. Models are generated as closure to some of the numerical codes, and they also provide physical insight for experiments. At the same time, codes which solve the complete Navier-Stokes equations can be used as a kind of numerical experiment from which far more extensive data can be obtained than ever could be obtained experimentally. This could provide physical insight into the complex processes that are taking place. These codes are also exercised against experimental data to assess the accuracy and applicability of models. Author

N87-20269*# Chinese Aeronautical Establishment, Beijing.
NUMERICAL STUDY OF COMBUSTION PROCESSES IN AFTERBURNERS **c25**
Xiaoqing Zhou and Xiaochun Zhang (Shenyang Aeroengine Research Inst., China.) *In* NASA- Lewis Research Center NASA-Chinese Aeronautical Establishment (CAE) Symposium 1986 p 7-30 (For primary document see N87-20267 13-07)
Avail: NTIS HC A01/MF A01 CSCL 21B

Mathematical models and numerical methods are presented for computer modeling of aeroengine afterburners. A computer code GEMCHIP is described briefly. The algorithms SIMPLER, for gas flow predictions, and DROPLET, for droplet flow calculations, are incorporated in this code. The block correction technique is adopted to facilitate convergence. The method of handling irregular shapes of combustors and flameholders is described. The predicted results for a low-bypass-ratio turbofan afterburner in the cases of gaseous combustion and multiphase spray combustion are provided and analyzed, and engineering guides for afterburner optimization are presented. Author

N87-20270*# National Aeronautics and Space Administration. Lewis Research Center, Cleveland, Ohio.
MODELING TURBULENT, REACTIG FLOW **c34**
Russell W. Claus *In its* NASA-Chinese Aeronautical Establishment (CAE) Symposium 1986 p 31-46 (For primary document see N87-20267 13-07)
Avail: NTIS HC A01/MF A01 CSCL 20D

Several of the approximations or models involved in the development of a numerical combustor flow code are examined. In the first section, the importance of numerical accuracy is illustrated, and the impact that improved-accuracy schemes have on slowing convergence is demonstrated. Solution algorithms that can speed convergence are discussed and some performance features of these algorithms are illustrated. A sample calculation displaying the importance of boundary conditions on a three-dimensional numerical prediction is presented. The inaccuracy of a current turbulence model in highly turbulent (nonequilibrium) regions is described. Finally, the surprisingly good performance of a six-flux model in describing radiation heat transfer is displayed. In all the areas examined, continued research is still needed, but valuable engineering tools are available today. Author

N87-20271*# Beijing Inst. of Aeronautics and Astronautics (China).
EXPERIMENTAL AND ANALYTICAL INVESTIGATION OF THE VARIATION OF SPRAY CHARACTERISTICS ALONG A RADIAL DISTANCE DOWNSTREAM OF A PRESSURE-SWIRL ATOMIZER **c34**
J. S. Chin, W. M. Li, and X. F. Wang *In* NASA- Lewis Research Center NASA-Chinese Aeronautical Establishment (CAE) Symposium 1986 p 47-62 (For primary document see N87-20267 13-07)
Avail: NTIS HC A01/MF A01 CSCL 20D

The variation of spray characteristics along a radial distance downstream of a pressure-swirl atomizer was measured by laser light-scattering technology. An analytical model was developed to predict the variation of spray characteristics along the radial distance. A comparison of the predicted and experimental data showed excellent agreement. Therefore, the spray model proposed, although relatively simple, is correct and can be used, with some expansion and modification of the prepared model, to predict more complicated spray systems. Author

N87-20272*# National Aeronautics and Space Administration. Lewis Research Center, Cleveland, Ohio.
TWO-PHASE FLOW **c34**
Robert R. Tacina *In its* NASA-Chinese Aeronautical Establishment (CAE) Symposium 1986 p 63-87 (For primary document see N87-20267 13-07)
Avail: NTIS HC A01/MF A01 CSCL 20D

An experimental program to characterize the spray from candidate nozzles for icing-cloud simulation is discussed. One canidate nozzle, which is currently used for icing research, has been characterized for flow and drop size. The median-volume diameter (MVD) from this air-assist nozzle is compared with correlations in the literature. The new experimental spray facility is discussed, and the drop-size instruments are discussed in detail. Since there is no absolute standard for drop-size measurements and there are other limitations, such as drop -size range and velocity range, several instruments are used and results are compared. A two-phase model was developed at Pennsylvania State University. The model uses the k-epsilon model of turbulence in the continous phase. Three methods for treating the discrete phase are used: (1) a locally homogeneous flow (LHF) model, (2) a deterministic separated flow (DSF) model, and (3) a stochastic separated flow (SSF) model. In the LHF model both phases have the same velocity and temperature at each point. The DSF model provides interphase transport but ignores the effects of turbulent fluctuations. In the SSF model the drops interact with turbulent eddies whose properties are determined by the k-epsilon turbulence model. The two-phase flow model has been extended to include the effects of evaporation and combustion. Author

N87-20273*# Gas Turbine Research Inst., Jiangyou (China).
COMBUSTION RESEARCH ACTIVITIES AT THE GAS TURBINE RESEARCH INSTITUTE **c25**
Zhongpu Shao *In* NASA- Lewis Research Center NASA-Chinese Aeronautical Establishment (CAE) Symposium 1986 p 89-111 (For primary document see N87-20267 13-07)
Avail: NTIS HC A01/MF A01 CSCL 21B

The Gas Turbine Research Institute (GTRI) is responsible mainly for basic research in aeronautical propulsion. An annular diffuser for the turbofan augmentor, combustor ignition performance, combustor airflow distribution, fuel injectors, a vaporizer fuel injector, and an airblast atomizer are discussed. Author

N87-20274*# National Aeronautics and Space Administration. Lewis Research Center, Cleveland, Ohio.
THERMODYNAMICS AND COMBUSTION MODELING **c77**
Frank J. Zeleznik *In its* NASA-Chinese Aeronautical Establishment (CAE) Symposium 1986 p 113-133 (For primary document see

N87-20267 13-07)
Avail: NTIS HC A01/MF A01 CSCL 20M

Modeling fluid phase phenomena blends the conservation equations of continuum mechanics with the property equations of thermodynamics. The thermodynamic contribution becomes especially important when the phenomena involve chemical reactions as they do in combustion systems. The successful study of combustion processes requires (1) the availability of accurate thermodynamic properties for both the reactants and the products of reaction and (2) the computational capabilities to use the properties. A discussion is given of some aspects of the problem of estimating accurate thermodynamic properties both for reactants and products of reaction. Also, some examples of the use of thermodynamic properties for modeling chemically reacting systems are presented. These examples include one-dimensional flow systems and the internal combustion engine. Author

N87-20275*# Shenyang Aeroengine Research Inst. (China).
EFFECT OF FLAME-TUBE HEAD STRUCTURE ON COMBUSTION CHAMBER PERFORMANCE
Minqqi Gu *In* NASA- Lewis Research Center NASA-Chinese Aeronautical Establishment (CAE) Symposium 1986 p 135-147 (For primary document see N87-20267 13-07)
Avail: NTIS HC A01/MF A01 CSCL 21E

The experimental combustion performance of a premixed, pilot-type flame tube with various head structures is discussed. The test study covers an extensive area: efficiency of the combustion chamber, quality of the outlet temperature field, limit of the fuel-lean blowout, ignition performance at ground starting, and carbon deposition. As a result of these tests, a nozzle was found which fits the premixed pilot flame tube well. The use of this nozzle optimized the performance of the combustion chamber. The tested models had premixed pilot chambers with two types of air-film-cooling structures, six types of venturi-tube structures, and secondary fuel nozzles with two small spray-cone angles. Author

N87-20276*# National Aeronautics and Space Administration. Lewis Research Center, Cleveland, Ohio.
EXPERIMENTS AND MODELING OF DILUTION JET FLOW FIELDS c34
James D. Holdeman *In its* NASA-Chinese Aeronautical Establishment (CAE) Symposium 1986 p 149-174 (For primary document see N87-20267 13-07)
Avail: NTIS HC A01/MF A01 CSCL 20D

Experimental and analytical results of the mixing of single, double, and opposed rows of jets with an isothermal or variable-temperature main stream in a straight duct are presented. This study was performed to investigate flow and geometric variations typical of the complex, three-dimensional flow field in the dilution zone of gas-turbine-engine combustion chambers. The principal results, shown experimentally and analytically, were the following: (1) variations in orifice size and spacing can have a significant effect on the temperature profiles; (2) similar distributions can be obtained, independent of orifice diameter, if momentum-flux ratio and orifice spacing are coupled; (3) a first-order approximation of the mixing of jets with a variable-temperature main stream can be obtained by superimposing the main-stream and jets-in-an-isothermal-crossflow profiles; (4) the penetration of jets issuing mixing is slower and is asymmetric with respect to the jet centerplanes, which shift laterally with increasing downstream distance; (5) double rows of jets give temperature distributions similar to those from a single row of equally spaced, equal-area circular holes; (6) for opposed rows of jets, with the orifice centerlines in line, the optimum ratio of orifice spacing to duct height is one-half the optimum value for single-side injection at the same momentum-flux ratiol and (7) for opposed rows of jets, with the orifice centerlines staggered, the optimum ratio of orifice spacing to duct height is twice the optimum value for single-side injection at the same momentum-flux ratio. Author

N87-20277*# National Aeronautics and Space Administration. Lewis Research Center, Cleveland, Ohio.
THEORETICAL KINETIC COMPUTATIONS IN COMPLEX REACTING SYSTEMS c77
David A. Bittker *In its* NASA-Chinese Aeronautical Establishment (CAE) Symposium 1986 p 175-189 (For primary document see N87-20267 13-07)
Avail: NTIS HC A01/MF A01 CSCL 20M

NASA Lewis' studies of complex reacting systems at high temperature are discussed. The changes which occur are the result of many different chemical reactions occurring at the same time. Both an experimental and a theoretical approach are needed to fully understand what happens in these systems. The latter approach is discussed. The differential equations which describe the chemical and thermodynamic changes are given. Their solution by numerical techniques using a detailed chemical mechanism is described. Several different comparisons of computed results with experimental measurements are also given. These include the computation of (1) species concentration profiles in batch and flow reactions, (2) rocket performance in nozzle expansions, and (3) pressure versus time profiles in hydrocarbon ignition processes. The examples illustrate the use of detailed kinetic computations to elucidate a chemical mechanism and to compute practical quantities such as rocket performance, ignition delay times, and ignition lengths in flow processes. Author

N87-20278*# Gas Turbine Research Inst., Jiangyou (China).
EXPERIMENTAL INVESTIGATION OF PILOTED FLAMEHOLDERS
C. F. Guo, Y. H. Zhang, and Q. M. Xie *In* NASA- Lewis Research Center NASA-Chinese Aeronautical Establishment (CAE) Symposium 1986 p 191-205 (For primary document see N87-20267 13-07)
Avail: NTIS HC A01/MF A01 CSCL 21E

Four configurations of piloted flameholders were tested. The range of flame stabilization, flame propagation, pressure oscillation during ignition, and pressure drop of the configurations were determined. Some tests showed a very strong effect of inlet flow velocity profile and flameholder geometry on flame stabilization. These tests led to the following conclusions. (1) The use of a piloted flameholder in the turbofan augmentor may minimize the peak pressure rise during ignition. At the present experimental conditions, delta P/P asterisk over 2 is less than 10 percent; therefore, the use of a piloted flameholder is a good method to realize soft ignition. (2) The geometry of the piloted flameholder and the amount of fuel injected into the flameholder have a strong effect on the pressure oscillation during ignition of the fuel-air mixture in the secondary zone. (3) Compared with the V-gutter flameholder with holes in its wall, the V-gutter flameholder without holes not only has advantages such as simple structure and good rigidity but offers a wide combustion stability limit and a high capability of igniting the fuel-air mixture of the secondary zone. Author

N87-20279*# National Aeronautics and Space Administration. Lewis Research Center, Cleveland, Ohio.
THE CHEMICAL SHOCK TUBE AS A TOOL FOR STUDYING HIGH-TEMPERATURE CHEMICAL KINETICS c35
Theodore A. Brabbs *In its* NASA-Chinese Aeronautical Establishment (CAE) Symposium 1986 p 207-224 (For primary document see N87-20267 13-07)
Avail: NTIS HC A01/MF A01 CSCL 14B

Although the combustion of hydrocarbons is our primary source of energy today, the chemical reactions, or pathway, by which even the simplest hydro-carbon reacts with atmospheric oxygen to form CO2 and water may not always be known. Furthermore, even when the reaction pathway is known, the reaction rates are always under discussion. The shock tube has been an important and unique tool for building a data base of reaction rates important in the combustion of hydrocarbon fuels. The ability of a shock wave to bring the gas sample to reaction conditions rapidly and homogeneously makes shock-tube studies of reaction kinetics extremely attractive. In addition to the control and uniformity of reaction conditions achieved with shock-wave methods, shock compression can produce gas temperatures far in excess of those in conventional reactors. Argon can be heated to well over

10000 K, and temperatures around 5000 K are easily obtained with conventional shock-tube techniques. Experiments have proven the validity of shock-wave theory; thus, reaction temperatures and pressures can be calculated from a measurement of the incident shock velocity. A description is given of the chemical shock tube and auxiliary equipment and of two examples of kinetic experiments conducted in a shock tube. Author

N87-20280*# National Aeronautics and Space Administration. Lewis Research Center, Cleveland, Ohio.
CONTINGENCY POWER FOR SMALL TURBOSHAFT ENGINES USING WATER INJECTION INTO TURBINE COOLING AIR
Thomas J. Biesiadny, Gary A. Klann, David A. Clark (Army Aviation Research and Development Command, Cleveland, Ohio.), and Brett Berger 1987 14 p Proposed for presentation at the 23rd Joint Propulsion Conference, San Diego, Calif., 29 Jun. - 2 Jul. 1987; sponsored by the AIAA, ASEE, ASME and SAE
(NASA-TM-89817; E-3462; NAS 1.15:89817; USAAVSCOM-TR-86-C-32; AIAA-87-1906) Avail: NTIS HC A02/MF A01 CSCL 21E

Because of one engine inoperative requirements, together with hot-gas reingestion and hot day, high altitude takeoff situations, power augmentation for multiengine rotorcraft has always been of critical interest. However, power augmentation using overtemperature at the turbine inlet will shorten turbine life unless a method of limiting thermal and mechanical stresses is found. A possible solution involves allowing the turbine inlet temperature to rise to augment power while injecting water into the turbine cooling air to limit hot-section metal temperatures. An experimental water injection device was installed in an engine and successfully tested. Although concern for unprotected subcomponents in the engine hot section prevented demonstration of the technique's maximum potential, it was still possible to demonstrate increases in power while maintaining nearly constant turbine rotor blade temperature. Author

N87-20281*# National Aeronautics and Space Administration, Washington, D.C.
THEORY AND DESIGN OF FLIGHT-VEHICLE ENGINES
V. T. Zhdanov, ed. and R. I. Kurziner, ed. Apr. 1987 139 p Transl. into ENGLISH of the book "Teoriya i Konstruktsiya Dvigateley Letatelnykh Apparatov" Academy of Sciences (USSR), Moscow, USSR, 1979 158 p Original language document was announced in IAA as 83A-22651 Transl. by Kanner (Leo) Associates, Redwood City, Calif.
(Contract NASw-4005)
(NASA-TM-88583; NAS 1.15:88583) Avail: NTIS HC A07/MF A01 CSCL 21E

Papers are presented on such topics as the testing of aircraft engines, errors in the experimental determination of the parameters of scramjet engines, the effect of the nonuniformity of supersonic flow with shocks on friction and heat transfer in the channel of a hypersonic ramjet engine, and the selection of the basic parameters of cooled GTE turbines. Consideration is also given to the choice of optimal total wedge angle for the acceleration of aerospace vehicles, the theory of an electromagnetic-resonator engine, the dynamic characteristics of the pumps and turbines of liquid propellant rocket engines in transition regimes, and a hierarchy of mathematical models for spacecraft control engines. IAA

N87-20282*# National Aeronautics and Space Administration. Lewis Research Center, Cleveland, Ohio.
PERFORMANCE AND EFFICIENCY EVALUATION AND HEAT RELEASE STUDY OF AN OUTBOARD MARINE CORPORATION ROTARY COMBUSTION ENGINE
H. L. Nguyen, H. E. Addy, T. H. Bond, C. M. Lee, and K. S. Chun Apr. 1987 24 p Presented at the International Congress and Exposition, Detroit, Mich., 23-27 Feb. 1987; sponsored by the Society of Automotive Engineers
(NASA-TM-89833; E-3488; NAS 1.15:89833) Avail: NTIS HC A02/MF A01 CSCL 21A

A computer simulation which models engine performance of the Direct Injection Stratified Charge (DISC) rotary engines was used to study the effect of variations in engine design and operating parameters on engine performance and efficiency of an experimental Outboard Marine Corporation (OMC) rotary combustion engine. Engine pressure data were used in a heat release analysis to study the effects of heat transfer, leakage, and crevice flows. Predicted engine data were compared with experimental test data over a range of engine speeds and loads. An examination of methods to improve the performance of the rotary engine using advanced heat engine concepts such as faster combustion, reduced leakage, and turbocharging is also presented. Author

N87-20283# Naval Air Development Center, Warminster, Pa. Aircraft and Crew Systems Technology Directorate.
AGARD (ADVISORY GROUP FOR AEROSPACE RESEARCH AND DEVELOPMENT) ENGINE DISC MATERIAL COOPERATIVE TEST
Eun U. Lee 31 Mar. 1986 61 p
(AD-A175533; NADC-86045-60) Avail: NTIS HC A04/MF A01 CSCL 11/6

Specimens, machined from a gas turbine engine fan disc of Ti-6Al-4V alloy, were subjected to fatigue testing, electrical potential drop measurements, and microstructural and fractographic examination. The fatigue crack initiation and growth, and fracture behavior were characterized, and the relationship between crack voltage and crack size was defined quantitatively. The microstructures and fractographs are typical of Ti-6Al-4V alloy forgings. This investigation was a part of NATO's AGARD Engine Disc Material Cooperative Test Project. GRA

N87-20284# Naval Air Propulsion Test Center, Trenton, N.J. Propulsion Engineering Dept.
DECOUPLED BELLMOUTH: AN ALTERNATE METHOD OF MEASURING THRUST IN THE SEA LEVEL TEST CELL Final Report, 1 Oct. 1984 - 30 Sep. 1985
Roman Deineka Aug. 1986 54 p
(AD-A175616; NAPC-PE-155) Avail: NTIS HC A04/MF A01 CSCL 21/5

This report evaluates an alternate method of measuring thrust in the sea level test cell. The method does not require a test cell thrust correction factor which is generally used with the conventional engine installation. In the decoupled bellmouth technique, the bellmouth is isolated from the thrust measuring system, and the inlet momentum is computed from the pressure measurements in the inlet duct. A TF34 engine was tested at an outdoor test site and in a test cell using both thrust accounting methods. Test results show the decoupled bellmouth method worked very well. The method can be used in any test cell or an outdoor site and should be considered as a good alternative to test cell correlations. GRA

N87-20285# Southwest Research Inst., San Antonio, Tex. Fuels and Lubricants Research Div.
THE PHYSICS OF FUEL SPRAYS. VOLUME 1: EXPERIMENTAL MEASUREMENTS Annual Report, Sep. 1985 - Sep. 1986
Lee G. Dodge 5 Dec. 1986 88 p
(Contract N00014-85-C-0841)
(AD-A175660; SWRI-8858/1-Vol-1) Avail: NTIS HC A05/MF A01 CSCL 21/4

The objective of this program is to develop a better understanding of gas-turbine-type fuel sprays under realistic high temperature and high pressure evaporating conditions, and also at altitude relight conditions. This includes developing computer models to predict spray behavior and evaporation rates and sophisticated diagnostics to verify these models. Progress includes: (1) Procedures for using the Aerometrics Phase/Doppler instrument and for processing the results have been developed to the point that the instrument can be used to provide benchmark quality data for spray model verification. Specifically, this instrument can be used to provide spatially-resolved drop size distributions, drop velocity distributions, and liquid volume-flux data. Problems in the liquid volume flux measurements close to the atomizer (less than 25 mm) are still being investigated. It was necessary to compare the

performance of the Aerometrics Phase/Doppler particle analyzer with the Malvern drop sizing instrument. Because these instruments sample the spray in different ways, techniques were developed to correctly average the overall spray characteristics from measurements of different types of instruments. (2) A new, atmospheric-pressure spray facility was designed and constructed. This facility features a low-turbulence air flow system and computer-controlled nozzle positioning for accurate measurements throughout the spray. (3) The effects of reduced air pressure on atomization were examined. GRA

N87-20286# National Aeronautical Establishment, Ottawa (Ontario).
HIGH TEMPERATURE PROTECTIVE COATINGS FOR AERO ENGINE GAS TURBINE COMPONENTS
P. C. Patnaik and J.-P. Immarigeon Sep. 1986 63 p
(AD-A176001; NAE-AN-42; NRC-26475) Avail: NTIS HC A04/MF A01 CSCL 11/3

Aluminide coatings have been widely used in the aircraft industries for the protection of gas turbine engine hot section components against oxidation and/or hot corrosion. This paper considers modes of coating degradation under conditions of cyclic oxidation, hot corrosion and corrosion-erosion interactions during service as well as the effects of interdiffusion between coating and substrate alloys either during service or coating application. It also discusses means of improving existing coatings as well as advanced coating systems currently under development. In assessing coating performance, consideration must be given to the influence coatings may have on substrate properties such as mechanical strength, resistance to creep and resistance to mechanical and thermal fatigue. Finally it is stressed that proven performance for a given coating/substrate combination is no guarantee that no deleterious reaction will occur, when the same coating is used with a different substrate alloy. Therefore, coating substitution requires requalification. GRA

N87-20287# Technische Hochschule, Aachen (West Germany). Inst. fuer Strahlantriebe und Turboarbeitsmachinen.
EXPERIMENTAL AND THEORETICAL INVESTIGATION OF THE FLOW PHENOMENA IN RETURN CHANNELS OF RADIAL COMPRESSOR STAGES, ESPECIALLY THOSE WITH SMALL CHANNEL WIDTH [EXPERIMENTELLE UND THEORETISCHE UNTERSUCHUNG DER STROEMUNGSVORGAENGE IN RUECK-FUEHRKANAELEN VON RADIALVERDICHTERSTUFEN, INSBESONDERE SOLCHER MIT GERINGEN KANALBREITEN]
H. E. Gallus and E. Rothstein Apr. 1985 146 p In GERMAN
(Contracts DFG-Ga-180/12-1; DFG-180/12-2; DFG-180/12-3)
(Mitt-85-01; ETN-87-99336) Avail: NTIS HC A07/MF A01

Radial compressor return channels with different flow rate characteristics and rotor outlet width were investigated. Compressor stages with very small flow characteristic quantities and correspondingly small channel widths, as applied in high pressure compress, in order to reduce the flow losses in the return channels were examined. The boundary conditions of the compressor stages are discussed. A model calculation allows to estimate the effect of losses in the return flow on the stage efficiency. A data evaluation method makes it possible to reduce the flow losses determined in model tests, to the required Reynolds number level. A procedure for the construction of return flow blades is presented. The experimental results show the effect of flow-mechanical and geometric parameters on the flow behavior and the development of losses in the return. ESA

08 AIRCRAFT STABILITY AND CONTROL

Includes aircraft handling qualities; piloting; flight controls; and autopilots.

For related information see also *05 Aircraft Design, Testing and Performance.*

N87-20288 Princeton Univ., N.J.
STABILITY REGIONS OF RELAXED STATIC STABILITY AIRCRAFT UNDER CONTROL SATURATION CONSTRAINTS Ph.D. Thesis
Prakash Chandra Shrivastava 1986 550 p
Avail: Univ. Microfilms Order No. DA8626183

Gains can be achieved in maneuvering performance and cruising flight fuel use if an aircraft is designed with low inherent stability. Limitations imposed by constraints on magnitudes and rates of control surface deflections on regions of stable operation of unstable aircraft are exposed. Shapes and sizes of stability regions are shown to depend upon types of singularities, feedback gains, control saturation limits, and command inputs. Analytical expressions for stability regions are possible only as special cases. Higher feedback gains increase sizes of stability regions. For non-zero commands, the stability regions of systems with saddle-point- and unstable-node-type singularities disappear when control deflections exceed saturation limits for desired command. Such is not the case for systems with unstable-focus-type singularities where with increasing commands, an inner limit cycle emerges within outer stability boundary, and it grows in size with commands until the two boundaries coincide. Effects of joint rate and displacement saturation are examined by a saddle-point-type singularity. Stability regions in phase plane of the control and unstable mode are found to be unstable limit cycles. Bandwidths have little influence on their sizes, which increase almost proportionately with rate limits. Upon imposition of displacement limits size reduction is considerable, and the size cannot be increased by increasing rate limits beyond a certain point. Larger stability regions result when control deflection is also fed back, and smaller regions are obtained when feedback gain is increased. Dissert. Abstr.

N87-20289*# Purdue Univ., West Lafayette, Ind. School of Aeronautics and Astronautics.
ANALYSIS OF NLR CONFIGURATIONS USING OCM FOR PILOT MODELING Interim Status Report
M. H. Drajeske 28 Apr. 1987 108 p
(Grant NAG4-1)
(NASA-CR-180656; NAS 1.26:180656) Avail: NTIS HC A06/MF A01 CSCL 01C

A summary of the results obtained from an analytic handling qualities analysis of the rate-command/attitude-hold aircraft configurations is presented. Pilot/vehicle performance was evaluated using an optimal control technique for pilot modeling. Numerical and graphical results for a closed-loop frequency-domain analysis are presented and discussed and comparisons with experimental results are made. Finally, the results are compared with those from another study that dealt with similar configurations. B.G.

N87-20290*# Boeing Commercial Airplane Co., Seattle, Wash.
DESIGN AND VERIFICATION BY NONLINEAR SIMULATION OF A MACH/CAS CONTROL LAW FOR THE NASA TCV B737 AIRCRAFT Final Report
Kevin R. Bruce Dec. 1986 68 p
(Contract NAS1-14880)
(NASA-CR-178029; NAS 1.26:178029) Avail: NTIS HC A04/MF A01 CSCL 01C

A Mach/CAS control system using an elevator was designed and developed for use on the NASA TCV B737 aircraft to support research in profile descent procedures and approach energy management. The system was designed using linear analysis techniques primarily. The results were confirmed and the system validated at additional flight conditions using a nonlinear 737 aircraft simulation. All design requirements were satisfied. Author

N87-20291*# National Aeronautics and Space Administration. Ames Research Center, Moffett Field, Calif.
MEAN-SQUARE ERROR BOUNDS FOR REDUCED-ERROR LINEAR STATE ESTIMATORS
Y. Baram and G. Kalit (Defence Dept., Israel.) Mar. 1987 8 p

(NASA-TM-89441; A-87157; NAS 1.15:89441) Avail: NTIS HC A02/MF A01 CSCL 01C

The mean-square error of reduced-order linear state estimators for continuous-time linear systems is investigated. Lower and upper bounds on the minimal mean-square error are presented. The bounds are readily computable at each time-point and at steady state from the solutions to the Ricatti and the Lyapunov equations. The usefulness of the error bounds for the analysis and design of reduced-order estimators is illustrated by a practical numerical example. Author

N87-20292# Georgia Inst. of Tech., Atlanta. School of Aerospace Engineering.

EFFECT OF DYNAMIC STALL AND ELASTIC PARAMETERS ON THE FUNDAMENTAL MECHANISMS OF HELICOPTER VIBRATIONS Final Report, 1 Sep. 1985 - 30 Sep. 1986

David A. Peters 1 Nov. 1986 82 p

(Contract DAAG29-85-K-0228)

(AD-A175561; ARO-23322.7-EG) Avail: NTIS HC A05/MF A01 CSCL 01/3

This research has dealt with the modeling and solution of rotary-wing dynamics. In the modeling area, it deals with elastic-blade models, ways to introduce rotor-body coupling, aerodynamic behavior near blade-tips, and the modeling of dynamic stall. In solution strategies, we have concentrated on new and improved Floquet methods, on innovative trim methodologies (such as auto-pilot and periodic shooting), on efficient formulation of equations, and on lifting -line and lifting-surface meshes. GRA

N87-20293# Royal Air Force Coll., Cranwell (England).

SIMULATION OF AN INTEGRATED FIRE AND FLIGHT CONTROL SYSTEM FOR AIR-TO-AIR GUNNERY M.S. Thesis

D. R. Smith 1986 158 p

(ETN-87-99479) Avail: NTIS HC A08/MF A01

A FORTRAN simulation of an integrated fire and flight control (IFFC) system was developed, based on the configuration of the Firefly system tested in an F-15B. The model simulates only the pitch channel of the system, using a simplified form of the short period pitching oscillation state equation. A choice of three forms of stability augmentation brings the basic aircraft dynamic characteristics within the Defense Standard limits. Because the model is assumed to have a fixed gun installation, the aircraft must itself be maneuvered to achieve correct weapon aiming and the overall system is therefore subject to kinematic closure. Simulations show that IFFC is a viable concept for new aircraft and for retrospective inclusion on existing types. There may not always be direct benefits in aiming accuracy, but IFC should result in a significant reduction in the pilot's workload, an enlargement of the engagement envelopes, and potentially an improvement in the overall cost-effectiveness of the complete weapons system. ESA

09 RESEARCH AND SUPPORT FACILITIES (AIR)

Includes airports, hangars and runways; aircraft repair and overhaul facilities; wind tunnels; shock tubes; and aircraft engine test stands.

For related information see also *14 Ground Support Systems and Facilities (Space)*.

N87-20294*# National Aeronautics and Space Administration. Langley Research Center, Hampton, Va.

COMPUTATIONS FOR THE 16-FOOT TRANSONIC TUNNEL, NASA, LANGLEY RESEARCH CENTER, REVISION 1

Charles E. Mercer, Bobby L. Berrier, Francis J. Capone, Alan M. Grayston (Wyle Labs., Inc., Hampton, Va.), and C. D. Sherman Jan. 1987 204 p

(NASA-TM-86319-Rev-1; NAS 1.15:86319-Rev-1) Avail: NTIS HC A10/MF A01 CSCL 14B

The equations used by the 16 foot transonic tunnel in the data reduction programs are presented in eight modules. Each module consists of equations necessary to achieve a specific purpose. These modules are categorized in the following groups: tunnel parameters; jet exhaust measurements; skin friction drag; balance loads and model attitudes calculations; internal drag (or exit-flow distributions); pressure coefficients and integrated forces; thrust removal options; and turboprop options. This document is a companion document to NASA TM-83186, A User's Guide to the Langley 16 Foot Transonic Tunnel, August 1981. Author

N87-20295*# National Aeronautics and Space Administration. Lewis Research Center, Cleveland, Ohio.

DETAILED FLOW SURVEYS OF TURNING VANES DESIGNED FOR A 0.1-SCALE MODEL OF NASA LEWIS RESEARCH CENTER'S PROPOSED ALTITUDE WIND TUNNEL

Royce D. Moore, Rickey J. Shyne, Donald R. Boldman, and Thomas F. Gelder Apr. 1987 151 p

(NASA-TP-2680; E-3294; NAS 1.60:2680) Avail: NTIS HC A08/MF A01 CSCL 14B

Detailed flow surveys downstream of the corner turning vanes and downstream of the fan inlet guide vanes have been obtained in a 0.1-scale model of the NASA Lewis Research Center's proposed Altitude Wind Tunnel. Two turning vane designs were evaluated in both corners 1 and 2 (the corners between the test section and the drive fan). Vane A was a controlled-diffusion airfoil and vane B was a circular-arc airfoil. At given flows the turning vane wakes were surveyed to determine the vane pressure losses. For both corners the vane A turning vane configuration gave lower losses than the vane B configuration in the regions where the flow regime should be representative of two-dimensional flow. For both vane sets the vane loss coefficient increased rapidly near the walls. Author

N87-20296*# National Aeronautics and Space Administration. Langley Research Center, Hampton, Va.

COMPUTATIONAL ANALYSIS AND PRELIMINARY REDESIGN OF THE NOZZLE CONTOUR OF THE LANGLEY HYPERSONIC CF4 TUNNEL

R. A. Thompson and Kenneth Sutton Mar. 1987 32 p

(NASA-TM-89042; L-16170; NAS 1.15:89042) Avail: NTIS HC A03/MF A01 CSCL 14B

A computational analysis, modification, and preliminary redesign study was performed on the nozzle contour of the Langley Hypersonic CF4 Tunnel. This study showed that the existing nozzle was contoured incorrectly for the design operating condition, and this error was shown to produce the measured disturbances in the exit flow field. A modified contour was designed for the current nozzle downstream of the maximum turning point that would provide a uniform exit flow. New nozzle contours were also designed for an exit Mach number and Reynolds number combination which matches that attainable in the Langley 20-Inch Mach 6 Tunnel. Two nozzle contours were designed: one having the same exit radius but a larger mass flow rate than that of the existing CF4 Tunnel, and the other having the same mass flow rate but a smaller exit radius than that of the existing CF4 Tunnel. Author

N87-20297*# General Dynamics/Convair, San Diego, Calif.

DESIGN STUDY OF ADVANCED MODEL SUPPORT SYSTEMS FOR THE NATIONAL TRANSONIC FACILITY (NTF)

Jan. 1987 68 p

(NASA Order L-997258)

(NASA-CR-178214; NAS 1.26:178214) Avail: NTIS HC A04/MF A01 CSCL 14B

It has long been recognized that the sting (or support system) is a very critical part of the model system. The designer is frequently faced with the tradeoff of minimizing sting size, thereby compromising facility and model safety, against a larger sting and the subsequent problems of sting interference effects. In the NASA Langley Research Center National Transonic Facility (NTF), this problem is accentuated by the severe environment of high pressure/low temperature, designed into the facility to provide the desired high Reynolds number. Compromises in the configuration geometry and/or limiting the test envelope are therefore contrary to the purposes and goals of the NTF and are unacceptable. The

results of an investigation aimed at improvements of 25% in both strength and Young's modulus of elasticity as compared to high strength cryogenically acceptable steels currently being used are presented. Various materials or combinations of materials were studied along with different design approaches. Design concepts were developed which included conventional material stings, advanced composites, and hybrid configurations. Candidate configurations are recommended. Author

N87-20298*# National Aeronautics and Space Administration. Ames Research Center, Moffett Field, Calif.
VISUAL DISPLAY AND ALARM SYSTEM FOR WIND TUNNEL STATIC AND DYNAMIC LOADS
Richard D. Hanly and James T. Fogarty (Raman Aeronautics Research and Engineering, Inc., Palo Alto, Calif.) Apr. 1987 10 p
(NASA-TM-89455; A-87105; NAS 1.15:89455) Avail: NTIS HC A02/MF A01 CSCL 14B

A wind tunnel balance monitor and alarm system developed at NASA Ames Research Center will produce several beneficial results. The costs of wind tunnel delays because of inadvertent balance damage and the costs of balance repair or replacement can be greatly reduced or eliminated with better real-time information on the balance static and dynamic loading. The wind tunnel itself will have enhanced utility with the elimination of overly cautious limits on test conditions. The microprocessor-based system features automatic scaling and 16 multicolored LED bargraphs to indicate both static and dynamic components of the signals from eight individual channels. Five individually programmable alarm levels are available with relay closures for internal or external visual and audible warning devices and other functions such as automatic activation of external recording devices, model positioning mechanisms, or tunnel shutdown. Author

N87-20299# Bristol Univ. (England). Dept. of Aeronautical Engineering.
AN INVESTIGATION INTO THE FACTORS AFFECTING THE FLOW QUALITY IN A SMALL SUCTION WIND TUNNEL B.S. Thesis
S. E. B. Lawson and A. P. R. Stewart Jun. 1986 46 p
(BU-344; ETN-87-99206) Avail: NTIS HC A03/MF A01

During testing of a wind tunnel designed to allow investigation of the dynamic interference on an airfoil, it was found that the tunnel itself was subject to large flow disturbances sufficient to prevent accurate measurements of the effects. Changes to the tunnel were made in order to investigate their relative contributions to turbulence alleviation. Measurements with a hot-wire probe system show that the turbulence can be reduced to under 0.7% by a combination of these changes. However, it is also shown that disturbances from the suction fan are a major cause of the tunnel turbulence and thus suggest that the tunnel/fan combination may not be suitable for measurement of the dynamic interference effects as originally intended. ESA

N87-20300# European Space Agency, Paris (France).
THE HIGH-SPEED CASCADE WIND TUNNEL - STILL AN IMPORTANT TEST FACILITY FOR TURBOMACHINERY BLADE INVESTIGATIONS
Heinz Hoheisel Nov. 1986 37 p Transl. into ENGLISH of "Der Hochgeschwindigkeits-Gitterwindkanel - Immernoch eine Wichtige Versuchsanlage fuer Untersuchungen an Turbomaschinenbeschaufellungen" DFVLR, Brunswick, West Gemany, report DFVLR-Mitt-86-11, Mar. 1986 Original language document was announced as N87-10878
(ESA-TT-1012; DFVRL-Mitt-86-11; ETN-87-99430) Avail: NTIS HC A03/MF A01; original German version available from DFVLR, Cologne, West Germany DM 14

The importance of the high speed cascade wind tunnel was demonstrated. Starting from the conception of this wind tunnel and the requirements for cascade wind tunnels in which compressible flows have to be studied, the usability and qualification of this test facility for research work is described with examples of turbine and compressor cascade investigations. Necessary additional equipment is discussed. ESA

12 ASTRONAUTICS (GENERAL)

For extraterrestrial exploration see *91 Lunar and Planetary Exploration.*

N87-20301*# National Aeronautics and Space Administration. Lyndon B. Johnson Space Center, Houston, Tex.
MANNED MARS MISSIONS: A WORKING GROUP REPORT
Michael B. Duke, ed. and Paul W. Keaton, ed. (Los Alamos National Lab., N. Mex.) May 1986 88 p Working Papers Presented at Huntsville, Alabama, 10-14 Jun. 1985
(NASA-TM-89214; NASA-M001; NAS 1.15:89214) Avail: NTIS HC A05/MF A01 CSCL 22A

The discussions of the Working Group (based in large part on working papers, which will shortly be published separately) are summarized. These papers cover a broad range of subjects which need to be addressed in the formulation of such a formidable enterprise as a manned Mars program. Science objective and operations; Mars surface infrastructure and activities; mission and system concepts and configurations; life sciences; impacts on the space infrastructure; and costs, schedules, and organizations are addressed. B.G.

N87-20302*# National Aeronautics and Space Administration. Goddard Space Flight Center, Greenbelt, Md.
THE 1986 GET AWAY SPECIAL EXPERIMENTER'S SYMPOSIUM
Lawrence R. Thomas, ed. and Frances L. Mosier, ed. Feb. 1987 236 p Symposium held in Greenbelt, Md., 7-8 Oct. 1986
(NASA-CP-2438; NAS 1.55:2438) Avail: NTIS HC A11/MF A01 CSCL 22A

The 1986 Get Away Special (GAS) Experimenter's Symposium will provide a formal opportunity for GAS Experimenter's to share the results of their projects. The focus of this symposium is on payloads that will be flown in the future. For individual titles, see N87-20303 through N87-20334.

N87-20303*# Defense Systems, Inc., McLean, Va.
TRACKING THE GLOMR SATELLITE **c13**
Keith W. Reiss and Jason C. ONeil *In* NASA. Goddard Space Flight Center The 1986 Get Away Special Experimenter's Symposium Feb. 1987 p 1-8 (For primary document see N87-20302 13-12)
Avail: NTIS HC A11/MF A01 CSCL 22A

The task of day-to-day low orbiting satellite tracking utilizing the NAVSPASUR orbital elements is discussed and methods for improving pass time predictions are presented. Estimates are needed for preprogramming of satellite-initiated communications scheduling which requires an accuracy of approximately 30 seconds. This can be achieved by removing the variance associated with the NAVSPASUR D sub 2 (decay) term. Finally, the shock evidenced in GLOMR's orbit on February 7, 1986 is documented and attributed to a severe solar storm with immediately enhanced drag. GLOMR's life expectancy in orbit is now estimated to have dropped approximately 17% by the end of orbit in early February, 1987. Author

N87-20304*# National Electric Co. of Venezuela, Caracas.
MANUFACTURING POLYMER THIN FILMS IN A MICROGRAVITY ENVIRONMENT **c29**
Ivan Vera *In* NASA. Goddard Space Flight Center The 1986 Get Away Special Experimenter's Symposium Feb. 1987 p 9-14 (For primary document see N87-20302 13-12)
Avail: NTIS HC A11/MF A01 CSCL 22A

This project represents Venezuela's first scientific experiment in space. The apparatus for the automatic casting of two polymer thin films will be contained in NASA's Payload No. G-559 of the Get Away Special program for a future orbital space flight in the U.S. Space Shuttle. Semi-permeable polymer membranes have

important applications in a variety of fields, such as medicine, energy, and pharmaceuticals and in general fluid separation processes, such as reverse osmosis, ultrafiltration, and electrodialysis. The casting of semi-permeable membranes in space will help to identify the roles of convection in determining the structure of these membranes. Author

N87-20305*# Alabama Univ., Huntsville. Consortium for Materials Development in Space.
PHASE PARTITIONING, CRYSTAL GROWTH, ELECTRODEPOSITION AND COSMIC RAY EXPERIMENTS IN MICROGRAVITY **c29**
Francis C. Wessling *In* NASA. Goddard Space Flight Center The 1986 Get Away Special Experimenter's Symposium Feb. 1987 p 15-22 (For primary document see N87-20302 13-12)
Avail: NTIS HC A11/MF A01 CSCL 22A

Five experiments are contained in one Get Away Special Canister (5 cu ft). The first utilizes microgravity to separate biological cells and to study the mechanism of phase partitioning in 12 separate cuvettes. Two experiments are designed to grow organic crystals by physical vapor transport. One experiment consists of eight electroplating cells with various chemicals to produce surfaces electroplated in microgravity. Some of the surfaces have micron sized particles of hard materials co-deposited during electrodeposition. The fifth experiment intercepts cosmic ray particles and records their paths on photographic emulsions. The first four experiments are controlled by an on-board C-MOS controller. The fifth experiment is totally passive. These are the first in Space. Their purpose is to create new commercial products with microgravity processing. Author

N87-20306*# National Aeronautics and Space Administration. Goddard Space Flight Center, Greenbelt, Md. Space Welding Project.
GAS TUNGSTEN ARC WELDING IN A MICROGRAVITY ENVIRONMENT: WORK DONE ON GAS PAYLOAD G-169 **c37**
Blake A. Welcher, Faysal A. Kolkailah, and Arthur H. Muir, Jr. (Rockwell International Corp., Thousand Oaks, Calif.) *In* NASA. Goddard Space Flight Center The 1986 Get Away Special Experimenter's Symposium Feb. 1987 p 23-29 (For primary document see N87-20302 13-12)
Avail: NTIS HC A11/MF A01 CSCL 11F

GAS payload G-169 is discussed. G-169 contains a computer-controlled Gas Tungsten Arc Welder. The equipment design, problem analysis, and problem solutions are presented. Analysis of data gathered from other microgravity arc welding and terrestrial Gas Tungsten Arc Welding (GTAW) experiments are discussed in relation to the predicted results for the GTAW to be performed in microgravity with payload G-169. Author

N87-20307*# Purdue Univ., West Lafayette, Ind. School of Technology.
USE OF LIGHTWEIGHT COMPOSITES FOR GAS PAYLOAD STRUCTURES **c24**
Mark B. Spencer *In* NASA. Goddard Space Flight Center The 1986 Get Away Special Experimenter's Symposium Feb. 1987 p 31-34 (For primary document see N87-20302 13-12)
Avail: NTIS HC A11/MF A01 CSCL 11D

A key element in the design of a small self-contained payload is the supporting structure. This structure must support the experiments and other components while using as little space and weight as possible. Hence, the structure material must have characteristics of being both strong and light. Aluminum was used for the structure on the first Purdue University payload, but consumed a relatively large percentage of the total payload weight. The current payload has a larger power supply requirement than did the previous payload. To allow additional weight for the batteries, a composite material has been chosen for the structure which has the required strength while being considerably lighter than aluminum. A radial fin design has been chosen for ease of composite material lay-up and its overall strength of design. A composite plate will connect the free ends of the fins and add strength and reduce vibration. The physical characteristics of the composite material and the method of open lay-up construction is described. Also discussed are the testing, modifications, and problems encountered during assembly of the experiments to the structure. Author

N87-20308*# Colorado Univ., Boulder. Get Away Special Project G-285
PHYCOMYCES IN SPACE: A PROBLEM IN BIOENGINEERING **c51**
Julie A. Schneringer *In* NASA. Goddard Space Flight Center The 1986 Get Away Special Experimenter's Symposium Feb. 1987 p 35-39 (For primary document see N87-20302 13-12)
Avail: NTIS HC A11/MF A01 CSCL 06B

Sustaining life with total automation is a difficult problem for GAS canisters. The length of time between setting the experiment and flight, the conditions of a completely sealed container, no guarantee on launch delay, orientation and the possibility of contamination all tend to exclude experiments with living matter. This experiment examines the growth of a nontoxic, everyday fungus, Phycomyces, in a microgravity environment. Data from this experiment will help define the mechanism by which plants determine the direction of gravity. The bioengineering problems were solved only after numerous tests and design changes. Phycomyces normally have a shelf life of approximately one week. Storing the fungus for two months, activating the fungus for growth and precise timing were the major obstacles. Solutions were found for storage by drying the fungus spores onto pieces of filter paper. Activation occurs when this filter paper is dropped onto the growth medium, via a solenoid system. The problem of timing is partially solved by growing more than one chamber of the fungus at different time intervals. This experiment proves that the simpler a design, the better it works. Author

N87-20309*# Norfolk Technical Vocational Center, Va.
NORSTAR PROJECT: NORFOLK PUBLIC SCHOOLS STUDENT TEAM FOR ACOUSTICAL RESEARCH **c71**
Ronald C. Fortunato *In* NASA. Goddard Space Flight Center The 1986 Get Away Special Experimenter's Symposium Feb. 1987 p 41-48 (For primary document see N87-20302 13-12)
Avail: NTIS HC A11/MF A01 CSCL 20A

Development of the NORSTAR (Norfolk Public Student Team for Acoustical Research) Project includes the definition, design, fabrication, testing, analysis, and publishing the results of an acoustical experiment. The student-run program is based on a space flight organization similar to the Viking Project. The experiment will measure the scattering transfer of momentum from a sound field to spheres in a liquid medium. It is hoped that the experimental results will shed light on a difficult physics problem - the difference in scattering cross section (the overall effect of the sound wave scattering) for solid spheres and hollow spheres of differing wall thicknesses. Author

N87-20310*# Telesat Canada, Ottawa (Ontario).
TOWARDS A BETTER MIRROR **c29**
David Hoffer *In* NASA. Goddard Space Flight Center The 1986 Get Away Special Experimenter's Symposium Feb. 1987 p 49-57 (For primary document see N87-20302 13-12)
Avail: NTIS HC A11/MF A01 CSCL 22A

Telesat's Getaway Special competition was designed to promote interest in space among high school students in Canada. The winning entry proposed the manufacture of mirrors in microgravity and to compare the optical properties of these mirrors with similar ones made on Earth. Telesat engineers designed and built the experiment which flew on the Atlantic shuttle on November 27, 1985. This paper outlines the design evolution, its implementation, the manufacture and test of the GAS and the results of the experiment. Author

N87-20311*# Ohio State Univ., Columbus. Dept. of Aeronautical and Astronautical Engineering.
PROGRESS ON THE OHIO STATE UNIVERSITY GET AWAY SPECIAL G-0318: DEAP **c29**
Nesrin Sarigul and A. J. Mortensen (Gould, Inc., Cleveland, Ohio.)

In NASA. Goddard Space Flight Center The 1986 Get Away Special Experimenter's Symposium Feb. 1987 p 59-62 (For primary document see N87-20302 13-12)
Avail: NTIS HC A11/MF A01 CSCL 22A

The Get Away Special program became a major presence at the Ohio State University with the award of GAS-0318 by the American Institute of Aeronautics and Astronautics. There are some twenty engineering researchers and students currently working on the project. GAS-0318 payload is an experimental manufacturing process known as Directional Electrostatic Accretion Process (DEAP). This high precision portable microgravity manufacturing method will revolutionize the manufacture and repair of spacecraft and space structures. The cost effectiveness of this process will be invaluable to future space development and exploration. Author

N87-20312*# Weber State Coll., Ogden, Utah. Center for AeroSpace Technology.
NUSAT UPDATE **c18**
Charles A. Bonsall *In* NASA. Goddard Space Flight Center The 1986 Get Away Special Experimenter's Symposium Feb. 1987 p 63-69 (For primary document see N87-20302 13-12)
Avail: NTIS HC A11/MF A01 CSCL 22B

This paper presents, in general terms, the results of the experiments with NUSAT I. These include what has been learned about the strengths of the original design, as well as improvements being incorporated into NUSAT II, which should be of interest to designers of future Get Away Special ejected satellites. This paper also presents an account of the formation of the Center for AeroSpace Technology (CAST) at Weber State College, which grew out of the NUSAT project, and some potential applications and markets for inexpensive, low orbit satellites which CAST has explored. Author

N87-20313*# Colorado Univ., Boulder. Getaway Special Project G-285.
SOPHISTICATED SOFTWARE SYSTEMS FOR SMALL SELF-CONTAINED SPACE SHUTTLE PAYLOAD G285 **c61**
Robert Burkhardt *In* NASA. Goddard Space Flight Center The 1986 Get Away Special Experimenter's Symposium Feb. 1987 p 71-78 (For primary document see N87-20302 13-12)
Avail: NTIS HC A11/MF A01 CSCL 09B

The increasing development of small microprocessor systems has allowed the use of more advanced software in the area of control systems. This paper discusses the development of software for small Space Shuttle Getaway Special Project payloads using payload G285 as a case example. The development process behind a space related software package (as in any software package) is a major factor. The design process for G285 is discussed in some detail along with the general scheme behind data acquisition and thermal environmental control for a space related payload. Additionally, key concepts in a software system concern the implementation of redundant systems, error detection, and error response. All of these factors are discussed. Author

N87-20314*# Utah State Univ., Logan. Center for Atmospheric and Space Sciences.
A SYSTEMS-LEVEL PERFORMANCE HISTORY OF GET AWAY SPECIALS AFTER 25 SPACE SHUTTLE MISSIONS
Rex W. Ridenoure *In* NASA. Goddard Space Flight Center The 1986 Get Away Special Experimenter's Symposium Feb. 1987 p 79-86 (For primary document see N87-20302 13-12)
Avail: NTIS HC A11/MF A01 CSCL 22A

Summarized are the results of a thorough performance study of Get Away Special (GAS) payloads conducted in 1986. During the study, a complete list of standard and non-standard GAS payloads vs. Shuttle mission was constructed, including specific titles for the experiments in each canister. A broad data base for each canister and each experiment was then compiled. Performance results were then obtained for all but a few experiments. The canisters and experiments were subsequently categorized according to the degree of experiment success. For those experiments experiencing failures or anomalies, several correlations and generalizations were extracted from individual subsystem performance data. Recommendations are made which may enhance the success and performance of future GAS payloads. Author

N87-20315*# National Aeronautics and Space Administration. Goddard Space Flight Center, Greenbelt, Md.
STS-61C, COLUMBIA FLIGHT Final Report **c32**
Edward F. Stluka *In its* The 1986 Get Away Special Experimenter's Symposium Feb. 1987 p 87-93 (For primary document see N87-20302 13-12)
Avail: NTIS HC A11/MF A01 CSCL 17B

The performance of the Marshall Amateur Radio Club Experiment (MARCE) is reviewed. The responses, from the World Wide Amateur Radio Ground Stations, who received the Columbia to Earth direct radio downlinks, are discussed. Likewise, the MARCE radio relay link from Columbia through the AMSAT OSCAR AO-10 satellite to Earth is reviewed. Author

N87-20316*# National Aeronautics and Space Administration. Goddard Space Flight Center, Greenbelt, Md.
USC/AIAA STUDENT GET AWAY SPECIAL PROJECT LIQUID DROPLET COLLECTOR EXPERIMENT **c34**
Raymond J. LeVesque, II *In its* The 1986 Get Away Special Experimenter's Symposium Feb. 1987 p 95-102 (For primary document see N87-20302 13-12)
Avail: NTIS HC A11/MF A01 CSCL 20D

This experimental payload was developed in order to observe, in a micro-gravity vacuum environment, the characteristics and stability of a thin fluid film flowing across a slightly curved surface. The test apparatus was designed based upon various ground-based thin film investigations, combined with the constraints imposed by the rigors of launch and the space environment. Testing of the fluid test article at atmospheric pressure and in vacuum verified the design provisions employed concerning ultra-low inlet pressure pump construction, as well as confirming expected pressure losses in the system. During the course of hardware development and construction modifications were required; however, the overall payload configuration remained largely unchanged. This will allow for modification and reflight of the apparatus based upon the findings of the initial flight. The specific applications of this experiment include Liquid Droplet Radiator development and various forms of material transport in vacuum. Author

N87-20317*# Saint Mary's Hospital, Milwaukee, Wis. Laser Program.
RESULTS OF THE JOINT UTILIZATION OF LASER INTEGRATED EXPERIMENTS FLOWN ON PAYLOAD GAS-449 ABOARD COLUMBIA MISSION 61-C **c36**
M. C. Muckerheide *In* NASA. Goddard Space Flight Center The 1986 Get Away Special Experimenter's Symposium Feb. 1987 p 103-110 (For primary document see N87-20302 13-12)
Avail: NTIS HC A11/MF A01 CSCL 20E

The high peak power neodymium YAG laser and the HeNe laser aboard GAS-449 have demonstrated the survivability of the devices in the micro-gravity, cosmic radiation, thermal, and shock environment of space. Some pharmaceuticals and other materials flown in both the active and passive status have demonstrated reduction in volume and unusual spectroscopic changes. X-ray detectors have shown cosmic particle hits with accompanying destruction at their interaction points. Some scattering in the plates is in evidence. Some results of both active and passive experiments on board the GAS-449 payload are evaluated. Author

N87-20318*# North Carolina Agricultural and Technical State Univ., Greensboro. Student Space Shuttle Program.
THE NORTH CAROLINA A AND T STATE UNIVERSITY STUDENT SPACE SHUTTLE PROGRAM Status Report, 1979-1986 **c29**
F. D. Hooker and S. T. Ahrens *In* NASA. Goddard Space Flight Center The 1986 Get Away Special Experimenter's Symposium Feb. 1987 p 111-118 (For primary document see N87-20302 13-12)

Avail: NTIS HC A11/MF A01 CSCL 22A

Inspired into being in 1979 by the late astronaut, Dr. Ronald McNair, the primary goal of this student centered program is to perform two experiments, Arthopod Development Study and Crystal Growth Study. Since 1979, 78 different students representing 12 majors have participated in every phase of development of the payload -- from coming up with the original ideas to final fabrication and testing. Students have also been involved in many extra activities such as presenting their results at annual meetings and hosting tours of our lab for local schools. The program has received extensive outside support in the form of funds, technical assistance and donated parts. The payload, made primarily out of aluminum, consists of a central column structure, a battery box, a crystal growth box, an arthropod development box, four control circuit boxes, and a thermograph box. The battery box contains 24, Eveready 6V, Alkaline batteries. The thermograph box contains 3 Ryan TempMentors. Fabrication of the payload is essentially complete and a complete testing program has been initiated.

Author

N87-20319*# Spar Aerospace Ltd., Toronto (Ontario).

BAKING THE FIRST BREAD IN SPACE **c29**

In NASA. Goddard Space Flight Center The 1986 Get Away Special Experimenter's Symposium Feb. 1987 p 119-126 (For primary document see N87-20302 13-12)

Avail: NTIS HC A11/MF A01 CSCL 22A

This Getaway Special program is a joint venture between Spar, Monarch flour and Telesat, with Telesat being responsible for the design, manufacture and implementation of the equipment. The purpose of the experiment is to investigate the behavior of bread yeast in the absence of gravity and in the presence of normal atmospheric pressure. The proposed design mixes flour, water and yeast on-orbit, allows the mixture to prove and then bakes it. This paper outlines the development history of the experiment, the various test programs and some of the problems encountered, with their solutions.

Author

N87-20320*# National Aeronautics and Space Administration. Goddard Space Flight Center, Greenbelt, Md.

HITCHHIKER-G: A NEW CARRIER SYSTEM FOR ATTACHED SHUTTLE PAYLOADS **c16**

T. C. Goldsmith *In its* The 1986 Get Away Special Experimenter's Symposium Feb. 1987 p 127-134 (For primary document see N87-20302 13-12)

Avail: NTIS HC A11/MF A01 CSCL 22B

A new carrier system has been developed for economical and quick response flight of small attached payloads on the space shuttle. Hitchhiker-G can accommodate up to 750 lb. of customer payloads in canisters or mounted to an exposed plate. The carrier connects to the orbiter's electrical systems and provides up to six customers with standard electrical services including power, real time telemetry, and commands. A transparent data and command system concept is employed to allow the customer to easily use his own ground support equipment and personnel to control his payload during integration and flight operations. The first Hitchhiker-G was successfully flown in January 1986 on STS 61C.

Author

N87-20321*# Purdue Univ., West Lafayette, Ind. School of Electrical Engineering.

MULTIPURPOSE MICROCONTROLLER DESIGN FOR PUGAS 2 **c60**

David M. Weber and Todd W. Deckard *In* NASA. Goddard Space Flight Center The 1986 Get Away Special Experimenter's Symposium Feb. 1987 p 135-140 (For primary document see N87-20302 13-12)

Avail: NTIS HC A11/MF A01 CSCL 09B

This paper will report on the past year's work on the development of the microcontroller design for the second Purdue University small self-contained payload. A first report on this effort was given at last year's conference by Ritter (1985). At that time, the project was still at the conceptual stage. Now a specific design has been set, prototyping has begun, and layout of the two-sided circuit board using CAD-techniques is nearing completion. A redesign of the overall concept of the circuit board was done to take advantage of the facilities available to students. An additional controller has been added to take large quantities of data concerning the shuttle environment during takeoff. The importance of setting a design time-line is discussed along with the electrical design considerations given to the controllers.

Author

N87-20322*# City Coll. of the City Univ. of New York. Dept. of Biology.

GEOTAXIS BASELINE DATA FOR DROSOPHILA **c51**

E. M. Schnebel, R. Bhargava, and J. Grossfield *In* NASA. Goddard Space Flight Center The 1986 Get Away Special Experimenter's Symposium Feb. 1987 p 141-148 (For primary document see N87-20302 13-12)

Avail: NTIS HC A11/MF A01 CSCL 06B

Geotaxis profiles for 20 Drosophila species and semispecies at different ages have been examined using a calibrated, adjustable slant board device. Measurements were taken at 5 deg intervals ranging from 0 deg to 85 deg. Clear strain and species differences are observed, with some groups tending to move upward (-geotaxis) with increasing angles, while others move downward (+geotaxis). Geotactic responses change with age in some, but not all experimental groups. Sample geotaxis profiles are presented and their application to ecological and aging studies are discussed. Data provide a baseline for future evaluations of the biological effects of microgravity.

Author

N87-20323*# Rupp (Charles C.), Huntsville, Ala.

MARSHALL AMATEUR RADIO CLUB EXPERIMENT (MARCE) POST FLIGHT DATA ANALYSIS **c32**

Charles C. Rupp *In* NASA. Goddard Space Flight Center The 1986 Get Away Special Experimenter's Symposium Feb. 1987 p 149-156 (For primary document see N87-20302 13-12)

Avail: NTIS HC A11/MF A01 CSCL 17B

The Marshall Amateur Radio Club Experiment (MARCE) data system, the data recorded during the flight of STS-61C, the manner in which the data was reduced to engineering units, and the performance of the student experiments determined from the data are briefly described.

Author

N87-20324*# California Polytechnic State Univ., San Luis Obispo.

CAL POLY SPACE PROJECT G-279 **c51**

David R. Farley *In* NASA. Goddard Space Flight Center The 1986 Get Away Special Experimenter's Symposium Feb. 1987 p 157-162 (For primary document see N87-20302 13-12)

Avail: NTIS HC A11/MF A01 CSCL 06B

The Cal Poly Space Project is an effort on the part of several highly motivated students to deploy a space canister which will examine the effects of microgravity on electroplating and immiscible metals. The experiments will be controlled and monitored by a specialized triple redundancy system developed to defer the possible electronic errors due to uncontrollable factors such as photons from the Sun. With the finalization of the payload design and the near completion of the data control system, the integration phase of the project is anticipated to be completed and the project ready for launching by early 1987. It is hoped that the experiments will lead to new insights in space research and also prove profitable to industry.

Author

N87-20325*# Colorado Univ., Boulder. Dept. of Aerospace Sciences.

THE GROWTH AND HARVESTING OF ALGAE IN A MICRO-GRAVITY ENVIRONMENT

Nancy L. Wiltberger *In* NASA. Goddard Space Flight Center The 1986 Get Away Special Experimenter's Symposium Feb. 1987 p 163-170 (For primary document see N87-20302 13-12)

Avail: NTIS HC A11/MF A01 CSCL 22A

Algae growth in a micro-gravity environment is an important factor in supporting man's permanent presence in space. Algae can be used to produce food, oxygen, and pure water in a manned space station. A space station is one example of a situation where a Controlled Ecological Life Support System (CELSS) is impera-

tive. In setting up a CELSS with an engineering approach at the Aerospace department of the University of Colorado, questions concerning algae growth in micro-g have arisen. The Get Away Special (GAS) Fluids Management project is a means through which many questions about the effects of a micro-g environment on the adequacy of growth rates, the viability of micro-organisms, and separation of gases and solids for harvesting purposes can be answered. In order to be compatible with the GAS tests, the algae must satisfy the following criteria: (1) rapid growth rates, (2) sustain viability over long periods of non-growth storage, and (3) very brief latency from storage to rapid growth. Testing indicates that the overall growth characteristics of Anacystis Nidulans satisfy the specifications of GAS's design constraints. In addition, data acquisition and the method of growth instigation are two specific problems being examined, as they will be encountered in interfacing with the GAS project. Flight testing will be two-fold, measurement of algae growth in micro-g and separation of algae from growth medium in an artificial gravitation field. Post flight results will provide information on algae viability in a micro-g environment as reflected by algal growth rates in space. Other post flight results will provide a basis for evaluating techniques for harvesting algae. The results from the GAS project will greatly assist the continuing effort of developing the CELSS and its applications for space. Author

N87-20326*# Medical Univ. of South Carolina, Charleston. Dept. of Pharmacology.

TO CATCH A COMET 2: TECHNICAL UPDATE ON CAN-DO **c53**

Thomas J. OBrien *In* NASA. Goddard Space Flight Center The 1986 Get Away Special Experimenter's Symposium Feb. 1987 p 171-178 (For primary document see N87-20302 13-12)
Avail: NTIS HC A11/MF A01 CSCL 05I

Since the presentation of, To Catch a Comet, was given at the last G.A.S. Symposium, many events have impacted the CAN-DO Comet Halley program. This paper summarizes the changes to the payload and its mission, including improvements in camera control and CAN-DO's participation in the Halley Armada. Author

N87-20327*# Medical Univ. of South Carolina, Charleston. Dept. of Pathology.

TO CATCH A CHILD'S IMAGINATION 2: EDUCATION UPDATE ON CAN-DO **c53**

James H. Nicholson *In* NASA. Goddard Space Flight Center The 1986 Get Away Special Experimenter's Symposium Feb. 1987 p 179-186 (For primary document see N87-20302 13-12)
Avail: NTIS HC A11/MF A01 CSCL 05I

At the G.A.S. Symposium last year, the Charleston County Public School CAN DO Project outlined an ambitious educational program revolving around the photography of Comet Halley from the Shuttle using a GAS canister. The target flight was STS 61-E scheduled for a March, 1986, launch. Such strict time constraints and highly specific mission requirements made the CAN DO program even more risky than normal. In spite of this, almost all of the planned educational goals were achieved, even after the postponement of all Shuttle activities in January of 1986. This follow-up paper summarizes the effects of events on the program as proposed and the attempts to carry out as many of the activities as possible. It is hoped that this paper will suggest constructive ways in which to cope with the delays and mishaps that are the invariable lot of pioneers who break new ground and attempt the new and untried. Author

N87-20328*# Weber State Coll., Ogden, Utah. Center for Aerospace Technology.

NUSAT 1 ATTITUDE DETERMINATION **c19**

Paul Talaga *In* NASA. Goddard Space Flight Center The 1986 Get Away Special Experimenter's Symposium Feb. 1987 p 187-191 (For primary document see N87-20302 13-12)
Avail: NTIS HC A11/MF A01 CSCL 14B

This paper presents the methods for attitude determination using the static wide angle field of view sensors of NUSAT 1. Some supporting analysis and operational results are given. The system gives at best a crude attitude determination. Author

N87-20329*# Weber State Coll., Ogden, Utah. Center for Aerospace Technology.

NUSAT 1 METHODS FOR RADAR FIELD STRENGTH MEASUREMENT **c32**

Paul Talaga *In* NASA. Goddard Space Flight Center The 1986 Get Away Special Experimenter's Symposium Feb. 1987 p 193-198 (For primary document see N87-20302 13-12)
Avail: NTIS HC A11/MF A01 CSCL 17B

The methods for obtaining the gain pattern of an Air Traffic Control Radar using the data collected by NUSAT 1 are presented. The basic equations for this are given; these require an independently determined satellite attitude. In addition we show how simultaneous measurements made by separate channels can be related to obtain a single axis attitude, i.e., the direction of propagation of the incident radiation, and the power density of the radiation. This is done by solving a system of three algebraic equations. Author

N87-20330*# Ecole Superieure d'Electricite, Gif-sur-Yvette (France). Lab. de Genie Electrique de Paris.

G-300: THE FIRST FRENCH GETAWAY SPECIAL MICROGRAVITY MEASUREMENTS OF FLUID THERMAL CONDUCTIVITY **c34**

J. C. Perron, P. Chretien, C. Garnier, and N. Lecaude *In* NASA. Goddard Space Flight Center The 1986 Get Away Special Experimenter's Symposium Feb. 1987 p 199-206 Original language document was announced in IAA as A87-15974 (For primary document see N87-20302 13-12)
Avail: NTIS HC A11/MF A01 CSCL 20D

Thermal conductivity measurements on liquids are difficult to perform on Earth because of thermal motions due to convection. In microgravity, the convection due to buoyancy is evanescent, and a strong reduction of Rayleigh and Nusselt numbers can be expected. Three low viscosity liquids are selected to carry out the measurements; distilled water (standard) and two silicone oils. A modified hot plate method with a simplified guard ring is used; the reduction of convective motions permitted the use in the experimental cells of larger interplate distances and/or temperature differences than in Earth measurements, improving the accuracy. Comparisons between Earth and orbit results may help to understand the convection occurrence in the cells. Thermal, vibrational, and EMI tests have proved that the design satisfies the NASA requirements. Author

N87-20331*# Deutsche Forschungs- und Versuchsanstalt fuer Luft- und Raumfahrt, Cologne (West Germany).

RECENT RESULTS FROM MAUS PAYLOADS **c16**

G. H. Otto and S. Staniek *In* NASA. Goddard Space Flight Center The 1986 Get Away Special Experimenter's Symposium Feb. 1987 p 207-213 (For primary document see N87-20302 13-12)
Avail: NTIS HC A11/MF A01 CSCL 22B

Project MAUS is a part of the German material sciences program and provides autonomous payloads for the Space Shuttle. These payloads are housed in canisters which are identical with those of NASA's Get-Away-Special program. The main components of the hardware are: a standard system consisting of power supply, experiment control, data acquisition and the experiment modules containing experiment specific hardware. Up to now, three MAUS modules with experiments from the area of material sciences have been flown as GAS payloads. Results will be reported from GAS Payload Number G-27 and G-28 flown aboard STS-51G. Author

N87-20332*# McDonnell-Douglas Astronautics Co., Huntsville, Ala.

MICROGRAVITY EFFECTS ON ELECTRODEPOSITION OF METALS AND METAL-CERMET MIXTURES **c29**

George W. Maybee, Clyde Riley (Alabama Univ., Huntsville.), and H. Dwain Coble *In* NASA. Goddard Space Flight Center The 1986 Get Away Special Experimenter's Symposium Feb. 1987 p

215-221 (For primary document see N87-20302 13-12)
Avail: NTIS HC A11/MF A01 CSCL 22A

An experimental system, designed to investigate the potential advantages of electrodeposition in microgravity, is being developed by the McDonnell Douglas Astronautics Company-Huntsville Division and the University of Alabama in Huntsville. It is intended to fly as an Orbiter payload when NASA resumes STS operations. The system will provide power, thermal conditioning, command and control for the production of electrodeposits; system performance data will be recorded for post-flight analysis. Plated metal surfaces will be created using simple electrolytic cells with pure metal electrodes immersed in aqueous electrolytic solutions. Crystalline structure and other properties will be analyzed to identify differences between samples produced in flight and those obtained from ground-based operations. Author

N87-20333*# Redstone Scientific Information Center, Redstone Arsenal, Ala.
GAS-007: FIRST STEP IN A SERIES OF EXPLORER PAYLOADS **c18**
Philip H. Kitchens *In* NASA. Goddard Space Flight Center The 1986 Get Away Special Experimenter's Symposium Feb. 1987 p 223-232 (For primary document see N87-20302 13-12)
Avail: NTIS HC A11/MF A01 CSCL 22B

As part of the NASA Get Away Special program for flying small, self-contained payloads onboard the Space Shuttle, the Alabama Space and Rocket Center (ASRC) in Huntsville has sponsored three such payloads for its Project Explorer. One of these is GAS-007, which was carried originally on STS mission 41-G in early October 1984. Due to an operational error it was not turned on and was, therefore, subsequently rescheduled and flown on mission 61-C. This paper will review Explorer's history, outline its experiments, present some preliminary experimental results, and describe future ASRC plans for Get Away Special activities, including follow-on Explorers GAS-105 and GAS-608. Author

N87-20334*# Tohoku Univ., Sendai (Japan). Faculty of Science.
IN SITU OBSERVATION OF MONO-MOLECULAR GROWTH STEPS ON AQUEOUS SOLUTION GROWN CRYSTALS AND THE TRANSPORT OF MOLECULES TO THE CRYSTALS **c76**
Katsuo Tsukamoto *In* NASA. Goddard Space Flight Center The 1986 Get Away Special Experimenter's Symposium Feb. 1987 p 233-238 (For primary document see N87-20302 13-12)
Avail: NTIS HC A11/MF A01 CSCL 20L

Direct in situ observation of mono-molecular growth steps on a crystal growing in an aqueous solution became possible. The combination of this method with high resolution Schlieren methods or interferometry, permits the growth mechanism of crystals to be investigated directly. Since the observation of growth steps on crystals is the most direct and sensitive way for investigating a crystal growth mechanism, it would contribute to revealing fundamental differences between the growth in space and on Earth. The method was recently extended to in situ observation of the growth processes at high temperatures (1800K). Author

N87-20335*# Science Applications International Corp., Schaumberg, Ill. Space Science Dept.
SATELLITE SERVICING MISSION PRELIMINARY COST ESTIMATION MODEL
Jan. 1987 38 p
(Contract NAS9-17207)
(NASA-CR-171978; NAS 1.26:171978; SAIC-87/1514; SAIC-1-120-778-C14) Avail: NTIS HC A03/MF A01 CSCL 22A

The cost model presented is a preliminary methodology for determining a rough order-of-magnitude cost for implementing a satellite servicing mission. Mission implementation, in this context, encompassess all activities associated with mission design and planning, including both flight and ground crew training and systems integration (payload processing) of servicing hardward with the Shuttle. A basic assumption made in developing this cost model is that a generic set of servicing hardware was developed and flight tested, is inventoried, and is maintained by NASA. This implies that all hardware physical and functional interfaces are well known and therefore recurring CITE testing is not required. The development of the cost model algorithms and examples of their use are discussed. B.G.

N87-20623# European Space Agency, Paris (France). Directorate of Space Station and Platforms.
THE COLUMBUS PROGRAM: AN OVERVIEW
D. J. Shapland *In its* Proceedings of the European Symposium on Polar platform Opportunities and Instrumentation for Remote-sensing (ESPOIR) Nov. 1986 p 11-17 (For primary document see N87-20621 13-43)
Avail: NTIS HC A07/MF A01

N87-20633# Science Research Council, Chilton (England).
REPORT OF THE ATMOSPHERE PANEL
J. E. Harries and H. Fischer (Technische Univ., Munich, West Germany.) *In* ESA Proceedings of the European Symposium on Polar platform Opportunities and Instrumentation for Remote-sensing (ESPOIR) Nov. 1986 p 75-77 (For primary document see N87-20621 13-43)
Avail: NTIS HC A07/MF A01

13 ASTRODYNAMICS

Includes powered and free-flight trajectories; and orbital and launching dynamics.

N87-20336 Illinois Univ., Urbana-Champaign.
A COMPARISON OF NONLINEAR FILTERS FOR ORBIT DETERMINATION AND ESTIMATION Ph.D. Thesis
Daryl Gene Boden 1986 111 p
Avail: Univ. Microfilms Order No. DA8701438

Compared are the performance of three filters when applied to the problem of orbit determination using satellite data obtained from ground based radar. The states estimated are the osculating classical orbital elements and the satellite ballistic coefficient. The dynamics used to propagate the state vector forward in time include the two-body acceleration plus perturbations due to atmospheric drag, the zonal harmonics in the geopotential through J sub 6, and the tesseral harmonics in the geopotential through J sub 44. The atmospheric density model used is an exponential model including diurnal variations and variations in the decimeter solar flux. The observations used to update the state vector estimates are slant range, azimuth and elevation relative to a radar site. The three filters investigated in the research are a nonlinear least squares filter, an Extended Kalman Filter, and a Gauss second order filter. Data are processed for three different satellites. The first is a high altitude (100km at perigee), non-circular (e = 0.015), orbit. The second satellite orbit is a low altitude (250km at perigee), non-circular (e = 0.01), orbit. The final orbit is a low altitude (300km), nearly circular (e = 0.0001), orbit. The filters are compared using four criteria; estimation errors, prediction errors, computer time of operation, and computer storage requirements. The Gauss second order filter is shown to provide a substantial improvement in orbit determination accuracy for satellites subject to significant perturbing accelerations. Dissert. Abstr.

N87-20303*# Defense Systems, Inc., McLean, Va.
TRACKING THE GLOMR SATELLITE
Keith W. Reiss and Jason C. ONeil *In* NASA. Goddard Space Flight Center The 1986 Get Away Special Experimenter's Symposium Feb. 1987 p 1-8 (For primary document see N87-20302 13-12)
Avail: NTIS HC A11/MF A01 CSCL 22A

N87-20671*# Space Command, Peterson AFB, Colo.
NORAD SATELLITE TRACKING
Joseph J. F. Liu *In* NASA. Marshall Space Flight Center Upper and Middle Atmospheric Density Modeling Requirements for Spacecraft Design and Operations Feb. 1987 p 89-94 (For primary

document see N87-20665 13-46)
Avail: NTIS HC A13/MF A01 CSCL 22A

14 GROUND SUPPORT SYSTEMS AND FACILITIES (SPACE)

Includes launch complexes, research and production facilities; ground support equipment, e.g., mobile transporters; and simulators.

For related information see also *09 Research and Support Facilities (Air).*

N87-20337 Department of the Navy, Washington, D. C.
ARRESTING AND RECOVERY SYSTEM FOR TEST MISSILES Patent
Robert E. Kennedy, inventor (to Navy) and James D. Neef, inventor (to Navy) Issued 12 Aug. 1986 10 p Supersedes N86-10198, AD-D011743 (24 - 01, p 36)
(AD-D012574; US-Patent-4,604,938; US-Patent-Appl-SN-637238; US-Patent-Class-89-1.8) Avail: US Patent and Trademark Office CSCL 16/1

A system for arresting and recovering test ballistic missiles is adaptable for use in an existing facility and with the existing arresting engine. A long loop of cable encircles a sheave on the nose-end of the test missile and is supported by sheaves mounted on the support structure. The ends of the cable loop are terminated on one side of a singletree device. The other side is connected by a single cable to the arresting engine. One end of the cable loop slidably engages with the singletree and has an end cap. As the test missile is launched the cable loop and singletree are drawn toward a ratchet mechanism which grasps the end cap. An intermittent pulling machine is disposed for anchoring one leg of the cable loop whereby the test missile may be later raised or lowered for recovery. The system effectively doubles the load carrying capacity of an existing arresting engine by providing mechanical advantage. GRA

15 LAUNCH VEHICLES AND SPACE VEHICLES

Includes boosters; operating problems of launch/space vehicle systems; and reusable vehicles.

For related information see also *20 Spacecraft Propulsion and Power.*

N87-20338 Maryland Univ., College Park.
AN APPLICATION OF COMPUTATIONAL FLUID DYNAMICS TO THE DESIGN OF OPTIMUM RAMJET POWERED MISSILE COMPONENTS Ph.D. Thesis
David Michael VanWie 1986 249 p
Avail: Univ. Microfilms Order No. DA8625752

In the design of a ramjet powered missile, the engineer is challenged with the development of engine components with optimum performance. The present research was aimed at the development of design tools which automatically generate aerodynamic geometries which are, in some sense, optimum. To accomplish the goal, computational fluid dynamic (CFD) tools were used to evaluate designs within a numerical optimization procedure. Starting from an initial design, the component geometry was modified continuously until a converged optimum was obtained. Numerous examples of the design procedure were completed, and, where possible, the results were validated against analysis results. The optimization procedure was shown to be practical in the design of minimum wave drag forebodies, maximum total pressure recovery inlets, and maximum thrust nozzles. In all example cases, the component performance was determined using MacCormack's explicit, finite-difference, marching technique to calculate the supersonic, inviscid flow-field around the component geometry. In the course of this research project, various nonlinear optimization procedures were investigated including the simplex method, the method of steepest descent, and the quasi-Newton method with BFGS updates. Questions concerning the figure of merit and off-design performance were also addressed. Dissert. Abstr.

N87-20339*# National Aeronautics and Space Administration. Langley Research Center, Hampton, Va.
EFFECTS OF SPACE PLASMA DISCHARGE ON THE PERFORMANCE OF LARGE ANTENNA STRUCTURES IN LOW EARTH ORBIT
Hans-Juergen C. Blume Feb. 1987 21 p
(NASA-TM-89118; NAS 1.15:89118) Avail: NTIS HC A02/MF A01 CSCL 20I

The anomalous plasma around spacecrafts in low Earth orbit represents the coma of an artificial comet. The plasma discharge is caused by an energetic disturbance of charged particles which were formerly in a state of equilibrium. The plasma can effect the passive and active radio frequency operation of large space antennas by inducing corona discharge or strong arcing in the antenna feeds. One such large space antenna is the 15-meter hoop column antenna which consists of a mesh membrane material (tricot knitted gold plated wire) reflector and carbon fiber tension cords. The atomic oxygen in the plasma discharge state can force the wire base metal particles through the gold lattice and oxydize the metal particles to build a Schottky-barrier contact at the point where the wires meet. This effect can cause strong deviations in the reflector performance in terms of antenna pattern and losses. Also, the carbon-fiber cords can experience a strength reduction of 30 percent over a 40-hour exposure time. Author

N87-20340*# Bionetics Corp., Hampton, Va.
AN ADVANCED TECHNOLOGY SPACE STATION FOR THE YEAR 2025, STUDY AND CONCEPTS Contractor Report, May-Nov. 1986
M. J. Queijo, A. J. Butterfield, W. F. Cuddihy, C. B. King, and P. A. Garn Mar. 1987 191 p
(Contract NAS1-18267)
(NASA-CR-178208; NAS 1.26:178208) Avail: NTIS HC A09/MF A01 CSCL 22B

A survey was made of potential space station missions that might exist in the 2020 to 2030 time period. Also, a brief study of the current state-of-the-art of the major subsystems was undertaken, and trends in technologies that could impact the subsystems were reviewed. The results of the survey and study were then used to arrive at a conceptual design of a space station for the year 2025. Factors addressed in the conceptual design included requirements for artificial gravity, synergies between subsystems, and the use of robotics. Suggestions are made relative to more in-depth studies concerning the conceptual design and alternative configurations. Author

N87-20341# Royal Air Force Coll., Cranwell (England). Dept. of Electrical and Electronic Engineering.
CONTROL ASPECTS OF THE LAUNCH PHASE OF A VERTICALLY-LAUNCHED SHORT-RANGE SURFACE-TO-AIR MISSILE M.S. Thesis
S. P. West 1986 120 p
(ETN-87-99478) Avail: NTIS HC A06/MF A01

A two dimensional mathematical model of a thrust vector controlled, vertically-launched missile suitable for use in a computer simulation is described. The program is written in FORTRAN 4 to run on the DEC-20 digital computer. The results obtained from this model are used to discover the design features necessary in a control system to make such a missile assume a horizontal trajectory. An autopilot is designed using classical methods to control the pitch attitude of the missile. The use of bang-bang rather than proportional control in the pitch autopilot loop is also investigated. A means of estimating the flight path angle from the pitch attitude is derived to allow control of flight path angle. The velocity control autopilot incorporating this estimator is examined as to the accuracy of the estimator and the retardation experienced

during turning. Improvements on the original design are made. Slew rate limitation, gain scheduling, and incidence limitation are introduced. ESA

N87-20606# Physics International Corp., San Leandro, Calif.
NUMERICAL SIMULATION OF ATLAS-CENTAUR STAGE-SEPARATION SHAPED CHARGE FIRING AND STRUCTURAL RESPONSE
Steven Hancock, David Davison, Jim Gordon, Pius Chao, Norm Viste (General Dynamics/Convair, San Diego, Calif.), and Jack Weber *In* Shock and Vibration Information Center The Shock and Vibration Bulletin. Part 3: Invited Papers, Pyrotechnic Shock, Pyrotechnic Shock Workshop Aug. 1986 p 45-57 (For primary document see N87-20602 13-39)
Avail: NTIS HC A07/MF A01 CSCL 20/13

16 SPACE TRANSPORTATION

Includes passenger and cargo space transportation, e.g., shuttle operations; and space rescue techniques.

For related information see also *03 Air Transportation and Safety* and *18 Spacecraft Design, Testing and Performance.* For space suits see *54 Man/System Technology and Life Support.*

N87-20342*# National Aeronautics and Space Administration. Lewis Research Center, Cleveland, Ohio.
FIRE SAFETY CONCERNS IN SPACE OPERATIONS
Robert Friedman 1987 13 p Prepared for presentation at the Joint Army-Navy-NASA-Air Force (JANNAF) Safety and Environmental Protection Subcommittee Meeting, Cleveland, Ohio, 4-7 May 1987
(NASA-TM-89848; E-3511; NAS 1.15:89848) Avail: NTIS HC A02/MF A01 CSCL 22A

This paper reviews the state-of-the-art in fire control techniques and identifies important issues for continuing research, technology, and standards. For the future permanent orbiting facility, the space station, fire prevention and control calls for not only more stringent fire safety due to the long-term and complex missions, but also for simplified and flexible safety rules to accommodate the variety of users. Future research must address a better understanding of the microgravity space environment as it influences fire propagation and extinction and the application of the technology of fire detection, extinguishment, and material assessment. Spacecraft fire safety should also consider the adaptation of methods and concepts derived from aircraft and undersea experience. Author

N87-20343*# Lockheed Missiles and Space Co., Huntsville, Ala. Engineering Center.
DEVELOPMENT OF A COMPUTATIONAL AERO/FLUIDS ANALYSIS SYSTEM Final Report
P. B. Kelley 30 Jan. 1987 24 p
(Contract NAS8-35774)
(NASA-CR-179046; NAS 1.26:179046; LMSC-HEC-TR-D065566) Avail: NTIS HC A02/MF A01 CSCL 22B

The Computational Aero/Fluids Analysis System (AFAS) provides the analytical capability to perform state-of-the-art computational analyses in two difficult fluid dynamics disciplines associated with the Space Shuttle program. This system provides the analysis tools and techniques for rapidly and efficiently accessing, analyzing, and reformulating the large and expanding external aerodynamic data base while also providing tools for complex fluid flow analyses of the SSME engine components. Both of these fluid flow disciplines, external aerodynamics and internal gasdynamics, required this capability to ensure that MSFC can respond in a timely manner as problems are encountered and operational changes are made in the Space Shuttle. B.G.

N87-20344*# Analytical Mechanics Associates, Inc., Hampton, Va.
POST-FLIGHT BET PRODUCTS FOR THE 2ND DISCOVERY ENTRY, STS-19 (51-A)
G. M. Kelly, J. G. McConnell, M. L. Heck, P. A. Troutman, L. A. Waters, and J. T. Findlay (Flight Mechanics and Control, Inc., Hampton, Va.) Apr. 1985 149 p
(Contract NAS1-17707)
(NASA-CR-172572; NAS 1.26:172572; AMA-85-5) Avail: NTIS HC A07/MF A01 CSCL 22B

The post-flight products for the second Discovery flight, STS-19 (51-A), are summarized. The inertial best estimate trajectory (BET), BT19D19/UN=169750N, was developed using spacecraft dynamic measurements from Inertial Measurement Unit 2 (IMU2) in conjunction with the best tracking coverage available for any of the earlier Shuttle entries. As a consequence of the latter, an anchor epoch was selected which conforms to an initial altitude of greater than a million feet. The Extended BET, ST19BET/UN=274885C, incorporated the previously mentioned inertial reconstructed state information and the Langley Atmospheric Information Retrieval System (LAIRS) atmosphere, ST19MET/UN=712662N, with some minor exceptions. Primary and back-up AEROBET reels are NK0165 and NK0201, respectively. This product was only developed over the lowermost 360 kft altitude range due to atmosphere problems but this relates to altitudes well above meaningful signal in the IMUs. Summary results generated from the AEROBET for this flight are presented with meaningful configuration and statistical comparisons from the previous thirteen flights. Modified maximum likelihood estimation (MMLE) files were generated based on IMU2 and the Rate Gyro Assembly/Accelerometer Assembly (RGA/AA), respectively. Appendices attached define spacecraft and physical constants utilized, show plots of the final tracking data residuals from the post-flight fit, list relevant parameters from the BET at a two second spacing, and retain for archival purpose all relevant input and output tapes and files generated. Author

N87-20345# Aerospace Corp., El Segundo, Calif. Aerophysics Lab.
LABORATORY INVESTIGATION OF LIGHTWEIGHT HEATER TAPE FOR SHUTTLE PROPELLANT TANK
Donald J. Spencer, Jerry F. Bott, and James S. Whittier 30 Sep. 1986 51 p
(Contract F04701-85-0086)
(AD-A175997; TR-0086(6930-01)-11; SD-TR-86-88) Avail: NTIS HC A04/MF A01 CSCL 13/1

Experimental measurements under simulated typical operating conditions have established that the addition of surface (or near-surface) lightweight mylar electrical heater tape to external tank (ET) sprayed-on-foam-insulation (SOFI) panels results in an efficient approximately 67 F (approx. 36 C) surface temperature rise for a 10-W/sq ft applied power per unit area of SOFI surface. Consideration was given to the application of the lightweight mylar heater tape used in these measurements to the ice critical areas of the ET. A cryogenically cooled power distribution system capable of providing a 10-w/sq ft heating rate was investigated for a configuration covering 8545/sq ft of ET area. Total onboard system weight was estimated to be approximately 33 lb with a total mylar heater tape weight of approximately 6 lb. GRA

N87-20320*# National Aeronautics and Space Administration. Goddard Space Flight Center, Greenbelt, Md.
HITCHHIKER-G: A NEW CARRIER SYSTEM FOR ATTACHED SHUTTLE PAYLOADS
T. C. Goldsmith *In its* The 1986 Get Away Special Experimenter's Symposium Feb. 1987 p 127-134 (For primary document see N87-20302 13-12)
Avail: NTIS HC A11/MF A01 CSCL 22B

N87-20331*# Deutsche Forschungs- und Versuchsanstalt fuer Luft- und Raumfahrt, Cologne (West Germany).
RECENT RESULTS FROM MAUS PAYLOADS
G. H. Otto and S. Staniek *In* NASA. Goddard Space Flight Center The 1986 Get Away Special Experimenter's Symposium Feb. 1987 p 207-213 (For primary document see N87-20302 13-12)
Avail: NTIS HC A11/MF A01 CSCL 22B

N87-20369# British Aerospace Public Ltd. Co., Stevenage (England). Space and Communications Div.
INFLUENCE CO-EFFICIENT TESTING AS A SUBSTITUTE FOR MODAL SURVEY TESTING OF LARGE SPACE STRUCTURES
T. F. Keates *In* AGARD Mechanical Qualification of Large Flexible Spacecraft Structures Jul. 1986 9 p (For primary document see N87-20355 13-18)
Avail: NTIS HC A12/MF A01

N87-20370# National Aeronautical Establishment, Ottawa (Ontario).
USE OF A VIDEO-PHOTOGRAMMETRY SYSTEM FOR THE MEASUREMENT OF THE DYNAMIC RESPONSE OF THE SHUTTLE REMOTE MANIPULATOR ARM
G. L. Basso and R. B. Kulchyski *In* AGARD Mechanical Qualification of Large Flexible Spacecraft Structures Jul. 1986 12 p (For primary document see N87-20355 13-18)
Avail: NTIS HC A12/MF A01

N87-20584*# National Aeronautics and Space Administration. Marshall Space Flight Center, Huntsville, Ala.
SAFE/DAE: MODAL TEST IN SPACE
T. E. Nesman and D. K. Reed *In* Shock and Vibration Information Center The Shock and Vibration Bulletin. Part 2: Modal Test and Analysis, Testing Techniques, Machinery Dynamics, Isolation and Damping, Structural Dynamics Aug. 1986 p 29-36 (For primary document see N87-20580 13-39)
Avail: NTIS HC A10/MF A01 CSCL 22B

17 SPACE COMM., SPACECRAFT COMM., COMMAND & TRACKING

Includes telemetry; space communications networks; astronavigation and guidance; and radio blackout.

For related information see also *04 Aircraft Communications and Navigation* and *32 Communications and Radar.*

N87-20346# Royal Air Force Coll., Cranwell (England). Dept. of Electrical and Electronics Engineering.
A STUDY OF THE METHODS USED TO CARRY OUT RF TELEMETRY TESTING OF SURFACE-TO-AIR MISSILES M.S. Thesis
A. R. Pritchard 1986 189 p
(ETN-87-99481) Avail: NTIS HC A09/MF A01

Radio frequency telemetry of surface to air missiles during the environmental, guidance and control, and homing phases was studied. The use of error detection codes in PCM - FM telemetry system is discussed. However, the low transmission bit rate, the expected bit error rate (BER) and the short flight duration imply that error detection codes are not necessary. The transmission problems caused by ionization of the air by the motor efflux were assessed. As these happen at the start of a flight when the range effects are low, ionization is not usually a significant problem. A single multiplexor hybrid PCM - FM / FM - FM is recommended. It is shown that as long as the range of the missile is < 40 km then a 3 W transmitter is adequate to transmit the data with an acceptable BER. ESA

18 SPACECRAFT DESIGN, TESTING AND PERFORMANCE

Includes satellites; space platforms; space stations; spacecraft systems and components such as thermal and environmental controls; and attitude controls.

For life support systems see *54 Man/System Technology and Life Support.* For related information see also *05 Aircraft Design, Testing and Performance, 39 Structural Mechanics,* and *16 Space Transportation.*

N87-20347 Massachusetts Univ., Amherst.
DYNAMIC AND THERMAL EFFECTS IN VERY LARGE SPACE STRUCTURES Ph.D. Thesis
Ramesh-Babu Malla 1986 326 p
Avail: Univ. Microfilms Order No. DA8701196

A mathematical formulation was developed for an axially flexible structure executing a planar motion in a general orbit in space in order to determine dynamic and thermal effects in the structure due to various disturbances in a space environment. The characteristic dimension of the structure is very large (of the order of a few kilometers). The influences of the differential gravitational forces, the radiation heating, and the radiation pressure forces were studied. Effects of these factors were studied on the structure's axial deformation, its attitude motion and its orbit simultaneously. Results are obtained for various initial conditions and physical parameter values. It is observed that the differential gravitational forces do not have any appreciable effects on the structure's axial length and its attitude motion. Thermal effects are significant in producing appreciable structural deformation, and they also affect the attitude motion of the structure considerably. The radiation pressure forces are very significant in changing attitude motion of the space structure, but it causes negligible effects in producing longitudinal deformation of the structure. All of the above factors have insignificant effects on the orbit of the structure chosen in this study. Of all the three external disturbances, the radiation pressure forces are found to be strongest in affecting the orbit of the structure. Dissert. Abstr.

N87-20348 Georgia Inst. of Tech., Atlanta.
STUDIES IN NONLINEAR STRUCTURAL DYNAMICS: CHAOTIC BEHAVIOR AND POYNTING EFFECT Ph.D. Thesis
Nandakishor Sadashiv Abhyankar 1986 237 p
Avail: Univ. Microfilms Order No. DA8628350

Nonlinear structural dynamics is one of the interdisciplinary fields used to predict and control the vibration of large space structures and flexible bodies. Transient response and steady state vibration constitute two integral parts of the field of structural dynamics. Specific problems consisting of the dynamic coupling of torsional and extensional deformations of a circular cylindrical bar and the chaotic forced vibration of buckled beams are addressed. Equations governing torsional and extensional coupling of waves for a finite hyperelastic cylindrical bar were formulated. Solutions are compared with available exact solutions. The period doubling and chaotic motion were studied for a simply supported buckled beam excited with periodic forcing function. The partial differential equations were solved directly by an explicit, stable finite difference scheme. Dissert. Abstr.

N87-20349*# National Aeronautics and Space Administration. Langley Research Center, Hampton, Va.
STRUCTURAL DESIGN OF AN IN-LINE BOLTED JOINT FOR THE SPACE SHUTTLE SOLID ROCKET MOTOR CASE SEGMENTS
John T. Dorsey, Peter A. Stein, and Harold G. Bush Mar. 1987 48 p
(NASA-TM-89027; NAS 1.15:89027) Avail: NTIS HC A03/MF A01 CSCL 20H

Results of a structural design study of an in-line bolted joint concept which can be used to assemble Space Shuttle Solid Rocket Motor (SRM) case segments are presented. Numerous parametric studies are performed to characterize the in-line bolted joint behavior as major design variables are altered, with the primary objective always being to keep the inside of the joint (where the O-rings are located) closed during the SRM firing. The resulting design has 180 1-inch studs, an eccentricity of -0.5 inch, a flange thickness of 3/4 inch, a bearing plate thickness of 1/4 inch, and the studs are subjected to a preload which is 70% of ultimate. The mass penalty per case segment joint for the in-line design is 346 lbm more than the weight penalty for the proposed capture tang fix. Author

N87-20350*# Martin Marietta Aerospace, Denver, Colo.
SHUTTLE/SPACELAB CONTAMINATION ENVIRONMENT AND

EFFECTS HANDBOOK Final Edition
L. E. Bareiss, R. M. Payton, and H. A. Papazian Washington NASA Mar. 1987 239 p
(Contract NAS8-35770)
(NASA-CR-4053; MCR-85-583; NAS 1.26:4053) Avail: NTIS HC A11/MF A01 CSCL 22B

This handbook is intended to assist users of the Spacelab/ Space Transportation System by providing contamination environments and effects information that may be of value in planning, designing, manufacturing, and operating a space flight experiment. A summary of available molecular and particulate contamination data on the Space Transportation System and its facilities is presented. Contamination models, contamination effects, and protection methods information are also presented. In addition to contamination, the effects of space environments at STS altitudes on spacecraft materials are included. Extensive references, bibliographies, and contacts are provided. This final edition contains data available through December 1986. Author

N87-20351*# McDonnell-Douglas Astronautics Co., St. Louis, Mo.
ADVANCED EVA SYSTEM DESIGN REQUIREMENTS STUDY: EVAS/SPACE STATION SYSTEM INTERFACE REQUIREMENTS
T. G. Woods 15 Nov. 1985 122 p
(Contract NAS9-17299)
(NASA-CR-171981; NAS 1.26:171981; MDC-W0070) Avail: NTIS HC A06/MF A01 CSCL 22B

The definition of the Extravehicular Activity (EVA) systems interface requirements and accomodations for effective integration of a production EVA capability into the space station are contained. A description of the EVA systems for which the space station must provide the various interfaces and accomodations are provided. The discussion and analyses of the various space station areas in which the EVA interfaces are required and/or from which implications for EVA system design requirements are derived, are included. The rationale is provided for all EVAS mechanical, fluid, electrical, communications, and data system interfaces as well as exterior and interior requirements necessary to facilitate EVA operations. Results of the studies supporting these discussions are presented in the appendix. B.G.

N87-20352*# National Aeronautics and Space Administration. Langley Research Center, Hampton, Va.
LARGE SPACE ANTENNAS: A SYSTEMS ANALYSIS CASE HISTORY
Lloyd S. Keafer, comp. and U. M. Lovelace, comp. Feb. 1987 19 p
(NASA-TM-89072; NAS 1.15:89072) Avail: NTIS HC A02/MF A01 CSCL 22B

The value of systems analysis and engineering is aptly demonstrated by the work on Large Space Antennas (LSA) by the NASA Langley Spacecraft Analysis Branch. This work was accomplished over the last half-decade by augmenting traditional system engineering, analysis, and design techniques with computer-aided engineering (CAE) techniques using the Langley-developed Interactive Design and Evaluation of Advanced Spacecraft (IDEAS) system. This report chronicles the research highlights and special systems analyses that focused the LSA work on deployable truss antennas. It notes developmental trends toward greater use of CAE techniques in their design and analysis. A look to the future envisions the application of improved systems analysis capabilities to advanced space systems such as an advanced space station or to lunar and Martian missions and human habitats. Author

N87-20353*# National Aeronautics and Space Administration. Lewis Research Center, Cleveland, Ohio.
LIQUID DROPLET RADIATOR DEVELOPMENT STATUS
K. Alan White, III [1987] 28 p Prepared for presentation at the 22nd Thermophysics Conference, Honolulu, Hawaii, 8-10 Jul. 1987; sponsored by AIAA
(NASA-TM-89852; E-3510; NAS 1.15:89852) Avail: NTIS HC A03/MF A01 CSCL 22B

Development of the Liquid Droplet Radiator (LDR) is described. Significant published results of previous investigators are presented, and work currently in progress is discussed. Several proposed LDR configurations are described, and the rectangular and triangular configurations currently of most interest are examined. Development of the droplet generator, collector, and auxiliary components are discussed. Radiative performance of a droplet sheet is considered, and experimental results are seen to be in very good agreement with analytical predictions. The collision of droplets in the droplet sheet, the charging of droplets by the space plasma, and the effect of atmospheric drag on the droplet sheet are shown to be of little consequence, or can be minimized by proper design. The LDR is seen to be less susceptible than conventional technology to the effects of micrometeoroids or hostile threats. The identification of working fluids which are stable in the orbital environments of interest is also made. Methods for reducing spacecraft contamination from an LDR to an acceptable level are discussed. Preliminary results of microgravity testing of the droplet generator are presented. Possible future NASA and Air Force missions enhanced or enabled by a LDR are also discussed. System studies indicate that the LDR is potentially less massive than heat pipe radiators. Planned microgravity testing aboard the Shuttle or space station is seen to be a logical next step in LDR development. Author

N87-20354# Air Force Systems Command, Wright-Patterson AFB, Ohio. Foreign Technology Div.
ATTITUDE MOTION OF TORQUE-FREE ASYMMETRIC DUAL-SPIN SPACECRAFT
Yang Haixing 26 Nov. 1986 24 p Transl. into ENGLISH from Lixua Xuebao (China—, v. 18, no. 1, 1986 p 65-73
(AD-A175531; FTD-ID(RS)T-1083-86) Avail: NTIS HC A02/MF A01 CSCL 22/1

From the law of conservation of angular momentum, this paper discusses the derivation of the first order attitude motion differential equation of a torque-free asymmetric dual-spin spacecraft with variables, the Euler angles and the angle of relative rotation. An exact analytical solution for the attitude motion without considering external torque is also obtained by means of the energy integral of the system. Based on that, the nutational stability of a dual-spin spacecraft is discussed when the rotor angular speed approaches zero. The nonstationary attitude motion of the dual-spin spacecraft through the unstable region while in the despinning process is also discussed. Some mistakes in the literature, are pointed out and corrected. GRA

N87-20355# Advisory Group for Aerospace Research and Development, Neuilly-Sur-Seine (France). Structures and Materials Panel.
MECHANICAL QUALIFICATION OF LARGE FLEXIBLE SPACECRAFT STRUCTURES
Loughton, England Jul. 1986 269 p In ENGLISH and FRENCH Meeting held in Oberammergau, West Germany, 9-13 Sep. 1985 (AD-A175529; AGARD-CP-397; ISBN-92-835-0396-1) Avail: NTIS HC A12/MF A01

An account is given of Conference Proceedings of a Specialists' Meeting held by the Structures and Materials Panel in Oberammergau in the Fall of 1985. The problems associated with the mechanical qualification of flexible spacecraft are discussed, and details of relevant methods and techniques are given. The final discussion highlights the difficulties associated with advanced methods of experimental and theoretical dynamic analysis and the handling of larger and larger amounts of data. For individual titles, see N87-20356 through N87-20374.

N87-20356*# National Aeronautics and Space Administration, Washington, D.C. Materials and Structures Div.
FUTURE TRENDS IN SPACECRAFT DESIGN AND QUALIFICATION
Samuel L. Venneri, Brantley R. Hanks (National Aeronautics and Space Administration. Langley Research Center, Hampton, Va.), and Larry D. Pinson *In* AGARD Mechanical Qualification of Large Flexible Spacecraft Structures Jul. 1986 9 p (For primary document see N87-20355 13-18)

Avail: NTIS HC A12/MF A01 CSCL 22A

Material and structures issues that must be resolved in order to develop the technology data base needed to design and qualify the next generation of large flexible spacecraft are discussed. This invoves the development of new ground test and analysis methods and the conduct of appropriate instrumented in-space flight experiments for final verification. A review of present understanding of material behavior in the space environment and identification of future needs is presented. The dynamic verification and subsequent qualification of a spacecraft structure currently rely heavily on ground-based tests, coupled with the verified analysis model. Future space structures, such as large antennas, Space Station and other large platforms, will be of sizes difficult to test using current ground test methods. In addition to size, other complex factors, such as low natural frequencies, lightweight construction and many structural joints, will also contribute significant problems to the test and qualification process in an Earth-gravity environment. These large spacecraft will also require new technology for controlling the configuration and dynamic deformations of the structures. Future trend in large flexible structures will also involve long-life design missions (10 to 20 years). In low earth orbit (LEO), materials will be subjected to repeated thermal cycles, ultraviolet radiation, atomic oxygen and vacuum. For high orbits such as geo-synchronous earth orbit (GEO), the materials will also be subjected to large doses of high energy electrons and protons. Understanding degradation and material stability over long-mission time periods will confront the designer with many issues that are unresolved today. Author

N87-20357# Messerschmitt-Boelkow-Blohm/Entwicklungspring Nord, Bremen (West Germany).

RECENT DEVELOPMENTS AND FUTURE TRENDS IN STRUCTURAL DYNAMIC DESIGN VERIFICATION AND QUALIFICATION OF LARGE FLEXIBLE SPACECRAFT

E. Hornung, E. Breitbach (Deutsche Forschungs- und Versuchsanstalt fuer Luft- und Raumfahrt, Goettingen, West Germany.), and H. Oery (Technische Univ., Aachen, West Germany.) *In* AGARD Mechanical Qualification of Large Flexible Spacecraft Structures Jul. 1986 43 p (For primary document see N87-20355 13-18)

Avail: NTIS HC A12/MF A01

A comprehensive dynamic verification concept is proposed, focusing on a multi-axis transient qualification test to be performed on the primary structure or on modular segments of it, respectively. First, practical experiences and development areas identified are addressed. Former existing barriers preventing the practical performance of this verification concepts are no longer relevant because of the extended analytical capabilities due to the positive developments in computer techniques and software and because of the availability of large multi-axis vibration simulators. A vital prerequisite for the applicability of this verification concept is the ability for analytical flightload identification and identification of the true dynamic characteristics on a high quality and reliability level. For this a comparative discussion is presented about the suitability of analytical methods for flightload predictions (shock spectra versus transient methods). The state of the art of design identification tests and of updating methods on mathematical models is summarized and discussed with respect to necessary development areas and the implementation into the proposed structure verification concept. First experience with this new verification cycle was made on a real satellite structure. The results and open development areas identified are discussed. Author

N87-20358# Societe Nationale Industrielle Aerospatiale, Cannes (France).

DYNAMIC MODELING AND OPTIMAL CONTROL DESIGN FOR LARGE FLEXIBLE SPACE STRUCTURES

L. Passeron, Ch. Garnier, and B. Sevennec *In* AGARD Mechanical Qualification of Large Flexible Spacecraft Structures Jul. 1986 14 p (For primary document see N87-20355 13-18)

Avail: NTIS HC A12/MF A01

Some advanced results in dynamic modeling and control areas are unifyingly reviewed. Dynamic modeling for complex assemblies of interconnected, rigid or flexible bodies subject to wide relative motions is achieved through a Lagrangian formulation using quasi-coordinates. Lagrange multipliers are explicitly eliminated by way of singular value decomposition resulting in a minimized set of equations. An original software program using element shape functions interfaces the dynamic model with NASTRAN-performed individual substructure analyses. Section 3 summarizes the now classical results in optimal control, while section 4 gives a comprehensive coverage of robustness aspects. Last section is devoted to model order reduction. The Internal Balancing Approach is generalized to systems with rigid body modes. Moreover, an error bound between full order and reduced order transfer function is evidenced, which bridges truncation and robustness. Author

N87-20359# MATRA Espace, Toulouse (France). Dept. of Satellite Engineering.

QUALIFICATION OF THE FAINT OBJECT CAMERA c35

Patrice Amadieu *In* AGARD Mechanical Qualification of Large Flexible Spacecraft Structures Jul. 1986 13 p (For primary document see N87-20355 13-18)

Avail: NTIS HC A12/MF A01

The Faint Object Camera (FOC) is presently integrated as one of the five Scientific Instruments in the NASA Space Telescope (ST) which after an extensive integration and tests campaign should be launched in 1986. The Space Telescope is an observatory of 13 metres long, 4.3 metres diameter and 11,000 kilogrammes which will be placed by the Space Shuttle in a 500 kms circular orbit. The Faint Object Camera installed at the ST focal plane is a complex instrument with a total weight of 320 kgs and overall dimensions 1 x 1 x 2.2 metres. A Structural/Thermal Model (STM) and flight model of the FOC have been built. The FOC/STM was subjected to an extensive test program with for the mechanical part, sine and random vibrations, acoustic noise and modal test. On the FOC/PFM, acoustic noise only was applied for workmanship verification. With the FOC integrated now in the Space Telescope, and considering the specimen overall dimensions, limited mechanical testing will be applied at ST level which will consist of modal survey and acoustic noise. Then at the end of the test program, the overall assembly will be shipped to Kenndey Space Center and launched. Author

N87-20360# Societe Nationale Industrielle Aerospatiale, Cannes (France).

DYNAMIC ANALYSIS OF DIRECT TELEVISION SATELLITE TV-SAT/TDF.1

Y. Plumat *In* AGARD Mechanical Qualification of Large Flexible Spacecraft Structures Jul. 1986 8 p (For primary document see N87-20355 13-18)

Avail: NTIS HC A12/MF A01

An application of the methods of analysis for the structural behavior of spacecraft whose bottom is affected by a vibrational environment is discussed. The application concerns the Direct Broadcast satellites TV-SAT and TDF.1, for which sine vibration qualification and acceptance are achieved through combination of the theoritical analysis (finite element method and frequential response) and of the experimental (sine vibrations test) verification of some subsystems and system assemblies. This procedure requires highly detailed mathematical models, which are validated by way of in depth correlation between the test predictions and test dynamic results. TV-SAT and TDF.1 satellites are a specially worthwhile illustration for the said type of studies as they are a pair of large, wholly European built spacecrafts whose structures are made up of several major subassemblies, namely: main body, propellant tanks, Antenna module complete with reflectors, solar array. Author

N87-20361*# Jet Propulsion Lab., California Inst. of Tech., Pasadena.

STRUCTURAL QUALIFICATION OF LARGE SPACECRAFT

Ben K. Wada *In* AGARD Mechanical Qualification of Large Flexible Spacecraft Structures Jul. 1986 19 p (For primary document see N87-20355 13-18)

Avail: NTIS HC A12/MF A01 CSCL 22A

Over the past twenty-five (25) years of the space program, the major challenge in the structural qualification of the primary structure has shifted from conducting a test that simulated the environment to accurately predicting the structural member loads in flight. Once the flight loads are avaliable, a number of different test methods are used to qualify the structure by subjecting it to the proper loads. The qualification challenge for future large spacecraft will be to adequately predict its dynamic characteristic in space to assure that it can be controlled to meet the mission objectives. A new test concept that may allow acquisition of modal data by ground tests for verification of mathematical models of large flexible space structures which can't be ground tested by conventional methods is discussed. Author

N87-20362# Rome Univ. (Italy). Dipt. Aerospaziale.
EFFECT OF MODAL DAMPING IN MODAL SYNTHESIS OF SPACECRAFT STRUCTURES
Luigi Balis Crema and Antonio Castellani *In* AGARD Mechanical Qualification of Large Flexible Spacecraft Structures Jul. 1986 11 p (For primary document see N87-20355 13-18)
Avail: NTIS HC A12/MF A01

In the modal synthesis of a large space structure, by a substructuring approach, a focal point is in the evaluation of the modal characteristics of the single components. As a matter of fact it is required to get the non-diagonal terms of the damping substructure matrix to acquire an efficient estimate of the damping characteristics of the whole structure. In this work it has been considered important to understand and to predict the physical causes of complex modes also in an elementary substructure as a sandwich carbon fiber plate. The results of the experimental work indicate that the modal analysis has to be gained in a very tight frequency range, with many averaged data, and the possibility of complex modes is increasing with the increase of the mode order. Author

N87-20363# Deutsche Forschungs- und Versuchsanstalt fuer Luft- und Raumfahrt, Goettingen (West Germany). Inst. of Aeroelasticity.
DYNAMIC QUALIFICATION OF SPACECRAFT BY MEANS OF MODAL SYNTHESIS
A. Bertram and P. Conrad (Messerschmitt-Boelkow-Blohm/ Entwicklungspring Nord, Bremen, West Germany.) *In* AGARD Mechanical Qualification of Large Flexible Spacecraft Structures Jul. 1986 11 p Sponsored in part by ESA/ESTEC (For primary document see N87-20355 13-18)
Avail: NTIS HC A12/MF A01

The dynamic qualification process is essentially based on tests: verification tests and qualification tests. In order to render ground testing feasible, the structure has to be subdivided into modules. After performing tests on the module level, the dynamic behavior of the entire structure is obtained by modal synthesis. The experience gained in applying modal synthesis concepts to simple models and spacecraft-type structures is discussed. It is shown that the success of a modal synthesis approach is considerably dependent on the input data, i.e., the results of the modal survey tests. Accordingly, test data requirements are outlined. Finally, the discussion includes the way in which the coupling analyses can be improved by precise consideration of the coupling conditions in substructure tests and calculations. Author

N87-20364# Centre National d'Etudes Spatiales, Toulouse (France).
LOW FREQUENCY VIBRATION TESTING ON SATELLITES
A. Girard, A. Mamode, and F. Mercier *In* AGARD Mechanical Qualification of Large Flexible Spacecraft Structures Jul. 1986 9 p In FRENCH; ENGLISH summary and title (For primary document see N87-20355 13-18)
Avail: NTIS HC A12/MF A01

Except the well known POGO phenomenon, the low frequency dynamic flight environment for a satellite consists of transient vibrations, mainly thrust transients. The qualification is generally achieved by a sine sweep on a shaker according to contractual specifications. Far from the POGO frequencies and near the main resonant frequencies of the satellite, notchings based on quasi static load criteria or launch vehicle/satellite coupled analysis results are applied to avoid overtesting. However this approach becomes unsatisfactory for complex structures with large appendages, where the initial specifications are widely modified, disturbing the qualification of secondary structures. In order to improve the representativity of these tests, transient vibration testing has been recently investigated. The feasability of such tests on electrodynamic shakers using digital control techniques was demonstrated several years ago and the main problem remaining prior to their operational use has been the definition of an adequate specification for satellite qualification purposes. Several approaches are presented, including shock synthesis, production of a specified transient, and simulation of the launch vehicle impedance. Author

N87-20365# Deutsche Forschungs- und Versuchsanstalt fuer Luft- und Raumfahrt, Goettingen (West Germany). Inst. of Aeroelasticity.
MODAL-SURVEY TESTING FOR SYSTEM IDENTIFICATION AND DYNAMIC QUALIFICATION OF SPACECRAFT STRUCTURES
N. Niedbal and H. Hueners *In* AGARD Mechanical Qualification of Large Flexible Spacecraft Structures Jul. 1986 13 p (For primary document see N87-20355 13-18)
Avail: NTIS HC A12/MF A01

Modal-survey testing is an increasingly common part of the qualification procedure for spacecraft structures, since it offers an experimental verification of normal mode parameters determined by dynamic finite-element anlaysis. Moreover, it permits identification of structural damping, knowledge of which is essential for reliable flight-load calculations. A state of the art survey of modern modal-survey testing is given here, covering the phase-resonance method and various phase-separation methods. The use of modal-survey results in the dynamic qualification of spacecraft structures is discussed, emphasizing the correlation of analytical and experimental modal data. This aspect has attracted growing interest in recent years, due to the obvious need for convenient tools that allow finite-element models to be updated with measured modal data. Author

N87-20366# Spar Aerospace Ltd., Weston (Ontario).
MODAL TESTING OF THE OLYMPUS DEVELOPMENT MODEL STOWED SOLAR ARRAY
S. Draisey, M. Elzeki, A. S. Jones, and G. Marks *In* AGARD Mechanical Qualification of Large Flexible Spacecraft Structures Jul. 1986 14 p (For primary document see N87-20355 13-18)
Avail: NTIS HC A12/MF A01

The modal testing portion of the structural verification of the stowed solar array configuration of the Olympus S/C, a high powered communication satellite is discussed. The Olympus S/C was designed for both Ariane and Shuttle launches. This versatility of launch configurations requires an emphasis on the ability to accurately predict loads and structural performance. The stowed array is comprised of: release mechanisms, a tip tensioning mechanism, a stowed astromast and a folded flexible blanket to which solar cells have been mounted. The blanket is held in place between a pallet and pressure plate. The prediction of accurate structural response for such a complicated arrangement from analytical data only would be difficult. Over the past few years Spar has undertaken several development studies in the area of modal analysis. Within these studies a technique, using base excitation of the structure has been established. The use of base input as the excitation for a modal test has provided an economical means of incorporating a modal test into a structural acceptance test procedure. Author

N87-20367# Politecnico di Milano (Italy). Dipt. di Ingegneria Aerospaziale.
ACTIVE STRUCTURAL CONTROLLERS EMULATING STRUCTURAL ELEMENTS BY ICUS
Amalia Ercoli Finzi, Massimiliano Lanz, and Paolo Mantegazza *In* AGARD Mechanical Qualification of Large Flexible Spacecraft Structures Jul. 1986 13 p (For primary document see N87-20355

13-18)
Avail: NTIS HC A12/MF A01

An approach is presented to the active control design of Large Space Structures that is based on the adoption of decentralized control units. These control units use colocated sensors and actuators and adopt a control law that generates forces proportional to local motions in order to emulate real structural elements, discrete tuning masses and grounding spring-damper combinations. Some numerical examples are used to demonstrate the application of the Independent Control Unit (ICU) concept to a beam and a plate for which the active structure controls are obtained by using a suboptimal design procedure. It is shown how the use of this type of control unit allows the development of an intrinsic fail-safe design. The results obtained with the application of the concepts developed here are demonstrated by their application to an experiment in which a thin beam, suspended from the ceiling, is controlled by different combinations of the independent analog control units making use of a velocity trasducer, an integrator and an electrodynamic actuator. Author

N87-20368# Industrieanlagen-Betriebsgesellschaft m.b.H., Ottobrunn (West Germany). Modal Testing Sect.
SPACECRAFT QUALIFICATION USING ADVANCED VIBRATION AND MODAL TESTING TECHNIQUES
K. Muehlbauer and U. Schildt *In* AGARD Mechanical Qualification of Large Flexible Spacecraft Structures Jul. 1986 9 p (For primary document see N87-20355 13-18)
Avail: NTIS HC A12/MF A01

The classical single-shaker vibration test has played a dominant role in the mechanical qualification of flexible spacecraft. Due to the substantially increased payload capacity of modern carrier vehicles the existing test facilities have reached their limits in terms of test article mass and size. These limits are being extended by implementing multi-shaker systems for uni-axial testing. At the same time digital data acquisition and analysis techniques are employed to get a better understanding of the test results and of the test article itself. An alternative approach which overcomes the limitations imposed by the test article size is the analytical qualification. Besides static testing this is in particular supported by modal testing accomplished on system or on sub-system level. For modal testing a broad spectrum of computerized or computer-based techniques is now available which are capable of meeting manifold requirements. The dynamic testing techniques mentioned here are outlined and illustrated using actual examples of installations and applications. Author

N87-20369# British Aerospace Public Ltd. Co., Stevenage (England). Space and Communications Div.
INFLUENCE CO-EFFICIENT TESTING AS A SUBSTITUTE FOR MODAL SURVEY TESTING OF LARGE SPACE STRUCTURES c16
T. F. Keates *In* AGARD Mechanical Qualification of Large Flexible Spacecraft Structures Jul. 1986 9 p (For primary document see N87-20355 13-18)
Avail: NTIS HC A12/MF A01

The American Space Transportation System is capable of placing large payload into low earth orbit. Since the presence of the payload has a significant effect on the behavior of the Shuttle under the low frequency and transient loading during launch and return, a flight loads analysis is performed using a mathematical model of the payload coupled to that of the Shuttle. The process of clearing a payload for launch involves performing this coupled analysis with a validated mathematical model of the payload. This validation usually includes modal survey testing on a structurally representative model which may also be used for static load testing. The advantages and disadvantages of modal survey testing (either fixed base or free/free) and of Static Influence Co-efficient (Flexibility) Testing are discussed. It is concluded that for parts of certain types of payload the latter is a cheaper and sufficient alternative to modal survey testing. Author

N87-20370# National Aeronautical Establishment, Ottawa (Ontario).
USE OF A VIDEO-PHOTOGRAMMETRY SYSTEM FOR THE MEASUREMENT OF THE DYNAMIC RESPONSE OF THE SHUTTLE REMOTE MANIPULATOR ARM c16
G. L. Basso and R. B. Kulchyski *In* AGARD Mechanical Qualification of Large Flexible Spacecraft Structures Jul. 1986 12 p (For primary document see N87-20355 13-18)
Avail: NTIS HC A12/MF A01

A video-photogrammetry system was used to obtain the dynamic response of the Canadian developed, space transportation system remote manipulator arm from video tape recordings of two space based test events - specifically, an auto-trajectory and a backup mode test sequence. The application of this system to this task represented a non-generic use in that no pre-launch preparations were made for implementing this technique. The procedures used to extract the response information from the video tapes are outlined. The stated resolution of the video-photogrammetry system is 1 part in 5000 (1 sigma) - typically, 0.03mm for a 12.5mm image plane size. Within this capability, the amplitude of the response for the auto-trajectory sequence was obtained with an estimated resolution of 1mm with a camera-to-object spacing of 2.18m; and for the backup mode, 3mm at a spacing of 13.78m. In both instances, dynamic parameters such as frequency and damping were readily derived from the response measurements. Author

N87-20371# Martin Marietta Aerospace, Denver, Colo.
BENEFITS OF PASSIVE DAMPING AS APPLIED TO ACTIVE CONTROL OF LARGE SPACE STRUCTURES
R. N. Gehling, H. W. Harcrow, and G. Morosow *In* AGARD Mechanical Qualification of Large Flexible Spacecraft Structures Jul. 1986 8 p (For primary document see N87-20355 13-18)
Avail: NTIS HC A12/MF A01

Active vibration and shape control of large space structures (LSS) has received a great deal of attention recently, while passive damping measures have been somewhat neglected. However, benefits may be derived from simultaneously considering both passive and active control measures to achieve certain performance requirements. Presented are results of a preliminary study of the role passive damping plays in the design and performance of active vibration control strategies. Passive dampers were incorporated into a representative LSS and their effect on candidate active control laws was investigated. Viscous dampers were implemented in time simulations with direct velocity feedback and optimal quadratic regulator control laws. The impact of passive damping on overall closed-loop performance, control system spill-over and robustness, and active control requirements was evaluated. Numerical results are presented for a representative model. The merit of designing a LSS to incorporate discrete passive dampers in the overall approach to vibration suppression is demonstrated through a reduction in demands placed upon an active control system. Author

N87-20372# Royal Netherlands Aircraft Factories Fokker, Schiphol-Oost. Space Div.
ACOUSTIC EFFECTS ON THE DYNAMIC OF LIGHTWEIGHT STRUCTURES c39
J. J. Wijker *In* AGARD Mechanical Qualification of Large Flexible Spacecraft Structures Jul. 1986 15 p (For primary document see N87-20355 13-18)
Avail: NTIS HC A12/MF A01

The influence of the acoustic effects (surrounding air) on the dynamic behavior of lightweight structures is discussed. Emphasis is given to: the unexpected dynamic characteristics as shown during test; simulation of the acoustic loading within the finite element representation (linear domain); and comparison of the measured dynamic characteristics (modal survey) with the adapted finite element results.

N87-20373# Industrieanlagen-Betriebsgesellschaft m.b.H., Ottobrunn (West Germany). Abteilung Maschinenbau und Fahrzeuge.
MULTI-AXIS VIBRATION TESTS ON SPACECRAFT USING HYDRAULIC EXCITERS

H. Hahn and W. Raasch *In* AGARD Mechanical Qualification of Large Flexible Spacecraft Structures Jul. 1986 23 p (For primary document see N87-20355 13-18)
Avail: NTIS HC A12/MF A01

Based on performance data that are specified for a spacecraft multi-axis hydraulic vibration test facility by ESA the feasibility of such a test facility is investigated. Technical problems and possible solutions concerning test table stiffness, elasticity of actuator oil column, actuator joints and oil consumption are discussed. More sophisticated problems may arise concerning the control and safety systems. The designed solutions include controllers for each individual actuator, controllers for a coordinated control of the multiple actuator system and a safety and monitoring system. The control system has to be based on a control strategy using a combination of analog fixed algorithm controllers and a digital variable algorithm controller both together performimg individual degree of freedom control including suitable decoupling procedures. The safety system has to be based on a triple redundancy concept for critical system components. It is recommended to built it by a digital multi-processor system. The investigations lead to the statement that multi-axis vibration tests of spacecrafts are realizable with respect to the necessary test equipment. Author

N87-20374# Air Force Flight Dynamics Lab., Wright-Patterson AFB, Ohio.
DEVELOPMENT OF PRECISION STRUCTURAL JOINTS FOR LARGE SPACE STRUCTURES
Harold C. Croop and Andrew R. Robertson (General Dynamics Corp., San Diego, Calif.) *In* AGARD Mechanical Qualification of Large Flexible Spacecraft Structures Jul. 1986 7 p (For primary document see N87-20355 13-18)
Avail: NTIS HC A12/MF A01

Many anticipated future space systems will employ deployable structural assemblies to meet the packaging constraints of the Space transporatation System. Recent developments in deployable structures are described relative to the use of advanced composite materials in the joint designs of such systems. Specific design requirements of interest are dimensional stability, zero free play, minimum weight, and thermal/electrical conductivity through the joints. Several design approaches are presented, along with results of material characterization tests. Author

N87-20375 Department of the Air Force, Washington, D.C.
PROPELLANT TANK RESUPPLY SYSTEM Patent
Thomas F. Schweickert, inventor (to Air Force) and George F. Orton, inventor (to Air Force) Issued 2 Sep. 1986 5 p Supersedes N85-13848, AD-D011288 (83 - 05, p 603)
(AD-D012559; US-Patent-4,609,169; US-Patent-Appl-SN-640636)
Avail: US Patent and Trademark Office CSCL 21/9

The present invention relates generally to improvements in attitude control systems (ACS) for spacecraft and more particularly to a novel propellant tank resupply system and method for increasing ACS propellant usage capability through resupply of the ACS tanks during operation of the engines of the primary propulsion system. GRA

N87-20376# Oscilloquartz S.A., Neuchatel (Switzerland).
NAVSAT TIME SYNCHRONIZATION SIMULATION STUDY
O. Busca Paris, France ESA Jan. 1986 136 p
(Contract ESA-5805/84-F-RD(SC))
(ESA-CR(P)-2305; ETN-87-99495) Avail: NTIS HC A07/MF A01

Frequency and time stability, and frequency standards are introduced, and time and frequency transfer from ground stations to a constellation of satellites is discussed. It is shown that the proposed state of the art system (SAT-TIME), applied to the initial NAVSAT satellite configuration with 12 hr period, can transfer to the satellite voltage controlled crystal oscillator time stability of < or = 100psec and a frequency stability of < or = 10 to the minus 14th power. The analysis is extended to proposed lower performance systems. ESA

N87-20312*# Weber State Coll., Ogden, Utah. Center for AeroSpace Technology.
NUSAT UPDATE
Charles A. Bonsall *In* NASA. Goddard Space Flight Center The 1986 Get Away Special Experimenter's Symposium Feb. 1987 p 63-69 (For primary document see N87-20302 13-12)
Avail: NTIS HC A11/MF A01 CSCL 22B

N87-20333*# Redstone Scientific Information Center, Redstone Arsenal, Ala.
GAS-007: FIRST STEP IN A SERIES OF EXPLORER PAYLOADS
Philip H. Kitchens *In* NASA. Goddard Space Flight Center The 1986 Get Away Special Experimenter's Symposium Feb. 1987 p 223-232 (For primary document see N87-20302 13-12)
Avail: NTIS HC A11/MF A01 CSCL 22B

N87-20577# Air Force Office of Scientific Research, Bolling AFB, Washington, D.C. Aerospace Sciences.
AIR FORCE BASIC RESEARCH IN DYNAMICS AND CONTROL OF LARGE SPACE STRUCTURES
Anthony K. Amos *In* Shock and Vibration Information Center The Shock and Vibration Bulletin. Part 1: Welcome, Invited Papers, Shipboard Shock, Blast and Ground Shock, Shock Testing and Analysis Aug. 1986 p 39-58 (For primary document see N87-20574 13-39)
Avail: NTIS HC A13/MF A01

N87-20581*# Jet Propulsion Lab., California Inst. of Tech., Pasadena.
MODAL TEST AND ANALYSIS: MULTIPLE TESTS CONCEPT FOR IMPROVED VALIDATION OF LARGE SPACE STRUCTURE MATHEMATICAL MODELS
B. K. Wada, C-P. Kuo, and R. J. Glaser *In* Shock and Vibration Information Center The Shock and Vibration Bulletin. Part 2: Modal Test and Analysis, Testing Techniques, Machinery Dynamics, Isolation and Damping, Structural Dynamics Aug. 1986 p 1-8 (For primary document see N87-20580 13-39)
Avail: NTIS HC A10/MF A01 CSCL 22B

N87-20625# European Space Agency. European Space Research and Technology Center, ESTEC, Noordwijk (Netherlands).
WORKING GROUP ON EARTH OBSERVATION REQUIREMENTS FOR THE POLAR ORBITING PLATFORM ELEMENTS OF THE INTERNATIONAL SPACE STATION (THE POPE WORKING GROUP)
N. deVilliers *In its* Proceedings of the European Symposium on Polar platform Opportunities and Instrumentation for Remote-sensing (ESPOIR) Nov. 1986 p 29-33 (For primary document see N87-20621 13-43)
Avail: NTIS HC A07/MF A01

N87-20627# European Space Agency. European Space Research and Technology Center, ESTEC, Noordwijk (Netherlands).
ESA COLUMBUS POLAR PLATFORM DESIGN CONCEPT
P. Wolf *In its* Proceedings of the European Symposium on Polar platform Opportunities and Instrumentation for Remote-sensing (ESPOIR) Nov. 1986 p 39-42 (For primary document see N87-20621 13-43)
Avail: NTIS HC A07/MF A01

N87-20628# European Space Agency, Paris (France).
SERVICING OF THE POLAR PLATFORM
G. Valentiny *In its* Proceedings of the European Symposium on Polar platform Opportunities and Instrumentation for Remote-sensing (ESPOIR) Nov. 1986 p 43-47 (For primary document see N87-20621 13-43)
Avail: NTIS HC A07/MF A01

N87-20629# European Space Agency. European Space Research and Technology Center, ESTEC, Noordwijk (Netherlands).
ORBIT CONFIGURATIONS
N. deVilliers *In its* Proceedings of the European Symposium Polar platform Opportunities and Instrumentation for Remote-sensing (ESPOIR) Nov. 1986 p 49-53 (For primary document see

N87-20621 13-43)
Avail: NTIS HC A07/MF A01

N87-20634# Deutsche Forschungs- und Versuchsanstalt fuer Luft- und Raumfahrt, Oberpfaffenhofen (West Germany).
LAND PANEL REPORT
J. Bodechtel and F. Lanzl *In* ESA Proceedings of the European Symposium on Polar platform Opportunities and Instrumentation for Remote-sensing (ESPOIR) Nov. 1986 p 79-83 (For primary document see N87-20621 13-43)
Avail: NTIS HC A07/MF A01

N87-20641# European Space Agency. European Space Research and Technology Center, ESTEC, Noordwijk (Netherlands).
PANEL REPORT ON THE POLAR PLATFORM SERVICING APPROACH AND ITS IMPLICATIONS
B. Pfeiffer *In its* Proceedings of the European Symposium on Polar platform Opportunities and Instrumentation for Remote-sensing (ESPOIR) Nov. 1986 p 107-108 (For primary document see N87-20621 13-43)
Avail: NTIS HC A07/MF A01

N87-20666*# National Aeronautics and Space Administration. Marshall Space Flight Center, Huntsville, Ala.
SATELLITE LIFETIME PREDICTION
Gerald Wittenstein *In its* Upper and Middle Atmospheric Density Modeling Requirements for Spacecraft Design and Operations Feb. 1987 p 15-37 (For primary document see N87-20665 13-46)
Avail: NTIS HC A13/MF A01 CSCL 22B

N87-20667*# Rockwell International Corp., Canoga Park, Calif. Rocketdyne International.
DENSITY UNCERTAINTY EFFECT ON COST OF SPACE STATION REBOOST Abstract Only
Walter Unterberg and Claus Meisl *In* NASA. Marshall Space Flight Center Upper and Middle Atmospheric Density Modeling Requirements for Spacecraft Design and Operations Feb. 1987 p 39-40 (For primary document see N87-20665 13-46)
Avail: NTIS HC A13/MF A01 CSCL 22B

N87-20668*# National Aeronautics and Space Administration. Marshall Space Flight Center, Huntsville, Ala.
SPACE STATION MOMENTUM MANAGEMENT
V. Buckalew and Miriam Hopkins *In its* Upper and Middle Atmospheric Density Modeling Requirements for Spacecraft Design and Operations Feb. 1987 p 41-57 (For primary document see N87-20665 13-46)
Avail: NTIS HC A13/MF A01 CSCL 22B

N87-20669*# National Aeronautics and Space Administration. Lyndon B. Johnson Space Center, Houston, Tex.
SPACE STATION CONTROL MOMENT GYRO CONTROL
Aldo Bordano *In* NASA. Marshall Space Flight Center Upper and Middle Atmospheric Density Modeling Requirements for Spacecraft Design and Operations Feb. 1987 p 59-71 (For primary document see N87-20665 13-46)
Avail: NTIS HC A13/MF A01 CSCL 22B

19 SPACECRAFT INSTRUMENTATION

For related information see also *06 Aircraft Instrumentation* and *35 Instrumentation and Photography.*

N87-20328*# Weber State Coll., Ogden, Utah. Center for Aerospace Technology.
NUSAT 1 ATTITUDE DETERMINATION
Paul Talaga *In* NASA. Goddard Space Flight Center The 1986 Get Away Special Experimenter's Symposium Feb. 1987 p 187-191 (For primary document see N87-20302 13-12)
Avail: NTIS HC A11/MF A01 CSCL 14B

N87-20624# Deutsche Forschungs- und Versuchsanstalt fuer Luft- und Raumfahrt, Oberpfaffenhofen (West Germany).
EUROPEAN UTILIZATION ASPECTS STUDIES
F. Schlude *In* ESA Proceedings of the European Symposium on Polar platform Opportunities and Instrumentation for Remote-sensing (ESPOIR) Nov. 1986 p 21-27 (For primary document see N87-20621 13-43)
Avail: NTIS HC A07/MF A01

N87-20637# European Space Agency, Paris (France).
PANEL REPORT ON MULTIDISCIPLINARY INSTRUMENTATION: NEW POSSIBILITIES
G. Duchossois *In its* Proceedings of the European Symposium on Polar platform Opportunities and Instrumentation for Remote-sensing (ESPOIR) Nov. 1986 p 95-97 (For primary document see N87-20621 13-43)
Avail: NTIS HC A07/MF A01

N87-20638# European Space Agency, Paris (France).
PANEL REPORT ON NEW APPROACHES TO CALIBRATION AND VALIDATION
S. Bruzzi *In its* Proceedings of the European Symposium on Polar platform Opportunities and Instrumentation for Remote-sensing (ESPOIR) Nov. 1986 p 99-100 (For primary document see N87-20621 13-43)
Avail: NTIS HC A07/MF A01

20 SPACECRAFT PROPULSION AND POWER

Includes main propulsion systems and components, e.g., rocket engines; and spacecraft auxiliary power sources.

For related information see also *07 Aircraft Propulsion and Power, 28 Propellants and Fuels, 44 Energy Production and Conversion,* and *15 Launch Vehicles and Space Vehicles.*

N87-20377 Purdue Univ., West Lafayette, Ind.
A NUMERICAL HEAT TRANSFER MODEL FOR AN ADVANCED SOLAR THERMAL PROPULSION SYSTEM Ph.D. Thesis
David Paul Miller 1986 202 p
Avail: Univ. Microfilms Order No. DA8700935

A numerical heat transfer model was developed for investigating the design of an advanced solar thermal thruster. The numerical model considered the interaction of conduction, convection and radiation transport mechanisms within a complex solar radiation absorption chamber. The numerical analysis was divided into three distinct models which considered the energy transmission in one-dimensional, two-dimensional and a quasi-three-dimensional fashion. The radiation characteristics in each model included absorption, emission and scattering effects. The flow and temperature distributions were predicted by each model and the results summarized for the parameters specified. Comparisons were provided for the three different models and good agreement was obtained between the 1-D, 2-D and quasi-3-D solutions and published results. The quasi-three-dimensional analysis provided the most realistic modelling of the physical processes in the absorption chamber. The loss mechanisms were best estimated by the quasi-3-D solution. The quasi-3-D modeling of the absorption chamber provided the best representation of the energy transmission in comparison to the 1-D and 2-D solutions. Dissert. Abstr.

N87-20378*# National Aeronautics and Space Administration. Lewis Research Center, Cleveland, Ohio.
CONCEPTUAL DESIGN AND INTEGRATION OF A SPACE STATION RESISTOJET PROPULSION ASSEMBLY
Robert R. Tacina 1987 19 p Prepared for presentation at the 23rd Joint Propulsion Conference, San Diego, Calif., 29 Jun. - 21 Jul. 1987; sponsored in part by AIAA, SAE, ASME and ASEE
(NASA-TM-89847; E-3483; NAS 1.15:89847) Avail: NTIS HC A02/MF A01 CSCL 21H

The resistojet propulsion module is designed as a simple, long life, low risk system offering operational flexibility to the space station program. It can dispose of a wide variety of typical space station waste fluids by using them as propellants for orbital maintenance. A high temperature mode offers relatively high specific impulse with long life while a low temperature mode can propulsively dispose of mixtures that contain oxygen or hydrocarbons without reducing thruster life or generating particulates in the plume. A low duty cycle and a plume that is confined to a small aft region minimizes the impacts on the users. Simple interfaces with other space station systems facilitate integration. It is concluded that there are no major obstacles and many advantages to developing, installing, and operating a resistojet propulsion module aboard the Initial Operational Capability (IOC) space station. Author

N87-20379*# National Aeronautics and Space Administration. Lewis Research Center, Cleveland, Ohio.
COMPARISON OF TWO PROCEDURES FOR PREDICTING ROCKET ENGINE NOZZLE PERFORMANCE
Kenneth J. Davidian 1987 16 p Proposed for presentation at the 23rd Joint Propulsion Conference, San Diego, Calif., 29 Jun. - 2 Jul. 1987; sponsored by AIAA, SAE, ASME and ASEE
(NASA-TM-89814; E-3458; NAS 1.15:89814) Avail: NTIS HC A02/MF A01 CSCL 21H

Two nozzle performance prediction procedures which are based on the standardized JANNAF methodology are presented and compared for four rocket engine nozzles. The first procedure required operator intercedence to transfer data between the individual performance programs. The second procedure is more automated in that all necessary programs are collected into a single computer code, thereby eliminating the need for data reformatting. Results from both procedures show similar trends but quantitative differences. Agreement was best in the predictions of specific impulse and local skin friction coefficient. Other compared quantities include characteristic velocity, thrust coefficient, thrust decrement, boundary layer displacement thickness, momentum thickness, and heat loss rate to the wall. Effects of wall temperature profile used as an input to the programs was investigated by running three wall temperature profiles. It was found that this change greatly affected the boundary layer displacement thickness and heat loss to the wall. The other quantities, however, were not drastically affected by the wall temperature profile change. Author

N87-20380*# National Aeronautics and Space Administration. Marshall Space Flight Center, Huntsville, Ala.
SOLAR ARRAY FLIGHT EXPERIMENT/DYNAMIC AUGMENTATION EXPERIMENT
Leighton E. Young and Homer C. Pack, Jr. Feb. 1987 72 p
(NASA-TP-2690; NAS 1.60:2690) Avail: NTIS HC A04/MF A01 CSCL 10A

This report presents the objectives, design, testing, and data analyses of the Solar Array Flight Experiment/Dynamic Augmentation Experiment (SAFE/DAE) that was tested aboard Shuttle in September 1984. The SAFE was a lightweight, flat-fold array that employed a thin polyimide film (Kapton) as a substrate for the solar cells. Extension/retraction, dynamics, electrical and thermal tests, were performed. Of particular interest is the dynamic behavior of such a large lightweight structure in space. Three techniques for measuring and analyzing this behavior were employed. The methodology for performing these tests, gathering data, and data analyses are presented. The report shows that the SAFE solar array technology is ready for application and that new methods are available to assess the dynamics of large structures in space. Author

N87-20381*# National Aeronautics and Space Administration. Lewis Research Center, Cleveland, Ohio.
EXPERIMENTAL THRUST PERFORMANCE OF A HIGH-AREA-RATIO ROCKET NOZZLE
Albert J. Pavli, Kenneth J. Kacynski, and Tamara A. Smith Apr. 1987 16 p Presented at the 23rd JANNAF Combustion Meeting, Hampton, Va., 20-24 Oct. 1986
(NASA-TP-2720; E-3236-1; NAS 1.60:2720) Avail: NTIS HC A02/MF A01 CSCL 21H

An experimental investigation was conducted to determine the thrust performance attainable from high-area-ratio rocket nozzles. A modified Rao-contoured nozzle with an expansion area of 1030 was test fired with hydrogen-oxygen propellants at altitude conditions. The nozzle was also tested as a truncated nozzle, at an expansion area ratio of 428. Thrust coefficient and thrust coefficient efficiency values are presented for each configuration at various propellant mixture ratios (oxygen/fuel). Several procedural techniques were developed permitting improved measurement of nozzle performance. The more significant of these were correcting the thrust for the aneroid effects, determining the effective chamber pressure, and referencing differential pressure transducers to a vacuum reference tank. Author

N87-20382*# National Aeronautics and Space Administration. Lewis Research Center, Cleveland, Ohio.
ARCJET COMPONENT CONDITIONS THROUGH A MULTI-START TEST
Frank M. Curran and Thomas W. Haag 1987 20 p Presented at the 19th International Electric Propulsion Conference, Colorado Springs, Colo., 11-13 May 1987; sponsored by AIAA, DGLR and JSASS
(NASA-TM-89857; E-3525; NAS 1.15:89857; AIAA-87-1060) Avail: NTIS HC A02/MF A01 CSCL 21H

A low power, dc arcjet thruster was tested for starting reliability using hydrogen-nitrogen mixtures simulating the decomposition products of hydrazine. More than 300 starts were accumulated in phases with extended burn-in periods interlaced. A high degree of flow stabilization was built into the arcjet and the power supply incorporated both rapid current regulation and a high voltage, pulsed starting circuit. A nominal current level of 10 A was maintained throughout the test. Photomicrographs of the cathode tip showed a rapid recession to a steady-state operating geometry. A target of 300 starts was selected, as this represents significantly more than anticipated (150 to 240), in missions of 10 yr or less duration. Weighings showed no apparent mass loss. Some anode erosion was observed, particularly at the entrance to the constrictor. This was attributed to the brief period during startup the arc mode attachment point spends in the high pressure region upstream of the nozzle. Based on the results obtained, startup does not appear to be performance or life limiting for the number of starts typical of operational satellite applications. Author

N87-20383*# National Aeronautics and Space Administration. Lewis Research Center, Cleveland, Ohio.
EXPERIMENTAL STUDY OF LOW REYNOLDS NUMBER NOZZLES
Stanley P. Grisnik, Tamara A. Smith, and Larry E. Saltz (Rocket Research Corp., Redmond, Wash.) 1987 13 p Presented at the 19th International Electric Propulsion Conference, Colorado Springs, Colo., 11-13 May 1987; sponsored by AIAA, DGLR and JSASS
(NASA-TM-89858; E-3526; NAS 1.15:89858; AIAA-87-0992) Avail: NTIS HC A02/MF A01 CSCL 21H

High-performance electrothermal thrusters operate in a low nozzle-throat Reynolds number regime. Under these conditions, the flow boundary layer occupies a large volume inside the nozzle, contributing to large viscous losses. Four nozzles (conical, bell, trumpet, and modified trumpet) and a sharp-edged orifice were evaluated over a Reynolds number range of 500 to 9000 with unheated nitrogen and hydrogen. The nozzles showed significant decreases in specific impulse efficiency with decreasing Reynolds number. At Reynolds numbers less than 1000, all four nozzles were probably filled with a large boundary layer. The discharge coefficient decreased with Reynolds number in the same manner as the specific impulse efficiency. The bell and modified trumpet nozzles had discharge coefficients 4 to 8 percent higher than those of the cone or trumpet nozzles. The Two-Dimensional Kinetics (TDK) nozzle analysis computer program was used to predict nozzle performance. The results were then compared to

the experimental results in order to determine the accuracy of the program within this flow regime. Author

N87-20384# Johns Hopkins Univ., Silver Spring, Md. Applied Physics Lab.
COMPOSITE MOTOR CASE NOMENCLATURE
T. L. Vandiver Dec. 1986 50 p
(Contract N00024-85-C-5301)
(AD-A176418; CPIA-Pub-454) Avail: NTIS HC A03/MF A01 CSCL 21/8

This document presents a list of recommended nomenclature pertaining to the design, fabrication, and testing of filament-wound rocket motor cases. It was prepared under the auspicies of the Testing and Inspection Panel of the JANNAF (Joint Army-Navy-NASA-Air Force) Composite Motor Case Subcommittee (CMCS). Author

23 CHEMISTRY AND MATERIALS (GENERAL)

No abstracts in this category.

24 COMPOSITE MATERIALS

Includes physical, chemical, and mechanical properties of laminates and other composite materials.
For ceramic materials see *27 Nonmetallic Materials.*

N87-20385# Virginia Polytechnic Inst. and State Univ., Blacksburg. Dept. of Engineering Science and Mechanics.
MECHANICAL AND THERMAL CHARACTERIZATION OF UNIDIRECTIONAL ARAMID/EPOXY Final Report, Nov. 1985 - Dec. 1986
Marek Jerzy Pindera, Zafer Gurdal, Jeffrey S. Hidde, and Carl T. Herakovich Feb. 1987 247 p Prepared for Aluminum Co. of America, Alcoa Center, Pa. and Center for Innovative Technology, Herndon, Va.
(Contract TC196810TC; Grant MAT-86-018)
(CCMS-86-08; VPI-86-29) Avail: NTIS HC A11/MF A01

The results of an extensive experimental investigation of the mechanical and thermal response of an aramid/epoxy unidirectional composite which is one of the constituents of currently produced ARALL laminates were summarized. The characterization of mechanical response of the supplied aramid/epocy system was performed at room temperature. Three different test methods were employed: the off-axis tension test, the Iosipescu shear test, and the offf-axis compression test. All tests were performed under monotonic and quasi-cyclic loading conditions in order to determine the initial elastic response and subsequent nonlinear response, including permanent strain accumulation as a function of the stress reversal level and failure. The results of the tests were summarized. B.G.

N87-20386*# National Aeronautics and Space Administration. Langley Research Center, Hampton, Va.
BASELINE TENSILE TESTS OF COMPOSITE MATERIALS FOR LDEF (LONG DURATION EXPOSURE FACILITY) EXPOSURE
William G. Witte Mar. 1987 62 p
(NASA-TM-89069; NAS 1.15:89069) Avail: NTIS HC A04/MF A01 CSCL 11D

Tensile specimens of five graphite fiber reinforced composite materials were tested at room temperature to provide baseline data for similar specimens exposed to the space environment in low-Earth orbit on the NASA Long Duration Exposure Facility. All specimens were 4-ply (+ or - 45 deg)s layups; at least five replicate specimens were tested for each parameter evaluated. Three epoxy-matrix materials and two polysulfone-matrix materials, several fiber volume fractions, and two sizes of specimen were evaluated. Stress-strain and Poisson's ratio-stress curves, ultimate stress, strain at failure, secant modulus at 0.004 strain, inplane shear stress-strain curves, and unidirectional shear modulus at .004 shear strain are presented. Author

N87-20387*# Pratt and Whitney Aircraft, East Hartford, Conn. Engineering Div.
ADVANCED COMPOSITE COMBUSTOR STRUCTURAL CONCEPTS PROGRAM Final Report
M. A. Sattar and R. P. Lohmann Dec. 1984 118 p
(Contract NAS3-23284)
(NASA-CR-174733; NAS 1.26:174733; PWA-5890-24) Avail: NTIS HC A06/MF A01 CSCL 11D

An analytical study was conducted to assess the feasibility of and benefits derived from the use of high temperature composite materials in aircraft turbine engine combustor liners. The study included a survey and screening of the properties of three candidate composite materials including tungsten reinforced superalloys, carbon-carbon and silicon carbide (SiC) fibers reinforcing a ceramic matrix of lithium aluminosilicate (LAS). The SiC-LAS material was selected as offering the greatest near term potential primarily on the basis of high temperature capability. A limited experimental investigation was conducted to quantify some of the more critical mechanical properties of the SiC-LAS composite having a multidirection 0/45/-45/90 deg fiber orientation favored for the combustor linear application. Rigorous cyclic thermal tests demonstrated that SiC-LAS was extremely resistant to the thermal fatigue mechanisms that usually limit the life of metallic combustor liners. A thermal design study led to the definition of a composite liner concept that incorporated film cooled SiC-LAS shingles mounted on a Hastelloy X shell. With coolant fluxes consistent with the most advanced metallic liner technology, the calculated hot surface temperatures of the shingles were within the apparent near term capability of the material. Structural analyses indicated that the stresses in the composite panels were low, primarily because of the low coefficient of expansion of the material and it was concluded that the dominant failure mode of the liner would be an as yet unidentified deterioration of the composite from prolonged exposure to high temperature. An economic study, based on a medium thrust size commercial aircraft engine, indicated that the SiC-LAS combustor liner would weigh 22.8N (11.27 lb) less and cost less to manufacture than advanced metallic liner concepts intended for use in the late 1980's. Author

N87-20388*# National Aeronautics and Space Administration, Washington, D.C.
COMPOSITES REVIEW
A. Hordonneau Apr. 1987 14 p Transl. into ENGLISH of Dossier Composites (Saint-Medard-en-Dalles, France), Jan. 1986 p 1-19 Previously announced as N86-28134 Transl. by Kanner (Leo) Associates, Redwood City, Calif. Original document was prepared by Societe Nationale Industrielle Aerospatiale, Saint-Medard-en-Dalles, France
(Contract NASw-4005)
(NASA-TT-20008; NAS 1.77:20008; SNIAS-861-430-108; ESA-86-87170) Avail: NTIS HC A02/MF A01 CSCL 11D

The properties and applications of composite materials are reviewed. Glass, carbon, Kevlar, ceramic, whisker, and metal fibers are discussed along with polyester, epoxy, polyimide, Peek, carbon, ceramic, and metal matrices. The quantitative distribution of high technology fiber in various applications is given. The role of aerospace industry in the development and promotion of composite utilization is discussed. Consumption trends indicate a rapid development of the composite market. Author

N87-20389*# National Aeronautics and Space Administration. Lewis Research Center, Cleveland, Ohio.
STRAIN ENERGY RELEASE RATES OF COMPOSITE INTERLAMINAR END-NOTCH AND MIXED-MODE FRACTURE: A SUBLAMINATE/PLY LEVEL ANALYSIS AND A COMPUTER CODE

R. R. Valisetty and C. C. Chamis Apr. 1987 88 p Presented at the 8th Symposium on Composite Materials Testing and Design, Charleston, S.C., 29 Apr. - 1 May 1986; sponsored by the American Society for Testing and Materials
(NASA-TM-89827; E-3476; NAS 1.15:89827) Avail: NTIS HC A05/MF A01 CSCL 11D

A computer code is presented for the sublaminate/ply level analysis of composite structures. This code is useful for obtaining stresses in regions affected by delaminations, transverse cracks, and discontinuities related to inherent fabrication anomalies, geometric configurations, and loading conditions. Particular attention is focussed on those layers or groups of layers (sublaminates) which are immediately affected by the inherent flaws. These layers are analyzed as homogeneous bodies in equilibrium and in isolation from the rest of the laminate. The theoretical model used to analyze the individual layers allows the relevant stresses and displacements near discontinuities to be represented in the form of pure exponential-decay-type functions which are selected to eliminate the exponential-precision-related difficulties in sublaminate/ply level analysis. Thus, sublaminate analysis can be conducted without any restriction on the maximum number of layers, delaminations, transverse cracks, or other types of discontinuities. In conjunction with the strain energy release rate (SERR) concept and composite micromechanics, this computational procedure is used to model select cases of end-notch and mixed-mode fracture specimens. The computed stresses are in good agreement with those from a three-dimensional finite element analysis. Also, SERRs compare well with limited available experimental data. Author

N87-20390*# National Aeronautics and Space Administration. Langley Research Center, Hampton, Va.
HIGH PERFORMANCE THERMOPLASTICS: A REVIEW OF NEAT RESIN AND COMPOSITE PROPERTIES
Norman J. Johnston and Paul M. Hergenrother Feb. 1987 14 p
(NASA-TM-89104; NAS 1.15:89104) Avail: NTIS HC A02/MF A01 CSCL 11D

A review was made of the principal thermoplastics used to fabricate high performance composites. Neat resin tensile and fracture toughness properties, glass transition temperatures (Tg), crystalline melt temperatures (Tm) and approximate processing conditions are presented. Mechanical properties of carbon fiber composites made from many of these thermoplastics are given, including flexural, longitudinal tensile, transverse tensile and in-plane shear properties as well as short beam shear and compressive strengths and interlaminar fracture toughness. Attractive features and problems involved in the use of thermoplastics as matrices for high performance composites are discussed. Author

N87-20391# Prairie View Agricultural and Mechanical Coll., Tex. Coll of Engineering.
STUDY OF THE NATURE OF FRACTURE FAILURE IN COMPOSITE MATERIALS Final Report, 1 May 1985 - 31 Aug. 1986
R. N. Rao 1 Dec. 1986 8 p
(Grant DAAG29-85-G-0123)
(AD-A175554; ARO-23440.2-EG-H) Avail: NTIS HC A02/MF A01 CSCL 11/6

The boron, aluminum composite material samples were cut to shape and subjected to push-pull type of loading under Instron Servo Hydrolic test system to failure. The failure surfaces were examined under electron microscope. The data collected under about ten experiments were used for an M.S.E. thesis of one graduate student. GRA

N87-20392# Army Military Personnel Center, Alexandria, Va.
CHARACTERIZING THERMAL/MECHANICAL PROPERTIES OF FILAMENT WOUND COMPOSITES Final Report
Bruce K. Fink 15 Jan. 1987 80 p
(AD-A176238) Avail: NTIS HC A05/MF A01 CSCL 11/4

The characterization of composites is a continuing process involving a wide variety of materials with different compositions, laminate geometries and fabrication processes. This thesis examines bench test methods for the determination of the linear coefficients of thermal expansion, residual stresses due to fabrication, and delamination strengths in S2-Glass/Epoxy and AS4 Graphite/Epoxy filament wound cylinders. Results from these tests are compared to finite element and closed form solutions. Test theory correlation is generally good. The slopes of temperature-strain curves are closely approximated by the linear coefficient of thermal expansion calculated for the laminates. Predicted values of residual stress are approximately equal to those determined by a simple bench test. Measured delamanation strengths were found to be considerably lower (35%) than other published data. GRA

N87-20393# Oak Ridge National Lab., Tenn. Metals and Ceramics Div.
ANALYSIS OF EXPERIMENTAL DETERMINATIONS OF THE THERMAL CONDUCTIVITY OF CBCF (CARBON-BONDED CARBON FIBER) INSULATION
R. E. Pawel, W. P. Eatherly, and J. M. Robbins Sep. 1986 65 p
(Contract DE-AC05-84OR-21400)
(DE87-004025; ORNL-6302) Avail: NTIS HC A04/MF A01

This report presents experimental data and addresses the extent of agreement between measurements of thermal conductivity of carbon-bonded carbon fiber (CBCF) insulation made by steady-state and transient heat flow methods. DOE

N87-20394# Sandia National Labs., Albuquerque, N. Mex.
MOISTURE ABSORPTION IN GRAPHITE/ORGANIC-MATRIX COMPOSITES
B. C. Odegard, Jr. Dec. 1986 17 p
(Contract DE-AC04-76DR-00789)
(DE87-004229; SAND-86-8248) Avail: NTIS HC A02/MF A01

Moisture absorption of graphite-epoxy composites in humid air was investigated and the results compared with similar data taken on a graphite-thermoplastic resin composite. The composite materials were: P75/3501-6, IM6/5217c, and AS4/PEEK. In addition, the P75/3501-6 was tested in both the as-cured and thermal cycled condition. The measured diffusivity values for the P75/3501-6 were in good agreement with earlier investigators. The thermoplastic resin, PEEK, absorbed moisture at a very low rate compared to the thermosetting resins which was expected. The P75/3501-6 composite exhibited the same diffusivity value for both the as-cured and thermally conditioned conditions. DOE

N87-20395# Allied Bendix Corp., Kansas City, Mo.
SCREENING TESTING FOR COMPOSITE PREPREGS Final Report
D. A. Carey Jan. 1987 30 p
(Contract DE-AC04-76DP-00613)
(DE87-004557; BDX-613-3642) Avail: NTIS HC A03/MF A01

Differential scanning calorimetry (DSC), rheometrics mechanical spectrometry (RMS), dielectric spectrometry (DS) and high pressure liquid chromatography (HPLC) were used to determine the level of advancement of a high-performance, carbon-fiber-reinforced epoxy composite. The experimental results indicated that the RMS, HPLC and DS methods can be used to assess the degree of advancement. DSC can be used to distinguish between as received prepreg and aged prepreg; however, from the DSC data, it is difficult to determine the degree of advancement. Acceptable parts were fabricated from preforms aged at -31°C over 397 days. Parts produced from compression molded preforms that were aged for longer than 19 days at room temperature under low or high humidities failed the thickness specification for production parts. DOE

N87-20396# Edgerton, Germeshausen and Grier, Inc., Idaho Falls, Idaho.
STUDIES OF STRESS WAVE PROPAGATION IN COMPOSITES
J. S. Epstein, V. A. Deason, and M. Abdallah (Hercules, Inc., Magna, Utah.) 1986 6 p Presented at the SEM Fall Meeting, Keystone, Colo., 2 Nov. 1986
(Contract DE-AC07-76ID-01570)
(DE87-001433; EGG-M-32786; CONF-8611110-1) Avail: NTIS HC A02/MF A01

Recent phenomenological developments in the use of dynam-

ic moire interferometry for the study of transient wave propagation on the free surface of graphite/epoxy composites are discussed. The technique of dynamic moire interferometry is briefly outlined. Experimental results are discussed in light of developed continuum theories for the propagation of transient waves in laminated anisotropic media. The emphasis of the discussion is on observed waveguide effects in laminated media. DOE

N87-20397# Sandia National Labs., Albuquerque, N. Mex.
RESIDUAL EFFECTS IN LAMINATED, CURVED, COMPOSITE PANELS
R. C. Reuter, Jr. Jan. 1987 20 p
(Contract DE-AC04-76DP-00789)
(DE87-005624; SAND-86-2759) Avail: NTIS HC A02/MF A01

Analytical techniques were employed to characterize residual effects induced in laminated, curved, composite panels during fabrication processing. The residual effects include circumferential residual stresses which develop while the laminated panel is in place over its mold, and a change in panel curvature which occurs following release of the panel from the mold and relief of the residual stresses. The analysis was utilized to predict the radius of a mold upon which panels could be fabricated so that they deform, upon release from the mold, to a predetermined radius of curvature. Sample panels were fabricated which provided experimental data and particle verification of the analytical methods developed. DOE

N87-20396# Office National d'Etudes et de Recherches Aerospatiales, Paris (France). Direction Scientifique des Materiaux.
DAMAGE IN CARBON-RESIN COMPOSITES: TRANSVERSAL CRACKING AND PEELING [ENDOMMAGEMENT DES COMPOSITES CARBONE/RESINE: FISSURATION TRANSVERSE ET DELAMINAGE]
J. P. Favre, P. Sigety, X. Marais, and J. C. Laizet Feb. 1986 100 p In FRENCH
(Contract DRET-85-34-001-BC-24)
(ONERA-RT-42/7086-M; ETN-87-99384) Avail: NTIS HC A05/MF A01

Measuring and detection of crack initiation and propagation in 0/90 deg lay-up carbon-epoxy composites were studied by X-radiography and acoustic emission methods. The analysis shows that many interferences such as edge effects and fiber breaking are not easily avoided. Several mechanisms are described and influence on the measurement method is analyzed. It is found that the composite fracture energy depends on the resin tenacity and on the presence of fibers. ESA

N87-20178# Societe Nationale Industrielle Aerospatiale, Toulouse (France). Composite Structure Design Dept.
A.T.R. 42 CARBON FIBRE FLAP REPAIR DESIGN AND INSPECTION
Guy Hellard *In* AGARD The Repair of Aircraft Structures Involving Composite Materials Oct. 1986 9 p (For primary document see N87-20174 13-01)
Avail: NTIS HC A11/MF A01

N87-20307*# Purdue Univ., West Lafayette, Ind. School of Technology.
USE OF LIGHTWEIGHT COMPOSITES FOR GAS PAYLOAD STRUCTURES
Mark B. Spencer *In* NASA. Goddard Space Flight Center The 1986 Get Away Special Experimenter's Symposium Feb. 1987 p 31-34 (For primary document see N87-20302 13-12)
Avail: NTIS HC A11/MF A01 CSCL 11D

N87-20586# Michigan State Univ., East Lansing. Dept. of Metallurgy, Mechanics, and Materials Science.
STRUCTURAL DEGRADATION OF IMPACTED GRAPHITE/EPOXY LAMINATES
Dahsin Liu, C. T. Sun (Florida Univ., Gainesville.), and L. E. Malvern *In* Shock and Vibration Information Center The Shock and Vibration Bulletin. Part 2: Modal Test and Analysis, Testing Techniques, Machinery Dynamics, Isolation and Damping, Structural Dynamics Aug. 1986 p 51-60 (For primary document see N87-20580 13-39)
Avail: NTIS HC A10/MF A01 CSCL 20/11

25 INORGANIC AND PHYSICAL CHEMISTRY

Includes chemical analysis, e.g., chromatography; combustion theory; electrochemistry; and photochemistry.

For related information see also *77 Thermodynamics and Statistical Physics.*

N87-20399*# National Aeronautics and Space Administration, Washington, D.C.
THEORETICAL AND EXPERIMENTAL INVESTIGATIONS OF IGNITION, COMBUSTION AND EXPANSION PROCESSES OF HYPERGOLIC LIQUID FUEL COMBINATIONS AT GAS TEMPERATURES UP TO 3000 DEG K Thesis - Rhein-Westfalia Technical Coll., 1967
Harry Schulz Mar. 1987 166 p Transl. into ENGLISH of German Thesis p 1-123 Original language document was announced in IAA as A69-20723 Transl. by SCITRAN, Santa Barbara, Calif.
(Contract NASw-4004)
(NASA-TM-88527; NAS 1.15:88527) Avail: NTIS HC A08/MF A01 CSCL 21B

The ignition, combustion, and expansion characteristics of hypergolic liquid propellant mixtures in small rocket engines are studied theoretically and experimentally. It is shown by using the Bray approximation procedure that the reaction H + OH + M = H2O + M (where M is the molecular mass of the gas mixture) has a strong effect on the combustion efficiency. Increases in recombination energies ranging from 30 to 65% were obtained when the rate of this reaction was increased by a factor of 10 in gas mixtures containing 90% oxygen. The effect of aluminum additions and various injection techniques on the combustion process is investigated. Author

N87-20400*# Systems Research Labs., Inc., Dayton, Ohio.
APPLICATION OF CARS TO SCRAMJET COMBUSTION Final Report
R. R. Antcliff Apr. 1987 32 p
(Contract NAS1-16562)
(NASA-CR-178245; NAS 1.26:178245; Rept-6657) Avail: NTIS HC A03/MF A01 CSCL 07D

A coherent anti-Stokes Raman spectroscopic (CARS) instrument has been developed for measuring simultaneously temperature and N2 - O2 species concentration in hostile flame environments. A folded BOXCARS arrangement was employed to obtain high spatial resolution. Polarization discrimination against the nonresonant background decreased the lower limits of O2 detectivity. The instrument has been primarily employed for validation of computational fluid-dynamics computer-model codes. Comparisons have been made to both the CHARNAL and TEACH codes on a hydrogen diffusion flame with good results. Author

N87-20401# European Space Agency, Paris (France).
THEORETICAL STUDY OF THE NONSTEADY COMBUSTION OF COMPOSITE FUEL DROPLETS
Francis Dupoirieux Nov. 1986 121 p Transl. into ENGLISH of "Etude Theorique de la Combustion Instationnaire de Gouttes de Combustible Composite" ONERA, Paris, France, report ONERA-NT-1983-3, 1983 Original language document was announced as N84-25781
(ESA-TT-868; ONERA-NT-1983-3; ETN-87-99424) Avail: NTIS HC A06/MF A01

A droplet combustion was constructed, based on the following assumptions: the droplet contains two distinct miscible fuels. The unsteady terms are included. The physical properties (thermal conductivity, mass diffusion coefficients) depend on gas phase composition and temperature. The effects of pressure variation are taken into account, with the pressure being either

given or computed. Since the combustion is assumed to be spherically symmetrical about the center, of the droplet, the convection due to a gas phase velocity far from the droplet cannot be taken into account. ESA

N87-20402# Office National d'Etudes et de Recherches Aerospatiales, Paris (France).
HIGH TEMPERATURE CO2 STUDY: ANTI-STOKES COHERENT RAMAN DIFFUSION AND INFRARED SPECTROSCOPY Ph.D. Thesis - Paris Univ. VI
Nicole Papineau 1986 106 p In FRENCH; ENGLISH summary Report will also be announced as translation (ESA-TT-1048)
(ONERA-P-1986-2; ISSN-0078-379X; ETN-87-99380) Avail: NTIS HC A06/MF A01

Coherent Anti-Stokes Raman scattering spectra were recorded at 300, 800, 1200, and 1500K with a 0.07 mm spectral resolution. Intense bands are located in this spectral region, coupled by Fermi resonance. The Q branches and the O and S branch lines of many vibration-rotation bands are assigned. A simulation of the experimental spectra at 300 and 800K was performed. Spectroscopic data compilations in the 4.3 and 2.7 micrometer regions were generated. These reproduce the experimental spectra up to 1500K in a satisfactory way. ESA

N87-20403# Institut National des Sciences Appliquees, Lyon (France). Lab. de Physicochimie Industrielle.
DETERMINATION OF THE TERNARY VISCOSITY DIAGRAM NaCl-KCl-LiCl BY THE FLOW METHOD Ph.D. Thesis [DETERMINATION DU DIAGRAMME DE VISCOSIE TERNAIRE NL-CACLCL-KCLCL-LLCICLCL PAR LA METHODE D'ECOULEMENT]
El Hassan Ballouki 1986 102 p In FRENCH
(INSA-IDTC1-8604; ETN-87-99405) Avail: NTIS HC A06/MF A01

The melt viscosity of two and three component mixtures was studied at a range of temperatures up to 900C using the vertical capillary flow method. The theoretical basis of the measurement method is reviewed. The curves of isoviscosity for 11 temperatures are presented. ESA

N87-20268*# National Aeronautics and Space Administration. Lewis Research Center, Cleveland, Ohio.
COMBUSTION RESEARCH IN THE INTERNAL FLUID MECHANICS DIVISION
Edward J. Muiarz *In its* NASA-Chinese Aeronautical Establishment (CAE) Symposium 1986 p 1-6 (For primary document see N87-20267 13-07)
Avail: NTIS HC A01/MF A01 CSCL 21B

N87-20269*# Chinese Aeronautical Establishment, Beijing.
NUMERICAL STUDY OF COMBUSTION PROCESSES IN AFTERBURNERS
Xiaoqing Zhou and Xiaochun Zhang (Shenyang Aeroengine Research Inst., China.) *In* NASA- Lewis Research Center NASA-Chinese Aeronautical Establishment (CAE) Symposium 1986 p 7-30 (For primary document see N87-20267 13-07)
Avail: NTIS HC A01/MF A01 CSCL 21B

N87-20273*# Gas Turbine Research Inst., Jiangyou (China).
COMBUSTION RESEARCH ACTIVITIES AT THE GAS TURBINE RESEARCH INSTITUTE
Zhongpu Shao *In* NASA- Lewis Research Center NASA-Chinese Aeronautical Establishment (CAE) Symposium 1986 p 89-111 (For primary document see N87-20267 13-07)
Avail: NTIS HC A01/MF A01 CSCL 21B

26 METALLIC MATERIALS

Includes physical, chemical, and mechanical properties of metals, e.g., corrosion; and metallurgy.

N87-20404*# McDonnell-Douglas Astronautics Co., St. Louis, Mo.
CONSOLIDATION PROCESSING PARAMETERS AND ALTERNATIVE PROCESSING METHODS FOR POWDER METALLURGY Al-Cu-Mg-X-X ALLOYS Final Report
K. K. Sankaran Feb. 1987 81 p
(Contract NAS1-16967)
(NASA-CR-178227; NAS 1.26:178227) Avail: NTIS HC A05/MF A01 CSCL 11F

The effects of varying the vacuum degassing parameters on the microstructure and properties of Al-4Cu-1Mg-X-X (X-X = 1.5Li-0.2Zr or 1.5Fe-0.75Ce) alloys processed from either prealloyed (PA) or mechanically alloyed (M) powder, and consolidated by either using sealed aluminum containers or containerless vacuum hot pressing were studied. The consolidated billets were hot extruded to evaluate microstructure and properties. The MA Li-containing alloy did not include Zr, and the MA Fe- and Ce-containing alloy was made from both elemental and partially prealloyed powder. The alloys were vacuum degassed both above and below the solution heat treatment temperature. While vacuum degassing lowered the hydrogen content of these alloys, the range over which the vacuum degassing parameters were varied was not large enough to cause significant changes in degassing efficiency, and the observed variations in the mechanical properties of the heat treated alloys were attributed to varying contributions to strengthening by the sub-structure and the dispersoids. Mechanical alloying increased the strength over that of alloys of similar composition made from PA powder. The inferior properties in the transverse orientation, especially in the Li-containing alloys, suggested deficiencies in degassing. Among all of the alloys processed for this study, the Fe- and Ce-containing alloys made from MA powder possessed better combinations of strength and toughness. Author

N87-20405*# National Aeronautics and Space Administration. Lewis Research Center, Cleveland, Ohio.
CREEP BEHAVIOR OF NIOBIUM ALLOY PWC-11 Final Report
R. H. Titran, T. J. Moore, and T. L. Grobstein 1987 11 p Presented at the 4th Symposium on Space Nuclear Power Systems, Albuquerque, N. Mex., 12-16 Jan. 1987; sponsored by New Mexico Univ.
(Contract DE-AI03-86SF-16310)
(NASA-TM-89834; DOE/NASA/16310-3; E-3306; NAS 1.15:89834) Avail: NTIS HC A02/MF A01 CSCL 11F

The high vacuum creep and creep-rupture behavior of a Nb-1Zr-.1C alloy (PWC 11) was investigated at 1350 and 1400 K with an applied stress of 40 MPa. The material was tested in the following four conditions: annealed (1 hr 1755 K/2 hr 1475 K); annealed plus EB welded; annealed plus aged for 1000 hr at 1350 or 1400 K; and annealed, welded, and aged. It was found that the material in the annealed state was the most creep-resistant condition tested, and that aging the alloy for 1000 hr without an applied stress greatly reduced that strength; however, it was still approximately three times as creep resistant as Nb-1Zr. Additionally, the EB weld region was stronger than the base metal in each condition tested, and phase extraction of the dispersed precipitate revealed the presence of a 70%ZrC-30%NbC cubic monocarbide phase. Author

N87-20406*# Lockheed-California Co., Burbank.
DEVELOPMENT OF POWDER METALLURGY 2XXX SERIES Al ALLOY PLATE AND SHEET MATERIALS FOR HIGH TEMPERATURE AIRCRAFT STRUCTURAL APPLICATIONS, FY 1983/1984 Final Technical Report, 30 Sep. 1982 - 31 Aug. 1984
D. J. Chellman Apr. 1985 78 p
(Contract NAS1-16048)
(NASA-CR-172521; NAS 1.26:172521; LR-30775) Avail: NTIS HC A05/MF A01 CSCL 11F

The objective of this investigation is to fabricate and evaluate PM 2124 Al alloy plate and sheet materials according to NASA program goals for damage tolerance and fatigue resistance. Previous research has indicated the outstanding strength-toughness relationship available with PM 2124 Al-Zr modified alloy compositions in extruded product forms. The range of processing conditions was explored in the fabrication of plate and sheet gage materials, as well as the resultant mechanical and metallurgical properties. The PM composition based on Al-3.70 Cu-1.85 Mg-0.20

Mn with 0.60 wt. pct. Zr was selected. Flat rolled material consisting of 0.250 in. thick plate was fabricated using selected thermal mechanical treatments (TMT). The schedule of TMT operations was designed to yield the extreme conditions of grain structure normally encountered in the fabrication of flat rolled products, specifically recrystallized and unrecrystallized. The PM Al alloy plate and sheet materials exhibited improved strength properties at thin gages compared to IM Al alloys, as a consequence of their enhanced ability to inhibit recrystallization and grain growth. In addition, the PM 2124 Al alloys offer much better combinations of strength and toughnessover equivalent IM Al. The alloy microstructures were examined by optical metallographic texture techniques in order to establish the metallurgical basis for these significant property improvements. Author

N87-20407*# National Aeronautics and Space Administration. Langley Research Center, Hampton, Va.
MATERIAL CHARACTERIZATION OF SUPERPLASTICALLY FORMED TITANIUM (Ti-6Al-2Sn-4Zr-2Mo) SHEET
William A. Ossa (PRC Kentron, Inc., Hampton, Va.) and Dick M. Royster 1987 38 p
(NASA-TP-2674; L-16115; NAS 1.60:2674) Avail: NTIS HC A03/MF A01 CSCL 11F

The aerospace industry has focused considerable interest on the near-alpha titanium alloy Ti-6Al-2Sn-4Zr-2Mo (Ti-6242) because of both its high-temperature properties and its superplastic forming (SPF) capabilities. This paper describes current research to characterize selected mechanical properties of Ti-6242 sheet in the SPF-strained condition, both with and without heat treatment, and compares the results with those obtained on as-received material. Tensile and creep tests were conducted, and metallographic analysis was performed to show the effect of 100 to 700 percent SPF strain on titanium properties. Analysis shows that as a result of SPF processing, both tensile and yield strengths, as well as elongation, are moderately reduced. Creep tests at 800 F and 1000 F show that the SPF processed material displays superior creep resistance compared with the as-received material. A post-SPF duplex-anneal heat treatment had no beneficial effect on tensile and creep properties. Author

N87-20408*# National Aeronautics and Space Administration. Lewis Research Center, Cleveland, Ohio.
BITHERMAL LOW-CYCLE FATIGUE BEHAVIOR OF A NiCoCrAlY-COATED SINGLE CRYSTAL SUPERALLOY
J. Gayda, T. P. Gabb, R. V. Miner, and G. R. Halford 1987 25 p Presented at the 1987 TMS-AIME Annual Meeting, Denver, Colo., 22-26 Feb. 1987
(NASA-TM-89831; E-3484; NAS 1.15:89831) Avail: NTIS HC A02/MF A01 CSCL 20B

Specimens of a single crystal superalloy, PWA 1480, both bare and coated with a NiCoCrAlY alloy, PWA 276, were tested in low-cycle fatigue at 650 and 1050 C, and in bithermal thermomechanical fatigue tests. In the two bithermal test types, tensile strain was imposed at one of the two temperatures and reversed in compression at the other. In the high-strain regime, lives for both bithermal test types approached that for the 650 C isothermal test on an inelastic strain basis, all being controlled by the low ductility of the superalloy at 650 C. In the low-strain regime, coating cracking reduced life in the 650 C isothermal test. The bithermal test imposing tension at 650 C, termed out-of-phase, also produced rapid surface cracking, but in both coated and bare specimens. Increased crack growth rates also occurred for the out-of-phase test. Increased lives in vacuum suggested that there is a large environmental contribution to damage in the out-of-phase test due to the 1050 C exposure followed by tensile straining at the low temperature. Author

N87-20409# Du Pont de Nemours (E. I.) and Co., Aiken, S.C.
GALVANIC CORROSION RESISTANCE OF WELDED DISSIMILAR NICKEL-BASE ALLOYS
R. A. Corbett, W. S. Morrison, and R. J. Snyder 1986 30 p Presented at the Symposium on Galvanic Corrosion, Phoenix, Ariz., 4 Nov. 1986
(Contract DE-AC09-76SR-00001)
(DE87-002656; DP-MS-86-111; CONF-861188-1) Avail: NTIS HC A03/MF A01

A program for evaluating the corrosion resistance of various dissimilar welded nickel-base alloy combinations is outlined. Alloy combinations included ALLCORR, Hastelloy C-276, Inconel 72 and Inconel 690. The GTAW welding process involved both high and minimum heat input conditions. Samples were evaluated in the as-welded condition, as well as after having been aged at various conditions of time and temperature. These were judged to be most representative of process upset conditions which might be expected. Corrosion testing evaluated resistance to an oxidizing acid and a severe service environment in which the alloy combinations might be used. Mechanical properties are also discussed. DOE

N87-20410# Technical Research Centre of Finland, Helsinki. Metallilaboratorio.
HYDROGEN EMBRITTLEMENT OF TITANIUM AND ITS ALLOYS: A LITERATURE REVIEW
Irina Aho-Mantila and Hannu Haenninen May 1986 82 p In FINNISH; ENGLISH summary
(DE87-750405; YJT-86-09) Avail: NTIS (US Sales Only) HC A05/MF A01

Hydrogen embrittlement data of titanium and its alloys is reviewed. Especially the results obtained in spent nuclear fuel repository conditions with commercially pure titanium and TiCode-12 alloy are examined. The results show that the mechanical properties of titanium are not much affected by hydrogen when tested by smooth specimens. Much greater effects can be expected with notched fracture mechanics specimens. However, only limited data is available. Hydrogen distribution in titanium is affected by stress, alloy composition and temperature gradients. In order to model the hydrogen-induced crack growth in titanium much more mechanistic work is needed especially to understand the behavior of hydrogen in crack tip stress field. DOE

N87-20411# Los Alamos National Lab., N. Mex.
MICROSTRUCTURE OF METASTABLE METALLIC ALLOY FILMS PRODUCED BY LASER BREAKDOWN CHEMICAL VAPOR DEPOSITION AND ION IMPLANTATION
S. K. Menon, T. R. Jervis, and M. Nastasi 1986 8 p Presented at the Materials Research Society Fall Meeting, Boston, Mass., 1 Dec. 1986
(Contract W-7405-eng-36)
(DE87-002914; LA-UR-86-3811; CONF-861207-15) Avail: NTIS HC A02/MF A01

Thin films produced by laser breakdown chemical vapor deposition from nickel and iron carbonyls and by implanting Ni foils with varying levels of C have been characterized by transmission electron microscopy. Decomposition of Ni(CO)4 produces polycrystalline films of fcc Ni and metastable ordered hexagonal Ni3C. This metastable phase is identical to that produced by gas carburization, rapid solidification of Ni-C melts, and ion implantation of C into Ni at low concentrations. Increasing the H2 content in the gas mixture during laser deposition reduces the grain size of the films significantly with grain sizes smaller than 10 nanometers produced. Laser decomposition of Fe(CO)5 produces films with islands of fcc gamma-Fe and finely dispersed metastable Fe3C (Cementite). In addition, the ferrous oxides Fe2O3 and Fe3O4 were found in these samples. Implants of C into pure Ni foils at 77 K and at a concentration of 35 at. % produced amorphous layers. Implants at the same dose at room temperature did not produce amorphous layers. DOE

N87-20412# Massachusetts Inst. of Tech., Cambridge. Dept. of Materials Science and Engineering.
MECHANISMS OF THE OXIDATION OF METALS AND ALLOYS: Annual Progress Report, 1 Jul. 1985 - 30 Jun. 1986
G. J. Yurek 27 Aug. 1986 23 p
(Contract DE-FG02-85ER-45179)
(DE87-003389; DOE/ER-45179/T1) Avail: NTIS HC A02/MF A01

Areas of research conducted during this period were oxidation/sulfidation of pure chromium, Fe-25 wt % Cr, and Fe-25 wt % Cr-10 wt % Al alloys, segregation of sulfur to grain boundaries in oxide scales, oxidation of rapidly solidified (crystalline) Fe-Cr-Ni-Si alloys, and oxidation of Cr-Y and Co-Cr-Y alloys. Work carried out in this program has demonstrated the occurrence of grain boundary segregation of sulfur in chromia and alumina scales and of yttrium in chromia scales. It has also been demonstrated that the segregated species cause a change in the growth rates of the scales, and, in the case of yttrium segregation, a change in growth mechanism and an increase in scale adherence. DOE

N87-20413# Oak Ridge National Lab., Tenn.
DUCTILITY AND FRACTURE BEHAVIOR OF POLYCRYSTALLINE NI3AI ALLOYS
C. T. Liu 1986 13 p Presented at the Materials Research Society Fall Meeting, Boston, Mass., 1 Dec. 1986
(Contract DE-AC05-84OR-21400)
(DE87-005340; CONF-861207-58) Avail: NTIS MF A01/MF A01

This paper provides a comprehensive review of the recent work on tensile ductility and fracture behavior of Ni3Al alloys tested at ambient and elevated temperatures. Polycrystalline Ni3Al is intrinsically brittle along grain boundaries, and the brittleness has been attributed to the large difference in valency, electronegativity, and atom size between nickel and aluminum atoms. Alloying with B, Mn, Fe, and Be significantly increases the ductility and reduces the propensity for intergranular fracture in Ni3Al alloys. Boron is found to be most effective in improving room-temperature ductility of Ni3Al with <24.5 at. % Al. The tensile ductility of Ni3Al alloys depends strongly on test environments at elevated temperatures, with much lower ductilities observed in air than in vacuum. The loss in ductility is accompanied by a change in fracture mode from transgranular to intergranular. This embrittlement is due to a dynamic effect involving simultaneously high localized stress, elevated temperature, and gaseous oxygen. The embrittlement can be alleviated by control of grain shape or alloying with chromium additions. All of the results are discussed in terms of localized stress concentration and grain boundary cohesion. DOE

N87-20414# Battelle Columbus Labs., Ohio.
HYDROGEN DEGRADATION OF PIPELINE STEELS Final Report
J. H. Holbrook, E. W. Collings, H. J. Cialone, and E. J. Drauglis Mar. 1986 163 p Prepared in cooperation with Brookhaven National Lab., Upton, N.Y.
(Contract DE-AC02-76CH-00016)
(DE87-005585; BNL-52049) Avail: NTIS HC A08/MF A01

The purpose of investigations conducted by Battelle Columbus Laboratories was to develop a research data base applicable to the problem of hydrogen degradation in pipeline steels. The findings would provide pipeline designers and operators with insight for developing specifications and procedures in the event available natural gas transmission/distribution systems are used for hydrogen transport. Fundamental investigations and data derived from sophisticated analytical and test procedures have been equated to practical field conditions and experiences as may be encountered should the hydrogen energy storage/transport option become an economic reality. DOE

N87-20415# Lawrence Livermore National Lab., Calif.
THE VARIATION OF SUBGRAIN MISORIENTATION IN ALUMINUM DEFORMED TO LARGE STEADY-STATE CREEP STRAINS
M. E. Kassner and M. E. McMahon 17 Nov. 1986 14 p Presented at the 3rd International Conference on Creep and Fracture of Engineering Materials and Structures, Swansea, England, 5 Apr. 1987 Prepared in cooperation with Naval Postgraduate School, Monterey, Calif.
(Contract W-7405-eng-48)
(DE87-003238; UCRL-94747; CONF-870447-1) Avail: NTIS HC A02/MF A01

Pure aluminum was deformed in torsion of 644 K to various steady-state strains up to 16.33. The character of the subgrain boundaries changes dramatically over steady state. As the torsion specimens are twisted, the original grains of the annealed aluminum spiral around the torsion axis and the axial width of the grains is reduced. The average misorientation angle of the low-angle boundaries is about 0.5° at onset of steady state (epsilon = 0.20). This increases by over a factor of 2 during steady state before reaching saturation at 1.2° at 1.2 strain. All this suggests that the details of the subgrain boundaries are not an important consideration in the rate-controlling process for creep. At the onset of steady state essentially all of the subgrain boundaries have small misorientation angles. If we replace one-third of these boundaries with high-angle boundaries (average misorientation of about 25°) and double the average misorientation of the remaining two-thirds, the flow stress is nearly unchanged. Results suggest that a description of the rate-controlling process for creep should consider the density of dislocations not associated with subgrain boundaries. DOE

N87-20416# Argonne National Lab., Ill.
APPARATUS FOR HIGH TEMPERATURE IN SITU LASER RAMAN SPECTROELECTROCHEMICAL STUDIES OF METAL CORROSION AND PASSIVATION IN AQUEOUS ENVIRONMENTS
W. Ruther, J. J. McMahon, and C. A. Melendres 1986 4 p Presented at the Electrochemical Society Fall Meeting, San Diego, Calif., 19 Oct. 1986
(Contract W-31-109-eng-38)
(DE87-004868; CONF-861068-17) Avail: NTIS HC A02

Apparatus for in situ Laser Raman Spectroscopy and electrochemical studies of corrosion and passivation phenomena on metals in high-temperature/high-pressure aqueous solutions has been constructed and is described. Results of investigations on lead in 7 X 10 to the -4 M Na2SO4 solution from 25 to 280 C are presented. Passivation of lead was found to persist up to 280 C; the surface film consisted mainly of PbSO4. Two other oxysulfate phases of lead have also been identified at open circuit and slightly more anodic potential. DOE

N87-20417# Oak Ridge National Lab., Tenn.
EFFECTS OF ELASTIC ANISOTROPY ON THE ANOMALOUS YIELD BEHAVIOR OF CUBIC ORDERED ALLOYS
M. H. Yoo 1986 7 p Presented at the Materials Research Society Fall Meeting, Boston, Mass., 1 Dec. 1986
(Contract DE-AC05-84OR-21400)
(DE87-005328; CONF-861207-54) Avail: NTIS HC A02/MF A01

The positive temperature dependence of yield stress in certain Li2 and B2 alloys, e.g., Ni3Al and beta'-CuZn, is analyzed on the basis of the nature of dislocation dissociations predicted by anisotropic elasticity theory. In the case of Ni3Al, the torque due to the tangential component of the elastic interaction between two superpartials as a major driving force for either the cross-slip pinning model or the force couplet model. The corresponding torque term is relatively unimportant in the B2 structure. The core transformation of individual superpartials may be important for the anomalous increase of yield stress in beta'-CuZn.. DOE

N87-20418# Rockwell International Corp., Golden, Colo.
IMPACT ENERGY RELATIONSHIPS FOR DIRECTLY ROLLED URANIUM STRIP
R. J. Jackson and J. R. Hammetter 26 Aug. 1986 19 p
(Contract DE-AC04-76DP-03533)
(DE87-005789; RFP-3862) Avail: NTIS HC A02/MF A01

Charpy V-notch impact energies were obtained from thermomechanically processed uranium strip. The thermomechanical process to improve material properties was to preheat a cast ingot at 630 C and roll it directly to final gauge on a nonheated mill. The degree of strengthening induced in the strip was varied by controlling the rate of cooling during rolling, and, hence the final pass temperatures. A direct correlation between rate of cooling during rolling and impact energy was found. Tensile properties and hardness were also obtained from the rolled strip and correlated with impact energies. A direct correlation was found between impact energies and ultimate tensile strength, tensile

elongation and reduction-in-area, and with indentation hardness. It is surprising that thermomechanically processed strip with the higher hardness, ultimate tensile strength, and elongation, also had the higher impact energy. It was concluded that warm and cold rolling deformations significantly enhance notched-bar impact toughness as well as the tensile strength and hardness of unalloyed uranium. DOE

N87-20419# Rockwell International Corp., Golden, Colo.
SUPERPLASTICITY OF METALS WITH SPECIAL REFERENCE TO Ti-6Al-4V
M. M. McDonald 11 Aug. 1986 12 p
(Contract DE-AC04-76DP-03533)
(DE87-005795; RFP-3909) Avail: NTIS HC A02/MF A01

A review of the literature on the phenomenon of superplasticity of metals has been conducted. Particular attention was paid to literature pertaining to Ti-6Al-4V. Areas of superplasticity addressed include metallurgical aspects of superplasticity, characterization of superplastic behavior, and a practical guide to approaching the superplastic forming of a given alloy into a given shape. DOE

27 NONMETALLIC MATERIALS

Includes physical, chemical, and mechanical properties of plastics, elastomers, lubricants, polymers, textiles, adhesives, and ceramic materials.

For composite materials see *24 Composite Materials*.

N87-20420# National Bureau of Standards, Gaithersburg, Md. Polymers Div.
INSTITUTE FOR MATERIALS SCIENCE ENGINEERING, POLYMERS: TECHNICAL ACTIVITIES 1986 Annual Report, 1 Oct. 1985 - 30 Sep. 1986
L. E. Smith and B. M. Fanconi Nov. 1986 103 p
(PB87-136693; NBSIR-86/3437) Avail: NTIS HC A06/MF A01 CSCL 11B

Technical Activities of the Polymers Division for Fy 86 are reviewed. Included are descriptions of the 6 Tasks of the Division, project reports, publications, and other technical activities. Topics addressed include: electrical properties; polymer standards and chemical performance; mechanical performance of polymers; processing and reliability of polymer composites; polymer blends; and dental and medical materials. GRA

N87-20421*# National Aeronautics and Space Administration. Lewis Research Center, Cleveland, Ohio.
INVESTIGATION OF PTFE TRANSFER FILMS BY INFRARED EMISSION SPECTROSCOPY AND PHASE-LOCKED ELLIPSOMETRY
James L. Lauer (Rensselaer Polytechnic Inst., Troy, N.Y.), Bruce G. Bunting, and William R. Jones, Jr. May 1987 16 p Prepared for presentation at the 1987 Annual Meeting of the American Society of Lubrication Engineers, Anaheim, Calif., 11-14 May 1987
(NASA-TM-89844; E-3505; NAS 1.15:89844) Avail: NTIS HC A02/MF A01 CSCL 20L

When a PTFE sheet was rubbed unidirectionally over a smooth surface of stainless steel an essentially monomolecular transfer film was formed. By ellipsometric and emission infrared spectroscopic techniques it was shown that the film was 10 to 15 A thick and birefringent. From the intensity differences of infrared bands obtained with a polarizer passing radiation polarized in mutually perpendicular planes, it was possible to deduce transfer film orientation with the direction of rubbing. After standing in air for several weeks the transfer films apparently increased in thickness by as much as threefold. At the same time both the index of refraction and the absorption index decreased. Examination of the surfaces by optical and electron microscopies showed that the films had become porous and flaky. These observations were consistent with previous tribological measurements. The coefficients of friction decreased with the formation of the transfer film but increased again as the film developed breaks. The applicability of the ellipsometric and polarized infrared emission techniques to the identification of monomolecular tribological transfer films of polymers such as PTFE has been demonstrated. Author

N87-20422*# National Aeronautics and Space Administration. Lewis Research Center, Cleveland, Ohio.
DEFORMATION AND FRACTURE OF SINGLE-CRYSTAL AND SINTERED POLYCRYSTALLINE SILICON CARBIDE PRODUCED BY CAVITATION
Kazuhisa Miyoshi, Shuji Hattori (Fukui Univ., Japan.), Tsunenori Okada, and Donald H. Buckley (Case Western Reserve Univ., Cleveland, Ohio.) 1987 25 p Proposed for presentation at the 1987 Joint Tribology Conference, San Antonio, Tex., 5-8 Oct. 1987; sponsored by the American Society of Lubrication Engineers and ASME
(NASA-TM-88981; E-3367; NAS 1.15:88981) Avail: NTIS HC A02/MF A01 CSCL 20B

An investigation was conducted to examine the deformation and fracture behavior of single-crystal and sintered polycrystalline SiC surfaces exposed to cavitation. Cavitation erosion experiments were conducted in distilled water at 25 C by using a magnetostrictive oscillator in close proximity (1 mm) to the surface of SiC. The horn frequency was 20 kHz, and the double amplitude of the vibrating disk was 50 microns. The results of the investigation indicate that the SiC (0001) surface could be deformed in a plastic manner during cavitation. Dislocation etch pits were formed when the surface was chemically etched. The number of defects, including dislocations in the SiC (0001) surface, increased with increasing exposure time to cavitation. The presence of intrinsic defects such as voids in the surficial layers of the sintered polycrystalline SiC determined the zones at which fractured grains and fracture pits (pores) were generated. Single-crystal SiC had superior erosion resistance to that of sintered polycrystalline SiC. Author

N87-20423*# National Aeronautics and Space Administration. Marshall Space Flight Center, Huntsville, Ala.
MICROGRAVITY CRYSTALLIZATION OF MACROMOLECULES: AN INTERIM REPORT AND PROPOSAL FOR CONTINUED RESEARCH
Benjamin E. Goldberg Dec. 1986 26 p
(NASA-TP-2671; NAS 1.60:2671) Avail: NTIS HC A03/MF A01 CSCL 20B

An initial investigation exploring the effects of gravity on the crystallization of macromolecular systems has been completed. Monodisperse poly(ethylene), molecular weight 48,000 was melted and recrystallized under gravitational conditions: 0, 1, and 2 g. No correlations to gravitational environment were noted for the 20 C/min melt, as monitored with a photodensitometer system. However, post-crystallization testing of the recrystallized samples revealed thicker samples with more regions of large, well defined spherulites for the zero gravity crystallization environment. The results of the post-crystallization analysis have been reviewed and the results related to nucleation concerns. Finally, birefringence data, consistent with, but not explained by, the nucleation scenarios is detailed, and further investigations are proposed. Author

N87-20424*# National Aeronautics and Space Administration, Washington, D.C.
BIOT THEORY AND ACOUSTICAL PROPERTIES OF HIGH POROSITY FIBROUS MATERIALS AND PLASTIC FOAMS
J. Allard and A. Aknine Apr. 1987 18 p Transl. into ENGLISH from Acustica (France), v. 56, no. 3, 1984 p 221-227 Transl. by The Corporate Word, Inc., Pittsburgh, Pa.
(Contract NASw-4006)
(NASA-TM-88575; NAS 1.15:88575) Avail: NTIS HC A02/MF A01 CSCL 11G

Experimental values of acoustic wave propagation constant and characteristic impedance in fibrous materials, and normal absorption for two plastic foams, were compared to theoretical predictions obtained with Biot's theory. The best agreement was

observed for fibrous materials between Biot's theory and Delany and Bazley experiments for a nearly zero mass coupling parameter. For foams, the lambda/4 structure resonance effect on absorption was calculated by using four-pole modelling of the medium. A significant mass coupling parameter is then necessary for obtaining agreement between the behavior of the measured absorption coefficients and the theoretical predictions. It is shown how the formalism used for predicting foams absorption coefficients may be used for studying the acoustic behavior of multi-layered media. Author

N87-20425*# National Aeronautics and Space Administration. Lewis Research Center, Cleveland, Ohio.
HOT CORROSION ATTACK AND STRENGTH DEGRADATION OF SIC AND SI(SUB)3N(SUB)4
James L. Smialek, Dennis S. Fox, and Nathan S. Jacobson Apr. 1987 12 p Presented at the 3rd Environmental Degradation of Engineering Materials, University Park, Pa., 13-15 Apr. 1987; sponsored by Pennsylvania State Univ.
(NASA-TM-89820; E-3466; NAS 1.15:89820) Avail: NTIS HC A02/MF A01 CSCL 11G

Thin films of Na2SO4 and Na2CO3 molten salt deposits were used to corrode sintered SiC and Si3N4 at 1000 C. The resulting attack produced pitting and grain boundary etching resulting in strength decreases ranging from 15 to 50 percent. Corrosion pits were the predominant sources of fracture. The degree of strength decrease was found to be roughly correlated with the depth of the pit, as predicted from fracture toughness considerations. Gas evolution and bubble formation were key aspects of pit formation. Many of the observations of furnace exposures held true in a more realistic burner rig test. Author

N87-20426*# National Aeronautics and Space Administration. Lewis Research Center, Cleveland, Ohio.
ADDITION POLYMERS FROM 1,4,5,8-TETRAHYDRO-1,4;5,8-DIEPOXYANTHRACENE AND Bis-DIENES: PROCESSABLE RESINS FOR HIGH TEMPERATURE APPLICATION
Mary Ann B. Meador [1987] 8 p Prepared for presentation at the 194th National Meeting of the American Chemical Society, New Orleans, La., 30 Aug. - 4 Sep. 1987
(NASA-TM-89838; E-3495; NAS 1.15:89838) Avail: NTIS HC A02/MF A01 CSCL 11B

1,4,5,8-Tetrahydro-1,4;5,8-diepoxyanthracene reacts with various anthracene endcapped polyimide oligomers to form Diels-Alder cycloaddition copolymers. The polymers are soluble in common organic solvents, and have molecular weights of approximately 21,000 to 32,000. Interestingly, these resins appear to be more stable in air then in nitrogen. This is shown to be due to a unique dehydration (loss of water ranges from 2 to 5 percent) at temperatures of 390 to 400 C to give thermo-oxidatively stable pentiptycene units along the polymer backbone. Because of their high softening points and good thermo-oxidative stability, the polymers have potential as processible, matrix resins for high temperature composite applications. Author

N87-20427# Detroit Univ., Mich. Polymer Inst.
ENERGY ABSORPTION OF POLYURETHANE BASED POLYMER ALLOYS Final Technical Report, 1 Jun. 1985 - 31 Aug. 1986
Bhavesh Muni, Bijan Sedghi, Irfan Raza, Daniel Klempner, and Kurt C. Frisch 27 Sep. 1986 15 p
(Contract DAAG29-85-K-0129)
(AD-A175542; ARO-22361.3-MS) Avail: NTIS HC A02/MF A01 CSCL 11/10

Interpenetrating polymer networks (IPNs) elastomers and foams composed of polyurethanes and epoxies were prepared by the simultaneous technique. Fillers and plasticizers were incorporated by random batch mixing. The PU/epoxy ratio was varied. Enhanced energy absorbing abilities were demonstrated by the dynamic mechanical spectroscopy results (broad and high tan behavior as a function of temperature). This was reflected in the mechanical and acoustical energy absorption of the foams. The effects of fillers and plasticizers were mixed. The component IPNs prepared from polyurethane, epoxy, and unsaturated polyester resulted in even broader tan delta behavior. GRA

N87-20428# Massachusetts Univ., Amherst. Dept. of Mechanical Engineering.
EROSION AND STRENGTH DEGRADATION IN ALUMINA
J. E. Ritter, L. Rosenfeld, and K. Jakus 1985 8 p Presented at the 4th International Conference on Wear of Materials, Vancouver, British Columbia, 14 Apr. 1985
(Contract DE-AC02-81ER-10950)
(DE87-003341; CONF-850415-5) Avail: NTIS HC A02/MF A01

The effect of multiparticle impact at 23, 700, 1000 C on the erosion and strength degradation of sintered alumina was determined. Impact damage at normal incidence was characterized by numerous small pits consistent with grain boundary cracking. Neither erosion rate nor strength degradation for normal impingement depended strongly on temperature. Although erosion rate increased with increasing kinetic energy of the impacting particle, strength degradation leveled off at high kinetic energies, contrary to predictions based on elastic/plastic fracture. An alternative theory, based on the observed damage morphology, assumes that the kinetic energy of the impacting particle goes into grain boundary cracking and the subsequent grain fallout creates a hemispherical pit with an annular crack. This model correctly predicts the dependency of both erosion rate and strength degradation on kinetic energy of the impacting particle. For impingement at low angles impact damage was primarily by a ductile plowing process. This caused erosion rates to be greater than that predicted based on the brittle chipping mode of erosion, but strength degradation was less because the shallow, elongated flaws are less severe than the impact pits. DOE

N87-20429# Research Inst. of National Defence, Stockholm (Sweden). Dept. 2.
ADHESION OF A SILICONE BASED INSULATING MATERIAL TO ROCKET MOTORS
Eva Ryden Nov. 1986 29 p In SWEDISH; ENGLISH summary (FOA-C-20635-2.1; ISSN-0347-3694; ETN-87-99438) Avail: NTIS HC A03/MF A01

Adhesion of an insulating material, consisting of 46% silicon elastomer, 50% silicon and silicon carbide, and 4% carbon fiber to an aluminum alloy containing among others Zn, Mg, Cu, Cr, and to an epoxy resin was investigated. Different test methods are described and discussed. Very good results are achieved: this can be seen on the fracture surfaces which in almost all experiments proved to be cohesive. The surface structure of the aluminum metal was only of limited importance. Choice of primer on epoxy resins was very important. ESA

28 PROPELLANTS AND FUELS

Includes rocket propellants, igniters, and oxidizers; their storage and handling procedures; and aircraft fuels.

For related information see also *07 Aircraft Propulsion and Power, 20 Spacecraft Propulsion and Power,* and *44 Energy Production and Conversion.*

N87-20430# Sandia National Labs., Albuquerque, N. Mex.
FEASIBILITY STUDY OF A SEMICONDUCTOR BRIDGE (SCB) FOR INITIATING PYROTECHNICS AND EXPLOSIVES
R. W. Bickes, Jr. and A. C. Schwarz Jan. 1987 27 p
(Contract DE-AC04-76DP-00789)
(DE87-004444; SAND-86-2617) Avail: NTIS HC A03/MF A01

Small metal bridgewires are traditionally used to initiate igniters, squibs, and actuators. This report describes a new initiation mode, a semiconductor bridge (SCB), which is 1/100 the volume of a wire bridge. Our studies indicate that order of magnitude reductions in threshold energy and function time are achievable with no loss in safety (base on no-fire data obtained). With appropriate designs, SCB's will function from a 10-volt power source; therefore, marriage to microelectronic switches, logic circuits, and firing sets appears

practical. Threshold initiation energies of 1.5 to 3.0 mJ, function times of 40 to 70 microseconds, and no-fire levels of 7.5 watts were achieved on devices loaded with the pyrotechnic, TiH/sub .65//KClO. The high explosives PETN, HNAB, and HMX deflagrated at comparable low energy levels. DOE

29 MATERIALS PROCESSING

Includes space-based development of products and processes for commercial applications.

For biological materials see *55 Space Biology.*

N87-20431*# National Aeronautics and Space Administration. Marshall Space Flight Center, Huntsville, Ala.
RAPID MELT/QUENCH FURNACE USING COMMERCIALLY AVAILABLE HARDWARE
Richard M. Poorman Mar. 1987 14 p
(NASA-TM-86590; NAS 1.15:86590) Avail: NTIS HC A02/MF A01 CSCL 22A

This report describes an off-the-shelf Orbital Tube Welder that can be easily used to melt and resolidify almost any electrically conductive material. This can be done on a KC-135 Aircraft within the microgravity period of one parabola. Melt sizes 3 mm diameter by 10 mm length and larger are feasible with most if not all materials. A highly reproducible, controlled, programmable heat and cool cycle can be provided. Sample measurements would have to be developed and could be as sophisticated or as simple as desired. These could include: optical and thermocouple temperature measurements, Peltier pulser for marking the solidification fronts, dimensional changes and whatever. Sample heat flows could be fixed over a very wide range being limited mostly by the cooling period, the desired sample size, and the 20 sec microgravity period of the KC-135 Aircraft parabola. Author

N87-20304*# National Electric Co. of Venezuela, Caracas.
MANUFACTURING POLYMER THIN FILMS IN A MICROGRAVITY ENVIRONMENT
Ivan Vera *In* NASA. Goddard Space Flight Center The 1986 Get Away Special Experimenter's Symposium Feb. 1987 p 9-14 (For primary document see N87-20302 13-12)
Avail: NTIS HC A11/MF A01 CSCL 22A

N87-20305*# Alabama Univ., Huntsville. Consortium for Materials Development in Space.
PHASE PARTITIONING, CRYSTAL GROWTH, ELECTRODEPOSITION AND COSMIC RAY EXPERIMENTS IN MICROGRAVITY
Francis C. Wessling *In* NASA. Goddard Space Flight Center The 1986 Get Away Special Experimenter's Symposium Feb. 1987 p 15-22 (For primary document see N87-20302 13-12)
Avail: NTIS HC A11/MF A01 CSCL 22A

N87-20310*# Telesat Canada, Ottawa (Ontario).
TOWARDS A BETTER MIRROR
David Hoffer *In* NASA. Goddard Space Flight Center The 1986 Get Away Special Experimenter's Symposium Feb. 1987 p 49-57 (For primary document see N87-20302 13-12)
Avail: NTIS HC A11/MF A01 CSCL 22A

N87-20311*# Ohio State Univ., Columbus. Dept. of Aeronautical and Astronautical Engineering.
PROGRESS ON THE OHIO STATE UNIVERSITY GET AWAY SPECIAL G-0318: DEAP
Nesrin Sarigul and A. J. Mortensen (Gould, Inc., Cleveland, Ohio.) *In* NASA. Goddard Space Flight Center The 1986 Get Away Special Experimenter's Symposium Feb. 1987 p 59-62 (For primary document see N87-20302 13-12)
Avail: NTIS HC A11/MF A01 CSCL 22A

N87-20318*# North Carolina Agricultural and Technical State Univ., Greensboro. Student Space Shuttle Program.
THE NORTH CAROLINA A AND T STATE UNIVERSITY STUDENT SPACE SHUTTLE PROGRAM Status Report, 1979-1986
F. D. Hooker and S. T. Ahrens *In* NASA. Goddard Space Flight Center The 1986 Get Away Special Experimenter's Symposium Feb. 1987 p 111-118 (For primary document see N87-20302 13-12)
Avail: NTIS HC A11/MF A01 CSCL 22A

N87-20319*# Spar Aerospace Ltd., Toronto (Ontario).
BAKING THE FIRST BREAD IN SPACE
In NASA. Goddard Space Flight Center The 1986 Get Away Special Experimenter's Symposium Feb. 1987 p 119-126 (For primary document see N87-20302 13-12)
Avail: NTIS HC A11/MF A01 CSCL 22A

N87-20332*# McDonnell-Douglas Astronautics Co., Huntsville, Ala.
MICROGRAVITY EFFECTS ON ELECTRODEPOSITION OF METALS AND METAL-CERMET MIXTURES
George W. Maybee, Clyde Riley (Alabama Univ., Huntsville.), and H. Dwain Coble *In* NASA. Goddard Space Flight Center The 1986 Get Away Special Experimenter's Symposium Feb. 1987 p 215-221 (For primary document see N87-20302 13-12)
Avail: NTIS HC A11/MF A01 CSCL 22A

31 ENGINEERING (GENERAL)

Includes vacuum technology; control engineering; display engineering; cryogenics; and fire prevention.

N87-20432# Naval Civil Engineering Lab., Port Hueneme, Calif.
PERFORMANCE OF RECYCLED ASPHALT CONCRETE AIRPORT PAVEMENT SURFACES Final Report, Aug. 1983 - May 1986
G. D. Cline and M. C. Hironaka Oct. 1986 38 p
(Contract DTFA01-83-Y-30593)
(DOT/FAA-PM-86-12; TN-N-1765) Avail: NTIS HC A03/MF A01

The objective of this research was to make an assessment of the relative performance of recycled versus new asphalt concrete pavement surfaces constructed for airport facilities. To make this assessment, pavement condition index (PCI) surveys and tests on core samples from the hot-mix recycled pavements located on the airports at Needles, California, and Valley City, North Dakota were conducted. Both pavements have a condition rating of very good. The survey and test data were compared with those for recycled highway and virgin material Navy airfield pavements. The recycle pavement at Needles is performing as good as those Navy pavements constructed with virgin material. The recycled pavement at Valley City has a higher deterioration rate than the Navy pavements but this could be attributed to the harsh climate found in North Dakota. The results of this study show that hot-mix recycling was successful at these airports but additional studies are required to determine the applicability of Asphalt Concrete (AC) recycling for reconstruction at all airports. Author

N87-20433# Army Cold Regions Research and Engineering Lab., Hanover, N. H.
RESILIENT MODULUS OF FREEZE-THAW AFFECTED GRANULAR SOILS FOR PAVEMENT DESIGN AND EVALUATION. PART 3: LABORATORY TESTS ON SOILS FROM ALBANY COUNTY AIRPORT
D. M. Cole, D. L. Bentley, G. D. Durell, and T. C. Johnson Feb. 1987 43 p Sponsored in part by FAA and Army
(Contract PHWA-8-3-0187)
(DOT/FAA-PM-84-16.3; CRREL-87-2) Avail: NTIS HC A03/MF A01

This is the third in a series of four reports on the laboratory and field testing of a number of road and airfield subgrades, covering the laboratory repeated-load triaxial testing of five soils in the frozen and thawed states and analysis of the resulting resilient modulus measurements. The laboratory testing procedures allow simulation of the gradual increase in stiffness found in frost-susceptible soils after thawing. The resilient modulus is expressed in a nonlinear model in terms of the applied stresses,

the soil moisture tension level (for unfrozen soil), the unfrozen water content (for frozen soil) and the dry density. The resilient modulus is about 10 GPa for the frozen material at temperatures in the range of -5 to -8 C. The decrease in modulus with increasing temperature was well-modeled in terms of the unfrozen water content. Upon thaw, the modulus dropped to about 100 MPa and generally increased with increasing confining stress and decreased with increasing principal stress ratio. The modulus also increased with the soil moisture tension level. The resilient Poisson's ratio did not appear to be a systematic function of any of the test variables. Author

N87-20434# Army Cold Regions Research and Engineering Lab., Hanover, N. H.
A FREEZE-THAW TEST TO DETERMINE THE FROST SUSCEPTIBILITY OF SOILS
Edwin J. Chamberlain Jan. 1987 97 p Sponsored in part by FAA and Army
(Contract FHWA-8-3-0187)
(DOT/FAA-PM-85-20; SR-87-1) Avail: NTIS HC A05/MF A01

A freezing test for determining the frost susceptibility of soils is presented to supplant the standard CRREL freezing test currently specified by the Corps of Engineers. This test reduces the time required to determine the frost susceptibility of a soil in half. It also allows for the determination of both the frost heave and thaw weakening susceptibilities and considers the effects of the freeze-thaw cycling. The freeze test eliminates much of the variability in test results caused by the human element by completely automating the temperature control and data observations. Author

N87-20435# Vibration Inst., Clarendon Hills, Ill.
THE SHOCK AND VIBRATION DIGEST, VOLUME 19, NO. 2 Monthly Report
Judith Nagle-Eshleman, ed. Feb. 1987 76 p
Avail: NTIS HC A05/MF A01

The Shock and Vibration Digest, Volume 19, No. 2, February 1987, contains articles on the following: Underwater Acoustic Modeling Techniques; and Recent Studies in Plate Vibrations: 1981 to 1985; Part 1. Classical Theory. It also contains numerous Book Reviews from fields related to shock and vibration. This is the first issue to be published by the Vibration Institute of Clarendon Hills, Illinois. The Shock and Vibration Digest was formerly published by The Shock and Vibration Center of the Naval Research Laboratory of Washington, D.C. For individual titles, see N87-20436 through N87-20437.

N87-20436# Ocean Data Systems, Inc., Rockville, Md. Defense Systems Div.
UNDERWATER ACOUSTIC MODELING TECHNIQUES **c71**
P. C. Etter *In* Vibration Inst. The Shock and Vibration Digest, Volume 19, No. 2 Feb. 1987 p 3-10 (For primary document see N87-20435 13-31)
Avail: NTIS HC A05/MF A01

This article reviews progress in the area of underwater acoustic modeling techniques since 1983. Emphasis is on developments of general interest to the Navy sonar modeling community including model refinements and specialized modeling applications. Author

N87-20437# Air Force Academy, Colo. Dept. of Engineering Mechanics.
RECENT STUDIES IN PLATE VIBRATIONS: 1981-1985. PART 1: CLASSICAL THEORY **c39**
A. W. Leissa *In* Vibration Inst. The Shock and Vibration Digest, Volume 19, No. 2 Feb. 1987 p 11-18 (For primary document see N87-20435 13-31)
Avail: NTIS HC A05/MF A01

This review article is the first of two summarizing recent studies in the free vibration of plates. The present one briefly summarizes 76 publications which appeared during the recent five year period (1981 to 1985) for plates which are governed by classical plate theory (thin, isotropic, homogeneous, linearly elastic, small displacements, etc). Accomplishments are reported for circular, rectangular, other quadrilateral, triangular, polygonal, and sectorial plates, as well as other shapes. Both theoretical and experimental studies are included. Complicating effects in plate vibrations will be assessed in a subsequent article. Author

N87-20438# Shock and Vibration Information Center (Defense), Washington, D. C.
THE SHOCK AND VIBRATION DIGEST, VOLUME 18, NO. 10 Monthly Report
Judith Nagle-Eshleman, ed. Oct. 1986 97 p
(AD-A175726) Avail: NTIS HC A05/MF A01 CSCL 20K

The Shock and Vibration Digest, Volume 18, No. 10, October 1986, contains articles on the following: (1) The digital processing of acceleration measurements for modal analysis; and (2) Stable response of damped linear systems -III. It also contains two Book Reviews on vibration-related subjects, and a comprehensive list of training courses associated with vibration technology. This is the last issue to be published by the Shock and Vibration Center of the Naval Research Laboratory of Washington, D.C. Henceforth, it is to be published by the Vibration Institute of Clarendon Hills, Illinois. For individual titles, see N87-20439 through N87-20440.

N87-20439# Carnegie-Mellon Univ., Pittsburgh, Pa. Dept. of Mechanical Engineering.
THE DIGITAL PROCESSING OF ACCELERATION MEASUREMENTS FOR MODAL ANALYSIS **c35**
C. W. deSilva *In* Shock and Vibration Information Center The Shock and Vibration Digest, Volume 18, No. 10 Oct. 1986 p 3-11 (For primary document see N87-20438 13-31)
Avail: NTIS HC A05/MF A01 CSCL 14/2

In modal testing dynamic responses are usually measured as acceleration signals. The corresponding displacement time histories are obtained through digital computation for subsequent modal analysis. Techniques used in this computation, i.e., data windowing, digital filtering, and double integration are described in this paper. Problems of aliasing distortion, leakage, numerical instability, and complementary-function effect are discussed; methods to reduce their influence are given. Typical results of data analysis are given. Author

N87-20440# Stevens Inst. of Tech., Hoboken, N. J. Dept. of Mechanical Engineering.
STABLE RESPONSE OF DAMPED LINEAR SYSTEMS, PART 3 **c39**
D. W. Nicholson *In* Shock and Vibration Information Center The Shock and Vibration Digest, Volume 18, No. 10 Oct. 1986 p 13-21 (For primary document see N87-20438 13-31)
Avail: NTIS HC A05/MF A01 CSCL 20K

The article is the third in a series of reviews focusing on the dynamic response of damped linear systems. Emphasis has been on response bounds under impulse excitation, step force excitation, harmonic force, and harmonic base motion. Both classical and nonclassical systems are discussed. A general bound is also reported using the one-sided Lipschitz constant. Finally, the close relation between system stability and numerical stability has been illustrated using Pade approximations. Author

N87-20441# Lawrence Livermore National Lab., Calif.
ENGINEERING THRUST AREAS, 1987
1987 34 p
(Contract W-7405-eng-48)
(DE87-004443; UCID-20366-87) Avail: NTIS HC A03/MF A01

This booklet contains descriptions of the activities of each thrust area and illustrates how thrust area innovations and advanced technologies support laboratory programs. The thrust areas are concerned with: computer code development; computer technologies; diagnostics and microelectronics engineering, dynamic systems and control; engineering modeling and simulation; fabrication technology; materials engineering; microwave and pulsed power; non-destructive evaluation; and remote sensing, image and signal engineering. DOE

N87-20442# Lawrence Livermore National Lab., Calif.
ELECTROFORMING WITH NICKEL, IRON, AND ALUMINUM
J. F. Lakner 15 Jul. 1986 76 p
(Contract W-7405-eng-48)
(DE87-005589; UCRL-53753) Avail: NTIS HC A05/MF A01

This is a manual of practical operating instructions for electroforming with the Watts-type nickel, iron, and aluminum baths. Collected here, in one volume, are many of the supposedly secret principles used by different manufacturers of electroformed parts. The author details the methods used to produce several types of electroformed shapes with lengths up to 30 in. and diameters as large as 8 in. In this illustrated manual, the author describes the apparatus; outlines the physical properties of electroplating baths and step-by step plating operations; provides analyses of electroformed products; addresses the difficulties encountered in the electrolysis process; describes mandrel design; and defines the machining and grinding techniques used. The author also describes how to produce steel shapes from iron that has first been electroformed and then carburized on a TiC mandrel. DOE

N87-20443# Bhabha Atomic Research Centre, Bombay (India).
CRYOGENIC REGENERATORS
1986 54 p
(DE87-701264; BARC-1301) Avail: NTIS (US Sales Only) HC A04/MF A01

Importance of regenerators in cryogenic refrigerators is highlighted. Design aspects of regenerator are reviewed and the factors involved in the selection of regenerator material are enumerated. Various methods used to calculate the heat transfer coefficient and regenerator effectiveness are mentioned. Variation of effectiveness with various parameters is calculated by a computer program using the ideal, Ackermann and Tipler formulae. Results are presented in graphical form. Listing of the computer program is given in the Appendix. DOE

N87-20444# National Bureau of Standards, Gaithersburg, Md.
INTERNATIONAL SYSTEM OF UNITS (SI)
D. T. Goldman and R. J. Bell Jul. 1986 61 p Prepared in cooperation with National Physical Lab., Teddington, England
(PB86-244159; NBS/SP-330) Avail: NTIS HC A04/MF A01; also available SOD HC $3.00 as 003-003-02739-1 CSCL 14B

The booklet is the United States edition of the English translation of the fifth edition of Le Systeme International d'Unites (SI), the definitive publication in the French language issued in 1985 by the International Bureau of Weights and Measures (BIPM). This U.S. edition, which conforms in substance with the British edition that follows the French text in the BIPM document is the result of a joint effort by the National Bureau of Standards (NBS) of the United States and the National Physical Laboratory (NPL) in the United Kingdom. GRA

N87-20445# Joint Publications Research Service, Arlington, Va.
USSR REPORT: PHYSICS AND MATHEMATICS
26 Jun. 1986 127 p Transl. into ENGLISH from various Russian articles
(JPRS-UPM-86-008) Avail: NTIS HC A07/MF A01

Articles from several Chinese publications are presented. Although all of the articles are collectively classified as physics and mathematics, several smaller classifications are made. Some of them are: Acoustics; Crystals, Laser glasses and semiconductors; Gas dynamics; Fluid dynamics; High temperature physics; Nuclear physics; Optics and spectroscopy; Plasma physics, etc. Two articles of primary importance are entitled: The laser strength of active elements made of gadolinium-scandium-gallium garnet (GSGG); and Organic photochrimic material for recording waveguide holograms. For individual titles, see N87-20446 through N87-20447.

N87-20446# Joint Publications Research Service, Arlington, Va.
THE LASER STRENGTH OF ACTIVE ELEMENTS MADE OF GADOLINIUM-SCANDIUM-GALLIUM GARNET (GSGG) c36
Yu. K. Kanileyko, Ye. V. Zharikov, V. V. Laptev, Yu. P. Minayev, V. N. Nikolayev, A. V. Sidorin, G. N. Toropkin, and I. A. Shcherbakov *In its* USSR Report: Physics and Mathematics 26 Jun. 1986 p 27-29 Transl. into ENGLISH from Kvantovaya Elektronika (Moscow, USSR), v. 12, no. 2, Feb. 1985 p 430-432 (For primary document see N87-20445 13-31)
Avail: NTIS HC A07/MF A01

The problem of the beam strength of the promising (Gadolinium-Scandium-Gallium Garnet) GSGG:Cr(3+), Nd(3+) crystals were examined for the first time. It is demonstrated that their high laser strength is not susceptible to gamma radiation. Based on studies of damage statistics, it is concluded that microdefects play the decisive role in the damage of GSGG:Cr(3+), Nd(3+) crystals. Author

N87-20447# Joint Publications Research Service, Arlington, Va.
ORGANIC PHOTOCHROMIC MATERIAL FOR RECORDING WAVEGUIDE HOLOGRAMS c35
Yu. A. Bykovskiy, V. A. Barachevskiy, Yu. V. Borodakiy, V. M. Kozenkov, V. L. Smirnov, and Yu. V. Shulev *In its* USSR Report: Physics and Mathematics 26 Jun. 1986 p 74-78 Transl. into ENGLISH from Kvantovaya Elektronika (Moscow, USSR), v. 11, no. 6, Jun. 1984 p 1250-1253 (For primary document see N87-20445 13-31)
Avail: NTIS HC A07/MF A01

A method of recording phase patterns and fixing them in organic photochromic waveguides was studied experimentally. On the basis of the method studied, the authors have recorded waveguide holograms and studied their selective properties and the spatial intensity distribution in the reconstructed beam. Ways are discussed to improve the selectivity of waveguide holograms. Author

32 COMMUNICATIONS AND RADAR

Includes radar; land and global communications; communications theory; and optical communications.

For related information see also *04 Aircraft Communications and Navigation* and *17 Space Communications, Spacecraft Communications, Command and Tracking.* For search and rescue see *03 Air Transportation and Safety,* and *16 Space Transportation.*

N87-20448*# National Aeronautics and Space Administration. Lewis Research Center, Cleveland, Ohio.
UNIQUE BIT-ERROR-RATE MEASUREMENT SYSTEM FOR SATELLITE COMMUNICATION SYSTEMS
Mary Jo Windmiller Mar. 1987 13 p
(NASA-TP-2699; E-3322; NAS 1.60:2699) Avail: NTIS HC A02/MF A01 CSCL 17B

Bit-error-rate measurements, necessary to assess the performance of communication systems and components, were required for the ground-based simulation and test bed of a Ka-band, satellite-switched time-division multiple access (SS-TDMA) satellite system at the NASA Lewis Research Center. This report discusses the requirements and design tradeoffs for that system and provides a description of its hardware design. Author

N87-20449*# Massachusetts Inst. of Tech., Cambridge. Research Lab. of Electronics.
RADAR SCENE GENERATION FOR TACTICAL DECISION AIDS Final Report, 15 Apr. 1986 - 14 Apr. 1987
J. A. Kong 28 Apr. 1987 7 p
(Grant NAG5-769)
(NASA-CR-180234; NAS 1.26:180234) Avail: NTIS HC A02/MF A01 CSCL 17I

The Mueller matrix and polarization covariance matrix for polarimetric radar systems was studied. The clutter is modeled by a layer of random permittivity, described by a three-dimensional correlation function, with variance, and horizontal and vertical correlation lengths. A general mixing formula was derived for discrete scatters immersed in a host medium. The results are applicable to general multiphase mixtures. The strong fluctuation theory was used to derive the backscattering cross sections, and

was further extended to include higher order co-polarized and cross-polarized moments. A two-layer anisotropic random medium model was developed for the active and passive remote sensing of ice fields. A three-layer random medium model was adopted to study the volume scattering effects for the active and passive microwave remote sensing of snow-covered ice fields. The snow layer was simulated by an isotropic random medium and the ice layer by an anisotropic random medium. The vegetation canopy and snow-covered ice field were studied with a three-layer model, an isotropic random medium layer overlying an anisotropic random medium. The dyadic Green's function of the three-layer medium and the scattered electromagnetic intensities with Born approximation were calculated. B.G.

N87-20450*# National Aeronautics and Space Administration. Lewis Research Center, Cleveland, Ohio.
A STUDY OF THE EFFECT OF GROUP DELAY DISTORTION ON AN SMSK SATELLITE COMMUNICATIONS CHANNEL
Robert J. Kerczewski Apr. 1987 39 p
(NASA-TM-89835; E-3491; NAS 1.15:89835) Avail: NTIS HC A03/MF A01 CSCL 17B

The effects of group delay distortion on an SMSK satellite communications channel have been investigated. Software and hardware simulations have been used to determine the effects of channel group delay variations with frequency on the bit error rate for a 220 Mbps SMSK channel. These simulations indicate that group delay distortions can significantly degrade the bit error rate performance. The severity of the degradation is dependent on the amount, type, and spectral location of the group delay distortion. Author

N87-20451# Mission Research Corp., Santa Barbara, Calif.
PROPAGATION OF RF SIGNALS THROUGH STRUCTURED IONIZATION. THEORY AND ANTENNA APERTURE EFFECT APPLICATIONS Technical Report, 1 Mar. 1985 - 1 May 1986
Roger A. Dana 15 May 1986 139 p
(Contract DNA001-85-C-0067)
(AD-A175522; MRC-R-976; DNA-TR-86-158) Avail: NTIS HC A07/MF A01 CSCL 20/14

This report presents a review of the theory of propagation of RF signals through random ionospheric disturbances that would result from high altitude chemical releases or nuclear detonations. Starting with Maxwell's equations, an analytic expression for the two-position, two-time, two-frequency mutual coherence function is derived for strong, anisotropic scattering conditions. The physics that are contained in this important function and the approximations that are used. The first is the usual frozen-in approximation which models the ionosphere as a rigid structure that drifts across the line-of-sight. The second, called the turbulent model, is developed in this report which decouples the spatial and temporal fluctuations in the ionosphere. This model may be more accurate at times before striations have formed in the ionosphere or when multiple layers of striations with different velocities are drifting across the line-of-sight. The second part of this report presents several new results and applications of the theory. The generalized power spectral density (GPSD), which is the Fourier transform of the mutual coherence function, is used to compute the second order statistics of the signal at the output of an anisotropic aperture antenna. Analytic results are presented for antennas with Gaussian beam profiles and numerical results are presented for uniformly weighted apertures. GRA

N87-20452# Columbia Univ., New York. Radiation Lab.
RESEARCH INVESTIGATION DIRECTED TOWARD EXTENDING THE USEFUL RANGE OF THE ELECTROMAGNETIC SPECTRUM Progress Report, 1 Oct. 1985 - 30 Sep. 1986
George W. Flynn and Richard M. Osgood, Jr. 31 Dec. 1986 208 p
(Contracts DAAG29-85-K-0049; F49620-84-K-0022; F49620-85-C-0067; DE-AC02-78ER-04940; N00014-78-C-0517; Grants AF-AFOSR-0013-84; NSF CHE-85-17460; NSF CHE-82-11593; NSF CHE-80-23747; NSF ECS-82-17677)
(AD-A175644; PR-36) Avail: NTIS HC A10/MF A01 CSCL 20/14

New developments have been achieved in the quantum generation and detection of light. The usual semiclassical theory of light detection turns out to be incomplete. The theory has been extended to include the possibility of feedback from the detector to the source which changes the theory substantially. In the revised theory the noise at the output of a detector can be below shot noise even though the incident light is classical, i.e., above shot noise. However, the action of such an electron current configured in an external feedback loop can be useful for converting Poisson light into amplitude-squeezed (sub-Poisson) light. A configuration making use of transitions between the energy levels of a quantum-well heterostructure has been developed. The noise properties of superlattice avalanche photodiodes (SAPD's) have been compared with those of conventional avalanche photodiodes (CAPD's) for the detection of both amplitude-squeezed light and conventional light. SAPD's are heterostructure devices constructed in such a way that principally one kind of carrier impact-ionizes. Performance and time response have been evaluated for lightware communication systems. These detectors exhibit promising characteristics. GRA

N87-20453# Air Force Systems Command, Wright-Patterson AFB, Ohio. Foreign Technology Div.
MATERIAL WITH ANISOTROPIC PROPERTIES FOR MAGNETIC SHIELDING PURPOSES
H. Schmid 8 Dec. 1986 16 p Transl. into ENGLISH of West German Patent, No. 884 659 (29 Apr. 1944) p 1-6
(AD-A175864; FTD-ID(RS)T-1203-86) Avail: NTIS HC A02/MF A01 CSCL 20/3

The following patent claim has been filed. Material with anisotropic properties, characterized by a construction for achieving high magnetic shielding effects by shielding cans, such that it consists of at least two planar elements in close succession and of thickness Delta, which cannot be divided any further into elements of the same kind, and the properties of the elements with respect to permeability, dielectric, and electric conductivity, firstly, are essentially the same in the plane of the elements, secondly, undergo at least one pronounced external fluctuation through the thickness Delta, and thirdly, are repeated from element to element so that, corresponding to the anisotropic behavior, the tensor ellipsoids belonging to the material tensors are ellipsoids of revolution whose axes of rotation are perpendicular to the elements. Material, characterized by the fact that the poor electrically conducting layer consists of an insulating material, is relatively thin, and is arranged so that it insulates the element's metallic layers and the element from each other. GRA

N87-20454# Computer Sciences Corp., Falls Church, Va. Systems Div.
FLEXIBLE SATELLITE COMMUNICATIONS SYSTEMS SIMULATOR STANDARD DEVICE GROUPS Final Report
D. W. Brown and J. L. Burgess Dec. 1986 198 p
(Contract DCA100-77-C-0020)
(AD-A175944) Avail: NTIS HC A09/MF A01 CSCL 17/2

This document contains the designs of the standard device groups (SDG) prepared for the Flexible Satellite Communications Systems Simulation (FSCSS). It contains updates to SDGs prepared for earlier versions of FSCSS and new SDG's prepared for version 4.0. FSCSS is a time domain simulation for accurately determining performance of satellite communications system principally in terms of bit error rate. SDGs are models of earth terminals, satellites and modems from the inventory of the Deense Satellite Communications System (DSCS). These ready-made SATCOM components ease the burden of a FSCSS user setting up large DSCS Systems within FSCSS. GRA

N87-20455# Mission Research Corp., Santa Barbara, Calif.
STOCHASTIC EFFECTS ON OBLIQUE HF (HIGH FREQUENCIES) PROPAGATION Technical Report, 7 Jan. 1984 - 31 Jan. 1986
L. J. Nickisch 31 Jan. 1986 101 p
(Contract DNA001-84-C-0253)
(AD-A176015; MRC-R-974; DNA-TR-86-74) Avail: NTIS

HC A06/MF A01 CSCL 20/12

A model for the calculation of the stochastic effects on transionospheric radio wave propagation due to structured ionization, developed in recent years, has been applied to internally reflected paths at high frequencies (HF). Measurements of signal spreading in the delay and doppler domains obtained by the HF Channel Probe experiment in the polar region were used to test the applicability of the transionospheric scintillation model to oblique, internal HF paths. Oblique soundings made by the Channel Probe experiment provide the ionospheric profile through which rays can be numerically traced and model calculations performed. A nonlinear regression routine is used to obtain model parameters providing the best fit to the data. Good fits are obtained and the resulting model parameters are consistent with independent measurements. GRA

N87-20456# Communications Research Centre, Ottawa (Ontario).
THE IN-SITU CALIBRATION OF A BILATERAL SPACE-FED PHASED ARRAY ANTENNA
E. K. Hung, N. R. Fines, and R. M. Turner Jun. 1983 38 p
(AD-A176069; CRC-1370) Avail: NTIS HC A03/MF A01

This report describes an in-situ technique to estimate the following parameters of a phased-array antenna: (1) the relative array-element excitation voltages, (2) the array-element tuning phases, and (3) the RF phase shifts at the array elements. This technique has several significant features. First, it involves the use of two auxiliary antennas. One is a passive antenna mounted close to the phased-array antenna. Its output is used to produce a reference phase for phase measurements. Second, it contains a technique to reduce the errors in phase estimates. Third, it takes note that beam steering uses phase sums of the form (phi k + Beta kl), where phi k is the tuning phase for the k-th array element and Beta kl is an RF phase shift of the array element, and pays special attention to reduce the errors associated with the estimates of these sums. Fourth, it assumes the use of a reasonably stable and strong CW source of commercially available quality. No other assumptions are made. GRA

N87-20457 Department of the Air Force, Washington, D.C.
TURNAROUND CONTROL FOR MECHANICALLY SCANNED RADAR ANTENNAS Patent
R. J. Bennett, inventor (to Air Force) Issued 9 Sep. 1986 8 p
Supersedes N85-10246, AD-D011238 (23 - 01, p 39)
(AD-D012563; US-Patent-4,611,210; US-Patent-Appl-SN-622614; US-Patent-Class-343-359) Avail: US Patent and Trademark Office CSCL 17/9

A programmed turnaround generator for a mechanically scanned antenna, to provide an n-bar scan pattern (n may be 1), with predetermined inputs to the generator comprising a desired turnaround time, a maximum excursion of the antenna in azimuth, and a start position for each bar, is mechanized using closed form equations. GRA

N87-20458 Department of the Air Force, Washington, D.C.
MAGNETOSTATIC WAVE FREQUENCY ANALYZER APPARATUS Patent
Robert E. Floyd, inventor (to Air Force) Issued 30 Sep. 1986 8 p Supersedes N85-14044, AD-D011249 (23 - 05, p 631)
(AD-D012558; US-Patent-4,614,919; US-Patent-Appl-SN-627699; US-Patent-Class-333-133) Avail: US Patent and Trademark Office CSCL 14/2

A magnetostatic wave frequency analyzer apparatus utilizing forward volume waves is presented. A single input transducer is arranged opposite a plurality of output transducers to receive the different frequencies of the generated magnetostatic forward volume wave. A geometric ground plane is positioned in the propagation path between the input transducer and the plurality of output transducers to demonstrate the propagation characteristics of magnetostatic forward volume waves (MSFVW) in the 2 to 6 GHz range. The waves were propagated in two inch diameter YIG La-doped films of varying thickness (20, 30, 40 microns). The waves were launched by the microstrip input transducers on an alumina substrate. Receiver transducers were also on the substrate, but placed approximately one inch away, in a semi-circle with 10 degrees of arc between adjacent transducers. Author (GRA)

N87-20459 Department of the Air Force, Washington, D.C.
ADAPTIVE MUTUAL INTERFERENCE SUPPRESSION METHOD Patent
Bernard N. ODonnell, inventor (to Air Force) Issued 23 Sep. 1986 14 p Supersedes N85-14024, AD-D011268 (23 - 05, p 628)
(AD-D012552; US-Patent-4,613,862; US-Patent-Appl-SN-624568; US-Patent-Class-343-17.1PF) Avail: US Patent and Trademark Office CSCL 17/9

A method is described which provides automatic self synchronization (in time) between multiple pulse repetition frequency (PRF), pulse Doppler radars. The synchronization technique time aligns data within a coherent look transmission (a group of pulses-typically milliseconds). This technique substantially eliminates sensitivity losses associated with blanking false alarms or detection from interfering radars transmitting (in time) at pulse repetition intervals (PRI) different than the host radar. An implementation of this method for a 2 PRF radar waveform is described although the technique may be extended to more than 2 PRF's. The technique provides an alternative approach to pulse shaping or multiple (different) frequencies to control MI but may be used in conjunction with these techniques to minimize sensitivity losses due to interference blanking. GRA

N87-20460# Sandia National Labs., Albuquerque, N. Mex.
ANALYSIS OF THE RECEIVING CHARACTERISTICS OF THE CIRCULAR DIFFRACTION ANTENNA WITH BOTH A FLUSH-MOUNTED AND A RECESSED CENTER POST
D. J. Riley Nov. 1986 81 p
(Contract DE-AC04-76DP-00789)
(DE87-003283; SAND-86-2398) Avail: NTIS HC A05/MF A01

A simplified model for analyzing the electromagnetic response of umbilical connectors and certain low-profile radar antennas is studied. The analysis is appropriate for approximating the response through several gigahertz. The integral equations which describe the TM symmetric modes are numerically solved, and several generic results are presented. Where applicable, comparison with analytic results is made. Corrections are made to some previous analytic results which have been found to be in error. DOE

N87-20461# Los Alamos National Lab., N. Mex.
FACTORS LIMITING THE OPERATION OF STRUCTURES UNDER HIGH GRADIENT
S. O. Schriber 1986 7 p Presented at the Linear Accelerator Conference, Stanford, Calif., 2 Jun. 1986
(Contract W-7405-eng-36)
(DE87-005132; LA-UR-86-3643; CONF-860629-68) Avail: NTIS HC A02/MF A01

Factors limiting the operation of rf structures under high-gradient conditions are described. Included are recent rf measurements at laboratories in Europe, Asia, and North America and how these measurements relate to earlier data as exemplified by the use of the Kilpatrick criterion (Kp). Operation limitations will cover mechanical, geometry, thermal, and surface constraints and the associated impact on structure design, fabrication, and material selection. Generally, structures operating continuous wave (100% duty factor) appear to be limited to peak surface fields at about twice the Kilpatrick limit, whereas pulsed structures operating with pulse lengths less than a millisecond can attain peak surface fields five times the Kilpatrick limit. DOE

N87-20462# Satel Conseil, Paris (France).
LAND MOBILE COMMUNICATIONS SATELLITE MISSION (LAMOCOSAMIS) TASK 1: MARKET STUDY
ESA Dec. 1985 170 p
(Contract ESA-6023/84-F-RD(SC))
(ESA-CR(P)-2302-Vol-1; ETN-87-99484) Avail: NTIS HC A08/MF A01

Land mobile communication service demand in Europe and the Mediterranean basin in the years 1995-2005 was estimated. A

traffic model was derived. There is an exploding demand for land mobile communications in Europe, with overwhelming preference for two way telephone services. The users survey shows a surprising lack of sensitivity to prices and tariffs, which widely contributed to the preeminence of the needs for telephone services. This demand justifies that every effort be made to develop as fast as possible a compatible pan-European terrestrial mobile system. If a large proportion of the needs may be satisfied by terrestrial mobile system solutions, the potential remaining needs for telephony, outside of the presently planned terrestrial mobile, which can be served only by satellite, even under the pessimistic economic scenario and high cost/tariff assumptions, requires a number of equivalent telephone circuits which cannot be achieved with available state of the art technology. ESA

N87-20463# Satel Conseil, Paris (France).
LAND MOBILE COMMUNICATIONS SATELLITE MISSIONS (LAMOCOSAMIS), EXECUTIVE SUMMARY
ESA 26 May 1986 22 p
(Contract ESA-6023/84-F-RD(SC))
(ESA-CR(P)-2302-Vol-6; ETN-87-99489) Avail: NTIS HC A02/MF A01

The potential needs for land mobile communications in Europe and the Mediterranean Basin in the years 1995 and 2005 were evaluated. Existing and planned cellular networks in Europe were reviewed to derive from them a hypothetical pan-European cellular network fulfilling a large proportion of these needs in the 1995-2005 time frame. Needs left unsatisfied by such a hypothetical network were identified, and satellite system solutions to fulfill these remaining needs were assessed. ESA

N87-20464# Italspazio, Rome (Italy).
LAND MOBILE SATELLITE COMMUNICATION SYSTEM. VOLUME 1: EXECUTIVE SUMMARY Final Report
C. Carnebianca, B. Pavesi, A. Tuozzi, and R. Capone Paris, France ESA Jun. 1986 24 p
(Contract ESA-6024/84-F-RD(SC))
(ITS-TR-043/86-Vol1; ESA-CR(P)-2303-Vol-1; ETN-87-99490) Avail: NTIS HC A02/MF A01

The economic value and salient technical and operational characteristics of a European Land Mobile Communication Satellite (LMCS), able to complement and supplement the demand for mobile services of Western European countries members of CEPT, foreseeable in the 1995-2005 time frame were evaluated. The expected traffic and markets for an LMCS were assessed. The satellite role was studied. ESA

N87-20465# Italspazio, Rome (Italy).
LAND MOBILE SATELLITE COMMUNICATION SYSTEM. VOLUME 2: TRAFFIC ANALYSIS AND MARKET DEMAND FOR THE LAND MOBILE COMMUNICATIONS SYSTEM IN THE EUROPEAN SCENARIO Final Report
C. Carnebianca, B. Pavesi, A. Tuozzi, and R. Capone Paris, France ESA Jun. 1986 105 p
(Contract ESA-6024/84-F-RD(SC))
(ITS-TR-043/86-Vol-2; ESA-CR(P)-2303-Vol-2; ETN-87-99491) Avail: NTIS HC A06/MF A01

The socioeconomic desirability in terms of market demand, technical economic feasibility, and price-performance for a Land Mobile Communication system ground based and/or satellite aided, able to satisfy the request of the traffic demand, foreseable in the 1995-2005 time frame, for the Western European countries was assessed. The criterion of economic value of the mobile system is considered as the driving element. The presence of gaps in the terrestrial system and reasonable traffic extrapolations suggest a very attractive role for a land mobile satellite communications mission. ESA

N87-20466# Ecole Nationale Superieure des Telecommunications, Paris (France). Dept. Systemes et Communications.
[ACTIVITIES REPORT OF THE DEPARTMENT OF SYSTEMS AND COMMUNICATIONS] Annual Report, 1985 [RAPPORT SCIENTIFIQUE 1985: DEPARTMENT SYSTEMES ET COMMUNICATIONS]
Jun. 1986 98 p In FRENCH
(ENST-86D002; ISSN-0751-1345; ETN-87-99400) Avail: NTIS HC A05/MF A01

Research in stochastic systems, treatment of numerical information, modeling techniques, speech recognition, pattern recognition, numerical communication theory, and architectures for signal processing are summarized. ESA

N87-20315*# National Aeronautics and Space Administration. Goddard Space Flight Center, Greenbelt, Md.
STS-61C, COLUMBIA FLIGHT Final Report
Edward F. Stluka *In its* The 1986 Get Away Special Experimenter's Symposium Feb. 1987 p 87-93 (For primary document see N87-20302 13-12)
Avail: NTIS HC A11/MF A01 CSCL 17B

N87-20323*# Rupp (Charles C.), Huntsville, Ala.
MARSHALL AMATEUR RADIO CLUB EXPERIMENT (MARCE) POST FLIGHT DATA ANALYSIS
Charles C. Rupp *In* NASA. Goddard Space Flight Center The 1986 Get Away Special Experimenter's Symposium Feb. 1987 p 149-156 (For primary document see N87-20302 13-12)
Avail: NTIS HC A11/MF A01 CSCL 17B

N87-20329*# Weber State Coll., Ogden, Utah. Center for Aerospace Technology.
NUSAT 1 METHODS FOR RADAR FIELD STRENGTH MEASUREMENT
Paul Talaga *In* NASA. Goddard Space Flight Center The 1986 Get Away Special Experimenter's Symposium Feb. 1987 p 193-198 (For primary document see N87-20302 13-12)
Avail: NTIS HC A11/MF A01 CSCL 17B

N87-20760# Selenia Industrie Elettroniche Associate S.p.A., Pomezia (Italy). Radar Div.
EXPERT SYSTEMS FOR DIAGNOSTIC PURPOSES, PROSPECTED APPLICATIONS TO THE RADAR FIELD
Riccardo Filippi *In its* Rivista Tecnica Selenia, Volume 10, Number 1 1986 p 1-10 (For primary document see N87-20759 13-61)
Avail: NTIS HC A04/MF A01

33 ELECTRONICS AND ELECTRICAL ENGINEERING

Includes test equipment and maintainability; components, e.g., tunnel diodes and transistors; microminiaturization; and integrated circuitry.

For related information see also *60 Computer Operations and Hardware* and *76 Solid-State Physics.*

N87-20467*# Ford Aerospace and Communications Corp., Palo Alto, Calif.
SATELLITE ANALOG FDMA/FM TO DIGITAL TDMA CONVERSION Final Report, May - Dec. 1986
T. Driggers, T. Nguyen, and V. Kolavennu Apr. 1987 72 p
(Contract NAS3-24890)
(NASA-CR-179605; NAS 1.26:179605; WDL-TR11068) Avail: NTIS HC A04/MF A01 CSCL 09C

The results of a study which investigated design issues regarding the use of analog to digital (A/D) conversion on board a satellite are presented. The need for A/D, and of course D/A as well, conversion arose from a satellite design which required analog FDMA/FM up and down links to/from a digitally modulated intersatellite link. There are also some advantages when one must interconnect a large number of various spot beams which are using analog, and therefore cannot take advantage of SS/TDMA switching among the beams, thus resulting in low fill factors. Various tradeoffs were performed regarding the implementation of on-board A/D processing, including mass, power, and costs. The various technologies which were considered included

flash ADCs, surface acoustic wave (SAW) devices, and digital signal processing (DSP) chips. Impact analyses were also performed to determine the effect on ground stations to convert to digital if the A/D approach were not implemented. Author

N87-20468*# National Aeronautics and Space Administration. Lewis Research Center, Cleveland, Ohio.
SYSTEM ARCHITECTURE OF MMIC-BASED LARGE APERTURE ARRAYS FOR SPACE APPLICATION
P. R. Herczfeld (Drexel Univ., Philadelphia, Pa.), M. Kam, R. R. Kunath, K. B. Bhasin, and N. LaPrade (Drexel Univ.,) Jan. 1987 12 p Presented at the O-E/LASE 87 Optoelectronics and Laser Applications in Science and Engineering, Los Angeles, Calif., 11-17 Jan. 1987; sponsored by the Society of Photo-Optical Instrumentation Engineers
(NASA-TM-89840; E-3482; NAS 1.15:89840) Avail: NTIS HC A02/MF A01 CSCL 09C

The persistent trend to use millimeter-wave frequencies for satellite communications presents the challenge to design large-aperture phased arrays for space applications. These arrays, which comprise 100 to 10,000 elements, are now possible due to the advent of lightwave technology and the availability of monolithic microwave integrated circuits. In this paper, system aspects of optically controlled array design are studied. In particular, two architectures for a 40 GHz array are outlined, and the main system-related issues are examined: power budget, synchronization in frequency and phase, and stochastic effects. Author

N87-20469*# National Aeronautics and Space Administration. Lewis Research Center, Cleveland, Ohio.
PROPAGATION CHARACTERISTICS OF SOME NOVEL CO-PLANAR WAVEGUIDE TRANSMISSION LINES ON GaAs AT MM-WAVE FREQUENCIES
Rainee N. Simons 1986 16 p Presented at the 1986 Conference on Millimeter Wave/Microwave Measurements and Standards for Miniaturized Systems, Redstone Arsenal, Ala., 6-7 Nov. 1986; sponsored by the Army Missile Command
(NASA-TM-89839; E-3335; NAS 1.15:89839) Avail: NTIS HC A02/MF A01 CSCL 09C

Three new Coplanar Waveguide (CPW) transmission lines, namely, Suspended CPW (SCPW), Stripline-like Suspended CPW (SSCPW) and Inverted CPW (ICPW), are proposed and also analyzed for their propagation characteristics. The substrate thickness, permittivity and dimensions of housing are assumed to be arbitrary. These structures have the following advantages over conventional CPW. Firstly, the ratio of guide wavelength to free space wavelength is closer to unity which results in larger dimensions and hence lower tolerances. Secondly, the effective dielectric constant is lower and hence the electromagnetic field energies are concentrated more in the air regions which should reduce attenuation. Thirdly, for a prescribed impedance level, the above structures have a wider slot width for identical strip width. Thus, low impedance lines can be achieved with reasonable slot dimensions. Fourthly, in an inverted CPW shunt mounting of active devices, such as Gunn and IMPATT diodes, between the strip and the metal trough is possible. This feature further enhances the attractiveness of the above structures. Lastly, an E-plane probe type transition from a rectangular waveguide to suspended CPW can also be easily realized. The computed results for GaAs at Ka-band illustrate the variation of normalized guide wavelength, effective dielectric constant and the characteristic impedance as a function of the: (1) frequency; (2) distance of separation between the trough side walls; (3) normalized strip and slot widths; and (4) normalized air gap. Author

N87-20470*# Martin Marietta Aerospace, Denver, Colo.
USERS MANUAL FOR NICKEL CADMIUM BATTERY EXPERT SYSTEM
Sep. 1986 10 p
(Contract NAS8-35922)
(NASA-CR-179032; NAS 1.26:179032; MCR-86-673) Avail: NTIS HC A02/MF A01 CSCL 10C

Presented is the User Manual for NICBES, Nickel Cadmium Battery Expert System. It documents the control for both NICBES subsystems; the Expert System and the Data-Handler. Author

N87-20471*# Martin Marietta Aerospace, Denver, Colo. Aerospace Div.
NICKEL CADMIUM BATTERY EXPERT SYSTEM Final Report
Nov. 1986 39 p
(Contract NAS8-35922)
(NASA-CR-179031; NAS 1.26:179031; MCR-85-641) Avail: NTIS HC A03/MF A01 CSCL 10C

The applicability of artificial intelligence methodologies for the automation of energy storage management, in this case, nickel cadmium batteries, is demonstrated. With the Hubble Space Telescope Electrical Power System (HST/EPS) testbed as the application domain, an expert system was developed which incorporates the physical characterization of the EPS, in particular, the nickel cadmium batteries, as well as the human's operational knowledge. The expert system returns not only fault diagnostics but also status and advice along with justifications and explanations in the form of decision support. Author

N87-20472*# Martin Marietta Aerospace, Denver, Colo. Aerospace Div.
PROGRAM MAINTENANCE MANUAL FOR NICKEL CADMIUM BATTERY EXPERT SYSTEM, VERSION 1
Oct. 1986 132 p
(Contract NAS8-35922)
(NASA-CR-179033; NAS 1.26:179033; MCR-86-675) Avail: NTIS HC A07/MF A01 CSCL 10C

The Nickel-Cadmium Battery Expert System (NICBES) is an expert system for fault diagnosis and advice of the nickel-cadmium batteries found in the Hubble Space Telescope (HST). The system application and security, equipment environment, and the program maintenance procedures are examined. B.G.

N87-20473*# Martin Marietta Aerospace, Denver, Colo.
REQUIREMENTS SPECIFICATION FOR NICKEL CADMIUM BATTERY EXPERT SYSTEM
Sep. 1986 37 p
(Contract NAS8-35922)
(NASA-CR-179034; NAS 1.26:179034; MCR-86-674) Avail: NTIS HC A03/MF A01 CSCL 10C

The requirements for performance, design, test, and qualification of a computer program identified as NICBES, Nickel Cadmium Battery Expert System, is established. The specific spacecraft power system configuration selected was the Hubble Space Telescope (HST) Electrical Power System (EPS) Testbed. Power for the HST comes from a system of 13 Solar Panel Arrays (SPAs) linked to 6 Nickel Cadmium Batteries which are connected to 3 Busses. An expert system, NICBES, will be developed at Martin Marietta Aerospace to recognize a testbed anomaly, identify the malfunctioning component and recommend a course of action. Besides fault diagnosis, NICBES will be able to evaluate battery status, give advice on battery status and provide decision support for the operator. These requirements are detailed. Author

N87-20474*# National Aeronautics and Space Administration. Lewis Research Center, Cleveland, Ohio.
DESIGN, FABRICATION AND PERFORMANCE OF SMALL, GRAPHITE ELECTRODE, MULTISTAGE DEPRESSED COLLECTORS WITH 200-W, CW, 8- TO 18-GHz TRAVELING-WAVE TUBES
Ben T. Ebihara and Peter Ramins Feb. 1987 22 p
(NASA-TP-2693; E-3099; NAS 1.60:2693) Avail: NTIS HC A02/MF A01 CSCL 09A

Small multistage depressed collectors (MDC's) which used pyrolytic graphite, ion-beam-textured pyrolytic graphite, and isotropic graphite electrodes were designed, fabricated, and evaluated in conjuntion with 200-W, continuous wave (CW), 8- to 18-GHz traveling-wave tubes (TWT's). The design, construction, and performance of the MDC's are described. The bakeout performance of the collectors, in terms of gas evolution, was indistinguishable from that of typical production tubes with copper

collectors. However, preliminary results indicate that some additional radiofrequency (RF) and dc beam processing time (and/or longer or higher temperature bakeouts) may be needed beyond that of typical copper electrode collectors. This is particularly true for pyrolytic graphite electrodes and for TWT's without appendage ion pumps. Extended testing indicated good long-term stability of the textured pyrolytic graphite and isotropic graphite electrode surfaces. The isotropic graphite in particular showed considerable promise as an MDC electrode material because of its high purity, low cost, simple construction, potential for very compact overall size, and relatively low secondary electron emission yield characteristics in the as-machined state. However, considerably more testing experience is required before definitive conclusions on its suitability for electronic countermeasure systems and space TWT's can be made. Author

N87-20475*# National Aeronautics and Space Administration. Lewis Research Center, Cleveland, Ohio.
REFERENCING IN FIBER OPTIC SENSING SYSTEMS
Grigory Adamovsky 1987 9 p Proposed for presentation at the Technical Symposium of Optics, Electro-Optics and Sensors, Orlando, Fla., 17-22 May 1987; sponsored by the Society of Photo-Optical Instrumentation Engineers
(NASA-TM-89822; E-3468; NAS 1.15:89822) Avail: NTIS HC A02/MF A01 CSCL 20F

Different techniques to account for losses induced by the environment on signals in intensity modulation fiber optic sensing systems are described and analyzed. Author

N87-20476*# National Aeronautics and Space Administration. Langley Research Center, Hampton, Va.
BUBBLE MEMORY MODULE FOR SPACECRAFT APPLICATION
P. J. Hayes, K. T. Looney, and C. D. Nichols Apr. 1985 107 p
(NASA-TM-86411; NAS 1.15:86411) Avail: NTIS HC A06/MF A01 CSCL 09A

Bubble domain technology offers an all-solid-state alternative for data storage in onboard data systems. A versatile modular bubble memory concept was developed. The key module is the bubble memory module which contains all of the storage devices and circuitry for accessing these devices. This report documents the bubble memory module design and preliminary hardware designs aimed at memory module functional demonstration with available commercial bubble devices. The system architecture provides simultaneous operation of bubble devices to attain high data rates. Banks of bubble devices are accessed by a given bubble controller to minimize controller parts. A power strobing technique is discussed which could minimize the average system power dissipation. A fast initialization method using EEPROM (electrically erasable, programmable read-only memory) devices promotes fast access. Noise and crosstalk problems and implementations to minimize these are discussed. Flight memory systems which incorporate the concepts and techniques of this work could now be developed for applications. Author

N87-20477*# National Aeronautics and Space Administration. Lewis Research Center, Cleveland, Ohio.
RESISTOJET CONTROL AND POWER FOR HIGH FREQUENCY ac BUSES
Robert P. Gruber 1987 33 p Presented at the 19th International Electric Propulsion Conference, Colorado Springs, Colo., 11-13 May 1987; sponsored by AIAA, DGLR and JSASS
(NASA-TM-89860; E-3527; NAS 1.15:89860; AIAA-87-0994) Avail: NTIS HC A03/MF A01 CSCL 09C

Resistojets are operational on many geosynchronous communication satellites which all use dc power buses. Multipropellant resistojets were selected for the Initial Operating Capability (IOC) Space Station which will supply 208 V, 20 kHz power. This paper discusses resistojet heater temperature controllers and passive power regulation methods for ac power systems. A simple passive power regulation method suitable for use with regulated sinusoidal or square wave power was designed and tested using the Space Station multipropellant resistojet. The breadboard delivered 20 kHz power to the resistojet heater. Cold start surge current limiting, a power efficiency of 95 percent, and power regulation of better than 2 percent were demonstrated with a two component, 500 W breadboard power controller having a mass of 0.6 kg. Author

N87-20478*# National Aeronautics and Space Administration. Langley Research Center, Hampton, Va.
DESCRIPTION OF A MAGNETIC BEARING TEST FIXTURE
Nelson J. Groom and William L. Poole Mar. 1987 23 p
(NASA-TM-89081; NAS 1.15:89081) Avail: NTIS HC A02/MF A01 CSCL 14B

A description of a microcomputer controlled magnetic bearing test fixture is presented. Parameters which are controlled are magnetic bearing current and gaps. Parameters which are measured are magnetic bearing gaps, magnetic flux in the bearing gaps, and bearing forces. The test fixture is configured for bearing elements similar to those used in a laboratory test model Annular Momentum Control Device (AMCD). Author

N87-20479*# National Aeronautics and Space Administration. Goddard Space Flight Center, Greenbelt, Md.
ANALYSIS OF 12 AH AEROSPACE NICKEL-CADMIUM CELLS FROM THE DESIGN VARIABLE PROGRAM
Kunigahalli L. Vasanth (Bowie State Coll., Md.) and George Morrow Apr. 1987 34 p
(NASA-TM-87774; NAS 1.15:87774; Rept-86BO186) Avail: NTIS HC A03/MF A01 CSCL 10C

The Design Variable Program of NASA/GSFC provided a systematic approach to evaluate the performance of 12 Ampere-Hour Nickel-Cadmium cells of different designs. Design Variables tested in this program included teflonated negative plates, silver treated negative plates, lightly loaded negative plates, positive plates with no cadmium treatment, plate design of 1968 utilizing old and new processing techniques and electrochemically impregnated positive plates. These cells were life cycled in a Low-Earth Orbit (LEO) regime for 3 to 4 years. Representative cells taken from the Design Variable Program were examined via chemical, electrochemical and surface analyses. The results indicate the following: (1) positive swelling and carbonate content in the electrolyte increase as a function of number of cycles; (2) electrolyte distribution follows a general order NEG greater than POS greater than SEP; (3) control and No PQ groups outperformed the rest of the groups; and (4) the polyproylene group exhibited heavy cadmium migration and poor performance. Author

N87-20480# Advanced Battery Group, Lancaster, N.Y.
SAFETY CHARACTERISTICS OF NON-LITHIUM BATTERY SYSTEMS, REVISION 1 Final Report, Oct. 1983 - Sep. 1984
Robert M. Murphy and Richard F. Bis Jul. 1986 297 p
(Contract N60921-84-C-0027)
(AD-A174577; NSWC-TR-84-302-Rev-1) Avail: NTIS HC A13/MF A01 CSCL 10/3

A study was conducted to determine the safety characteristics for both primary and secondary non-lithium battery systems. Of particular interest was the behavior of these battery systems when subjected to the electrical and thermal abuse testing procedures (i.e., short circuit, forced overdischarge, and incineration). Also included are the safety/hazard characteristics associated with charging primary batteries and overdischarging secondary batteries. This report also summarizes the manufacture, electrical performance, failure mechanisms, self-discharge, and applications for twenty-two primary and nineteen secondary battery systems. GRA

N87-20481# Carnegie-Mellon Univ., Pittsburgh, Pa. Dept. of Electrical and Computer Engineering.
MULTILEVEL REPRESENTATION AND SIMULATION FOR VLSI DESIGN Final Report, 23 May 1983 - 22 May 1986
S: W. Director and D. E. Thomas 26 Nov. 1986 18 p
(Contract DAAG29-83-K-0083)
(AD-A175663; ARO-20060.6-EL) Avail: NTIS HC A02/MF A01 CSCL 09/5

Integrated circuit design has become almost impossible without circuit and system level simulation programs. Simulators at the

circuit level produce performance data that allows the circuits to be functionally verified, optimized, and their performance evaluated. The size and complexity of integrated circuits has increased greatly since the first circuit simulators were designed. Because large circuits need to be simulated as thoroughly as small ones, the time spent simulating larger circuits has increased dramatically. Consequently, simulation tools that can efficiently simulate large circuits are needed. In this regard, work under this contract has focussed on the improvement of the mixed circuit/logic simulator SAMSON, as well as the development of new approaches to simulation. At the system level, simulators also produce data that allow the system architecture to be functionally verified, optimized and evaluated. Because of the ever larger systems being designed for implementation on an integrated circuit chip, there is a need for higher performance system level simulators. In this regard, work under this contract has also focussed on the development of new approaches to system level simulation. A study of the use of hardware accelerators in this application is described. GRA

N87-20482# Marconi Electronic Devices Ltd., Lincoln (England).
OPTICALLY TUNED MILLIMETER-WAVE CW. IMPATT SOURCE Final Technical Report
J. F. Singleton, S. Brunt, and A. J. Seeds Apr. 1986 50 p
(Contract DAJA45-84-C-0045)
(AD-A175838; TR-85) Avail: NTIS HC A03/MF A01 CSCL 09/1

The main objective of the contract was to carry out a one year feasibility study on the use of an optical signal to control the operating frequency of a millimetre-wave IMPATT oscillator. The study involved a theoretical analysis of optical tuning in IMPATT diodes, computer modelling of optical tuning behavior, including transient behavior, and experimental measurements on a W-Band optically controlled oscillator. An analytic theory of optical tuning in IMPATT oscillators has been developed, leading to a simple equation relating the change in oscillator frequency to the optically injected current. Major predictions of the optically injected current that the proportionality constant varies as the reciprocal of the oscillator Q factor and that avalanche multiplication increases the optical tuning effect significantly at the higher oscillator voltage swings. It is predicted that a 5mW semiconductor laser would produce a tuning range of the order of 1% in a W-Band IMPATT oscillator having a Q of 200. GRA

N87-20483 Department of the Air Force, Washington, D.C.
LOW PASS PI SECTION DIGITAL PHASE SHIFTER APPARATUS Patent
Binboga S. Yarman, inventor (to Air Force) Issued 30 Sep. 1986 5 p Supersedes N86-25710, AD-D012093 (24 - 16, p 2582)
(AD-D012553; US-Patent-4,614,921; US-Patent-Appl-SN-767446; US-Patent-Class-333-139) Avail: US Patent and Trademark Office CSCL 09/5

A low pass Pi section digital phase shifter apparatus having an inductor and a diode connected in series between two identical parallel circuits is described. The parallel circuits connect to the series inductor/diode circuit at both the input and output and each circuit has inductor connected in parallel with a capacitor and a diode to provide balanced insertion loss at each diode switching state. When the diodes of the circuit are in the forward biased state they act as closed short circuit switches. When the diodes are reversed biased, the inductance in the series circuit resonates with the diode capacitance to provide a short circuit path to the RF signal to pass the center frequency of the RF signal at the desired phase. GRA

N87-20484# Ames Lab., Iowa.
ELECTRON TUNNELING STUDIES OF Mo/(SUB)1-xRe/(SUP)x/: ENHANCEMENT OF SUPERCONDUCTIVITY BY A RESONANCE MODE Ph.D. Thesis
D. P.C. Shum Nov. 1986 112 p
(Contract W-7405-eng-82)
(DE87-003048; IS-T-1246) Avail: NTIS HC A06/MF A01

It is well-known that a heavy impurity atom in a lattice of light atoms induces a lower frequency in-band resonance mode in the vibrational spectrum. The exact effect of such a mode on the lattice spectrum has not previously been reported and effects of such modes on superconductivity have not previously been described. Sputtered thin films of bcc Mo(sub 1-x)Re(sub x), 0.2 less than x less than 0.4, have been prepared for this study because the Re atom is almost twice as heavy as Mo. High quality MoRe(Al2O3)Pb tunnel junctions on these films have been made with an in situ deposited and subsequently oxidized thin Al layer as barrier. Three phonon peaks were observed directly in the dV/dI and d sup2 V/dI sup 2 curves. The alpha sup2 F (omega) spectra, determined from the data through the Eliashberg theory of superconductivity, all show an anomalous low energy peak, in addition to the Mo-derived transverse and longitudinal phonon peaks. This peak appears near 14 MeV, in agreement with the Brout-Visscher theory and with neutron scattering data which first indicated the Re resonance mode in Mo(sub .85)Re(sub .15). We show that the resonance mode contributes strongly to alpha sup 2F (omega) and to strong coupling delta(=2 Delta/k sub B T sub c - 3.53 greater than 0. delta increases with lambda(sub R), the Re contribution to the electron-phonon coupling constant lambda. The dependence of the anomalous softening and width of the resonance mode on lambda(sub R) fit the Yu-Anderson theory of local phonon screening by a Fermi gas of electrons treated as Tomonaga bosons. These results explain the low N(O), high T(sub c) behavior of Mo(sub .6)Re(sub .4). DOE

N87-20485# Ames Lab., Iowa.
PROXIMITY-INDUCED JOSEPHSON EFFECT AND ITS APPLICATION TO HEAVY FERMION SUPERCONDUCTOR UBe-13 Ph.D. Thesis
S. Han Nov. 1986 131 p
(Contract W-7405-eng-82)
(DE87-003049; IS-T-1244) Avail: NTIS HC A07/MF A01

A new effect between a superconductor with superconducting transition temperature T(sub cs) and a normal metal N (T(sub cn)) (or another superconductor with T(sub cn)<T(sub cs)) has been experimentally observed and theoretically explained. That is when S and N are brought together to form a weak link the Josephson effect can occur in this SN system even in the temperature range T(sub cn) less than T less than T(sub cs), when the N side is in the normal state. The temperature dependence of the Josephson critical current I(sub c)(T) of the SN point contact junctions have been studied experimentally. The experiments have been performed on Ta/Mo, Ta/UBe-13 and Nb/Ta point contacts, etc. The theoretical model is based on the linearized Gor'kov equation (or linearized Ginzburg-Landau equation) combined with de Gennes boundary conditions. This model is applicable only in the vicinity of the T(sub c) of the SN system. Thus, we studied I(sub c)(T) of the SN junctions near their T(sub c). Good agreement between experimental data and theoretical result is obtained. Along with the recent discovery of the superconductivity in heavy fermion materials CeCu2Si2, UBe-13, and Upt3, the old question of p-wave pairing superconductivity is raised again. Among these three heavy fermion superconductors UBe-13 is thought to be the best candidate for odd parity pairing. The proximity-induced Josephson effect is employed to investigate the pairing state of UBe-13.The results are found to favor an odd parity bulk superconducting ground state in UBe-13. DOE

N87-20486# Oak Ridge National Lab., Tenn.
A RESEARCH PROGRAM TO ASSESS THE IMPACT OF THE ELECTROMAGNETIC PULSE ON ELECTRIC POWER SYSTEMS
B. W. McConnell and P. R. Barnes 1987 9 p Presented at the EMC Symposium and Exhibition Special Seminar: EMP Effects on Power Systems, Zurich, Switzerland, 3 Mar. 1987
(Contract DE-AC05-84OR-21400)
(DE87-002415; CONF-870305-2) Avail: NTIS HC A02/MF A01

A strong electromagnetic pulse (EMP) with an electric-field component on the order of tens of kilovolts per meter is produced by a nuclear detonation in or above the atmosphere. This paper presents an overview and a summary of the results to date of a program formulated to address the research and development of technologies and systems required to assess and reduce the impact of EMP on electric power systems. The technologies and

systems being considered include simulation models, methods of assessment, definition of required experiments and data, development of protective hardware, and the creation or revision of operating and control procedures. Results to date include the development of relatively simple unclassified EMP environment models, the development of methods for extending EMP coupling models to the large transmission and distribution network associated with the electric power system, and the performance of a parametric study of HEMP induced surges using an appropriate EMP environment. An experiment to investigate the effect of corona on the coupling of EMP to conductors has been defined and has been performed in an EMP simulator. Experiments to determine the response of key components to simulated EMP surges and an investigation of the impact of steep-front, short-duration impulse on a selected number of the insulation systems used in electric power systems apparatus are being performed. DOE

N87-20487# Argonne National Lab., Ill.
HIGH-TEMPERATURE FUEL CELLS
R. D. Pierce 1986 17 p Presented at the Electrochemical Sciences Conference, Cleveland, Ohio, 14 Sep. 1986
(Contract W-31109-eng-38)
(DE87-004870; CONF-8609230-1) Avail: NTIS HC A02/MF A01

The DOE is about to embark on the development and demonstration of a prototype molten carbonate fuel cell (MCFC) stack of 0.1 to 0.5 MW. This engineering effort will be complemented by base technology and component development contracts sponsored by DOE and EPRI. The tubular solid oxide fuel cell (SOFC) concept under development by Westinghouse is being tested in multikilowatt generators. Cell endurance and cost are the major issues for both concepts. ANL is developing the monolithic SOFC concept with laboratory-scale cell arrays. Continued development of advanced ceramic fabrication technology is the major thrust of that program. DOE

N87-20488# Argonne National Lab., Ill.
BATTERIES FOR HYBRID VEHICLES OR OTHER HIGH-POWER APPLICATIONS
J. F. Miller, J. Lee, and C. C. Christianson 1986 8 p Presented at the 8th International Electric Vehicle Symposium, Washington, D.C., 20 Oct. 1986
(Contract W-31109-eng-38)
(DE87-004928; CONF-8610122-12) Avail: NTIS HC A02

Argonne National Laboratory conducted a study to identify promising battery designs for application in future hybrid vehicles (HVs). A preliminary set of battery requirements for HVs was established using information available from previous studies and also by contacting potential HV developers worldwide. The consensus of the information obtained indicated that, as compared with the electric vehicle battery, the HV battery will be smaller and lighter, must have higher power capability per unit weight and will, on the average, be discharged at higher rates. Based upon the preliminary battery requirements, many different battery technologies proposed for the hybrid-vehicle mission were evaluated. Although no existing battery presently developed satisfies all of the preliminary requirements, the analysis has shown that several battery types, with appropriate redesign and development, are good candidates for meeting the hybrid-vehicle application requirements. DOE

N87-20489# Argonne National Lab., Ill.
TEMPERATURE EFFECTS ON NICKEL/IRON BATTERY CHARACTERISTICS
W. H. DeLuca, A. F. Tummillo, R. L. Biwer, F. Hornstra, and C. C. Christianson 1986 8 p Presented at the 8th International Electric Vehicle Symposium, Washington, D.C., 20 Oct. 1986
(Contract W-31109-eng-38)
(DE87-004930; CONF-8610122-13) Avail: NTIS HC A02

The performance of an improved Ni/Fe electric vehicle battery applications was measured at ambient temperatures of 0, 25 and 50°C for a range of overcharge levels (3 to 80%), open-circuit stand times (0 to 4 h), and charge (1 to 6 h) and discharge (1 to 3 h) rates. Charges and discharges were also performed at different battery operating temperatures to differentiate the effects of temperature on battery charge acceptance and available discharge capacity. The results show that the discharge capacity increases with an increase in the operating temperature, but that the charge acceptance is maximal at 25°C. DOE

N87-20490# Department of Energy, Morgantown, W. Va.
FEASIBILITY OF A PHOSPHORIC ACID FUEL CELL BASIC TECHNOLOGY PROGRAM
Feb. 1987 15 p
(DE87-001045; DOE/METC-87-6075) Avail: NTIS HC A02/MF A01

Large reductions in PAFC power plant installed costs and other significant benefits are possible with the present technology if power plant production rates achieve significant levels. However, the required rates cannot currently be met because of low market penetration. Utilities will not commit to this alternative method of power production without convincing evidence that PAFC power plant performance, reliability, and economics are acceptable risks. A private sector demonstration initiative aimed at this issue is currently underway. A modest parallel R and D program could produce cost reductions and performance improvements that will leverage the industry demonstration program to substantially greater market success. DOE has completed a feasibility study, requested by the 99th Congress, which identified discrete areas of research in the PAFC and the associated benefits expected from such research. Consensus has been reached by all participants in the Fuel Cell Program that a focussed research program could be developed and implemented to achieve those benefits and readily permit their incorporation into power plants offered by the manufacturers in the mid 1990's at the completion of the demo program. DOE

N87-20491# Pacific Northwest Labs., Richland, Wash.
SODIUM SULFUR BATTERY: AN OVERVIEW
R. K. Sen and A. L. Landgrebe Jan. 1987 10 p Presented at the Symposium on Sodium Sulfur Batteries, San Diego, Calif., 16 Oct. 1986
(Contract DE-AC06-76RL-01830)
(DE87-004920; PNL-SA-14579; CONF-8610232-1) Avail: NTIS HC A02/MF A01

High theoretical specific energy values are expected from batteries with low equivalent weight reactants and large electronegativity differences. Alkali metals, acting as the negative electrode, and the chalcogenides as the positive electrode, potentially could produce a battery with high specific energy density. Weber and Kummer demonstrated such a battery using sodium and sulfur as the two electrode materials. The key to the development of this battery was the discovery that solid electrolytes such as beta-alumina conducts sodium ions efficiently. Since then other glassy materials have been shown to be adequate conductors of sodium ions as well. Based on these two types of electrolytes, three approaches to the design of the sodium/sulfur battery have evolved. This paper provides a brief overview of these design approaches. DOE

N87-20492# Argonne National Lab., Ill.
MONOLITHIC FUEL CELL DEVELOPMENT
D. C. Fee, P. E. Blackburn, D. E. Busch, T. D. Claar, D. W. Dees, J. Dusek, T. E. Easler, W. A. Ellingson, B. K. Flandermeyer, and R. J. Fousek 1986 5 p Presented at the Fuel Cell Seminar, Tucson, Ariz., 26 Oct. 1986
(Contract W-31-109-eng-38)
(DE87-004926; CONF-861008-6) Avail: NTIS HC A02/MF A01

A new fuel cell design, called the monolithic fuel cell, is being developed at Argonne. The monolithic design employs the same thin ceramic components used in other oxide fuel cells in a strong, lightweight honeycomb structure of small cells, and thus can achieve very high power per unit mass or volume. The light weight and low volume, as well as the efficiency and reliability of electrical systems, are advantageous in space and terrestrial systems. DOE

N87-20493# Argonne National Lab., Ill.
MORPHOLOGICAL CHANGES IN THE SULFUR ELECTRODE OF LIFECYCLE-TESTED Na/S CELLS
J. A. Smaga 1986 12 p Presented at the Electrochemical Society Fall Meeting, San Diego, Calif., 19 Oct. 1986
(Contract W-31-109-eng-38)
(DE87-004961; CONF-861068-14) Avail: NTIS HC A02/MF A01

Morphological studies of the sulfur electrode have provided important insights into the factors that influence the performance of Na/S cells. The observed compositional gradients indicate that multiple reaction fronts arise within the electrode during cycling through the two-liquid compositional range. Present models predicting this behavior inadequately describe the location of these fronts. The pattern of changes in Na and S distribution is repeated with each charge-discharge cycle; however, the morphology is progressively altered by corrosion products, especially the migratory compounds of NaAlS2 and NaCrS2. As a result of a cycle-dependent transport mechanism, the latter compound becomes concentrated in the electrode adjacent to the electrolyte. Cells that fail because of electrolyte fractures form solid sodium polysulfides within the sulfur electrode. On occasion, the uncontrolled growth of solid phases undermines the integrity of the container. DOE

N87-20494# Research Inst. of National Defence, Linkoeping (Sweden). Dept. 3.
FABRICATION OF MICROWAVE DEVICES ON ULTRATHIN ACTIVE GaAs SUBSTRATES
Dennis Soederberg, Ulf Dahlgren, Staffan Rudner, Thorwald Andersson (Chalmers Univ. of Technology, Goeteborg, Sweden.), and Johan Westin Nov. 1986 34 p
(FOA-C-30431-3.2; ISSN-0347-3708; ETN-87-99439) Avail: NTIS HC A03/MF A01; Research Intitute of National Defence, Stockholm, Sweden KR 50

A fabrication process for a microstrip structure on a 5 micron thick n-doped GaAs active substrate was designed. The resulting distributed Gunn diode is intended to be used as a voltage controlled oscillator. The process includes molecular beam epitaxy growth of active layers, selective etching using a GaAlAs etchstop layer, and the formation of an integral heat sink. The process has 30 discrete steps and takes a week to produce a device. The technology could also be used in the fabrication of other high power devices such as power FET's. ESA

N87-20495# Research Inst. of National Defence, Linkoeping (Sweden). Dept. 3.
A THEORETICAL AND EXPERIMENTAL STUDY OF CYLINDRICAL DIELECTRIC RESONATORS AND THEIR APPLICATIONS TO MICROWAVE OSCILLATORS
Jan Svedin Nov. 1986 75 p
(FOA-C-30434-3.2; ISSN-0347-3708; ETN-87-99440) Avail: NTIS HC A04/MF A01; Research Institute of National Defence, Stockholm, Sweden KR 50

A method for calculating the TE sub 01 delta-mode resonant frequencies and field patterns of a shielded cylindrical dielectric resonator mounted on a microstrip substrate coupled to a microstrip line is presented. Experimental results confirm the accuracy of the method to be within 1% of average error. The calculation of and the relations between quality factors are outlined. Experimental results of the coupling coefficient as a function of the distance between resonator and microstrip line are given. Serial and parallel feedback oscillators using dielectric resonators were studied. The serial feedback type shows the best overall performance. One serial feedback oscillator constructed shows output power of 12 dBm, temperature stability of 1 MHz (0 to 100 C), a noise figure of minus 75 dBc at 10 kHz off-carrier, and a second harmonic of minus 28 dBc. ESA

N87-20496# Ecole Nationale Superieure des Telecommunications, Paris (France).
LINEARIZATION OF GaAs FIELD EFFECT TRANSISTOR POWER AMPLIFIERS IN HYPERFREQUENCES Ph.D. Thesis [LINEARISATION DES AMPLIFICATEURS DE PUISSANCE A TRANSISTORS A EFFET DE CHAMP GLCAALCS EN HYPERFREQUENCES]
Andre Loembe 18 Jun. 1986 217 p In FRENCH
(ENST-86E007; ISSN-0751-1353; ETN-87-99401) Avail: NTIS HC A10/MF A01

Methods to characterize the nonlinearities in hyperfrequency devices are studied showing that nonlinear transformation techniques are efficient to evaluate distorsions and intermodulation of GaAs MESFET power amplifiers. A computer program was developed to model and simulate the multicarrier behavior. This behavior can be deduced from transfer characteristics determinations (power and phase) for a single carrier. Examples of synthesis and implementation are given. ESA

34 FLUID MECHANICS AND HEAT TRANSFER

Includes boundary layers; hydrodynamics; fluidics; mass transfer; and ablation cooling.

For related information see also *02 Aerodynamics* and *77 Thermodynamics and Statistical Physics.*

N87-20497 California Inst. of Tech., Pasadena.
THE EFFECTS OF LARGE-EDDY MANIPULATOR DEVICES ON THE TURBULENT SPOT AND THE TURBULENT BOUNDARY LAYER Ph. D. Thesis
Stephen Taylor 1986 121 p
Avail: Univ. Microfilms Order No. DA8623959

Recent experimental studies indicate that the net drag reductions can be achieved in a turbulent boundary layer by placing a tandem configuration of large-eddy manipulator blades in the outer region of the boundary layer. However, the mechanisms responsible for the observed wall-shear reductions are not well understood. A fundamental argument is made regarding the source of the observed wall-shear reductions. The implication is that the momentum deficit in the wake of the manipulator is a prominent contributor to the observed wall-shear reductions, not necessarily that the ability of the large eddies to transport momentum is hampered. The behavior of the wall shear downstream of the device, obtained using hot-film wall-shear sensors, is consistent with the entrainment, mixing, and consequent deceleration of low-momentum fluid from the wake of the manipulator. With the aid of direct measurement of wall shear, an upper bound is placed on the attainable net drag reduction by establishing a lower bound for the device drag. Efforts were made to explain the observed effects in terms of turbulent structure. Some effects of a three-dimensional manipulator were explored. Dissert. Abstr.

N87-20498 Missouri Univ., Columbia.
A HOLOGRAPHIC INTERFEROMETRY STUDY OF AN AXISYMMETRIC SHOCK-WAVE/BOUNDARY-LAYER STRONG INTERACTION FLOW Ph.D. Thesis
Stephen Emil Dunagan 1986 274 p
Avail: Univ. Microfilms Order No. DA8625943

An experimental study of the axisymmetric shock wave/turbulent boundary layer strong interaction flow generated in the vicinity of a cylinder-cone intersection was conducted. The present data are useful in the documentation and understanding of compressible turbulent strong-interaction flows, and are part of a more general effort to improve turbulence modeling for compressible two- and three-dimensional strong viscous/inviscid interactions. The primary emphasis was on the application of the holographic interferometry technique to these flow cases. The density field was deduced from an interferometric analysis based on the Abel transform. Supporting data were obtained using a 2-D laser velocimeter, as well as mean wall pressure and oil flow measurements. The attached flow case was observed to be steady, while the separated cases exhibited shock unsteadiness. Comparisons with Navier-Stokes computations using a two equation turbulence model are presented. The utility of holographic interferometry is illustrated for detailed instantaneous flow field

characterization and provides documented data useful in the evaluation of computational schemes. Dissert. Abstr.

N87-20499 Michigan Univ., Ann Arbor.
NUMERICAL SIMULATION OF SEPARATED FLOWS PAST BLUFF BODIES Ph.D. Thesis
Andreas Neophytou Alexandrou 1986 141 p
Avail: Univ. Microfilms Order No. DA8621243

The steady two-dimensional flow past bluff bodies is simulated numerically using a hybrid Eulerian-Lagrangian model. The boundary layer effects, such as the location of the separation points and the rate of the generation of vorticity, are determined by a boundary layer solver. This solver uses Prandtl's boundary layer equations transformed by the Falkner-Skan transformation and then solved using a cubic spline approximation and a mean weighted residual technique. The vorticity generated at separation is discretized into elemental point vortices and convected downstream into the wake in a Lagrangian manner. The wake is modeled in a finite Eulerian computational domain using a modified Cloud-in-Cell (CIC) method. The velocity field at each time step is obtained as a solution to the rotationality condition using the finite element method in a cartesian mesh with nine-node elements and biquadratic shape functions. The biquadratic shape functions introduce a higher order interpolation scheme for the distribution of the vorticity at the nodal points than the bilinear (area) interpolation used in the original CIC method. The higher order interpolation as used in the CIC formulation performs better than the bilinear interpolation of the original method. This is demonstrated by the simulation of an isolated Rankine vortex. The ability of the CIC method to simulate the dynamics of vortex structures is also tested for the cases of flow past a flat plate and a circular cylinder.
Dissert. Abstr.

N87-20500*# National Aeronautics and Space Administration. Langley Research Center, Hampton, Va.
STABILITY, TRANSITION AND TURBULENCE Final Report
M. Y. Hussaini Feb. 1987 22 p Submitted for publication
(Contract NAS1-18107)
(NASA-CR-178258; ICASE-87-9; NAS 1.26:178258) Avail: NTIS HC A02/MF A01 CSCL 20D

A glimpse is provided of the research program in stability, transition and turbulence based on numerical simulations. This program includes both the so-called abrupt and the restrained transition processes. Attention is confined to the prototype problems of channel flow and the parallel boundary layer in the former category and the Taylor-Couette flow in the latter category. It covers both incompressible flows and supersonic flows. Some representative results are presented. Author

N87-20501*# Universities Space Research Association, Boulder, Colo.
PREDICTION OF RECIRCULATION ZONES IN ISOTHERMAL COAXIAL JET FLOWS RELEVANT TO COMBUSTORS
M. Nallasamy Washington NASA Apr. 1987 23 p
(Contract NAS8-35918)
(NASA-CR-4064; NAS 1.26:4064) Avail: NTIS HC A02/MF A01 CSCL 20D

The characteristics of the recirculation zones in confined coaxial turbulent jets are investigated numerically employing the kappa - epsilon turbulence model. The geometrical arrangement corresponds to the experimental study of Owen (AIAA J. 1976) and the investigation is undertaken to provide information for isothermal flow relevant to combustor flows. For the first time, the shape, size, and location of the recirculation zones for the above experimental configuration are correctly predicted. The processes leading to the observed results are explained. Detailed comparisons of the prediction with measurements are made. It is shown that the recirculation zones are very sensitive to the central jet exit configuration and the velocity ratio of the jets. Author

N87-20502*# National Aeronautics and Space Administration. Langley Research Center, Hampton, Va.
THE FULLY NONLINEAR DEVELOPMENT OF GOERTLER VORTICES IN GROWING BOUNDARY LAYERS
Philip Hall (Exeter Univ., England.) and William D. Lakin (Old Dominion Univ., Norfolk, Va.) Mar. 1987 36 p
(Contract NAS1-18107)
(NASA-CR-178268; ICASE-87-16; NAS 1.26:178268) Avail: NTIS HC A03/MF A01 CSCL 20D

The fully nonlinear development of small wavelength Goertler vortices in a growing boundary layer is investigated using a combination of asymptotic and numerical methods. The starting point for the analysis is the weakly nonlinear theory of Hall (1982b) who discussed the initial development of small amplitude vortices in a neighborhood of the location where they first become linearly unstable. That development is unusual in the context of nonlinear stability theory in that it is not described by the Stuart-Watson approach. In fact the development is governed by a pair of coupled nonlinear partial differential evolution equations for the vortex flow and the mean flow correction. Here the further development of this interaction is considered for vortices so large that the mean flow correction driven by them is as large as the basic state. Surprisingly it is found that such a nonlinear interaction can still be described by asymptotic means. It is shown that the vortices spread out across the boundary layer and effectively drive the boundary layer. In fact the system obtained by writing down the equations for the fundamental component of the vortex generate a differential equation for the basic state. Thus the mean flow adjusts so as to make these large amplitude vortices locally neutral. Moreover in the region where the vortices exist the mean flow has a square-root profile and the vortex velocity field can be written down in closed form. The upper and lower boundaries of the region of vortex activity are determined by a free-boundary problem involving the boundary layer equations. In general it is found that this region ultimately includes almost all of the original boundary layer and much of the free-stream. In this situation the mean flow has essentially no relationship to the flow which exists in the absence of the vortices. Author

N87-20503*# Flow Research, Inc., Kent, Wash.
TURBULENCE CONTROL ON AN AIRBORNE LASER PLATFORM Final Technical Report, 1 Jan. - 30 Jun. 1986
Mohamed Gad-el-Hak Mar. 1987 55 p
(Contract NAS1-18213)
(NASA-CR-178249; NAS 1.26:178249; Rept-365) Avail: NTIS HC A04/MF A01 CSCL 20D

An active flow control device to generate large-scale, periodic structures in a turbulent shear flow is developed. Together with adaptive optics, the device may be used on airborne laser platforms to reduce or eliminate optical distortion caused by the turbulence in the aircraft's boundary layer. A cyclic jet issuing from a spanwise slot is used to collect the turbulent boundary layer for a finite time and then release all of the flow instantaneously in one large eddy that convects downstream. Flow visualization and hot-film probe measurements are used together with pattern recognition algorithms to demonstrate the viability of the flow control method. A flat plate towed in a water channel is used as a test bed. The instantaneous velocity signal is used to compute important statistical quantities of the random velocity field, such as the mean, the root-mean-square, the spectral distribution, and the probability density function. When optimized for a given boundary layer, it is shown that the cyclic jet will produce periodic structures that are similar to the random, naturally occurring ones. These structures seem to trigger the onset of bursting events near the wall of the plate. Thus, the present device generates periodic structures in both the outer and inner regions of a turbulent boundary layer.
Author

N87-20504*# National Aeronautics and Space Administration. Lewis Research Center, Cleveland, Ohio.
A FINITE DIFFERENCE SCHEME FOR THREE-DIMENSIONAL STEADY LAMINAR INCOMPRESSIBLE FLOW
Danny P. Hwang and Hung T. Huynh 1987 16 p Proposed for presentation at the 5th International Conference on Numerical Methods in Laminar and Turbulent Flow, Montreal, Quebec, 6-10 Jul. 1987; sponsored by Concordia Univ., P and W Canada,

International Journal for Numerical Methods in Fluids
(NASA-TM-89851; E-3513; NAS 1.15:89851) Avail: NTIS HC A02/MF A01 CSCL 20D

A finite difference scheme for three-dimensional steady laminar incompressible flows is presented. The Navier-Stokes equations are expressed conservatively in terms of velocity and pressure increments (delta form). First order upwind differences are used for first order partial derivatives of velocity increments resulting in a diagonally dominant matrix system. Central differences are applied to all other terms for second order accuracy. The SIMPLE pressure correction algorithm is used to satisfy the continuity equation. Numerical results are presented for cubic cavity flow problems for Reynolds numbers up to 2000 and are in good agreement with other numerical results. Author

N87-20505# Sverdrup Technology, Inc., Arnold Air Force Station, Tenn.
CONVERSION OF ARO-1 TO AN IMPLICIT NAVIER-STOKES SOLVER Final Report, 1 Oct. 1983 - 1 Oct. 1986
Karl R. Kneile AEDC Dec. 1986 32 p
(AD-A175967; AEDC-TR-86-45) Avail: NTIS HC A03/MF A01 CSCL 20/4

The purpose of this report is to describe the development of an implicit Navier Stodes solver (KM1) based upon modification of an existing explicit Euler code known as ARO-1. The report narrates the steps of the conversion, relates the lessons learned along the way, and highlights the algorithm's advantages and shortcomings. The goal upon inception of this work was to develop an efficient Navier Stokes solver, capable of solving complex three dimensional (3 D) internal flow problems. It was to be modeled after the ARO-1 code because of ARO-1's established flexibility and robustness. While the KM1 code successfully solved the flow problems that were tried, it does not have the anticipated robustness that was expected. Considerable user interaction was required to obtain solutions for certain complex 3=D problems. The code has taken a backseat to a more robust code recently acquired. The KM1 code is still in its developmental form, and there are no plans for converting the code to a production format. GRA

N87-20506# Los Alamos National Lab., N. Mex.
APPLICATION OF A LASER-INDUCED BREAKDOWN TIME-OF-FLIGHT TECHNIQUE IN A FLOW DIAGNOSTIC IN A CO2 FREE-JET EXPANSION
P. J. Wantuck and D. E. Hof 1986 4 p Presented at the OSA/APS International Laser Science Conference, Seattle, Wash., 20 Oct. 1986
(Contract W-7405-eng-36)
(DE87-002890; LA-UR-86-4052; CONF-861038-1) Avail: NTIS HC A02/MF A01

A time-of-flight velocity technique utilizing ions formed by the process of laser-induced (1.064 microns) breakdown has been used to measure axial flow speeds in a CO2 free-jet expansion. For the nozzle stagnation pressure and temperature employed (p0 approx. = 200 torr, T0 approx. = 298K), the axial flow speed is on the order of 630 m/s. DOE

N87-20507# Lawrence Livermore National Lab., Calif.
CALCULATION OF RAYLEIGH-TAYLOR FLOWS USING VORTEX BLOBS
R. M. Kerr Oct. 1986 12 p Presented at the 3rd International Conference on Stratified Flows, Pasadena, Calif., 3 Feb. 1987
(Contract W-7405-eng-48)
(DE87-002551; UCRL-95629; CONF-870235-2) Avail: NTIS HC A02/MF A01

A modification of a boundary-integral method is used to study the single-scale Rayleigh-Taylor instability for arbitrary Atwood number. Smoothing the Green's function using vortex blobs suppresses singularities in the curvature and other modifications are designed to extend the calculation through several singular events. The method successfully follows the development of a single mode to states with asymptotic velocities for the bubble and spike that depend on Atwood number and are independent of the blob size. Incipient droplet formation is observed. DOE

N87-20508# Los Alamos National Lab., N. Mex.
A PREDICTOR-CORRECTOR METHOD FOR CALCULATION OF INCOMPRESSIBLE FLUID FLOW DYNAMICS
B. A. Kashiwa Nov. 1986 29 p
(Contract W-7405-eng-36)
(DE87-003804; LA-10854-MS) Avail: NTIS HC A03/MF A01

A new method for solution of the time-dependent, incompressible fluid conservation equations is presented. The method is distinguished from other computational techniques for incompressible flows by its use of the same control volume for mass and momentum, rather than mass and momentum control volumes that are staggered in space. Employing coincident control volumes for mass and momentum makes the velocity and pressure appear as cell-centered variables. The use of a cell-centered velocity and pressure is made possible by use of a predictor-corrector formulation that is implicit in the pressure term in both predictor and corrector phases of the computation. The particular predictor-corrector technique presented here is modeled after the method introduced by MacCormack for compressible flows. Hence, the scheme is second-order accurate in both space and time, and can be used on a computational grid of arbitrary polygons. In multiphase flow computations, use of coincident control volumes for both mass and momentum means that the velocity can be defined as the ratio of momentum per unit volume in a consistent fashion. DOE

N87-20509# Oak Ridge National Lab., Tenn.
ON THE USE OF CORLIB SUBROUTINES FOR THE SOLUTION OF A MODEL FLUID FLOW PROBLEM
S. Thompson Dec. 1986 58 p
(Contract DE-AC05-84OR-21400)
(DE87-005285; ORNL/TM-10038) Avail: NTIS HC A04/MF A01

This report describes the use of several subroutines from the CORLIB core mathematical subroutine library for the solution of a model fluid flow problem. The model consists of the Euler partial differential equations. The equations are spatially discretized using the method of pseudo-characteristics. The resulting system of ordinary differential equations is then integrated using the method of lines. The stiff ordinary differential equation solver LSODE (2) from CORLIB is used to perform the time integration. The non-stiff solver ODE (4) is used to perform a related integration. The linear equation solver subroutines DECOMP and SOLVE are used to solve linear systems whose solutions are required in the calculation of the time derivatives. The monotone cubic spline interpolation subroutines PCHIM and PCHFE are used to approximate water properties. The report describes the use of each of these subroutines in detail. It illustrates the manner in which modules from a standard mathematical software library such as CORLIB can be used as building blocks in the solution of complex problems of practical interest. DOE

N87-20510# European Space Agency, Paris (France).
NUMERICAL AND OPTICAL EXPERIMENTS ON THE WEISSENBERG EFFECT
Georg Eitelberg Nov. 1986 85 p Transl. into ENGLISH of "Numerische und Optische Experimente zum Weissenberg-Effekt" DFVLR, Goettingen, West Germany, report DFVLR-FB-84-04, 1984 Original language document was announced as N84-25992
(ESA-TT-879; DFVLR-FB-84-04; ETN-87-99425) Avail: NTIS HC A05/MF A01; original German version available from DFVLR, Cologne, West Germany DM 29.50

The axisymmetric creeping shear flow of a second order fluid in the annulus between two coaxially mounted cylinders, with the inner cylinder rotating, is studied. The shape of the free liquid surface, dependent on the material and geometry parameters, is numerically calculated and experimentally measured by means of holographic interferometry. Viscous heating and the existence of a secondary flow in the cylindrical geometry are considered. ESA

N87-20511# Office National d'Etudes et de Recherches Aerospatiales, Paris (France). Direction Scientifique de la Resistance des Structures.
TWO-DIMENSIONAL FLOW COMPUTATION IN STRAIGHT BLADE ARRAYS Final Report [CALCUL DES ECOULEMENTS BIDIMENSIONNELS EN GRILLE D'AUBES RECTILIGNES]
G. D. Mortchelewicz Mar. 1986 22 p In FRENCH
(Contract DRET-85-34-001)
(ONERA-RT-35/1621-RY-053-R; ETN-87-99388) Avail: NTIS HC A02/MF A01

The contribution of viscous effects to reducing turbomachinery flow stability is studied. The separation of the boundary layer at the leading edge is analyzed. A computation method is proposed to estimate the flow modifications starting from experimental pressure distribution data measured on a single blade or on a straight blade array. ESA

N87-20512# Centre d'Etudes Aerodynamiques et Thermiques, Poitiers (France). Lab. d'Etudes Aerodynamiques.
STUDY OF THE DEVELOPMENT OF A COMPRESSIBLE TURBULENT BOUNDARY LAYER ON A POROUS AND ROUGH WALL Final Report [ETUDE DU DEVELOPPEMENT D'UNE COUCHE LIMITE TURBULENTE COMPRESSIBLE SUR UNE PAROI RUGUEUSE ET POREUSE]
A. Stassinopoulos and R. Leblanc Jun. 1986 90 p In FRENCH
(Contract DRET-84-057)
(ETN-87-99390) Avail: NTIS HC A05/MF A01

A method to estimate the development of a boundary layer on a flat wall in the presence of mass transfer is studied. It follows the analysis of the interaction of a shock wave with a boundary layer subjected to either aspiration or blowing. The experimental set up, including mass transfer mechanisms, is described. The computational approach is based on finite difference theory. The efficiency of the proposed method to compute the turbulent boundary layer in the presence of mass transfer is discussed.ESA

N87-20513# Centre d'Etudes Aerodynamiques et Thermiques, Poitiers (France). Lab. d'Etudes Aerodynamiques.
EXPERIMENTAL EVALUATION OF SUB-CELL TURBULENT MODELS. SPACE-TIME CORRELATIONS IN A MIXING LAYER Final Report [EVALUATION EXPERMENTALE DES MODELES DE TURBULENCE SOUS-MAILLE. CORRELATIONS SPATIO-TEMPORELLES DANS UNE COUCHE DE MELANGE]
J. Delville, H. Garem, and J. P. Bonnet Jul. 1986 100 p In FRENCH
(Contract DRET-84-057)
(ETN-87-99391) Avail: NTIS HC A05/MF A01

In the frame of a larger program to solve the two dimensional unsteady Navier-Stokes equation using finite difference theory, an experimental study to optimize the measurements in the verification of sub-cell mixing layer models is presented. The problems involved are analyzed and discussed. The sensors used in anemometric measurements are described. The results constitute an experimental data base for model verification once the analysis tools are developed. The Townsend and the Lumley correlation analysis methods are discussed. Another study result is the definition of the limits of the equivalent filter concept. ESA

N87-20212# MATRA Service Aerodynamique, Velizy-Villacoublay (France).
SIMULATION OF A JET DEFLECTION SYSTEM WITH THE AID OF THE EULER EQUATIONS [SIMULATION D'UN SYSTEME DE DEVIATION DE JAT A L'AIDE DES EQUATIONS D'EULER]
M. Bredif, J. J. Chattot, C. Koeck, and P. Werle *In* AGARD Applications of Computational Fluid Dynamics in Aeronautics Nov. 1986 11 p In FRENCH (For primary document see N87-20199 13-02)
Avail: NTIS HC A19/MF A01

N87-20213# Dornier-Werke G.m.b.H., Friedrichshafen (West Germany). Theoretical Aerodynamic Group.
NUMERICAL SIMULATION OF INTERNAL AND EXTERNAL INVISCID AND VISCOUS 3-D FLOW FIELDS
Stefan Leicher *In* AGARD Applications of Computational Fluid Dynamics in Aeronautics Nov. 1986 27 p (For primary document see N87-20199 13-02)
Avail: NTIS HC A19/MF A01

N87-20222*# National Aeronautics and Space Administration. Ames Research Center, Moffett Field, Calif.
USING THE BOUNDARY-LAYER EQUATIONS IN THREE-DIMENSIONAL VISCOUS FLOW SIMULATION
William R. VanDalsem and Joseph L. Steger *In* AGARD Applications of Computational Fluid Dynamics in Aeronautics Nov. 1986 12 p Previously announced as N86-28061 (For primary document see N87-20199 13-02)
Avail: NTIS HC A19/MF A01

N87-20223# Office National d'Etudes et de Recherches Aeronautiques, Paris (France).
COMPUTATION OF THREE-DIMENSIONAL FLOWS BY VISCOUS-INVISCID INTERATION USING THE MZM METHOD
M. Lazareff and J. C. LeBalleur *In* AGARD Applications of Computational Fluid Dynamics in Aeronautics Nov. 1986 15 p In FRENCH; ENGLISH summary (For primary document see N87-20199 13-02)
Avail: NTIS HC A19/MF A01

N87-20270*# National Aeronautics and Space Administration. Lewis Research Center, Cleveland, Ohio.
MODELING TURBULENT, REACTIG FLOW
Russell W. Claus *In its* NASA-Chinese Aeronautical Establishment (CAE) Symposium 1986 p 31-46 (For primary document see N87-20267 13-07)
Avail: NTIS HC A01/MF A01 CSCL 20D

N87-20271*# Beijing Inst. of Aeronautics and Astronautics (China).
EXPERIMENTAL AND ANALYTICAL INVESTIGATION OF THE VARIATION OF SPRAY CHARACTERISTICS ALONG A RADIAL DISTANCE DOWNSTREAM OF A PRESSURE-SWIRL ATOMIZER
J. S. Chin, W. M. Li, and X. F. Wang *In* NASA- Lewis Research Center NASA-Chinese Aeronautical Establishment (CAE) Symposium 1986 p 47-62 (For primary document see N87-20267 13-07)
Avail: NTIS HC A01/MF A01 CSCL 20D

N87-20272*# National Aeronautics and Space Administration. Lewis Research Center, Cleveland, Ohio.
TWO-PHASE FLOW
Robert R. Tacina *In its* NASA-Chinese Aeronautical Establishment (CAE) Symposium 1986 p 63-87 (For primary document see N87-20267 13-07)
Avail: NTIS HC A01/MF A01 CSCL 20D

N87-20276*# National Aeronautics and Space Administration. Lewis Research Center, Cleveland, Ohio.
EXPERIMENTS AND MODELING OF DILUTION JET FLOW FIELDS
James D. Holdeman *In its* NASA-Chinese Aeronautical Establishment (CAE) Symposium 1986 p 149-174 (For primary document see N87-20267 13-07)
Avail: NTIS HC A01/MF A01 CSCL 20D

N87-20316*# National Aeronautics and Space Administration. Goddard Space Flight Center, Greenbelt, Md.
USC/AIAA STUDENT GET AWAY SPECIAL PROJECT LIQUID DROPLET COLLECTOR EXPERIMENT
Raymond J. LeVesque, II *In its* The 1986 Get Away Special Experimenter's Symposium Feb. 1987 p 95-102 (For primary document see N87-20302 13-12)
Avail: NTIS HC A11/MF A01 CSCL 20D

N87-20330*# Ecole Superieure d'Electricite, Gif-sur-Yvette (France). Lab. de Genie Electrique de Paris.
G-300: THE FIRST FRENCH GETAWAY SPECIAL MICROGRAVITY MEASUREMENTS OF FLUID THERMAL CONDUCTIVITY
J. C. Perron, P. Chretien, C. Garnier, and N. Lecaude *In* NASA.

Goddard Space Flight Center The 1986 Get Away Special Experimenter's Symposium Feb. 1987 p 199-206 Original language document was announced in IAA as A87-15974 (For primary document see N87-20302 13-12)
Avail: NTIS HC A11/MF A01 CSCL 20D

35 INSTRUMENTATION AND PHOTOGRAPHY

Includes remote sensors; measuring instruments and gages; detectors; cameras and photographic supplies; and holography.

For aerial photography see *43 Earth Resources and Remote Sensing.* For related information see also *06 Aircraft Instrumentation,* and *19 Spacecraft Instrumentation.*

N87-20514*# National Aeronautics and Space Administration. Langley Research Center, Hampton, Va.
A SIMPLIFIED METHOD FOR DETERMINING HEAT OF COMBUSTION OF NATURAL GAS
Jag J. Singh, Hoshang Chegini (Old Dominion Univ., Norfolk, Va.), and Gerald H. Mall (Computer Sciences Corp., Hampton, Va.) Apr. 1987 15 p
(NASA-TP-2682; L-16261; NAS 1.60:2682) Avail: NTIS HC A02/MF A01 CSCL 14B

A simplified technique for determination of the heat of combustion of natural gas has been developed. It is a variation of the previously developed technique wherein the carrier air, in which the test sample was burnt, was oxygen enriched to adjust the mole fraction of oxygen in the combustion product gases up to that in the carrier air. The new technique eliminates the need for oxygen enrichment of the experimental mixtures and natural gas samples and has been found to predict their heats of combustion to an uncertainty of the order of 1 percent. Author

N87-20515*# National Aeronautics and Space Administration. Lewis Research Center, Cleveland, Ohio.
PRETEST UNCERTAINTY ANALYSIS FOR CHEMICAL ROCKET ENGINE TESTS
Kenneth J. Davidian 1987 16 p Presented at the 33rd International Instrumentation Symposium, Las Vegas, Nev., 3-8 May 1987; sponsored by the Instrument Society of America
(NASA-TM-89819; E-3465; NAS 1.15:89819) Avail: NTIS HC A02/MF A01 CSCL 14B

A parametric pretest uncertainty analysis has been performed for a chemical rocket engine test at a unique 1000:1 area ratio altitude test facility. Results from the parametric study provide the error limits required in order to maintain a maximum uncertainty of 1 percent on specific impulse. Equations used in the uncertainty analysis are presented. Author

N87-20516*# National Aeronautics and Space Administration. Lewis Research Center, Cleveland, Ohio.
A COMPUTER CONTROLLED SIGNAL PREPROCESSOR FOR LASER FRINGE ANEMOMETER APPLICATIONS
Lawrence G. Oberle Mar. 1987 28 p Presented at the Conference on the Use of Computers in Laser Velocimetry, Saint-Louis, France
(NASA-TM-88982; E-3452; NAS 1.15:88982) Avail: NTIS HC A03/MF A01 CSCL 14B

The operation of most commercially available laser fringe anemometer (LFA) counter-processors assumes that adjustments are made to the signal processing independent of the computer used for reducing the data acquired. Not only does the researcher desire a record of these parameters attached to the data acquired, but changes in flow conditions generally require that these settings be changed to improve data quality. Because of this limitation, on-line modification of the data acquisition parameters can be difficult and time consuming. A computer-controlled signal preprocessor has been developed which makes possible this optimization of the photomultiplier signal as a normal part of the data acquisition process. It allows computer control of the filter selection, signal gain, and photo-multiplier voltage. The raw signal from the photomultiplier tube is input to the preprocessor which, under the control of a digital computer, filters the signal and amplifies it to an acceptable level. The counter-processor used at Lewis Research Center generates the particle interarrival times, as well as the time-of-flight of the particle through the probe volume. The signal preprocessor allows computer control of the acquisition of these data.Through the preprocessor, the computer also can control the hand shaking signals for the interface between itself and the counter-processor. Finally, the signal preprocessor splits the pedestal from the signal before filtering, and monitors the photo-multiplier dc current, sends a signal proportional to this current to the computer through an analog to digital converter, and provides an alarm if the current exceeds a predefined maximum. Complete drawings and explanations are provided in the text as well as a sample interface program for use with the data acquisition software. Author

N87-20517*# National Aeronautics and Space Administration. Langley Research Center, Hampton, Va.
AERODYNAMIC MEASUREMENTS AND THERMAL TESTS OF A STRAIN-GAGE BALANCE IN A CRYOGENIC WIND TUNNEL
Richmond P. Boyden, Alice T. Ferris, William G. Johnson, Jr., David A. Dress, and Acquilla S. Hill Apr. 1987 87 p
(NASA-TM-89039; L-16208; NAS 1.15:89039) Avail: NTIS HC A05/MF A01 CSCL 14B

An internal strain-gage balance designed and constructed in Europe for use in cryogenic wind tunnels has been tested in the Langley 0.3-Meter Transonic Cryogenic Tunnel. Part of the evaluation was made at equilibrium balance temperatures and it consisted of comparing the data taken at a tunnel stagnation temperature of 300 K with the data taken at 200 K and 110 K while maintaining either the Reynolds number or the stagnation pressure. A sharp-leading-edge delta-wing model was used to provide the aerodynamic loading for these tests. Results obtained with the balance during the force tests were found to be accurate and repeatable both with and without the use of a convection shield on the balance. An additional part of this investigation involved obtaining data on the transient temperature response of the balance during both normal and rapid changes in the tunnel stagnation temperature. The variation of the temperature with time was measured at three locations on the balance near the physical locations of the strain gages. The use of a convection shield significantly increased the time required for the balance to stabilize at a new temperature during the temperature response tests.
Author

N87-20518# State Univ. of New York, Buffalo.
PROGRESS IN THE DEVELOPMENT OF HOLOGRAPHIC SCHEME FOR PAIR CORRELATION ESTIMATION Final Report 10 Sep. 1984 - 9 Sep. 1986
Peter D. Scott and David T. Shaw 1 Nov. 1986 39 p Prepared in cooperation with Southeastern Center for Electrical Engineering Education, Inc., St. Cloud, Fla.
(Contract DAAG29-84-K-0199)
(AD-A175573; ARO-21818.4-GS) Avail: NTIS HC A03/MF A01 CSCL 20/6

Progress on the development of a methodology for estimation of pair correlation function from holographic data is reviewed. During the reported grant year, efforts have focused on the automation of holographic data reduction and extension of our previously reported digital signal processing approach to the splitbeam (off axis) case. The former is a necessary prerequisite to insure objective, accurate, and cost effective use of holograms, while the latter permits somewhat higher densities than the on axis technique. GRA

N87-20519 Department of the Air Force, Washington, D.C.
DIFFRACTION DIFFUSION SCREEN WITH HOLOGRAPHICALLY SUPPRESSED ZERO-ORDER BEAM Patent
Mao-Jin Chern, inventor (to Air Force) and Ronald T. Smith, inventor (to Air Force) Issued 9 Sep. 1986 6 p Supersedes N85-19387,

AD-D011445 (25 - 10, p 1487)
(AD-D012565; US-Patent-4,610,499; US-Patent-Appl-SN-667194; US-Patent-Class-350-37) Avail: US Patent and Trademark Office CSCL 20/6

A diffusing screen of a transmission hologram located adjacent to a diffraction optics directional diffusing screen suppresses zero order light from the diffusing screen thereby providing a device having the advantages of a directional diffusing screen but which does not have the disadvantages associated with zero order light. GRA

N87-20520 Department of the Air Force, Washington, D.C.
ATMOSPHERIC CONTRAST TRANSMITTANCE MONITOR Patent
Richard W. Johnson, inventor (to Air Force) Issued 30 Sep. 1986 7 p Supersedes N84-34083, AD-D011167 (22 - 23, p 3798)
(AD-D012555; US-Patent-4,614,429; US-Patent-Appl-SN-610142) Avail: US Patent and Trademark Office CSCL 20/6

An atmospheric contrast transmittance monitor is described which comprises an electro-optical system including three solid state transducer assemblies interfaced with a small dedicated microcompressor for control of the system in either semi-automatic or operator interactive modes for real time monitoring of the optical state of the atmosphere, one assembly comprising a compact multi-channel nephelometer of novel configuration for providing directional volume scattering function measurements on atmospheric samples, and a pair of staring fisheye lens scanners and associated detectors for scanning the upper and lower hemisphere radiance distributions. The system requires only a few hundred watts of input power and is less than one meter in length overall, and, operating in pulsed mode, has been used to measure the scattering characteristics of clear-day room air, with adequate sensitivity to suggest the capability of measurements approaching .00001/m i.e., sea level molecular. Author (GRA)

N87-20521# Technische Univ., Brunswick (West Germany). Naturwissenschaftlichen Fakultaet.
PRELIMINARY EXAMINATION OF THE CONSTRUCTION OF LASER GYROSCOPES WITH REDUCED LOCK-IN THRESHOLD Ph.D. Thesis [VORUNTERSUCHUNGEN ZUM AUFBAU VON LASERKREISELN MIT VERMINDERTER LOCK-IN-SCHWELLE]
Rolf Gauert 1985 173 p In GERMAN
(ETN-87-99016) Avail: NTIS HC A08/MF A01

Ring laser equations were evaluated with a view to the lock-in threshold. Lock-in threshold measurements were performed on two different ring lasers backscattering on laser mirrors was investigated. The examination of the differential stability shows that the calculated lock-in threshold largely corresponds to the limit between the stable and unstable state as described by the ring laser equation system. The difficulties involved in solving this equation system are pointed out; further investigations are required to develop suitable algorithms. ESA

N87-20180# Norges Tekniske Hoegskole, Trondheim. Dept. of Physics.
TV-HOLOGRAPHY: A PROMISING INSPECTION TOOL FOR ANALYSIS OF COMPOSITE MATERIALS
Ole J. Lokberg, Jan T. Malmo, and Arvid Strand (Conspectum A/S, Trondheim, Norway.) *In* AGARD The Repair of Aircraft Structures Involving Composite Materials Oct. 1986 7 p (For primary document see N87-20174 13-01)
Avail: NTIS HC A11/MF A01

N87-20279*# National Aeronautics and Space Administration. Lewis Research Center, Cleveland, Ohio.
THE CHEMICAL SHOCK TUBE AS A TOOL FOR STUDYING HIGH-TEMPERATURE CHEMICAL KINETICS
Theodore A. Brabbs *In its* NASA-Chinese Aeronautical Establishment (CAE) Symposium 1986 p 207-224 (For primary document see N87-20267 13-07)
Avail: NTIS HC A01/MF A01 CSCL 14B

N87-20359# MATRA Espace, Toulouse (France). Dept. of Satellite Engineering.
QUALIFICATION OF THE FAINT OBJECT CAMERA
Patrice Amadieu *In* AGARD Mechanical Qualification of Large Flexible Spacecraft Structures Jul. 1986 13 p (For primary document see N87-20355 13-18)
Avail: NTIS HC A12/MF A01

N87-20447# Joint Publications Research Service, Arlington, Va.
ORGANIC PHOTOCHROMIC MATERIAL FOR RECORDING WAVEGUIDE HOLOGRAMS
Yu. A. Bykovskiy, V. A. Barachevskiy, Yu. V. Borodakiy, V. M. Kozenkov, V. L. Smirnov, and Yu. V. Shulev *In its* USSR Report: Physics and Mathematics 26 Jun. 1986 p 74-78 Transl. into ENGLISH from Kvantovaya Elektronika (Moscow, USSR), v. 11, no. 6, Jun. 1984 p 1250-1253 (For primary document see N87-20445 13-31)
Avail: NTIS HC A07/MF A01

N87-20439# Carnegie-Mellon Univ., Pittsburgh, Pa. Dept. of Mechanical Engineering.
THE DIGITAL PROCESSING OF ACCELERATION MEASUREMENTS FOR MODAL ANALYSIS
C. W. deSilva *In* Shock and Vibration Information Center The Shock and Vibration Digest, Volume 18, No. 10 Oct. 1986 p 3-11 (For primary document see N87-20438 13-31)
Avail: NTIS HC A05/MF A01 CSCL 14/2

N87-20608# Wilson (Jon), San Juan Capistrano, Calif.
STATE-OF-THE-ART ACCELEROMETER CHARACTERISTICS FOR PYROTECHNIC SHOCK MEASUREMENT
Jon Wilson *In* Shock and Vibration Information Center The Shock and Vibration Bulletin. Part 3: Invited Papers, Pyrotechnic Shock, Pyrotechnic Shock Workshop Aug. 1986 p 71-76 (For primary document see N87-20602 13-39)
Avail: NTIS HC A07/MF A01 CSCL 14/2

N87-20609# TRW Electronics and Defense Sector, Redondo Beach, Calif.
ZERO-SHIFTED ACCELEROMETER OUTPUTS
Arnold Galef *In* Shock and Vibration Information Center The Shock and Vibration Bulletin. Part 3: Invited Papers, Pyrotechnic Shock, Pyrotechnic Shock Workshop Aug. 1986 p 77-80 (For primary document see N87-20602 13-39)
Avail: NTIS HC A07/MF A01 CSCL 14/2

36 LASERS AND MASERS

Includes parametric amplifiers.
For related information see also *76 Solid-State Physics.*

N87-20522*# National Aeronautics and Space Administration. Langley Research Center, Hampton, Va.
CLOSED-CYCLE, FREQUENCY-STABLE CO2 LASER TECHNOLOGY
Carmen E. Batten, ed., Irvin M. Miller, ed., George M. Wood, Jr., ed., and David V. Willetts, ed. (Royal Signals and Radar Establishment, Malvern, England.) Apr. 1987 279 p Workshop held in Hampton, Va., 10-12 Jun. 1986
(NASA-CP-2456; L-16271; NAS 1.55:2456) Avail: NTIS HC A13/MF A01 CSCL 20E

These proceedings contain a collection of papers and comments presented at a workshop on technology associated with long-duration closed-cycle operation of frequency-stable, pulsed carbon dioxide lasers. This workshop was held at the NASA Langley Research Center June 10 to 12, 1986. The workshop, jointly sponsored by the National Aeronautics and Space Administration (NASA) and the Royal Signals and Radar Establishment (RSRE), was attended by 63 engineers and scientists from the United States and the United Kingdom. During the 2 1/2 days of the workshop, a number of issues relating to obtaining frequency-stable operation and to the catalytic control of laser gas chemistry were discussed, and specific recommendations concerning future

activities were drafted. For individual titles, see N87-20523 through N87-20542.

N87-20523*# Royal Signals and Radar Establishment, Malvern (England).
REVIEW OF THE FREQUENCY STABILIZATION OF TEA CO2 LASER OSCILLATORS
David V. Willetts *In* NASA. Langley Research Center Closed-Cycle, Frequency-Stable CO2 Laser Technology Apr. 1987 p 11-21 (For primary document see N87-20522 13-36)
Avail: NTIS HC A13/MF A01 CSCL 20E

Most applications of TEA CO2 lasers in heterodyne radar systems require that the transmitter has a high degree of frequency stability. This ensures good Doppler resolution and maximizes receiver sensitivity. However, the environment within the device is far from benign with fast acoustic and electrical transients being present. Consequently the phenomena which govern the frequency stability of pulsed lasers are quite different from those operative in their CW counterparts. This review concentrates on the mechanisms of chirping within the output pulse; pulse to pulse frequency drift may be eliminated by frequency measurement and correction on successive pulses. It emerges that good stability hinges on correct cavity design. The energy-dependent laser-induced frequency sweep falls dramatically as mode diameter is increased. Thus, it is necessary to construct resonators with good selectivity for single mode operation while having a large spot size. Author

N87-20524*# Royal Signals and Radar Establishment, Malvern (England).
LARGE MODE RADIUS RESONATORS
Michael R. Harris *In* NASA. Langley Research Center Closed-Cycle, Frequency-Stable CO2 Laser Technology Apr. 1987 p 23-31 (For primary document see N87-20522 13-36)
Avail: NTIS HC A13/MF A01 CSCL 20E

Resonator configurations permitting operation with large mode radius while maintaining good transverse mode discrimination are considered. Stable resonators incorporating an intracavity telescope and unstable resonator geometries utilizing an output coupler with a Gaussian reflectivity profile are shown to enable large radius single mode laser operation. Results of heterodyne studies of pulsed CO2 lasers with large (11mm e sup-2 radius) fundamental mode sizes are presented demonstrating minimal frequency sweeping in accordance with the theory of laser-induced medium perturbations. Author

N87-20525*# National Aeronautics and Space Administration. Marshall Space Flight Center, Huntsville, Ala.
WIND VELOCITY MEASUREMENT ACCURACY WITH HIGHLY STABLE 12 mJ/PULSE HIGH REPETITION RATE CO2 LASER MASTER OSCILLATOR POWER AMPLIFIER
James W. Bilbro, Steven C. Johnson, and Jeffry Rothermel (Universities Space Research Association, Huntsville, Ala.) *In* NASA. Langley Research Center Closed-Cycle, Frequency-Stable CO2 Laser Technology Apr. 1987 p 33-45 (For primary document see N87-20522 13-36)
Avail: NTIS HC A13/MF A01 CSCL 20E

A coherent CO2 lidar operating in a master oscillator power amplifier configuration (MOPA) is described for both ground-based and airborne operation. Representative data taken from measurements against stationary targets in both the ground-based and airborne configurations are shown for the evaluation of the frequency stability of the system. Examples of data are also given which show the results of anomalous system operation. Overall results demonstrate that velocity measurements can be performed consistently to an accuracy of + or - 0.5 m/s and in some cases + or - 0.1 m/s. Author

N87-20526*# Spectra Technology, Inc., Bellevue, Wash.
ANALYSIS OF INTRAPULSE CHIRP IN CO2 OSCILLATORS
Stephen E. Moody, Russell G. Berger, and William J. Thayer, III *In* NASA. Langley Research Center Closed-Cycle, Frequency-Stable CO2 Laser Technology Apr. 1987 p 47-53 (For primary document see N87-20522 13-36)
Avail: NTIS HC A13/MF A01 CSCL 20E

Pulsed single-frequency CO2 laser oscillators are often used as transmitters for coherent lidar applications. These oscillators suffer from intrapulse chirp, or dynamic frequency shifting. If excessive, such chirp can limit the signal-to-noise ratio of the lidar (by generating excess bandwidth), or limit the velocity resolution if the lidar is of the Doppler type. This paper describes a detailed numerical model that considers all known sources of intrapulse chirp. Some typical predictions of the model are shown, and simple design rules to minimize chirp are proposed. Author

N87-20527*# Jet Propulsion Lab., California Inst. of Tech., Pasadena.
FREQUENCY STABILIZATION IN INJECTION CONTROLLED PULSED CO2 LASERS
Robert T. Menzies and Gerard M. Ancellet *In* NASA. Langley Research Center Closed-Cycle, Frequency-Stable CO2 Laser Technology Apr. 1987 p 55-63 (For primary document see N87-20522 13-36)
Avail: NTIS HC A13/MF A01 CSCL 20E

Longitudinal mode selection by injection has been demonstrated as a viable technique for tailoring a TEA-CO2 laser with pulse energies of a Joule or greater to fit the requirements of a coherent lidar transmitter. Once reliable generation of single-longitudinal-mode (SLM) pulses is obtained, one can study the intrapulse frequency variation and attempt to determine the sources of frequency sweeping, or chirp. These sources include the effect of the decaying plasma, the thermal gradient due to the energy dissipation associated with the laser mechanism itself, and the pressure shift of the center frequency of the laser transition. The use of the positive-branch unstable resonator as an efficient means of coupling a discharge with transverse spatial dimensions of the order of centimeters to an optical cavity mode introduces another concern: namely, what can be done to emphasize transverse mode discrimination in an unstable resonator cavity while maintaining high coupling efficiency. These issues are briefly discussed in the paper, and representative experimental examples are included. Author

N87-20528*# United Kingdom Atomic Energy Authority, Harwell (England).
THE OXIDATION OF CARBON MONOXIDE USING A TIN OXIDE CATALYST
Christopher F. Sampson and Nicholas J. Gudde *In* NASA. Langley Research Center Closed-Cycle, Frequency-Stable CO2 Laser Technology Apr. 1987 p 65-76 (For primary document see N87-20522 13-36)
Avail: NTIS HC A13/MF A01 CSCL 20E

This paper outlines some of the steps involved in the development by the United Kingdom Atomic Energy Authority (UKAEA) of a catalytic device for the recombination of carbon monoxide and oxygen in a CO2 laser system. It contrasts the differences between CO oxidation for air purification and for laser environmental control, but indicates that there are similarities between the physical specifications. The principal features of catalytic devices are outlined and some experimental work described. This includes measurements concerning the structure and mechanical properties of the artifact, the preparation of the catalyst coating and its interaction with the gaseous environment. The paper concludes with some speculation about the method by which the reaction actually occurs. Author

N87-20529*# Marconi Avionics Ltd., Borehamwood (England). Applied Physics Div.
HIGH REPETITION RATE SEALED CO2 TEA LASERS USING HETEROGENEOUS CATALYSTS
H. T. Price and S. R. Shaw *In* NASA. Langley Research Center Closed-Cycle, Frequency-Stable CO2 Laser Technology Apr. 1987 p 77-84 Sponsored by DCVD (For primary document see N87-20522 13-36)
Avail: NTIS HC A13/MF A01 CSCL 20E

The significant operational advantages offered by CO2 lasers,

operating in the 10.6 micron region of the spectrum, over current solid state lasers, emitting in the near IR region, have prompted increased interest in the development of compact, reliable, rugged CO2 laser sources. Perhaps the most critical aspect associated with achieving a laser compatible with military use is the development of lasers which require no gas replenishment. Sealed, single shot, CO2 TEA lasers have been available for a number of years. Stark et al were first to demonstrate reliable sealed operation in single shot CO2 TEA lasers in 1975 using gas catalysis. GEC Avionics reported the compact, environmentally qualified, MKIII CO2 TEA laser with a pulse life of greater than 10 to the 6th power pulses in 1980. A sealed laser lifetime of greater than 10 to the 6th power pulses is acceptable for single shot cases, such as direct detection rangefinders for tank laser sights. However, in many other applications, such as tracking of fast moving targets, it is essential that a repetition rate of typically 30Hz to 100Hz is employed. In such cases, a pulse lifetime of 10 to the 6th power pulses is no longer sufficient and a minimum pulse lifetime 10 to the 7th power pulses is essential to ensure a useful service life. In 1983 Stark el al described a sealed, 100Hz CO2 TEA laser, with a life of greater than 2.6 x 10 to the 6th power, which employed heterogeneous catalysis. Following this pioneering work, GEC Avionics has been engaged in the development of sealed high repetition rate lasers with a pulse lifetime of 20 million pulses.

Author

N87-20530*# Illinois Univ., Chicago.

CO OXIDATION STUDIES OVER SUPPORTED NOBLE METAL CATALYSTS AND SINGLE CRYSTALS: A REVIEW

Dirk Boecker and Richard D. Gonzalez *In* NASA. Langley Research Center Closed-Cycle, Frequency-Stable CO2 Laser Technology Apr. 1987 p 85-102 (For primary document see N87-20522 13-36)
Avail: NTIS HC A13/MF A01 CSCL 20E

The catalytic oxidation of CO over noble metal catalysts is reviewed. Results obtained on supported noble metal catalysts and single crystals both at high pressures and under UHV conditions are compared. The underlying causes which result in surface instabilities and multiple steady-state oscillations are considered, in particular, the occurrence of hot spots. CO islands of reactivity, surface oxide formation and phase transformations under oscillatory conditions are discussed. Author

N87-20531*# California Univ., San Diego, La Jolla. Dept. of Chemical Engineering.

CHEMICAL ENGINEERING DESIGN OF CO OXIDATION CATALYSTS

Richard K. Herz *In* NASA. Langley Research Center Closed-Cycle, Frequency-Stable CO2 Laser Technology Apr. 1987 p 103-112 (For primary document see N87-20522 13-36)
Avail: NTIS HC A13/MF A01 CSCL 20E

How a chemical reaction engineer would approach the challenge of designing a CO oxidation catalyst for pulsed CO2 lasers is described. CO oxidation catalysts have a long history of application, of course, so it is instructive to first consider the special requirements of the laser application and then to compare them to the characteristics of existing processes which utilize CO oxidation catalysts. All CO2 laser applications require a CO oxidation catalyst with the following characteristics: (1) active at stoichiometric ratios of O2 and CO, (2) no inhibition by CO2 or other components of the laser environment, (3) releases no particulates during vibration or thermal cycling, and (4) long lifetime with a stable activity. In all applications, low consumption of power is desirable, a characteristic especially critical in aerospace applications and, thus, catalyst activity at low temperatures is highly desirable. High power lasers with high pulse repetition rates inherently require circulation of the gas mixture and this forced circulation is available for moving gas past the catalyst. Low repetition rate lasers, however, do not inherently require gas circulation, so a catalyst that did not require such circulation would be favorable from the standpoint of minimum power consumption. Lasers designed for atmospheric penetration of their infrared radiation utilize CO2 formed from rare isotopes of oxygen and this application has the additional constraint that normal abundance oxygen isotopes in the catalyst must not exchange with rare isotopes in the gas mixture. Author

N87-20532*# National Aeronautics and Space Administration. Langley Research Center, Hampton, Va.

CATALYSTS FOR LONG-LIFE CLOSED-CYCLE CO2 LASERS

David R. Schryer, Barry D. Sidney, Irvin M. Miller, Robert V. Hess, George M. Wood, Carmen E. Batten, Lewis G. Burney, Ronald F. Hoyt, Patricia A. Paulin, Kenneth G. Brown (Old Dominion Univ., Norfolk, Va.) et al *In its* Closed-Cycle, Frequency-Stable CO2 Laser Technology Apr. 1987 p 113-119 (For primary document see N87-20522 13-36)
Avail: NTIS HC A13/MF A01 CSCL 20E

Long-life, closed-cycle operation of pulsed CO2 lasers requires catalytic CO-O2 recombination both to remove O2, which is formed by discharge-induced CO2 decomposition, and to regenerate CO2. Platinum metal on a tin (IV) oxide substrate (Pt/SnO2) has been found to be an effective catalyst for such recombination in the desired temperature range of 25 to 100 C. This paper presents a description of ongoing research at NASA-LaRC on Pt/SnO2 catalyzed CO-O2 recombination. Included are studies with rare-isotope gases since rare-isotope CO2 is desirable as a laser gas for enhanced atmospheric transmission. Results presented include: (1) achievement of 98% to 100% conversion of a stoichiometric mixture of CO and O2 to CO2 for 318 hours (greater than 1 x 10 to the 6th power seconds), continuous, at a catalyst temperature of 60 C, and (2) development of a technique verified in a 30-hour test, to prevent isotopic scrambling when CO-18 and O-18(2) are reacted in the presence of a common-isotope Pt/Sn O-16(2) catalyst. Author

N87-20533*# Pennsylvania State Univ., University Park. Dept. of Chemical Engineering.

STRONG METAL-SUPPORT INTERACTIONS

M. Albert Vannice *In* NASA. Langley Research Center Closed-Cycle, Frequency-Stable CO2 Laser Technology Apr. 1987 p 121-140 (For primary document see N87-20522 13-36)
Avail: NTIS HC A13/MF A01 CSCL 20E

It has been demonstrated that synergistic metal-support effects can occur which markedly enhance specific activity and alter selectivity in certain reactions. Because of the presence of such effects in certain reactions conducted under reducing conditions (that is, under H2 pressure), but not others, the creation of unique sites at the metal-support interface seems to be the best model at the present time to explain this behavior. The postulation of these sites, which are specific for a certain reactant such as CO, provides an effective explanation for the higher methanation rates that have been reported over some catalysts. The creation of these sites in the adlineation zone is facilitated by hydrogen spillover from the metal surface, and this same process can also enhance the reduction of many oxide supports. Although oxygen spillover is much less probable due to its higher heat of adsorption, it is much less well understood and the possibility of rate enhancements in CO oxidation caused by special interface sites cannot be discounted at the present time. Consequently, this seems to be an important area of future research. Author

N87-20534*# University of Southern California, Los Angeles. Dept. of Chemical Engineering.

REACTION RATE OSCILLATIONS DURING CATALYTIC CO OXIDATION: A BRIEF OVERVIEW

T. T. Tsotsis and R. C. Sane *In* NASA. Langley Research Center Closed-Cycle, Frequency-Stable CO2 Laser Technology Apr. 1987 p 141-152 (For primary document see N87-20522 13-36)
Avail: NTIS HC A13/MF A01 CSCL 20E

It is not the intent here to present a comprehensive review of the dynamic behavior of the catalytic oxidation of CO. This reaction is one of the most widely studied in the field of catalysis. A review paper by Engel and Ertl has examined the basic kinetic and mechanistic aspects, and a comprehensive paper by Razon and Schmitz was recently devoted to its dynamic behavior. Those interested in further study of the subject should consult these reviews and a number of general review papers on catalytic reaction

dynamics. The goal is to present a brief overview of certain interesting aspects of the dynamic behavior of this reaction and to discuss a few questions and issues, which are still the subject of study and debate. Author

N87-20535*# Teledyne Water Pik, Fort Collins, Colo. Research and Development.
CHARACTERIZATION OF THE LTC CATALYST: PERFORMANCE AGAINST COMMON AIR POLLUTANTS
Marcia F. Collins *In* NASA. Langley Research Center Closed-Cycle, Frequency-Stable CO2 Laser Technology Apr. 1987 p 153-163 (For primary document see N87-20522 13-36)
Avail: NTIS HC A13/MF A01 CSCL 20E

One of the important qualities of the Low-Temperature Catalyst (LTC) is the rapid oxidation of carbon monoxide to carbon dioxide under a wide variety of conditions. The catalytic material is a palladium-copper activated complex which reacts with various contaminant molecules through a continuous oxidation/reduction cycle. The alumina substrate enhances LTC activity with its favorable surface chemistry and very high surface area. About 10 percent surface water is necessary to facilitate the oxidation of CO. This reaction shows a log-log dependence on contact time, suggesting a Langmuir-Hinshelwood mechanism. In the tube tests, LTC removed 90 to 100 percent of contaminating carbon monoxide in the temperature region of 20 to 4000 C, and at ambient over a range of 25 to 65 percent relative humidity. In contrast, NO2 is chemisorbed by the LTC/alumina material--the amount strongly dependent on temperature increases but independent of humidity. The LTC catalyst has demonstrated excellent capability to remove an important variety of hazardous pollutant gases which are common factors to poor indoor air quality. The Instapure Air Filtration System incorporates the LTC catalyst in a 50:50 mixture with activated carbon to effectively remove particulate, odors, and hazardous gases at room temperature and humidities. The ability to remove hazardous gases is unique for the category of portable air filtration equipment. The wide variety of pollutant gases that LTC removes suggests that catalytic technology is adaptable to a considerable range of commercial and industrial applications.
Author

N87-20536*# General Motors Research Labs., Warren, Mich. Physical Chemistry Dept.
ALUMINA-SUPPORTED Pd-Ag CATALYSTS FOR LOW-TEMPERATURE CO AND METHANOL OXIDATION
R. W. McCabe *In* NASA. Langley Research Center Closed-Cycle, Frequency-Stable CO2 Laser Technology Apr. 1987 p 165-178 (For primary document see N87-20522 13-36)
Avail: NTIS HC A13/MF A01 CSCL 20E

Pd-Ag bimetallic catalysts, supported on gamma-Al2O3, have been evaluated as exhaust catalysts for methanol-fueled vehicles. Laboratory studies have shown that a 0.01% Pd-5% Ag catalyst has greater CO and CH3OH oxidation activity than either 0.01% Pd or 5% Ag catalysts alone. Moreover, Pd and Ag interact synergistically in the bimetallic catalyst to produce greater CO and CH3OH oxidation rates and lower yields of methanol partial oxidation products than expected from a mixture of the single-component catalysts. The Pd-Ag synergism results from Pd promoting the rate of O2 adsorption and reaction with CO and CH3OH on Ag. Rate enhancement by the bimetallic catalyst is greatest at short reactor residence times where the oxygen adsorption rate limits the overall reaction rate. Author

N87-20537*# Florida Univ., Gainesville. Dept. of Chemical Engineering.
A REVIEW OF TIN OXIDE-BASED CATALYTIC SYSTEMS: PREPARATION, CHARACTERIZATION AND CATALYTIC BEHAVIOR
Gar B. Hoflund *In* NASA. Langley Research Center Closed-Cycle, Frequency-Stable CO2 Laser Technology Apr. 1987 p 179-192 (For primary document see N87-20522 13-36)
Avail: NTIS HC A13/MF A01 CSCL 20E

This paper reviews the important aspects of the preparation, characterization and catalytic behavior of tin oxide-based catalytic systems including doped tin oxide, mixed oxides which contain tin oxide, Pt supported on tin oxide and Pt/Sn supported on alumina. These systems have a broad range of applications and are continually increasing in importance. However, due to their complex nature, much remains to be understood concerning how they function catalytically. Author

N87-20538*# National Aeronautics and Space Administration. Langley Research Center, Hampton, Va.
RARE ISOTOPE STUDIES INVOLVING CATALYTIC OXIDATION OF CO OVER PLATINUM-TIN OXIDE
Billy T. Upchurch (Science and Technology Corp., Hampton, Va.), George M. Wood, Jr., Robert V. Hess, and Ronald F. Hoyt *In its* Closed-Cycle, Frequency-Stable CO2 Laser Technology Apr. 1987 p 193-197 (For primary document see N87-20522 13-36)
Avail: NTIS HC A13/MF A01 CSCL 20E

Results of studies utilizing normal and rare oxygen isotopes in the catalytic oxidation of carbon monoxide over a platinum-tin oxide catalyst substrate are presented. Chemisorption of labeled carbon monoxide on the catalyst followed by thermal desorption yielded a carbon dioxide product with an oxygen-18 composition consistent with the formation of a carbonate-like intermediate in the chemisorption process. The efficacy of a method developed for the oxygen-18 labeling of the platinum-tin oxide catalyst surface for use in closed cycle pulsed care isotope carbon dioxide lasers is demonstrated for the equivalent of 10 to the 6th power pulses at 10 pulses per second. Author

N87-20539*# National Aeronautics and Space Administration. Langley Research Center, Hampton, Va.
STUDIES OF CO OXIDATION ON Pt/SnO2 CATALYST IN A SURROGATE CO2 LASER FACILITY
Carmen E. Batten, Irvin M. Miller, Patricia A. Paulin, and Jacqueline Schryer (Old Dominion Univ., Norfolk, Va.) *In its* Closed-Cycle, Frequency-Stable CO2 Laser Technology Apr. 1987 p 199-209 (For primary document see N87-20522 13-36)
Avail: NTIS HC A13/MF A01 CSCL 20E

Samples of 1% Pt/SnO2 catalyst were exposed to a stoichiometric gas mixture of 1% CO and 1.2% O2 in helium over a range of flowrates from 5 to 15 sccm and temperatures from 338 to 394 Kelvin. Reaction rate constants for the catalytic oxidation of carbon monoxide and their temperature dependence were determined and compared with previous literature values. Author

N87-20540*# National Aeronautics and Space Administration. Langley Research Center, Hampton, Va.
STUDIES OF LONG-LIFE PULSED CO2 LASER WITH Pt/SnO2 CATALYST
Barry D. Sidney *In its* Closed-Cycle, Frequency-Stable CO2 Laser Technology Apr. 1987 p 211-218 (For primary document see N87-20522 13-36)
Avail: NTIS HC A13/MF A01 CSCL 20E

Closed-cycle CO2 laser testing with and without a catalyst and with and without CO addition indicate that a catalyst is necessary for long-term operation. Initial results indicate that CO addition with a catalyst may prove optimal, but a precise gas mix has not yet been determined. A long-term run of 10 to the 6th power pulses using 1.3% added CO and a 2% Pt on SnO2 catalyst yields an efficiency of about 95% of open-cycle steady-state power. A simple mathematical analysis yields results which may be sufficient for determining optimum running conditions. Future plans call for testing various catalysts in the laser and longer tests, 10 to the 7th power pulses. A Gas Chromatograph will be installed to measure gas species concentration and the analysis will be slightly modified to include neglected but possibly important parameters. Author

N87-20541*# National Aeronautics and Space Administration. Langley Research Center, Hampton, Va.
CHARACTERIZATION OF Pt/SnO2 CATALYSTS FOR CO OXIDATION
K. G. Brown (Old Dominion Univ., Norfolk, Va.), J. Schryer, D. R. Schryer, B. T. Upchurch (Science and Technology Corp., Hampton,

Va.), G. M. Wood, I. M. Miller, B. D. Sidney, C. E. Batten, and P. A. Paulin *In its* Closed-Cycle, Frequency-Stable CO2 Laser Technology Apr. 1987 p 219-225 (For primary document see N87-20522 13-36)
Avail: NTIS HC A13/MF A01 CSCL 20E

Results are presented of surface characterization of 2% and 1% (w/w) Pt on SnO2 catalysts which are being used in promoting the oxidation of CO in pulsed CO2 lasers. The N2 adsorption BET surface area for both catalysts is 6.9 sq m/g. The CO chemisorbed area at 313K is 0.17 sq m/g and 0.062 sq m/g for the 2% and 1% catalysts, respectively. Monitoring the reaction between CO and O2 by the same technique, at the same temperature yields a turn-over frequency (TOF) for the 2% catalyst of 2.7 x 100 molecules of CO2/site/s and for the 1% catalyst a value of 1.2 x 100. The ratio of the TOFs for the two catalysts is 2.2 which is approximately the ratio of the Pt loading. Author

N87-20542*# Defence Research Establishment Valcartier (Quebec).
AN OVERVIEW OF DREV'S ACTIVITIES ON PULSED CO2 LASER TRANSMITTERS: FREQUENCY STABILITY AND LIFETIME ASPECTS
James Cruickshank, Paul Pace, and Pierre Mathieu *In* NASA. Langley Research Center Closed-Cycle, Frequency-Stable CO2 Laser Technology Apr. 1987 p 227-232 (For primary document see N87-20522 13-36)
Avail: NTIS HC A13/MF A01 CSCL 20E

After introducing the desired features in a transmitter for laser radar applications, the output characteristics of several configurations of frequency-stable TEA-CO2 lasers are reviewed. Based on work carried out at the Defence Research Establishment Valcartier (DREV), output pulses are examined from short cavity lasers, CW-TEA hybrid lasers, and amplifiers for low power pulses. It is concluded that the technique of injecting a low-power laser beam into a TEA laser resonator with Gaussian reflectivity mirrors should be investigated because it appears well adapted to producing high energy, single mode, low chirp pulses. Finally, a brief report on tests carried out on catalysts composed of stannic oxide and noble metals demonstrates the potential of these catalysts, operating at close to room temperature, to provide complete closed-cycle laser operation. Author

N87-20543 Department of the Navy, Washington, D. C.
OPERATION OF TRANSVERSELY EXCITED N2O LASERS Patent
Wayne T. Whitney, inventor (to Navy) and Hiroshi Hara, inventor (to Navy) Issued 16 Sep. 1986 5 p Supersedes N85-19409, AD-D011488 (23 - 10, p 1490)
(AD-D012583; US-Patent-4,612,642; US-Patent-Appl-SN-651399; US-Patent-Class-372-60) Avail: US Patent and Trademark Office CSCL 20/5

An improved method and apparatus is described for producing high power, high efficiency pulsed TEA laser energy and N2O wavelengths by suppressing discharge arc formation with H2 or CO that is added to the N2O lasing medium. . GRA

N87-20544# Sandia National Labs., Albuquerque, N. Mex.
ETCHING OF LINbO3 BY LASER-DRIVEN FUSION OF SALTS
Carol I. H. Ashby and P. J. Brannon 1986 6 p Presented at the Materials Research Society Fall Meeting, Boston, Mass., 1 Dec. 1986
(Contract DE-AC04-76DP-00789)
(DE87-003033; SAND-86-1395C; CONF-861207-12) Avail: NTIS HC A02/MF A01

Lithium niobate exhibits low reactivity with most chemical etchants. Consequently, etching a LiNbO3 surface to produce optical structures such as ridge waveguides or grooves for fiber coupling normally requires relatively slow processes such as ion milling. We have developed a laser-driven chemical etching process for etching highly unreactive ionic solids based on the fusion of salts in the molten phase which can be more than 100 times faster than ion milling rates. This process involves spatially localized melting of LiNbO3 by higher-power density laser pulses with photon energies in excess of the band gap of LiNbO3. While molten, LiNbO3 undergoes reaction with a surface coating of KF to form niobium oxyfluoride anions by fusion of the salts. The resulting solid is highly water soluble. The insolubility of LiNbO3 permits subsequent removal of only the irradiated area by rinsing in water. Surface morphology is determined by laser density. The process exhibits a wavelength dependence. DOE

N87-20545# Oak Ridge National Lab., Tenn.
OPPORTUNITIES AND PROBLEMS IN WAVELENGTH TUNABLE LASERS BASED ON VACANCY DEFECTS IN REFRACTORY OXIDES
Y. Chen, V. M. Orera, R. Gonzalez, and C. Ballesteros Oct. 1986 31 p Presented at the 5th Europhysical Topical Conference on Lattice Defects in Ionic Materials, Madrid, Spain, 8 Sep. 1986
(Contract DE-AC05-84OR-21400)
(DE87-002406; CONF-8609138-4) Avail: NTIS HC A03/MF A01

The primary methods for producing vacancies in the refractory oxides for tunable lasers are neutron irradiation and thermochemical reduction at high temperatures. The latter offers several distinct advantages. However, there are two serious problems: long-lived phosphorescence from anion vacancies and crystal darkening. The former is shown to be due to H(-) ions which serve as metastable electron traps to form H(-2) ions (proton with three electrons occupying oxygen vacancy sites). The localized vibrational modes and electronic transitions of the H(-2) ions have been identified. Photoconversion between F and F(+) centers is shown to involve H(-) in equilibrium H(-2) conversion. The crystal darkening is shown by analytical electron microscopy techniques to be due to scattering from metallic precipitates containing primarily iron. DOE

N87-20546# Sandia National Labs., Albuquerque, N. Mex.
INJECTION-SEEDING STUDIES OF DIODE LASER ARRAY BEHAVIOR
J. P. Hohimer, G. R. Hadley, and A. Owyoung 1987 5 p Presented at the Southwest Optics Conference, Albuquerque, N. Mex., 9 Feb. 1987
(Contract DE-AC04-76DP-00789)
(DE87-002051; SAND-86-2458C; CONF-870220-3) Avail: NTIS HC A02/MF A01

By optical injection seeding of diode laser arrays with the output from a narrowband tunable master oscillator, we are able to actively probe these devices and study their inter-element coupling behavior and eigenmodes. DOE

N87-20547# Brookhaven National Lab., Upton, N. Y.
A RING-CAVITY FOR A QUADRUPLED Nd-YAG LASER
G. Matone 1987 17 p
(Contract DE-AC02-76CH-00016)
(DE87-004175; BNL-39049; LEGS-TN-15) Avail: NTIS HC A02/MF A01

The important characteristics of the proposed storage-ring cavity for green light to be used in the quadrupling of Nd-YAG laser are discussed. These include the attainable infrared power densities, the expected ir-to-green and green-to-uv conversion efficiencies, and the equilibrium uv power levels analyzed assuming both rectangular and gaussian shaped pulses. This analysis demonstrates that in all cases, an equilibrium in the green power stored is very quickly achieved and average uv power levels of approximately 20 W are possible. DOE

N87-20548# Sandia National Labs., Albuquerque, N. Mex.
LASER SPECTROSCOPY AND GAS-PHASE CHEMISTRY IN CVD
P. Ho, W. G. Breiland, and M. E. Coltrin 1986 2 p Presented at the 2nd ASME/JSME Thermal Engineering Conference, Honolulu, Hawaii, 22 Mar. 1987
(Contract DE-AC04-76DP-00789)
(DE86-007392; SAND-86-0440C; CONF-870304-1) Avail: NTIS HC A02/MF A01

The experimental work involves the use of laser spectroscopic techniques for in situ measurements on the gas phase in a chemical vapor deposition reactor. The theoretical part of the program

consists of a computer model of the coupled fluid mechanics and gas-phase chemical kinetics of silane decomposition and subsequent reactions of intermediate species. The laser measurements provide extensive data for thoroughly testing the predictive capabilities of the model. DOE

N87-20549# Bettis Atomic Power Lab., West Mifflin, Pa.
AN AUTOMATED TWO-DIMENSIONAL LASER VELOCIMETER SYSTEM
B. B. Ibrahim and R. B. Hammond Feb. 1987 15 p
(Contract DE-AC11-76PN-00014)
(DE87-005625; WAPD-TM-1616) Avail: NTIS HC A02/MF A01

This document describes a laser velocimeter - minicomputer data acquisition system that is used in the measurement of fluid velocity. An automated traversing mechanism is also described. The data collection, processing, calculation and display of velocity plots in real-time is the principal feature of this system. DOE

N87-20317*# Saint Mary's Hospital, Milwaukee, Wis. Laser Program.
RESULTS OF THE JOINT UTILIZATION OF LASER INTEGRATED EXPERIMENTS FLOWN ON PAYLOAD GAS-449 ABOARD COLUMBIA MISSION 61-C
M. C. Muckerheide *In* NASA. Goddard Space Flight Center The 1986 Get Away Special Experimenter's Symposium Feb. 1987 p 103-110 (For primary document see N87-20302 13-12)
Avail: NTIS HC A11/MF A01 CSCL 20E

N87-20446# Joint Publications Research Service, Arlington, Va.
THE LASER STRENGTH OF ACTIVE ELEMENTS MADE OF GADOLINIUM-SCANDIUM-GALLIUM GARNET (GSGG)
Yu. K. Kanileyko, Ye. V. Zharikov, V. V. Laptev, Yu. P. Minayev, V. N. Nikolayev, A. V. Sidorin, G. N. Toropkin, and I. A. Shcherbakov *In its* USSR Report: Physics and Mathematics 26 Jun. 1986 p 27-29 Transl. into ENGLISH from Kvantovaya Elektronika (Moscow, USSR), v. 12, no. 2, Feb. 1985 p 430-432 (For primary document see N87-20445 13-31)
Avail: NTIS HC A07/MF A01

37 MECHANICAL ENGINEERING

Includes auxiliary systems (nonpower); machine elements and processes; and mechanical equipment.

N87-20550 Fraunhofer-Inst. fuer Betriebsfestigkeit, Darmstadt (West Germany).
CRITERIA AND METHODOLOGY FOR LIGHTWEIGHT DESIGN OF VEHICLE COMPONENTS
V. Grubisic 15 Jul. 1986 78 p
(LBF-TB-176(1986); ISSN-0721-5320; ETN-87-99332) Copyright. Avail: Issuing Activity

Criteria for lightweight design of vehicle components and the methodology for the service strength analysis are presented. Methods for the analysis of operational loads and stresses and for fatigue life prediction are treated. Procedures to determine the service fatigue life and proof-out tests are described. ESA

N87-20551# Instituto de Pesquisas Espaciais, Sao Jose dos Campos (Brazil).
AUTOMATION AND ROBOTICS [AUTOMATICA E ROBOTICA]
Atair RiosNeto Dec. 1986 20 p In PORTUGUESE Presented at the Miniconference of the 38th Annual Conference of the SBPC, Curitiba, Parana, Brazil, 9-16 Jul. 1986
(INPE-4088-PRE/1033) Avail: NTIS HC A02/MF A01

A general description is given of automation (either control and automation or automatic control). This characterization is in the form of definitions and basic ideas, where automation is regarded as a technical - scientific area in search of artificial solutions for automatic control systems, i.e., substituting physical terms for human actions, and the acquisition, transmission, and processing of information. The structural elements and types of schemes usually utilized in the control and automation systems are presented. Criteria are adopted, beginning with the most scientific and technical and proceeding to applied technologies. Automation is classified into 8 groups of activities. The classification is most explicit concerning the area of robotics, one of the basic descriptions of automation. A preliminary review of robotics follows, i.e., the robot, its basic elements and operation. The origins, classifications, and uses of robots are analyzed as well as the present state of robotics and current technological problems of robotic systems. Author

N87-20552*# Akron Univ., Ohio. Dept. of Mechanical Engineering.
FLEXIBILITY EFFECTS ON TOOTH CONTACT LOCATION IN SPIRAL BEVEL GEAR TRANSMISSIONS
P. C. Altidis and M. Savage Washington NASA Mar. 1987 201 p
(Grant NAG3-55; DA Proj. 1L1-61102-AH-45)
(NASA-CR-4055; E-3360; NAS 1.26:4055) Avail: NTIS HC A10/MF A01 CSCL 13I

An analytical method to predict the shift of the contact ellipse between the meshing teeth in a spiral bevel gear set is presented in this report. The contact ellipse shift of interest is the motion of the nominal tooth contact location on each tooth from the ideal pitch point to the point of contact between the two teeth considering the elastic motions of the gears and their supporting shafts. This is the shift of the pitch point from the ideal, unloaded position on each tooth to the nominal contact location on the tooth when the gears are fully loaded. It is assumed that the major contributors of this motion are the elastic deflections of the gear shafts, the slopes of the shafts under load and the radial deflections of the four gear shaft bearings. The motions of the two pitch point locations on the pinion and the gear tooth surfaces are calculated in a FORTRAN program which also calculates the size and orientation of the Hertzian contact ellipse on the tooth faces. Based on the curvatures of the two spiral bevel gear teeth and the size of the contact ellipse, the program also predicts the basic dynamic capacity of the tooth pair. A complete numerical example is given to illustrate the use of the program. Author

N87-20553*# Texas A&M Univ., College Station. Dept. of Mechanical Engineering.
HYBRID METHODS FOR ROTORDYNAMIC ANALYSIS
Sherif T. Noah Dec. 1986 54 p
(Contract NAS8-36182)
(NASA-CR-179035; NAS 1.26:179035) Avail: NTIS HC A04/MF A01 CSCL 13K

Effective procedures are presented for the response analysis of the Space Shuttle Main Engine turbopumps under transient loading conditions. Of particular concern is the determination of the nonlinear response of the systems to rotor imbalance in presence of bearing clearances. The proposed procedures take advantage of the nonlinearities involved being localized at only a few rotor/housing coupling joints. The methods include those based on integral formulations for the incremental solutions involving the transition matrices of the rotor and housing. Alternatively, a convolutional representation of the housing displacements at the coupling points is proposed which would allow performing the transient analysis on a reduced model of the housing. The integral approach is applied to small dynamical models to demonstrate the efficiency of the approach. For purposes of assessing the numerical integration results for the nonlinear rotor/housing systems, a numerical harmonic balance procedure is developed to enable determining all possible harmonic, subharmonic, and nonperiodic solutions of the systems. A brief account of the Fourier approach is presented as applied to a two degree of freedon rotor-support system. Author

N87-20554*# Boeing Aerospace Co., Seattle, Wash.
NASA/MSFC LARGE STRETCH PRESS STUDY
M. W. Choate, W. P. Nealson, G. C. Jay, and W. D. Buss Apr. 1985 138 p
(Contract NAS8-35969)
(NASA-CR-180376; NAS 1.26:180376; D180-27884-3) Avail: NTIS

HC A07/MF A01 CSCL 13I

The Mueller matrix and polarization covariance matrix for polarimetric radar systems were studied. The clutter is modeled by a layer of random permittivity, described by a three-dimensional correlation function, with variance, and horizontal and vertical correlation lengths. Theoretical predictions were matched with experimental data for vegetation fields. A general mixing formula was derived for discrete scatters immersed in a host medium. The results are applicable to general multiphase mixtures. The strong fluctuation theory was used to derive the backscattering cross sections and was further extended to include higher order co-polarized and cross-polarized moments. A two-layer anisotropic random medium model was developed for the active and passive microwave remote sensing of ice fields. A three-layer random medium model was adopted to study the volume scattering effects for the active and passive microwave remote sensing of snow-covered fields. The snow layer was simulated by an isotropic random medium and the ice layer by an anisotropic random medium. The vegetation canopy and snow-covered ice field were studied with a three-layer model, an isotropic random medium layer overlying an anisotropic random medium. The dyadic Green's function of the three-layer medium and the scattered electromagnetic intensities with Born approximation were calculated. B.G.

N87-20555*# National Aeronautics and Space Administration. Lewis Research Center, Cleveland, Ohio.

VIBRATION CHARACTERISTICS OF OH-58A HELICOPTER MAIN ROTOR TRANSMISSION

David G. Lewicki and John J. Coy Apr. 1987 18 p

(NASA-TP-2705; E-3368; NAS 1.60:2705; AVSCOM-TR-86-C-42) Avail: NTIS HC A01/MF A01 CSCL 01C

Experimental vibration tests covering a range of torque and speed conditions were performed on the OH-58A helicopter main rotor transmission at the NASA Lewis Research Center. Signals from accelerometers located on the transmission housing were analyzed by using Fourier spectra, power spectral density functions, and averaging techniques. Most peaks of the Fourier spectra occurred at the spiral bevel and planetary gear mesh harmonics. The highest level of vibration occurred at the spiral bevel meshing frequency. Transmission speed and vibration measurement location had a significant effect on measured vibration; transmission torque and measurement direction had a small effect. Author

N87-20556*# National Aeronautics and Space Administration. Lewis Research Center, Cleveland, Ohio.

EXPERIMENTAL AND ANALYTICAL EVALUATION OF DYNAMIC LOAD AND VIBRATION OF A 2240-kW (300-hp) ROTORCRAFT TRANSMISSION

Fred K. Choy, Dennis P. Townsend, and Fred B. Oswald Mar. 1987 18 p Presented at the Design Engineering Conference and Show, Chicago, Ill., 2-5 Mar. 1987; sponsored by ASME

(NASA-TM-88975; E-3380; NAS 1.15:88975) Avail: NTIS HC A02/MF A01 CSCL 13I

A dynamic analysis of a 2240-kW (3000-hp) helicopter planetary system is presented. Results from both analytical and experimental studies show good correlation in gear-tooth loads. A parametric study indicates that the mesh damping ratio has a significant effect on maximum gear tooth load, stress, and vibration. Correlation with experimental results indicates that the Sun-planet mesh damping ratio can significantly differ from the planet ring mesh damping ratio. A numerical fast Fourier transform (FFT) procedure was applied to examine the mesh load components in the frequency domain and the magnitudes of multiple tooth pass frequencies excited by nonsynchronous meshing of the planets. Effects of tooth-spacing errors and tooth-profile modifications with tip relief are examined. A general discussion of results and correlation with the experimental study are also presented. Author

N87-20557*# George Washington Univ., Washington, D.C. School of Engineering and Applied Science.

INVESTIGATION OF THERMAL-FLUID MECHANICAL CHARACTERISTICS OF THE CAPILLARY PUMP AND THE PUMPED TWO-PHASE LOOP Semiannual Status Report, 1 Sep. 1986 - 28 Feb. 1987

Ali M. Kiper 15 Apr. 1987 40 p

(Grant NAG5-834)

(NASA-CR-180509; NAS 1.26:180509) Avail: NTIS HC A03/MF A01 CSCL 13K

This first semi-annual report summarized progress made on NASA Goddard Space Flight Center (GSFC) Grant NAG 5-834 during the period September 1, 1986 to February 28, 1987. The goal of the project is to gain a better understanding of the transient behavior of the Capillary Pump Loop (CPL) developed and tested by the GSFC. The investigation is directed toward development of analytical models to represent the transient thermal-fluid mechanic processes occurring in different parts of the CPL engineering model. Evaluation of the available test data has been the starting point for the investigation. Based on results of this evaluation, supplementary tests will be conducted by using a CPL test system already operational in the Heat Transfer laboratory of the university. Of particular interest is the oscillatory behavior of the CPL engineering model exhibited during some of the earlier test runs conducted at NASA-GSFC and Johnson Space Center (JSC). Author

N87-20558# Southwest Research Inst., San Antonio, Tex. Fuels and Lubricants Research Facility.

COMPARISON OF 6.2L ARCTIC AND STANDARD FUEL INJECTION PUMPS USING JP-8 FUEL Interim Report, Feb. - Oct. 1986

Alan F. Montemayor and Edwin C. Owens Oct. 1986 37 p

(Contracts DAAK70-85-C-0007; DA Proj. 1L2-63104-D-150)

(AD-A175597; BFLRF-218) Avail: NTIS HC A03/MF A01 CSCL 21/4

Use of MIL-T-83133 JP-8 aviation turbine fuel (NATO F-34) in compression-ignition engines is being investigated. In previous engine-dynamometer tests, JP-8 was compatible with the 6V-53T and NHC-250 engines but tests with the 6.2L engine indicated that the JP-8 fuel may cause premature fuel injection pump deterioration, resulting in a change in maximum fuel delivery volume and retarding the injection timing. The fuel injection pump manufacturer has experienced premature wear problems with their pumps when operated on low viscosity fuels, such as JP-8 in cold climates and now offers an arctic fuel injection pump designed to operate with lower viscosity fuels. This program sought to determine if that pump is superior to the standard pump in preventing premature wear with JP-8 fuel. Results of 200-hour test indicate that the arctic pump performed better than the standard pump in injection timing change (caused by internal drive tang wear), while the standard pump was better in governor thrust washer wear. GRA

N87-20559# Mound Lab., Miamisburg, Ohio.

CHEMISTRY OF GLASS-CERAMIC TO METAL BONDING FOR HEADER APPLICATIONS PART 2: HYDROGEN BUBBLE FORMATION DURING GLASS-CERAMIC TO METAL SEALING

S. M. Craven, D. P. Kramer, and W. E. Moddeman 3 Dec. 1986 17 p

(Contract DE-AC04-76DP-00053)

(DE87-004041; MLM-3403) Avail: NTIS HC A02/MF A01

During the formation of a glass-ceramic to metal seal with nickel-based superalloy Inconel 718, hydrogen bubble formation was observed in the glass-ceramic. This bubble formation was caused by the reaction of dissolved metals with adsorbed water, all of which are in the glass-ceramic. The dissolved metals are present in the glass from dissociation of the Inconel 718, and the water is present in the glass prior to seal formation. To inhibit bubble formation, the glass-ceramic was spiked with 1 wt % CuO. This spiking allowed competing reactions to occur, thus causing the formation of copper and/or CuO in the glass-to-metal interface and reducing bubble formation. Spiking with 1 wt % CrO also inhibited bubble formation. Thermodynamic data suggest that hydrogen formation is responsible for bubbles in a wide variety of seal systems, including glass-to-metal seals in which the metal is or contains iron, manganese, chromium, niobium, titanium, or aluminum. DOE

N87-20560# Oak Ridge National Lab., Tenn.
EFFECTS OF FORCE REFLECTION ON SERVOMANIPULATOR TASK PERFORMANCE
J. V. Draper, W. E. Moore, J. N. Herndon, and B. S. Weil 1986 19 p Presented at the International Topical Meeting on Remote Systems and Robotics in Hostile Environments, Pasco, Wash., 29 Mar. 1987
(Contract DE-AC05-84OR-21400)
(DE87-003008; CONF-870301-4) Avail: NTIS HC A02/MF A01

This paper reports results of a testing program that assessed the impact of force reflection on servomanipulator task performance. The testing program compared three force-reflection levels: 4 to 1 (four units of force on the slave produce one unit of force at the master controller), 1 to 1, and infinity to 1 (no force reflection). Time required to complete tasks, rate of occurrence of errors, the maximum force applied to task components, and variability in forces during completion of representative remote handling tasks were used as dependent variables. Operators exhibited lower error rates, lower peak forces, and more consistent application of forces using force reflection than they did without it. These data support the hypothesis that force reflection provides useful information for servomanipulator operators. DOE

N87-20561# Edgerton, Germeshausen and Grier, Inc., Idaho Falls, Idaho.
EXPERIMENTAL MEASUREMENT OF THIN PLATE SS 304 GTAW WELD POOL SURFACE TEMPERATURES
H. G. Kraus 1987 28 p Presented at the 68th Annual American Welding Society Convention, Chicago, Ill., 22 Mar. 1987
(Contract DE-AC07-76ID-01570)
(DE87-004545; EGG-M-17586; CONF-870372-1) Avail: NTIS HC A03/MF A01

The optical spectral radiometric/laser reflectance method was used to noninvasively measure arc-side GTAW weld pool surface temperatures for 1.5 mm thick plate SS 304. Weld pool surface temperature isothermal contour and topology plots, as well as lengthwise centerline temperature profiles, were generated for welder currents of 38, 50, and 70 A; welder voltages of 7.5, 8.0 and 8.5 V, respectively; and welding speeds of 0.423, 1.270, and 2.540 mm/s (1, 3, and 6 in/min), respectively. Purpose of the work was to investigate the possibility of constitutional supercooling in the tail region of the weld pools. The peak weld pool temperatures in the range of 2000 to 2800 K were often found to lead the electrode instead of lag it. These results were compared to those for experimental measurements of electron beam welds and predictions based on vaporization theory. Under most conditions, no two weld pools are alike and that the concept of quasi-steady-state pools does not represent reality. They are instead dynamically (stochastically) varying about mean value representative characteristics. No evidence of tail region constitutional supercooling was found. DOE

N87-20306*# National Aeronautics and Space Administration. Goddard Space Flight Center, Greenbelt, Md. Space Welding Project.
GAS TUNGSTEN ARC WELDING IN A MICROGRAVITY ENVIRONMENT: WORK DONE ON GAS PAYLOAD G-169
Blake A. Welcher, Faysal A. Kolkailah, and Arthur H. Muir, Jr. (Rockwell International Corp., Thousand Oaks, Calif.) *In* NASA. Goddard Space Flight Center The 1986 Get Away Special Experimenter's Symposium Feb. 1987 p 23-29 (For primary document see N87-20302 13-12)
Avail: NTIS HC A11/MF A01 CSCL 11F

N87-20588# United Technologies Research Center, East Hartford, Conn.
IMPLEMENTATION OF ACTIVE FORCE CONTROL FOR ROBOTS SUBJECT TO DYNAMIC LOADING
R. Hollowell, R. Guile, P. FitzPatrick, and S. Foley *In* Shock and Vibration Information Center The Shock and Vibration Bulletin. Part 2: Modal Test and Analysis, Testing Techniques, Machinery Dynamics, Isolation and Damping, Structural Dynamics Aug. 1986 p 81-88 (For primary document see N87-20580 13-39)
Avail: NTIS HC A10/MF A01 CSCL 20/11

N87-20591# Cepstrum Engeharia Ltda., Sao Paulo (Brazil).
A NEW APPROACH FOR GEARBOX MODELLING IN FINITE ELEMENT ANALYSES OF TORSIONAL VIBRATION OF GEAR-BRANCHED PROPULSION SYSTEMS
H. F. Tavares and V. Prodonoff (PETROBRAS Research Center, Rio de Janeiro, Brazil.) *In* Shock and Vibration Information Center The Shock and Vibration Bulletin. Part 2: Modal Test and Analysis, Testing Techniques, Machinery Dynamics, Isolation and Damping, Structural Dynamics Aug. 1986 p 117-125 (For primary document see N87-20580 13-39)
Avail: NTIS HC A10/MF A01 CSCL 20/11

38 QUALITY ASSURANCE AND RELIABILITY

Includes product sampling procedures and techniques; and quality control.

N87-20562*# National Aeronautics and Space Administration. Lewis Research Center, Cleveland, Ohio.
THE ACOUSTO-ULTRASONIC APPROACH
Alex Vary [1987] 30 p Prepared for presentation at the Conference on Acousto-Ultrasonics: Theory and Application, Blacksburg, Va., 12-15 Jul. 1987; sponsored in part by NASA and American Society for Nondestructive Testing
(NASA-TM-89843; E-3504; NAS 1.15:89843) Avail: NTIS HC A03/MF A01 CSCL 14D

The nature and underlying rationale of the acousto-ultrasonic approach is reviewed, needed advanced signal analysis and evaluation methods suggested, and application potentials discussed. Acousto-ultrasonics is an NDE technique combining aspects of acoustic emission methodology with ultrasonic simulation of stress waves. This approach uses analysis of simulated stress waves for detecting and mapping variations of mechanical properties. Unlike most NDE, acousto-ultrasonics is less concerned with flaw detection than with the assessment of the collective effects of various flaws and material anomalies. Acousto-ultrasonics has been applied chiefly to laminated and filament-wound fiber reinforced composites. It has been used to assess the significant strength and toughness reducing effects that can be wrought by combinations of essentially minor flaws and diffuse flaw populations. Acousto-ultrasonics assesses integrated defect states and the resultant variations in properties such as tensile, shear, and flexural strengths and fracture resistance. Matrix cure state, porosity, fiber orientation, fiber volume fraction, fiber-matrix bonding, and interlaminar bond quality are underlying factors. Author

N87-20563# Edgerton, Germeshausen and Grier, Inc., Idaho Falls, Idaho.
RISK EVALUATIONS OF AGING PHENOMENA: THE LINEAR AGING RELIABILITY MODEL AND ITS EXTENSIONS
W. E. Vesely 28 Oct. 1986 18 p Presented at the 14th Water Reactor Safety Information Meeting, Gaithersburg, Md., 27 Oct. 1986
(Contract DE-AC07-76ID-01570)
(DE87-002607; EGG-M-34086; CONF-8610135-11) Avail: NTIS HC A02/MF A01

A model for component failure rates due to aging mechanisms has been developed from basic phenomenological considerations. In the treatment, the occurrences of deterioration are modeled as following a Poisson process. The severity of damage is allowed to have any distribution, however the damage is assumed to accumulate independently. Finally, the failure rate is modeled as being proportional to the accumulated damage. Using this treatment, the linear aging failure rate model is obtained. The applicability of the linear aging model to various mechanisms is discussed. The model can be extended to cover nonlinear and dependent aging phenomena. The implementability of the linear

aging model is demonstrated by applying it to the aging data collected in NRC's Nuclear Plant Aging Research (NPAR) Program. The applications show that aging as observed in collected data have significant effects on the component failure probability and component reliability when aging is not effectively detected and controlled by testing and maintenance. DOE

39 STRUCTURAL MECHANICS

Includes structural element design and weight analysis; fatigue; and thermal stress.

For applications see *05 Aircraft Design, Testing and Performance* and *18 Spacecraft Design, Testing and Performance.*

N87-20564 Virginia Polytechnic Inst. and State Univ., Blacksburg.
MODELING AND CONTROL OF FLEXIBLE STRUCTURES Ph.D. Thesis
Jeffrey Kent Bennighof 1986 137 p
Avail: Univ. Microfilms Order No. DA8625796

Topics in the modeling and control of large flexible structures are examined. In the finite element convergence toward the natural modes and frequencies of a structure, it was found that two mechanisms limiting the accuracy of higher modes, are, first, a decrease in the number of active degrees of freedom for higher mode approximations due to orthogonality constraints, and, second, the fact that lower computed, rather than actual, eigenfunctions appear in the orthogonality constraints, so that inaccuracy in lower modes inhibits convergence to higher modes. Refining the elements using the hierarchial p-version proves to be far superior to refining the mesh, as demonstrated by numerical examples. A method is presented for solving the algebraic eigenvalue problem for a structure, which combines attractive features of the subspace iteration method and the component-mode synthesis methods. The effectiveness of modal control (IMSC) and direct feedback control are investigated for suppressing traveling waves on a string and on a beam, both with slight material damping. Dissert. Abstr.

N87-20565*# National Aeronautics and Space Administration. Lewis Research Center, Cleveland, Ohio.
CALCULATION OF THERMOMECHANICAL FATIGUE LIFE BASED ON ISOTHERMAL BEHAVIOR
Gary R. Halford and James F. Saltsman 1987 22 p Prepared for presentation at the 5th National Congress on Pressure Vessel and Piping Technology, San Diego, Calif., 28 Jun. - 2 Jul. 1987; sponsored by ASME
(NASA-TM-88864; E-2940; NAS 1.15:88864) Avail: NTIS HC A02/MF A01 CSCL 20K

The isothermal and thermomechanical fatigue (TMF) crack initiation response of a hypothetical material was analyzed. Expected thermomechanical behavior was evaluated numerically based on simple, isothermal, cyclic stress-strain - time characteristics and on strainrange versus cyclic life relations that have been assigned to the material. The attempt was made to establish basic minimum requirements for the development of a physically accurate TMF life-prediction model. A worthy method must be able to deal with the simplest of conditions: that is, those for which thermal cycling, per se, introduces no damage mechanisms other than those found in isothermal behavior. Under these assumed conditions, the TMF life should be obtained uniquely from known isothermal behavior. The ramifications of making more complex assumptions will be dealt with in future studies. Although analyses are only in their early stages, considerable insight has been gained in understanding the characteristics of several existing high-temperature life-prediction methods. The present work indicates that the most viable damage parameter is based on the inelastic strainrange. Author

N87-20566*# National Aeronautics and Space Administration. Lewis Research Center, Cleveland, Ohio.
SHOT PEENING FOR TI-6AI-4V ALLOY COMPRESSOR BLADES
Gerald A. Carek Apr. 1987 9 p
(NASA-TP-2711; E-3430; NAS 1.60:2711) Avail: NTIS HC A01/MF A01 CSCL 20K

A text program was conducted to determine the effects of certain shot-peening parameters on the fatigue life of the Ti-6Al-4V alloys as well as the effect of a demarcation line on a test specimen. This demarcation line, caused by an abrupt change from untreated surface to shot-peened surface, was thought to have caused the failure of several blades in a multistage compressor at the NASA Lewis Research Center. The demarcation line had no detrimental effect upon bending fatigue specimens tested at room temperature. Procedures for shot peening Ti-6Al-4V compressor blades are recommended for future applications. Author

N87-20567*# National Aeronautics and Space Administration. Langley Research Center, Hampton, Va.
MODELING OF JOINTS FOR THE DYNAMIC ANALYSIS OF TRUSS STRUCTURES
W. Keith Belvin May 1987 43 p
(NASA-TP-2661; L-16163; NAS 1.60:2661) Avail: NTIS HC A03/MF A01 CSCL 20K

An experimentally-based method for determining the stiffness and damping of truss joints is described. The analytical models use springs and both viscous and friction dampers to simulate joint load-deflection behavior. A least-squares algorithm is developed to identify the stiffness and damping coefficients of the analytical joint models from test data. The effects of nonlinear joint stiffness such as joint dead band are also studied. Equations for predicting the sensitivity of beam deformations to changes in joint stiffness are derived and used to show the level of joint stiffness required for nearly rigid joint behavior. Finally, the global frequency sensitivity of a truss structure to random perturbations in joint stiffness is discussed. Author

N87-20568*# National Aeronautics and Space Administration. Marshall Space Flight Center, Huntsville, Ala.
SPACE STATION STRUCTURES AND DYNAMICS TEST PROGRAM
Carleton J. Moore, John S. Townsend, and Edward W. Ivey Mar. 1987 47 p
(NASA-TP-2710; NAS 1.60:2710) Avail: NTIS HC A03/MF A01 CSCL 20K

The design, construction, and operation of a low-Earth orbit space station poses unique challenges for development and implementation of new technology. The technology arises from the special requirement that the station be built and constructed to function in a weightless environment, where static loads are minimal and secondary to system dynamics and control problems. One specific challenge confronting NASA is the development of a dynamics test program for: (1) defining space station design requirements, and (2) identifying the characterizing phenomena affecting the station's design and development. A general definition of the space station dynamic test program, as proposed by MSFC, forms the subject of this report. The test proposal is a comprehensive structural dynamics program to be launched in support of the space station. The test program will help to define the key issues and/or problems inherent to large space structure analysis, design, and testing. Development of a parametric data base and verification of the math models and analytical analysis tools necessary for engineering support of the station's design, construction, and operation provide the impetus for the dynamics test program. The philosophy is to integrate dynamics into the design phase through extensive ground testing and analytical ground simulations of generic systems, prototype elements, and subassemblies. On-orbit testing of the station will also be used to define its capability. Author

N87-20569*# Auburn Univ., Ala. Dept. of Aerospace Engineering.
INITIAL INVESTIGATIONS INTO THE DAMPING CHARACTERISTICS OF WIRE ROPE VIBRATION ISOLATORS Final Technical Report

M. A. Cutchins, J. E. Cochran, Jr., K. Kumar, N. G. Fitz-Coy, and M. L. Tinker 29 Apr. 1987 89 p
(Grant NAG8-532)
(NASA-CR-180698; NAS 1.26:180698) Avail: NTIS HC A05/MF A01 CSCL 20K

Passive dampers composed of coils of multi-strand wire rope are investigated. Analytical results range from those produced by complex NASTRAN models to those of a Coulomb damping model with variable friction force. The latter agrees well with experiment. The Coulomb model is also utilized to generate hysteresis loops. Various other models related to early experimental investigations are described. Significant closed-form static solutions for physical properties of single-and multi-strand wire ropes are developed for certain specific geometries and loading conditions. NASTRAN models concentrate on model generation and mode shapes of 2-strand and 7-strand straight wire ropes with interfacial forces.
Author

N87-20570*# National Aeronautics and Space Administration. Langley Research Center, Hampton, Va.
STRUCTURES AND DYNAMICS DIVISION RESEARCH AND TECHNOLOGY PLANS FOR FY 1987 AND ACCOMPLISHMENTS FOR FY 1986
Kay S. Bales Mar. 1987 108 p
(NASA-TM-89141; NAS 1.15:89141) Avail: NTIS HC A06/MF A01 CSCL 20K

This paper presents the Objectives, FY 1987 Plans, Approach, and FY 1987 Milestones for the Structures and Dynamics Division's research programs. FY 1986 Accomplishments are presented where applicable. This information is useful in program coordination with other governmental organizations in areas of mutual interest.
Author

N87-20571# Princeton Univ., N. J. Dept. of Civil Engineering.
INCLINED PILEUP OF EDGE DISLOCATIONS NEAR THE CRACK TIP
A. C. Eringen and G. D. Dhondt 3 Dec. 1986 38 p
(Contract DAAL03-86-K-0019)
(AD-A175610; ARO-22967.2-EG) Avail: NTIS HC A03/MF A01 CSCL 20/11

The formation of a plastic zone, in the form of a linear array of inclined edge dislocations in front of a mode crack in plane strain, is studied. The direction of the force field on an edge dislocation due to the crack load allows for the determination of the plastic zone as a function of the inclination angle. The dislocation distribution along the plastic zone is found from force equilibrium considerations. The results show the presence of a dislocation free zone (DFZ) and a shrinking of the plastic zone size with greater angle of inclination. The latter angle does not seem to influence the DFZ size. The way in which we determined the stress field allows us to study the influence of defects on the plastic zone formation.
GRA

N87-20572# Michigan State Univ., East Lansing. Coll. of Engineering.
THEORETICAL INVESTIGATIONS OF SHEAR BAND FORMATION IN FINITE ELASTICITY Final Report, 1 Oct. 1983 - 30 Sep. 1986
C. O. Horgan and R. Abeyaratne 15 Nov. 1986 14 p
(Contract DAAG29-83-K-0145)
(AD-A175657; ARO-19872.9-EG) Avail: NTIS HC A02/MF A01 CSCL 20/11

This work concerned various types of failure mechanisms arising due to large strains in solid materials. Specifically, it addressed issues related to loss of stability, shear localization, void nucleation, stress concentrations and crack-tip deformations. The foregoing failure processes have been investigated analytically within the contexts of finite elasticity and finite strain plasticity theories. The inherently nonlinear phenomena examined in this research program are of crucial importance for understanding the mechanical behavior of solid materials subjected to the increasing demands of military technology.
GRA

N87-20573# Geo-Centers, Inc., Suitland, Md.
LOAD BIAXIALITY AND FRACTURE: A TWO-SIDED HISTORY OF COMPLEMENTING ERRORS
John Eftis and Mitchell I. Jolles 14 Nov. 1986 59 p
(AD-A175972; NRL-MR-5875) Avail: NTIS HC A04/MF A01 CSCL 20/11

It is the view of many engineers associated with fracture mechanics, materials science and mechanical design, that for bodies containing plane cracks, loads that are applied in a direction that is parallel to the plane of the crack, in addition to the tensile load acting in the direction perpendicular to it, can have no influence upon the fracture behavior of the body. This point of view has persisted for the past sixty years or so, and still continues to persist, despite the paucity of experimental evidence in support of it. This paper traces the two-sided historical genesis of this notion. It shows how a series of errors, both in the calculation of the elastic strain energy appearing in Griffith's global crack instability hypothesis and in the evolution of Irwin's local theory of the crack-tip elastic stress intensity, have, by coincidence, had the particular effect of nullifying the presence of the loads that are applied to the crack. The mishaps associated with one theory are, in a sense, complementary to the entirely different set of errors that cause this same null effect to appear in the other theory, in that they give the appearance between the two theories in this regard.
GRA

N87-20574# Shock and Vibration Information Center (Defense), Washington, D. C.
THE SHOCK AND VIBRATION BULLETIN. PART 1: WELCOME, INVITED PAPERS, SHIPBOARD SHOCK, BLAST AND GROUND SHOCK, SHOCK TESTING AND ANALYSIS
Aug. 1986 297 p Proceedings of the 56th Shock and Vibration Symposium, Monterey, Calif., 22-24 Oct. 1985
(AD-A175224; SVIC-Bull-56-Pt-1) Avail: NTIS HC A13/MF A01

Topics addressed include: solid mechanics; shock mechanics; dynamics and control of large space structures; structural dynamic response analysis methods; shipborne shock; blast and ground shock; and shock testing and analysis. For individual titles, see N87-20575 through N87-20579.

N87-20575# Office of Naval Research, Arlington, Va. Solids and Structures Group.
SOLID MECHANICS PROGRAM AT ONR
Alan S. Kushner *In* Shock and Vibration Information Center The Shock and Vibration Bulletin. Part 1: Welcome, Invited Papers, Shipboard Shock, Blast and Ground Shock, Shock Testing and Analysis Aug. 1986 p 3-20 (For primary document see N87-20574 13-39)
Avail: NTIS HC A13/MF A01

A brief description was made on the Office of Naval Research's philosophy of basic research and the current program in solid mechanics (fundamental solid mechanics, failure mechanics, fluid-structure interaction, and structural mechanics), along with a few examples.
B.G.

N87-20576# Army Materials Technology Lab., Watertown, Mass. Shock and Mechanics Team.
ARMY RESEARCH IN SHOCK MECHANICS
John F. Mescall and Richard Shea *In* Shock and Vibration Information Center The Shock and Vibration Bulletin. Part 1: Welcome, Invited Papers, Shipboard Shock, Blast and Ground Shock, Shock Testing and Analysis Aug. 1986 p 21-38 (For primary document see N87-20574 13-39)
Avail: NTIS HC A13/MF A01

The U.S. Army Materials Technology Laboratory (MTL) has mission responsibility for managing the Army's technology base programs in structural materials, solid mechanics, and materials testing. One of the MTL's major programs is in armor/anti-armor materials. A key ingredient of this program is shock mechanics research. The research seeks to understand the mechanisms associated with the complex processes of projectile impact of targets and explosives-metal interaction. The analytical basis for research in shock mechanics is presented. Several of the

mechanisms, test procedures, and applications of the research are discussed. Author

N87-20577# Air Force Office of Scientific Research, Bolling AFB, Washington, D.C. Aerospace Sciences.
AIR FORCE BASIC RESEARCH IN DYNAMICS AND CONTROL OF LARGE SPACE STRUCTURES **c18**
Anthony K. Amos *In* Shock and Vibration Information Center The Shock and Vibration Bulletin. Part 1: Welcome, Invited Papers, Shipboard Shock, Blast and Ground Shock, Shock Testing and Analysis Aug. 1986 p 39-58 (For primary document see N87-20574 13-39)
Avail: NTIS HC A13/MF A01

The Air Force Basic Research in dynamics and control of large space structures addresses several of the many scientific and technological issues relating to the development and operation of very large and sophisticated high performance systems in the relatively unfamiliar space environment. The design challenge has motivated most of the ongoing research to date. It is perceived that these have evolved modeling concepts, computational algorithms, and performance/stability criteria capable of supporting the design process. However, analytical and experimental methods and the experience data base needed to support the validation of designs prior to commitment to launch are still sparse or nonexistent. The program is therefore in the process of shifting emphasis from the synthesis to the simulation objectives of the technologies. It is entended to embark on the development of modeling and computational capabilities needed to perform high fidelity simulation of orbital dynamics including operational maneuvers and developmental functions of deployment and assembly. B.G.

N87-20578# Imperial Coll. of Science and Technology, London (England). Dynamics Group.
STATE-OF-THE-ART ASSESSMENT OF STRUCTURAL DYNAMIC RESPONSE ANALYSIS METHODS (DYNAS)
D. J. Ewins and M. Imregun *In* Shock and Vibration Information Center The Shock and Vibration Bulletin. Part 1: Welcome, Invited Papers, Shipboard Shock, Blast and Ground Shock, Shock Testing and Analysis Aug. 1986 p 59-90 (For primary document see N87-20574 13-39)
Avail: NTIS HC A13/MF A01

Following interest in surveys to assess current capabilities in the field of measuring structural dynamic data, a study (codename DYNAS) was undertaken to make a corresponding assessment of dynamic analysis prediction methods. A test structure was designed and its specification distributed to a number of organization who have undertaken a structural dynamic analysis of it. The first phase of results from the DYNAS survey were collected and compared and are presented, including modal properties and various response characteristics (both frequency responses and transient response histories). The results from 12 submissions are found to exhibit a wide range of levels of agreement. It is concluded that although accurate analyses are possible, a number of techniques used by participants in the survey did not produce reliable results. Some form of self-assessment is considered desirable for such complex dynamic analysis tasks. Author

N87-20579# Admiralty Research Establishment, Portland (England).
THE DYNAS SURVEY. PART 2: A PARTICIPANT'S VIEW
R. W. Windell *In* Shock and Vibration Information Center The Shock and Vibration Bulletin. Part 1: Welcome, Invited Papers, Shipboard Shock, Blast and Ground Shock, Shock Testing and Analysis Aug. 1986 p 91-100 (For primary document see N87-20574 13-39)
Avail: NTIS HC A13/MF A01

Various possible finite element modeling solutions for the DYNAS structure are explored. Solutions and modeling assumptions are presented and final predictions are compared with measured data. Good agreement is demonstrated for the soft impact with poor agreement for the hard impact due to modeling limitations. Author

N87-20580# Shock and Vibration Information Center (Defense), Washington, D. C.
THE SHOCK AND VIBRATION BULLETIN. PART 2: MODAL TEST AND ANALYSIS, TESTING TECHNIQUES, MACHINERY DYNAMICS, ISOLATION AND DAMPING, STRUCTURAL DYNAMICS
Aug. 1986 216 p Proceedings of the 56th Symposium on Shock and Vibration, Monterey, Calif., 22-24 Oct. 1985
(AD-A175225; SVIC-Bull-56-Pt-2) Avail: NTIS HC A10/MF A01 CSCL 20/11

The proceedings of the 56th Shock and Vibration Symposium are presented. Part 2 of the conference was divided into several areas of study: Modal test and analysis; Testing techniques; Machinery dynamics; Isolation and damping; Structural dynamics; and Fatigue and acoustics. For individual titles, see N87-20581 through N87-20601.

N87-20581*# Jet Propulsion Lab., California Inst. of Tech., Pasadena.
MODAL TEST AND ANALYSIS: MULTIPLE TESTS CONCEPT FOR IMPROVED VALIDATION OF LARGE SPACE STRUCTURE MATHEMATICAL MODELS **c18**
B. K. Wada, C-P. Kuo, and R. J. Glaser *In* Shock and Vibration Information Center The Shock and Vibration Bulletin. Part 2: Modal Test and Analysis, Testing Techniques, Machinery Dynamics, Isolation and Damping, Structural Dynamics Aug. 1986 p 1-8 (For primary document see N87-20580 13-39)
Avail: NTIS HC A10/MF A01 CSCL 22B

For the structural dynamic analysis of large space structures, the technology in structural synthesis and the development of structural analysis software have increased the capability to predict the dynamic characteristics of the structural system. The various subsystems which comprise the system are represented by various displacement functions; the displacement functions are then combined to represent the total structure. Experience has indicated that even when subsystem mathematical models are verified by test, the mathematical representations of the total system are often in error because the mathematical model of the structural elements which are significant when loads are applied at the interconnection points are not adequately verified by test. A multiple test concept, based upon the Multiple Boundary Condition Test (MBCT), is presented which will increase the accuracy of the system mathematical model by improving the subsystem test and test/analysis correlation procedure. Author

N87-20582# Nanjing Aeronautical Inst. (China). Structural Vibration Research Lab.
THE ALGORITHM AND APPLICATION OF A NEW MULTI-INPUT-MULTI-OUTPUT MODAL PARAMETER IDENTIFICATION METHOD
Zhang Lingmi and Hiroshi Kanda (Yanmar Diesel Engine Co., Osaka, Japan.) *In* Shock and Vibration Information Center The Shock and Vibration Bulletin. Part 2: Modal Test and Analysis, Testing Techniques, Machinery Dynamics, Isolation and Damping, Structural Dynamics Aug. 1986 p 11-19 (For primary document see N87-20580 13-39)
Avail: NTIS HC A10/MF A01 CSCL 20/11

A new multi-input/multi-output modal parameter identification method is presented that makes direct and simultaneous use of multiple frequency response function data with respect to multiple reference locations to estimate a global set of modal frequencies, damping ratios, mode shapes and modal participation factors. By employing the singular-value decomposition technique, the rank of the frequency response function matrix, i.e., the approximate number of effective modes in the frequency range of interests, is determined. A minimum-order system matrix is calculated by principal component decomposition and generalized inverse techniques. Modal parameters are then extracted by solving a standard eigenvalue problem. Author

N87-20583# TRW Space Technology Labs., Redondo Beach, Calif. Engineering and Test Div.
MODAL PARAMETER IDENTIFICATION USING ADAPTIVE

DIGITAL FILTERS
B. H. Wendler *In* Shock and Vibration Information Center The Shock and Vibration Bulletin. Part 2: Modal Test and Analysis, Testing Techniques, Machinery Dynamics, Isolation and Damping, Structural Dynamics Aug. 1986 p 21-27 (For primary document see N87-20580 13-39)
Avail: NTIS HC A10/MF A01 CSCL 20/11

Recent advances in the use of adaptive digital filters has shown promise in their application as stochastic models of dynamic structures. Certain classes of digital filters allow modeling the structure as a set of Z-transform filters. The filter model can be analyzed using 3-transform methods for frequency, damping, and modal residues to define mode shapes. The Auto Regressive Moving Average (ARMA) filter formulation as selected for study. A closed solution for computing the ARMA residues is demonstrated. Author

N87-20584*# National Aeronautics and Space Administration. Marshall Space Flight Center, Huntsville, Ala.
SAFE/DAE: MODAL TEST IN SPACE c16
T. E. Nesman and D. K. Reed *In* Shock and Vibration Information Center The Shock and Vibration Bulletin. Part 2: Modal Test and Analysis, Testing Techniques, Machinery Dynamics, Isolation and Damping, Structural Dynamics Aug. 1986 p 29-36 (For primary document see N87-20580 13-39)
Avail: NTIS HC A10/MF A01 CSCL 22B

In September of 1984, NASA performed a series of experiments on orbit with a large solar wing attached to the Space Shuttle orbiter. These experiments, the Solar Array Flight Experiment (SAFE), mark the first tests of a large space structure in space. Extension, retraction, and dynamic tests had to be performed in space due to the fragility of the solar array. Due to the extendable and retractable design of the solar array, accelerometers and associated wires could not be used; therefore, remote sensing, the Dynamics Augmentation Experiment (DAE), was added to the SAFE program. The DAE uses a remote sensor based on star tracker technology to measure the dynamic response of the solar array. The DAE sensor tracked 18 targets on the solar array during free-decay response to a transient excitation. An overview of the SAFE/DAE is presented, highlighting analysis results from the remotely sensed data. Modal parameter estimates from the remotely sensed data were computed using the complex exponential and polyreference techniques. Author

N87-20585# Sandia National Labs., Albuquerque, N. Mex.
TESTING TECHNIQUES. RANDOM VARIATION OF MODAL FREQUENCIES: EXPERIMENTS AND ANALYSIS
Thomas L. Paez, Linda J. Branstetter, and Danny L. Gregory *In* Shock and Vibration Information Center The Shock and Vibration Bulletin. Part 2: Modal Test and Analysis, Testing Techniques, Machinery Dynamics, Isolation and Damping, Structural Dynamics Aug. 1986 p 37-48 (For primary document see N87-20580 13-39)
Avail: NTIS HC A10/MF A01 CSCL 20/11

When a mechanical system is subjected to a dynamic environment it executes dynamic response, and the character of the response depends on the features of the excitation and the structural system parameters. In order to predict the structural system response, it is necessary to know both the excitation and structural system characters. The modal frequencies are among the most basic system properties and are often used in dynamic analysis. Frequently, one or more structural parameters is random, and this causes the modal frequencies to vary randomly. This investigation shows how random variation in modal frequencies can be estimated using a combination of experiments and analysis. One experimental and three numerical examples are presented. Author

N87-20586# Michigan State Univ., East Lansing. Dept. of Metallurgy, Mechanics, and Materials Science.
STRUCTURAL DEGRADATION OF IMPACTED GRAPHITE/EPOXY LAMINATES c24
Dahsin Liu, C. T. Sun (Florida Univ., Gainesville.), and L. E. Malvern *In* Shock and Vibration Information Center The Shock and Vibration Bulletin. Part 2: Modal Test and Analysis, Testing Techniques, Machinery Dynamics, Isolation and Damping, Structural Dynamics Aug. 1986 p 51-60 (For primary document see N87-20580 13-39)
Avail: NTIS HC A10/MF A01 CSCL 20/11

Graphite/epoxy laminates fabricated from Hercules' AS4/3501-6 prepreg tape were studied. The investigations included three different symmetric laminations of cross-ply plates: 3-layer, 5-layer, and 15-layer. Each square specimen was clamped around four edges and impacted at the center by a blunted steel impactor, 9.5 mm in diameter and 25.4 mm in length. The delamination areas caused by impact were measured by ultrasonic C-scan and X-ray radiography. The fundamental vibration frequency and damping coefficient of each cantilever plate before and after impact were measured by a Fast Fourier Transform (FFT) analyzer. After these nondestructive tests, every impacted specimen was subjected to a three-point bend test for the measurements of residual stiffness and residual strength. Results show the possibility of using the changes in damping coefficient and vibration frequency as nondestructive evaluations for damaged composite plates. Author

N87-20587# Institut National des Sciences Appliquees de Lyon, Villeurbanne (France). Lab. de Mecanique des Structures.
MACHINERY DYNAMICS: PREDICTION OF NATURAL FREQUENCIES OF FLEXIBLE SHAFT-DISC SYSTEM
P. Bremand, G. Ferraris, and M. Lelanne *In* Shock and Vibration Information Center The Shock and Vibration Bulletin. Part 2: Modal Test and Analysis, Testing Techniques, Machinery Dynamics, Isolation and Damping, Structural Dynamics Aug. 1986 p 71-79 (For primary document see N87-20580 13-39)
Avail: NTIS HC A10/MF A01 CSCL 20/11

Today the dynamic behavior of rotors must be predicted with the greatest care. The influence of disc flexibility on the natural frequencies of rotors is studied. The rotors considered here are made of a shaft, symmetric bearings and flexible disc. The kinetic and strain energies of the element are calculated, the finite element method is used and the Lagrange's equations applied. The solution of the equations is performed through a modal method. The application is an industrial gas turbine. Its natural frequencies as a function of the speed of rotation are obtained, which gives critical speeds. Author

N87-20588# United Technologies Research Center, East Hartford, Conn.
IMPLEMENTATION OF ACTIVE FORCE CONTROL FOR ROBOTS SUBJECT TO DYNAMIC LOADING c37
R. Hollowell, R. Guile, P. FitzPatrick, and S. Foley *In* Shock and Vibration Information Center The Shock and Vibration Bulletin. Part 2: Modal Test and Analysis, Testing Techniques, Machinery Dynamics, Isolation and Damping, Structural Dynamics Aug. 1986 p 81-88 (For primary document see N87-20580 13-39)
Avail: NTIS HC A10/MF A01 CSCL 20/11

A force control servo for robotic machining was designed and studied based on structural and servo dynamic tests. Results of the studies indicate the feasibility of robotic chamfering using force control and the need for considering robot structural modes in stable force control design. An autoregressive moving average identification technique was used to develop a procedure for model parameter identification from digital sampled impulse response data. A gain scheduling technique is described for achieving stable force control during light metal cutting, while compensating for varying robot structural modes. Author

N87-20589# Texas A&I Univ., Kingsville. Mechanical Engineering.
FORCE MAGNITUDE AND ANGULAR VELOCITY FLUCTUATION REDUCTION IN A SPRING-RESTRAINED, FLEXIBLY-SUPPORTED FOUR-BAR MECHANICAL LINKAGE
Robert A. McLauchlan and Seung Ho Hong *In* Shock and Vibration Information Center The Shock and Vibration Bulletin. Part 2: Modal Test and Analysis, Testing Techniques, Machinery Dynamics, Isolation and Damping, Structural Dynamics Aug. 1986 p 89-106 (For primary document see N87-20580 13-39)

Avail: NTIS HC A10/MF A01 CSCL 20/11

Linear restraining spring potential energy storage elements and flexible vibration isolator support systems were investigated as passive devices to control the highly-nonlinear motion of a planar four-bar mechanical linkage. Specific design/performance indices considered for the spring-restrained, flexibly-supported linkage were: (1) Shaft angular speed variation over time; (2) Internal reaction force magnitudes; and (3) Forces transmitted to the base of the linkage mechanism. The design study was based upon the numerical solution in the time domain of the state vector equation for the four-bar mechanical linkage system. The state-vector equation was developed using Lagrange's form of D'Alembert's principle. Three different linkage systems were considered as follows: (1) Four-bar linkage, rigidly mounted without restraining spring (Model 1); (2) Four-bar linkage, rigidly supported with restraining spring (and damper) (Model 2); and (3) Four-bar linkage, flexibly-supported with restraining spring (and damper) (Model 3). Frequency responses of the shaft angular velocities, etc., were also obtained using the Fast Fourier Transform of the time domain results. Author

N87-20590# Embassy of India, Washington, D.C.

BLADE DAMPING MEASUREMENTS IN A SPIN RIG WITH NOZZLE PASSING EXCITATION SIMULATED BY ELECTRO-MAGNETS

J. S. Rao, K. Gupta (Indian Inst. of Tech., New Delhi.), and N. Vyas *In* Shock and Vibration Information Center The Shock and Vibration Bulletin. Part 2: Modal Test and Analysis, Testing Techniques, Machinery Dynamics, Isolation and Damping, Structural Dynamics Aug. 1986 p 109-115 (For primary document see N87-20580 13-39)

Avail: NTIS HC A10/MF A01 CSCL 20/11

Experimental determination of overall damping in a rotating turbine disc-blade system was studied. A test spin rig was designed and fabricated. Nozzle Passing Excitation is simulated by electro-magnets. Transient excitation of rotating blades is caused by suddenly shutting off the excitation to the rotating blades. Frequency analysis of the transient blade response gives the necessary information about the modal damping in several modes. The variation of modal damping with the speed of rotation and strain amplitude is obtained. Author

N87-20591# Cepstrum Engeharia Ltda., Sao Paulo (Brazil).

A NEW APPROACH FOR GEARBOX MODELLING IN FINITE ELEMENT ANALYSES OF TORSIONAL VIBRATION OF GEAR-BRANCHED PROPULSION SYSTEMS c37

H. F. Tavares and V. Prodonoff (PETROBRAS Research Center, Rio de Janeiro, Brazil.) *In* Shock and Vibration Information Center The Shock and Vibration Bulletin. Part 2: Modal Test and Analysis, Testing Techniques, Machinery Dynamics, Isolation and Damping, Structural Dynamics Aug. 1986 p 117-125 (For primary document see N87-20580 13-39)

Avail: NTIS HC A10/MF A01 CSCL 20/11

A new modelling procedure for use in analyses of torsional vibration of gear-branched propulsion systems is presented. The method has evolved from considerations on the use of constrained finite element equilibrium equations. It is shown that the process of modelling gearboxes can be carried out through a simple modification of the mass, stiffness and damping matrices of the elements situated immediately after every branch. Starting with a development valid for straight-geared systems, the procedure is then extended to account for gear-branched systems and idler gears. An example is included in order to show a practical application. Author

N87-20592# Hieber Engineering, Watching, N.J.

ISOLATION AND DAMPING: A GRAPHICAL METHOD OF DETERMINING THE RESPONSE OF THE CASCADED TWO DEGREE OF FREEDOM SYSTEM

George M. Hieber *In* Shock and Vibration Information Center The Shock and Vibration Bulletin. Part 2: Modal Test and Analysis, Testing Techniques, Machinery Dynamics, Isolation and Damping, Structural Dynamics Aug. 1986 p 127-138 (For primary document see N87-20580 13-39)

Avail: NTIS HC A10/MF A01 CSCL 20/11

There are many occassions when a designer has to install a load onto an existing base structure. If the dynamic characteristics of the load and of the base structure are known individually, the question is: what will happen to the dynamic response of the load when it is connected to the base to form a new system? Assuming the net system results in a configuration that can be modeled as a two degree of freedom system, there are graphical methods available to determine the resulting system frequencies but no quick way to estimate the response amplitude of the load without setting up and solving the appropriate equations. A method is presented here where the maximum response of the load can be obtained graphically. The graphics are valid for Qs from 4 to 400. The ratio of load weight to base weight can range from less than 0.001 to 10. The ratio of natural frequencies of load to base (before installation of load) can range from 0.1 to greater than 10. The results show that two widely held points of view regarding two degree of freedom response should be moderated somewhat. Author

N87-20593# Air Force Wright Aeronautical Labs., Wright-Patterson AFB, Ohio.

TEMPERATURE SHIFT CONSIDERATIONS FOR DAMPING MATERIALS

Lynn Rogers *In* Shock and Vibration Information Center The Shock and Vibration Bulletin. Part 2: Modal Test and Analysis, Testing Techniques, Machinery Dynamics, Isolation and Damping, Structural Dynamics Aug. 1986 p 139-145 Presented at the 56th Shock and Vibration Symposium, Oct. 1985 (For primary document see N87-20580 13-39)

Avail: NTIS HC A10/MF A01 CSCL 20/11

For the temperature shift function for a particular damping material to be obtained, it must be implicitly defined by a set of complex modulus data. Historical procedures have been marginal because frequency ranges have not been adequate. A new procedure for such data is proposed based on the slope of the temperature shift function, on a fractional model of complex modulus and on apparent activation energy considerations. Author

N87-20594# Concordia Univ., Montreal (Quebec). Dept. of Mechanical Engineering.

EFFECTIVENESS OF ON-OFF DAMPER IN ISOLATING DYNAMICAL SYSTEMS

S. Rakheja and S. Sanka *In* Shock and Vibration Information Center The Shock and Vibration Bulletin. Part 2: Modal Test and Analysis, Testing Techniques, Machinery Dynamics, Isolation and Damping, Structural Dynamics Aug. 1986 p 147-156 (For primary document see N87-20580 13-39)

Avail: NTIS HC A10/MF A01 CSCL 20/11

Concepts of vibration isolation through an on-off damper is investigated. A number of on-off damper control schemes are proposed and analyzed for their isolation performance. The vibration isolation characteristics of the proposed on-off dampers are evaluated through computer simulations and compared to that of a passive damper. Effectiveness of the on-off damper is investigated for single degree-of-freedom system with rigid as well as elastically coupled damper. Isolation characteristics of Ruzicka relaxation isolator and Snowdon's two inertia vibration isolation system with on-off damping are evaluated and compared to the optimal passive isolators. Isolation performance of on-off damper is also investigated for multi-degrees-of-freedom dynamical systems. Author

N87-20595# Los Alamos National Lab., N. Mex.

STRUCTURAL DYNAMICS: BUCKLING OF RING-STIFFENED CYLINDRICAL SHELLS WITH DYNAMIC LOADS

T. A. Butler, W. E. Baker, and C. D. Babcock (California Inst. of Tech., Pasadena.) *In* Shock and Vibration Information Center The Shock and Vibration Bulletin. Part 2: Modal Test and Analysis, Testing Techniques, Machinery Dynamics, Isolation and Damping, Structural Dynamics Aug. 1986 p 157-165 Sponsored by Nuclear Regulatory Commission (For primary document see N87-20580

13-39)
Avail: NTIS HC A10/MF A01 CSCL 20/11

Buckling of a ring-stiffened, thin-walled cylinder from dynamic base excitation was investigated in a combined experimental/numerical program. A polycarbonate (Lexan) cylinder was excited with single-frequency harmonic transients to determine the peak base acceleration levels required to induce buckling. Buckling was identified using recorded signals from strain gages and accelerometers, with high-speed video records, and by audibility. Experimental results are compared with numerical results obtained using a freezing-in-time technique. The numerical method is based on modal analysis techniques combined with a statically determined buckling interaction curve. Results of the study indicate that, for the particular types of transients studied, this freezing-in-time technique provides a conservative prediction of when buckling will occur. Author

N87-20596# Indian Inst. of Tech., New Delhi. Dept. of Mechanical Engineering.
FORCED VIBRATIONS OF STRINGER STIFFENED DAMPED SANDWICH PANEL
N. Kavi and N. T. Asnani *In* Shock and Vibration Information Center The Shock and Vibration Bulletin. Part 2: Modal Test and Analysis, Testing Techniques, Machinery Dynamics, Isolation and Damping, Structural Dynamics Aug. 1986 p 167-178 (For primary document see N87-20580 13-39)
Avail: NTIS HC A10/MF A01 CSCL 20/11

Transfer matrix method to determine response of a stiffened sandwich panel consisting of elastic face layers sandwiching viscoelastic core, to a deterministic harmonic loading was developed. A rectangular sandwich panel with arbitrary number of stringers placed at equal or unequal spacings was considered with the edges perpendicular to stringers simply supported and the edges parallel to stringers with arbitrary boundary conditions. The principle of the correspondence of linear viscoelasticity was applied to take account of the viscoelastic damping. Vibration response of a sandwich panel with two equally spaced stringers to a sinusoidal excitation was determined and values of the resonant frequencies and associated model loss factors are reported. Author

N87-20597# University of Central Florida, Orlando. Dept. of Mechanical Engineering and Aerospace Sciences.
STRUCTURAL DYNAMIC REANALYSIS USING RITZ VECTORS
L. Kitis and W. D. Pilkey (Virginia Univ., Charlottesville.) *In* Shock and Vibration Information Center The Shock and Vibration Bulletin. Part 2: Modal Test and Analysis, Testing Techniques, Machinery Dynamics, Isolation and Damping, Structural Dynamics Aug. 1986 p 179-181 (For primary document see N87-20580 13-39)
Avail: NTIS HC A10/MF A01 CSCL 20/11

The objective is to indicate how structural dynamic reanalysis can be done when Ritz vectors are used in mode superposition. Reanalysis methodology gives system response as a function of design parameters without a complete analysis for each parameter change. The generation of Ritz vectors for use in reanalysis requires the solution of linear algebraic equations and an eigenvalue problem of reduced order. An efficient method of formulation and solution of these problems is described. Author

N87-20598# Waterloo Univ. (Ontario). Dept. of Civil and Mechanical Engineering.
FATIGUE AND ACOUSTICS: PREDICTION OF METAL FATIGUE USING MINER'S RULE
H. H. E. Leipholz *In* Shock and Vibration Information Center The Shock and Vibration Bulletin. Part 2: Modal Test and Analysis, Testing Techniques, Machinery Dynamics, Isolation and Damping, Structural Dynamics Aug. 1986 p 183-190 (For primary document see N87-20580 13-39)
Avail: NTIS HC A10/MF A01 CSCL 20/11

The concept of a modified Woehler curve is introduced and used for the prediction of metal fatigue. First, a method is presented by which the modified curve can actually be obtained. Then, experimental evidence is given of the high precision of a fatigue life prediction by means of an equation which involves the values N sub i provided by the Woehler curve. In the last section, it is indicated how this derived equation can be modified to yield another equation. This equation is applicable for fatigue life prediction in the case where the load is a stochastic one. Author

N87-20599# Spar Aerospace Ltd., Ste-Anne-de-Bellevue (Quebec).
OPTIMIZATION OF AEROSPACE STRUCTURES SUBJECTED TO RANDOM VIBRATION AND FATIGUE CONSTRAINTS c05
V. K. Jha, T. S. Sankar (Concordia Univ., Montreal, Quebec.), and R. B. Bhat *In* Shock and Vibration Information Center The Shock and Vibration Bulletin. Part 2: Modal Test and Analysis, Testing Techniques, Machinery Dynamics, Isolation and Damping, Structural Dynamics Aug. 1986 p 193-200 (For primary document see N87-20580 13-39)
Avail: NTIS HC A10/MF A01 CSCL 20/11

Aerospace structures have to be designed with very strict reliability requirements, at the same time these structures should be as light as possible in weight to minimize the cost of launching into space. These structures are often subjected to random excitations with power spectral density varying in an arbitrary manner in the frequency domain. With the advent of the space shuttle, it is likely that these structures may have to be designed to withstand many launches, and hence fatigue will be an important factor along with other considerations while optimizing the design. An approach for handling and incorporating fatigue design constraints in optimizing aerospace structures is presented. Miner's criterion of cumulative fatigue damage was used to formulate the fatigue constraint to ensure that the total expected fatigue damage over the required period of fatigue life does not exceed unity. The fatigue constaint is used in conjunction with other probabilistic constraints such as those on displacements, stresses and on component sizes, when subjected to random vibration loads, to arrive at an optimum design. An optimum design of a typical satellite antenna structure was realized using the proposed approach. Author

N87-20600# Northrop Corp., Hawthorne, Calif. Electronics Div.
EVALUATION OF VIBRATION SPECIFICATIONS FOR STATIC AND DYNAMIC MATERIAL ALLOWABLES
S. P. Bhatia and J. H. Schmidt *In* Shock and Vibration Information Center The Shock and Vibration Bulletin. Part 2: Modal Test and Analysis, Testing Techniques, Machinery Dynamics, Isolation and Damping, Structural Dynamics Aug. 1986 p 201-207 (For primary document see N87-20580 13-39)
Avail: NTIS HC A10/MF A01 CSCL 20/11

A technique was developed previously to correlate sine, shock and random specifications for selecting the highest load or acceleration producing environment for comparison with the static (yield or ultimate) material allowables. The proposed method extends the above technique so that it not only allows for the direct comparison between sine, shock and random environments using a static (yield) allowable, but also makes this comparison more comprehensive by accounting for fatigue producing environments and the corresponding lower dynamic (fatigue) material allowables. The concept of equivalent stress for random vibrations is introduced. The proposed technique allows for a quick and an accurate assessment of the worst vibration environment using both the static and dynamic allowables, helps selection of alternate materials and provides the direction that detailed structural analysis must proceed. Author

N87-20601# Air Force Systems Command, Wright-Patterson AFB, Ohio.
SUPERSONIC FLOW INDUCED CAVITY ACOUSTICS c71
Leonard L. Shaw *In* Shock and Vibration Information Center The Shock and Vibration Bulletin. Part 2: Modal Test and Analysis, Testing Techniques, Machinery Dynamics, Isolation and Damping, Structural Dynamics Aug. 1986 p 209-216 (For primary document see N87-20580 13-39)
Avail: NTIS HC A10/MF A01 CSCL 20/11

A wind tunnel test was performed on a cavity model with

variable length and depth. It was tested at three supersonic Mach numbers of 1.5, 2.16 and 2.86. Four unit Reynolds numbers, 1.0, 2.0, 3.0, 4.0 million were tested. The model was tested at two angles of attack and two yaw angles. Two cavity widths were tested. Acoustic data were obtained for almost all combinations of the test parameters. Strong acoustic resonance was obtained for many of the configurations and all three Mach numbers. Levels as high as 165 dB were measured. Reynolds number was shown to strongly affect excitation of specific resonant modes. Angle of attack affected the levels as well as yaw. An important result of the effort is the affect of model scale. It was shown that by changing the cavity size, but keeping all other parameters equal, change in the flow induced acoustic levels as large as 20 dB can occur. As much of the acoustic data as possible is documented so that the data trends will be available for the user. Author

N87-20602# Shock and Vibration Information Center (Defense), Washington, D. C.
THE SHOCK AND VIBRATION BULLETIN. PART 3: INVITED PAPERS, PYROTECHNIC SHOCK, PYROTECHNIC SHOCK WORKSHOP
Aug. 1986 144 p Proceedings of 56th Symposium on Shock and Vibration, Monterey, Calif., 22-24 Oct. 1985
(AD-A175226; SVIC-Bull-56-Pt-3) Avail: NTIS HC A07/MF A01 CSCL 20/11

Topics addressed include: pyrotechnic shock; numerical simulation of Atlas-Centaur stage-separation; vibroacoustic data base management system; technology assessment of accelerometer characteristics; effects of data shock filtering; resonant plate simulation techniques; multiaxis transient shock simulation; and testing techniques. For individual titles, see N87-20603 through N87-20614.

N87-20603# Aerospace Corp., Los Angeles, Calif.
VIEWS OF THE WORLD OF PYROTECHNIC SHOCK
Charles Moening *In* Shock and Vibration Information Center The Shock and Vibration Bulletin. Part 3: Invited Papers, Pyrotechnic Shock, Pyrotechnic Shock Workshop Aug. 1986 p 3-28 (For primary document see N87-20602 13-39)
Avail: NTIS HC A07/MF A01 CSCL 20/11

Lessons learned in 27 years of aerospace engineering experience are reviewed. Flight failure data is examined. It was concluded that vibration and shock testing should maintain its present standards. B.G.

N87-20604# Shock and Vibration Information Center (Defense), Washington, D. C.
THE PRE-PULSE IN PYROSHOCK MEASUREMENT AND ANALYSIS
A. E. Galef *In* Shock and Vibration Information Center The Shock and Vibration Bulletin. Part 3: Invited Papers, Pyrotechnic Shock, Pyrotechnic Shock Workshop Aug. 1986 p 29-32 (For primary document see N87-20602 13-39)
(Contract F04704-84-C-0064)
Avail: NTIS HC A07/MF A01 CSCL 20/11

Accelerometers are usually incapable of faithful measurement of the nearly instantaneous velocity change occurring when a structure is subjected to excitation that closely approaches a true impulse (as is often the case with pyrotechnic or X-ray induced shocks). The imperfect accelerometer behavior can lead to a serious error in the shock spectrum calculated from it. A method of correcting for one of the common accelerometer insufficiencies is provided. Author

N87-20605*# Jet Propulsion Lab., California Inst. of Tech., Pasadena.
SUPER*ZIP (LINEAR SEPARATION) SHOCK CHARACTERISTICS
Kurng Y. Chang and Dennis L. Kern *In* Shock and Vibration Information Center The Shock and Vibration Bulletin. Part 3: Invited Papers, Pyrotechnic Shock, Pyrotechnic Shock Workshop Aug. 1986 p 33-42 Sponsored by NASA (For primary document see N87-20602 13-39)
Avail: NTIS HC A07/MF A01 CSCL 20K

Super*Zip is a high load carrying pyrotechnic device which separates ring-shroud structure without contamination. Explosive separation devices, such as Super*Zip, employed during the spacecraft launch phase and space flight generate a shock environment that could have a deleterious effect on the spacecraft hardware. The results of a series of tests designed to study the dynamic characteristic (and hence the shock response level) produced by detonation of the Super*Zip joint are presented. Tests performed include separation of straight and curved panels and of complete full-ring bands for spacecraft systems. Data obtained from these tests have provided qualitative indications of the shock response levels for different test configurations. During the study, considerable effort was extended to evaluate the shock directivity, distance attenuation, boundary condition effects, and firing-to-firing variations. Representative results are shown and the information can be used as a reference base for analytical predictions as well as flight equipment design requirements. Author

N87-20606# Physics International Corp., San Leandro, Calif.
NUMERICAL SIMULATION OF ATLAS-CENTAUR STAGE-SEPARATION SHAPED CHARGE FIRING AND STRUCTURAL RESPONSE **c15**
Steven Hancock, David Davison, Jim Gordon, Pius Chao, Norm Viste (General Dynamics/Convair, San Diego, Calif.), and Jack Weber *In* Shock and Vibration Information Center The Shock and Vibration Bulletin. Part 3: Invited Papers, Pyrotechnic Shock, Pyrotechnic Shock Workshop Aug. 1986 p 45-57 (For primary document see N87-20602 13-39)
Avail: NTIS HC A07/MF A01 CSCL 20/13

Numerical simulations were made of a flexible linear shaped charge missile stage separation system. Both the shaped charge firing and the missile structural response are modeled in detail. The numerical approach is verified by good agreement with laboratory ballistic pendulum tests and full scale stage separation tests. Parameter studies with the model have helped to identify a particular sensitivity of peak stress to a gap dimension. Author

N87-20607# Lockheed Missiles and Space Co., Sunnyvale, Calif.
A VIBROACOUSTIC DATABASE MANAGEMENT SYSTEM AND ITS APPLICATION FOR A PYROSHOCK DATABASE **c82**
W. Henricks and Y. Albert Lee *In* Shock and Vibration Information Center The Shock and Vibration Bulletin. Part 3: Invited Papers, Pyrotechnic Shock, Pyrotechnic Shock Workshop Aug. 1986 p 63-68 (For primary document see N87-20602 13-39)
Avail: NTIS HC A07/MF A01 CSCL 20/13

The development of a pyroshock database management system is proposed. A candidate data structure for this system is developed from that of a similar system previously configured for vibroacoustic data. Author

N87-20608# Wilson (Jon), San Juan Capistrano, Calif.
STATE-OF-THE-ART ACCELEROMETER CHARACTERISTICS FOR PYROTECHNIC SHOCK MEASUREMENT **c35**
Jon Wilson *In* Shock and Vibration Information Center The Shock and Vibration Bulletin. Part 3: Invited Papers, Pyrotechnic Shock, Pyrotechnic Shock Workshop Aug. 1986 p 71-76 (For primary document see N87-20602 13-39)
Avail: NTIS HC A07/MF A01 CSCL 14/2

A brief history, a brief summary of a user survey, and a brief summary of a manufacturer's survey that was conducted to find the state-of-the-art for pyrotechnic shock measurements are presented. It provides a chart summarizing the characteristics of several different accelerometers. Author

N87-20609# TRW Electronics and Defense Sector, Redondo Beach, Calif.
ZERO-SHIFTED ACCELEROMETER OUTPUTS **c35**
Arnold Galef *In* Shock and Vibration Information Center The Shock and Vibration Bulletin. Part 3: Invited Papers, Pyrotechnic Shock, Pyrotechnic Shock Workshop Aug. 1986 p 77-80 (For primary document see N87-20602 13-39)

Avail: NTIS HC A07/MF A01 CSCL 14/2

It is claimed that the commonly appearing zero-shift in pyroshock data is usually a symptom of a malfunctioning measurement system, so that the data can not be repaired (by high-pass filtering or equivalent) unless tests can be devised that permit the demonstration that the system is operating in a linear mode in all respects other than the shift. The likely cause of the zero-shift and its prevention are discussed. Author

N87-20610# Rockwell International Corp., Canoga Park, Calif. Rocketdyne Div.

QUESTIONABLE EFFECTS OF SHOCK DATA FILTERING

Paul R. Strauss *In* Shock and Vibration Information Center The Shock and Vibration Bulletin. Part 3: Invited Papers, Pyrotechnic Shock, Pyrotechnic Shock Workshop Aug. 1986 p 81-83 (For primary document see N87-20602 13-39)

Avail: NTIS HC A07/MF A01 CSCL 20/11

Measurements of pyrotechnic shock events are unpredictable and often unexplainable. Filtering of accelerometer signals is used and misused in processing the data. An attempt is made to show the effects of some filtering processes. A sample case of an electrically simulated measurement is presented to exemplify the effect of filtering on the Shock Response Spectrum, the final data product. Author

N87-20611# TRW Electronics and Defense Sector, Redondo Beach, Calif.

COMPARISON OF RESPONSE FROM DIFFERENT RESONANT PLATE SIMULATION TECHNIQUES

Robert E. Morse *In* Shock and Vibration Information Center The Shock and Vibration Bulletin. Part 3: Invited Papers, Pyrotechnic Shock, Pyrotechnic Shock Workshop Aug. 1986 p 85-116 (For primary document see N87-20602 13-39)

Avail: NTIS HC A07/MF A01 CSCL 20/11

Two applications of the resonant plate technique are examined. The development of each system is discussed, and the responses are compared. B.G.

N87-20612# Sandia National Labs., Albuquerque, N. Mex.

THE CONTROLLED RESPONSE OF RESONATING FIXTURES USED TO SIMULATE PYROSHOCK ENVIRONMENTS

Neil T. Davie *In* Shock and Vibration Information Center The Shock and Vibration Bulletin. Part 3: Invited Papers, Pyrotechnic Shock, Pyrotechnic Shock Workshop Aug. 1986 p 119-124 (For primary document see N87-20602 13-39)

Avail: NTIS HC A07/MF A01 CSCL 20/11

The test techniques used at Sandia National Laboratories for simulating pyrotechnic shock on components are described. It is a resonating fixture approach, sometimes known as a hammer test. Information is brought together that was available separately, and adds details, not previously published, which should enable the reproduction of these techniques for use. Author

N87-20613# Agbabian Associates, El Segundo, Calif.

MULTI-AXIS TRANSIENT SHOCK SIMULATION USING MECHANICAL PULSE GENERATORS

F. B. Safford *In* Shock and Vibration Information Center The Shock and Vibration Bulletin. Part 3: Invited Papers, Pyrotechnic Shock, Pyrotechnic Shock Workshop Aug. 1986 p 125-132 (For primary document see N87-20602 13-39)

Avail: NTIS HC A07/MF A01 CSCL 20/11

Pyrotechnic shock is represented by a very short time duration, accelerations into 1000 g levels, and a wide frequency band up to 10 kHz. The current technology of laboratory simulation test machines is hard pressed to repetitively meet these requirements in one axis and much less so in two or three axes simultaneously. A biaxial transient shock machine under development for the U.S. Army ERADCOM is described and shows potential to adequately meet these pyrotechnic requirements in two-axes with extension to three-axes. Author

N87-20614# McDonnell-Douglas Corp., Huntington Beach, Calif.

SUMMARY OF TESTING TECHNIQUES

Dan Powers *In* Shock and Vibration Information Center The Shock and Vibration Bulletin. Part 3: Invited Papers, Pyrotechnic Shock, Pyrotechnic Shock Workshop Aug. 1986 p 135-142 (For primary document see N87-20602 13-39)

Avail: NTIS HC A07/MF A01 CSCL 20/11

The use of flight structures or flight-like structures and general-purpose machines that can be used to simulate a pyrotechnic shock environment that was generated from a wide range of vehicles are discussed. B.G.

N87-20615# Ceskoslovenska Akademie Ved, Brno. Ustav Fyzikaini Metalurgie.

CREEP AND CREEP FRACTURE: CONFERENCE PROCEEDINGS [CREEP A LOM PRI CREEPU: SBORNIK PREDNASEK, CAST 2]

Sep. 1985 15 p In CZECHOSLOVAKIAN Proceedings of the 5th National Seminar on Creep and Creep Fracture, Kuparovice, Czechoslovakia, 21 Oct. 1985

(DE87-780056; INIS-mf-10517; CONF-8510384-Pt-2) Avail: NTIS (US Sales Only) HC A02/MF A01

Individual papers in this meeting have been abstracted separately. Two papers are presented in Czech with references. DOE

N87-20616# Stuttgart Univ. (West Germany). Inst. fuer Mechanik (Bauwesen).

NUMERICAL INVESTIGATIONS OF GEOMETRICALLY NONLINEAR SHELL KINETICS Ph.D. Thesis [NUMERISCHE UNTERSUCHUNGEN ZUR GEOMETRISCH NICHTLINEAREN SCHALENKINETIK]

Karl Baitinger 1986 149 p In GERMAN

(ETN-87-99019) Avail: NTIS HC A07/MF A01

A simple but efficient method suited for the numerical investigation of the nonlinear supporting behavior of thin, dynamically loaded, elastic shells was developed. The variational equation of thin shells was deduced using a mixed formulation of the d'Alembert-principle. The discretization of this equation with respect to space and time leads to nonlinear algebraic equations. The advantages of the variational formulation are that lower derivatives occur and that boundary conditions can be taken into account in a simple way. Simple assumptions in the space discretization using independent approximations lead to useful results. All the unknowns of a time stop are determined from quantities calculated in previous time steps (explicit method). An inversion of large matrices is not required. The usefulness of the method in comparison with analytical approximation was demonstrated in an example with thin plates. Stability phenomena can be correctly analyzed. ESA

N87-20617# Office National d'Etudes et de Recherches Aerospatiales, Paris (France). Direction Scientifique de la Resistance des Structures.

A MODEL FOR THE DEGRADATION OF COMPOSITE STRUCTURES Final Report [UN MODELE DE DEGRADATION POUR LES STRUCTURES COMPOSITES]

R. Girard Jun. 1986 29 p In FRENCH

(Contract DRET-85-34-001)

(ONERA-RT-30/3043-RY-057-R; ETN-87-99382) Avail: NTIS HC A03/MF A01

The degeneration of a single laminate layer was characterized using a criterion to define load levels and a redefinition of the degraded layer behavior. The model is implemented in a finite element code considering the successive degradation of individual layers until total breakdown. The model was tested on a composite panel problem, showing that it is a good starting point for model development. ESA

N87-20372# Royal Netherlands Aircraft Factories Fokker, Schiphol-Oost. Space Div.

ACOUSTIC EFFECTS ON THE DYNAMIC OF LIGHTWEIGHT STRUCTURES

J. J. Wijker *In* AGARD Mechanical Qualification of Large Flexible Spacecraft Structures Jul. 1986 15 p (For primary document

see N87-20355 13-18)
Avail: NTIS HC A12/MF A01

N87-20437# Air Force Academy, Colo. Dept. of Engineering Mechanics.
RECENT STUDIES IN PLATE VIBRATIONS: 1981-1985. PART 1: CLASSICAL THEORY
A. W. Leissa *In* Vibration Inst. The Shock and Vibration Digest, Volume 19, No. 2 Feb. 1987 p 11-18 (For primary document see N87-20435 13-31)
Avail: NTIS HC A05/MF A01

N87-20440# Stevens Inst. of Tech., Hoboken, N. J. Dept. of Mechanical Engineering.
STABLE RESPONSE OF DAMPED LINEAR SYSTEMS, PART 3
D. W. Nicholson *In* Shock and Vibration Information Center The Shock and Vibration Digest, Volume 18, No. 10 Oct. 1986 p 13-21 (For primary document see N87-20438 13-31)
Avail: NTIS HC A05/MF A01 CSCL 20K

N87-20762# Selenia Industrie Elettroniche Associate S.p.A., Pomezia (Italy). Defense Systems Div.
AN APPLICATION OF RAYLEIGH'S METHOD TO THE FAST CALCULATION OF THE FIRST VIBRATION FREQUENCY OF A MISSILE LAUNCHER CELL
Gian Fabrizio Venarucci and Armando Peruzzi *In its* Rivista Tecnica Selenia, Volume 10, Number 1 1986 p 25-31 (For primary document see N87-20759 13-61)
Avail: NTIS HC A04/MF A01

42 GEOSCIENCES (GENERAL)

No abstracts in this category.

43 EARTH RESOURCES AND REMOTE SENSING

Includes remote sensing of earth resources by aircraft and spacecraft; photogrammetry; and aerial photography.

For instrumentation see *35 Instrumentation and Photography.*

N87-20618 Bayerische Akademie der Wissenschaften, Munich (West Germany). Bayerische Kommission fuer die Internationale Erdmessung.
REPORT ON THE SPECIAL PROGRAM 78 SATELLITE GEODESY OF THE TECHNICAL UNIVERSITY OF MUNICH Progress Report, 1984-1985 [DIE ARBEITEN DES SONDERFORSCHUNGSBEREICHES 78 SATELLITENGEODAESIE DER TECHNISCHEN UNIVERSITAET MUENCHEN 1984 UND 1985]
Manfred Schneider 1986 346 p In GERMAN
(Astron-Geodaet-Arb-48; ISBN-3-7696-9791-X; ISSN-0340-7691; ETN-87-98974) Copyright. Avail: Issuing Activity

In the project, laser range finding software and sequential storage system development for satellite observation, the thermal behavior and radiation quality of an Nd-glass slab laser, laser and receiver developments, and a concept for a Moon and satellite laser range finder were studied. A mobile laser range finder was examined. The operation and development of a receiver unit for radio interferometry was investigated. Microwave Doppler and global positioning measurements were performed. Universal time, terrestrial, meteorological, and seismological supplemental measurements were conducted. Gradiometer concepts were examined. The influence of lithosphere boundary waves on the geoid was studied. In the field of the Earth-Moon systems dynamics ephemeride calculations, satellite orbits and laser time-of-flight, satellite gradiometry, the Newton-Euler equation of motion, and relativistic effects were investigated. The astrometric and geodetic-geophysical application of interferometric methods was examined.
ESA

N87-20619 Delaware Univ., Newark.
REAL-TIME CROP ASSESSMENT USING COLOR THEORY AND SATELLITE DATA Ph.D. Thesis
Russell Andrew Ambroziak 1986 219 p
Avail: Univ. Microfilms Order No. DA8629273

A new color coordinate system for satellite image display is developed and applied to crop monitoring using AVHRR data over the African Sahel. The system, called the Ambroziak Color Coordinate System (ACCS), is the result of applying color theory, models of human vision, and analyses of the unique constraints put on remote sensing for agriculture by the interaction of the vegetation's and atmosphere's time scales of change. The new color system allows real-time quantitative analysis of crops to be done in support of regional and national food security programs. The need for such a system is demonstrated by the severe food shortages in parts of Africa over the past several years and the delayed reports of existing problems. Based on the analysis of the strengths and weaknesses of false color IR images in existing crop monitoring systems which use remotely sensed data, the steps necessary to improve the usefulness of the image without sacrificing its strengths are outlined. The result is the development of the ACCS. The ACCS is then used to produce high resolution, effective cumulative rainfall analyses of the African Sahel and Horn regions.
Dissert. Abstr.

N87-20620 Wisconsin Univ., Madison.
THE USE OF VISIBLE DATA FOR IMPROVING VAS SATELLITE SOUNDINGS Ph.D. Thesis
Gin-Rong Liu 1986 143 p
Avail: Univ. Microfilms Order No. DA8623686

An improved method for handling clouds in the process of retrieving atmospheric vertical sounding from VAS geostationary radiance observations is developed, tested, and applied. The method makes use of visible data for the first time, permitting estimates of fractional cloud amount for each 8-16 Km infrared field of view (FOV) using high resolution, 1 Km, visible data. Cloud top pressure is calculated using the CO2 slicing method or directly from the VAS observed 11 micron window channel overcast brightness temperature and the temperature profile. Cloud emissivity is obtained from the cloud level atmospheric temperature, which corresponds to the cloud top pressure derived from the CO2 slicing method, and VAS 11 micron window channel brightness temperature. With the aid of effective cloud amount and cloud top pressure, the proper clear and cloudy weighting functions of the radiative transfer equation (RTE) are specified, and a direct physical inverse solution (e.g., the simultaneous physical retrieval method) of the RTE is used to produce vertical temperature and moisture soundings. In addition to giving cloud amount, cloud top temperature, cloud emissivity, and cloud top pressure estimates, the surface skin temperature is also estimated as part of the temperature and water vapor profile retrieval process. The results obtained from its application are compared with the surface hourly reports, radiosonde observations and sounding determinations by the CIMSS (Cooperative institute for Meteorological Satellite Studies) operational method of profile retrieval. The intercomparisons reveal significant improvements both in the reliability and accuracy in atmospheric profile retrieval using visible channel data.
Dissert. Abstr.

N87-20621# European Space Agency, Paris (France).
PROCEEDINGS OF THE EUROPEAN SYMPOSIUM ON POLAR PLATFORM OPPORTUNITIES AND INSTRUMENTATION FOR REMOTE-SENSING (ESPOIR)
E. J. Rolfe, ed. and B. Battrick, ed. Nov. 1986 127 p Symposium held in Avignon, France, 16-18 Jun. 1986
(ESA-SP-266; ISSN-0379-6566; ETN-87-99434) Avail: NTIS HC A07/MF A01

European activities in preparing the Columbus polar platforms;

United States cooperation with Europe; atmosphere, land, ocean/ice, and solid Earth missions; and platform instruments, calibrating, data management, orbit configuration, and servicing were discussed. For individual titles, see N87-20622 through N87-20641.

N87-20622# European Space Agency. European Space Research and Technology Center, ESTEC, Noordwijk (Netherlands).
THE EARTH OBSERVATION ACTIVITIES OF THE EUROPEAN SPACE AGENCY AND THE USE OF THE POLAR PLATFORM OF THE INTERNATIONAL SPACE STATION
B. Pfeiffer *In its* Proceedings of the European Symposium on Polar platform Opportunities and Instrumentation for Remote-sensing (ESPOIR) Nov. 1986 p 7-10 (For primary document see N87-20621 13-43)
Avail: NTIS HC A07/MF A01

The Meteosat, ERS-1, and Earthnet programs are reviewed. The long term follow-on programs are outlined. Space infrastructure elements of ESA and their use for Earth observation are described. User requirements and ESA policy for a polar Earth observations platform are discussed. ESA

N87-20623# European Space Agency, Paris (France). Directorate of Space Station and Platforms.
THE COLUMBUS PROGRAM: AN OVERVIEW c12
D. J. Shapland *In its* Proceedings of the European Symposium on Polar platform Opportunities and Instrumentation for Remote-sensing (ESPOIR) Nov. 1986 p 11-17 (For primary document see N87-20621 13-43)
Avail: NTIS HC A07/MF A01

The origins and content of the Columbus program are reviewed. The candidate elements to be studied in phase B2 are described: a pressurized module/laboratory permanently attached to the Space Station core; a man-tended free flyer (pressurized module plus resource module); a polar platform; and a co-orbiting platform based on Eureca technology and experience. A scenario and schedule of events is suggested and discussed in the framework of a total European plan. The importance of user requirements is stressed. ESA

N87-20624# Deutsche Forschungs- und Versuchsanstalt fuer Luft- und Raumfahrt, Oberpfaffenhofen (West Germany).
EUROPEAN UTILIZATION ASPECTS STUDIES c19
F. Schlude *In* ESA Proceedings of the European Symposium on Polar platform Opportunities and Instrumentation for Remote-sensing (ESPOIR) Nov. 1986 p 21-27 (For primary document see N87-20621 13-43)
Avail: NTIS HC A07/MF A01

Starting from a synthesis of space station user data needs, a minimum instrumentation scenario was derived. Grouping of these instruments gave application oriented missions which led to two model missions that can be realized on an international two polar platform system. ESA

N87-20625# European Space Agency. European Space Research and Technology Center, ESTEC, Noordwijk (Netherlands).
WORKING GROUP ON EARTH OBSERVATION REQUIREMENTS FOR THE POLAR ORBITING PLATFORM ELEMENTS OF THE INTERNATIONAL SPACE STATION (THE POPE WORKING GROUP) c18
N. deVilliers *In its* Proceedings of the European Symposium on Polar platform Opportunities and Instrumentation for Remote-sensing (ESPOIR) Nov. 1986 p 29-33 (For primary document see N87-20621 13-43)
Avail: NTIS HC A07/MF A01

A polar platform specification for Earth observations was defined. It features 2 platforms in coordinated Sun-synchronous orbits at an altitude of 800 km (morning and afternoon orbits); a multidisciplinary payload divided between the platforms growing from 2.4 tons initially (per platform) through 3.6 tons at the first servicing to a mature amount of 4.8 tons per platform at the second service point; and servicing every 2 to 3 yr, adding new payloads and upgrading payloads. The power requirements grow from 2 to 2.5 KW initially, through 4 KW, to 6 KW. The data rates of up to several hundred megabits per second are compatible with: direct downlinking, and the proposed European Data Relay Satellite System; the lower data rates generated globally are compatible with on-board recording techniques. ESA

N87-20626# Centre National d'Etudes Spatiales, Toulouse (France). SPOT IMAGE.
REMOTE SENSING APPLICATIONS: COMMERCIAL ISSUES AND OPPORTUNITIES FOR SPACE STATION
G. Brachet *In* ESA Proceedings of the European Symposium on Polar platform Opportunities and Instrumentation for Remote-sensing (ESPOIR) Nov. 1986 p 35-37 (For primary document see N87-20621 13-43)
Avail: NTIS HC A07/MF A01

The SPOT program is reviewed and the long term prospects beyond SPOT-4 are assessed. Management, legal, and commercial aspects are emphasized. ESA

N87-20627# European Space Agency. European Space Research and Technology Center, ESTEC, Noordwijk (Netherlands).
ESA COLUMBUS POLAR PLATFORM DESIGN CONCEPT c18
P. Wolf *In its* Proceedings of the European Symposium on Polar platform Opportunities and Instrumentation for Remote-sensing (ESPOIR) Nov. 1986 p 39-42 (For primary document see N87-20621 13-43)
Avail: NTIS HC A07/MF A01

The Columbus polar platform (PPF) system requirements, configuration, payload complement model, subsystem concepts, and operational aspects are discussed. The PPF is intended to be a large general purpose spacecraft supporting scientific and operational users in a high inclination Earth orbit. Earth observations represent a large percentage of the potential user community, whose requirements essentially determine the design and performance of the PPF. The PPF design is planned to be relatively classical and conservative except for technology for an on-orbit servicing, maintenance, and upgrading capability to extend the life of this large vehicle, and in particular repair, upgrade, and modernize in-orbit the user instruments on board of the PPF, and to bring new instruments up to the PPF at determined intervals after the launch of the spacecraft and its initial payload complement. ESA

N87-20628# European Space Agency, Paris (France).
SERVICING OF THE POLAR PLATFORM c18
G. Valentiny *In its* Proceedings of the European Symposium on Polar platform Opportunities and Instrumentation for Remote-sensing (ESPOIR) Nov. 1986 p 43-47 (For primary document see N87-20621 13-43)
Avail: NTIS HC A07/MF A01

The use of the ESA shuttle Hermes to service the Columbus space station polar platform is discussed. In-orbit servicing is required to achieve the 20 yr specified lifetime for the platform. Hermes can carry 4 people and a 2 ton payload. A typical servicing scenario is presented. ESA

N87-20629# European Space Agency. European Space Research and Technology Center, ESTEC, Noordwijk (Netherlands).
ORBIT CONFIGURATIONS c18
N. deVilliers *In its* Proceedings of the European Symposium Polar platform Opportunities and Instrumentation for Remote-sensing (ESPOIR) Nov. 1986 p 49-53 (For primary document see N87-20621 13-43)
Avail: NTIS HC A07/MF A01

The International Space Station polar platform orbit is discussed. The effect of orbit class, number of orbits, nodal equatorial crossing times, altitude, repeat cycles (linked to altitude), relative phasing of platforms (linked to repeat cycles), and additional platforms are considered. A pair of platforms in Sun synchronous orbit, one in a morning orbit, the other an afternoon is proposed. ESA

N87-20630# European Space Agency. ESRIN, Frascati (Italy).
PAYLOAD DATA MANAGEMENT SCHEME PLANNED FOR

EARTH OBSERVATION SENSORS TO BE FLOWN ON THE POLAR PLATFORMS IN THE FRAMEWORK OF THE SPACE STATION/COLUMBUS PROGRAM
L. Marelli *In its* Proceedings of the European Symposium on Polar platform Opportunities and Instrumentation for Remote-sensing (ESPOIR) Nov. 1986 p 55-61 (For primary document see N87-20621 13-43)
Avail: NTIS HC A07/MF A01

Data transmission to the ground from the Columbus polar platform; data acquisition and recording; data processing and dissemination; data archive/retrieval; and user interfaces are discussed. ESA

N87-20631# European Space Agency. European Space Research and Technology Center, ESTEC, Noordwijk (Netherlands).
COOPERATION OF THE INTERNATIONAL SPACE STATION PARTNERS IN THE PREPARATION OF THE USE OF SPACE STATION ELEMENTS FOR EARTH OBSERVATION (PLATFORM AND PAYLOAD ASPECTS) **c84**
B. Pfeiffer *In its* Proceedings of the European Symposium on Polar platform Opportunities and Instrumentation for Remote-sensing (ESPOIR) Nov. 1986 p 65-67 (For primary document see N87-20621 13-43)
Avail: NTIS HC A07/MF A01

Space station elements and launch/services means for polar missions are discussed. European interests are identified. Items for further study and coordination between space station partners are suggested. Potential polar platform instruments, and their providers, are listed. ESA

N87-20632# European Space Agency, Paris (France).
USA-EUROPE COORDINATION AND COOPERATION ACTIVITIES: ANNOUNCEMENTS OF OPPORTUNITY **c84**
G. Duchossois *In its* Proceedings of the European Symposium on Polar platform Opportunities and Instrumentation for Remote-sensing (ESPOIR) Nov. 1986 p 69-71 (For primary document see N87-20621 13-43)
Avail: NTIS HC A07/MF A01

International Space Station polar platform Announcements of Opportunity objectives, content, schedule, evaluation and selection process, address, funding sources, data access and rights, as discussed and agreed within the Coordination Group are outlined. ESA

N87-20633# Science Research Council, Chilton (England).
REPORT OF THE ATMOSPHERE PANEL **c12**
J. E. Harries and H. Fischer (Technische Univ., Munich, West Germany.) *In* ESA Proceedings of the European Symposium on Polar platform Opportunities and Instrumentation for Remote-sensing (ESPOIR) Nov. 1986 p 75-77 (For primary document see N87-20621 13-43)
Avail: NTIS HC A07/MF A01

Policy issues governing the planning of an atmospheric element of a European Polar Platform program were debated. Instrument payloads and observation strategies are suggested. ESA

N87-20634# Deutsche Forschungs- und Versuchsanstalt fuer Luft- und Raumfahrt, Oberpfaffenhofen (West Germany).
LAND PANEL REPORT **c18**
J. Bodechtel and F. Lanzl *In* ESA Proceedings of the European Symposium on Polar platform Opportunities and Instrumentation for Remote-sensing (ESPOIR) Nov. 1986 p 79-83 (For primary document see N87-20621 13-43)
Avail: NTIS HC A07/MF A01

International Space Station polar platform sensor configurations and missions are suggested. The platforms should maintain the capability for operational land remote sensing using optical sensors; improve the capability of optical sensors in terms of radiometric and spatial resolution, coverage, stereoscopic capability, etc.; improve experimental capabilities for allweather remote sensing of land with microwave sensors, to provide an operational capability similar to that of optical sensors; optimize the integration of microwave and optical data; set up demonstration programs in renewable resources, achieve operational status in the 1990s; and promote fundamental research activities. ESA

N87-20635# Meteorological Office, Bracknell (England).
OCEAN-ICE PANEL REPORT **c48**
T. D. Allan and A. Morel *In* ESA Proceedings of the European Symposium on Polar platform Opportunities and Instrumentation for Remote-sensing (ESPOIR) Nov. 1986 p 85-88 (For primary document see N87-20621 13-43)
Avail: NTIS HC A07/MF A01

Ocean/ice objectives, payload, observation strategy, and data management of Columbus are outlined. Ocean/ice objectives for Columbus should provide continuity to routine remote sensing of the global oceans and ice caps, and over European coastal zones; prepare for an operational system following the experimental and/or pre-operational satellite systems planned to be launched over the next 5yr; develop and test techniques and concepts; provide improved scientific, social and economic benefits; and foster international, interagency cooperative programs aimed at the routine monitoring of the environment. ESA

N87-20636# Belgian Royal Observatory, Brussels.
SOLID EARTH PANEL REPORT
P. Paquet *In* ESA Proceedings of the European Symposium on Polar platform Opportunities and Instrumentation for Remote-sensing (ESPOIR) Nov. 1986 p 89-91 (For primary document see N87-20621 13-43)
Avail: NTIS HC A07/MF A01

Investigations of geokinematics, Earth gravity, and geomagnetism by Columbus polar platforms are discussed. Candidate techniques for solid Earth missions, and support from solid Earth studies for Earth observations are considered. ESA

N87-20637# European Space Agency, Paris (France).
PANEL REPORT ON MULTIDISCIPLINARY INSTRUMENTATION: NEW POSSIBILITIES **c19**
G. Duchossois *In its* Proceedings of the European Symposium on Polar platform Opportunities and Instrumentation for Remote-sensing (ESPOIR) Nov. 1986 p 95-97 (For primary document see N87-20621 13-43)
Avail: NTIS HC A07/MF A01

The utility of active microwave sensors, passive microwave sensors, high and medium resolution optical sensors, and active optics/laser sensors for the Columbus polar platform Earth observations was assessed. Recommendations concerning SAR, radar altimeters, wind scatterometers, rain radiometers and scatterometers, and microwave radiometers are made. ESA

N87-20638# European Space Agency, Paris (France).
PANEL REPORT ON NEW APPROACHES TO CALIBRATION AND VALIDATION **c19**
S. Bruzzi *In its* Proceedings of the European Symposium on Polar platform Opportunities and Instrumentation for Remote-sensing (ESPOIR) Nov. 1986 p 99-100 (For primary document see N87-20621 13-43)
Avail: NTIS HC A07/MF A01

The impact of the Columbus polar platform system on calibration and validation; the impact of availability of the space station system (including a coorbiting platform), and the impact of servicing were discussed. ESA

N87-20639# European Space Agency. ESRIN, Frascati (Italy).
DATA MANAGEMENT PANEL REPORT
L. Marelli *In its* Proceedings of the European Symposium on Polar platform Opportunities and Instrumentation for Remote-sensing (ESPOIR) Nov. 1986 p 101-102 (For primary document see N87-20621 13-43)
Avail: NTIS HC A07/MF A01

Data gathering, data processing and dissemination, data archiving and retrieval, and user support services for the Columbus space station polar platforms are discussed. ESA

N87-20640# European Space Agency. European Space Research and Technology Center, ESTEC, Noordwijk (Netherlands).

THE ORBIT CONFIGURATION PANEL REPORT
D. deVilliers *In its* Proceedings of the European Symposium on Polar platform Opportunities and Instrumenation for Remote-sensing (ESPOIR) Nov. 1986 p 103-106 (For primary document see N87-20621 13-43)
Avail: NTIS HC A07/MF A01

The effects on Columbus polar platforms of class of orbits, number of orbits/platforms, nodal crossing times, orbit altitudes, repeat cycles, impact of an additional platform, and impact of having two half-sized platforms in each orbit are reviewed. The impact on meteorological sounders of reducing the altitude; possible choices of repeat cycles and the extent to which compromises can be found because of the conflicts with altitude; and a four-platform scenario, concentrating on the improvements possible in repeat cycles and the altitude choices available should be investigated. ESA

N87-20641# European Space Agency. European Space Research and Technology Center, ESTEC, Noordwijk (Netherlands).
PANEL REPORT ON THE POLAR PLATFORM SERVICING APPROACH AND ITS IMPLICATIONS c18
B. Pfeiffer *In its* Proceedings of the European Symposium on Polar platform Opportunities and Instrumentation for Remote-sensing (ESPOIR) Nov. 1986 p 107-108 (For primary document see N87-20621 13-43)
Avail: NTIS HC A07/MF A01

Preventive maintenance for polar-platform subsystems and instruments; corrective maintenance for polar-platform subsystems and instruments in the event of failure(s); enhancement of polar-platform capabilities beyond the initial orbit configuration; long-duration missions involving high-repetitivity of Earth observation data; and performing such missions on a cost-effective basis were discussed. A servicing approach and implications and user requirements were reviewed. ESA

N87-20642# Air/Ocean Remote Sensing Co., San Diego, Calif.
SIMULATION OF WIND GRADIENT ERRORS IN NROSS (NAVY REMOTE OCEAN SENSING SYSTEM) RADAR SCATTEROMETER DATA IN A SIMPLIFIED GEOMETRY Final Report, May - Sep. 1986
James L. Mueller Aug. 1986 48 p
(Contract N62271-86-M-0235)
(AD-A175754; AO1-1(ST1); NEPRF-CR-86-05) Avail: NTIS HC A03/MF A01 CSCL 17/9

A set of simplified case studies is used to illuminate the effect of spatial gradients in normalized radar cross section (NRCS) on the accuracy of NRCS at NROSS (Navy Remote Ocean Sensing System) scatterometer (NSCAT) cell centroids, and at wind vector retrieval grid points displaced from the centroid. Values of linear and quadratic variables s(x,y) are estimated at the centroid and at a point displaced from the centroid of a parallelogram cell, using first the mean value (S) over the cell (a nearest neighbor or binning approach) and then a bilinear interpolation estimator Si(x,y). Isoparametric finite elements are used to take cell shape into account in the interpolation. At cell centroids with linear fields s(x,y), errors are negligible using either (S) or Si(x,y). At cell centroids with nonlinear fields s(x,y), errors using (S) and Si(x,y) both approach 0.5% (with interpolation errors being slightly less) at spatial gradients of 0.1 dB/km. At displaced points with linear fields s(x,y), errors using interpolation Si(x,y) are negligible at all gradients, but error using cell means (S) exceeds 6% at gradients of 0.1 dB/km. At displaced points with nonlinear fields s(x,y), error using interpolation Si(x,y) approaches 2%, while error using cell means (S) exceeds 7%, near spatial gradients of 0.1 dB/km. The simulated errors associated with binning are large, and interpolation yields much better accuracy. GRA

N87-20643# Oak Ridge National Lab., Tenn.
THE 3-D WORLD MODELLING WITH UPDATING CAPABILITY BASED ON COMBINATORIAL GEOMETRY
M. Goldstein, F. G. Pin, G. deSaussure, and C. R. Weisbin 1987 11 p Presented at the Workshop on Space Telerobotics, Pasadena, Calif., 20 Jan. 1987
(Contract DE-AC05-84OR-21400)
(DE87-004257; CONF-870134-1) Avail: NTIS HC A02/MF A01

This paper describes a 3-D world modeling technique using range data. Range data quantify the distances from the sensor focal plane to the object surface, i.e., the 3-D coordinates of discrete points on the object surface are known. The approach proposed herein for 3-D world modeling is based on the Combinatorial Geometry (CG) Method which is widely used in Monte Carlo particle transport calculations. First, each measured point on the object surface is surrounded by a small sphere with a radius determined by the range to that point. Then, the 3-D shapes of the visible surfaces are obtained by taking the (Boolean) union of all the spheres. The result is an unambiguous representation of the object's boundary surfaces. The pre-learned partial knowledge of the environment can be also represented using the CG Method with a relatively small amount of data. Using the CG type of representation, distances in desired directions to boundary surfaces of various objects are efficiently calculated. This feature is particularly useful for continuously verifying the world model against the data provided by a range finder, and for integrating range data from successive locations of the robot during motion. The efficiency of the proposed approach is illustrated by simulations of a spherical robot in a 3-D room in the presence of moving obstacles and inadequate prelearned partial knowledge of the environment. DOE

44 ENERGY PRODUCTION AND CONVERSION

Includes specific energy conversion systems, e.g., fuel cells; global sources of energy; geophysical conversion; and windpower.

For related information see also *07 Aircraft Propulsion and Power, 20 Spacecraft Propulsion and Power,* and *28 Propellants and Fuels.*

N87-20644*# Jet Propulsion Lab., California Inst. of Tech., Pasadena.
FLAT-PLATE SOLAR ARRAY PROJECT OF THE US DEPARTMENT OF ENERGY'S NATIONAL PHOTOVOLTAICS PROGRAM: TEN YEARS OF PROGRESS
Elmer Christensen Oct. 1985 105 p Sponsored in part by NASA and DOE
(NASA-CR-180507; NAS 1.26:180507) Avail: NTIS HC A06/MF A01 CSCL 10A

The Flat-Plate Solar Array (FSA) Project, a Government-sponsored photovoltaics project, was initiated in January 1975 (previously named the Low-Cost Silicon Solar Array Project) to stimulate the development of PV systems for widespread use. Its goal then was to develop PV modules with 10% efficiency, a 20-year lifetime, and a selling price of $0.50 per peak watt of generating capacity (1975 dollars). It was recognized that cost reduction of PV solar-cell and module manufacturing was the key achievement needed if PV power systems were to be economically competitive for large-scale terrestrial use. Author

N87-20645*# Jet Propulsion Lab., California Inst. of Tech., Pasadena.
SUMMARY OF FLAT-PLATE SOLAR ARRAY PROJECT DOCUMENTATION: ABSTRACTS OF PUBLISHED DOCUMENTS, 1975-1986, REVISION 1
M. J. Phillips Sep. 1986 217 p Sponsored in part by NASA and DOE
(NASA-CR-180401-Rev-1; JPL-Pub-82-79-Rev-1;
Rept-5101-221-Rev-1; NAS 1.26:180401-Rev-1;
DOE/JPL-1012-76-Rev-1) Avail: NTIS HC A10/MF A01 CSCL 10A

Abstracts of final reports, or the latest quarterly or annual, of the Flat-Plate Solar Array (FSA) Project Contractor of Jet Propulsion Laboratory (JPL) in-house activities are presented. Also presented is a list of proceedings and publications, by author, of work

connected with the project. The aim of the program has been to stimulate the development of technology that will enable the private sector to manufacture and widely use photovoltaic systems for the generation of electricity in residential, commercial, industrial, and Government applications at a cost per watt that is competitive with utility generated power. FSA Project activities have included the sponsoring of research and development efforts in silicon refinement processes, advanced silicon sheet growth techniques, higher efficiency solar cells, solar cell/module fabrication processes, encapsulation, module/array engineering and reliability, and economic analyses. Author

N87-20646*# Jet Propulsion Lab., California Inst. of Tech., Pasadena.
FLAT-PLATE SOLAR ARRAY PROJECT. VOLUME 1: EXECUTIVE SUMMARY Final Report
W. Callaghan and R. McDonald Oct. 1986 29 p Sponsored in part by NASA, DOE, NSF and ERDA
(Contract DE-A101-85-CE-89008)
(NASA-CR-180658; JPL-Pub-86-31-Vol-1; NAS 1.26:180658; DOE/JPL-1012-125-Vol-1) Avail: NTIS HC A03/MF A01 CSCL 10A

In 1975, the U.S. Government contracted the Jet Propulsion Lab. to develop, by 1985, in conjunction with industry, the photovoltaics (PV) module and array technology required for widespread use of photovoltaics as a significant terrestrial energy source. As a result, a project that eventually became known as the Flat Plate Solar Array (FSA) Project was formed to manage an industry, university, and Government team to perform the necessary research and development. The original goals were to achieve widespread commercial use of PV modules and arrays through the development of technology that would allow them to be profitably sold for $1.07/peak watts (1985 dollars). A 10% module conversion efficiency and a 20 year lifetime were also goals. It is intended that the executive summary provide the means by which one can gain a perspective on 11 years of terrestrial photovoltaic research and development conducted by the FSA Project. Author

N87-20647*# Jet Propulsion Lab., California Inst. of Tech., Pasadena.
FLAT-PLATE SOLAR ARRAY PROJECT. VOLUME 2: SILICON MATERIAL Final Report
R. Lutwack Oct. 1986 73 p Sponsored part by NASA
(Contract DE-A101-85CE-89008)
(NASA-CR-180659; JPL-Pub-86-31-Vol-2; NAS 1.26:180659; DOE/JPL-1012-125-Vol-2) Avail: NTIS HC A04/MF A01 CSCL 10A

The goal of the Silicon Material Task, a part of the Flat Plate Solar Array (FSA) Project, was to develop and demonstate the technology for the low cost production of silicon of suitable purity to be used as the basic material for the manufacture of terrestrial photovoltaic solar cells. Summarized are 11 different processes for the production of silicon that were investigated and developed to varying extent by industrial, university, and Government researchers. The silane production section of the Union Carbide Corp. (UCC) silane process was developed completely in this program. Coupled with Siemens-type chemical vapor deposition reactors, the process was carried through the pilot stage. The overall UCC process involves the conversion of metallurgical-grade silicon to silane followed by decomposition of the silane to purified silicon. The other process developments are described to varying extents. Studies are reported on the effects of impurities in silicon on both silicon-material properties and on solar cell performance. These studies on the effects of impurities yielded extensive information and models for relating specific elemental concentrations to levels of deleterious effects. Author

N87-20648*# Jet Propulsion Lab., California Inst. of Tech., Pasadena.
FLAT-PLATE SOLAR ARRAY PROJECT. VOLUME 3: SILICON SHEET: WAFERS AND RIBBONS Final Report
A. Briglio, K. Dumas, M. Leipold, and A. Morrison Oct. 1986 132 p Sponsored in part by NASA and DOE
(NASA-CR-180661; JPL-Pub-86-31-Vol-3; NAS 1.26:180661; DOE/JPL-1012-125-Vol-3) Avail: NTIS HC A07/MF A01 CSCL 10A

The primary objective of the Silicon Sheet Task of the Flat-Plate Solar Array (FSA) Project was the development of one or more low cost technologies for producing silicon sheet suitable for processing into cost-competitive solar cells. Silicon sheet refers to high purity crystalline silicon of size and thickness for fabrication into solar cells. Areas covered in the project were ingot growth and casting, wafering, ribbon growth, and other sheet technologies. The task made and fostered significant improvements in silicon sheet including processing of both ingot and ribbon technologies. An additional important outcome was the vastly improved understanding of the characteristics associated with high quality sheet, and the control of the parameters required for higher efficiency solar cells. Although significant sheet cost reductions were made, the technology advancements required to meet the task cost goals were not achieved. Author

N87-20649*# Jet Propulsion Lab., California Inst. of Tech., Pasadena.
FLAT-PLATE SOLAR ARRAY PROJECT. VOLUME 4: HIGH-EFFICIENCY SOLAR CELLS Final Report
M. Leipold, L. Cheng, T. Daud, A. Mokashi, D. Burger, E. Christensen, ed., J. Murry, ed., and I. Bengelsdorf, ed. Oct. 1986 68 p Sponsored in part by NASA and DOE
(Contract DE-A101-85CE-89008)
(NASA-CR-180662; JPL-Pub-86-31-Vol-4; NAS 1.26:180662; DOE/JPL-1012-125-Vol-4) Avail: NTIS HC A04/MF A01 CSCL 10A

The High Efficiency Solar Cell Task was assigned the objective of understanding and developing high efficiency solar cell devices that would meet the cost and performance goals of the Flat Plate Solar Array (FSA) Project. The need for research dealing with high efficiency devices was considered important because of the role efficiency plays in reducing price per watt of generated energy. The R&D efforts conducted during the 1982 to 1986 period are summarized to provide understanding and control of energy conversion losses associated with crystalline silicon solar cells. New levels of conversion efficiency were demonstrated. Major contributions were made both to the understanding and reduction of bulk and surface losses in solar cells. For example, oxides, nitrides, and polysilicon were all shown to be potentially useful surface passivants. Improvements in measurement techniques were made and Auger coefficients and spectral absorption data were obtained for unique types of silicon sheets. New modelling software was developed including a program to optimize a device design based on input characteristics of a cell. Author

N87-20650*# Jet Propulsion Lab., California Inst. of Tech., Pasadena.
FLAT-PLATE SOLAR ARRAY PROJECT. VOLUME 5: PROCESS DEVELOPMENT Final Report
B. Gallagher, P. Alexander, and D. Burger Oct. 1986 71 p Sponsored in part by NASA and DOE
(Contract DE-A101-85CE-89008)
(NASA-CR-180663; JPL-Pub-86-31-Vol-5; NAS 1.26:180663; DOE/JPL-1012-125-Vol-5) Avail: NTIS HC A04/MF A01 CSCL 10A

The goal of the Process Development Area, as part of the Flat-Plate Solar Array (FSA) Project, was to develop and demonstrate solar cell fabrication and module assembly process technologies required to meet the cost, lifetime, production capacity, and performance goals of the FSA Project. R&D efforts expended by Government, Industry, and Universities in developing processes capable of meeting the projects goals during volume production conditions are summarized. The cost goals allocated for processing were demonstrated by small volume quantities that were extrapolated by cost analysis to large volume production. To provide proper focus and coverage of the process development effort, four separate technology sections are discussed: surface preparation, junction formation, metallization, and module assembly. Author

N87-20651*# Jet Propulsion Lab., California Inst. of Tech., Pasadena.
FLAT-PLATE SOLAR ARRAY PROJECT. VOLUME 6: ENGINEERING SCIENCES AND RELIABILITY Final Report
R. G. Ross, Jr. and M. I. Smokler Oct. 1986 98 p Sponsored in part by NASA and DOE
(Contract DE-A101-85CE-89008)
(NASA-CR-180664; JPL-Pub-86-31-Vol-6; NAS 1.26:180664; DOE/JPL-1012-125-Vol-6) Avail: NTIS HC A05/MF A01 CSCL 10A

The Flat-Plate Solar Array (FSA) Project activities directed at developing the engineering technology base required to achieve modules that meet the functional, safety, and reliability requirements of large scale terrestrial photovoltaic systems applications are reported. These activities included: (1) development of functional, safety, and reliability requirements for such applications; (2) development of the engineering analytical approaches, test techniques, and design solutions required to meet the requirements; (3) synthesis and procurement of candidate designs for test and evaluation; and (4) performance of extensive testing, evaluation, and failure analysis of define design shortfalls and, thus, areas requiring additional research and development. A summary of the approach and technical outcome of these activities are provided along with a complete bibliography of the published documentation covering the detailed accomplishments and technologies developed. Author

N87-20652*# Jet Propulsion Lab., California Inst. of Tech., Pasadena.
FLAT-PLATE SOLAR ARRAY PROJECT. VOLUME 7: MODULE ENCAPSULATION Final Report
E. Cuddihy, C. Coulbert, A. Gupta, and R. Liang Oct. 1986 78 p Sponsored in part by NASA and DOE
(Contract DE-A101-85CE-89008)
(NASA-CR-180665; JPL-Pub-86-31-Vol-7; NAS 1.26:180665; DOE/JPL-1012-125-Vol-7) Avail: NTIS HC A05/MF A01 CSCL 10A

The objective of the Encapsulation Task was to develop, demonstrate, and qualify photovoltaic (PV) module encapsulation systems that would provide 20 year (later decreased to 30 year) life expectancies in terrestrial environments, and which would be compatible with the cost and performance goals of the Flat-Plate Solar Array (FSA) Project. The scope of the Encapsulation Task included the identification, development, and evaluation of material systems and configurations required to support and protect the optically and electrically active solar cell circuit components in the PV module operating environment. Encapsulation material technologies summarized include the development of low cost ultraviolet protection techniques, stable low cost pottants, soiling resistant coatings, electrical isolation criteria, processes for optimum interface bonding, and analytical and experimental tools for evaluating the long term durability and structural adequacy of encapsulated modules. Field testing, accelerated stress testing, and design studies have demonstrated that encapsulation materials, processes, and configurations are available that meet the FSA cost and performance goals. Author

N87-20653*# Jet Propulsion Lab., California Inst. of Tech., Pasadena.
FLAT-PLATE SOLAR ARRAY PROJECT. VOLUME 8: PROJECT ANALYSIS AND INTEGRATION Final Report
P. McGuire and P. Henry Oct. 1986 41 p Sponsored in part by NASA, DOE,
(Contract DE-A101-85CE-89008)
(NASA-CR-180695; JPL-Pub-86-31-Vol-8; NAS 1.26:180695; DOE/JPL-1012-125-Vol-8) Avail: NTIS HC A03/MF A01 CSCL 10A

Project Analysis and Integration (PA&I) performed planning and integration activities to support management of the various Flat-Plate Solar Array (FSA) Project R&D activities. Technical and economic goals were established by PA&I for each R&D task within the project to coordinate the thrust toward the National Photovoltaic Program goals. A sophisticated computer modeling capability was developed to assess technical progress toward meeting the economic goals. These models included a manufacturing facility simulation, a photovoltaic power station simulation and a decision aid model incorporating uncertainty. This family of analysis tools was used to track the progress of the technology and to explore the effects of alternative technical paths. Numerous studies conducted by PA&I signaled the achievement of milestones or were the foundation of major FSA project and national program decisions. The most important PA&I activities during the project history are summarized. The PA&I planning function is discussed and how it relates to project direction and important analytical models developed by PA&I for its analytical and assessment activities are reviewed. Author

N87-20654# Los Alamos National Lab., N. Mex.
FUEL CELLS IN TRANSPORTATION
J. R. Huff and H. S. Murray Jan. 1987 8 p Presented at the Annual Battery Conference on Application and Advances, Long Beach, Calif., 13 Jan. 1987
(Contract W-7405-eng-36)
(DE87-003746; LA-UR-86-4296; CONF-870111-2) Avail: NTIS HC A02/MF A01

Fuel cells have been considered for use in transportation applications for a number of years. They are attractive because they offer a mode of reducing US dependency on petroleum. Fuel cell performance at present has been assessed for applicability to vehicle power plants. Types of fuels that might be used and their effect on selection of a fuel cell technology have been considered. Simulation of a city bus using a hybrid fuel cell/battery power plant indicates that adequate performance can be obtained with current technology. DOE

N87-20655# Argonne National Lab., Ill.
CHARACTERIZATION OF MONOLITHIC FUEL CELL COMPONENTS
D. W. Dees and F. C. Mrazek Oct. 1986 4 p Presented at the Fuel Cell Seminar, Tucson, Ariz., 26 Oct. 1986
(Contract W-31109-eng-38)
(DE87-004929; CONF-861008-5) Avail: NTIS HC A02/MF A01

Electrochemical characterization of materials and components is an important part of the monolithic fuel cell development effort. The bulk electrical/ionic conductivity of all cell materials has been determined over the range of temperatures (800 to 1000°C) and oxygen pressures (0.2 to 10^{-18} atm). A series of ac impedance studies has been performed on various three-layer (anode/electrolyte/cathode) composite samples. A complex impedance diagram for one of the composites is given. While current densities up to 2.2 A/cm² have been observed, further increases are possible through reduced interfacial resistances. DOE

N87-20656# Stirling Technology Co., Richland, Wash.
CONCEPTUAL DESIGN OF A SOLAR ELECTRIC ADVANCED STIRLING POWER SYSTEM Monthly Progress Report, 1-31 Jan. 1987
M. A. White and A. T. Brown Feb. 1987 29 p Prepared in cooperation with Mechanical Technology, Inc., Latham, N.Y. and Thermacore, Inc., Lancaster, Pa.
(Contracts DE-AT04-85AL-33408; DE-AI04-80AL-13137)
(DE87-005036; DOE/AL-33408/T3) Avail: NTIS HC A03/MF A01

The objective is to develop a high confidence conceptual design for a free-piston Stirling engine based system designed to deliver 25 kW of three-phase electric power to a utility grid when coupled to the 11 meter Test Bed Concentrator (TBC) at SNLA. Further objectives include a design life of 60,000 hours, minimum life cycle cost and dynamic balancing. The approach used to achieve these objectives is to utilize a hermetically sealed Stirling hydraulic concept based on technology developed to an advanced level during the past 19 years for an artificial heart power source. Such engines and critical metal bellows components have demonstrated operating times in the desired range. This approach provides full film hydraulic lubrication of all sliding parts, simple construction with conventional manufacturing tolerances, proven hydraulically

coupled counterbalancing, and simple but effective power control to follow insolation variations. Other advantages include use of commercially available hydraulic motors and rotary alternators which can be placed on the ground to minimize suspended weight. The output from several engine/concentrator modules can be directed to one large motor/alternator for further cost savings. Three monthly progress reports for the same period, January 1 to January 31, 1987, are compiled within this document. DOE

N87-20657# Societe Nationale Industrielle Aerospatiale, Cannes (France). Div. Systemes Balistiques et Spatiaux.
THE CONCENTRATION PRINCIPLE APPLIED TO SPACEBORNE SOLAR ARRAYS. AGORA MISSION: STUDIES SYNTHESIS
R. Laget Paris, France ESA 27 Jan. 1986 44 p
(Contract ESA-5978/84-NL-PB(SC))
(SNIAS-959-CA/CG; ESA-CR(P)-2291-Vol-2; ETN-87-99483) Avail: NTIS HC A03/MF A01

Studies that led to selection of the distributed 25 kW SARA LOUVRE concept for the solar cell generator to be flown on the AGORA asteroid mission, and the major characteristics of such a spaceborne solar array are summarized. In the SARA LOUVRE concept, a parabolic cross section reflector concentrates incident light over the rear face of the identical, preceding reflector dish. The whole set of reflectors is pivotally commanded, thus compensating the effects of depointing. Geometric concentration factor is 10. End of life power level at 2.5 AU is 4.5 kW. ESA

45 ENVIRONMENT POLLUTION

Includes atmospheric, noise, thermal, and water pollution.

N87-20658*# Bionetics Corp., Cocoa Beach, Fla.
EFFECTS OF SPACE SHUTTLE LAUNCHES STS-1 THROUGH STS-9 ON TERRESTRIAL VEGETATION OF JOHN F. KENNEDY SPACE CENTER, FLORIDA
P. A. Schmalzer, C. R. Hinkle, D. Breininger, W. M. Knott, III, ed. (National Aeronautics and Space Administration. John F. Kennedy Space Center, Cocoa Beach, Fla.), and A. M. Koller, Jr., ed. Sep. 1985 46 p
(Contract NAS10-10285)
(NASA-TM-83103; NAS 1.15:83103) Avail: NTIS HC A03/MF A01 CSCL 13B

Space Shuttle launches produce a cloud containing hydrochloric acid (HCl), aluminum oxide (Al_2O_3), and other substances. Acidities of less than 0.5 pH have been measured routinely in association with the launch cloud. In an area of about 22 ha regularly exposed to the exhaust cloud during most Shuttle launches, acute vegetation damage has resulted from the first nine Shuttle launches. Changes include loss of sensitive species, loss of plant community structure, reduction in total cover, and replacement of some species by weedy invaders. Community level changes define a retrogressive sequence. One-time impacts to strand and dune vegetation occurred after launches of STS-8 and STS-9. Acute vegetation damage occurred especially to sensitive species. Within six months, however, recovery was nearly complete. Sensitivity of species to the launch cloud was partially predicted by previous laboratory studies. Far-field acidic and dry fallout from the cloud as it rises to stabilization and moves with the prevailing winds causes vegetation spotting. Damage from this deposition is minor; typically at most 1% to 5% of leaf surface area is affected. No plant mortality or community changes have occurred from far-field deposition. Author

N87-20659# Research Inst. of National Defence, Linkoeping (Sweden). Dept. 3.
POTENTIAL OF LASER REMOTE SENSING OF OIL BELOW WATER SURFACE
Ove Steinvall Nov. 1986 19 p
(FOA-C-30435-3.1; ISSN-0347-3708; ETN-87-99441) Avail: NTIS HC A02/MF A01

An airborne pollution-monitoring system with a laser bathymeter to detect the oil and a laser fluoresensor for verification is proposed. It is estimated that such a system can have a depth range of 10 m in coastal waters. ESA

46 GEOPHYSICS

Includes aeronomy; upper and lower atmosphere studies; ionospheric and magnetospheric physics; and geomagnetism.

For space radiation see *93 Space Radiation.*

N87-20660 Purdue Univ., West Lafayette, Ind.
NUMERICAL SIMULATION OF AIR MASS MODIFICATION OVER THE EAST CHINA SEA DURING THE WINTER SEASON Ph.D. Thesis
Wu-Ron Hsu 1986 148 p
Avail: Univ. Microfilms Order No. DA8700901

Air mass modification over the East China Sea during cold air outbreaks in the winter season was simulated by utilizing a high-resolution numerical model. The model includes most of the major physical processes, such as, surface exchange of heat and moisture between water and air; condensation and evaporation; and vertical turbulent transfer of heat, moisture, and momentum. The simulated convective boundary layer (CBL) consists of a surface layer, a subcloud layer, and a cloud layer. It is capped by an inversion with strong temperature and moisture gradients. Mesoscale cellular convection (MCC) embedded within the convective layer moves along with the mean wind. The average aspect ratio of the cells is 17.5, which agrees with observed aspect ratios for convective cells over the East China Sea. The upward convective motion correlates very well with the appearance of clouds, higher temperature, and higher moisture content in the CBL. The distribution of specific humidity during the passage of the surface front reveals the moisture being pushed upward along the frontal surface as observed. The cold and dry air behind the cold front is quickly modified by strong convection over the warm water surface, especially over the Kuroshio Current. A cloud-free region exists near the coast where the CBL is too shallow for clouds to develop. A layer of stratocumulus forms downstream from the cloud-free region. The depth of the CBL increases toward the Kuroshio Current due to strong heat and moisture fluxes from the water surface. The CBL reached an almost quasi-steady state about 36 hours after the surface front passed through Naha in the simulation. Dissert. Abstr.

N87-20661# Instituto de Pesquisas Espaciais, Sao Jose dos Campos (Brazil).
MAGNETOTELLURIC MEASUREMENTS IN ANTARCTICA [MEDIDAS MAGNETOTELURICAS NA ANTARTICA]
N. B. Trivedi, A. L. Padilha, and M. J. F. Barbosa Nov. 1986 16 p In PORTUGUESE Presented at the Brazilian Congress of Geology, Goiania, Brazil, Oct. 1986 Sponsored in part by the National Fund for Scientific and Technological Development
(INPE-4058-PRE/1017) Avail: NTIS HC A02/MF A01

In the period of 2/14/86 to 3/7/86, during the 4th Brazilian Scientific Expedition to Antarctica, organized through the CIRM (Comissao Interministerial para Recursos do Mar), Station Commander Ferraz, (62 deg 5 min S, 58 deg 23.5 min W), magnetotelluric measurements were accomplished in 120 second intervals for DC. This measurement complemented the former, accomplished in the preceeding year between 20 and 400 seconds and although it presented excellent agreement in the overlapping intervals, it was a difficult interpretation. A Hilbert transformation technique was utilized for solving this problem, which brought to mind similar obtained resistivity values. The preliminary results encountered were presented and discussed. Author

N87-20662*# Massachusetts Inst. of Tech., Cambridge. Earth Resources Lab.
THE INTERPRETATION OF CRUSTAL DYNAMICS DATA IN TERMS OF PLATE INTERACTIONS AND ACTIVE TECTONICS

OF THE ANATOLIAN PLATE AND SURROUNDING REGIONS IN THE MIDDLE EAST Annual Report, 15 Mar. 1986 - 14 Mar. 1987
M. Nafi Toksoz 10 Apr. 1987 134 p
(Grant NAG5-753)
(NASA-CR-180501; NAS 1.26:180501) Avail: NTIS HC A07/MF A01 CSCL 08G

The primary effort in this study during the past year has been directed along two separate lines: (1) expanding finite element models to include the entire Anatolian plate, the Aegean Sea and the Northeastern Mediterranean Sea, and (2) investigating the relationship between fault geometry and earthquake activity for the North Anatolian and similar strike-slip faults (e.g., San Andreas Fault). Both efforts are designed to provide an improved basis for interpreting the Crustal Dynamics measurements NASA has planned for this region. The initial phases of both investigations have been completed and the results are being prepared for publication. These investigations are described briefly. Author

N87-20663*# National Aeronautics and Space Administration. Langley Research Center, Hampton, Va.
AIRBORNE LIDAR MEASUREMENTS OF EL CHICHON STRATOSPHERIC AEROSOLS, JANUARY 1984
M. Patrick McCormick and M. T. Osborn (ST Systems Corp., Hampton, Va.) Apr. 1987 49 p
(NASA-RP-1175; L-16234; NAS 1.61:1175) Avail: NTIS HC A03/MF A01 CSCL 04A

A lidar-equipped NASA Electra aircraft was flown in January 1984 between the latitude of 38 and 90 deg N. One of the primary purposes of this mission was to determine the spatial distribution and aerosol characteristics of El Chichon produced stratospheric material. Lidar data from that portion of the flight mission between 38 deg N and 77 deg N is presented. Representative profiles of lidar backscatter ratio, a plot of the integral backscattering function versus latitude, and contours of backscatter mixing ratio versus altitude and latitude are given. In addition, tables containing numerical values of the backscatter ratio and backscattering function versus altitude are applied for each profile. These data clearly show that material produced by the El Chichon eruptions of late March-early April 1982 had spread throughout the latitudes covered by this mission, and that the most massive portion of the material resided north of 55 deg N and was concentrated below 17 km in a layer that peaked at 13 to 15 km. In this latitude region, peak backscatter ratios at a wavelength of 0.6943 microns were approximately 3 and the peak integrated backscattering function was about 15 X 10 to the -4/sr corresponding to a peak optical depth of approximately 0.07. This report presents the results of this mission in a ready-to-use format for atmospheric and climatic studies. Author

N87-20664*# Lunar and Planetary Inst., Houston, Tex.
WILSON CYCLE STUDIES Semiannual Report, 15 Jul. 1986 - 15 Jan. 1987
1987 7 p
(Grant NAG5-585)
(NASA-CR-180503; NAS 1.26:180503) Avail: NTIS HC A02/MF A01 CSCL 08E

Continents originate by the sweeping together of island arcs. Continental and island arc crusts are dominated by rocks of comparable compositional and density ranges, evidence of the operation of this process is abundant in the geological record, and can be seen in action today in Indonesia. Lineaments within continents are attributable to a small number of processes of continent formation and modification, but interactions among these processes may produce complex patterns. Author

N87-20665*# National Aeronautics and Space Administration. Marshall Space Flight Center, Huntsville, Ala.
UPPER AND MIDDLE ATMOSPHERIC DENSITY MODELING REQUIREMENTS FOR SPACECRAFT DESIGN AND OPERATIONS
M. H. Davis, ed. (Universities Space Research Association, Boulder, Colo.), R. E. Smith, ed., and D. L. Johnson, ed. Feb. 1987 290 p Workshop held in Huntsville, Ala., 19-21 1985
(Contract NAS8-36400)
(NASA-CP-2460; M-548; NAS 1.55:2460) Avail: NTIS HC A13/MF A01 CSCL 04A

Presented and discussed are concerns with applications of neutral atmospheric density models to space vehicle engineering design and operational problems. The area of concern which the atmospheric model developers and the model users considered, involved middle atmosphere (50 to 90 km altitude) and thermospheric (above 90 km) models and their engineering application. Engineering emphasis involved areas such as orbital decay and lifetime prediction along with attitude and control studies for different types of space and reentry vehicles. For individual titles, see N87-20666 through N87-20688.

N87-20666*# National Aeronautics and Space Administration. Marshall Space Flight Center, Huntsville, Ala.
SATELLITE LIFETIME PREDICTION **c18**
Gerald Wittenstein *In its* Upper and Middle Atmospheric Density Modeling Requirements for Spacecraft Design and Operations Feb. 1987 p 15-37 (For primary document see N87-20665 13-46)
Avail: NTIS HC A13/MF A01 CSCL 22B

Satellite lifetime predictions are critically dependent on the ability to forecast future solar and geomagnetic activity. These quantities are inputs to the atmospheric model with which values of atmospheric density are computed along a projected orbital path. Density values are combined with the predicted ballistic coefficient timeline to compute drag and predict decay histories. The major uncertainty in making predictions that pertain to the time periods that are years in the future is in the solar and geomagnetic activity projections, although the ballistic coefficient is also frequently in doubt. The study concludes that while present density models are adequate for planning, the inputs to them, particularly solar/geomagnetic activity indices, are unreliable.
Author

N87-20667*# Rockwell International Corp., Canoga Park, Calif. Rocketdyne International.
DENSITY UNCERTAINTY EFFECT ON COST OF SPACE STATION REBOOST Abstract Only **c18**
Walter Unterberg and Claus Meisl *In* NASA. Marshall Space Flight Center Upper and Middle Atmospheric Density Modeling Requirements for Spacecraft Design and Operations Feb. 1987 p 39-40 (For primary document see N87-20665 13-46)
Avail: NTIS HC A13/MF A01 CSCL 22B

If the space station is designed for operation in a nominal atmosphere for ten years and the atmosphere is two-sigma higher than nominal during the entire ten year period, the impact would be an additional cost of $70.1 million, based on a resupply cost of $3200/lb. A cost analysis of the space station fuel consumption with reboost is presented. Author

N87-20668*# National Aeronautics and Space Administration. Marshall Space Flight Center, Huntsville, Ala.
SPACE STATION MOMENTUM MANAGEMENT **c18**
V. Buckalew and Miriam Hopkins *In its* Upper and Middle Atmospheric Density Modeling Requirements for Spacecraft Design and Operations Feb. 1987 p 41-57 (For primary document see N87-20665 13-46)
Avail: NTIS HC A13/MF A01 CSCL 22B

Gravity gradient stabilization is planned for the space station. Torques arise from air-drag since the center of pressure is not the same as the center of mass of the satellite. The magnitude of these torques varies depending upon the orientation of the solar panels. Adjustments are made through the use of CMG's (Control Moment Gyros). In time, if the CMG's saturate, torque must be bled off using thrusters; however, that is undesirable because it expends propellant and contaminates the local environment. The task of the engineer is to design the CMG's to handle the aerodynamic torques and design the configuration of the spacecraft to prevent, if possible, CMG saturation. For this application the long-term atmospheric density trends are of less importance than the rate of change of density within an orbit. In

principle, CMG's could be designed for the worst case of maximum solar activity, but the penalty for overdesign is excess mass and cost. In summary, present models are inadequate for this application with the greatest need being a reliable prediction of maximum rates-of-change of density within an orbit. Author

N87-20669*# National Aeronautics and Space Administration. Lyndon B. Johnson Space Center, Houston, Tex.
SPACE STATION CONTROL MOMENT GYRO CONTROL c18
Aldo Bordano *In* NASA. Marshall Space Flight Center Upper and Middle Atmospheric Density Modeling Requirements for Spacecraft Design and Operations Feb. 1987 p 59-71 (For primary document see N87-20665 13-46)
Avail: NTIS HC A13/MF A01 CSCL 22B

The potential large center-of-pressure to center-of-gravity offset of the space station makes the short term, within an orbit, variations in density of primary importance. The large range of uncertainty in the prediction of solar activity will penalize the design, developments, and operation of the space station. Author

N87-20670*# National Aeronautics and Space Administration. Marshall Space Flight Center, Huntsville, Ala.
HUBBLE SPACE TELESCOPE c89
G. Nurre *In its* Upper and Middle Atmospheric Density Modeling Requirements for Spacecraft Design and Operations Feb. 1987 p 73-87 (For primary document see N87-20665 13-46)
Avail: NTIS HC A13/MF A01 CSCL 03A

The Hubble Space Telescope will employ magnetic torque controllers, which make use of the Earth's magnetic field augmented by four reaction wheels. DC torques are easily allowed for, but variations, orbit by orbit, can result in excessive wheel speeds which can excite vibratory modes in the telescope structure. If the angular momentum from aerodynamic sources exceeds its allocation of 100 Nms, the excess has to come out of the maneuvering budget since the total capacity of the momentum storage system is fixed at 500 Nms. This would mean that maneuvers could not be made as quickly, and this would reduce the amount of science return. In summary, there is a definite need for a model that accurately portrays short term (within orbit) variations in density for use in angular momentum management analyses. It would be desirable to have a simplified model that could be used for planning purposes; perhaps applicable only over a limited altitude range (400 to 700 km) and limited latitude band. Author

N87-20671*# Space Command, Peterson AFB, Colo.
NORAD SATELLITE TRACKING c13
Joseph J. F. Liu *In* NASA. Marshall Space Flight Center Upper and Middle Atmospheric Density Modeling Requirements for Spacecraft Design and Operations Feb. 1987 p 89-94 (For primary document see N87-20665 13-46)
Avail: NTIS HC A13/MF A01 CSCL 22A

NORAD routinely tracks about 6000 orbiting objects. During the last 30 days of orbital time, prior to reentry, special perturbations are used in the orbital update procedure. Besides routine orbit determination, NORAD does special tasks such as predicting satellite orbit conjunctions within 20 km, ephimerides of weather satellites, satellite decay predictions and other studies. Since their mission is operational, they do not store the data from their analyses. The ballistic coefficient is not known for most of the orbiting objects. If a ballistic coefficient were derived that was consistent with one density model, it might give erroneous results if used with a different density model. Given the ballistic coefficient, density values could, in principle, be obtained from their tracking data. The densities would represent an integrated mean over the orbital path near perigee. They would be model dependent and would not necessarily represent the real density. In summary, the primary need is for reliable forecasts of solar flux (F10.7) and geomagnetic activity (Ap) in the 1 to 4 week time scale. Forecasts over longer time spans would also be useful for special projects. Author

N87-20672*# Space Command, Peterson AFB, Colo. Directorate of Astrodynamics.
NORAD/SPACECMD COMMENTS CONCERNING THE ATMOSPHERIC DENSITY MODELS Abstract Only
Joseph J. F. Liu *In* NASA. Marshall Space Flight Center Upper and Middle Atmospheric Density Modeling Requirements for Spacecraft Design and Operations Feb. 1987 p 95 (For primary document see N87-20665 13-46)
Avail: NTIS HC A13/MF A01 CSCL 04A

Recent models do not produce more accurate neutral densities (although they require more computer time), regardless of the level of solar activity. This implies that there has been no measurable improvement of the calculation of neutral density since the early 60s. With known solar flux and geomagnetic activity (Ap) inputs, the density evaluation needs improvement. For highly eccentric orbits which span low to high altitude, the accuracy generated which has an altitude limitation of 1000 km remains comparable with those obtained by more recent models. This implies that either the density at 1000 km and above is insignificant or that the values provided by the recent models at high altitudes may not be reliable or both. Prediction accuracies obtained through the use of precision data from the Defense Mapping Agency are generally comparable to those obtained by using operational sensor data. This implies that the prediction accuracy problem is not necessarily caused by less accurate observations. The definition of the mean solar flux F10.7 is not universal. Author

N87-20673*# National Center for Atmospheric Research, Boulder, Colo.
ORBITAL ATMOSPHERIC PHYSICS AND DYNAMICS
Raymond Roble and Timothy Killeen (Michigan Univ., Ann Arbor.) *In* NASA. Marshall Space Flight Center Upper and Middle Atmospheric Density Modeling Requirements for Spacecraft Design and Operations Feb. 1987 p 99-100 (For primary document see N87-20665 13-46)
Avail: NTIS HC A13/MF A01 CSCL 04A

There are two ways of modeling the upper atmosphere. One is the empirical model that makes use of experimental data on means and excursions from the mean and fits the data in a self-consistent manner. The other approach is to deal directly with the physical processes. This is difficult since what is happening is extremely complex. Data measured using an interferometer to give Doppler shifts of airglow lines showed 300 to 800 m/sec winds with a complex structure in the upper region of the thermosphere at high latitudes. Ionospheric electric fields, strongly influenced by interaction with the solar wind, drive the ionized component and large neutral winds result due to momentum transfer between the charged particles and the neutrals. Frictional heating results from movement of ions through the neutrals, which also influences the compositional structure. These are examples of the complex interactions involved. The NCAR General Circulation Model (tropospheric) was adapted for use at thermospheric altitudes: the Thermospheric General Circulation Model (TGCM). The model makes use partly of primitive equations and partly of empirical data for some quantities such as electron density, magnetic field, and ion drift. Author

N87-20674*# Smithsonian Astrophysical Observatory, Cambridge, Mass.
LIMITATIONS TO MODELING THE THERMOSPHERE AND EXOSPHERE Abstract Only
John Slowey *In* NASA. Marshall Space Flight Center Upper and Middle Atmospheric Density Modeling Requirements for Spacecraft Design and Operations Feb. 1987 p 109 (For primary document see N87-20665 13-46)
Avail: NTIS HC A13/MF A01 CSCL 04A

Correlations were noted between solar 10cm radio flux, the indices of geomagnetic activity, and what happens in the atmosphere. There are also correlations between events in the troposphere and density in the thermosphere. Gravity waves in the thermosphere are not handled in existing models. A reasonable estimate is that they contribute perhaps ten percent to the deviation between model density values and the effective density

as it influences satellite orbital motion. Another factor is atmospheric composition which influences density through the different scale heights of components of different molecular weight in this regime. Author

N87-20675*# National Aeronautics and Space Administration. Goddard Space Flight Center, Greenbelt, Md.
EMPIRICAL MODELING OF THE THERMOSPHERE: AN OVERVIEW
A. Hedin *In* NASA. Marshall Space Flight Center Upper and Middle Atmospheric Density Modeling Requirements for Spacecraft Design and Operations Feb. 1987 p 111-122 (For primary document see N87-20665 13-46)
Avail: NTIS HC A13/MF A01 CSCL 04A

A summary is given of thermospheric density modeling history and standard atmospheres. In particular, the approaches of the Jacchia and MSIS models were compared and contrasted. It was concluded that the Jacchia models are best if drag is the primary concern. MSIS is superior for variations in composition and temperature variations and comparison with theoretical models is facilitated by the use of spherical harmonics, which also provide a simple and consistent way of obtaining simplifications. Advantages and disadvantages of both models are listed and discussed. Author

N87-20676*# Air Force Geophysics Lab., Hanscom AFB, Mass.
REQUIREMENTS FOR IMPROVED MODELING OF THE ORBITAL ATMOSPHERE
Frank A. Marcos *In* NASA. Marshall Space Flight Center Upper and Middle Atmospheric Density Modeling Requirements for Spacecraft Design and Operations Feb. 1987 p 123-138 (For primary document see N87-20665 13-46)
Avail: NTIS HC A13/MF A01 CSCL 04A

Satellite accelerometer data are available for seven time periods during the period 1974 to the present. All seasons and latitudes up to 83 deg are covered. Deviations between the accelerometer data and current models are greatest for high geographic latitudes and high geomagnetic index, although about a 15 percent standard deviation persists between the models and the accelerometer data even at low latitudes and geomagnetically quiet times. Accelerometer data give density times the ballistic coefficient and it is therefore necessary to estimate the time-line of the ballistic coefficient in order to obtain density. Author

N87-20677*# National Oceanic and Atmospheric Administration, Boulder, Colo. Space Environment Lab.
FORECASTS OF SOLAR AND GEOMAGNETIC ACTIVITY c92
JoAnn Joselyn *In* NASA. Marshall Space Flight Center Upper and Middle Atmospheric Density Modeling Requirements for Spacecraft Design and Operations Feb. 1987 p 141-149 (For primary document see N87-20665 13-46)
Avail: NTIS HC A13/MF A01 CSCL 03B

Forecasts of solar and geomagnetic activity are critical since these quantities are such important inputs to the thermospheric density models. At this time in the history of solar science there is no way to make such a forecast from first principles. Physical theory applied to the Sun is developing rapidly, but is still primitive. Techniques used for forecasting depend upon the observations over about 130 years, which is only twelve solar cycles. It has been noted that even-numbered cycles systematically tend to be smaller than the odd-numbered ones by about 20 percent. Another observation is that for the last 12 cycle pairs, an even-numbered sunspot cycle looks rather like the next odd-numbered cycle, but with the top cut off. These observations are examples of approximate periodicities that forecasters try to use to achieve some insight into the nature of an upcoming cycle. Another new and useful forecasting aid is a correlation that has been noted between geomagnetic indices and the size of the next solar cycle. Some best estimates are given concerning both activities. Author

N87-20678*# National Aeronautics and Space Administration. Marshall Space Flight Center, Huntsville, Ala.
NASA/MSFC PREDICTION TECHNIQUES c92
Robert E. Smith *In its* Upper and Middle Atmospheric Density Modeling Requirements for Spacecraft Design and Operations Feb. 1987 p 151-153 (For primary document see N87-20665 13-46)
Avail: NTIS HC A13/MF A01 CSCL 03B

The NASA/MSFC method of forecasting is more formal than NOAA's. The data is smoothed by the Lagrangian method and linear regression prediction techniques are used. The solar activity period is fixed at 11 years--the mean period of all previous cycles. Interestingly, the present prediction for the time of the next solar minimum is February or March of 1987, which, within the uncertainties of two methods, can be taken to be the same as the NOAA result. Author

N87-20679*# National Aeronautics and Space Administration. Lyndon B. Johnson Space Center, Houston, Tex.
USERS OF MIDDLE ATMOSPHERE MODELS REMARKS
Joe Gamble *In* NASA. Marshall Space Flight Center Upper and Middle Atmospheric Density Modeling Requirements for Spacecraft Design and Operations Feb. 1987 p 157-179 (For primary document see N87-20665 13-46)
Avail: NTIS HC A13/MF A01 CSCL 04A

The procedure followed for shuttle operations is to calculate descent trajectories for each potential shuttle landing site using the Global Reference Atmosphere Model (GRAM) to interactively compute density along the flight path 100 times to bound the statistics. The purpose is to analyze the flight dynamics, along with calculations of heat loads during reentry. The analysis program makes use of the modified version of the Jacchia-70 atmosphere, which includes He bulges over the poles and seasonal latitude variations at lower altitudes. For the troposphere, the 4-D Model is used up to 20 km, Groves from 30 km up to 90 km. It is extrapolated over the globe and faired into the Jacchia atmosphere between 90 and 115 km. Since data on the Southern Hemisphere was lacking, what was done was that the data was flipped over and lagged 6 months. Sometimes when winds are calculated from pressure data in the model there appear to be discontinuities. Modelers indicated that the GRAM was not designed to produce winds, but good wind data is needed for the landing phase of shuttle operations. Use of atmospheric models during reentry is one application where it is obvious that a single integrated atmosphere model is required. Author

N87-20680*# National Aeronautics and Space Administration. Lyndon B. Johnson Space Center, Houston, Tex.
UTILIZATION OF GLOBAL REFERENCE ATMOSPHERE MODEL (GRAM) FOR SHUTTLE ENTRY
Kent Joosten *In* NASA. Marshall Space Flight Center Upper and Middle Atmospheric Density Modeling Requirements for Spacecraft Design and Operations Feb. 1987 p 181-193 (For primary document see N87-20665 13-46)
Avail: NTIS HC A13/MF A01 CSCL 04A

At high latitudes, dispersions in values of density for the middle atmosphere from the Global Reference Atmosphere Model (GRAM) are observed to be large, particularly in the winter. Trajectories have been run from 28.5 deg to 98 deg. The critical part of the atmosphere for reentry is 250,000 to 270,000 ft. 250,000 ft is the altitude where the shuttle trajectory levels out. For ascending passes the critical region occurs near the equator. For descending entries the critical region is in northern latitudes. The computed trajectory is input to the GRAM, which computes means and deviations of atmospheric parameters at each point along the trajectory. There is little latitude dispersion for the ascending passes; the strongest source of deviations is seasonal; however, very wide seasonal and latitudinal deviations are exhibited for the descending passes at all orbital inclinations. For shuttle operations the problem is control to maintain the correct entry corridor and avoid either aerodynamic skipping or excessive heat loads. Author

N87-20681*# McDonnell-Douglas Corp., St. Louis, Mo.
USE OF THE 4D-GLOBAL REFERENCE ATMOSPHERE MODEL (GRAM) FOR SPACE SHUTTLE DESCENT DESIGN
S. M. McCarty *In* NASA. Marshall Space Flight Center Upper and Middle Atmospheric Density Modeling Requirements for

Spacecraft Design and Operations Feb. 1987 p 195-201 (For primary document see N87-20665 13-46)
Avail: NTIS HC A13/MF A01 CSCL 04A

The method of using the Global Reference Atmosphere Model (GRAM) mean and dispersed atmospheres to study skipout/overshoot requirements, to characterize mean and worst case vehicle temperatures, study control requirements, and verify design was discussed. Landing sites in these analyses range from 65 N to 30 S, while orbit inclinations vary from 20 deg to 98 deg. The primary concern was that they cannot use as small vertical steps in the reentry calculation as desired because the model predicts anomalously large density shear rates for very small vertical step sizes. The winds predicted by the model are not satisfactory. This is probably because they are geostrophic winds and because the model has an error in the computation of winds in the equatorial regions. Author

N87-20682*# National Aeronautics and Space Administration. Lyndon B. Johnson Space Center, Houston, Tex.
AERO-ASSISTED ORBITAL TRANSFER VEHICLE (AOTV)
Oliver Hill *In* NASA. Marshall Space Flight Center Upper and Middle Atmospheric Density Modeling Requirements for Spacecraft Design and Operations Feb. 1987 p 203-219 (For primary document see N87-20665 13-46)
Avail: NTIS HC A13/MF A01 CSCL 04A

The AOTV will make use of the atmosphere to provide braking on return from a planetary mission or geosynchronous orbit. The minimum altitude for aerobraking is typically 255,000 ft at the equator. Time of the braking maneuver is typically 480 sec from 400,000 ft to 255,000 ft and back out - about 8 min. The problem is to design a control system that will be able to handle density irregularities such as those that have shown up in shuttle data near 280,000 ft. To obtain data, one has to use model-produced statistics or information obtained during the atmospheric transit time. The Global Reference Atmosphere Model (GRAM) appears to bracket the shuttle data, but it is not clear that the statistics are correct. The model-data exhibits strong density shears over small step size that are probably an artifact. Author

N87-20683*# National Aeronautics and Space Administration. Langley Research Center, Hampton, Va.
OVERVIEW OF SHUTTLE DATA ON DENSITY
Robert Blanchard *In* NASA. Marshall Space Flight Center Upper and Middle Atmospheric Density Modeling Requirements for Spacecraft Design and Operations Feb. 1987 p 221-227 (For primary document see N87-20665 13-46)
Avail: NTIS HC A13/MF A01 CSCL 04A

The HiRAP (High Resolution Accelerometer Package) used on the Shuttle is described and examples of flight-derived density-altitude profiles are compared to the 1976 Standard Atmosphere. By flying an accelerometer along with a mass spectrometer it is possible to obtain the drag coefficients for the Shuttle. However, problems may arise due to contamination in the near-shuttle environment. Author

N87-20684*# Flight Mechanics and Control, Inc., Hampton, Va.
SHUTTLE DERIVED ATMOSPHERE
John Findlay *In* NASA. Marshall Space Flight Center Upper and Middle Atmospheric Density Modeling Requirements for Spacecraft Design and Operations Feb. 1987 p 229-243 (For primary document see N87-20665 13-46)
Avail: NTIS HC A13/MF A01 CSCL 04A

The shuttle descends along a rather shallow path, thus providing some information on the horizontal structure of the atmosphere. Small scale structures were suggested (shears, potholes). The best estimates of the shuttle drag coefficient and projected areas are used to go from accelerometer data to density through the use of BET's (Best Estimated Trajectories). Data are from the IMU's (Inertial Measurement Unit) and the HiRAP (High Resolution Accelerometer Package). Author

N87-20685*# Alaska Univ., Fairbanks.
GRAVITY WAVES
David Fritts *In* NASA. Marshall Space Flight Center Upper and Middle Atmospheric Density Modeling Requirements for Spacecraft Design and Operations Feb. 1987 p 245-246 (For primary document see N87-20665 13-46)
Avail: NTIS HC A13/MF A01 CSCL 04A

Gravity waves contributed to the establishment of the thermal structure, small scale (80 to 100 km) fluctuations in velocity (50 to 80 m/sec) and density (20 to 30%, 0 to peak). Dominant gravity wave spectrum in the middle atmosphere: x-scale, less than 100 km; z-scale, greater than 10 km; t-scale, less than 2 hr. Theorists are beginning to understand middle atmosphere motions. There are two classes: Planetary waves and equatorial motions, gravity waves and tidal motions. The former give rise to variability at large scales, which may alter apparent mean structure. Effects include density and velocity fluctuations, induced mean motions, and stratospheric warmings which lead to the breakup of the polar vortex and cooling of the mesosphere. On this scale are also equatorial quasi-biennial and semi-annual oscillations. Gravity wave and tidal motions produce large rms fluctuations in density and velocity. The magnitude of the density fluctuations compared to the mean density is of the order of the vertical wavelength, which grows with height. Relative density fluctuations are less than, or of the order of 30% below the mesopause. Such motions may cause significant and variable convection, and wind shear. There is a strong seasonal variation in gravity wave amplitude. Additional observations are needed to address and quantify mean and fluctuation statistics of both density and mean velocity, variability of the mean and fluctuations, and to identify dominant gravity wave scales and sources as well as causes of variability, both temporal and geographic. Author

N87-20686*# Georgia Inst. of Tech., Atlanta.
THE GRAM-3 MODEL
C. G. Justus *In* NASA. Marshall Space Flight Center Upper and Middle Atmospheric Density Modeling Requirements for Spacecraft Design and Operations Feb. 1987 p 255-272 (For primary document see N87-20665 13-46)
Avail: NTIS HC A13/MF A01 CSCL 04A

The Global Reference Atmosphere Model (GRAM) is under continuous development and improvement. GRAM data were compared with Middle Atmosphere Program (MAP) predictions and with shuttle data. An important note: Users should employ only step sizes in altitude that give vertical density gradients consistent with shuttle-derived density data. Using too small a vertical step size (finer then 1 km) will result in what appears to be unreasonably high values of density shears but what in reality is noise in the model. Author

N87-20687*# Air Force Geophysics Lab., Hanscom AFB, Mass.
MIDDLE ATMOSPHERE DENSITY AND MODELS
K. Champion *In* NASA. Marshall Space Flight Center Upper and Middle Atmospheric Density Modeling Requirements for Spacecraft Design and Operations Feb. 1987 p 273-280 (For primary document see N87-20665 13-46)
Avail: NTIS HC A13/MF A01 CSCL 04A

The 80 to 130 km altitude region is our old ignorosphere, the region of the atmosphere that no one seems to be interested in and yet the critical region for shuttle entry and atmospheric braking. Comparison between the Air Force reference atmosphere and Shuttle Inertial Measurement Units data shows large fluctuations at high latitudes. New data sources are available now, such as the Arecibo and Millstone Hill ionospheric scatter radars. In the 20 to 80 km altitude range there is a reasonable quantity of data on the mean atmosphere, however, infomation on diurnal variability is needed. In the 20 to 80 km altitude range data is needed to identify systematic variations and models for the regions are preliminary. Unpredictable variations are observed: turbulence, storm effects, gravity waves. Author

N87-20688*# California Univ., Fullerton. Dept. of Geological Sciences.
SIX REASONS WHY THERMOSPHERIC MEASUREMENTS AND MODELS DISAGREE

Kenneth Moe *In* NASA. Marshall Space Flight Center Upper and Middle Atmospheric Density Modeling Requirements for Spacecraft Design and Operations Feb. 1987 p 291-303 (For primary document see N87-20665 13-46)
Avail: NTIS HC A13/MF A01 CSCL 04A

The differences between thermospheric measurements and models are discussed. Sometimes the model is in error and at other times the measurements are, but it also is possible for both to be correct, yet have the comparison result in an apparent disagreement. These reasons are collected for disagreement, and, whenever possible, methods of reducing or eliminating them are suggested. The six causes of disagreement discussed are: actual errors caused by the limited knowledge of gas-surface interactions and by in-track winds; limitations of the thermospheric general circulation models due to incomplete knowledge of the energy sources and sinks as well as incompleteness of the parameterization which must be employed; and limitations imposed on the empirical models by the conceptual framework and the transient waves. Author

N87-20689*# National Aeronautics and Space Administration. Marshall Space Flight Center, Huntsville, Ala.
YOSEMITE CONFERENCE ON IONOSPHERIC PLASMA IN THE MAGNETOSPHERE: SOURCES, MECHANISMS AND CONSEQUENCES, MEETING REPORT
D. L. Gallagher, J. L. Burch (Southwest Research Inst., Houston, Tex.), D. M. Klumpar (Lockheed Missiles and Space Co., Palo Alto, Calif.), T. E. Moore, and J. H. Waite, Jr. Feb. 1987 11 p The 6th Biennial Conference was held in Yosemite, Calif., 3-6 Feb. 1986
(NASA-TM-86589; NAS 1.15:86589) Avail: NTIS HC A02/MF A01 CSCL 04A

The sixth biennial Yosemite topical conference and the first as a Chapman Conference was held on February 3 to 6, 1986. Due to the recent changes in our perception of the dynamics of the ionospheric/magnetospheric system, it was deemed timely to bring researchers together to discuss and contrast the relative importance of solar versus terrestrial sources of magnetospheric plasma. Although the solar wind was once thought to dominate the supply of plasma in the Earth's magnetosphere, it is now thought that the Earth's ionosphere is a significant contributor. Polar wind and other large volume outflows of plasma have been seen at relatively high altitudes over the polar cap and are now being correlated with outflows found in the magnetotail. The auroral ion fountain and cleft ion fountain are examples of ionospheric sources of plasma in the magnetosphere, observed by the Dynamics Explorer 1 (DE 1) spacecraft. The conference was organized into six sessions: four consisting of prepared oral presentations, one poster session, and one session for open forum discussion. The first three oral sessions dealt separately with the three major topics of the conference, i.e., the sources, mechanisms, and consequences of ionospheric plasma in the magnetosphere. A special session of invited oral presentations was held to discuss extraterrestrial ionospheric/magnetospheric plasma processes. The poster session was extended over two evenings during which presenters discussed their papers on a one-on-one basis. The last session of the conferences was reserved for open discussions of those topics or ideas considered most interesting or controversial. Author

N87-20690*# National Aeronautics and Space Administration. Goddard Space Flight Center, Greenbelt, Md.
CRUSTAL DYNAMICS PROJECT DATA ANALYSIS, 1986. VOLUME 1: FIXED STATION VLBI GEODETIC RESULTS
C. Ma and J. W. Ryan Mar. 1987 211 p Submitted for publication
(NASA-TM-87806; Rept-87B0118; NAS 1.15:87806) Avail: NTIS HC A10/MF A01 CSCL 08G

The Goddard VLBI group reports the results of analyzing 361 Mark III VLBI data sets from fixed observatories through the end of 1985 which are available to the Crustal Dynamics Project. All POLARIS/IRIS full-day data sets are included. The mobile VLBI sites at Platteville, Colorado; Penticton, British Columbia; and Yellowknife, Northwest Territories are also included since these occupations bear on the study of plate stability. Two large solutions, GLB027 and GLB028, were used to obtain site/baseline evolutions and earth rotation parameters, respectively. Source positions and nutation offsets were also adjusted in each solution. The results include 23 sites and 101 baselines. Author

N87-20691# Naval Ocean Systems Center, San Diego, Calif.
LOWTRAN MODELING OF NEAR-HORIZON INFRARED SKY RADIANCES IN THE PRESENCE OF CLOUDS Research Report, Oct. 1985 - Sep. 1986
H. G. Hughes Sep. 1986 13 p
(AD-A175661; NOSC/TD-988) Avail: NTIS HC A02/MF A01 CSCL 17/5

A set of infrared (8 to 12 micrometer) sky radiances and meteorological (radiosonde) measurements are used to test the utility of the LOWTRAN 6 radiance algorithm to predict infrared sky radiances close to the horizon when clouds are present. The effects of clouds on the calculated radiances at the optical horizon are shown to be minimal but must be properly included at slightly higher elevations. Although the measurements pertain to good surface visibility conditions, small contributions by aerosols must be included in the LOWTRAN 6 calculations in order to match the measured radiances. This points out the possibility of inferring an appropriate (but not unique) vertical aerosol size distribution model from remotely sensed sky radiances. A deficiency in the radiance algorithm at a zenith angle of 90 degrees was noted, and its sensitivity to the number of lower layers used in the atmospheric model is discussed. GRA

N87-20692# Science Applications International Corp., McLean, Va.
SPECTRAL CHARACTERISTICS OF INTERCHANGE TURBULENCE IN THE IONOSPHERE
A. B. Hassam (Maryland Univ., College Park.), W. Hall (Columbia Univ., New York.), J. D. Huba, and M. J. Keskinen 22 Oct. 1986 55 p
(AD-A175975; NRL-MR-5793) Avail: NTIS HC A04/MF A01 CSCL 04/1

The spectral characteristics of turbulence associated with the magnetized plasma Rayleigh Taylor instability in the presence of a background neutral gas are studied. Particular attention is paid to comparing the spectra obtained in the ion neutral collision dominated case with the spectra from the ion inertia dominated case. A saturated level of turbulence is obtained for a model system confined between conducting boundaries with an imposed density gradient between the boundaries. The potential spectrum in the collisional case shows a marked anisotropy in contrast to that in the inertial case which is isotropic and exhibits Kolmogorov scaling. The anisotropy in the collisional case is attributed to the viscous nature of the turbulence and the consequent suppression of inertial overshoots. Application of these results to ionospheric turbulence is discussed. GRA

N87-20693# Instituto de Pesquisas Espaciais, Sao Jose dos Campos (Brazil).
NUCLEAR GEOPHYSICS IN SPACE AND ATMOSPHERIC RESEARCH AT INPE/BRAZIL
D. J. R. Nordemann, E. B. Pereira, E. V. A. Marinho, and F. SircilliNeto May 1986 15 p In PORTUGUESE
(DE87-700426; INPE-3883) Avail: NTIS (US Sales Only) HC A02/MF A01

In recent years, INPE's research in Nuclear Geophysics has developed in fields of interest to the Institute, the scientific community and the society in general. In the space research field a contribution has been made to the history of meteorite falls on our planet and its possible collision with large meteorites, which may have been the cause of important effects such as biological extinction and extraterrestrial matter gathering. In atmospheric research, spatial and temporal variations of radon measurements in the lower atmosphere permit correlations from micrometeorology to mesoscale phenomena, related to the dynamics of air masses. DOE

N87-20694# Purdue Univ., West Lafayette, Ind. Dept. of Physics.
THE FIFTH FORCE
E. Fischbach, D. Sudarsky, A. Szafer, C. Talmadge, and S. H. Aronson 1986 12 p Presented at the 23rd International Conference on High-Energy Physics, Berkeley, Calif., 16 Jul. 1986 Prepared in cooperation with Washington Univ., Seattle.; Brookhaven National Lab., Upton, NY.;European Organization for Nuclear Research, Geneva (Switzerland).
(Contract DE-AC02-76CH-00016)
(DE87-004612; BNL-39062; CONF-860701-70) Avail: NTIS HC A02/MF A01

We present a phenomenological description of the fifth force which focuses on the implications of the existing data from satellite and geophysical measurements of gravity, the Eoetvoes experiment, decays into hyperphotons, and the energy-dependence of the K(0) - anti-K(0) parameters. DOE

N87-20695# Goettingen Univ. (West Germany). Mathematisch-Naturwissenschaflichen Fachbereiche.
AMPLIFICATION OF AN ELECTRON DENSITY PERTURBATION IN THE POLAR E LAYER, INDUCED BY STRONG HF WAVES Ph.D. Thesis [VERSTAERKUNG EINER DURCH STARKE HF-WELLEN INDUZIERTEN ELEKTRONENDICHTESTOERUNG IN DER POLAREN E-SCHICHT]
Johannes Stecker 1985 99 p In GERMAN
(ETN-87-99014) Avail: NTIS HC A05/MF A01

The interpretation of ionospheric plasma modification experiments using HF waves was studied. The experiments were conducted in the polar E layer, thus in the region of the local electron density maximum with an average extension from 90 to 140 km. A model based on the description of quiescent polar arcs was used. The HF-heating-induced electron density perturbation excites currents parallel to the Earth's magnetic field which cause flow instabilities above a certain threshold. The numerical calculation shows that the ionospheric parameters are more important than the magnetospheric ones, and that instabilities only occur under very special conditions. For times >100 sec, a second perturbation splits off from the original one, propagates away from the heating region, and further behaves as a free perturbation. Improvements for the model are proposed. ESA

47 METEOROLOGY AND CLIMATOLOGY

Includes weather forecasting and modification.

N87-20696 Purdue Univ., West Lafayette, Ind.
THE EFFECT OF LATENT HEAT ON KINETIC ENERGY CONVERSIONS ASSOCIATED WITH SOUTH PACIFIC CYCLONES Ph.D. Thesis
Deirdre Mary Kann 1986 180 p
Avail: Univ. Microfilms Order No. DA8700909

Three cyclones which formed in the South Pacific Convergence Zone (SPCZ) during January 1979 are studied using ECMWF FGGE Level III-b analyses. The FGGE analyses made the study of these cyclones possible for the first time. One cyclone remained in the tropics, the other two propagated southeastward along the western edge of the SPCZ and took on frontal characteristics while still in the subtropics. Analyses of the structure of the SPCZ verify that the region was an active baroclinic zone during the period of study. Temperature anomalies and precipitating convection suggest that latent heat plays an important role in the SPCZ. Vertical velocities partitioned into adiabatic and diabatic components confirm that the forcing by moist processes dominates over that due to dry processes. The role that latent heat has in the life cycles of each cyclone is examined by calculating two terms in the eddy kinetic energy budget: (1) CE, a baroclinic-type conversion, and (2) CK, a barotropic-type conversion. These terms are calculated using the partitioned vertical velocities. Results show that CE is an order of magnitude larger than CK, indicating that baroclinic processes dominate over barotropic processes in both terms. Dissert. Abstr.

N87-20697 Saint Louis Univ., Mo.
DYNAMICAL AND THERMODYNAMICAL CHARACTERISTICS OF A SQUALL-LINE DETERMINED FROM DUAL-DOPPLER DATA Ph.D. Thesis
Jen-Hong (Jeff) Lin 1986 176 p
Avail: Univ. Microfilms Order No. DA8628800

Dual-Doppler wind data at 1630 and 1634 CST for the 6 June 1979 convective storm in Oklahoma, obtained from the National Severe Storms Laboratory, are used to investigate the dynamic and thermodynamic characteristics of the storm during the investigation time. The horizontal storm-relative winds are obtained on a gridded array with 1 km intervals using the Barnes' objective scheme. Vertical velocities were computed from the anelastic continuity equation by integrating downward from the storm's top with variational adjustment. In order to learn the advantage of the variational technique and the effect of smoothing, a series of ten experiments were conducted. The findings demonstrated that the variational method is far better than the kinematic method. A further reduction of relative errors was obtained through smoothing in radial velocity before calculation of the pressure and temperature fields. Results show that the gust front (GF) is mainly responsible for vigorous convection in the storm. Three-dimensional kinematic trajectory calculations further reveal some structural features of the storm in the lower layers, which are in agreement with the overall findings in the storm structure. Dissert. Abstr.

N87-20698 Washington Univ., Seattle.
THE MESOSCALE ORGANIZATION, DYNAMICS, AND EVOLUTION OF THE MARINE PLANETARY BOUNDARY LAYER DURING COLD AIR OUTBREAKS Ph.D. Thesis
Bernard A. Walter, Jr. 1986 219 p
Avail: Univ. Microfilms Order No. DA8626711

Satellite imagery along with aricraft data collected off the east coast of the U.S. and over the Bering Sea are used to study the evolution of organized mesoscale convection with fetch during cold air outbreaks. Comparisons between satellite photos of cloud formations during cold air outbreaks and results from Rayleigh-Benard laboratory experiments show a number of simularities. Satellite photos show three distinct regions offshore where particular mesoscale convection regimes dominate, while Rayleigh-Benard studies show a transition to different convection forms as the Rayleigh number is increased. Aircraft data from over the Bering Sea show a different situation in that cloud streets present at the ice edge, although broadening with distance downstream, still maintain their two dimensional nature. Calculation of an atmospheric Rayleigh number using a value of the eddy viscosity obtained from the aircraft data resulted in the placement of broad bounds on values of the atmospheric Rayleigh number for different convective regimes. Comparison of aircraft observations of boundary layer growth with fetch during cold outbreaks with results from a layer-averaged airmass modification model showed the inability of the model to adequately predict the large entrainment velocities actually present in strong air mass modification conditions. Dissert. Abstr.

N87-20699*# Universities Space Research Association, Boulder, Colo.
WIND AND TURBULENCE DATA FOR DEVELOPMENT OF DESIGN CRITERIA FOR UNMANNED HIGH-ALTITUDE LOW-SPEED ENDURANCE AIRCRAFT
Stanley I. Adelfang Washington NASA Apr. 1987 128 p
(Contract NAS8-34010)
(NASA-CR-4065; NAS 1.26:4065) Avail: NTIS HC A07/MF A01 CSCL 04B

The wind environment for the ascent/descent and cruise modes of unmanned aircraft designed for long duration low speed station keeping operation at high altitude is described. Six study sites are used to characterize the wind in geographic areas. A nominal ascent altitude versus time function is used in the development of wind speed exceedance/duration statistics. Wind

statistics at cruise altitude are derived based on a nominal cruise altitude that does not exceed 21 km and is a function of the minimum 50 percentile wind speed. The site specific data is supplemented by hemispheric scale data obtained from other published studies. Significant variability of winds aloft as a function of location, altitude, and season is indicated. Cruise altitude selection based on analysis of winds aloft data over operations areas is suggested because of the variability of the altitude of the minimum wind speed with latitude. Atmospheric turbulence criteria, as published in Terrestrial Environment (Climatic) Criteria Guidelines for Use in Aerospace Vehicle Development, 1982 Revision, NASA TM-82473, are suggested for the ascent and cruise modes of operation. Author

N87-20700*# Universities Space Research Association, Huntsville, Ala.
LINEAR BAROCLINIC INSTABILITY IN THE PRESENCE OF LARGE SCALE TOPOGRAPHY
Nathaniel Dunton Reynolds Washington NASA Mar. 1987 111 p
(Contract NAS8-36474)
(NASA-CR-4057; NAS 1.26:4057) Avail: NTIS HC A06/MF A01 CSCL 04B

The effect of a planetary-scale, wavenumber 2 topography on baroclinically active disturbances is investigated for a channel domain in a two-layer, quasi-geostrophic context. When the lower-layer zonal velocity is nonzero, the topography influences the disturbances by forcing a stationary wave, and the topography and the forced wave influence the growth rates and the spatial structures of the time-dependent solutions. The case of zero zonal velocity in the lower layer was also investigated, for which no forced wave exists. Asymptotic forms of the equations, valid when the topographic effect (governed by the ratio of the nondimensional topographic height to the rotational Froude number) is small, are used to obtain both the stationary and time-dependent solutions. The latter are also obtained using a numerical approach, in which is determined the eigenvalues and eigenfunctions of a matrix representing the dynamical equations. Agreement is good between the two approaches. Recent laboratory experiments with a baroclinic annulus in which there is a false bottom with wavenumber 2 topography, are used to select governing parameters. The simultaneous presence of a stationary forced wave of wavenumber 2 and a time-dependent baroclinic wave of wavenumber 4, which has wavenumber 2 and 6 sidebands due to the topography, yields a flow field that exhibits some principal features of the laboratory experiments. The position of the forced wave and the location of an excursion in latitude of the storm track show qualitative resemblance to those features observed in the atmosphere. Author

N87-20701*# National Aeronautics and Space Administration. Goddard Space Flight Center, Greenbelt, Md.
ON REQUIREMENTS FOR A SATELLITE MISSION TO MEASURE TROPICAL RAINFALL
Otto W. Thiele, ed. Apr. 1987 67 p
(NASA-RP-1183; NAS 1.61:1183) Avail: NTIS HC A04/MF A01 CSCL 04B

Tropical rainfall data are crucial in determining the role of tropical latent heating in driving the circulation of the global atmosphere. Also, the data are particularly important for testing the realism of climate models, and their ability to simulate and predict climate accurately on the seasonal time scale. Other scientific issues such as the effects of El Nino on climate could be addressed with a reliable, extended time series of tropical rainfall observations. A passive microwave sensor is planned to provide information on the integrated column precipitation content, its areal distribution, and its intensity. An active microwave sensor (radar) will define the layer depth of the precipitation and provide information about the intensity of rain reaching the surface, the key to determining the latent heat input to the atmosphere. A visible/infrared sensor will provide very high resolution information on cloud coverage, type, and top temperatures and also serve as the link between these data and the long and virtually continuous coverage by the geosynchronous meteorological satellites. The unique combination of sensor wavelengths, coverages, and resolving capabilities together with the low-altitude, non-Sun synchronous orbit provide a sampling capability that should yield monthly precipitation amounts to a reasonable accuracy over a 500- by 500-km grid. Author

N87-20702# Air Command and Staff Coll., Maxwell AFB, Ala.
AFGWC'S ADVANCED WEATHER ANALYSIS AND PREDICTION SYSTEM (AWAPS)
James G. Stobie Jun. 1986 72 p
(AD-A172801; ACSC-86-2405; AWS-TN-86/001) Avail: NTIS HC A04/MF A01 CSCL 04/2

Described are the three computer models used in the Air Force Global Weather Central's Advanced Weather Analysis and Prediction System (AWAPS) and how they interact to form a production cycle. These models are the High Resolition Analysis Systems (HIRAS), the Global Spectral Model (GSWM), and the Relocatable Window Model (RWM). Also given is a brief introduction to the basics of numerical weather prediction. GRA

N87-20703# East Anglia Univ., Norwich (England). Climatic Research Unit.
MONTHLY MEAN PRESSURE RECONSTRUCTIONS FOR EUROPE (BACK TO 1780) AND NORTH AMERICA (TO 1958)
P. D. Jones, T. M. L. Wigley, and K. R. Briffa Feb. 1987 104 p
(Contract DE-FG02-86ER-60397)
(DE87-005556; DOE/ER-60397/H1) Avail: NTIS HC A06/MF A01

Monthly grid-point pressure data are reconstructed from station records of air temperature, precipitation and pressure for Europe, back to 1780, and North America, back to 1858. The reconstructions are based on a principal components regression technique which relates surface pressure patterns to those of the temperature, precipitation and station pressure data. The relationships are derived over a calibration period and the results are tested with independent data from another period. To illustrate the results examples are given of pressure anomalies over Europe during 1816 (the year without a summer), anomalies over both Europe and North America for January and November 1862 (months with particularly strong anomalies), and anomalies over North America during 1884 (the year after Krakatau). The reconstructions are compared with other monthly mean pressure maps produced by Lamb and Johnson (1966) for Europe for 1780 to 1872 and for North America for 1858 to 1898, and by Kington (1980) for Europe for 1781 to 1785. Both of these map series show systematic biases relative to the present reconstructions. The reconstructed data are available on magnetic tape. DOE

N87-20704# European Space Agency, Paris (France).
A BISPECTRAL METHOD FOR THE DETERMINATION OF THE ALTITUDE OF ICE CLOUDS
Werner Pollinger and Peter Wendling Nov. 1986 57 p Transl. into ENGLISH of "Eine bispektrale Methode zur Hohenbestimmung von Eiswolken" DFVLR, Oberphaffenhofen, West Germany, report DFVLR-FB-86-03, Dec. 1985 Original language document was announced as N86-32072 Original contains color illustrations
(ESA-TT-993; DFVLR-FB-86-03; ETN-87-99428) Avail: NTIS HC A04/MF A01; original German version available from DFVLR, Cologne, West Germany DM 36.50

A bispectral method for the height determination of optically thin ice clouds from satellite measurements at two adjacent points of an ice cloud layer was developed. Using two wavelengths in the spectral range of the water vapor band at 6.3 microns and in the window range at 11 microns, a transcendental equation was derived under the assumption that both points of the cloud have the same temperature but different optical thickness. The solution of the transcendental equation yields the cloud temperature, and the height via the temperature profile which must be known. The effect of the water vapor above the cloud is corrected for using a radiation transfer model. ESA

N87-20705# Office National d'Etudes et de Recherches Aerospatiales, Paris (France).
DEFINITION AND USE OF SENSORS FOR MEASURING ELECTRICAL CONDUCTIVITY IN THUNDERCLOUDS Ph.D. Thesis - Paris Univ. VI, France
P. Gondot 1986 61 p In FRENCH; ENGLISH summary Report will also be announced as translation (ESA-TT-1047)
(ONERA-NT-1986-4; ISSN-0078-3781; ETN-87-99381) Avail: NTIS HC A04/MF A01

The electrical behavior of a convective cloud is related to global parameters like the atmospheric electric field and to local phenomena like the electric charge of hydrometeors and the electric ionic conductivity of the medium. Different sensors were designed and installed on an aircraft. The experimental devices are described and results of the airborne experiments are presented. A positive monopole zone of ionic density was detected in clear sky at the edge of convective clouds, at 6000 m altitude. ESA

N87-20706# Office National d'Etudes et de Recherches Aerospatiales, Paris (France). Direction de la Physique Generale.
LIGHTNING STRIKES ON AIRCRAFT. EXPLOITATION OF LANDES (FRANCE)-FRONT '84 CAMPAIGN AND COMPLEMENTARY DEVELOPMENT OF AIRBORNE ELECTRICAL SENSORS Final Report [FOUDROIEMENTS DES AERONEFS. EXPLOITATION DE LA CAMPAGNE LANDES-FRONT 84 ET DEVELOPPEMENT COMPLEMENTAIRE DE CAPTEURS ELECTRIQUES EMBARQUABLES]
P. Laroche, A. Bondiou, A. Delannoy, P. Gondot, and P. Richard Aug. 1986 160 p In FRENCH
(Contract DRET-85-001)
(ONERA-RF-91/7154-PY; ETN-87-99383) Avail: NTIS HC A08/MF A01

The localization of atmospheric discharges obtained by a 300 MHz electromagnetic interferometer are compared to the radar signatures giving the precipitation rate and wind fields inside the convective cells. The data are complemented by onboard measurements of electric field and hydrometeors, made using sensors placed on the structure of a Transall aircraft. Results show a clear correlation between Doppler radar and interferometric simultaneous images. Electrical simultaneous onboard measurements such as electric field, ionic conductivity, precipitation charges, are, as suspected, strongly correlated. ESA

N87-20707# Office National d'Etudes et de Recherches Aerospatiales, Paris (France). Direction de la Physique Generale.
STUDY OF SURFACE DISCHARGES Final Report [ETUDE DES DECHARGES DE SURFACE]
S. Larigaldie, H. LecourtdeBeru, J. Surget, A. Brunet, F. Faure, J. P. Marque, and D. Veyrat Jun. 1986 93 p In FRENCH
(Contract DRET-85-001)
(ONERA-RF-11/7236-PY; ETN-87-99387) Avail: NTIS HC A05/MF A01

Surface discharges are studied including atmospheric pressure discharge final phase, discharges at low pressure (some mb) and high vacuum discharges (0.00001 Torr). The first is equivalent to a reflected wave process propagating in an ionized environment. The last case is characteristic of phenomena observed on geostationary satellites. It is shown that the existing models describing the atmospheric discharge propagation do not explain adequately the experimental evidence. ESA

N87-20708# Joint Publications Research Service, Arlington, Va.
CHINA REPORT: SCIENCE AND TECHNOLOGY
1 Jul. 1986 92 p Transl. into ENGLISH from various Chinese articles
(JPRS-CST-86-025) Avail: NTIS HC A05/MF A01

Topics addressed include: national developments; physical sciences; applied sciences; life sciences; environmental quality; scientists and scientific organizations; and thermophysics. For individual titles, see N87-20709 through N87-20709.

N87-20709# Joint Publications Research Service, Arlington, Va.
HYDROLOGIC FEATURES IN CYCLONIC EDDY REGION OF NORTHERN EAST CHINA SEA IN COLD SEASONS
Zongxin Ding *In its* China Report: Science and Technology (JPRS-CST-86-025) 1 Jul. 1986 p 56-63 Transl. into ENGLISH from Haiyang Kexue (Beijing, China), v. 9, no. 5, 9 Sep. 1985 p 1-4 (For primary document see N87-20708 13-47)
Avail: NTIS HC A05/MF A01

A detailed analysis was made on the data collected from October 1979 to April 1980 in the northern East China Sea. The appearance of the low salinity region signifies that the Huanghai Sea coastal current no longer enters the northern part of the East China Sea, thus creating an enclosed counterclockwise loop in the southern part of the Huanghai Sea. The region covered by the counterclockwise loop, which originally extended into the East China Sea, is drastically reduced. This low salinity region is an important piece of evidence in studying the variation of the circulation in the Huanghai Sea and the East China Sea. B.G.

48 OCEANOGRAPHY

Includes biological, dynamic, and physical oceanography; and marine resources.

For related information see also *43 Earth Resources and Remote Sensing.*

N87-20710 Wisconsin Univ., Madison.
A TECHNIQUE TO ESTIMATE THE OCEAN SURFACE ENERGY FLUX USING VAS MULTISPECTRAL DATA Ph.D. Thesis
John Joseph Bates 1986 164 p
Avail: Univ. Microfilms Order No. DA8605676

A technique is developed to estimate the ocean surface energy flux from multispectral (visible and infrared) data obtained from the visible and infrared spin scan radiometer atmospheric sounder (VAS) on the geostationary GOES satellite. The technique is designed for application in the tropics. The shortwave flux is estimated by application of a simple physical model to visible data. The longwave flux is calculated using a statistical regression algorithm specifically tailored to model tropical cumulus clouds. In order to estimate the latent heat flux, the bulk parameterization is used with the sea surface temperature (SST), low-level moisture, and low-level wind speed, as inputs. Simulation and in-situ matches are used to estimate the expected errors of the method. The model was tested through its application to a case study using several days of data from November of 1982 and 1983 in the eastern tropical Pacific, in order to examine a large SST signal (the El Nino Southern Oscillation, ENSO). The results showed that almost all features on the individual analyses were significant to the 2 sigma level, but that few significant features remained on the difference fields for latent heat flux and net heat flux.
Dissert. Abstr.

N87-20711# Woods Hole Oceanographic Institution, Mass.
DYNAMIC PRESENTATION OF LONG. TERM UPPER OCEAN STUDY (LOTUS) DATA USING VIDEOTAPE
Ellyn T. Montgomery Sep. 1986 35 p
(Contracts N00014-76-C-0197; N00014-84-C-0134)
(AD-A175535; WHOI-86-33) Avail: NTIS HC A03/MF A01 CSCL 09/2

In order to show efficiently the large amount of data obtained during the Long Term Upper Ocean Study (LOTUS), a new method of data presentation was developed. Three data variables can be included in a simple color contour plot, but if successive color contour plots are recorded on videotape, a fourth variable, time, can also be shown. This report documents the process of making a videotape presenting scientific data in this way, from raw data to finished videotape. The videotape shows internal wave kinetic energy versus frequency and depth; the time variation of the videotape displays real time variation in the ratio of 14/30 second to one week, or about 1 month of data very 2 seconds. GRA

N87-20712# Naval Ocean Research and Development Activity, Bay St. Louis, Miss.
TESTING AND COMPARISON OF SEVERAL MIXED-LAYER MODELS Final Report
Paul J. Martin May 1986 36 p
(AD-A175959; NORDA-143) Avail: NTIS HC A03/MF A01 CSCL 08/10

Several models of the upper mixed layer of the ocean (Mellor-Yamada Level 2 and 2 1/2, Niiler, Garwood, Price, and Therry-Lacarrere) were compared using (a) idealized forcing that consisted of cases of wind deepening, heating, and cooling, (b) data from Ocean Stations November and Papa, (c) data taken during the Mixed-Layer Experiment (MILE), and (d) data taken from R/P FLIP in the spring of 1980 about 400 km off California. Comparisons with both idealized and observed forcing show the differences among the models to be significant. Differences are especially noticeable for the deepening of the mixed layer in the fall and winter due to wind mixing and convection, and for the shallowing of the mixed layer during light winds and strong heating. Although evaluation of the models is complicated by uncertainties (primarily with regard to advective effects and forcing), the results suggest certain deficiences in some of the mixing parameterizations. GRA

N87-20713# Woods Hole Oceanographic Institution, Mass.
MOORED CURRENT METER AND TEMPERATURE-PRESSURE RECORDER MEASUREMENTS FROM THE WESTERN NORTH ATLANTIC (HIGH ENERGY BENTHIC BOUNDARY LAYER AND ABYSSAL CIRCULATION EXPERIMENTS 1983-1984), VOLUME 39
Ellen Levy and Susan A. Tarbell Apr. 1986 45 p
(Contracts N00014-82-C-0019; N00014-76-C-0197; Grant NSF OCE-82-14925)
(AD-A176014; WHOI-86-14) Avail: NTIS HC A03/MF A01 CSCL 08/3

Summaries of long-term current, temperature and pressure measurements from moored instruments in the western North Atlantic are presented. The moorings were set in March 1983 and retrieved seventeen months later. Composite plots of filtered time series are presented. GRA

N87-20714# Naval Postgraduate School, Monterey, Calif.
WIND-CURRENT RELATIONSHIPS IN THE OPTOMA DOMAIN OFF THE NORTHERN CALIFORNIA COAST M.S. Thesis
Steven J. Summers Sep. 1986 81 p
(AD-A176019) Avail: NTIS HC A05/MF A01 CSCL 04/2

The oceanic response to time-dependent wind forcing approximately 100-200 km off the Northern California coast is examined through cross-spectrum analysis of current and wind time series. Current meter records 10 months in length from three moorings in deep water 100-200 km off the coast are analyzed in conjunction with surface wind analyses from the Fleet Numerical Oceanography Center. Coherence is found between atmospheric and oceanic variables in the locally forced band (1-10 day period), in the planetary wave band (10-30 day period), and at low frequency (greater than 30 day period), though not in all of these bands for all records. The barotropic and first baroclinic dynamical modes appear to respond to wind forcing at different frequencies for two of the moorings analyzed. There is coherence between alongshore divergence and temperature fluctuations 100 km farther offshore, consistent with offshore advection by current filaments. Evidence of the Sverdrup balance is found for some periods greater than 18 days in the form of coherence between wind stress curl and the current component parallel to the local potential vorticity gradient. Complex bottom topography and the influence of coastal processes in the vicinity of the current meter moorings appear to greatly complicate the flow. There appears to be significant mesoscale variability in the region at scales too small to be resolved by the 100 km spacing of the OPTOMA moorings. GRA

N87-20715# Naval Underwater Systems Center, New London, Conn.
ACOUSTIC SCATTERING FROM COMPOSITE WIND-WAVE SURFACES II: BACKSCATTER CROSS SECTIONS AND DOPPLER EFFECTS AT HIGH FREQUENCIES AND SMALL ANGLES FOR 'BUBBLE-FREE' REGIMES
David Middleton 22 Jul. 1986 71 p
(AD-A176081; NUSC-TR-7635) Avail: NTIS HC A04/MF A01 CSCL 20/1

The present study continues the investigation of the author embodied in NUSC Technical Document TD-78205. Here we are again concerned with underwater acoustic scattering from the random moving wind-wave surface of the ocean. In particular, we are concerned with high frequency O(5-20 kHz), small grazing angle configurations O(5-25), and near-surface as well as volume regimes which are bubble-free vis-a-vis surface effects. Our efforts here are specifically directed to the calculation of doppler shift an doppler spread produced by the wind-driven ocean surface. Included also is a summary of a more complete model of the soliton scattering mechanism originally postulated and described. This more complete model is based on recent work of Middleton and Mellen. GRA

N87-20716# Old Dominion Univ., Norfolk, Va.
CONTINENTAL SHELF PROCESSES AFFECTING THE OCEANOGRAPHY OF THE SOUTH ATLANTIC BIGHT Progress Report, 1 Jun. 1986 - 31 May 1987
L. P. Atkinson Jan. 1987 52 p
(Contract DE-FG05-85ER-60348)
(DE87-005303; DOE/ER-60348/5) Avail: NTIS HC A04/MF A01

As part of a study of continental shelf processes affecting the oceanography of the South Atlantic Bight, data collected during the Spring 1985 SPREX field experiment was processed and analyzed. The goals of the analyses were to: (1) determine the distribution of temperature, salinity, nutrients, and humid fluorescence such that flow fields and distributions of variables could be related to wind forcing events; (2) determine the time change in nutrient concentration and salinity at selected current meter locations; and (3) evaluate the usefulness of tritium as a fresh water tracer in the nearshore region of the South Atlantic Bight. DOE

N87-20717# Joint Publications Research Service, Arlington, Va.
CHINA REPORT: SCIENCE AND TECHNOLOGY
11 Feb. 1987 102 p Transl. into ENGLISH from various Chinese articles
(JPRS-CST-87-005) Avail: NTIS HC A06/MF A01

Articles from several Chinese publications are presented. The articles cover a wide range of topics in the science and technology field, from national developments to physical sciences and applied sciences. The two articles which are of special interest are entitled: Numerical simulation of storm surges in the East China Sea; and Mathematical model of steady state circulation in the South China Sea. For individual titles, see N87-20718 through N87-20719.

N87-20718# Joint Publications Research Service, Arlington, Va.
NUMERICAL SIMULATION OF STORM SURGES IN THE EAST CHINA SEA
Jingyong Wang *In its* China Report: Science and Technology 11 Feb. 1987 p 61-70 Transl. into ENGLISH from Shandong Haiyang Xueyuan Xuebao (Qingdao, China). Vol. 15, No. 3, 15 Sep. 1985 p 40-47 (For primary document see N87-20717 13-48) Avail: NTIS HC A06/MF A01

A depth averaged numerical storm surge model was used to simulate the East China Sea under the influence of a Pacific Ocean typhoon. The influence of the Changjiang River's discharge is included in the model. Data on typhoon 8114 were used to simulate the rise in water level at Wusong station. The calculated water level results for a large area show wavelike propagation. The numerical calculation indicates that the phase velocity of the wave is about 23 m/sec. One explanation currently offered for the rise in the water level near shore during storm surges is that when the waves from a remote disturbance reach the coast, the amplification effect of shallow water produces high water levels close to shore. It is evident from the computation results presented

that there is some truth in this explanation. If the numerical model presented were used to calculate the rises in water level produced by all possible types of typhoon, it would provide an excellent supplement to the historically used prediction method. Author

N87-20719# Joint Publications Research Service, Arlington, Va.
MATHEMATICAL MODEL OF STEADY-STATE CIRCULATION IN THE SOUTH CHINA SEA
Jia Wang *In its* China Report: Science and Technology 11 Feb. 1987 p 71-83 Transl. into ENGLISH from Shandong Haiyang Xueyuan Xuebao (Qingdao, China), v. 15, no. 3, 15 Sep. 1985 p 22-32 (For primary document see N87-20717 13-48)
Avail: NTIS HC A06/MF A01

The beta-plane wind curl thermohaline gradient model is extended to a model representing the actual South China Sea area as a multiply connected region and simulates the winter and summer circulation in the sea. The calculations take account of wind stress, the thermohaline effect, bottom topography, and boundary forces. A fast convergence technique was used in the calculations, and nonlinear effects were further elucidated on the basis of the linear model. Author

N87-20720# Joint Publications Research Service, Arlington, Va.
CHINA REPORT: SCIENCE AND TECHNOLOGY
7 Aug. 1986 111 p Transl. into ENGLISH from various Chinese articles
(JPRS-CST-86-031) Avail: NTIS HC A06/MF A01

Topics addressed include: cyclonic eddies; spectral analysis of waves; effect of sound velocity in ocean sediments; wind-wave prediction models; frequency spectrum estimation of sea water; Chinese language microcomputer; square-loop antennas; and undulator for an electron storage ring. For individual titles, see N87-20721 through N87-20726.

N87-20721# Joint Publications Research Service, Arlington, Va.
EXISTENCE SEEN OF CYCLONIC EDDY IN NORTHERN EAST CHINA SEA
Baoren Zaho *In its* China Report: Science and Technology 7 Aug. 1986 p 1-11 Transl. into ENGLISH from Haiyang Yu Huzao (Beijing, China), v. 16, no. 3, May 1985 p 240-248 (For primary document see N87-20720 13-48)
Avail: NTIS HC A06/MF A01

The results of the surveys conducted in the cyclonic eddy zone in northern East China Sea in recent years are briefly summarized. Based on the temperature field, mass field, and flow field measured in these surveys, cyclonic eddy did exist in the area southwest of Cheju Island during this period. The residual current vector obtained in the survey was plotted with those measured in the past in the same season, resulting in a complete cyclonic eddy flow field. In addition, fundamental characteristics of the Huanghai Sea coastal current in northern East China Sea are also discussed. The results further confirm that the diagnosis that this cyclonic eddy exists year round and its position is stable is correct. Author

N87-20722# Joint Publications Research Service, Arlington, Va.
SPECTRAL ANALYSIS OF WAVES IN GULF OF TONKIN DESCRIBED
Wenzhi Wang *In its* China Report: Science and Technology 7 Aug. 1986 p 12-26 Transl. into ENGLISH from Nanhai Haiyang Kexue Jikan (Beijing, China), no. 2, Oct. 1981 p 79-92 (For primary document see N87-20720 13-48)
Avail: NTIS HC A06/MF A01

Although much was accomplished in the study of sea-wave spectrum, its spectrum form is not yet unified. The various spectrum representations that were proposed give results that are quite different from one another. Therefore, it is extremely important to analyze the observed wave spectra of a selected area of the sea. On the one hand, it will produce knowledge about the composition of the wave spectrum of a certain sea zone, which will be useful for areas such as constructions at sea, shipbuilding, and wave forecasting. On the other hand, it will provide information helpful to the comprehensive efforts in the theoretical study of sea-wave spectrum. Spectrum calculations were performed on 12 wave records from a fixed site in the Gulf during the passing of a stormy cold wave and a preliminary analysis and discussion of the results are presented. Among the 12 calculated correlation function graphs, some are not perfect. Either they don't oscillate along the time axis or they are far from approaching zero. These differences are probably due to insufficient measuring time and the presence of the zero-line drifting phenomenon, which is discussed. Author

N87-20723# Joint Publications Research Service, Arlington, Va.
PHYSICAL, MECHANICAL EFFECT OF VELOCITY OF SOUND IN OCEAN SEDIMENTS
Yuanbo Liang and Bo Lu *In its* China Report: Science and Technology 7 Aug. 1986 p 27-40 Transl. into ENGLISH from Haiyang Xuebao (Beijing, China), v. 7, no. 1, 15 Jan. 1985 p 111-119 (For primary document see N87-20720 13-48)
Avail: NTIS HC A06/MF A01

The use of acoustical methods to obtain information on the physical-mechanical properties of the ocean floor sedimentary layer is one of the fast developing ocean floor research methods in recent years. Observations during the last 10 to 20 years using the electon microscopic technology have led to the discovery of a few important microscopic characteristics of sedimentation; for example, the condition of granular sediment buildup, the pore structure, and the aspect ratio of pores. All these have effects which cannot be overlooked when considering the propagation characteristics of sound in ocean floor sediments, particularly in terms of the velocity of sound. In order to clarify the structure of ocean floor sedimentation and the physical mechanism of the mechanical factors that influence the propagation characteristics of sound, the relationship between the microscopic structure of sediment and the macroscopic acoustical phenomena. Also, taking one representative area of the continental shelf in the northwest section of the South China Sea as an example, regression analysis was performed on a set of test data from 17 test sites. Author

N87-20724# Joint Publications Research Service, Arlington, Va.
COMPARISON OF DEEPWATER WIND-WAVE PREDICTION MODELS
Bingxiang Wang, Jiuzi Zhang, and Guiqiu Wu *In its* China Report: Science and Technology 7 Aug. 1986 p 41-55 Transl. into ENGLISH from Shandong Haiyang Xueyuan Xuebao (Qingdao, China), v. 15, no. 3, 15 Sep. 1985 p 1-11 (For primary document see N87-20720 13-48)
Avail: NTIS HC A06/MF A01

Presently, there are about 36 models used in deep-water wind-wave forecasting by incomplete statisitics. To select from among these models 12 that are more important and currently employed are confirmed by field observations, and are compared with each other. The calculation based on the 12 were compared with wind data; so far as the cases examined are concerned. The accuracy of the results given by Wang's model are superior to those of the other 11 models. In order to investigate typhoon waves at station Xiaomaidao at 1800 hours 30 August 1939, the above approaches to wave prediction are used to hindcast again; the wave height on a basis of Wang's model is found to be more consistent with a 50 year return period wave at the wave station than those found for the existing models. According to the prediction technique of hurricane waves, the wave height and period of the most probable first highest wave within the area of the typhoon are estimated at about 39 meters and 24 seconds, respectively. Author

N87-20725# Joint Publications Research Service, Arlington, Va.
METHODS OF FREQUENCY SPECTRUM ESTIMATION OF SEA WATER COMPARED
Decai Jiang and Xinsheng Gao *In its* China Report: Science and Technology 7 Aug. 1986 p 56-68 Transl. into ENGLISH from Shandong Haiyang Xueyuan Xuebao (Qingdao, China), v. 15, no. 3, 15 Sep. 1985 p 12-21 (For primary document see N87-20720 13-48)
Avail: NTIS HC A06/MF A01

The principle of Maximum Entropy Method (MEM) is briefly introduced. The determination of the length of prediction filter is discussed in the case of MEM being used for estimating the spectrum of sea wave (wind wave, mixed wave) profile. The quality of the spectrum estimation with MEM and convential methods is also dealt with under the condition of the same sampling interval and the same sample capacity. It is shown that the MEM has higher resolution, especially for the short series of wave profile records, it is much better than conventional. Author

N87-20726# Joint Publications Research Service, Arlington, Va.
PHASE SPEED OF WIND-WAVE COMPONENT STUDIED
Delun Xu *In its* China Report: Science and Technology 7 Aug. 1986 p 69-77 Transl. into ENGLISH from Shandong Haiyang Xueyuan Xuebao (Qingdao, China), v. 15, no. 3, 15 Sep. 1985 p 33-39 (For primary document see N87-20720 13-48)
Avail: NTIS HC A06/MF A01

Measurements of phase speed of wind-wave components were made by the cross-spectrum method, separation distance between the two probes for measuring surface elevations being 2 cm. The measured data indicate that the relationship between phase speed and frequency varies with wind speed and water depth. For one extreme condition, low wind and deep water, it obeys basically the classical linear dispersion relation. For the other extreme condition, high wind and shallow water, the components are nondispersive, all traveling with the same speed as the component with spectrum-peak frequency. For medium conditions, the dispersion relations have some forms between the two extreme cases. The measured result can be interpreted on the basis of a refined spectral model, which consists of the contributions of both dispersive and nondispersive wave with the effect of the drift current included. At low wind and in deep water, the wave field in of low nonlinearity: free waves are dominant and, hence, the wave components are dispersive and obey the classical dispersion relation. At high wind and in shallow water, the wave field has high nonlinearity. In this case, forced waves dominate over free waves and the wave components appear to be nondispersive. Author

N87-20635# Meteorological Office, Bracknell (England).
OCEAN-ICE PANEL REPORT
T. D. Allan and A. Morel *In* ESA Proceedings of the European Symposium on Polar platform Opportunities and Instrumentation for Remote-sensing (ESPOIR) Nov. 1986 p 85-88 (For primary document see N87-20621 13-43)
Avail: NTIS HC A07/MF A01

51 LIFE SCIENCES (GENERAL)

N87-20727*# National Aeronautics and Space Administration. Marshall Space Flight Center, Huntsville, Ala.
LIQUID DROP STABILITY FOR PROTEIN CRYSTAL GROWTH IN MICROGRAVITY
Robert B. Owen, Beth H. Broom, Robert S. Snyder, and Ron Daniel Apr. 1987 17 p
(NASA-TP-2724; NAS 1.60:2724) Avail: NTIS HC A02/MF A01 CSCL 06B

It is possible to grow protein crystals for biomedical research in microgravity by deploying a protein-rich solution from a syringe, forming a drop in which crystallization can occur with the proper degree of supersaturation. Drop stability is critical to the success of this research, due to the large drop sizes which can be achieved in space. In order to determine the type of syringe tips most suitable to support these large drops, tests were performed during brief periods of weightlessness onboard the NASA KC-135 low-gravity simulation aircraft. The drops were analyzed using three simple models in which the samples were approximated by modified pendulum and spring systems. It was concluded that the higher frequency systems were the most stable, indicating that of the syringes utilized, a disk-shaped configuration provided the most stable environment of low-gravity protein crystal growth. Author

N87-20728# Brandeis Univ., Waltham, Mass.
EFFECT OF LIGHT AND DEVELOPMENT OF PHOTOSYNTHETIC CELLS Final Report
M. Gibbs 1986 11 p
(Contract DE-AC02-76ER-03231)
(DE87-005183; DOE/ER-03231/10) Avail: NTIS HC A02/MF A01

Green algae exposed to an anaerobic environment adapt to a hydrogen metabolism and can photooxidize H2O to H2 and O2 as well as carbon compounds to H2 and CO2. The products from fermentation of chloroplastic starch included acetate, formate, ethanol, CO2, H2, glycerol, and lactate. Light caused an increase in H2 and CO2 and decreases in acetate and ethanol. Aerobically isolated algal chloroplasts adapted to a hydrogen metabolism where H2 was evolved. The oxyhydrogen reaction was not detected in the chloroplasts. Acetate is photoassimilated anaerobically by Chlamydomonas cells to lipid, carbohydrate, CO2, and H2 with a stoichiometry indicating a light-dependent anaerobic glyoxylate cycle as the primary assimilatory pathway. DOE

N87-20729# Midwest Research Inst., Golden, Colo.
MICROALGAE CULTURE COLLECTION, 1986-1987
W. Barclay, J. Johansen, P. Chelf, N. Nagle, P. Roessler, and P. Lemke Dec. 1986 153 p
(Contract DE-AC02-83CH-10093)
(DE87-005578; SERI/SP-232-3079) Avail: NTIS HC A08/MF A01

The SERI Microalgae Culture Collection provides a repository for strains identified or developed for mass culture biomass production and makes these strains readily available to the research community. The strains in the collection have been selected for their potential in biomass fuel applications, and many produce significant quantities of cellular storage lipids. All of the newly added strains have been recently isolated by SERI and its subcontractors in organized screening programs. Many have been tested in outdoor mass culture systems, and several have demonstrated excellent performance as biomass producers. The strains added to the collection this year have been isolated from inland saline waters and marine waters. We believe that the strains in this collection can provide a source of extremely useful organisms, both for laboratory experimentation and for mass culture research. Most of the strains are currently nonaxenic. Again this year, cultures will be shipped free of charge to interested researchers. An important function of the culture collection catalog, in addition to listing the available strains, is to provide culture and performance data for each of the organisms. By collecting a summary of the requirements and characteristics of these organisms, we hope to allow requestors of cultures to begin productive research with a minimum of preliminary work on culture techniques. DOE

N87-20308*# Colorado Univ., Boulder. Get Away Special Project G-285
PHYCOMYCES IN SPACE: A PROBLEM IN BIOENGINEERING
Julie A. Schneringer *In* NASA. Goddard Space Flight Center The 1986 Get Away Special Experimenter's Symposium Feb. 1987 p 35-39 (For primary document see N87-20302 13-12)
Avail: NTIS HC A11/MF A01 CSCL 06B

N87-20322*# City Coll. of the City Univ. of New York. Dept. of Biology.
GEOTAXIS BASELINE DATA FOR DROSOPHILA
E. M. Schnebel, R. Bhargava, and J. Grossfield *In* NASA. Goddard Space Flight Center The 1986 Get Away Special Experimenter's Symposium Feb. 1987 p 141-148 (For primary document see N87-20302 13-12)
Avail: NTIS HC A11/MF A01 CSCL 06B

N87-20324*# California Polytechnic State Univ., San Luis Obispo.
CAL POLY SPACE PROJECT G-279

David R. Farley *In* NASA. Goddard Space Flight Center The 1986 Get Away Special Experimenter's Symposium Feb. 1987 p 157-162 (For primary document see N87-20302 13-12)
Avail: NTIS HC A11/MF A01 CSCL 06B

N87-20741# Joint Publications Research Service, Arlington, Va.
EFFECT OF LONG-TERM SPACEFLIGHT ON RAT BRAIN POLYAMINE CONTENT
R. A. Tigranyan and V. Yu. Kovalev *In its* USSR Report: Space Biology and Aerospace Medicine, Vol. 20, No. 3, May - Jun. 1986 (JPRS-USB-86-005) 15 Aug. 1986 p 74-79 Transl. into ENGLISH from Kosmicheskaya Biologiya i Aviakosmicheskaya Meditsina (Moscow, USSR), v. 20, no. 3, May Jun. 1986 p 53-57 (For primary document see N87-20731 13-52)
Avail: NTIS HC A08/MF A01

52 AEROSPACE MEDICINE

Includes physiological factors; biological effects of radiation; and effects of weightlessness on man and animals.

N87-20730*# National Aeronautics and Space Administration. Lyndon B. Johnson Space Center, Houston, Tex.
RADIATION PROTECTION GUIDELINES FOR SPACE MISSIONS
R. J. M. Fry (Oak Ridge National Lab., Tenn.) and D. S. Nachtwey 1986 17 p Presented at the Hanford Life Sciences Symposium on Radiation Protection: A Look to the Future, Celebrating Four Decades of Research at Hanford, Richland, Wash., 21 Oct. 1986 (Contract DE-AC05-84OR-21400)
(NASA-TM-89278; NAS 1.15:89278; DE87-002815; CONF-861044-5) Avail: NTIS HC A02/MF A01 CSCL 06R

NASA's current radiation protection guidelines date from 1970, when the career limit was set at 400 rem. Today, using the same approach, but with the current risk estimates, a considerably lower career limit would obtain. Also, there is considerably more information about the radiation environments to be experienced in different missions than previously. Since 1970 women have joined the ranks. For these and other reasons it was necessary to reexamine the radiation protection guidelines. This task was undertaken by the National Council on Radiation Protection and Measurements Scientific Committee 75 (NCRP SC 75). Below the magnetosphere the radiation environment varies with altitude and orbit inclination. In outer space missions galactic cosmic rays, with the small but important heavy ion component, determine the radiation environment. The new recommendations for career dose limits, based on lifetime excess risk of cancer mortality, take into account age at first exposure and sex. The career limits range from 100 rem (4.0Sv) for a 24 year old female to 400 rem for a 55 year old male compared to the previous single limit of 400 rem (4.0 Sv). The career limit for the lens of the eye was reduced from 600 to 400 rem (6.0 to 4.0 Sv.) DOE

N87-20731# Joint Publications Research Service, Arlington, Va.
USSR REPORT: SPACE BIOLOGY AND AEROSPACE MEDICINE, VOLUME 20, NO. 3, MAY - JUNE 1986
O. G. Gazenko, ed. 15 Aug. 1986 154 p Transl. into ENGLISH of Kosmicheskaya Biologiya i Aviakosmicheskaya Meditsina (Moscow, USSR), v. 20, no. 3, May Jun. 1986 96 p
(JPRS-USB-86-005) Avail: NTIS HC A08/MF A01

USSR Report: Space Biology and Aerospace Medicine, vol. 20, No. 3, May to June 1986 contains articles on the following: the 25th Anniversary of Soviet Manned Spaceflight; flight safety; space motion sickness; spacecrew work capacity; spacecrew blood lipids; vestibular stability; respiration restraints; effects of long term spaceflight; effect of hypoxia on DNA synthesis; electrodermal conductivity; human brain bioelectricity; and spatial orientation. For individual titles, see N87-20732 through N87-20746.

N87-20732# Joint Publications Research Service, Arlington, Va.
SPACE BIOLOGY AND MEDICINE ON THE TWENTY-FIFTH ANNIVERSARY OF THE FIRST SPACEFLIGHT OF YURIY ALEKSEYEVICH GAGARIN
O. G. Gazenko, N. N. Gurovskiy, and A. A. Gyurdzhian *In its* USSR Report: Space Biology and Aerospace Medicine, Vol. 20, No. 3, May - Jun. 1986 (JPRS-USB-86-005) 15 Aug. 1986 p 1-11 Transl. into ENGLISH from Kosmicheskaya Biologiya i Aviakosmicheskaya Meditsina (Moscow, USSR), v. 20, no. 3, May Jun. 1986 p 4-12 (For primary document see N87-20731 13-52)
Avail: NTIS HC A08/MF A01

Soviet Space exploration has come a long way in the quarter century that has elapsed after the historical day of the flight of Yu. A. Gagarin on 12 April 1961. The first flight, which lasted only 108 min, was to determine human capacities under conditions prevailing in space. As of 1 January 1986, Soviet cosmonauts had made 109 manned flights involving 60 people. Some of the participants had been in space 2 to 3 and even 5 times (V. A. Dzhanibekov). The Salyut orbital stations became a permanent space research laboratory. The crew consisting of L. D. Kizim, V. A. Solovyev and O. Yu. Atkov worked in space for 237 days. V. A. Dzhanibekov and V. P. Savinykh were able to find and dock with the inactive Salyut-7 station in space, repair it and completely restore its work capacity. In the 25 years that have passed since the first flight, space science has become a solid part of life, an inseparable element of the scientific, economic and sociocultural life of mankind. The file of organizations that are planning spaceflights is full of applications for investigations in the interests of the most diverse scientific disciplines and the national economy. Author

N87-20733# Joint Publications Research Service, Arlington, Va.
STAGES OF DEVELOPMENT OF THE PROBLEM OF FLIGHT SAFETY IN AVIATION MEDICINE
V. A. Ponomarenko *In its* USSR Report: Space Biology and Aerospace Medicine, Vol. 20, No. 3, May - Jun. 1986 (JPRS-USB-86-005) 15 Aug. 1986 p 12-20 Transl. into ENGLISH from Kosmicheskaya Biologiya i Aviakosmicheskaya Meditsina (Moscow, USSR), v. 20, no. 3, May Jun. 1986 p 12-19 (For primary document see N87-20731 13-52)
Avail: NTIS HC A08/MF A01

Aviation medicine is a direct participant in technological progress in aviation. The high level of development of aviation equipment at the present stage would be inconceivable without adequate solution of problems of its control by man. In past years, aviation medicine was enriched with new theoretical conceptions and vast practical experience in the area of assuring flight safety. New growth points emerged, both in aviation medicine proper and at its boundaries with allied disciplines in engineering psychology and ergonomics. Organization of protection of man on the basis of providing an optimum environment was recognized as the key direction of scientific research at the first stage of development of aviation medicine, since in essence it determined the assurance of human vital functions and work capacity. Practical implementation of the basic ideas of protection of an individual connected into a technological system was based not only on advances in applied physiology, but new investigative methods that permitted gaining deeper understanding of the biological bases of adaptation to a unique environment and disclosure of mechanisms and patterns that control processes of interaction between the environment and man. Author

N87-20734# Joint Publications Research Service, Arlington, Va.
INTERLABYRINTHINE ASYMMETRY, VESTIBULAR DYSFUNCTION AND SPACE MOTION SICKNESS
G. I. Gorgiladze, G. I. Samarin, and I. I. Bryanov *In its* USSR Report: Space Biology and Aerospace Medicine, Vol. 20, No. 3, May - Jun. 1986 (JPRS-USB-86-005) 15 Aug. 1986 p 21-38 Transl. into ENGLISH from Kosmicheskaya Biologiya i Aviakosmicheskaya Meditsina (Moscow, USSR), v. 20, no. 3, May Jun. 1986 p 19-31 (For primary document see N87-20731 13-52)
Avail: NTIS HC A08/MF A01

Data suggest that a disorder in the labyrinthine paired function can be regarded as the factor responsible for the initiation and development of space motion sickness. This concept is based on

the assumption that in the norm the vestibular function is to a certain extent asymmetric which is made up for by a compensatory center in the central nervous system. Exposure to an unusual space environment leads to a disorder of this compensation and development of a new vestibular asymmetry. This exposure involves: elimination of the difference in the weight of otolith membranes, disorder of the canal-otolith interaction, asymmetric blood-CSF changes, distinct interhemispheric asymmetry, and general stress. Vestibular asymmetry developing in the weightless state may become sufficient for the generalization of afferent impulsation to normal stimuli and development of a strong reaction. Adaptation to weightlessness occurs due to rearrangements of the compensatory center responsible for lower vestibular asymmetry. The compensatory mechanisms evolved in weightlessness continue to function during a certain time interval after recovery. They facilitate a re-initiation of vestibular asymmetry and motion sickness that is mainly provoked by head movements, as in the weightless state. Author

N87-20735# Joint Publications Research Service, Arlington, Va.
EVALUATION OF PHYSICAL WORK CAPACITY OF COSMONAUTS ABOARD SALYUT-6 STATION
V. A. Tishler, A. V. Yeremin, V. I. Stepantsov, and I. I. Funtova *In its* USSR Report: Space Biology and Aerospace Medicine, Vol. 20, No. 3, May - Jun. 1986 (JPRS-USB-86-005) 15 Aug. 1986 p 39-45 Transl. into ENGLISH from Kosmicheskaya Biologiya i Aviakosmicheskaya Meditsina (Moscow, USSR), v. 20, no. 3, May Jun. 1986 p 31-35 (For primary document see N87-20731 13-52)
Avail: NTIS HC A08/MF A01

Electrocardiograms of Salyut-6 prime crewmembers recorded during their exercises on a bicycle ergometer and treadmill are presented. ECG were recorded by a portable tape recorder Cardiocassette and transmitted to the Earth via the radiocommunication channel. This procedure helped to better understand cardiovascular adaptation to different workloads, including submaximal, as well as reserve abilities of the body at various flight stages. This can be used advantageously to correct and control the training process as well as to predict the cardiovascular status at the final flight stage. Author

N87-20736# Joint Publications Research Service, Arlington, Va.
OPERATOR WORK CAPACITY IN TRACKING SYSTEM WHEN SUBMITTED TO ANTIORTHOSTATIC HYPOKINESIA c54
L. S. Khachaturyants and A. K. Yepishkin *In its* USSR Report: Space Biology and Aerospace Medicine, Vol. 20, No. 3, May - Jun. 1986 (JPRS-USB-86-005) 15 Aug. 1986 p 46-51 Transl. into ENGLISH from Kosmicheskaya Biologiya i Aviakosmicheskaya Meditsina (Moscow, USSR), v. 20, no. 3, May Jun. 1986 p 36-39 (For primary document see N87-20731 13-52)
Avail: NTIS HC A08/MF A01

It is shown that the work capacity of head-down tilted operators performing sensorimotor pursuit depends on the health of their central nervous system (CNS). The operators who react to the exposure showing moderate predominance of excitation processes display the best work capacity. Author

N87-20737# Joint Publications Research Service, Arlington, Va.
BLOOD LIPIDS AND INCIDENCE OF LIPEMIA IN FLIGHT PERSONNEL
S. A. Bugrov, R. K. Kiselev, R. V. Beleda, V. I. Plakhatnyuk, N. N. Artamonov, A. P. Ivanchikov, and V. A. Tsyganok *In its* USSR Report: Space Biology and Aerospace Medicine, Vol. 20, No. 3, May - Jun. 1986 (JPRS-USB-86-005) 15 Aug. 1986 p 52-57 Transl. into ENGLISH from Kosmicheskaya Biologiya i Aviakosmicheskaya Meditsina (Moscow, USSR), v. 20, no. 3, May Jun. 1986 p 39-43 (For primary document see N87-20731 13-52)
Avail: NTIS HC A08/MF A01

The content of cholesterol and triglycerides was measured in healthy pilots. Over 1500 subjects were examined and age-related norms of the parameter were established. They were compared with published data. Physiological variations of cholesterol and triglycerides were related to age, height and body weight. The authors developed a method for diagnosing hyperlipidemia based on the agreement or disagreement between experimentally measured and theoretically calculated values. The authors maintain that hyperlipidemia can be diagnosed if the difference between the real and expected values is over 10%. The authors calculated the incidence of hyperlipidemia in all subjects examined (over 2100) and found that it was high: even in pilots of the age group 20 to 29 years hyperlipidemia occurred in 30% of the subjects. Author

N87-20738# Joint Publications Research Service, Arlington, Va.
LINK BETWEEN ASYMMETRY OF OPTOKINETIC NYSTAGMUS, OPTOVESTIBULAR AND VESTIBULOVEGETATIVE STABILITY
V. K. Grigorova *In its* USSR Report: Space Biology and Aerospace Medicine, Vol. 20, No. 3, May - Jun. 1986 (JPRS-USB-86-005) 15 Aug. 1986 p 58-61 Transl. into ENGLISH from Kosmicheskaya Biologiya i Aviakosmicheskaya Meditsina (Moscow, USSR), v. 20, no. 3, May Jun. 1986 p 43-45 (For primary document see N87-20731 13-52)
Avail: NTIS HC A08/MF A01

Comparative quantitative analysis of physiological asymmetry of the optokinetic nystagmus produced predominantly by central optokinetic stimulation (field of vision = 30 deg) or peripheral stimulation (field of vision = 110 deg) reveals an objective correlation between the asymmetry coefficient of the central optokinetic nystagmus with respect to the angular velocity of its slow phase and susceptibility to motion sickness caused by Coriolis and pseudo-Coriolis acceleration, the nystagmus velocity being up to 4 deg/sec. Author

N87-20739# Joint Publications Research Service, Arlington, Va.
PHYSIOLOGICAL MECHANISMS LIMITING EXTERNAL RESISTANCE TO RESPIRATION
M. A. Tikhonov and N. M. Asyamolova *In its* USSR Report: Space Biology and Aerospace Medicine, Vol. 20, No. 3, May - Jun. 1986 (JPRS-USB-86-005) 15 Aug. 1986 p 62-68 Transl. into ENGLISH from Kosmicheskaya Biologiya i Aviakosmicheskaya Meditsina (Moscow, USSR), v. 20, no. 3, May Jun. 1986 p 45-50 (For primary document see N87-20731 13-52)
Avail: NTIS HC A08/MF A01

A study was performed on 8 healthy male subjects to investigate the effect of nonelastic resistance 6-40 GPa (the air flow velocity being 90 1/min) on the duration of proprioceptive reflexes of respiratory muscles, volume and velocity parameters of forced exhalation. Resistance of 15 and 25 GPa combined with a workload of 100 to 150 W increased the duration of proprioceptive reflexes from 0.18 + or - 0.015 to 0.29 + or - 0.012 sec and to 0.38 + or - 0.06 sec, respectively, which indicates fatigue of respiratory muscles. Resistance of 25 GPa reduced significantly (by 55%) the maximum volume velocity of forced exhalation and increased its duration by 31%, the exhalation volume decreasing insignificantly (by 6%). The major factor limiting man's tolerance to external respiration resistance is functional deficiency of proprioceptive regulation of respiration and strength and velocity of respiratory muscles. Author

N87-20740# Joint Publications Research Service, Arlington, Va.
EFFECT OF HEMADSORPTION ON RHEOLOGICAL PARAMETERS OF BLOOD DURING SEVEN-DAY ANTIORTHOSTATIC HYPOKINESIA AND IN VITRO STUDIES
I. B. Goncharov, A. P. Ivanov, A. F. Davydkin, and Zh. M. Kudryashova *In its* USSR Report: Space Biology and Aerospace Medicine, Vol. 20, No. 3, May - Jun. 1986 (JPRS-USB-86-005) 15 Aug. 1986 p 69-74 Transl. into ENGLISH from Kosmicheskaya Biologiya i Aviakosmicheskaya Meditsina (Moscow, USSR), v. 20, May - Jun. 1986 p 50-53 (For primary document see N87-20731 13-52)
Avail: NTIS HC A08/MF A01

The effect of hemosorption of blood rheology was examined in 9 healthy men exposed to head-down tilt (-8 deg). Venous-venous hemosorption was performed on tilt day 7 using activated charcoal SKN-2M. It was found that by tilt day 7 rheological parameters increased significantly and returned to the norm after 2-hour hemoperfusion through activated charcoal. This shows

that hemosorption produces a beneficial effect on blood rheology and microcirculation which is indicated by a direct examination of eye microvessels. Experimental in vitro studies using oxygenated and nonoxygenated donor's blood demonstrated that hemosorption combined with blood oxygenation can noticeably increase the effectiveness of perfusion on the whole. Author

N87-20741# Joint Publications Research Service, Arlington, Va.
EFFECT OF LONG-TERM SPACEFLIGHT ON RAT BRAIN POLYAMINE CONTENT c51
R. A. Tigranyan and V. Yu. Kovalev *In its* USSR Report: Space Biology and Aerospace Medicine, Vol. 20, No. 3, May - Jun. 1986 (JPRS-USB-86-005) 15 Aug. 1986 p 74-79 Transl. into ENGLISH from Kosmicheskaya Biologiya i Aviakosmicheskaya Meditsina (Moscow, USSR), v. 20, no. 3, May Jun. 1986 p 53-57 (For primary document see N87-20731 13-52)
Avail: NTIS HC A08/MF A01

The concentration of polyamines, i.e., putrescine, spermidine and spermine, was measured in different brain compartments of rats flown for 18.5 days on Cosmos-1129. Exposure to space flight led to changes in the polyamine content that were the most distinct in medulla oblongata. It is suggested that the changes develop as a result of a chronic stress associated with the effects of weightlessness. Author

N87-20742# Joint Publications Research Service, Arlington, Va.
EFFECT OF HYPOXIA ON DNA SYNTHESIS AND COLLAGENT CONTENT OF REGENERATING SKIN
G. V. Khomullo, V. I. Lotova, A. N. Chernyayev, and I. N. Vinogradov *In its* USSR Report: Space Biology and Aerospace Medicine, Vol. 20, No. 3, May - Jun. 1986 (JPRS-USB-86-005) 15 Aug. 1986 p 80-85 Transl. into ENGLISH from Kosmicheskaya Biologiya i Aviakosmicheskaya Meditsina (Moscow, USSR), v. 20, no. 3, May Jun. 1986 p 57-61 (For primary document see N87-20731 13-52)
Avail: NTIS HC A08/MF A01

During chronic hypoxia DNA synthesis in various areas of the regenerating skin decreased. Inhibition of epithelial and connective-tissue elements was accompanied by suppression of collagenogenesis, which finally led to longer-term wound healing. Author

N87-20743# Joint Publications Research Service, Arlington, Va.
ELECTRODERMAL CONDUCTIVITY IN MAN AND MONKEYS
A. T. Neborskiy and G. S. Belkaniya *In its* USSR Report: Space Biology and Aerospace Medicine, Vol. 20, No. 3, May - Jun. 1986 (JPRS-USB-86-005) 15 Aug. 1986 p 86-95 Transl. into ENGLISH from Kosmicheskaya Biologiya i Aviakosmicheskaya Meditsina (Moscow, USSR), v. 20, no. 3, May Jun. 1986 p 61-68 (For primary document see N87-20731 13-52)
Avail: NTIS HC A08/MF A01

The topographic and functional correlation of acupuncture skin zones on the limbs of humans (99 healthy subjects) and monkeys (64 adult hamadryas baboons and rhesus monkeys) was compared by measuring the electric conductivity of the skin (ECS). The profile of the ECS was found to be an informative and sensitive integrated indicator of the functional state of the body and of the autonomic nervous system. The ECS showed seasonal variations and relief differences with respect to the two phases of the menstrual cycle in women. It also displayed distinct differences between men and women as well as species differences between men, hamadryas baboons and rhesus monkeys. The high differential informativeness of the ECS is indicated by the functional differences of the primate body under various constraint conditions. The anatomical and topographic correlation of acupuncture skin zones and similarity of ECS characteristics in man and monkeys suggest that the formation of functional characteristics of the ECS in various types of primates has a common philogenetic basis. It is concluded that monkeys can be used as an adequate experimental model for further evaluation of the ECS as a method to measure and diagnose functional and pathological changes in the body. Author

N87-20744# Joint Publications Research Service, Arlington, Va.
INTERPRETATION OF RIGHT HEART KINETOCARDIOGRAM
V. A. Degtyarev, A. Ya. Kormer, V. A. Rogov, V. Ye. Tolpekin, L. P. Tsyganov, V. N. Ragozin, Ye. Yu. Shcherbakov, and Z. A. Kirillova *In its* USSR Report: Space Biology and Aerospace Medicine, Vol. 20, No. 3, May - Jun. 1986 (JPRS-USB-86-005) 15 Aug. 1986 p 96-99 Transl. into ENGLISH from Kosmicheskaya Biologiya i Aviakosmicheskaya Meditsina (Moscow, USSR), v. 20, no. 3, May Jun. 1986 p 69-71 (For primary document see N87-20731 13-52)
Avail: NTIS HC A08/MF A01

On the basis of ultrasonic Doppler valvulocardiography of 20 healthy men and catheterization of the right heart of 15 patients with acute large-focal myocardial infarction, the development of elements of the right kinetocardiograms (KCG sub r) is explored. Comparison of kinetocardiograms of the right heart with ultrasonic and catheterization data has demonstrated that KCG sub r can be used to examine right heart contractions of cosmonauts and pilots in flight and on the ground as well as of patients to diagnose pathologies of the right compartments of the heart. Author

N87-20745# Joint Publications Research Service, Arlington, Va.
DYNAMICS OF BIOELECTRIC ACTIVITY OF HUMAN BRAIN IN A CONTINUOUS WAKING STATE
V. P. Tychina and A. P. Nechayev *In its* USSR Report: Space Biology and Aerospace Medicine, Vol. 20, No. 3, May - Jun. 1986 (JPRS-USB-86-005) 15 Aug. 1986 p 135-140 Transl. into ENGLISH from Kosmicheskaya Biologiya i Aviakosmicheskaya Meditsina (Moscow, USSR), vol. 20, no. 3, May Jun. 1986 p 88-91 (For primary document see N87-20731 13-52)
Avail: NTIS HC A08/MF A01

Electroencephalographic parameters can be used to detect early signs of fatigue, which is of practical importance. Experiments were carried out on three healthy men to identify a limited number of symptoms allowing a rapid evaluation of operator's work capacity. The subjects were kept in long-term isolation. The study revealed general trends and individual variations in brain bioelectrical activities that reflected their performance during continuous work with natural sleep deprivation for three days. Author

N87-20746# Joint Publications Research Service, Arlington, Va.
NEW BOOK DEALS WITH SPATIAL ORIENTATION
A. A. Gyurdzhian and Yu. Yu. Shipkov *In its* USSR Report: Space Biology and Aerospace Medicine, Vol. 20, No. 3, May - Jun. 1986 (JPRS-USB-86-005) 15 Aug. 1986 p 141-144 Transl. into ENGLISH from Kosmicheskaya Biologiya i Aviakosmicheskaya Meditsina (Moscow, USSR), v. 20, no. 3, May Jun. 1986 p 91-93 (For primary document see N87-20731 13-52)
Avail: NTIS HC A08/MF A01

The collection is compiled on the basis of the proceedings of a conference on spatial orientation (SO) and space perception, which convened at the University of Minnesota on 14 to 16 July 1980. The book consists of the following 5 sections: (1) comparative physiological, comparative psychological and age-related aspects of SO; (2) SO in some groups of people (the mentally retarded and elderly); (3) ability to use maps and space perception mechanisms; (4) language and space perception; (5) space perception and processing of information about space. Author

53 BEHAVIORAL SCIENCES

Includes psychological factors; individual and group behavior; crew training and evaluation; and psychiatric research.

N87-20747*# National Aeronautics and Space Administration. Ames Research Center, Moffett Field, Calif.
HUMAN-DISPLAY INTERACTIONS: CONTEXT-SPECIFIC BIASES
Mary Kister Kaiser and Dennis R. Proffitt (Virginia Univ., Charlottesville.) Apr. 1987 25 p
(NASA-TM-89430; A-87118; NAS 1.15:89430) Avail: NTIS HC A02/MF A01 CSCL 05I

Recent developments in computer engineering have greatly

enhanced the capabilities of display technology. As displays are no longer limited to simple alphanumeric output, they can present a wide variety of graphic information, using either static or dynamic presentation modes. At the same time that interface designers exploit the increased capabilities of these displays, they must be aware of the inherent limitation of these displays. Generally, these limitations can be divided into those that reflect limitations of the medium (e.g., reducing three-dimensional representations onto a two-dimensional projection) and those reflecting the perceptual and conceptual biases of the operator. The advantages and limitations of static and dynamic graphic displays are considered. Rather than enter into the discussion of whether dynamic or static displays are superior, general advantages and limitations are explored which are contextually specific to each type of display.
Author

N87-20326*# Medical Univ. of South Carolina, Charleston. Dept. of Pharmacology.
TO CATCH A COMET 2: TECHNICAL UPDATE ON CAN-DO
Thomas J. OBrien *In* NASA. Goddard Space Flight Center The 1986 Get Away Special Experimenter's Symposium Feb. 1987 p 171-178 (For primary document see N87-20302 13-12)
Avail: NTIS HC A11/MF A01 CSCL 05I

N87-20327*# Medical Univ. of South Carolina, Charleston. Dept. of Pathology.
TO CATCH A CHILD'S IMAGINATION 2: EDUCATIONAL UPDATE ON CAN-DO
James H. Nicholson *In* NASA. Goddard Space Flight Center The 1986 Get Away Special Experimenter's Symposium Feb. 1987 p 179-186 (For primary document see N87-20302 13-12)
Avail: NTIS HC A11/MF A01 CSCL 05I

54 MAN/SYSTEM TECHNOLOGY AND LIFE SUPPORT

Includes human engineering; biotechnology; and space suits and protective clothing.

For related information see also *16 Space Transportation.*

N87-20748 Department of the Navy, Washington, D. C.
AUTOMATED ANTHROPOMETRIC DATA MEASUREMENT SYSTEM Patent
William F. Moroney, inventor (to Navy), James C. Bartholomew, inventor (to Navy), Clifford M. Cagle, inventor (to Navy), and Robert E. Hughes, inventor (to Navy) Issued 5 Aug. 1986 8 p Supersedes N86-33017, AD-D012299 (24 - 24, p 3777)
(AD-D012575; US-Patent-4,603,486; US-Patent-Appl-SN-788371; US-Patent-Class-33-512) Avail: US Patent and Trademark Office CSCL 06/14

An automated anthropometric data measurement system is described which includes a standing measuring assembly and a seated measuring assembly to determine pertinent anthropometric features of aviators being screened for assignment to particularly suitable aircraft. Both assemblies have a plurality of position sensors and measuring probes which are selectively placed by an operator upon the aviator, each measuring probe producing a digital data signal indicative of the particular feature measured when selective position sensors indicate body contact. The signals are then collected by a microcomputer which compares them to a predetermined population and outputs the compared data to magnetic storage media.
GRA

N87-20749# Oak Ridge National Lab., Tenn.
INTEGRATED DIGITAL CONTROL AND MAN-MACHINE INTERFACE FOR COMPLEX REMOTE HANDLING SYSTEMS
J. C. Rowe, R. F. Spille, and S. D. Zimmermann Dec. 1986 24 p Presented at the International Topical Meeting on Remote Systems and Robotics in Hostile Environments, Pasco, Wash., 29 Mar. 1987
(Contract DE-AC05-84OR-21400)
(DE87-003002; CONF-870301-7) Avail: NTIS HC A02/MF A01

The Advanced Integrated Maintenance System (AIMS) is part of a continuing effort within the Consolidated Fuel Reprocessing Program at Oak Ridge National Laboratory to develop and extend the capabilities of remote manipulation and maintenance technology. The AIMS is a totally integrated approach to remote handling in hazardous environments. State-of-the-art computer systems connected through a high-speed communication network provide a real-time distributed control system that supports the flexibility and expandability needed for large integrated maintenance applications. A Man-Machine Interface provides high-level human interaction through a powerful color graphics menu-controlled operator console. An auxiliary control system handles the real-time processing needs for a variety of support hardware. A pair of dedicated fiber-optic-linked master/slave computer system control the Advanced Servomanipulator master/slave arms using powerful distributed digital processing methods. The FORTH language was used as a real-time operating and development environment for the entire system, and all of these components are integrated into a control room concept that represents the latest advancements in the development of remote maintenance facilities for hazardous environments.
DOE

N87-20750# Oak Ridge National Lab., Tenn.
ADVANCED REMOTE HANDLING FOR FUTURE APPLICATIONS: THE ADVANCED INTEGRATED MAINTENANCE SYSTEM
J. N. Herndon, C. T. Kring, and J. C. Rowe 1986 26 p Presented at the International Topical Meeting on Remote Systems and Robotics in Hostile Environments, Pasco, Wash., 29 Mar. 1987
(Contract DE-AC05-84OR-21400)
(DE87-003004; CONF-870301-5) Avail: NTIS HC A03/MF A01

The Consolidated Fuel Reprocessing Program at Oak Ridge National Laboratory has been developing advanced techniques for remote maintenance of future US fuel reprocessing plants. The developed technology has a wide spectrum of application for other hazardous environments. These efforts are based on the application of teleoperated, force-reflecting servomanipulators for dexterous remote handling with television viewing for large-volume hazardous applications. These developments fully address the nonrepetitive nature of remote maintenance in the unstructured environments encountered in fuel reprocessing. This paper covers the primary emphasis in the present program; the design, fabrication, installation, and operation of a prototype remote handling system for reprocessing applications, the Advanced Integrated Maintenance System.
DOE

N87-20751# Joint Publications Research Service, Arlington, Va.
USSR REPORT: LIFE SCIENCES. BIOMEDICAL AND BEHAVIORAL SCIENCES
10 Feb. 1987 86 p Transl. into ENGLISH from various Russian articles
(JPRS-UBB-87-003) Avail: NTIS HC A05/MF A01

Topics addressed include: agrotechnology; biochemistry; radiation biology; psychology; public health; physiology; pharmacology and toxicology; microbiology; medicine; laser bioeffects; immunology; genetics; epidemiology; and environments. For individual titles, see N87-20752 through N87-20752.

N87-20752# Joint Publications Research Service, Arlington, Va.
INVESTIGATION OF MICROSTRUCTURE OF ARBITRARY MOTIONS OF OPERATOR
G. G. Tsulaya, M. V. Khvingiya, I. F. Chekirda, and V. V. Danilovtsev *In its* USSR Report: Life Sciences. Biomedical and Behavioral Sciences (JPRS-UBB-87-003) 10 Feb. 1987 p 16-19 Transl. into ENGLISH from Soobshcheniya Akademii Nauk Gruzinskoy SSR (Tbilisi, USSR), v. 121, no. 2, Feb. 1986 p 369-372 (For primary document see N87-20751 13-54)
Avail: NTIS HC A05/MF A01

Under normal conditions, alternating micromotor processes are inherent to the human body in any physiological and functional state. These processes are mainly connected with changes in the joint angle (physiological tremor). The purpose of the present

research is to study the spectral composition of a tremor and the microstructure of random motions connected with the control tasks of an operator. Operator activity tasks involved the execution of multidimensional tracking of a dynamic object with different dynamic characteristics. It was shown that the activity of an operator executing a control process is accompanied by tremors and microoscillations during any conscious movement. The tremors correspond to a fixed position or a shift of the control stick. In addition, these oscillations embrace a wide frequency spectrum with a changing frequency and amplitude of the harmonics. There is every basis to propose that the oscillations depend on the physiological and psychological states of the operator. B.G.

N87-20736# Joint Publications Research Service, Arlington, Va.
OPERATOR WORK CAPACITY IN TRACKING SYSTEM WHEN SUBMITTED TO ANTIORTHOSTATIC HYPOKINESIA
L. S. Khachaturyants and A. K. Yepishkin *In its* USSR Report: Space Biology and Aerospace Medicine, Vol. 20, No. 3, May - Jun. 1986 (JPRS-USB-86-005) 15 Aug. 1986 p 46-51 Transl. into ENGLISH from Kosmicheskaya Biologiya i Aviakosmicheskaya Meditsina (Moscow, USSR), v. 20, no. 3, May Jun. 1986 p 36-39 (For primary document see N87-20731 13-52)
Avail: NTIS HC A08/MF A01

55 SPACE BIOLOGY

Includes exobiology; planetary biology; and extraterrestrial life.

No abstracts in this category.

59 MATHEMATICAL AND COMPUTER SCIENCES (GENERAL)

N87-20753*# Norfolk State Coll., Va. Research Foundation.
MACSYMA USAGE AT LANGLEY, REVISION 1
Sandra Jean DeLoatch Jan. 1987 61 p
(Contract NAS1-16921)
(NASA-CR-172518; NAS 1.26:172518) Avail: NTIS HC A04/MF A01 CSCL 12A

MACSYMA, a large and versatile symbolic manipulation system, is discussed in relation to its access and use at NASA, Langley Research Center. The report provides introductory information for new users, descriptions of the available resources for new and experienced users, and illustrations of selected features of the MACSYMA computing environment. Author

N87-20754*# National Aeronautics and Space Administration. Langley Research Center, Hampton, Va.
CUMULATIVE REPORTS AND PUBLICATIONS THROUGH DECEMBER 31, 1986 Final Report
Feb. 1987 53 p
(Contracts NAS1-18107; NAS1-17070; NAS1-17130; NAS1-15810; NAS1-16394; NAS1-14101; NAS1-14472)
(NASA-CR-178257; NAS 1.26:178257) Avail: NTIS HC A04/MF A01 CSCL 12A

This document contains a complete list of ICASE Reports. Since ICASE Reports are intended to be preprints of articles that will appear in journals or conference proceedings, the published reference is included when it is available. Author

N87-20755*# National Aeronautics and Space Administration. Langley Research Center, Hampton, Va.
A COMPUTER SIMULATOR FOR DEVELOPMENT OF ENGINEERING SYSTEM DESIGN METHODOLOGIES
S. L. Padula and J. Sobieszczanski-Sobieski Feb. 1987 18 p
(NASA-TM-89109; NAS 1.15:89109) Avail: NTIS HC A02/MF A01 CSCL 12A

A computer program designed to simulate and improve engineering system design methodology is described. The simulator mimics the qualitative behavior and data couplings occurring among the subsystems of a complex engineering system. It eliminates the engineering analyses in the subsystems by replacing them with judiciously chosen analytical functions. With the cost of analysis eliminated, the simulator is used for experimentation with a large variety of candidate algorithms for multilevel design optimization to choose the best ones for the actual application. Thus, the simulator serves as a development tool for multilevel design optimization strategy. The simulator concept, implementation, and status are described and illustrated with examples. Author

N87-20756*# National Aeronautics and Space Administration. Langley Research Center, Hampton, Va.
AN ASYMPTOTIC ANALYSIS OF SUPERSONIC REACTING MIXING LAYERS
T. L. Jackson (Old Dominion Univ., Norfolk, Va.) and M. Y. Hussaini Mar. 1987 17 p
(Contract NAS1-18107)
(NASA-CR-178266; ICASE-87-17; NAS 1.26:178266) Avail: NTIS HC A02/MF A01 CSCL 12A

The purpose of this paper is to present an asymptotic analysis of the laminar mixing of the simultaneous chemical reaction between parallel supersonic streams of two reacting species. The study is based on a one-step irreversible Arrhenius reaction and on large activation energy asymptotics. Essentially it extends the work of Linan and Crespo to include the effect of free shear and Mach number on the ignition regime, the deflagration regime and the diffusion flame regime. It is found that the effective parameter is the product of the characteristic Mach number and a shear parameter. Author

60 COMPUTER OPERATIONS AND HARDWARE

Includes hardware for computer graphics, firmware, and data processing.

For components see *33 Electronics and Electrical Engineering.*

N87-20757# Florida Univ., Gainesville. Database Systems Research and Development Center.
A DYNAMIC MULTICOMPUTER SYSTEM FOR MANAGING SCIENTIFIC AND ENGINEERING DATABASES Final Technical Report, 1 Aug. 1984 - 31 Jul. 1986
S. Y. W. Su Sep. 1986 19 p
(Contract DE-FG05-84ER-13285)
(DE87-002497; DOE/ER-13285/T1) Avail: NTIS HC A02/MF A01

Research and accomplishments are summarized in the following four areas: (1.1) Architectural Design of a Dyamically Partitionable Multicomputer System with Switchable Main Memory Modules (SM3); (1.2) Performance Analysis of SM3; (1.3) Simulation of Operations in SM3; and (1.4) Parallel Algorithms for Matrix Computations Using SM3. The architecture of SM3 is based on three key concepts, viz., switchable memory, partitionable common bus, and global control lines. DOE

N87-20758# Office National d'Etudes et de Recherches Aerospatiales, Paris (France).
[ACTIVITIES REPORT IN COMPUTER SCIENCE] Annual Report, 1985
Oct. 1986 12 p
(ETN-87-99377) Avail: NTIS HC A02/MF A01

The Aeronautique computer network; extension of the scientific computation systems; parallelizing computation of the unsteady

flow of a real fluid around an airfoil; and solving Poisson's equation in 3D on the parallel computation system are described. ESA

N87-20321*# Purdue Univ., West Lafayette, Ind. School of Electrical Engineering.
MULTIPURPOSE MICROCONTROLLER DESIGN FOR PUGAS 2
David M. Weber and Todd W. Deckard *In* NASA. Goddard Space Flight Center The 1986 Get Away Special Experimenter's Symposium Feb. 1987 p 135-140 (For primary document see N87-20302 13-12)
Avail: NTIS HC A11/MF A01 CSCL 09B

61 COMPUTER PROGRAMMING AND SOFTWARE

Includes computer programs, routines, algorithms, and specific applications, e.g., CAD/CAM.

N87-20759# Selenia Industrie Elettroniche Associate S.p.A., Pomezia (Italy). Education and Training Dept.
RIVISTA TECNICA SELENIA, VOLUME 10, NUMBER 1
Adriana Marzi, ed. 1986 52 p Original contains color illustrations
(ETN-87-99091) Avail: NTIS HC A04/MF A01

Expert systems for diagnostic purposes applied to radar; avionic and defense systems logistic support standardization and cost effectiveness; an application of Rayleigh's method to the fast calculation of the first vibration frequency of a missile cell; and automatic graphics applied to antenna computer aided design are discussed. For individual titles, see N87-20760 through N87-20763.

N87-20760# Selenia Industrie Elettroniche Associate S.p.A., Pomezia (Italy). Radar Div.
EXPERT SYSTEMS FOR DIAGNOSTIC PURPOSES, PROSPECTED APPLICATIONS TO THE RADAR FIELD c32
Riccardo Filippi *In its* Rivista Tecnica Selenia, Volume 10, Number 1 1986 p 1-10 (For primary document see N87-20759 13-61)
Avail: NTIS HC A04/MF A01

Expert systems applied to fault diagnosis, particularly electrical circuit troubleshooting, are introduced. Diagnostic systems consisting of sequences of rules of the symptom-disease type (rule based system) and systems based upon a physical and functional description of the unit subjected to fault diagnosis are treated. Application of such systems to radar equipment troubleshooting, in particular to the transmitter, is discussed. ESA

N87-20761# Selenia Industrie Elettroniche Associate S.p.A., Pomezia (Italy). Engineering.Support Dept.
ON MODERN AVIONIC AND DEFENSE SYSTEMS LOGISTIC SUPPORT STANDARDIZATION AND COST EFFECTIVENESS c06
Vincenzo Buontempo *In its* Rivista Tecnica Selenia, Volume 10, Number 1 1986 p 11-24 Original contains color illustrations (For primary document see N87-20759 13-61)
Avail: NTIS HC A04/MF A01

Hardware and software standardization available on avionic systems; and the effectiveness of a maintenance philosophy and concepts (elimination of the second maintenance level) are discussed. The results can be extended to naval and ground defense systems. ESA

N87-20762# Selenia Industrie Elettroniche Associate S.p.A., Pomezia (Italy). Defense Systems Div.
AN APPLICATION OF RAYLEIGH'S METHOD TO THE FAST CALCULATION OF THE FIRST VIBRATION FREQUENCY OF A MISSILE LAUNCHER CELL c39
Gian Fabrizio Venarucci and Armando Peruzzi *In its* Rivista Tecnica Selenia, Volume 10, Number 1 1986 p 25-31 (For primary document see N87-20759 13-61)
Avail: NTIS HC A04/MF A01

The first natural vibration frequency of a missile cell is calculated using an energy method. ESA

N87-20763# Selenia Industrie Elettroniche Associate S.p.A., Pomezia (Italy). Antennas Lab.
AUTOMATIC GRAPHICS APPLIED TO ANTENNA COMPUTER AIDED DESIGN
Massimo Biagi and Paolo deVincenti *In its* Rivista Tecnica Selenia, Volume 10, Number 1 1986 p 32-49 (For primary document see N87-20759 13-61)
Avail: NTIS HC A04/MF A01

Antenna design programs in FORTRAN 4 which utilize the Tektronix Plot 10 system graphic routine are shown. The programs are available on Univac 1100/80 computer. ESA

N87-20764*# National Aeronautics and Space Administration. Langley Research Center, Hampton, Va.
A SYSTEM FOR ROUTING ARBITRARY DIRECTED GRAPHS ON SIMD ARCHITECTURES
Sherryl Tomboulian Mar. 1987 25 p
(Contract NAS1-18107)
(NASA-CR-178265; ICASE-87-14; NAS 1.26:178265) Avail: NTIS HC A02/MF A01 CSCL 09B

There are many problems which can be described in terms of directed graphs that contain a large number of vertices where simple computations occur using data from connecting vertices. A method is given for parallelizing such problems on an SIMD machine model that is bit-serial and uses only nearest neighbor connections for communication. Each vertex of the graph will be assigned to a processor in the machine. Algorithms are given that will be used to implement movement of data along the arcs of the graph. This architecture and algorithms define a system that is relatively simple to build and can do graph processing. All arcs can be transversed in parallel in time O(T), where T is empirically proportional to the diameter of the interconnection network times the average degree of the graph. Modifying or adding a new arc takes the same time as parallel traversal. Author

N87-20765*# National Aeronautics and Space Administration. Langley Research Center, Hampton, Va.
THE FAULT-TREE COMPILER
Anna L. Martensen (PRC Kentron, Inc., Hampton, Va.) and Ricky W. Butler Jan. 1987 40 p
(NASA-TM-89098; NAS 1.15:89098) Avail: NTIS HC A03/MF A01 CSCL 09B

The Fault Tree Compiler Program is a new reliability tool used to predict the top event probability for a fault tree. Five different gate types are allowed in the fault tree: AND, OR, EXCLUSIVE OR, INVERT, and M OF N gates. The high level input language is easy to understand and use when describing the system tree. In addition, the use of the hierarchical fault tree capability can simplify the tree description and decrease program execution time. The current solution technique provides an answer precise (within the limits of double precision floating point arithmetic) to the five digits in the answer. The user may vary one failure rate or failure probability over a range of values and plot the results for sensitivity analyses. The solution technique is implemented in FORTRAN; the remaining program code is implemented in Pascal. The program is written to run on a Digital Corporation VAX with the VMS operation system. Author

N87-20766*# National Aeronautics and Space Administration. Lewis Research Center, Cleveland, Ohio.
TIME-PARTITIONING SIMULATION MODELS FOR CALCULATION ON PARALLEL COMPUTERS
Edward J. Milner, Richard A. Blech, and Rodrick V. Chima 1987 15 p Proposed for presentation at the 1987 Summer Computer Simulation Conference, Montreal, Quebec, 27-30 Jul. 1987; sponsored by the Society for Computer Simulation
(NASA-TM-89850; E-3517; NAS 1.15:89850) Avail: NTIS HC A02/MF A01 CSCL 09B

A technique allowing time-staggered solution of partial differential equations is presented in this report. Using this technique,

called time-partitioning, simulation execution speedup is proportional to the number of processors used because all processors operate simultaneously, with each updating of the solution grid at a different time point. The technique is limited by neither the number of processors available nor by the dimension of the solution grid. Time-partitioning was used to obtain the flow pattern through a cascade of airfoils, modeled by the Euler partial differential equations. An execution speedup factor of 1.77 was achieved using a two processor Cray X-MP/24 computer. Author

N87-20200# National Aerospace Lab., Amsterdam (Netherlands).
FLEXIBLE GRID GENERATION FOR COMPLEX GEOMETRIES IN TWO SPACE DIMENSIONS BASED ON VARIATIONAL PRINCIPLES
B. Oskam and G. H. Huizing *In* AGARD Applications of Computational Fluid Dynamics in Aeronautics Nov. 1986 14 p Sponsored by Netherlands Agency for Aerospace Programs (For primary document see N87-20199 13-02)
Avail: NTIS HC A19/MF A01

N87-20201# Aircraft Research Association Ltd., Bedford (England).
A DISCUSSION ON A MESH GENERATION TECHNIQUE APPLICABLE TO COMPLEX GEOMETRIES
N. P. Weatherill, J. A. Shaw, C. R. Forsey, and K. E. Rose *In* AGARD Applications of Computational Fluid Dynamics in Aeronautics Nov. 1986 12 p Sponsored by Ministry of Defence and British Aerospace (For primary document see N87-20199 13-02)
Avail: NTIS HC A19/MF A01

N87-20202# Dornier-Werke G.m.b.H., Friedrichshafen (West Germany). Theoretical Aerodynamic Group.
NUMERICAL GRID GENERATION AROUND COMPLETE AIRCRAFT CONFIGURATIONS
Willy Fritz *In* AGARD Applications of Computational Fluid Dynamics in Aeronautics Nov. 1986 8 p (For primary document see N87-20199 13-02)
Avail: NTIS HC A19/MF A01

N87-20203*# National Aeronautics and Space Administration. Ames Research Center, Moffett Field, Calif.
GEOMETRY DEFINITION AND GRID GENERATION FOR A COMPLETE FIGHTER AIRCRAFT
Thomas A. Edwards *In* AGARD Applications of Computational Fluid Dynamics in Aeronautics Nov. 1986 12 p Previously announced as N86-28050 (For primary document see N87-20199 13-02)
Avail: NTIS HC A19/MF A01 CSCL 09B

N87-20204# Royal Aircraft Establishment, Farnborough (England). Aerodynamics Dept.
AN ASSESSMENT OF THE USE OF LOW-ORDER PANEL METHODS FOR THE CALCULATION OF SUPERSONIC FLOWS
J. S. Smith and D. S. Woodward *In* AGARD Applications of Computational Fluid Dynamics in Aeronautics Nov. 1986 8 p (For primary document see N87-20199 13-02)
Avail: NTIS HC A19/MF A01

N87-20313*# Colorado Univ., Boulder. Getaway Special Project G-285.
SOPHISTICATED SOFTWARE SYSTEMS FOR SMALL SELF-CONTAINED SPACE SHUTTLE PAYLOAD G285
Robert Burkhardt *In* NASA. Goddard Space Flight Center The 1986 Get Away Special Experimenter's Symposium Feb. 1987 p 71-78 (For primary document see N87-20302 13-12)
Avail: NTIS HC A11/MF A01 CSCL 09B

62 COMPUTER SYSTEMS

Includes computer networks and special application computer systems.

N87-20767*# National Aeronautics and Space Administration. Lewis Research Center, Cleveland, Ohio.
THE HYPERCLUSTER: A PARALLEL PROCESSING TEST-BED ARCHITECTURE FOR COMPUTATIONAL MECHANICS APPLICATIONS
Richard A. Blech 1987 11 p Proposed for presentation at the Summer Computer Simulation Conference, Montreal, Canada, 27-30 Jul. 1987; sponsored by the Society for Computer Simulation
(NASA-TM-89823; E-3469; NAS 1.15:89823) Avail: NTIS HC A02/MF A01 CSCL 09B

The development of numerical methods and software tools for parallel processors can be aided through the use of a hardware test-bed. The test-bed architecture must be flexible enough to support investigations into architecture-algorithm interactions. One way to implement a test-bed is to use a commercial parallel processor. Unfortunately, most commercial parallel processors are fixed in their interconnection and/or processor architecture. In this paper, we describe a modified n cube architecture, called the hypercluster, which is a superset of many other processor and interconnection architectures. The hypercluster is intended to support research into parallel processing of computational fluid and structural mechanics problems which may require a number of different architectural configurations. An example of how a typical partial differential equation solution algorithm maps on to the hypercluster is given. Author

N87-20768*# National Aeronautics and Space Administration. Langley Research Center, Hampton, Va.
A LANCZOS EIGENVALUE METHOD ON A PARALLEL COMPUTER
Susan W. Bostic and Robert E. Fulton (Georgia Inst. of Tech., Atlanta.) Mar. 1987 20 p
(NASA-TM-89097; NAS 1.15:89097) Avail: NTIS HC A02/MF A01 CSCL 09B

Eigenvalue analyses of complex structures is a computationally intensive task which can benefit significantly from new and impending parallel computers. This study reports on a parallel computer implementation of the Lanczos method for free vibration analysis. The approach used here subdivides the major Lanczos calculation tasks into subtasks and introduces parallelism down to the subtask levels such as matrix decomposition and forward/backward substitution. The method was implemented on a commercial parallel computer and results were obtained for a long flexible space structure. While parallel computing efficiency for the Lanczos method was good for a moderate number of processors for the test problem, the greatest reduction in time was realized for the decomposition of the stiffness matrix, a calculation which took 70 percent of the time in the sequential program and which took 25 percent of the time on eight processors. For a sample calculation of the twenty lowest frequencies of a 486 degree of freedom problem, the total sequential computing time was reduced by almost a factor of ten using 16 processors. Author

N87-20769*# National Aeronautics and Space Administration. Langley Research Center, Hampton, Va.
PERFORMANCE STUDIES OF THE MULTIGRID ALGORITHMS IMPLEMENTED ON HYPERCUBE MULTIPROCESSOR SYSTEMS
Vijay K. Naik and Shlomo Taasan Jan. 1987 22 p
(Contract NAS1-18107)
(NASA-CR-178237; ICASE-87-5; NAS 1.26:178237) Avail: NTIS HC A02/MF A01 CSCL 09B

In this paper, we analyze and compare the performance on a hypercube multiprocessor of some of the major multigrid techniques used in practice. The model problem considered here is that of solving the 2-D incompressible Navier-Stokes equations representing the flow between two parallel plates. Results obtained by implementing the different multigrid schemes on an iPSC are presented. Effects on the overall performance of various parameters of the algorithms, of the partitioning strategies employed, and

of some of the characteristics of the underlying architecture are discussed. Author

N87-20770*# National Aeronautics and Space Administration. Langley Research Center, Hampton, Va.
A PRELIMINARY TRANSIENT-FAULT EXPERIMENT ON THE SIFT COMPUTER SYSTEM
Ricky W. Butler and Carl R. Elks (PRC Kentron, Inc., Hampton, Va.) Feb. 1987 43 p
(NASA-TM-89058; NAS 1.15:89058) Avail: NTIS HC A03/MF A01 CSCL 09B

This paper presents the results of a preliminary experiment to study the effectiveness of a fault-tolerant system's ability to handle transient faults. The primary goal of the experiment was to develop the techniques to measure the parameters needed for a reliability analysis of the SIFT computer system which includes th effects of transient faults. A key aspect of such an analysis is the determination of the effectiveness of the operating system's ability to discriminate between transient and permanent faults. A detailed description of the preliminary transient fault experiment along with the results from 297 transient fault injections are given. Although not enough data was obtained to draw statistically significant conclusions, the foundation has been laid for a large-scale transient fault experiment. Author

N87-20771# Washington State Univ., Pullman.
PARALLEL PROCESSING OF NETWORKS Final Technical Report
Narsingh Deo 15 Nov. 1986 8 p
(Contract DAAG29-82-K-0107)
(AD-A175641; ARO-18360.18-EL) Avail: NTIS HC A02/MF A01 CSCL 09/2

Recent advancements in hardware technology have made it attractive to use many processors in parallel that cooperate and coordinate their efforts to solve a problem much faster. Such parallel computers are currently being developed, designed and experimented with. A few, with limited parallelism, are available as commercial products, such as, Intel's iPSC, NCUBE, Sequent's Balance 8000 and 21000. It appears certain that computers are going to be in wide use in the 1990's. However, the art of designing parallel algorithms is far behind that of sequential algorithms. The goal of this project was to develop strategies for designing parallel algorithms and computer programs for a certain class of problems consisted of various graph problems that arise on large, sparse, real-life transportation and communication networks. The parallel computer deemed most suited for such problems is a multiple-instruction, multiple-data stream (MIMD) machine. GRA

N87-20772# Argonne National Lab., Ill. Computing Services.
GUIDE TO SHARING PERSONAL COMPUTER RESOURCES VIA LOCAL AREA NETWORKS, REVISED
L. Winkler Aug. 1986 70 p
(Contract W-31-109-eng-38)
(DE86-016088; ANL/TM-438-Rev) Avail: NTIS HC A04/MF A01

This Guide is for professional staff who commonly need computing tools on personal computers, minicomputers, mainframe computers, and supercomputers. It provides information and recommendations about personal computer local area networks in the context of the larger scheme of computing tools and services at the Laboratory. The material presented here is for the person considering installation of a personal computer local area network. Chapter 1 introduces the reader to the concept of personal computer local area networks and provides background material on networking. Chapter 2 summarizes Computing Services' evaluation of personal computer local area networking in general terms. Chapter 3 describes the technical and functional details of Computing Services' Personal Computer Local Area Network Evaluation and Demonstration Project. Chapters 4 and 5 are for individuals who are familiar with personal computing and who will be responsible for establishing a local area network. Chapter 4 covers technical issues relating to the prototype network installation in Building 221. Chapter 5 warns potential users what to expect when establishing a local area network. DOE

63 CYBERNETICS

Includes feedback and control theory, artificial intelligence, robotics and expert systems.

For related information see also *54 Man/System Technology and Life Support.*

N87-20773# Oak Ridge National Lab., Tenn.
A VIRTUAL-TIME OPERATING-SYSTEM SHELL FOR A HYPERCUBE IN ROBOTICS APPLICATIONS
J. R. Einstein, J. Barhen, and D. Jefferson 1986 8 p Presented at the SPIE's Cambridge Symposium on Optical and Optoelectronic Engineering: Advanced in Intelligent Robotics Systems, Cambridge, Mass., 26 Oct. 1986 Prepared in cooperation with California Univ., Los Angeles
(Contract DE-AC05-84OR-21400)
(DE87-004256; CONF-8610215-2) Avail: NTIS HC A02/MF A01

Hypercube multiprocessors possess many attributes advantageous for autonomous, intelligent robots which operate in time-critical fashion in hostile environments. However, their message-passing architecture presents certain difficulties in rapid changes of plans in response to unpredictable events in the environment. The status of a virtual-time operating-system shell, providing functions which facilitate such responses, is described. DOE

N87-20774# Oak Ridge National Lab., Tenn.
THE OAK RIDGE NATIONAL LABORATORY'S ROBOTICS AND INTELLIGENT SYSTEMS PROGRAM
S. A. Meacham 23 Jan. 1987 8 p Presented at the Roane-Anderson Economic Council Meeting, Oak Ridge, Tenn., 23 Jan. 1987
(Contract DE-AC05-84OR-21400)
(DE87-004627; CONF-870148-1) Avail: NTIS HC A02/MF A01

The goals of the newly formed Robotics and Intelligent Systems Program are discussed. The application of the remote systems technology developed by the Consolidated Fuel Reprocessing Program for the Department of Energy is presented. The activities (satellite refueling and space station truss assembly) with the National Aeronautics and Space Administration are presented in a videotape format with narration by the presenter. The goals of technology transfer to the private sector and the potential positive impact on the community conclude the oral presentation. DOE

N87-20775# Technische Univ., Brunswick (West Germany). Fakultaet fuer Maschinenbau und Elektrotechnik.
ADAPTIVE CONTROL WITH A NONPARAMETRIC MODEL FOR THE CONTROLLED SYSTEM Ph.D. Thesis [SELBSTEINSTELLENDE REGELUNG MIT NICHTPARAMETRISCHEM MODELL DER STRECKE]
Georg Fromme 1985 179 p In GERMAN
(ETN-87-99015) Avail: NTIS HC A09/MF A01

The application of the principle of the nonparametric model for control systems to adaptive controllers was investigated. The model construction via the convolution integral, the convolution sum, the structure of the nonparametric model, and the determination of the weight function are presented. It is shown that the nonparametric model is suited as a basis for adaptive controllers; its efficiency and that of the optimization procedure are demonstrated by practical test results. The time series controller, in the form of a nonrecursive high order filter, developed on the basis of the nonparametric model proves to be suited for the development of controllers. The proposed adaptive filters can only be economically realized using a microcomputer which allows a practical application of the control and optimization methods. ESA

N87-20776# Oxford Univ. (England). Dept. of Engineering Science.
CHARACTERISTIC DECOMPOSITION AND THE MULTIVARIABLE GENERALIZATION OF PREDICTIVE SELF-TUNING CONTROL
D. J. Cloud and B. Kouvaritakis 1986 48 p
(OUEL-1651/86; ETN-87-99459) Avail: NTIS HC A03/MF A01

A multivariable generalization of the concept of long-range

predictive control is presented. The proposed algorithm relies on a characteristic subsystem description of the system which reduces the multivariable control problem to a set of scalar problems so that existing single-input/single-output algorithms can be directly applied. This provides the user with the same flexibility in controling the individual loops of the multivariable system as that associated with standard scalar implementations. The result is a multivariable self-tuning algorithm that achieves loop-by-loop control in a true, generalized Nyquist framework. ESA

64 NUMERICAL ANALYSIS

Includes iteration, difference equations, and numerical approximation.

N87-20777*# National Aeronautics and Space Administration. Langley Research Center, Hampton, Va.
INVERSE PROBLEMS IN THE MODELING OF VIBRATIONS OF FLEXIBLE BEAMS Final Report
H. T. Banks, R. K. Powers, and I. G. Rosen Feb. 1987 24 p Submitted for publication
(Contracts NAS1-17070; NAS1-18107)
(NASA-CR-178259; ICASE-87-10; NAS 1.26:178259) Avail: NTIS HC A02/MF A01 CSCL 12A

The formulation and solution of inverse problems for the estimation of parameters which describe damping and other dynamic properties in distributed models for the vibration of flexible structures is considered. Motivated by a slewing beam experiment, the identification of a nonlinear velocity dependent term which models air drag damping in the Euler-Bernoulli equation is investigated. Galerkin techniques are used to generate finite dimensional approximations. Convergence estimates and numerical results are given. The modeling of, and related inverse problems for the dynamics of a high pressure hose line feeding a gas thruster actuator at the tip of a cantilevered beam are then considered. Approximation and convergence are discussed and numerical results involving experimental data are presented. Author

N87-20778*# National Aeronautics and Space Administration. Langley Research Center, Hampton, Va.
PIECEWISE LINEAR APPROXIMATION FOR HEREDITARY CONTROL PROBLEMS Final Report
Georg Propst Jan. 1987 75 p Submitted for publication
(Contracts NAS1-17070; NAS1-18107)
(NASA-CR-178260; ICASE-87-11; NAS 1.26:178260) Avail: NTIS HC A04/MF A01 CSCL 12A

Finite dimensional approximations are presented for linear retarded functional differential equations by use of discontinuous piecewise linear functions. The approximation scheme is applied to optimal control problems when a quadratic cost integral has to be minimized subject to the controlled retarded system. It is shown that the approximate optimal feedback operators converge to the true ones both in case the cost integral ranges over a finite time interval as well as in the case it ranges over an infinite time interval. The arguments in the latter case rely on the fact that the piecewise linear approximations to stable systems are stable in a uniform sense. This feature is established using a vector-component stability criterion in the state space R(n) x L(2) and the favorable eigenvalue behavior of the piecewise linear approximations. Author

N87-20779*# National Aeronautics and Space Administration. Langley Research Center, Hampton, Va.
A PRACTICAL ASSESSMENT OF SPECTRAL ACCURACY FOR HYPERBOLIC PROBLEMS WITH DISCONTINUITIES Final Report
David A. Kopriva Dec. 1986 24 p Submitted for publication
(Contract NAS1-18107)
(NASA-CR-178226; ICASE-86-82; NAS 1.26:178226) Avail: NTIS HC A02/MF A01 CSCL 12A

Physical and transform space filtering has been applied to the Fourier spectral collocation solution of the constant coefficient scalar wave equation with a discontinuous initial condition. High order accuracy can be extracted from the unfiltered solution. Smooth, high order Fourier space filtering gives expected polynomial order solutions away from the discontinuity. Spectral accuracy is observed with the physical space filter of Gottlieb and Tadmor. Author

N87-20780*# National Aeronautics and Space Administration. Langley Research Center, Hampton, Va.
REMARKS ON THE STABILITY ANALYSIS OF REACTIVE FLOWS
B. Scheurer (Commissariat a l'Energie Atomique, Villeneuve-Saint-Georges, France.) Mar. 1987 22 p
(Contract NAS1-18107)
(NASA-CR-178269; ICASE-87-18; NAS 1.26:178269) Avail: NTIS HC A02/MF A01 CSCL 12A

A simple model of compressible reacting flow is studied. First, a dispersion relation is derived for the linearized problem making a distinction between frozen and equilibrium sound speed. Second, the stability of the Von Neumann-Richtmyer scheme applied to this model is studied. A natural generalization of the C.F.L. condition is found. Author

N87-20781*# National Aeronautics and Space Administration. Langley Research Center, Hampton, Va.
ACOUSTIC GRAVITY WAVES: A COMPUTATIONAL APPROACH
S. I. Hariharan (Akron Univ., Ohio.) and P. K. Dutt Mar. 1987 27 p
(Contract NAS1-18107; Grants NAG1-624; NSF DMS-86-04047)
(NASA-CR-178270; ICASE-87-19; NAS 1.26:178270) Avail: NTIS HC A03/MF A01 CSCL 12A

This paper discusses numerical solutions of a hyperbolic initial boundary value problem that arises from acoustic wave propagation in the atmosphere. Field equations are derived from the atmospheric fluid flow governed by the Euler equations. The resulting original problem is nonlinear. A first order linearized version of the problem is used for computational purposes. The main difficulty in the problem as with any open boundary problem is in obtaining stable boundary conditions. Approximate boundary conditions are derived and shown to be stable. Numerical results are presented to verify the effectiveness of these boundary conditions. Author

N87-20782*# National Aeronautics and Space Administration. Langley Research Center, Hampton, Va.
ON LIPSCHITZ CONTINUITY OF NONLINEAR DIFFERENTIAL OPERATORS
Stephen L. Keeling Mar. 1987 13 p
(Contract NAS1-18107)
(NASA-CR-178263; ICASE-87-12; NAS 1.26:178263) Avail: NTIS HC A02/MF A01 CSCL 12A

In connection with approximations for nonlinear evolution equations, it is standard to assume that nonlinear terms are at least locally Lipschitz continuous. However, it is shown here that f = f(X,del sub u(X)) is Lipschitz continuous from the subspace W sup 1, infinity is a subset of L sub 2 into W sup 1,2, and maps W sup 2, infinity into W sup 1, infinity, if and only if f is affine with W sup 1, infinity coefficients. In fact, a local version of this claim is proved. Author

N87-20783*# National Aeronautics and Space Administration. Langley Research Center, Hampton, Va.
GALERKIN/RUNGE-KUTTA DISCRETIZATIONS FOR SEMILINEAR PARABOLIC EQUATIONS
Stephen L. Keeling Mar. 1987 32 p
(Contract NAS1-18107)
(NASA-CR-178264; ICASE-87-13; NAS 1.26:178264) Avail: NTIS HC A03/MF A01 CSCL 12A

A new class of fully discrete Galerkin/Runge-Kutta methods is constructed and analyzed for semilinear parabolic initial boundary value problems. Unlike any classical counterpart, this class offers

arbitrarily high, optimal order convergence. In support of this claim, error estimates are proved, and computational results are presented. Furthermore, it is noted that special Runge-Kutta methods allow computations to be performed in parallel so that the final execution time can be reduced to that of a low order method.
Author

N87-20784*# National Aeronautics and Space Administration, Washington, D.C.
ALGEBRA AND TOPOLOGY FOR APPLICATIONS TO PHYSICS
S. S. Rozhkov Apr. 1987 33 p Transl. into ENGLISH of Algebra i Topologiya dlya Fizicheskikh Prilozheniy (Kiev, USSR), Preprint no. 30, 1985 56 p Previously announced in IAA as A86-49343 Transl. by Kanner (Leo) Associates, Redwood City, Calif. Original document was prepared by Institut Fiziki, Academy of Sciences of the Ukrainian SSR, Kiev (USSR)
(Contract NASw-4005)
(NASA-TT-20056; NAS 1.77:20056) Avail: NTIS HC A03/MF A01 CSCL 12A

The principal concepts of algebra and topology are examined with emphasis on applications to physics. In particular, attention is given to sets and mapping; topological spaces and continuous mapping; manifolds; and topological groups and Lie groups. The discussion also covers the tangential spaces of the differential manifolds, including Lie algebras, vector fields, and differential forms, properties of differential forms, mapping of tangential spaces, and integration of differential forms. Author

N87-20785*# National Aeronautics and Space Administration. Ames Research Center, Moffett Field, Calif.
EIGENSYSTEM ANALYSIS OF CLASSICAL RELAXATION TECHNIQUES WITH APPLICATIONS TO MULTIGRID ANALYSIS
Harvard Lomax and Catherine Maksymiuk Mar. 1987 78 p
(NASA-TM-88377; A-86432; NAS 1.15:88377) Avail: NTIS HC A05/MF A01 CSCL 12A

Classical relaxation techniques are related to numerical methods for solution of ordinary differential equations. Eigensystems for Point-Jacobi, Gauss-Seidel, and SOR methods are presented. Solution techniques such as eigenvector annihilation, eigensystem mixing, and multigrid methods are examined with regard to the eigenstructure. Author

N87-20786# Los Alamos National Lab., N. Mex.
THREE-BODY CALCULATIONS AT LOS ALAMOS
J. L. Friar 1986 11 p Presented at the European Workshop on Few Body Physics, Rome, Italy, 7 Oct. 1986
(Contract W-7405-eng-36)
(DE87-001959; LA-UR-86-3455; CONF-8610196-3) Avail: NTIS HC A02/MF A01

This work was motivated by four goals: (1) by working in configuration space, where intuition is greatest, investigate graphically those trinucleon properties which are determined by specific features of wave functions; (2) produce benchmark calculations against which new techniques and numerical methods can be measured; (3) investigate the effect of the Coulomb interaction between the two protons in ^{3}He and in the p-d system; (4) systematically investigate the various trinucleon observables. Configuration space is particularly well-suited for investigating the Coulomb problem. The singularity and discontinuity problems associated with the Coulomb (momentum space) t-matrix are transformed into boundary condition problems in configuration space. One simply adds the Coulomb potential to the strong interaction. In order to produce accurate numerical solutions powerful techniques were adopted which have not frequently been used in nuclear physics. These spline methods together with collocation techniques combine the power of Gaussian quadrature procedures with the flexibility and strength of finite element approaches to solving partial differential equations. The union of these methods allows one to calculate wavefunctions at the same qualitative level of accuracy as the eigenvalues. Observables can therefore be calculated with considerable confidence. DOE

N87-20205# Office National d'Etudes et de Recherches Aerospatiales, Paris (France).
NEW NUMERICAL TECHNIQUES IN THE METHOD OF SINGULARITIES FOR APPLICATION TO COMPLEX THREE-DIMENSIONAL CONFIGURATIONS [TECHNIQUES NUMERIQUES NOUVELLES DANS LES METHODES DE SINGULARITES POUR L'APPLICATION A DES CONFIGURATIONS TRIDIMENSIONNELLES COMPLEXES]
T. H. Le, Y. Morchoisne, and J. Ryan *In* AGARD Applications of Computational Fluid Dynamics in Aeronautics Nov. 1986 22 p In FRENCH Original language document was announced in IAA as A87-21085 (For primary document see N87-20199 13-02)
Avail: NTIS HC A19/MF A01

N87-20211# Naval Surface Weapons Center, Silver Spring, Md. Applied Mathematics Branch.
A SECOND ORDER GODUNOV METHOD FOR TACTICAL MISSILES
A. B. Wardlaw, Jr. and S. F. Davis *In* AGARD Applications of Computational Fluid Dynamics in Aeronautics Nov. 1986 10 p (For primary document see N87-20199 13-02)
Avail: NTIS HC A19/MF A01

65 STATISTICS AND PROBABILITY

Includes data sampling and smoothing; Monte Carlo method; and stochastic processes.

N87-20787# Center for Mathematics and Computer Science, Amsterdam (Netherlands). Dept. of Mathematical Statistics.
A NEW APPROACH TO LEAST SQUARES ESTIMATION, WITH APPLICATIONS
Sara A. vandeGeer Mar. 1986 21 p
(CWI-MS-R8602; ETN-87-99244) Avail: NTIS HC A02/MF A01

The regression model y=g(x) I epsilon and least squares estimation are studied. By making use of empirical process theory, it is shown that the essential condition for L consistency of the least squares estimator of g is an entropy condition on the class of possible regression functions. This result is applied in parametric and nonparametric regression. ESA

N87-20788# Politecnico di Milano (Italy). Dipt. di Elettronica.
STRUCTURAL PROPERTIES OF LINEAR PERIODIC SYSTEMS
Sergio Bittanti 1986 32 p Revised
(Rept-86-004-Rev; ETN-87-99355) Avail: NTIS HC A03/MF A01

The structural properties of linear periodic continuous-time and discrete time systems are reviewed. Reachability and controllability subspaces; the length of the time interval required to perform the reachability and controllability transition; modal (spectral) characterizations; and stabilizability and detectability are discussed. ESA

N87-20789# Center for Mathematics and Computer Science, Amsterdam (Netherlands). Dept. of Mathematical Statistics.
UNIQUENESS OF GIBBS MEASURES AND ABSORPTION PROBABILITIES
H. C. P. Berbee Aug. 1986 15 p
(CWI-MS-R8610; ETN-87-99530) Avail: NTIS HC A02/MF A01

Gibbs measures are studied using a Markov chain on the non-negative integers. Uniqueness of Gibbs measures follows from absorption of the chain at (0). To this end a certain inequality is derived. For one-dimensional systems this improves a uniqueness result of Ruelle and it is for models near the 1/rsq interaction Ising model a natural improvement of other results.
ESA

66 SYSTEMS ANALYSIS

Includes mathematical modeling; network analysis; and operations research.

N87-20790*# National Aeronautics and Space Administration. Ames Research Center, Moffett Field, Calif.

ESTIMABILITY AND REGULABILITY OF LINEAR SYSTEMS
Yoram Baram and Thomas Kailath (Stanford Univ., Calif.) Feb. 1987 31 p
(NASA-TM-89427; A-87100; NAS 1.15:89427) Avail: NTIS HC A03/MF A01 CSCL 12B

A linear state-space system will be said to be estimable if in estimating its state from its output the posterior error covariance matrix is strictly smaller than the prior covariance matrix. It will be said to be regulable if the quadratic cost of state feedback control is strictly smaller than the cost when no feedback is used. These properties, which are shown to be dual, are different from the well known observability and controllability properties of linear systems. Necessary and sufficient conditions for estimability and regulability are derived for time variant and time invariant systems, in discrete and continuous time. Author

N87-20791# Rensselaer Polytechnic Inst., Troy, N.Y.
A SELF CRITICAL APPROACH TO DATA ANALYSIS AND MODEL BUILDING Final Report, 9 Jul. 1981 - 15 Jun. 1986
A. S. Paulson 1 Sep. 1986 948 p
(Contract DAAG29-81-K-0110)
(AD-A175640; ARO-18072.9-MA) Avail: NTIS HC A99/MF A02 CSCL 12/1

New methods related to model construction and evolution are introduced. The most frequently encountered specific cases are treated in substantial detail, e.g., experimental design layouts, regression, proportional hazards models, etc. The ultimate development is a generalization of the standard likelihood procedures for complete, censored, and binary data. This development includes estimation procedures, a test of hypothesis procedures (asymptotic), and an objective test of adequacy for specific models. These objective tests require the development of special tables, some of which are given in this report. A close connection of the generalized likelihood with Fourier methods had been observed and exploited to arrive at the formal definition of the generalized likelihood. A number of results of independent interests are obtained via, and for Fourier concepts. The idea of a sensitivity analysis of a model is paramount throughout: if the process of extraction of information from data vis-a-vis a tentative model is changed slightly, then the summarization or specification of this model should also change only slightly. Because our methods feed the estimation process back through the (tentative) model, the generalized likelihood procedures have been termed self-or model critical. Author (GRA)

67 THEORETICAL MATHEMATICS

Includes topology and number theory.

N87-20792# Gosudarstvennyi Komitet po Ispolzovaniyu Atomnoi Energii, Serpukhov (USSR). Inst. Fiziki Vysokikh Ehnergij.
GRAVITATIONAL COLLAPSE IN RELATIVISTIC THEORY OF GRAVITATION
A. A. Vlasov and A. A. Logunov 1985 20 p In RUSSIAN
(DE87-700730; IFVE-OTF-85-167) Avail: NTIS (US Sales Only) HC A02/MF A01

It is shown that in the relativistic theory of gravitation, unlike GTR, the process of the massive body compression by gravitational forces has been stopped at the finite density of matter for the final period of the proper time. This phenomenon of gravitational kernel may be understood when analyzing the motion of a probe particle in the gravitational field of the speherically symmetric body in Minkowski space. DOE

70 PHYSICS (GENERAL)

For precision time and time interval (PTTI) see *35 Instrumentation and Photography;* for geophysics, astrophysics or solar physics see *46 Geophysics, 90 Astrophysics,* or *92 Solar Physics.*

N87-20793# Massachusetts Inst. of Tech., Cambridge. Lab. for Computer Science.
INFORMATION-PRESERVING MODELS OF PHYSICS AND COMPUTATION Final Report
1986 17 p
(Contract DE-AC02-83ER-13082)
(DE87-005354; DOE/ER-13082/1) Avail: NTIS HC A02/MF A01

This research pertains to discrete dynamical systems, as embodied by cellular automata, reversible finite-difference equations, and reversible computation. The research has strengthened the cross-fertilization between physics, computer science and discrete mathematics. It has shown that methods and concepts of physics can be exported to computation. Conversely, fully discrete dynamical systems have been shown to be fruitful for representing physical phenomena usually described with differential equations - cellular automata for fluid dynamics has been the most noted example of such a representation. At the practical level, the fully discrete representation approach suggests innovative uses of computers for scientific computing. The originality of these uses lies in their non-numerical nature: they avoid the inaccuracies of floating-point arithmetic and bypass the need for numerical analysis. DOE

71 ACOUSTICS

Includes sound generation, transmission and attenuation. For noise pollution see *45 Environment Pollution.*

N87-20794*# National Aeronautics and Space Administration. Langley Research Center, Hampton, Va.
AN EVALUATION OF ACTIVE NOISE CONTROL IN A CYLINDRICAL SHELL
R. J. Silcox, H. C. Lester, and S. B. Abler (Joint Inst. for Advancement of Flight Sciences, Hampton, Va.) Feb. 1987 28 p Presented at the ASME Winter Annual Meeting, Anaheim, Calif., 7-12 Dec. 1986
(NASA-TM-89090; NAS 1.15:89090) Avail: NTIS HC A03/MF A01 CSCL 20A

The physical mechanisms governing the use of active noise control in an extended volume of a cylindrical shell are discussed. Measured data was compared with computer results from a previously derived analytical model based on an infinite shell theory. For both the analytical model and experiment, the radiation of the external monopoles is coupled to the internal acoustic field through the radial displacement of the thin, elastic cylindrical shell. An active noise control system was implemented in the cylinder using a fixed array of discrete monopole sources, all of which lie in the plane of the exterior noise sources. Good agreement between measurement and prediction was obtained for both internal pressure response and overall noise reduction. Attenuations in the source plane greater than 15 dB were recorded along with a uniformly quieted noise environment over the entire length of the experimental model. Results indicate that for extended axial forcing distributions or very low shell damping, axial arrays of control sources may be required. Finally, the Nyquist criteria for the number of azimuthal control sources is shown to provide for effective control over the full cylinder cross section. Author

N87-20795*# National Aeronautics and Space Administration. Langley Research Center, Hampton, Va.
DOCUMENTATION OF THE SPACE STATION/AIRCRAFT ACOUSTIC APPARATUS
Sherman A. Clevenson Feb. 1987 32 p
(NASA-TM-89111; NAS 1.15:89111) Avail: NTIS

HC A03/MF A01 CSCL 20A

This paper documents the design and construction of the Space Station/Aircraft Acoustic Apparatus (SS/AAA). Its capabilities both as a space station acoustic simulator and as an aircraft acoustic simulator are described. Also indicated are the considerations which ultimately resulted in man-rating the SS/AAA. In addition, the results of noise surveys and reverberation time and absorption coefficient measurements are included. Author

N87-20796 British Broadcasting Corp., London (England). Engineering Div.

A SURVEY OF ACHIEVED LEVELS OF AIRBORNE SOUND INSULATION IN BROADCASTING STUDIO CENTRES

D. J. Meares Feb. 1987 12 p

(BBC-RD-1987/1) Avail: BBC, Kingswood Warren, Tadworth, Surrey, England

A survey was performed on results from field measurements over the past fifteen years of the sound insulation of partitions in the technical areas of studio centers. The conduct of that survey is outlined and some examples of the acoustic performance of partitions are given. Author

N87-20797*# National Aeronautics and Space Administration. Langley Research Center, Hampton, Va.

AIRCRAFT NOISE SYNTHESIS SYSTEM: VERSION 4 USER INSTRUCTIONS

David A. McCurdy, Brenda M. Sullivan (Bionetics Corp., Hampton, Va.), and Robert E. Grandle Feb. 1987 31 p

(NASA-TM-89089; NAS 1.15:89089) Avail: NTIS HC A03/MF A01 CSCL 20A

A modified version of the Aircraft Noise Synthesis System with improved directivity and tonal content modeling has been developed. The synthesis system is used to provide test stimuli for studies of community annoyance to aircraft flyover noise. The computer-based system generates realistic, time-varying audio simulations of aircraft flyover noise at a specified observer location on the ground. The synthesis takes into account the time-varying aircraft position relative to the observer; specified reference spectra consisting of broadband, narrowband, and pure tone components; directivity patterns; Doppler shift; atmospheric effects; and ground effects. These parameters can be specified and controlled in such a way as to generate stimuli in which certain noise characteristics such as duration or tonal content are independently varied while the remaining characteristics such as broadband content are held constant. The modified version of the system provides improved modeling of noise directivity patterns and an increased number of pure tone components. User instructions for the modified version of the synthesis system are provided. Author

N87-20798*# National Aeronautics and Space Administration. Langley Research Center, Hampton, Va.

EXPERIMENTAL VALIDATION OF A TWO-DIMENSIONAL SHEAR-FLOW MODEL FOR DETERMINING ACOUSTIC IMPEDANCE

Tony L. Parrott, Willie R. Watson, and Michael G. Jones (PRC Kentron, Inc., Hampton, Va.) May 1987 50 p

(NASA-TP-2679; L-16203; NAS 1.60:2679) Avail: NTIS HC A03/MF A01 CSCL 20A

Tests were conducted to validate a two-dimensional shear-flow analytical model for determining the acoustic impedance of a liner test specimen in a grazing-incidence, grazing-flow environment. The tests were limited to a test specimen chosen to exhibit minimal effects of grazing flow so that the results obtained by using the shear-flow analytical model would be expected to match those obtained from normal-incidence impedance measurements. Impedances for both downstream and upstream sound propagation were generally consistent with those from normal-incidence measurements. However, sensitivity of the grazing-incidence impedance to small measurement or systematic errors in propagation constant varied dramatically over the range of test frequencies. Author

N87-20799# Federal Aviation Administration, Washington, D.C. Office of Environment and Energy.

THE 1985 SMALL PROPELLER-DRIVEN AIRCRAFT NOISE TEST PROGRAM

Kenneth E. Jones Oct. 1985 41 p

(AD-A175596; DOT/FAA/EE-85-8) Avail: NTIS HC A03/MF A01 CSCL 20/1

The international aviation community is currently reviewing noise certification procedure for small propeller-driven aircraft. Under discussion is a proposal to substitute a ground-plane microphone for the currently specified elevated microphone as a means of suppressing spectral irregularities. Given the strong low and mid-range tonal frequencies attendent to propeller-driven aircraft, the constructive/destructive interference pattern in an aircraft frequency spectrum can result in inconsistent certification test results for aircraft with different blade passage frequencies. The Federal Aviation Administration conducted flight tests during the summer of 1985 to compare noise levels measured at four feet to ground-plane levels as a function of the blade passage frequency. A preliminary assessment of the data acquired during the flight tests is presented. A more comprehensive analysis of the test results will be documented in the final report. Three flight tests were performed using a Cessna 210, Cessna Caravan I, and a (Beechcraft) U.S. NAVY T-34C. A vertical array (3.75 to 7.0 ft.) of microphones and a range of test RPMs were used to test the theoretical prediction of the ground reinforcement effect. As a secondary objective, the microphones were redeployed in horizontal arrays to test for a difference in variability between elevated and ground-plane microphones. DOE

N87-20800# European Space Agency, Paris (France).

NOISE MEASUREMENTS ON THE HELICOPTER BK 117 DESIGN. WEIGHTED NOISE LEVELS AND INFLUENCE OF AIRSPEED

Wolf R. Splettstoesser, Klaus P. Anders, and Karl-Heinz Spiegel Nov. 1986 90 p Transl. into ENGLISH of "Schallmessungen an der Hubschrauberneuentwicklung BK 117 - Bewertete Laermpegel und Einfluss der Fluggeschwindigkeit" DFVLR, Brunswick, West Germany, report DFVLR-Mitt-81-18, 1981 Original language document was announced as N8219957

(ESA-TT-748; DFVLR-Mitt-81-18; ETN-87-99423) Avail: NTIS HC A05/MF A01; original German version available from DFVLR, Cologne, West Germany DM 22.95

Noise measurements on the prototype helicopter BK 117 were performed in strict compliance with the proposed international Civil Aviation Organization regulations for noise certification of helicopters. Measurement procedure, noise data acquisition, analysis and reduction as well as applied correction procedures are described. Effective perceived noise levels (EPNL) and other noise descriptors were evaluated and related to the proposed noise limits. Additional level flyover tests with variable airspeed were conducted to investigate the resulting effect on the EPNL and other noise measures. ESA

N87-20801# National Oceanic and Atmospheric Administration, Boulder, Colo. Wave Propagation Lab.

HARPA: A VERSATILE THREE-DIMENSIONAL HAMILTONIAN RAY-TRACING PROGRAM FOR ACOUSTIC WAVES IN THE ATMOSPHERE ABOVE IRREGULAR TERRAIN

R. M. Jones, J. P. Riley, and T. M. Georges Aug. 1986 410 p

(PB87-132031; NOAA/SW/MT-87/001A) Avail: NTIS HC A18/MF A01 CSCL 20A

The modular FORTRAN 77 computer program traces the three-dimensional paths of acoustic rays through continuous model atmospheres by numerically integrating Hamilton's equations (a differential expression of Fermat's principle). The user specifies an atmospheric model by writing closed-form formulas for its three-dimensional wind and temperature (or sound speed) distribution, and by defining the height of the reflecting terrain vs. geographic latitude and longitude. Some general-purpose models are provided, or users can readily design their own. In addition to computing the geometry of each raypath, HARPA can calculate pulse travel time, phase time, Doppler shift (if the medium varies in time), absorption, and geometrical path length. The program prints a step-by-step account of a ray's progress. The 410-page

documentation describes the ray-tracing equations and the structure of the program, and provides complete instructions, illustrated by a sample case. GRA

N87-20309*# Norfolk Technical Vocational Center, Va.
NORSTAR PROJECT: NORFOLK PUBLIC SCHOOLS STUDENT TEAM FOR ACOUSTICAL RESEARCH
Ronald C. Fortunato *In* NASA. Goddard Space Flight Center The 1986 Get Away Special Experimenter's Symposium Feb. 1987 p 41-48 (For primary document see N87-20302 13-12)
Avail: NTIS HC A11/MF A01 CSCL 20A

N87-20436# Ocean Data Systems, Inc., Rockville, Md. Defense Systems Div.
UNDERWATER ACOUSTIC MODELING TECHNIQUES
P. C. Etter *In* Vibration Inst. The Shock and Vibration Digest, Volume 19, No. 2 Feb. 1987 p 3-10 (For primary document see N87-20435 13-31)
Avail: NTIS HC A05/MF A01

N87-20601# Air Force Systems Command, Wright-Patterson AFB, Ohio.
SUPERSONIC FLOW INDUCED CAVITY ACOUSTICS
Leonard L. Shaw *In* Shock and Vibration Information Center The Shock and Vibration Bulletin. Part 2: Modal Test and Analysis, Testing Techniques, Machinery Dynamics, Isolation and Damping, Structural Dynamics Aug. 1986 p 209-216 (For primary document see N87-20580 13-39)
Avail: NTIS HC A10/MF A01 CSCL 20/11

72 ATOMIC AND MOLECULAR PHYSICS

Includes atomic structure, electron properties, and molecular spectra.

N87-20802*# National Aeronautics and Space Administration, Washington, D.C.
KINETIC MODEL FOR THE VIBRATIONAL ENERGY EXCHANGE IN FLOWING MOLECULAR GAS MIXTURES Ph.D. Thesis
F. Offenhaeuser Mar. 1987 97 p Transl. into ENGLISH of "Kinestisches Modell fuer den Schwingungsenergieaustausch in Stroemenden Moleskuelgasgemischen" Stuttgart (West Germany), 13 Feb. 1985 p 1-101 Original language document was announced in IAA as A86-27827 Transl. by The Corporate Word, Pittsburgh, Pa. Original document was prepared by Stuttgart Univ., West Germany
(Contract NASw-4006)
(NASA-TM-88500; NAS 1.15:88500) Avail: NTIS HC A05/MF A01 CSCL 20H

The present study is concerned with the development of a computational model for the description of the vibrational energy exchange in flowing gas mixtures, taking into account a given number of energy levels for each vibrational degree of freedom. It is possible to select an arbitrary number of energy levels. The presented model uses values in the range from 10 to approximately 40. The distribution of energy with respect to these levels can differ from the equilibrium distribution. The kinetic model developed can be employed for arbitrary gaseous mixtures with an arbitrary number of vibrational degrees of freedom for each type of gas. The application of the model to CO2-H2ON2-O2-He mixtures is discussed. The obtained relations can be utilized in a study of the suitability of radiation-related transitional processes, involving the CO2 molecule, for laser applications. It is found that the computational results provided by the model agree very well with experimental data obtained for a CO2 laser. Possibilities for the activation of a 16-micron and 14-micron laser are considered. Author

N87-20803# Netherlands Energy Research Foundation, Petten.
CAPTURE OF THERMAL NEUTRONS B10 AND LI6: APPLICATIONS IN SPECTROSCOPY AND IN THE STUDY OF WEAK NUCLEON INTERACTIONS
P. J. J. Kok Jul. 1986 92 p
(ECN-184; ETN-87-99216) Avail: NTIS HC A05/MF A01

Investigation of excited states of Li7 by means of thermal neutrons capture; investigation of excited states of B11 and Li7 by means of thermal neutron capture on B10 nuclei; and an investigation of the admixture of strong and weak interactions in the B10 (n, alpha) reaction with slow neutrons are described. For individual titles, see N87-20804 through N87-20807.

N87-20804# Netherlands Energy Research Foundation, Petten.
GENERAL INTRODUCTION TO CAPTURE OF THERMAL NEUTRONS IN B10 AND LI6: APPLICATIONS IN SPECTROSCOPY AND IN THE STUDY OF WEAK NUCLEON INTERACTIONS
P. J. J. Kok *In its* Capture of Thermal Neutrons in B10 and Li: Applications in Spectroscopy and in the Study of Weak Nucleon Interactions Jul. 1986 p 9-22 (For primary document see N87-20803 13-72)
Avail: NTIS HC A05/MF A01

The neutron beam facilities and capture gamma ray spectroscopy at a high flux reactor are outlined. Thermal capture in B10 and Li6 nuclei is described. Knowledge from the (n, alpha gamma) experiments is used for the analysis of a parity violation experiment. ESA

N87-20805# Netherlands Energy Research Foundation, Petten. Nuclear Structure Group.
INVESTIGATION OF EXCITED STATES OF LI7 BY MEANS OF THERMAL NEUTRON CAPTURE
P. J. J. Kok, K. Abrahams, H. Postma (Technische Hogeschool, Delft, Netherlands.), and W. J. Huiskamp (Leiden Univ., Netherlands.) *In its* Capture of Thermal Neutrons in B10 and Li6: Applications in Spectroscopy and in the Study of Weak Nucleon Interactions Jul. 1986 p 23-43 (For primary document see N87-20803 13-72)
Avail: NTIS HC A05/MF A01

Capture of unpolarized thermal neutrons was used to gain information on the Li7 level scheme. The decay scheme of Li7 was studied through the Li6 (n, gamma) Li7 reaction. Three gamma-transitions were observed and placed. The binding energy value of this reaction is Q = 7251.02(9) keV. Investigation of radiation from excited Li7 produced by the B10 (n, alpha) Li7 reaction, made it possible to deduce a lifetime of the 478 keV level of Li7 = 102 + or - 5 fs. This value agrees with previous less accurate independent values and an average could be made in order to reduce the error further. The analysis of the peak shape of the 478 keV transition offers a method for estimating the size of boron grains embedded in other materials. ESA

N87-20806# Netherlands Energy Research Foundation, Petten. Nuclear Structure Group.
INVESTIGATION OF EXCITED STATES OF B11 AND LI7 BY MEANS OF THERMAL NEUTRON CAPTURE ON B10 NUCLEI
P. J. J. Kok, J. B. M. deHaas, K. Abrahams, H. Postma (Technische Hogeschool, Delft, Netherlands.), and W. J. Huiskamp (Leiden Univ., Netherlands.) *In its* Capture of Thermal Neutrons in B10 and Li6: Applications in Spectroscopy and in the Study of Weak Nucleon Interactions Jul. 1986 p 45-75 Submitted for publication (For primary document see N87-20803 13-72)
Avail: NTIS HC A05/MF A01

The gamma-radiation from the B10 (n, gamma) reaction was studied using an unpolarized target. More accurate values for energies of transitions in B11 are determined. No new levels are found. The Q value of 11454.1(2) keV agrees with earlier experiments. The cross section is 0.29(4) barn, a factor 5 more accurate than earlier experiments. The B10 (n, alpha) Li7 reaction, leading to the 478 keV state in Li7 was studied by polarized B10 nuclei and polarized neutrons. The resulting anisotropy in the directional distribution of the Li7 particles manifests itself in the Doppler broadening of the 478 keV line. Analysis of the line shape shows that the reaction proceeds for greater than 96% through the J = 7/2 channel of B11 in case of destructive channel interference of the J = 5/2 channel. Constructive channel interference is only possible if the reaction proceeds for greater than 99.5% through the J = 7/2 channel. Outcoming alpha and Li7 particles are

emitted predominantly in directions perpendicular to the nuclear orientation axis. ESA

N87-20807# Netherlands Energy Research Foundation, Petten. Nuclear Structure Group.
AN INVESTIGATION OF THE ADMIXTURE OF STRONG AND WEAK INTERACTIONS IN THE B10 (N, ALPHA) LI7 REACTION WITH SLOW NEUTRONS
P. J. J. Kok, F. Stecher-Rasmussen, K. Abrahams, O. N. Ermakov (Institute for Theoretical and Experimental Physics, Moscow, USSR.), J. L. Karpikhin, P. A. Krupchitsky, G. A. Lobov, V. F. Pereplitsa, H. Postma (Technische Hogeschool, Delft, Netherlands.), and W. J. Huiskamp (Leiden Univ., Netherlands.) *In its* Capture of Thermal Neutrons in B10 and Li6: Applications in Spectroscopy and in the Study of Weak Nucleon Interactions Jul. 1986 p 77-94 Submitted for publication (For primary document see N87-20803 13-72)
Avail: NTIS HC A05/MF A01

The weak nucleon-nucleon interaction was studied by an investigation of the forward-backward asymmetry of alpha-particle emission after capture of longitudinally polarized thermal neutrons by B10 nuclei. No asymmetry effects are observed for the two possible alpha transitions. The upper limits for the asymmetries at a 99.9% confidence level ere 0.0000057 for the direct transition to the ground state and 0.000001 for the transition to the 478 keV excited state of Li7. These limits suggest that the respective weak interaction matrix element is smaller than or of the order of 2.6 eV, which is well within the range of expectations. ESA

N87-20808# Stockholm Univ. (Sweden). Inst. of Physics.
A MODEL AND COMPUTER CODE FOR THE MONTE CARLO SIMULATION OF RELATIVISTIC ELECTRON AND POSITRON PENETRATION THROUGH MATTER
M. Ismail and D. Liljequist Oct. 1986 73 p
(USIP-86-11; ETN-87-99105) Avail: NTIS HC A04/MF A01

A model and Monte Carlo code were developed as a subroutine dealing with electron and positron transport in a computer program simulating the response of a multimaterial nuclear detector. The variable scattering angle model and the variable screened Rutherford model are used for scattering. In both models, an artificial mean free path with fixed, computationally convenient length is used. The method is similar to the multiple scattering approximation in that simulation is performed in steps of a finite length considerably larger than the mean free path. Electronic collision energy loss is considered partly by discrete events, partly by the continuous slowing down approximation (csda). Characteristic features of relativistic electron transmission, energy loss distributions, straggling, angular distributions, and trajectories were studied. ESA

N87-20809# Technische Hogeschool Twente, Enschede (Netherlands).
NOBLE-GAS ION BOMBARDMENT ON CLEAN SILICON SURFACES STUDIED USING ELLIPSOMETRY AND DESORPTION Ph.D. Thesis
Antonius Hendricus Maria Holtslag 16 Dec. 1986 183 p Sponsored by the Foundation for Fundamental Research on Matter, and the Netherlands Organization for the Advancement of Pure Research
(B8672200; ETN-87-99319) Avail: NTIS HC A09/MF A01

The influence of low-energy noble-gas ion bombardement on clean silicon surfaces was studied. At a low dose and at a high dose quite different behaviors are observed, finally resulting in a steady state. The low-dose behavior reflects the amorphism (a loss of long-range order) of the original c-Si surface layer. In order to explain the high-dose behavior, desorption experiments were carried out; information concerning the anneal behavior of the damaged implanted surface layer is obtained. During an anneal-step up to 800 C of the damaged layer, the noble gas is driven out and a recovery from damage occurs, resulting in the initial cristalline state. Upon termination of ion bombardment changing ellipsometric values, called self-anneal behavior, are still observed. ESA

N87-20810# Technische Hogeschool Twente, Enschede (Netherlands).
ADSORPTION OF ATOMIC OXYGEN (N2O) ON CLEAN SILICON SURFACES AND ITS INFLUENCE ON THE SURFACE STATE DENSITY; A COMPARISON WITH O2 Ph.D. Thesis
Enrico George Keim 1986 148 p
(B8668354; ETN-87-99320) Avail: NTIS HC A07/MF A01

The interaction of molecular oxygen (O2) and nitrous oxide (N2O) with the Si(100)2x1, (111)7x7 and (110)5x1 surfaces was studied in an ultrahigh vacuum system, the crystal temperature being 300 K, the gases being admitted into the reaction chamber at pressures ranging from 10 to the minus 8th power to 0.005 Torr. The geometric nature of the oxygen covered Si(100), (111) and (110) surfaces is described. ESA

N87-20811# Technische Univ., Munich (West Germany). Fakultaet fuer Physik.
GROUND-STATE PROTON RADIOACTIVITY IN THE DOMAIN OF NEUTRON-POOR NUCLEI HEAVIER THAN TIN Ph.D. Thesis [GRUNDZUSTANDS-PROTONENRADIOAKTIVITAET IM GEBIET NEUTRONENARMER KERNE OBERHALB DES ZINNS]
Albrecht Gillitzer 1985 83 p In GERMAN
(ETN-87-99342) Avail: NTIS HC A05/MF A01

The ground-state proton radioactivity in the domain of neutron-poor nuclei with an atomic number above 50 was investigated. In order to allow the observation of short-lived decays in the nsec range, a large-area, annular gas detector system with a parallel-plate avalanche counter was built, it has a detection probability better than 90% for protons. A 250 MeV Ni58-beam was used to bombard Ni58, Fe54, and Cr50 targets. The dependence of the measured half life on the decay energy and on the angular momentum of the emitted proton was investigated using a WKB calculation for an optical-model-potential; the agreement between measurement and calculation is variable. ESA

N87-20812# Helsinki Univ. of Technology, Espoo (Finland). Lab. of Physics.
STUDIES OF X-RAY SATELLITES IN SODIUM, MAGNESIUM, ALUMINUM, ARGON, AND IRON Ph.D. Thesis
Esko Mikkola 1986 42 p
(ETN-87-99364) Avail: NTIS HC A03/MF A01

Energies and intensities of K alpha, Beta, and alpha h satellites were determined in electron or in photon excitation. The spectra were measured with high resolution in sodium, magnesium, aluminum, argon, and iron (welding fumes). Energies of X-ray transitions: KLn to Ln+1 (n=0, 1, 2) core x-ray transitions, KLn to LnV (n=0, 1, 2) band spectra, K2Ln to KLn+1 (n=0, 1) hypersatellites and KL2, 3 (n=1, 2) radiative electron rearrangement (RER) transitions were determined. The relative intensities of the electron excited KL(2) multiplets show marked deviations from the statistical population of initial states, in contrast to the KL multiplets. Results indicate that the relative intensities of the multiplet bands within a K Beta satellite group (KLn to LnV) neither follow the experimental population of initial states nor statistical intensity ratios. This means that the atomic picture does not fully explain the relative valence band intensities in these light elements. The energy separation K Beta 1,3-K Beta' is the most sensitive parameter for the determination of the valence of iron in the most common welding fumes. ESA

73 NUCLEAR AND HIGH-ENERGY PHYSICS

Includes elementary and nuclear particles; and reactor theory.

For space radiation see *93 Space Radiation.*

N87-20813*# Alabama A & M Univ., Normal. Dept. of Physics.
STATISTICAL ANALYSIS OF SECONDARY PARTICLE DISTRIBUTIONS IN RELATIVISTIC NUCLEUS-NUCLEUS COLLISIONS
Stephen C. McGuire Washington NASA Mar. 1987 44 p

(Grant NAG8-027)
(NASA-CR-4054; NAS 1.26:4054) Avail: NTIS HC A03/MF A01 CSCL 20H

The use is described of several statistical techniques to characterize structure in the angular distributions of secondary particles from nucleus-nucleus collisions in the energy range 24 to 61 GeV/nucleon. The objective of this work was to determine whether there are correlations between emitted particle intensity and angle that may be used to support the existence of the quark gluon plasma. The techniques include chi-square null hypothesis tests, the method of discrete Fourier transform analysis, and fluctuation analysis. We have also used the method of composite unit vectors to test for azimuthal asymmetry in a data set of 63 JACEE-3 events. Each method is presented in a manner that provides the reader with some practical detail regarding its application. Of those events with relatively high statistics, Fe approaches 0 at 55 GeV/nucleon was found to possess an azimuthal distribution with a highly non-random structure. No evidence of non-statistical fluctuations was found in the pseudo-rapidity distributions of the events studied. It is seen that the most effective application of these methods relies upon the availability of many events or single events that possess very high multiplicities. Author

74 OPTICS

N87-20814*# National Aeronautics and Space Administration. Langley Research Center, Hampton, Va.
SOLAR POWER ABSORPTION IN A GLASS TUBE
Michael D. Williams Apr. 1987 16 p
(NASA-TM-89063; L-16055; NAS 1.15:89063) Avail: NTIS HC A02/MF A01 CSCL 20F

The optics of a glass tube to be used in near-Earth space at the focus of a solar concentrator has been examined, and an equation for the power absorbed from multiple-reflected light beams in the tube wall has been developed. The equation has been used to calculate the power absorbed by a highly transmissive form of fused silica. The equilibrium temperature reached by the tube with only radiative cooling has also been examined, and it shows a significant rise with large solar concentrations. The results apply specifically to cylindrical containment vessels for space-based solar-pumped lasers and generally to any similarly irradiated tubes. Author

N87-20815 Department of the Air Force, Washington, D.C.
FLY'S EYE SENSOR NONLINEAR SIGNAL PROCESSING Patent
Richard T. Schneider, inventor (to Air Force) Issued 9 Sep. 1986 11 p Supersedes N85-14684, AD-D011290 (23 - 05, p 729)
(AD-D012564; US-Patent-4,611,124; US-Patent-Appl-SN-620211; (US-Patent-Class-250-578) Avail: US Patent and Trademark Office CSCL 20/6

This document describes a multiaperture fly's eye optical signal transducing apparatus employing nonlinear electrical signal processing located adjacent the optical transducers in a multifunction integrated circuit device. The processed signals have enhanced low-level contrast and attenuated high contrast. Utilization examples, mathematical equations and related characteristic curves are also included along with exemplary circuit diagrams. Author (GRA)

N87-20816# Lawrence Livermore National Lab., Calif.
INTEGRATED OPTICAL DEVICES FOR HIGH SPEED DIAGNOSTICS
G. M. McWright Apr. 1986 26 p Presented at the Society of Photo-Optical Instrumentation Advanced Institute on Broadband Photonic Sensors, Howey-in-the-Hills, Fla., 7 Apr. 1986
(Contract W-7405-eng-48)
(DE87-003160; UCRL-94402; CONF-8604292-1) Avail: NTIS HC A03/MF A01

The design, fabrication, and evaluation of high speed directional coupler waveguide modulators for application to diagnostic systems is discussed. DOE

N87-20817# Bhabha Atomic Research Centre, Bombay (India).
DEVELOPMENT OF OPTICAL THIN FILM TECHNOLOGY FOR LASERS AND SYNCHROTRON RADIATION
1985 13 p
(DE87-701254; BARC-1281) Avail: NTIS (US Sales Only) HC A02/MF A01

Dielectric multilayer optical thin film devices play an important role not only in the working of lasers but also in different front line research activities using high power lasers and high intensity synchrotron radiation sources. Facilities were recently set up in the Spectroscopy Division to develop the optical thin film design and fabrication technologies indigeneously. Using the facilities thin film devices for different laser applications working in the wavelength range from 300 nm to 1064 nm were developed. Different technical aspects involved in the technology development are briefly described. DOE

75 PLASMA PHYSICS

Includes magnetohydrodynamics and plasma fusion.
For ionospheric plasmas see *46 Geophysics*. For space plasmas see *90 Astrophysics*.

N87-20818# Nagoya Univ. (Japan). Inst. of Plasma Physics.
INVESTIGATION OF LOW-CURRENT-DENSITY NANOSECOND ELECTRON BEAM DIODE
Naiyan Wang (Academia Sinica, Beijing, China.), Yusuke Kubota, and Akira Miyahara Aug. 1986 25 p
(IPPJ-T-36) Avail: NTIS HC A02/MF A01

An investigation of the low-current-density cold-cathode diode distinguished by nonself-convergent electron flow and the absence of applied magnetic field is described. Diode voltage and current can be easily adjusted by changing the diode separation due to the absence of the prepulse, while pulse-to-pulse reproducibility is rather good. The diode is coupled directly to a co-axial Marx generator. The energy conversion efficiency is high reaching to 61% and it strongly depends on the impedance of the diode. The maximum current density on the anode foil is obtained in the range from 100 to 200 A/sq cm. Author

76 SOLID-STATE PHYSICS

Includes superconductivity.
For related information, see also *33 Electronics and Electrical Engineering* and *36 Lasers and Masers*.

N87-20819 Howard Univ., Washington, D. C.
A STUDY OF III-V SEMICONDUCTOR PROCESSING EMPLOYING HIGH PURITY EPITAXIAL GALLIUM ARSENIDE Ph.D. Thesis
Moses Terlumun Asom 1985 152 p
Avail: Univ. Microfilms Order No. DA8627917

As the quest for new III-V semiconductor devices and improvements on current devices continues, it is necessary to examine the effects of processing on the starting materials and on the devices. An often used processing step requires thermal treatment. We have conducted numerous studies on GaAs epitaxial materials grown by liquid phase and molecular beam epitaxial techniques. Epitaxial layers of carrier concentration ranging from 10(14) to 10(17) cm(-3) were thermally treated at temperatures from 700 C to 950 C for thirty minutes. The thermal treatment involved capped and uncapped samples. The treated layers were characterized via conventional Hall measurements, capacitance-voltage, photoluminescence (PL) and deep level transient spectroscopy (DLTS) measurements. Results observed include: Hall mobility degradation of up to 50% of the starting material, increases in compensation

ratio and decreases in surface carrier concentration resulting in type conversion for low doped layers annealed at higher temperatures, e.g., in excess of 850 C. PL results indicated relative decreases in PL intensity of the 1.514, 1.484, 1.479 eV peaks and an appearance of the 1.407 eV peak for n-type materials annealed at higher temperatures (T greater than 850 C). DLTS measurements showed a higher temperature defect, with its location in energy close to mid-gap. Dissert. Abstr.

N87-20820*# Continuum, Inc., Huntsville, Ala.
COMPUTATIONAL ANALYSES OF CRYSTAL GROWTH Final Report
Youssef M. Dakhoul Jan. 1987 63 p
(Contract NAS8-36483)
(NASA-CR-179027; NAS 1.26:179027; CI-FR-0102) Avail: NTIS HC A04/MF A01 CSCL 20B

Two important aspects of Hg/Cd/Te crystal growth processes are discussed. First, the thermal field and second, the fluid movement in the melt zone. The thermal analysis includes numerical calculation of axisymmetric heat conduction within the sample. It also includes a three-dimensional radiation model to calculate the radiative heat exchange between the furnace and the crystal as determined by the complex geometry of the furnace and the adiabatic shield. The thermal analysis also includes a crystal conductivity which is dependent on temperature and composition. To tackle the fluid flow aspect of the problem, an attempt was made to use a newly developed incompressible flow code based on the slight compressibility, and hence the finite sound speed, of all real fluids. Author

N87-20821*# National Aeronautics and Space Administration. Lewis Research Center, Cleveland, Ohio.
RAPID THERMAL ANNEALING OF AMORPHOUS HYDROGENATED CARBON (a-C:H) FILMS
Samuel A. Alterovitz, John J. Pouch, and Joseph D. Warner Apr. 1987 8 p Presented at the Spring Meeting of the Materials Research Society, Anaheim, Calif., 21-25 Apr. 1987
(NASA-TM-89859; E-3519; NAS 1.15:89859) Avail: NTIS HC A02/MF A01 CSCL 20L

Amorphous hydrogenated carbon (a-C:H) films were deposited on silicon and quartz substrates by a 30 kHz plasma discharge technique using methane. Rapid thermal processing of the films was accomplished in nitrogen gas using tungsten halogen light. The rapid thermal processing was done at several fixed temperatures (up to 600 C), as a function of time (up to 1800 sec). The films were characterized by optical absorption and by ellipsometry in the near UV and the visible. The bandgap, estimated from extrapolation of the linear part of a Tauc plot, decreases both with the annealing temperature and the annealing time, with the temperature dependence being the dominating factor. The density of states parameter increases up to 25 percent and the refractive index changes up to 20 percent with temperature increase. Possible explanations of the mechanisms involved in these processes are discussed. Author

N87-20822# Palisades Inst. for Research Services, Inc., N.Y.
THE US WORKSHOP ON THE PHYSICS AND CHEMISTRY OF MERCURY CADMIUM TELLURIDE: EXTENDED ABSTRACTS Final Report
Leonard H. Klein Nov. 1986 232 p Workshop held in Dallas, Tex., 7-9 Oct. 1986
(Grant DAAL03-86-G-0175)
(AD-A175593; ARO-23894.1-EL) Avail: NTIS HC A11/MF A01 CSCL 20/12

Topics at the workshop sessions included band offsets, heterointerfaces, physical properties of lattices, structural properties of superlattices, impurities and defects, surfaces and interfaces, structural physics and electronic properties. GRA

N87-20823 Department of the Navy, Washington, D. C.
LIQUID PHASE EPITAXY (LPE) OF SILICON CARBIDE Patent
Arrigo Addamiano, inventor (to Navy) Issued 30 Sep. 1986 5 p Supersedes N86-13191, AD-D011825 (24 - 03, p 530)
(AD-D012571; US-Patent-4,614,672; US-Patent-Appl-SN-741784; US-Patent-Class-427-249) Avail: US Patent and Trademark Office CSCL 20/2

A method is described for making cubic SiC devices comprising the steps of preparing a preform consisting of high purity Si on which a layer of cubic SiC has been deposited by CVD; transferring the preform to a furnace containing a molten bath of Si saturated with SiC at a temperature of between 1600-1800C., the saturation being insured by the use of a high purity graphite crucible for the Si; dipping the Si-SiC preform into the molten bath and allowing deposition of more cubic SiC on the SiC layer by reducing the temperature of the already formed cubic SiC layer from the preparing step in relation to the rest of the molten bath. Additional steps include adding P-type or N-type dopants to the molten bath or into the CVD process and repeating the above mentioned steps to create cubic SiC homojunctions; and eliminating any Si adhering to the surface of the cubic SiC layer. Author (GRA)

N87-20824# Oak Ridge National Lab., Tenn.
THE EFFECTS OF HEAVY DOPING ON THE ELECTRONIC STATES IN SEMICONDUCTORS
B. E. Sernelius Jan. 1987 90 p Presented at the International Solid State Physics Workshop, Santiago, Chile, 1 Jan. 1987 Prepared in cooperation with Tennessee Univ., Knoxville
(Contract DE-AC05-84OR-21400)
(DE87-004421; CONF-870144-1) Avail: NTIS HC A05/MF A01

The physics of semiconductors is reviewed. Topics included in the discussion are energy of the dopant system (kinetic energy in a many-valley semiconductor, exchange energy in an ellipsoidal Fermi volume, energy in a polar semiconductor), self energy shifts, band-gap narrowing, and piezo experiments. DOE

N87-20825# Argonne National Lab., Ill.
HIGHLIGHTS FROM THE PHYSICS IN METALLIC SUPERLATTICES
I. K. Schuller Sep. 1986 8 p Presented at the 7th International Conference on Ternary Compounds, Snowmass, Colo., 1 Sep. 1986
(Contract W-31-109-eng-38)
(DE87-004657; CONF-8609160-2) Avail: NTIS HC A02/MF A01

Some highlights are presented from the physics that has been studied using metallic superlattices as model systems. These include unique structural aspects, anomalous elastic constants, electron localization, matching of superconducting vortices to the superlattice periodicity, dimensional crossover and development of magnon bands in magnetic superlattices. The results illustrate that these model systems can be tuned to study physics at different length scales. DOE

N87-20826# Argonne National Lab., Ill.
HIGH FIELD PROPERTIES OF SnMo6S8 AND PbMo6S8 RIBBONS PREPARED USING A VAPOR TRANSPORT TECHNIQUE
D. W. Capone, II, D. G. Hinks, and D. L. Brewe Sep. 1986 5 p Presented at the Applied Superconductivity Conference (ASC '86), Baltimore, Md., 28 Sep. 1986
(Contract W-31-109-eng-38)
(DE87-004707; CONF-860914-33) Avail: NTIS HC A02

Superconducting ribbons of SnMo6S8 and PbMo6S8 have been produced using a one step vapor transport technique. In this process Sn or Pb vapor and H2S gas react at the surface of a Mo substrate at elevated temperatures to form a uniform coating of Chevrel phase. SEM micrographs show the film on the ribbons to be composed of small (less than or equal to 0.5 microns) single-crystal rhombohedra of Chevrel phase. Critical currents for the SnMo6S8 ribbons are similar to that achieved in PbMo6S8 by other techniques (approx 1 x 10 to the 4th power A/sq cm at 19 T and 4.2 K). The performance of the PbMo6S8 is severely degraded. An explanation for this is based on larger intrinsic strain effects in the PbMo6S8. DOE

N87-20827# State Univ. of New York, Stony Brook. Dept. of Materials Science and Engineering.
DISLOCATION REACTIONS AT GRAIN BOUNDARIES IN LI2

ORDERED ALLOYS
A. H. King and M. H. Yoo 1986 6 p Presented at the Materials Research Society Fall Meeting, Boston, Mass., 1 Dec. 1986 Prepared in cooperation with ORNL, Tenn.
(Contract DE-AC05-84OR-21400)
(DE87-005713; CONF-861207-68) Avail: NTIS MF A01

The characteristics of perfect grain boundary dislocations in ordered alloys are discussed, and consideration is given to the possible formation of perfect and imperfect grain boundary dislocations by the impingement of crystal lattice dislocations. It is shown that many dislocation reactions at grain boundaries in ordered alloys are made unfavorable if chemical co-ordination must be maintained in the structure of the grain boundary. This leads to a suggestion that the effect of boron in the grain boundaries of Ni3Al is to reduce the importance of chemical ordering, and thus to promote deformation by allowing greater freedom for dislocation reactions to occur. DOE

N87-20828# Technische Hogeschool Twente, Enschede (Netherlands).
DEEP ION IMPLANTATION FOR BIPOLAR SILICON DEVICES; INVESTIGATIONS INTO THE USE OF THE THIRD DIMENSION Ph.D. Thesis
Antoni Johan Houthaan 16 Dec. 1986 133 p Sponsored by the Foundation for Fundamental Research on Matter, the Foundation for Technical Research, and the Netherlands Organization for the Advancement of Pure Research
(B8672201; ETN-87-99318) Avail: NTIS HC A07/MF A01

Ion implantations with energies up to 1 MeV were used in the realization of bipolar semiconductor devices for digital applications. An Integrated Injection Logic (IIL) structure, and five different of memory devices were investigated. All devices operate vertically, thus using the third dimension in silicon. It is shown that deep ion implantations can create vertically stacked npnp-devices that can be used as a vertical variant of IIL, named Buried Injector Logic (BIL). Epi-layers are avoided. Measurements and device simulation show that subnanosecond BIL gate-delay can be projected when lateral device areas are less than 25 sq microns. The BIL has all the merits attached to other forms of Vertical Injection Logic (or Substrate Fed Logic) as layout facilitation and the absence of powerlines on the silicon surface. The structure seems suitable for the realization of high density static RAM if switching currents are confined to pass through the on surface metallization. ESA

N87-20829# Helsinki Univ. of Technology, Espoo (Finland). Dept. of Technical Physics.
NONLINEAR DYNAMICS OF SOME CONDENSED MATTER DEVICES AND MATERIALS Ph.D. Thesis
R. K. Ritala 1986 29 p
(ETN-87-99363) Avail: NTIS HC A03/MF A01

Chaotic dynamics of periodically driven rf superconducting quantum interference devices; instabilities and chaotic solutions of the current biased dc superconducting interference device; tangential bifurcation and critical indices in a josephson junction; chaotic dynamics of nonideally driven simple oscillators; nonuniversal critical behavior in a model for charge-density-wave dynamics; and mode-locking in an infinite set of coupled circle maps were studied. The utility of bifurcation theory and the applicability of the universality of one dimensional mapping were examined. The effect of the number of degrees of freedom, and the possibility of observing chaos experimentally were investigated. ESA

N87-20334*# Tohoku Univ., Sendai (Japan). Faculty of Science.
IN SITU OBSERVATION OF MONO-MOLECULAR GROWTH STEPS ON AQUEOUS SOLUTION GROWN CRYSTALS AND THE TRANSPORT OF MOLECULES TO THE CRYSTALS
Katsuo Tsukamoto *In* NASA. Goddard Space Flight Center The 1986 Get Away Special Experimenter's Symposium Feb. 1987 p 233-238 (For primary document see N87-20302 13-12)
Avail: NTIS HC A11/MF A01 CSCL 20L

77 THERMODYNAMICS AND STATISTICAL PHYSICS

Includes quantum mechanics; theoretical physics; and Bose and Fermi statistics.

For related information see also *25 Inorganic and Physical Chemistry* and *34 Fluid Mechanics and Heat Transfer.*

N87-20830# Hiroshima Univ., Takehara (Japan). Research Inst. for Theoretical Physics.
ON THE DE SITTER AND NARIAI SPACE-TIMES IN A GENERALIZED THEORY OF GRAVITATION
Hidekazu Nariai Jul. 1985 7 p
(DE86-703483; RRK-85-20) Avail: NTIS (US Sales Only) HC A02/MF A01

A possibility of obtaining the de sitter and Nariai space-times in a generalized theory of gravitation (which was in succession proposed by Utiyama-DeWitt, Parker-Fulling-Hu and Gurovich-Starobinski) is examined. It is shown that the generalized theory with a suitable fixation of three parameters admit both space-times, just like the general theory of relativity. DOE

N87-20831# Bhabha Atomic Research Centre, Bombay (India). Water Chemistry Div.
THERMODYNAMIC DATA OF INTERMETALLIC COMPOUNDS
1984 28 p
(DE87-701244; BARC-1244) Avail: NTIS (US Sales Only) HC A03/MF A01

The data are presented in the alphabetical order of the chemical symbol for the elements. Each table presents the data of a group of binary intermetallic compounds with a common first component. For example, Table 1 shows the data of all binaries of silver. The table lists the properties indicated. For completeness, the experimental methods used in obtaining the data are also listed in the remarks column. The units are kJ mol/sup -1/ for all energy quantities and J K/sup -1/ mol/sup -1/ for entropies. DOE

N87-20832# Netherlands Energy Research Foundation, Petten.
TRANSIENT HEAT TRANSFER TO SUPERCRITICAL HELIUM AT LOW TEMPERATURES Thesis - Technische Hogeschool, Delft, The Netherlands
Willem Berend Bloem 1986 207 p
(ETN-87-99321) Avail: NTIS HC A10/MF A01

Transient heat transfer to a forced flow of supercritical helium flowing through a rectangular copper tube with a hydraulic diameter of 5 mm was studied. The transient heat transfer coefficient is, apart from time, a function of the helium properties thermal conductivity, density, and specific heat. Although these properties depend strongly on pressure and temperature, the temperature increase during a heat pulse is nearly the same at different helium pressures at 4.2 K. At higher bulk inlet temperatures differences occur. It is recommended to work at high pressures because the heat absorption of helium is relatively large with increasing temperature; there is a small probability of pressure oscillations; and when the inlet bulk temperature is greater than 4.2 K the heat absorption by helium still increases when the temperature rises. The heat transfer improves at Reynolds numbers greater than 100,000. ESA

N87-20274*# National Aeronautics and Space Administration. Lewis Research Center, Cleveland, Ohio.
THERMODYNAMICS AND COMBUSTION MODELING
Frank J. Zeleznik *In its* NASA-Chinese Aeronautical Establishment (CAE) Symposium 1986 p 113-133 (For primary document see N87-20267 13-07)
Avail: NTIS HC A01/MF A01 CSCL 20M

N87-20277*# National Aeronautics and Space Administration. Lewis Research Center, Cleveland, Ohio.
THEORETICAL KINETIC COMPUTATIONS IN COMPLEX REACTING SYSTEMS
David A. Bittker *In its* NASA-Chinese Aeronautical Establishment

(CAE) Symposium 1986 p 175-189 (For primary document see N87-20267 13-07)
Avail: NTIS HC A01/MF A01 CSCL 20M

80 SOCIAL SCIENCES (GENERAL)

Includes educational matters.

No abstracts in this category.

81 ADMINISTRATION AND MANAGEMENT

Includes management planning and research.

N87-20833* National Aeronautics and Space Administration, Washington, D.C.
MANAGEMENT: A BIBLIOGRAPHY FOR NASA MANAGERS
Apr. 1987 70 p
(NASA-SP-7500(21); NAS 1.21:7500(21)) Avail: NTIS HC A04 CSCL 05A

This bibliography lists 664 reports, articles and other documents introduced into the NASA scientific and technical information system in 1986. Items are selected and grouped according to their usefulness to the manager as manager. Citations are grouped into ten subject categories: human factors and personnel issues; management theory and techniques; industrial management and manufacturing; robotics and expert systems; computers and information management; research and development; economics, costs, and markets; logistics and operations management; reliability and quality control; and legality, legislation, and policy. Author

N87-20834*# Houston Univ., Tex. Dept. of Industrial Engineering.
AN INVESTIGATION OF TRANSITIONAL MANAGEMENT PROBLEMS FOR THE NSTS Annual Report
John L. Hunsucker and Japhet S. Law 15 Jan. 1987 405 p
(Contract NAS9-17315)
(NASA-CR-171979; NAS 1.26:171979) Avail: NTIS HC A18/MF A01 CSCL 05A

Analysis and recommendations were provided to the National Space Transportation System (NSTS) on managing the transition from a research and development (R/D) structure to an operational structure. Summaries of published literature on the theory and applications of transition, or change management, and the results of interviews with additional industry personnel whose organizations either have gone through or are now going through change are contained. The issues of flight rates and the flight decision are addressed. The use of a computer simulation model to analyze the effect of varying different parameters on the flight rate was also discussed. The issue of NASA's changing demographics was examined and why this may be a cause for concern. The impact of the whole shuttle system structure on the Challenger accident was presented along with the highlights of the Rogers Commission Report. The proposed reorganization of the NSTS management structure is discussed and how this transition from R/D to operations can be performed. B.G.

N87-20835# East Carolina Univ., Greenville, N.C. Dept. of Mathematics.
A STOCHASTIC APPROACH TO PROJECT PLANNING IN AN R AND D ENVIRONMENT Final Report
S. J. Seyedghasemipour Feb. 1987 105 p
(Contract DE-AS19-84BC-10828)
(DE87-005347; DOE/BC-10828/2) Avail: NTIS HC A06/MF A01

This study describes a simulation approach to project planning in an R and D environment by network model. GERT (Graphical Evaluation and Review Technique), a network model, was utilized for the modeling of a hypothetical research and development project. GERT is a network model capable of including randomness in activity duration, probabilistic branching, feedback loop, and multiple terminate node in a project planning. These capabilities make it more suitable for modeling of research and development projects than the previous approaches such as CPM and PERT. SLAM II simulation language is utilized for simulation of the network model. SLAM II is a simulation language which heavily relies on GASP IV and Q-GERTS with powerful modeling capability in a single integrated framework. The simulation is performed on a hypothetical standard research and development project. Two cases of project planning are considered. In the first case, the traditional simulation of network model of the hypothetical R and D project is performed. In the second case, learning factor is incorporated in the simulation process. Learning factor, in the context of project planning, means the mean and variance of a probability distribution representing an activity duration is discounted (reduced) every time that activity is repeated. The results and statistics of each case study concerning expected duration of successful completion of the project, probability of washouts, and realization time of milestones are presented in details. The differences between two cases (i.e., with and without learning factor) are discussed. DOE

N87-20836# Office National d'Etudes et de Recherches Aerospatiales, Paris (France).
[ACTIVITIES REPORT IN AEROSPACE RESEARCH] Annual Report, 1985
Sep. 1986 17 p
(ETN-87-99378) Avail: NTIS HC A02/MF A01

The management and administration, organization, operational departments, and patents of the French national aerospace research administration are described. ESA

82 DOCUMENTATION AND INFORMATION SCIENCE

Includes information management; information storage and retrieval technology; technical writing; graphic arts; and micrography.

For computer documentation see *61 Computer Programming and Software.*

N87-20837# Ecole Nationale Superieure des Telecommunications, Paris (France). Dept. Informatique.
EVALUATION OF THE PERFORMANCE OF A GEOGRAPHICALLY DISTRIBUTED DATA BASE MANAGEMENT SYSTEM USING STOCHASTIC PETRI NETS [EVALUATION DES PERFORMANCES D'UN SGBDR AU MOYEN DE RDPSC]
Alexandre Zenie 1986 19 p In FRENCH Presented at the Workshop on Computer Performance Evaluation, Sophia Antipolis, France, 28-30 Apr. 1986
(ENST-86C002; ISSN-0751-1337; ETN-87-99399) Avail: NTIS HC A02/MF A01

Colored stochastic Petri nets were used to model and evaluate the analytical performance of a data base system. Labels, transitions, and associated probability measure are colored. The extension of stochastic Petri nets permits simplification of both the base model and the associated stochastic process, while results are obtained easier and faster than using standard stochastic Petri nets. ESA

N87-20899*# Applied Research Corp., Landover, Md.
SEARCHING THE UVSP DATABASE AND A LIST OF EXPERIMENTS SHOWING MASS MOTIONS
William Thompson *In* NASA. Goddard Space Flight Center Coronal and Prominence Plasmas Dec. 1986 p 191-196 (For primary document see N87-20871 13-92)
Avail: NTIS HC A19/MF A01 CSCL 05B

N87-20607# Lockheed Missiles and Space Co., Sunnyvale, Calif.
A VIBROACOUSTIC DATABASE MANAGEMENT SYSTEM AND ITS APPLICATION FOR A PYROSHOCK DATABASE
W. Henricks and Y. Albert Lee *In* Shock and Vibration Information Center The Shock and Vibration Bulletin. Part 3: Invited Papers, Pyrotechnic Shock, Pyrotechnic Shock Workshop Aug. 1986 p 63-68 (For primary document see N87-20602 13-39)
Avail: NTIS HC A07/MF A01 CSCL 20/13

83 ECONOMICS AND COST ANALYSIS

Includes cost effectiveness studies.

No abstracts in this category.

84 LAW, POLITICAL SCIENCE AND SPACE POLICY

Includes NASA appropriation hearings; aviation law; space law and policy; international law; international cooperation; and patent policy.

N87-20838# Committee on Science and Technology (U. S. House).
ASSURED ACCESS TO SPACE: 1986
Washington GPO 1987 864 p Hearings before the Subcommittee on Space Science and Applications of the Committee on Science and Technology, 99th Congress, 2d Session, no. 164, 26 Feb.; 6, 19 Mar.; 17, 21, 25 Jul.; 13-14 Aug. 1986
(GPO-60-627) Avail: Subcommittee on Space Science and Applications

With the loss of the Challenger, the Nation lost more than 25% of its launch capacity. The capacity of a three-orbiter fleet was assessed and the size and impact of the schedule disruption was determined. The question of proper mix of expendable launchers and orbiters, as well as the implications that this loss will have on efforts to commercialize both expendables and orbiters was addressed. The issues of assured access to space were examined. B.G.

N87-20631# European Space Agency. European Space Research and Technology Center, ESTEC, Noordwijk (Netherlands).
COOPERATION OF THE INTERNATIONAL SPACE STATION PARTNERS IN THE PREPARATION OF THE USE OF SPACE STATION ELEMENTS FOR EARTH OBSERVATION (PLATFORM AND PAYLOAD ASPECTS)
B. Pfeiffer *In its* Proceedings of the European Symposium on Polar platform Opportunities and Instrumentation for Remote-sensing (ESPOIR) Nov. 1986 p 65-67 (For primary document see N87-20621 13-43)
Avail: NTIS HC A07/MF A01

N87-20632# European Space Agency, Paris (France).
USA-EUROPE COORDINATION AND COOPERATION ACTIVITIES: ANNOUNCEMENTS OF OPPORTUNITY
G. Duchossois *In its* Proceedings of the European Symposium on Polar platform Opportunities and Instrumentation for Remote-sensing (ESPOIR) Nov. 1986 p 69-71 (For primary document see N87-20621 13-43)
Avail: NTIS HC A07/MF A01

85 URBAN TECHNOLOGY AND TRANSPORTATION

Includes applications of space technology to urban problems; technology transfer; technology assessment; and surface and mass transportation.

For related information see also *03 Air Transportation and Safety, 16 Space Transportation,* and *44 Energy Production and Conversion.*

No abstracts in this category.

88 SPACE SCIENCES (GENERAL)

No abstracts in this category.

89 ASTRONOMY

Includes radio, gamma-ray, and infrared astronomy, and astrometry.

N87-20839 Princeton Univ., N. J.
A SYSTEMATIC SEARCH FOR MILLISECOND PULSARS Ph.D. Thesis
David J. Segelstein 1986 62 p
Avail: Univ. Microfilms Order No. DA8626182

A systematic search for pulsars was performed, covering approximately 300 square degrees of sky, with sensitivity to periods as short as 0.6 ms. We detected 19 known pulsars and 5 new ones, one of which is a millisecond pulsar--PSR 1855 + 09, with rotational period 5.3 ms and dispersion measure 13.3 pc cm(-3), indicating that it is a nearby object. It is evidently in a binary system, although its orbital parameters are not yet known with certainty. The sensitivity of our search is such that we can rule out the existence of a large population of high flux density pulsars such as PSR 1937 + 21. However, the possibility of a population of weaker objects, such as the previously known PSR 1953 + 29 and the new PSR 1855 + 09, is suggested. Our findings support the arguments for the origin of the short periods of these pulsars which rely on mass accretion from a companion object. Strategies for further searching are proposed. Dissert. Abstr.

N87-20840*# Smithsonian Astrophysical Observatory, Cambridge, Mass.
A NORMAL INCIDENCE X-RAY TELESCOPE Semiannual Progress Report, 1 May 1985 - 31 Oct. 1986
Leon Golub Jan. 1987 23 p
(Grant NAGw-397)
(NASA-CR-180107; NAS 1.26:180107; SAPR-6; SAPR-7; SAPR-8)
Avail: NTIS HC A02/MF A01 CSCL 03A

The postflight performance evaluation of the X-ray telescope was summarized. All payload systems and subsystems performed well within acceptable limits, with the sole exception of the light-blocking prefilters. Launch, flight and recovery were performed in a fully satisfactory manner. The payload was recovered in a timely manner and in excellent condition. The prefilter performance analysis showed that no X-ray images were detected on the processed flight film. Recommendations for improved performance are listed. B.G.

N87-20841*# National Aeronautics and Space Administration. Ames Research Center, Moffett Field, Calif.
AN ASTROMETRIC FACILITY FOR PLANETARY DETECTION

ON THE SPACE STATION
Kenji Nishioka, Jeffrey D. Scargle, and John J. Givens Apr. 1987 16 p Presented at the 4th International Symposium on Optical and Optoelectronic Applied Science Engineering, The Hague, Netherlands, 28 Mar. - 3 Apr. 1987
(NASA-TM-89436; A-87133; NAS 1.15:89436) Avail: NTIS HC A02/MF A01 CSCL 03A

An Astrometric Telescope Facility (ATF) for planetary detection is being studied as a potential space station initial operating capability payload. The primary science objective of this mission is the detection and study of planetary systems around other stars. In addition, the facility will be capable of other astrometric measurements such as stellar motions of other galaxies and highly precise direct measurement of stellar distance within the Milky Way Galaxy. The results of a recently completed ATF preliminary systems definition study are summarized. Results of this study indicate that the preliminary concept for the facility is fully capable of meeting the science objective without the development of any new technologies. A simple straightforward operations approach was developed for the ATF. A real-time facility control is not normally required, but does maintain a near real-time ground monitoring capability for the facility and science data stream on a full-time basis. Facility observational sequences are normally loaded once a week. In addition, the preliminary system is designed to be fail-safe and single-fault tolerant. Routine interactions by the space station crew with the ATF will not be necessary, but onboard controls are provided for crew override as required for emergencies and maintenance. Author

N87-20842*# Texas Univ., Austin. Office of Sponsored Programs.
FIDUCIAL REFERENCE FOR THE HIPPARCOS REFERENCE SYSTEM Final Report, 1 Feb. 1984 - 31 Jan. 1987
R. L. Duncombe Jan. 1987 72 p
(Grant NAGw-233)
(NASA-CR-180250; NAS 1.26:180250) Avail: NTIS HC A04/MF A01 CSCL 03A

The groundwork was prepared for observations by the Hubble Space Telescope (HST) to tie the coordinate system of the European Astrometry Satellite HIPPARCOS to an extragalactic (VLBI) reference frame, and to determine the rotation of the HIPPARCOS frame with respect to the extragalactic frame. A total of 90 Extragalactic Optical Objects (EGOs) were determined in the vicinity (angular separation less than 18 arcminutes) of 160 HIPPARCOS stars (brighter than about 11.0 magnitude, mostly SAO stars brighter than 10.5), evenly distributed over the sky, to be used to tie the HIPPARCOS system to the Extragalactic Reference Frame. The pairs are to be observed with the HST Fine Guidance Sensors (FGS), sometimes in conjunction with the HST Planetary Camera, in order to determine the relative positions and motions of the individual HIPPARCOS stars with respect to the EGOs. The data base which contains the optical information used to generate the HST Guaranteed Observing Time (GTO) proposal is included. B.G.

N87-20843# Sandia National Labs., Albuquerque, N. Mex.
A GONDOLA AND POINTING SYSTEM FOR A GAMMA RAY TELESCOPE
A. D. Sayers and M. C. Dowdican Nov. 1986 33 p
(Contract DE-AC04-76DP-00789)
(DE87-004561; SAND-86-0964) Avail: NTIS HC A03/MF A01

Details are reported of a gondola for carrying a gamma telescope during balloon flight and protecting it upon landing, and also of the mechanical drives needed to point the telescope with the required accuracy and stability needed to make precise measurements. The gondola is approximately 8' x 8' at its base and 16' tall, made of aluminum tubing and bar, and weighing about 800 lb. The pointing system is an elevation over azimuth arrangement which allows 360 degrees of azimuth and from zenith to 20 degrees above horizontal for elevation. DOE

N87-20844# Los Alamos National Lab., N. Mex.
LINEAR NONADIABATIC PULSATIONS OF HOMOGENEOUS ZAMS STARS
J. H. Cahn (Illinois Univ., Urbana.), A. N. Cox, and D. A. Ostlie (Weber State Coll., Ogden, Utah.) 11 Aug. 1986 5 p Presented at the Stellar Pulsation Conference, Los Alamos, N. Mex., 11 Aug. 1986 Prepared in cooperation with Illinois Univ., Urbana. Weber State Coll., Ogden, UT.
(Contract W-7405-eng-36)
(DE87-003722; LA-UR-86-4116; CONF-8608130-10) Avail: NTIS HC A02/MF A01

Current uncertainty about the most massive observed stars has led to a reexamination of the most massive star that is stable against radial pulsation. The nuclear energy generation equations in the LNA linear, nonadiabatic code have been considerably improved, so that it is now appropriate to redo the study to determine the maximum mass of Zero Age Main Sequence Stars (ZAMS) star that will be stable against pulsation. DOE

N87-20845# Academy of Sciences of the Ukrainian SSR, Kiev.
UBVRI-PHOTOMETRY OF THE ANTIFLARE STARS V586 ORI AND IU ORI
G. U. Kovalchuk 1986 24 p In RUSSIAN
(DE87-700760; ITF-86-29-R) Avail: NTIS (US Sales Only) HC A02/MF A01

The results of photoelectric UBVRI-observations of the antiflare stars V586 Ori and IU Ori done in 1979 to 1983 are presented. A random deep weakening up to 2/sup m/(V) are the main process of variability. The decrease of variable star brightness is interpreted under the assumption that a global weakening of brightness is due to the appearance in a close proximity to variable stars of the absorbing matter clouds. DOE

N87-20670*# National Aeronautics and Space Administration. Marshall Space Flight Center, Huntsville, Ala.
HUBBLE SPACE TELESCOPE
G. Nurre *In its* Upper and Middle Atmospheric Density Modeling Requirements for Spacecraft Design and Operations Feb. 1987 p 73-87 (For primary document see N87-20665 13-46)
Avail: NTIS HC A13/MF A01 CSCL 03A

90 ASTROPHYSICS

Includes cosmology; celestial mechanics; space plasmas; and interstellar and interplanetary gases and dust.
For related information see also *75 Plasma Physics.*

N87-20846 California Univ., Santa Barbara.
PROBLEMS IN QUANTUM COSMOLOGY Ph.D. Thesis
Piotr Amsterdamski 1986 126 p
Avail: Univ. Microfilms Order No. DA8629471

The standard cosmological model is reviewed and shown not to be self-sufficient in that it requires initial conditions which are most likely to be supplied by quantum cosmology. The possible approaches to the issue of intitial conditions for cosmology are then discussed. Three separate problems related to this isssue are considered. First, the possibility of inflation is investigated in detail by analyzing the evolution of metric perturbations and fluctuations in the expectation value of a scalar field prior to a phase transition; finite temperature effects are also included. Since the inhomogeneities were damped well before the onset of a phase transition, it is concluded that an inflation was possible. Next, the effective action of neutrino and photon fields is calculated for homogeneous spacetimes with small anisotropy, and is shown that quantum corrections to the action due to these fields influence the evolution of an early Universe in the same way as do the analogus correction terms arising from a conformally invariant scalar which has been previously studied. It is thus concluded that the physical processes of neutrino and photon production could rapidly dissipate any anisotropy in an early Universe. Finally, the question of an early anisotropy is also discussed in a framework of Hartle-Hawking wave function of the Universe. A wavefunction of a Bianchi IX type Universe is calculated in a

semiclassical approximation for a model with a cosmological constant, and by solving the Wheeler-DeWitt equation numerically for a model with classical radiation. It is shown that an anisotropic Universe is very unlikely, and that the expectation value of the anisotropy energy density decreases very fast as the Universe expands. Dissert. Abstr.

N87-20847 Massachusetts Univ., Amherst.
THE ACCELERATION AND DISSOLUTION OF STARS MOVING THROUGH THE BLACKBODY RADIATION OF A COLLAPSING UNIVERSE Ph.D. Thesis
Alice L. Argon 1986 79 p
Avail: Univ. Microfilms Order No. DA8701133

This dissertation deals with the motion and ablation of stars in the collapse phase of a closed Friedmann universe. Stars are initially accelerated due to the collapse of space. Radiation drag becomes increasingly important, however, and in most of the cases considered leads to maximum speeds and rapid deceleration. The external blackbody radiation also leads to mass loss, which acts as an additional accelerating mechanism. Three species of degenerate stars are considered: black dwarfs (BD), white dwarfs (WD), and neutron stars (NS). Each is assumed to have a non-degenerate, ionized atmosphere. In the star's rest frame the external blackbody radiation appears highly anisotropic, with most of the radiation entering the atmosphere through a narrow cone centered on the forward direction (opposite to the direction of motion). This radiation is Compton scattered. Atmospheric electrons (and hence ions) are accelerated azimuthally. After having travelled about one quarter of a circumference, they detach themselves from the star and stream away. The atmosphere is constantly replenished by upwelling from the interior. Mass loss then is a result of mechanical forces and is not due to thermal boiling. Four optical depths are considered for each species: 0, 1, 2, and 3. Maximum speeds and related temperatures are given for BD0, BD1, WD0, WD1, WD2, NS0, NS1, NS2 and NS3. Dissert. Abstr.

N87-20848 Texas Univ., Austin.
CARBON AND NITROGEN ABUNDANCES ALONG THE EVOLUTIONARY SEQUENCE OF M67 Ph.D. Thesis
Jeffery Allan Brown 1986 318 p
Avail: Univ. Microfilms Order No. DA8700171

A spectroscopic study of stars in the old galactic star cluster M67 was made to find the first dredge-up, that stage of stellar evolution where the surface abundances of carbon and nitrogen are altered by convective mixing with material processed by the CN cycle in the stellar interior. A high-resolution study of three bright cluster stars was made to determine the oxygen abundance of the cluster. Techniques and linelists for large-scale spectrum synthesis of the CHA x X delta v = 0 and CN B x X delta v = 1 bands were developed and used to determine the C/N abundance ratio in giant and subgiant stars. Nineteen M67 stars were analyzed with this method. It was found that the C/N ratio changes abruptly at the elbow in the cluster Hertzsprung-Russell diagram; at (BxV)sub 0 = 0.94 the C/N ratio drops by about 0.6 dex between M sub v approx. = + 3.5 and M sub v approx. = + 2.8. If probable systematic errors are allowed for, the C/N ratio does not change elsewhere on the cluster evolutionary sequence. The location of this change in the Hertzsprung Russell diagram is in accordance with theoretical predictions of stellar evolution although the amount of change in C/N is greater than that predicted by standard evolution calculations. Dissert. Abstr.

N87-20849 Illinois Univ., Urbana-Champaign.
THE STAR-FORMING PROPERTIES OF VIOLENTLY INTERACTING GALAXIES Ph.D. Thesis
Howard Alan Bushouse 1986 163 p
Avail: Univ. Microfilms Order No. DA8701446

The effects of galaxy-galaxy collisions on star formation are investiated for a large, morphologically selected sample of strongly interacting disk-type galaxies. Current star formation rates, stellar contents, and spatial distributions of star forming sites are explored on both global and nuclear scales via narrow-band imaging and spectrophotometry. The implications of this work are four-fold. First, the disk regions of galaxies are not strongly affected (in terms of star formation) as a result of an interaction with a close companion. Second, when interaction-induced activity does occur, it is primarily seen as an enhancement in the star formation rate in and around the nuclear regions of a galaxy. Third, exotic forms of nuclear activity, such as Seyferts, are not optically detectable in this sample of interacting galaxies. Fourth, while the observations agree in general with theoretical models, no explanations exist for (1) those galaxies that have not experienced any significant levels of star formation activity for a length of time comparable to the dynamical timescale for interactions, and (2) the overall lack of Seyfert and LINER nuclei in the sample. Dissert. Abstr.

N87-20850 Washington Univ., Seattle.
PRE-COMPACTION IRRADIATION OF METEORITES Ph.D. Thesis
Marc William Caffee 1986 191 p
Avail: Univ. Microfilms Order No. DA8626368

In the four meteorites studied the non-irradiated grains show the nominal amount of spallogenic Ne and Ar expected from recent galactic cosmic ray exposure. Two conclusions follow from these observations: (1) The quantity of spallogenic Ne and Ar in the irradiated grains is far more than can be explained by reasonable pre-compaction exposures to galactic cosmic rays. If the pre-compaction irradiation occurred in a regolith, the exposure to galactic cosmic rays would have to last several hundred m.y. for some of the grains. Similarly long ages would result if the source of the protons were solar flares with a particle flux similar to modern-day solar flares. These exposure durations are incompatible with current models for the pre-compaction irradiation of gas-rich meteorites. (2) There is always a correlation between solar flare tracks and pre-compaction spallogenic Ne and Ar. This correlation is surprising, considering the difference in range of these two effects. These two observations may be explained if the energetic particle flux at the time of irradiation was considerably higher than the modern-day flux and the track-producing ions and spallogenic protons have a similar range. These requirements could be met by an active early (T-Tauri) Sun where the solar energetic particles are responsible for both heavy-ion tracks and spallation-produced Ne and Ar. However, if an active early Sun is responsible for the pre-compaction spallation Ne and Ar then this irradiation necessarily occurred early in the history of the solar system since the duration of increased activity is short. To address this problem we performed Ar-40 to Ar-39 analyses of individual irradiated and non-irradiated grains from Kapoeta. Dissert. Abstr.

N87-20851 California Univ., Los Angeles.
COMPUTER SIMULATION AND ANALYSIS OF SPATIAL GALAXY DISTRIBUTIONS Ph.D. Thesis
Arati Chokshi 1986 195 p
Avail: Univ. Microfilms Order No. DA8629879

Monte Carlo techniques were employed to simulate detailed and realistic fields of galaxies in a variety of model universes extending to a maximum redshift of z = 10. The simulated data were treated as real data and extensive analysis were carried out. The interest was in developing analytical tools that would work with confusion limited data sets (which would typify high redshift galaxy ensembles) and also provide information on cosmological effects that are important at high redshifts, such as the effects due to stellar evolution in galaxies and those due to geometry of space-time. Special attention was paid to the infrared behavior of galaxies and in particular the role of infrared colors as distance indicators was carefully scrutinized. Dissert. Abstr.

N87-20852 Massachusetts Univ., Amherst.
THE MAGNETIC AND TURBULENT EVOLUTION OF THE TAURUS MOLECULAR CLOUD Ph.D. Thesis
Mark C. Hemeon-Heyer 1986 177 p
Avail: Univ. Microfilms Order No. DA8701168

The role of the interstellar magnetic field in the dynamics of C(13)OJ = 1 - 0 emission to delineate gas morphology and kinematics and polarization of background starlight to determine the magnetic field direction within the Taurus Molecular Cloud

Complex is investigated. The signature for a dynamically significant magnetic field is a rotating, flattened cloud with the rotational and minor axes parallel to the direction of the magnetic field. It was found that molecular regions characterized by mean densities less that 100/cu cm exhibit such magnetic signatures and are likely a result of magnetically dominated evolution. Dissert. Abstr.

N87-20853 Texas Univ., Austin.
A NUMERICAL STUDY OF SOME SPHERICALLY-SYMMETRIC AND AXISYMMETRIC COSMOLOGICAL MODELS Ph.D. Thesis
Katherine Ann Holcomb 1986 246 p
Avail: Univ. Microfilms Order No. DA8700206

Two computer codes whose purpose is the study of inhomogeneous cosmological models are described. The first code assumes spherical symmetry, whereas the second is more general assuming only axisymmetry. Both codes are based upon the 3+1 decomposition of Arnowitt, Deser, and Misner. With this approach, general relativity is cast into a dynamical form which has proved fruitful for numerical solution. The conformal approach of York is employed to solve the initial-value problem. Gauge conditions are set in order to write the three-metric in the simplest possible form. Constant-mean-curvature time slicing is used to determine the foliation of spacelike hypersurfaces. In the case of spherical symmetry, the three-metric is put into diagonal form. A fully-constrained evolution is performed. The code has full hydrodynamical capabilities. Outer boundary conditions are applied by requiring that the metric become the Friedmann-Robertson-Walker metric appropriate to the matter energy density at the edge of the computational mesh. The code tests carried out are discussed. The axisymmetric code is based upon a code developed by Wilson and Dykema and by Evans to treat the problem of nonspherical gravitational collapse in asymptotically-flat spacetimes. Appropriate modifications were made to permit cosmological models to be studied. The three-metric is put into quasi-isotropic form, leaving two metric variables for which we must solve. One, the conformal factor, is determined by the Hamiltonian constraint. The other represents the single dynamical degree of freedom allowed by our symmetries. A partially-constrained evolution is employed in which only the Hamiltonian constraint is enforced on each time slice. Only the study of gravitational radiation in a vacuum cosmological context is attempted. Dissert. Abstr.

N87-20854 Rensselaer Polytechnic Inst., Troy, N.Y.
MOLECULAR CLOUDS IN THE OUTER GALAXY Ph. D. Thesis
Kathryn N. Mead 1986 250 p
Avail: Univ. Microfilms Order No. DA8700145

Physical conditions and related star forming activities were investigated in molecular clouds in the outer galaxy. Thirty-five molecular clouds were mapped in the CO(J = 1-0) line at lambda = 2.6 mm. Ten of these were mapped in (13)CO(J = 1-0) and CO(J = 2-1) (lambda = 1.3 mm). Far infrared continuum emission from dust was detected in four of six clouds searched and radio continuum emission from HII regions was mapped in 15 of 17 observed clouds. On a large scale, the CO emission follows the HI warp and there appears to be an arm at R approx. 13 kpc, coincident with a feature in the HI surface density distribution. Studying individual clouds reveals the following results. (1) Linestrength (T sub R*) ratios of the (12)CO(J = 1-0) and (13)CO(J = 1-0) lines at and near the cloud peaks are typically between 3 and 6, indicating that the CO is optically thick. (2) Qualitative analyses of the CO(J = 1-0 and J = 2-1) line-strengths in the envelopes indicate low kinetic temperatures in the clouds. (3) Peak T sub R*'s are found to decrease somewhat with an increase in galactocentric distance, R, indicating that the peaks are beam diluted. (4) Most clouds lie between R = 11.5 kpc and R = 14 kpc. At larger R's few clouds were found; and they have drastically lower linestrengths, indicating that the CO at R greater than 14.5 kpc is either sparse or cold. (5) An average cloud is 40 pc in the longest dimension. (6) Most clouds have masses from 10(4). 10(5) solar mass (7) Continuum emission was detected in four of six clouds searched in the infrared and 15 of 17 clouds searched at 6 cm. Spectral types of embedded stars derived from the continuum data were between O7 and B3; most were B1 or B2. Dissert. Abstr.

N87-20855 Princeton Univ., N. J.
TIMING MILLISECOND PULSARS Ph.D. Thesis
Lloyd Alexander Rawley 1986 108 p
Avail: Univ. Microfilms Order No. DA8629457

UHF timing observations of the millisecond pulsar PSR 1937 + 21 were conducted with the 73000 sq m telescope of the Arecibo Observatory since October 1984 using a multichannel signal averager built for the purpose and described herein. A two-hour dual-frequency observation measures the pulsar rotation phase at one instant with 275 ns accuracy. The timing results determine the pulsar's celestial proper motion and place a 2 sigma lower limit of 2 kpc on its distance. The integrated electron density along the line of sight to the pulsar is shown to vary by 1 part in 10 to the 5th power on time scales of order 6 months. Time residuals from the astrometric fit have the properties of a flicker phase modulation, a type of noise indicative of measurement errors (probably instrumental) rather than pulsar rotation instabilities or gravitational waves. The local energy density in gravitational waves of period approx. 3 years must be less than 3 x 10 to the -35 power g/cu cm. The other two known millisecond pulsars, PSRs 1953 + 29 and 1855 + 09, have also been timed. The secular increase in the rotation period of PSR 1953 + 29, the smallest such increase yet measured, implies an unusually small surface magnetic field of 4 X 10 to the 8th power G for this pulsar, very close to that derived for PSR 1937 + 21, despite the fact that PSR 1953 + 29 is in a binary system and PSR 1937 + 21 is not. These pulsars probably have similar histories involving spin-up by accretion. The rate of period increase of PSR 1855 + 09 may be even smaller, but a few more months of data are needed to determine it precisely. PSR 1955 + 09 is potentially nearly as good a clock as PSR 1937 + 21. Dissert. Abstr.

N87-20856 California Inst. of Tech., Pasadena.
ABUNDANCES AND KINEMATICS OF K GIANTS IN THE GALACTIC NUCLEAR BULGE Ph.D. Thesis
Robert Michael Rich 1986 211 p
Avail: Univ. Microfilms Order No. DA8623948

Spectroscopy and photometry was obtained for 100 K giants in Baade's Window at l = 1 deg, b = -4 deg. The abundance distribution of the nuclear bulge K giants was derived relative to 45 stars of known abundance. The abundances run from -1 to nearly +1 dex, with a peak at 0.3 dex, or twice the solar abundance. Of the 88 stars with derived abundances, 22% exceeded the abundance of the most metal rich local K giants; 50% exceeded the solar abundance, and 10% were metal poor (less than -0.6 dex). Radial velocities were measured for 53 nuclear bulge K giants which also have derived abundances. Their velocity dispersion is 104 km/sec. The mean velocity is -19 + or - 14 km/sec. The abundance distribution function is found to be fit very well by the simple model of chemical evolution with complete gas consumption. No evidence was found that either the metal rich or metal poor stars follow the galactic rotation curve; hence neither population appears to be rotation supported. Optical and infrared photometry is presented for nuclear bulge K giants. The colors of these stars are shown to be too hot for their derived metal abundances. Analysis of color-magnitude diagrams in bulge fields at -4 deg (Baade's Window) and -8 deg shows that there cannot be a 1 Gyr old population of main sequence stars in the galactic bulge. A turnoff population is detected at -8 deg, and comparison with isochrones indicates that the population is older than 5 Gyr. For the first [illegible], there is a clear indication of a horizontal branch, or globular cluster feature in the luminosity function of the galactic bulge. Dissert. Abstr.

N87-20857 New Mexico State Univ., Las Cruces.
STATISTICAL PROPERTIES OF BARIUM STARS Ph.D. Thesis
Jon Eric Hakkila 1986 148 p
Avail: Univ. Microfilms Order No. DA8626089

Barium stars are G- and K-giant stars with atmospheric

excesses of s-process elements, and a broadband spectral depression in the blue portion of the spectrum. The strength of the wavelength 4554 Ball line is used as a classification parameter known as the barium intensity. These stars apparently belong to a young-disk population from analyses of both the solar reflex motion and their residual velocity distribution, which implies that they have an upper mass limit of around three solar masses. There is no apparent correlation of barium intensity with either luminosity or kinematic properties. The barium stars appear to be preferentially distributed in the direction of the local spiral arm, but show no preference to associate with or avoid the direction of the galactic center. The distribution in absolute magnitude combined with starcount analyses implies that these stars are slightly less numerous than previously believed. Barium stars show infrared excesses which correlate with their barium intensities. Barium intensities can be identified from DDO photometric colors to approximately the same accuracy as obtained from the more tedious method of spectral analysis. This could prove to be a useful survey tool for the future identification of these stars.
Dissert. Abstr.

N87-20858 California Univ., Berkeley.
RING GALAXIES: AN INVESTIGATION OF THE PHYSICAL CONDITIONS IN CLOSELY INTERACTING SYSTEMS Ph.D. Thesis
Norbert Alan Jeske 1986 241 p
Avail: Univ. Microfilms Order No. DA8624803

A radio and optical study of 28 ring galaxies was performed. The radio data consist of VLA continuum maps at 20, 6, and 2 cm and Arecibo 21 cm line spectra. The optical data consist of long slit CCD spectra, aperture spectra, and CCD direct images. Infrared data from the IRAS survey and published X-ray data from the Einstein X-ray observatory were also incorporated. Optical emission line fluxes were measured and compared to the radio continuum position, flux density, and spectral index information to determine the emission mechanisms present in ring galaxies. The strongest sources of radio continuum emission were found to be nonthermal emission from compact sources. Optical line emission from HII regions as well as from gas excited by nonthermal excitation mechanisms was found. Dissert. Abstr.

N87-20859 Princeton Univ., N. J.
SELF-CONSISTENT MODELS OF PERFECT TRIAXIAL GALAXIES Ph.D. Thesis
Thomas Stuart Statler 1986 247 p
Avail: Univ. Microfilms Order No. DA8626185

The self-consistent problem for the triaxial mass model known as the perfect ellipsoid is treated numerically. Schwarzschild's method is applied to 21 perfect ellipsoids of various axis ratios, using an unbiased catalogue of 1065 orbits to match the density of mass model at 240 points. The extent of the space of mathematically allowed solutions for each figure is mapped out by using linear programming to maximize linear combinations of the x and z components of the angular momentum. Lucy's iterative method is used to obtain smooth solutions in the interiors of the solution spaces. The major results are given and discussed.
Dissert. Abstr.

N87-20860*# Virginia Univ., Charlottesville. Dept. of Applied Mathematics.
COLLISIONAL DYNAMICS OF PERTURBED PARTICLE DISKS IN THE SOLAR SYSTEM Annual Technical Progress Report
W. W. Roberts and G. R. Stewart 25 Mar. 1987 11 p
(Grant NAGw-929)
(NASA-CR-180497; NAS 1.26:180497; UVA/528253/AM87/101)
Avail: NTIS HC A02/MF A01 CSCL 03B

Investigations of the collisional evolution of particulate disks subject to the gravitational perturbation of a more massive particle orbiting within the disk are underway. Both numerical N-body simulations using a novel collision algorithm and analytical kinetic theory are being employed to extend our understanding of perturbed disks in planetary rings and during the formation of the solar system. Particular problems proposed for investigation are: (1) The development and testing of general criteria for a small moonlet to clear a gap and produce observable morphological features in planetary rings; (2) The development of detailed models of collisional damping of the wavy edges observed on the Encke division of Saturn's A ring; and (3) The determination of the extent of runaway growth of the few largest planetesimals during the early stages of planetary accretion. Author

N87-20861# Instituto de Pesquisas Espaciais, Sao Jose dos Campos (Brazil).
MEASUREMENTS OF IRIDIUM AND THE HYPOTHESIS OF METEORITIC IMPACT AS THE END OF THE CRETACEOUS PERIOD M.S. Thesis [MEDIDAS DE IRIDIO E A HIPOTESE DO IMPACTO METEORITICO DO FIM DO CRETACEO]
Francisco SircilliNeto Dec. 1986 113 p In PORTUGUESE
(INPE-4070-TDL/248) Avail: NTIS HC A06/MF A01

Analysis methods applied for neutron activation and radiochemistry for determination of trace elements, iridium and gold, were utilized in cosmochemistry. The concentrations analyzed were in the parts per billion band. The analysis by neutron activation determined the concentration of 1.5 gram irradiated iridium sample during 32 hours in thermal flux as 10 to the 13th power neutrons/sq cm/sec. Gamma spectrometry was performed on the samples in the course of 10 to 12 hours after 40 days of decay. In the analysis by radiochemical neutron activation, the method of chemical separation of noble metals through coprecipitation with tellurium (Stockman, 1983) was used for determination of gold and iridium. The first preliminary data of iridium in sedimentary rocks, collected in the National Territory was obtained with the application of neutron activation analysis method. These determinations of iridium are important for checking, in future work, an hypothesis of asteroidal impact as the cause of the large mass extinction observed in the transitional Cretaceous/Tertiary period (Alvarez et al, 1980) utilizing samples collected in the Southern Hemisphere. Author

N87-20862# Maryland Univ., College Park.
AN INVESTIGATION OF THE STRONG PRINCIPLE OF EQUIVALENCE THROUGH THE USE OF FREELY FALLING GEOCENTRIC COORDINATES Ph.D. Thesis
Mark Douglas Somers 1986 131 p
Avail: Univ. Microfilms Order No. DA8629014

The strong equivalence principle (as stated in Will (1981)) is investigated by developing a transformation from a system of coordinates at rest relative to the Sun to a freely falling inertial coordinate system at rest relative to the Earth. The transformation is used to transform the metric, the n-body equation of motion and the light-time equation to the new coordinates. As any terms that contain solar quantities in the transformed equations represent violations of the strong equivalence principle, proposals for experiments to measure these terms are discussed. The parameterized post-Newtonian formalism is employed throughout to facilitate the discussion, and limits on some of the associated parameters are derived based on the possible results of the proposed experiments. Dissert. Abstr.

N87-20863# Los Alamos National Lab., N. Mex.
MHD WAVES DETECTED BY ICE AT DISTANCES > 28 X 10 km FROM COMET HALLEY: COMETARY OR SOLAR WIND ORIGIN
B. T. Tsurutani, A. L. Brinca, E. J. Smith, R. M. Thorne, F. L. Scarf, J. T. Gosling, and F. M. Ipavich 1986 7 p Presented at the 20th ESLAB Symposium, Heidelberg, West Germany, 27 Oct. 1986 Prepared in cooperation with JPL, Pasadena, Calif., TRW Space Technology Labs., Redondo Beach, Calif. and Maryland Univ., College Park
(Contract W-7405-eng-36)
(DE87-005122; LA-UR-87-39; CONF-8610207-6) Avail: NTIS HC A02

Spectral analyses of the high resolution magnetic field data are employed to determine if there is evidence of cometary heavy ion pickup when ICE was closest to Halley, approx 28 x 10 to the 6th power km. No evidence is found for the presence of heavy

ion cyclotron waves. However, from this search, two new wave modes are discovered in the solar wind: electromagnetic ion cyclotron waves and drift mirror mode waves. Both modes have scales of 10 to 60 s (1 to 6 T(sub p)) in the spacecraft frame. The possibility of wave generation by cometary hydrogen pickup is explored. Theoretical arguments and further experimental evidence indicates that cometary origin is improbable. The most likely source is plasma instabilities associated with solar wind stream-stream interactions. VLF electrostatic emissions are found to occur in field minima or at gradients of the drift mirror structures. Possible generation mechanisms of drift mirror mode waves, cyclotron waves and electrostatic waves are discussed. DOE

N87-20864# California Univ., Berkeley. Dept. of Astronomy.
THE LARGE-SCALE PECULIAR VELOCITY FIELD IN FLAT MODELS OF THE UNIVERSE
N. Vittorio and M. S. Turner Oct. 1986 18 p Prepared in cooperation with Fermi National Accelerator Lab., Batavia, Ill. and Chicago Univ., Ill.
(Contract DE-AC02-76CH-03000)
(DE87-005402; FNAL/Pub-86/79-A) Avail: NTIS HC A02/MF A01

The inflationary Universe scenario predicts a flat Universe and both adiabatic and isocurvature primordial density perturbations with the Zel'dovich spectrum. The two simplest realizations, models dominated by hot or cold dark matter, seem to be in conflict with observations. Flat models are examined with two components of mass density, where one of the components of mass density is smoothly distributed and the large-scale (greater than or equal to 10h/1 MpC) peculiar velocity field for these models is considered. For the smooth component relativistic particles, a relic cosmological term, and light strings are considered. At present the observational situation is unsettled; but, in principle, the large-scale peculiar velocity field is a very powerful discriminator between these different models. DOE

N87-20865# Fermi National Accelerator Lab., Batavia, Ill.
DOUBLE INFLATION: A POSSIBLE RESOLUTION OF THE LARGE-SCALE STRUCTURE PROBLEM
M. S. Turner, J. V. Villumsen, N. Vittorio, J. Silk, and R. Juszkiewicz Nov. 1986 22 p Prepared in cooperation with California Inst. of Tech., Pasadena, Rome Univ., Italy, and California Univ., Berkeley
(Contract DE-AC02-76CH-03000)
(DE87-005403; FNAL/Pub-86/158-A) Avail: NTIS HC A02/MF A01

A model is presented for the large-scale structure of the universe in which two successive inflationary phases resulted in large small-scale and small large-scale density fluctuations. This bimodal density fluctuation spectrum in an Omega = 1 universe dominated by hot dark matter leads to large-scale structure of the galaxy distribution that is consistent with recent observational results. In particular, large, nearly empty voids and significant large-scale peculiar velocity fields are produced over scales of approx 100 Mpc, while the small-scale structure over less than or equal to 10 Mpc resembles that in a low density universe, as observed. Detailed analytical calculations and numerical simulations are given of the spatial and velocity correlations. DOE

N87-20866# Fermi National Accelerator Lab., Batavia, Ill.
THERMAL PRODUCTION OF NOT SO INVISIBLE AXIONS IN THE EARLY UNIVERSE
M. S. Turner Oct. 1986 12 p Prepared in cooperation with Chicago Univ., Ill.
(Contract DE-AC02-76CH-03000)
(DE87-005404; FNAL/Pub-86/150-A) Avail: NTIS HC A02/MF A01

We find that for Peccei-Quinn symmetry-breaking scales less than or equal to 2 x 10 to the 8th power GeV (corresponding to axion masses greater than or equal to 3 x 10 to the -2 eV) thermal production of axions in the early Universe (via the Primakoff and photoproduction processes) dominates coherent production by a factor of about 1200 (m(sub a)/eV) sup 2.175. The photon luminosity from the decays of these relic axions leads to a model-independent upper limit to the axion mass of order 2 to 5 eV. If the axion mass saturates this bound, relic axion decays may well be detectable. DOE

N87-20867# European Space Agency, Paris (France).
ENCOUNTER 86: AN INTERNATIONAL RENDEZVOUS WITH HALLEY'S COMET
Norman Longdon, ed. Nov. 1986 71 p Original contains color illustrations
(ESA-BR-27; ISSN-0250-1589; ETN-87-99432) Avail: NTIS HC A04/MF A01

Images of Halley's comet from the American, Russian, European, and Japanese missions of 1986 and from historical documents are presented. International cooperation in planning and executing the missions, and scientific highlights are described. ESA

N87-20868*# Jet Propulsion Lab., California Inst. of Tech., Pasadena.
STEEPENED MAGNETOSONIC WAVES IN THE HIGH BETA PLASMA SURROUNDING COMET-GIACOBINI-ZINNER
B. T. Tsurutani, E. J. Smith, R. M. Thorne, J. T. Gosling, and H. Matsumoto 1986 6 p Presented at the 20th ESLAB Symposium, Heidelberg, West Germany, 27 Oct. 1986 Prepared in cooperation with Los Alamos National Lab., N. Mex.; California Univ., Los Angeles.;Kyoto Univ. (Japan) Sponsored by NASA
(Contract W-7405-eng-36)
(NASA-CR-180614; NAS 1.26:180614; DE87-005123; LA-UR-87-38; CONF-8610207-8) Avail: NTIS MF A01/MF A01 CSCL 03B

We extend the previous studies of intense hydromagnetic waves at Giacobini-Zinner to investigate the mode and direction of wave propagation. Simultaneous high-resolution measurements of electron density fluctuations demonstrate that the long period (approx. 100 s) waves are propagating in the magnetosonic mode. Principal axis analyses of the long period waves and accompanying partial rotations show that the sum of the wave phase rotations is 360 C, indicating that both are parts of the same wave oscillation. From the time sequence of the steepened waveforms observed by the International Cometary Explorer (ICE), we demonstrate that the waves must propagate towards the sun with C/sub ph/ is less than V/sub sw/. All available observations are consistent with wave generation by the resonant ion ring or ion beam instability which predicts right-hand polarized waves propagating in the ion beam (solar) direction. The large amplitudes (delta polarized B/absolute value of B is approx.0(1)) and small scale sizes (rotational discontinuities) of the cometary waves suggest that rapid pitch-angle scattering and energy transfer with energetic ions should oc cur. Since the waves are highly compressive, delta absolute value of B/absolute value of B = 0(0.5), one can also anticipate first-order Fermi acceleration. DOE

91 LUNAR AND PLANETARY EXPLORATION

Includes planetology; and manned and unmanned flights.
For spacecraft design or space stations see *18 Spacecraft Design, Testing and Performance.*

N87-20869 Maryland Univ., College Park.
OBSERVATIONS OF SUNWARD AND TAILWARD ION STREAMING IN THE MAGNETOTAIL OF JUPITER WITH VOYAGER 2 Ph. D. Thesis
Dale Calvin Brown 1985 173 p
Avail: Univ. Microfilms Order No. DA8625676

Energetic ions in the Jovian magnetotail were studied using the LECP instrument onboard Voyager 2. Seven periods of ion streaming, indicative of ion acceleration in progress in the magnetotail, were found inside the magnetopause between 90 to 170 R sub j from Jupiter. The study of these ion streams leads to two conclusions. Averaging over time and with a reasonable estimate of the spatial size of the ion streams, it was found that

on the order of 10 to the 23rd power ions/sec with E equal to or greater than 100 keV/nuc are accelerated and transported towards the inner magnetosphere. This rate of ion acceleration is sufficient to populate the inner Jovian magnetosphere using 1% of the observed sunward streaming ions. Dissert. Abstr.

92 SOLAR PHYSICS

Includes solar activity, solar flares, solar radiation and sunspots.

For related information see *93 Space Radiation.*

N87-20870 Princeton Univ., N. J.
THEORY AND SIMULATION OF THE EVOLUTION OF THE LARGE-SCALE SOLAR MAGNETIC FIELD Ph.D. Thesis
Carl Richard DeVore 1986 100 p
Avail: Univ. Microfilms Order No. DA8629443

The evolution of the Sun's large-scale magnetic field is modeled by a transport equation which describes the effects of differential rotation, meridional circulation, and supergranular diffusion on the field at the photosphere. This equation is solved analytically and numerically to investigate three aspects of solar magnetic behavior. The axisymmetric solutions to the transport equation which approximate the distribution of flux near the time of sunspot minimum were calculated. Then the evolution of several bipolar magnetic regions were simulated over a few solar rotational periods, using digital magnetic-field measurements to initialize the model and to evaluate the results. The evolution of the Sun's mean line-of-sight magnetic field over an eight-year interval during sunspot cycle 21, using nominal values of the transport parameters and estimated properties of the emerging bipolar regions are simulated. The findings support the hypothesis that the Suns's large-scale magnetic field can be understood as resulting from the transport of flux emerging in sunspot groups. Dissert. Abstr.

N87-20871*# National Aeronautics and Space Administration. Goddard Space Flight Center, Greenbelt, Md.
CORONAL AND PROMINENCE PLASMAS
Arthur I. Poland, ed. Dec. 1986 435 p Workshop held in Greenbelt, Md., 9-11 Apr. 1985 and 8-10 Apr. 1986
(NASA-CP-2442; Rept-86BO536; NAS 1.55:2442) Avail: NTIS HC A19/MF A01 CSCL 03B

Various aspects of solar prominences and the solar corona are discussed. The formation of prominences, prominence diagnostics and structure, prominence dissappearance, large scale coronal structure, coronal diagnostics, small scale coronal structure, and non-equilibrium/coronal heating are among the topics covered. For individual titles, see N87-20872 through N87-20945.

N87-20872*# National Aeronautics and Space Administration. Marshall Space Flight Center, Huntsville, Ala.
SOME CRUCIAL CORONA AND PROMINENCE OBSERVATIONS
E. A. Tandberg-Hanssen *In* NASA. Goddard Space Flight Center Coronal and Prominence Plasmas Dec. 1986 5-8 (For primary document see N87-20871 13-92)
Avail: NTIS HC A19/MF A01 CSCL 03B

A number of theories and hypotheses are currently being developed to explain the often complex behavior of corona and prominence plasmas. In order to test the theories and hypotheses certain crucial observations are necessary. Some of these observations are examined and a few conclusions are drawn. Corona mass balance, corona and prominence classifications, prominence formation and stability, and coronal mass ejection are dicussed. Author

N87-20873*# Chicago Univ., Ill. Dept. of Physics.
HEATING OF THE STELLAR CORONA
E. N. Parker *In* NASA. Goddard Space Flight Center Coronal and Prominence Plasmas Dec. 1986 p 9-20 (For primary document see N87-20871 13-92)
(Grant NGL-14-001-001)
Avail: NTIS HC A19/MF A01 CSCL 03B

The present state of development of the theory of coronal heating is summarized. Coronal heating is the general cause of stellar X-ray emission, and it is also the cause of stellar mass loss in most stars. Hence a quantitive theory of coronal heating is an essential part of X-ray astronomy, and the development of a correct theory of coronal heating should be a primary concern of X-ray astronomers. The magnetohydrodynamical effects involved in coronal heating are not without interest in their own right, representing phenomena largely unknown in the terrestrial laboratory. Until these effects can be evaluated and assembled into a comprehensive theory of coronal heating for at least one star, the interpretation of the X-ray emissions of all stars is a phenomenological study at best, based on arbitrary organization and display of X-ray luminosity against bolometric luminosity, rotation rate, etc. The sun provides the one opportunity to pursue the exotic physical effects that combine to heat a stellar corona. Author

N87-20874*# New Hampshire Univ., Durham. Space Science Center.
FORMATION AND SUPPORT OF PROMINENCE
T. G. Forbes *In* NASA. Goddard Space Flight Center Coronal and Prominence Plasmas Dec. 1986 p 21-26 (For primary document see N87-20871 13-92)
(Grant NAGw-76)
Avail: NTIS HC A19/MF A01 CSCL 03B

A short introduction is given to the concepts discussed by the group on the formation and support of prominences. Only quiescent and long-lived active region prominences were considered, since transient prominence phenomena, such as sprays, surges, H alpha flare-loops, and coronal rain, are dynamically distinct from long-lived, prominences. Stable prominences (which are often referred to as filaments when seen against the disk) can be subdivided into three categories, namely active region prominences, quiescent prominences and polar crown prominences. The third category is closely related to the second since a quiescent prominence will eventually evolve into a polar crown prominence if it lasts long enough. The distinction between the first and second categories is not sharp either since intermediates exist here as well (Martin, 1973). Author

N87-20875*# California Univ., Irvine. Dept. of Physics.
THE GROWTH OF RADIATIVE FILAMENTATION MODES IN SHEARED MAGNETIC FIELDS
Gerard VanHoven *In* NASA. Goddard Space Flight Center Coronal and Prominence Plasmas Dec. 1986 p 27-31 Sponsored in part by NSF (For primary document see N87-20871 13-92)
Avail: NTIS HC A19/MF A01 CSCL 03B

Observations of prominences show them to require well-developed magnetic shear and to have complex small-scale structure. Researchers show here that these features are reflected in the results of the theory of radiative condensation. Researchers studied, in particular, the influence of the nominally negligible contributions of perpendicular (to B) thermal conduction. They find a large number of unstable modes, with closely spaced growth rates. Their scale widths across B show a wide range of longitudinal and transverse sizes, ranging from much larger than to much smaller than the magnetic shear scale, the latter characterization applying particularly in the direction of shear variation. Author

N87-20876*# Observatoire de Paris-Meudon (France).
CAN PROMINENCES FORM IN CURRENT SHEETS
J. M. Malherbe and T. G. Forbes (New Hampshire Univ., Durham.) *In* NASA. Goddard Space Flight Center Coronal and Prominence Plasmas Dec. 1986 p 33-39 (For primary document see N87-20871 13-92)
(Grants NAGw-76; NSF ATM-85-07035)
Avail: NTIS HC A19/MF A01 CSCL 03B

Two-dimensional numerical simulations of the formation of cold condensations in a vertical current sheet have been performed using the radiative, resistive MHD equations with line-tied boundary conditions at one end of the sheet. Prominence-like condensations are observed to appear above and below an X-line produced by

the onset of the tearing-mode instability. Cooling in the sheet is initiated by Ohmic decay, with the densest condensations occurring in the region downstream of a fast-mode shock. This shock, which is due to the line-tied boundary conditions, terminates one of the two supermagnetosonic reconnection jets that develop when the tearing is fully developed. The condensation properties of shock waves, which may trigger or considerably enhance the conditions for thermal condensation are emphasized. Author

N87-20877*# National Aeronautics and Space Administration. Marshall Space Flight Center, Huntsville, Ala.
CONDENSATION MODES IN MAGNETIZED PLASMAS
Chang-Hyuk An *In* NASA. Goddard Space Flight Center Coronal and Prominence Plasmas Dec. 1986 p 41-45 (For primary document see N87-20871 13-92)
Avail: NTIS HC A19/MF A01 CSCL 03B

Condensation modes in magnetized cylindrical plasmas, with concentration on how magnetic field affects the stability were studied. It is found that the effects of magnetic field (shear, twist, and strength) on the condensation modes are different depending on the wave vector. For modes whose wave vector is not perpendicular to magnetic field lines the plasma motion is mainly along the field lines; the effects of magnetic field on the modes are negligible except on the heat flow parallel to the field line. For a mode which is localized near a surface where the wave vector is perpendicular to the field line, the plasma moves perpendicular to the line carrying the field line into the condensed region; magnetic field affects the mode by building up magnetic pressure in the condensed region. The stability of condensation modes strongly depends on how density and temperature vary with field twist. The stable nature of global quiescent prominence magnetic configurations implies that prominences form for low field twist for which ideal MHD modes are stable; plasma temperature should increase with field twist for stable prominence formation. Author

N87-20878*# Alabama Univ., Huntsville.
FILAMENT FORMATION DUE TO PHOTOSPHERIC SHEAR
S. T. Wu and Y. C. Xiao *In* NASA. Goddard Space Flight Center Coronal and Prominence Plasmas Dec. 1986 p 47-50 (For primary document see N87-20871 13-92)
(Contract NAS8-33528; Grants NAGw-9; NAG8-053)
Avail: NTIS HC A19/MF A01 CSCL 03B

Recently, Wu et al. (1983, 1986) developed a three-dimensional, time-dependent axisymmetric ideal magnetohydrodynamic (MHD) model which has been used to study lower solar atmospheric response due to photospheric motion. They have shown that various observed solar features can be formed from these numerical simulation experiments. Some work currently in progress which has resulted from a specific numerical simulation experiment is reported. These results may elucidate the possible physical mechanism of formation of filament. Author

N87-20879*# National Aeronautics and Space Administration. Marshall Space Flight Center, Huntsville, Ala.
FORMATION OF ACTIVE REGION AND QUIESCENT PROMINENCE MAGNETIC FIELD CONFIGURATIONS
C.-H. An, J. J. Bao (Alabama Univ., Huntsville.), and S. T. Wu *In* NASA. Goddard Space Flight Center Coronal and Prominence Plasmas Dec. 1986 5 p Sponsored in part by National Academy of Sciences/National Research Council, Washington, D.C. (For primary document see N87-20871 13-92)
(Grants NAGw-9; NAG8-053)
Avail: NTIS HC A19/MF A01 CSCL 03B

To investigate the formation of prominences, researchers studied chromospheric mass injection into an overlying coronal dipole magnetic field using a 2-D ideal magnetohydrodynamic (MHD) numerical model. Researchers propose that active region prominences are formed by chromospheric plasmas injected directly into the overlying coronal magnetic field and that quiescent prominences are formed by plasmas evaporated at the interface between spicules and corona. Hence, for the simulation of an active region prominence magnetic field we inject the mass from one side, but use a symmetric mass injection to form a quiescent prominence field configuration. Researchers try to find optimum conditions for the formation of Kippenhahn-Schuluter(K-S) type field configuration for stable support of the injection plasmas. They find that the formation of K-S type field configuration by mass injection requires a delicate balance between injection velocity, density, and overlying magnetic fields. These results may explain why a prominence does not form on every neutral line. Author

N87-20880*# National Aeronautics and Space Administration. Goddard Space Flight Center, Greenbelt, Md.
NUMERICAL SIMULATIONS OF A SIPHON MECHANISM FOR QUIESCENT PROMINENCE FORMATION
A. I. Poland, J. T. Mariska (Naval Research Lab., Washington, D. C.), and J. A. Klimchuk *In its* Coronal and Prominence Plasmas Dec. 1986 p 57-61 Sponsored in part by Navy (For primary document see N87-20871 13-92)
Avail: NTIS HC A19/MF A01 CSCL 03B

Quiescent prominences represent a significant challenge to our understanding of the flow of mass and energy in the outer layers of the solar atmosphere. A small number of quiescent prominences contain as much mass as the entire corona (Athay, 1976). The problem then is how to get that much material into the relatively small volume of a prominence and maintain it at a temperature of 10,000 K in close proximity to material at one million K. The thermal insulation to conduction provided by the magnetic field explains the disparate temperatures. The mass source problem is less well understood. One method for supplying mass to the prominence is to siphon it from the chromosphere. The siphon mechanism begins with a magnetic loop that evolves into a configuration with a gravitational well, such as that described by Kippenhahn and Schluter (1957). This could be formed, for example, by a twist in the magnetic field. A gravitational well could also be formed by a condensation induced sag in the field. This could further enhance the condensation process. Once this well has formed, or as it is forming, the material in the well area of the loop must cool and condense to the point where radiative losses exceed any heat input. Additional material must also flow into the well from the underlying chromosphere to supply the mass required to form the prominence. One example from a series of numerical simulations that were performed to study the formation of quiescent prominences is presented. Author

N87-20881*# Oslo Univ. (Norway). Inst. of Theoretical Astrophysics.
ALFVEN-WAVE DISSIPATION: A SUPPORT MECHANISM FOR QUIESCENT PROMINENCES
Eberhart Jensen *In* NASA. Goddard Space Flight Center Coronal and Prominence Plasmas Dec. 1986 p 63-67 (For primary document see N87-20871 13-92)
Avail: NTIS HC A19/MF A01 CSCL 03B

High resolution filtergrams or spectrograms of the main body of quiescent prominences often show a very vivid dynamical picture that cannot be reconciled with static models. Even if large differences exist between individual prominences in this respect, at least parts of the prominence are usually found to be in a 'choppy', turbulent state. Evidence for systematic flows are found in local regions in the prominence and also in the transition zone in the surroundings. These two regions are probably decoupled magnetically. Alfven waves are generally believed to be responsible for the heating in the upper chromosphere and corona (Hollweg 1986). Since evidence for the presence of Alfven-waves has also been found in the solar wind field, it is highly probable that such waves are generated in the convection zone of the sun and propagated outwards in the solar atmosphere wherever a proper magnetic field is present to carry the waves. The most basic magnetic formations in the solar atmosphere are simple loops. They occur all over the solar surface and cover a large range of magnetic field strengths. Loops with the strongest magnetic fields are found in active regions. It is to be expected that the Alfven-wave flux which is channelled into the loops from below, could show considerable variation both with heliocentric latitude, with time and

locally between neighbouring loops. What happens when a magnetic loop is exposed to the appropriate Alfven-wave flux required to heat the upper solar atmosphere is examined. Author

N87-20882*# National Center for Atmospheric Research, Boulder, Colo. High Altitude Observatory.
STATIC CURRENT-SHEET MODELS OF QUIESCENT PROMINENCES
F. Wu and B. C. Low *In* NASA. Goddard Space Flight Center Coronal and Prominence Plasmas Dec. 1986 p 69-72 (For primary document see N87-20871 13-92)
Avail: NTIS HC A19/MF A01 CSCL 03B

A particular class of theoretical models idealize the prominence to be a discrete flat electric-current sheet suspended vertically in a potential magnetic field. The weight of the prominence is supported by the Lorentz force in the current sheet. These models can be extended to have curved electric-current sheets and to vary three-dimensionally. The equation for force balance is 1 over 4 pi (del times B) times Bdel p- p9 z=zero. Using Cartesian coordinates we take, for simplicity, a uniform gravity with constant acceleration g in the direction -z. If we are interested not in the detailed internal structure of the prominence, but in the global magnetic configuration around the prominence, we may take prominence plasma to be cold. Consideration is given to how such equilibrium states can be constructed. To simplify the mathematical problem, suppose there is no electric current in the atmosphere except for the discrete currents in the cold prominence sheet. Let us take the plane z =0 to be the base of the atmosphere and restrict our attention to the domain z greater than 0. The task we have is to solve for a magnetic field which is everywhere potential except on some free surface S, subject to suit able to boundary conditions. The surface S is determined by requiring that it possesses a discrete electric current density such that the Lorentz force on it is everywhere vertically upward to balance the weight of the material m(S). Since the magnetic field is potential in the external atmosphere, the latter is decoupled from the magnetic field and its plane parallel hydrostatic pressure and density can be prescribed. Author

N87-20883*# California Inst. of Tech., Pasadena. Solar Astronomy.
RECENT OBSERVATIONS OF THE FORMATION OF FILAMENTS
Sara F. Martin *In* NASA. Goddard Space Flight Center Coronal and Prominence Plasmas Dec. 1986 p 73-80 (For primary document see N87-20871 13-92)
(Grants NGL-05-002-034; NAG5-766; NSF ATM-82-11002; AF-AFOSR-0018-82)
Avail: NTIS HC A19/MF A01 CSCL 03B

Two examples of the formation of small filaments in H alpha are described and illustrated. In both cases, the formation is seen to be the spontaneous appearance of strands of absorbing mass that evolve from no previous structure. The initial development of the filaments appears to consist of the accumulation of these absorptive strands along approximately parallel paths in a channel between large-scale, opposite polarity magnetic fields on either side of the filaments. The strands exhibit continuous changes in shape and degree of absorption which can be due to successive condensations resulting in new strands, mass motions within the strands, and outflow of the mass from the strands. For at least several hours before the formation of both filaments, small-scale fragments of opposite polarity, line-of-sight magnetic flux adjacent to or immediately below the filaments, and at the ends of the filaments, were cancelling. This type of magnetic flux disappearance continued during the development of the filaments and is commonly observed in association with established filaments. Cancellation is interpreted as an important evolutionary change in the magnetic field that can lead to configurations suitable for the formation of filaments. Author

N87-20884*# National Center for Atmospheric Research, Boulder, Colo. High Altitude Observatory.
ON THE FORMATION OF ACTIVE REGION PROMINENCES (H ALPHA FILAMENTS)
Bogdan Rompolt and Thomas Bogdan *In* NASA. Goddard Space Flight Center Coronal and Prominence Plasmas Dec. 1986 p 81-87 Sponsored in part by NSF (For primary document see N87-20871 13-92)
Avail: NTIS HC A19/MF A01 CSCL 03B

Analysis of sequential H alpha images of active region prominence formation suggests that simple large-scale photospheric mass-motions may play a key role in the formation of these long, thin, H alpha filaments. Author

N87-20885*# Centre National de la Recherche Scientifique, Verrieres-Le Buisson (France). Lab. de Physique Stellaire et Planetaire
DIAGNOSTICS AND STRUCTURE
J. C. Vial *In* NASA. Goddard Space Flight Center Coronal and Prominence Plasmas Dec. 1986 7 p (For primary document see N87-20871 13-92)
Avail: NTIS HC A19/MF A01 CSCL 03B

The structure of prominences and the diagnostic techniques used to evaluate their physical parameters are discussed. These include electron temperature, various densities (n sub p, n sub e, n sub I), ionization degree, velocities, and magnetic field vector. UV and radio measurements have already evidenced the existence of different temperature regions, corresponding to different geometrical locations, e.g., the so called Prominence-Corona (P-C) interface. Velocity measurements are important for considering formation and mass balance of prominences but there are conflicting velocity measurements which have led to the basic question: what structure is actually observed at a given wavelength; what averaging is performed within the projected slit area during the exposure time? In optically thick lines, the question of the formation region of the radiation along the line of sight is also not a trivial one. The same is true for low resolution measurements of the magnetic field. Coupling diagnostics with structure is now a general preoccupation. Author

N87-20886*# Oslo Univ. (Norway). Inst. of Theoretical Astrophysics.
TEMPERATURES OF QUIESCENT PROMINENCES MEASURED FROM HYDROGEN PASCHEN AND CaII IR LINES
Oddbjorn Engvold and Nils Brynildsen *In* NASA. Goddard Space Flight Center, Coronal and Prominence Plasmas Dec. 1986 p 97-107 Sponsored in part by Norwegian Research Council for Scicences and the Humanities (For primary document see N87-20871 13-92)
Avail: NTIS HC A19/MF A01 CSCL 03B

During 12 to 17 September 1983 a number of prominences were observed with the McMatch solar telescope of National Solar Observatories, using the Fourier transform spectrometer with a InSb detector (Brault 1979). The present study refers to three prominences observed 13 and 14 September. Prominence A: Large quiescent prominence at S28 E90 Prominence B. Stable prominence in weakly enhanced magnetic region at about NO8 E90 Prominence C: Quiescent prominence at N30 E90. Spectra were obtained at a total of 15 different locations in the three prominences in the wavelength range lambda, lambda 7740 to 14,000 Angstroms. The observed differences between T sub exc and T sub kin are hardly significant. Researchers conclude that the two methods for temperature determination when applied to optically thin lines give reasonably consistent results, i.e., the population of the excited levels of hydrogen is collisionally controlled. The well known increase in T and V towards the edge of equiescent prominences (Hirayama 1964) is not corroborated by the present data. One explanation for this could be that prominence A is atypical. The optical thickness of prominence emission lines tends to increase from center to edges as demonstrated by the case of He I lambda 10830 angstroms. If line opacity plays a significant role in earlier center to edge determinations of T and V, a smaller variation would be expected from measurements in optically thin lines, such as in the present case. Author

N87-20887*# Tokyo Astronomical Observatory, Mitaka (Japan).
DARK FILAMENTS OBSERVED AT 8.3mm AND 3.1mm WAVELENGTH
E. Hiei, M. Ishiguro, T. Kosugi, and K. Shibasaki (Nagoya Univ., Toyokawa, Japan.) *In* NASA. Goddard Space Flight Center Coronal and Prominence Plasmas Dec. 1986 p 109-116 (For primary document see N87-20871 13-92)
Avail: NTIS HC A19/MF A01 CSCL 03B

Mapping of the sun was made at 3.1mm (98 GHz) and 8.3mm (36 GHz) wavelengths with a 45m dish radio telescope at the Nobeyama Cosmic Radio Observatory. The depressions associated with large H alpha filaments are derived to be -0.2 at 8.3mm and -0.05 at 3.1mm, which are darker than the values inferred by Raoult et al. (1979). Author

N87-20888*# Maryland Univ., College Park. Astronomy Program.
VLA OBSERVATIONS OF SLAR FILAMENTS AT 6 AND 20 CM WAVELENGTHS
M. R. Kundu *In* NASA. Goddard Space Flight Center Coronal and Prominence Plasmas Dec. 1986 p 117-120 (For primary document see N87-20871 13-92)
(Grants NAG5-511; NgR21-002-199; NSF ATM-84-15388)
Avail: NTIS HC A19/MF A01 CSCL 03B

Using the Very Large Array we have observed several solar filaments at 1.5 and 5 GHz. The brightness temperatures of the filaments are 4-5 x 10 K at 20 cm and 1.5-1.6 x 10,000 K at 6 cm. The maximum temperature depressions appear to be associated with H alpha filaments. Comparison with He 10830 angstrons spectroheliogram shows that 20 cm temperature depressions correspond to the regions of reduced intensity in the He 10830 angstrons around filaments, which correspond to coronal cavities. We have studied the temperature and density structure of the transition sheath between the filament and the surrounding corona assuming that the energy radiated away is balanced by the energy conducted from the corona. Researchers find that the observations can be better explained by a model having a pressure gradient in the transition sheath around the filament. Author

N87-20889*# California Inst. of Tech., Pasadena. Solar Astronomy.
THE MICROWAVE STRUCTURE OF QUIESCENT SOLAR FILAMENTS AT HIGH RESOLUTION
Dale E. Gary *In* NASA. Goddard Space Flight Center Coronal and Prominence Plasmas Dec. 1986 121-125 (For primary document see N87-20871 13-92)
(Grant NSF ATM-83-09955)
Avail: NTIS HC A19/MF A01 CSCL 03B

High resolution very low altitude maps of a quiescent filament at three frequencies are presented. The spatial resolution (approx. 15' at 1.45 GHz, approx. 6' at 4.9 GHz, and approx. 2' at 15 GHz) is several times better than previously attained. At each frequency, the filament appears as a depression in the quiet Sun background. The depression is measurably wider and longer in extent than the corresponding H alpha filament at 1.45 GHz and 4.9 GHz, indicating that the depression is due in large part to a deficit in coronal density associated with the filament channel. In contrast, the shape of the radio depression at 15 CHz closely matches that of the H alpha filament. In addition, the 15 GHz map shows enhanced emission along both sides of the radio depression. A similar enhancement is seen in an observation of a second filament 4 days later, which suggests that the enhancement is a general feature of filaments. Possible causes of the enhanced emission are explored. Author

N87-20890*# Maryland Univ., College Park. Astronomy Program.
INTERPRETATION OF THE PROMINENCE DIFFERENTIAL EMISSIONS MEASURE FOR 3 GEOMETRIES
E. J. Schmahl and F. Q. Orrall (Hawaii Univ., Honolulu.) *In* NASA. Goddard Space Flight Center Coronal and Prominence Plasmas Dec. 1986 p 127-133 (For primary document see N87-20871 13-92)
Avail: NTIS HC A19/MF A01 CSCL 03B

Researchers have used prominence extreme ultraviolet line intensities observed from Skylab to derive the differential emission measure Q(T) in the prominence-corona (PC) interface from 3 x 10,000 to 3 times 1 million K, including the effects of Lyman Continuum absorption. Using lines both shortward and longward of the Lyman limit, researchers have estimated the importance of absorption as function of temperature. The magnitude of the absorption, as well as its rate of increase as a function of temperature, place limits on the thread scales and the character of the interfilar medium. Researchers have calculated models based on three assumed geometries: (1) threads with hot sheaths and cool cores; (2) isothermal threads; and (3) threads with longitudinal temperature gradients along the magnetic field. Comparison of the absorption computed from these models with the observed absorption in prominences shows that none of the geometries is totally satisfactory. Author

N87-20891*# National Optical Astronomy Lab. Tucson, Ariz.
THE PROMINENCE-CORONA INTERFACE AND ITS RELATIONSHIP TO THE CHROMOSPHERE-CORONA TRANSITION
Douglas Rabin *In* NASA. Goddard Space Flight Center Coronal and Prominence Plasmas Dec. 1986 p 135-142 (For primary document see N87-20871 13-92)
Avail: NTIS HC A19/MF A01 CSCL 03B

The classical model of the chromosphere-corona transition does not account for the observed behavior of the differential emission measure for T approx. less than 100,000 K. Several models have been proposed to resolve this discrepancy in physically different ways. Because the observed differential emission measure at the prominence-corona interface is on average nearly the same as in the chromosphere-corona transition, prominences offer a fresh testing ground for models tailored to the chromosphere-corona transition. The researcher considered three such models and concluded that none extends in a natural way to the environment of prominences. The researcher advanced a simple idea involving thermal conduction both along and across the magnetic field from the corona into cool threads. Author

N87-20892*# Observatoire de Paris-Meudon (France).
THERMAL STABILITY ANALYSIS OF THE FINE STRUCTURE OF SOLAR PROMINENCES
Pascal Demoulin, Jean-Marie Malherbe, Brigitte Schmieder, and Mickael A. Raadu (Royal Inst. of Tech., Stockholm, Sweden.) *In* NASA. Goddard Space Flight Center Coronal and Prominence Plasmas Dec. 1986 p 143-147 (For primary document see N87-20871 13-92)
Avail: NTIS HC A19/MF A01 CSCL 03B

The linear thermal stability of a 2D periodic structure (alternatively hot and cold) in a uniform magnetic field is analyzed. The energy equation includes wave heating (assumed proportional to density), radiative cooling and both conduction parallel and orthogonal to magnetic lines. The equilibrium is perturbed at constant gas pressure. With parallel conduction only, it is found to be unstable when the length scale 1// is greater than 45 Mn. In that case, orthogonal conduction becomes important and stabilizes the structure when the length scale is smaller than 5 km. On the other hand, when the length scale is greater than 5 km, the thermal equilibrium is unstable, and the corresponding time scale is about 10,000 s: this result may be compared to observations showing that the lifetime of the fine structure of solar prominences is about one hour; consequently, our computations suggest that the size of the unresolved threads could be of the order of 10 km only. Author

N87-20893*# Tokyo Astronomical Observatory, Mitaka (Japan).
THE DENSITY AND THICKNESS OF QUIESCENT PROMINENCES
Tadashi Hirayama *In* NASA. Goddard Space Flight Center Coronal and Prominence Plasmas Dec. 1986 p 149-153 (For primary document see N87-20871 13-92)

Avail: NTIS HC A19/MF A01 CSCL 03B

The electron density was determined for a number of quiescent prominences at various positions from the Stark effect. It was found that the intensity ratio of Mg I emission lines to SrII lines is independent of the observed electron density in the range of ten to the 10.2 power to 10 to the 11.4 power cm-3. This contrasts with Landman's (1984) theoretical expectation that the ratio is proportional to the electron density. From the intensity of Balmer lines and the electron density, it is inferred that the true diameter of a thread in prominence of high electron density may be smaller than 0.2'. The averaged total number density of hydrogen N sub H sub of was found to be 3-6 times 10 to the 11th power cm-3, leading to a total gas pressure P =0.6 dyn cm-2 and a total density of approx. 10 to the minus twelth power g cm-3. Landman's large value of N sub H approx. 6 times 10 to the 12th power and P sub g approx. 6 may have resulted either from the fact that he has treated very bright prominences and/or from the derivation of the high electron density for all prominences he studied. Author

N87-20894*# Ceskoslovenska Akademie Ved, Ondrejov. Astronomical Inst.

PARTIAL REDISTRIBUTION EFFECTS IN THE FORMATION OF HYDROGEN LINES IN QUIESCENT PROMINENCES

P. Heinzel, P. Gouttebroze (Centre National de la Recherche Scientifique, Verrieres-Le Buisson, France.), and J. C. Vial *In* NASA. Goddard Space Flight Center Coronal and Prominence Plasmas Dec. 1986 p 155-167 (For primary document see N87-20871 13-92)

Avail: NTIS HC A19/MF A01 CSCL 03B

Departures from complete frequency redistribution (CRD) in hydrogen lines are investigated for solar prominences. Partial redistribution effects (PRD) are found both in the wings (their already known lowering) and in the central part of the L alpha line; a new feature is evidenced here: the partially coherent scattering in the near wings of the line leads to a double-peaked profile mirroring the incident solar radiation. With a low density model, we obtain a good agreement with OSO 8 observed profiles. On the contrary, the PRD computed L beta profile (lower density, no reversal) departs from the observed one, a result which calls for more progress in terms of non-LTE transfer and modelling. Author

N87-20895*# Ceskoslovenska Akademie Ved, Ondrejov. Astronomical Inst.

NON-LTE HYDROGEN-LINE FORMATION IN MOVING PROMINENCES

P. Heinzel and B. Rompolt (National Center for Atmospheric Research, Boulder, Colo.) *In* NASA. Goddard Space Flight Center Coronal and Prominence Plasmas Dec. 1986 p 163-167 (For primary document see N87-20871 13-92)

Avail: NTIS HC A19/MF A01 CSCL 03B

The behavior of hydrogen-line brightness variations, depending on the prominence-velocity changes were investigated. By solving the NON-Local thermodynamic equilibrium (LTE) problem for hydrogen researchers determine quantitatively the effect of Doppler brightening and/or Doppler dimming (DBE, DDE) in the lines of Lyman and Balmer series. It is demonstrated that in low-density prominence plasmas, DBE in H alpha and H beta lines can reach a factor of three for velocities around 160 km/sec, while the L alpha line exhibits typical DDE. L beta brightness variations follow from a combined DBE in the H alpha and DDE in L alpha and L beta itself, providing that all relevant multilevel interlocking processes are taken into account. Author

N87-20896*# Oslo Univ. (Norway). Inst. of Theoretical Astrophysics

VERTICAL MOTIONS IN THE QUIESCENT PROMINENCES OBSERVED IN THE He I LAMBDA10830ANGSTROM LINE

Oddbjorn Engvold and Stephen L. Keil (Sacramento Peak Observatory, Sunspot, N. Mex.) *In* NASA. Goddard Space Flight Center Coronal and Prominence Plasmas Dec. 1986 p 169-175 (For primary document see N87-20871 13-92)

Avail: NTIS HC A19/MF A01 CSCL 03B

The observations contain two-dimensional spectral scans of a total of 17 different prominences on the solar disk from the period 3 to 9 May 1981, using the main spectrograph of the solar vacuum telescope at Sacramento Peak. The following conclusions may be drawn from the data: (1) Blue shifts are much more common than red shifts. In many cases more than 90 per cent of the projected prominence area is associated with blue shifts. (2) The darkest prominence regions show the largest blue shift (v less than 3 km s-1). (3) Red shifts are most commonly seen at prominence edges. (4) The general pattern of prominence velocity persists for several hours. On the scale of about 10 arcsec and less, changes are detectable in the course of 2 to 5 minutes. The observed predominance of the blue shifts is largely in agreement with earlier results from H alpha (cf. Martres et al. 1981). It cannot, however, be concluded definitely that the observed shift really represents a net flow of matter. The situation could possibly be analogous to that of the solar transition region where lines such as C IV lambda 1548 angstroms seem to indicate a net inflow, which can hardly be true, at velocities greater than 4 km s(-1) in the quiet Sun (Athay et al. 1983; Gurman and Athay 1983). If the typical structure element of the prominence is sub-resolution, i.e., 2 to 3 arcsec or worse, as in the present case, an apparent net shift could result if the ascending and the decending elements have different temperature and/or pressure. Different lines could then indicate different flow velocities and even opposite directions. Author

N87-20897*# National Aeronautics and Space Administration. Goddard Space Flight Center, Greenbelt, Md.

CONSTRAINTS ON FILAMENT MODELS DEDUCED FROM DYNAMICAL ANALYSIS

G. Simon (Observatoire de Paris-Meudon, France.), B. Schmieder, P. Demoulin, J. M. Malherbe, and A. I. Poland *In its* Coronal and Prominence Plasmas Dec. 1986 p 177-182 (For primary document see N87-20871 13-92)

Avail: NTIS HC A19/MF A01 CSCL 03B

The conclusions deduced from simultaneous observations with the Ultra-Violet Spectrometer and Polarimeter (UVSP) on the Solar Maximum Mission satellite, and the Multichannel Subtractive Double Pass (MSPD) spectrographs at Meudon and Pic du Midi observatories are presented. The observations were obtained in 1980 and 1984. All instruments have almost the same field of view and provide intensity and velocity maps at two temperatures. The resolution is approx. 0.5 to 1.5' for H alpha line and 3' for C IV. The high resolution and simultaneity of the two types of observations allows a more accurate description of the flows in prominences as functions of temperature and position. The results put some contraints on the models and show that dynamical aspects must be taken into account. E.R.

N87-20898*# Naval Research Lab., Washington, D. C. Center for Space Research.

C IV DOPPLER SHIFTS OBSERVED IN ACTIVE REGION FILAMENTS

J. A. Klimchuk *In* NASA. Goddard Space Flight Center Coronal and Prominence Plasmas Dec. 1986 p 183-190 Sponsored in part by NSF (For primary document see N87-20871 13-92)

Avail: NTIS HC A19/MF A01 CSCL 03B

The Doppler shift properties of 21 active region filaments were studied using C IV Dopplergram data. Most are associated with corridors of weak magnetic field that separate opposite polarity strong fields seen in photospheric magnetograms. A majority of the filaments are relatively blue shifted, although several lie very close to the dividing lines between blue and red shift. Only one filament in the samples is clearly red shifted. A new calibration procedure for Dopplergrams indicates that sizable zero point offsets are often required. The center-to-limb behavior of the resulting absolute Doppler shifts suggests that filament flows are usually quite small. It is possible that they vanish. Author

N87-20899*# Applied Research Corp., Landover, Md.

SEARCHING THE UVSP DATABASE AND A LIST OF EXPERIMENTS SHOWING MASS MOTIONS c82

William Thompson *In* NASA. Goddard Space Flight Center Coronal

and Prominence Plasmas Dec. 1986 p 191-196 (For primary document see N87-20871 13-92)
Avail: NTIS HC A19/MF A01 CSCL 05B

Since the Solar Maximum Mission (SMM) satellite was launched, a large database has been built up of experiments using the Ultraviolet Spectrometer and Polarimeter (UVSP) instrument. Access to this database can be gained through the SMM Vax 750 computer at Goddard Space Flight Center. One useful way to do this is with a program called USEARCH. This program allows one to make a listing of different types of UVSP experiments. It is evident that this program is useful to those who would wish to make use of UVSP data, but who don't know what data is available. Therefore it was decided to include a short description of how to make use of the USEARCH program. Also described, but not included, is a listing of all UVSP experiments showing mass motions in prominences and filaments. This list was made with the aid of the USEARCH program. E.R.

N87-20900*# National Aeronautics and Space Administration. Marshall Space Flight Center, Huntsville, Ala.
ON THE EXISTENCE OF OSCILLATIONS IN SOLAR FILAMENTS OBSERVED IN H ALPHA AND C IV LINES
B. Schmieder (Observatoire de Paris-Meudon, France.), J. M. Malherbe, P. Mein, and E. Tandberg-Hanssen *In* NASA. Goddard Space Flight Center Coronal and Prominence Plasmas Dec. 1986 (For primary document see N87-20871 13-92)
Avail: NTIS HC A19/MF A01 CSCL 03B

Time sequence observations of filaments in both the H alpha line and the 1548 A C IV line were analyzed with the Fourier transform technique in the frequency range (1 - 10 mHz). No oscillation is detected in filaments except at the footpoints where a steady velocity gradient is large. The energy is probably due to convective motions rather than pressure oscillations. Author

N87-20901*# Florence Univ. (Italy). Inst. di Astronomia.
MEASUREMENTS OF MAGNETIC FIELDS IN SOLAR PROMINENCES
Egidio Landi DegliInnocenti *In* NASA. Goddard Space Flight Center Coronal and Prominence Plasmas Dec. 1986 p 203-207 (For primary document see N87-20871 13-92)
Avail: NTIS HC A19/MF A01 CSCL 03B

Magnetic fields can be measured, in solar prominences, by means of two different basic mechanisms that are responsible for the introduction (or the reduction) of a given amount of polarization in spectral lines: these are the Zeeman effect and the Hanle effect. Through the splitting of the magnetic components of a spectral line, the Zeeman effect is capable of introducing a certain amount of circular polarization across the line profile. The Hanle effect consist of a modification of the linear polarization that is induced in spectral lines by the anisotropic illumination of the prominence plasma by the photospheric radiation field. These two effects are briefly discussed. E.R.

N87-20902*# Observatoire de Paris-Meudon (France). Lab. de Physique Atomique et Moleculaire et dInstrumentation en Astrophysique.
MAGNETIC FIELD VECTOR AND ELECTRON DENSITY DIAGNOSTICS FROM LINEAR POLARIZATION MEASUREMENTS IN 14 SOLAR PROMINENCES
V. Bommier *In* NASA. Goddard Space Flight Center Coronal and Prominence Plasmas Dec. 1986 p 209-213 (For primary document see N87-20871 13-92)
Avail: NTIS HC A19/MF A01 CSCL 03B

The Hanle effect is the modification of the linear polarization parameters of a spectral line due to the effect of the magnetic field. It has been successfully applied to the magnetic field vector diagnostic in solar prominences. The magnetic field vector is determined by comparing the measured polarization to the polarization computed, taking into account all the polarizing and depolarizing processes in line formation and the depolarizing effect of the magnetic field. The method was applied to simultaneous polarization measurements in the Helium D3 line and in the hydrogen beta line in 14 prominences. Four polarization parameters are measured, which lead to the determination of the three coordinates of the magnetic field vector and the electron density, owing to the sensitivity of the hydrogen beta line to the non-negligible effect of depolarizing collisions with electrons and protons of the medium. A mean value of 1.3 x 10 to the 10th power cu. cm. is derived in 14 prominences. Author

N87-20903*# National Oceanic and Atmospheric Administration, Boulder, Colo. Space Environment Lab.
FILAMENT DISAPPEARANCES
William J. Wagner *In* NASA. Goddard Space Flight Center Coronal and Prominence Plasmas Dec. 1986 p 215-219 (For primary document see N87-20871 13-92)
Avail: NTIS HC A19/MF A01 CSCL 03B

The phenomenon of the sudden filament disappearance (Disparition Brusque) is a familiar one to observers at H alpha telescopes. Nevertheless, the importance in Disparition Brusques (DB) continues to grow for several reasons which are cited in the discussion. It is reported that there seems to be more interest on building and maintain filaments than in destroying them. As a consequence, this sub-group is smaller than most of the others. All the same, progress in this area of filament disapperences seems steady and assured. The importance and interest in DBs is discussed and future directions are indicated. Author

N87-20904*# National Aeronautics and Space Administration. Goddard Space Flight Center, Greenbelt, Md.
THE HEATING OF FILAMENTS AS A DISAPPEARANCE PROCESS
Z. Mouradian, M. J. Martres, and I. Soru-Escaut *In* NASA. Goddard Space Flight Center Coronal and Prominence Plasmas Dec. 1986 p221-223 (For primary document see N87-20871 13-92)
Avail: NTIS HC A19/MF A01 CSCL 03B

The sudden disappearance of filaments, commonly called Disparition Brusque (DB) is of two types: (1) the well known ejection of cool prominence material in the corona, i.e., a dynamic process (BDd) and (2) the heating of the prominence plasma. When the hydrogen of the filament becomes ionised, then the filament start to be visible in EUV lines keeping the same shape and position as the cool one. This process which is a thermic disapperence was named DB thermic (DBt). Successive disappearances and condensations of a quiescent filament from 13 to 17 of June 1973 was studied. This observation was provided by two instruments on Skylab ATM satellite. These observations of disappearances and condensations are discussed. E.R.

N87-20905*# Observatoire de Paris-Meudon (France).
ON THE THERMAL DURABILITY OF SOLAR PROMINENCES, OR HOW TO EVAPORATE A PROMINENCE
J. M. Malherbe and T. G. Forbes (New Hampshire Univ., Durham.) *In* NASA. Goddard Space Flight Center Coronal and Prominence Plasmas Dec. 1986 p 225-228 (For primary document see N87-20871 13-92)
(Grant NAGw-76)
Avail: NTIS HC A19/MF A01 CSCL 03B

The thermal disappearance of solar prominences under strong perturbations due to wave heating, Ohmic heating, viscous heating or conduction was investigated. Specifically, how large a thermal perturbation is needed to destroy a stable thermal equilibrium was calculated. It was found that the prominence plasma appears to be thermally very rugged. Its cold equilibrium may most likely be destroyed by either strong magnetic heating or conduction in a range of parameters which is relevant to flares. Author

N87-20906*# Observatoire de Paris-Meudon (France).
FILAMENT ERUPTION CONNECTED TO PROTOSPHERIC ACTIVITY
G. Simon, L. Gesztelyi (Hungarian Academy of Sciences, Debrecen.), B. Schmieder, and N. Mein *In* NASA. Goddard Space Flight Center Coronal and Prominence Plasmas Dec. 1986 p 229-233 (For primary document see N87-20871 13-92)
Avail: NTIS HC A19/MF A01 CSCL 03B

Two cases of activation of filaments that occured in regions of intense magnetic activity was studied. The simultaneous observations from Debrecen Observatory (white light and H alpha filtergram), and from Meudon Observatory (magnetogram, MSDP dopplergram and intensity maps in H alpha) gave a complementary set of data from which can be produced evidence of the influence of the photospheric magnetic field on the destabilization process of the filaments. On June 22, 1980, the eruption of the filament is associated with the motion of pores, which are manifestations of emerging flux knots. On September 3, 1980, the twisting motions in the filament are associated to the birth of a pore in its neighborhood. These observations are discussed. E.R.

N87-20907*# Los Alamos National Lab., N. Mex.
MAGNETIC FIELD RE-ARRANGEMENT AFTER PROMINENCE ERUPTION
R. A. Kopp and G. Poletto (Florence Univ., Italy.) *In* NASA. Goddard Space Flight Center Coronal and Prominence Plasmas Dec. 1986 p 235-239 Previously announced as N87-13382 (For primary document see N87-20871 13-92)
Avail: NTIS HC A19/MF A01 CSCL 03B

It has long been known that magnetic reconnection plays a fundamental role in a variety of solar events. Although mainly invoked in flare problems, large scale loops interconnecting active regions, evolving coronal hole boundaries, the solar magnetic cycle itself, provide different evidence of phenomena which involve magnetic reconnection. A further example might be given by the magnetic field rearrangement which occurs after the eruption of a prominence. Since most often a prominence reforms after its disappearance and may be observed at about the same position it occupied before erupting, the magnetic field has to undergo a temporary disruption of relax back, via reconnection, to a configuration similar to the previous one. The above sequence of events is best observable in the case of two ribbon (2-R) flares but most probably is associated with all filament eruptions. Even if the explanation of the magnetic field rearrangement after 2-R flares in terms of reconnection is generally accepted, the lack of a 3-dimensional model capable of describing the field reconfiguration, has prevented, up to now, a thorough analysis of its topology as traced by H alpha/x ray loops. A numerical technique is presented which enables oneto predict and visualize the reconnected configuration, at any time, and therefore allows one to make a significant comparison of observations and model predictions throughout the whole process. Author

N87-20908*# National Aeronautics and Space Administration. Goddard Space Flight Center, Greenbelt, Md.
A DYNAMIC MODEL OF FILAMENT ERUPTIONS AND TWO RIBBON FLARES
N. Paul M. Kuin and Piet C. H. Martens *In its* Coronal and Prominence Plasmas Dec. 1986 p 241-248 (For primary document see N87-20871 13-92)
Avail: NTIS HC A19/MF A01 CSCL 03B

Two basically different models for the filament equilibrium by Kippenhahn and Schluter (1957) and Kuperus and Raadu (1974) have appeared in the literature. A further analyses by van Tend and Kuperus (1978) added the force due to the horizontal component of the background field to the Kuperus and Raadu model. In order to obtain a better model which actually describes these phenomena, the evolution of the filament has to be considered in detail. A first attempt was recently presented by Kaastra. Kaastra did not formulate the precise energy balance equations for the problem, as is done in the present work. In the present model not only the force balance, but also the energy balance of the filament is taken into account. Thus a fully closed system of equations is obtained, that describes the evolution of the filament, first in force equilibrium during the current build-up phase, then in the non-equilibrium phase before the eruption, and the eruption itself. A neutral point appears above the photospheric surface in the non-equilibrium phase, but long before the eruption. It was found that although the filament itself may be in non-equilibrium, the evolution may still be slow up to the height where the eruption takes place. The eruption of the filament itself causes a large induced electric field at the neutral point which leads to the observed flare phenomena. E.R.

N87-20909*# Maryland Univ., College Park. Astronomy Program.
LARGE SCALE STRUCTURE OF THE CORONA
M. R. Kundu *In* NASA. Goddard Space Flight Center Coronal and Prominence Plasmas Dec. 1986 p 249-251 (For primary document see N87-20871 13-92)
Avail: NTIS HC A19/MF A01 CSCL 03B

This is an introduction to this section of the proceedings. In this section is a brief description of some radio results obtained with meter-decameter radioheliograph. An optical study based upon synoptic data of polarized brightness (pB), H alpha line filtergrams and large scale B-fields is presented. This is followed by two papers on the interpretation of coronal mass ejection (CME) and modeling of three dimensional coronas. E.R.

N87-20910*# Maryland Univ., College Park. Astronomy Program.
LARGE SCALE STRUCTURE OF THE SUN'S RADIO CORONA
M. R. Kundu *In* NASA. Goddard Space Flight Center Coronal and Prominence Plasmas Dec. 1986 p 253-256 (For primary document see N87-20871 13-92)
(Grant NAG5-752; Contract F19628-83-K004)
Avail: NTIS HC A19/MF A01 CSCL 03B

Results of studies of large scale structures of the corona at long radio wavelengths are presented, using data obtained with the multifrequency radioheliograph of the Clark Lake Radio Observatory. It is shown that features corresponding to coronal streamers and coronal holes are readily apparent in the Clark Lake maps. Author

N87-20911*# Observatoire de Paris-Meudon (France).
SYNOPTIC STUDY OF THE CORONA AT METER WAVELENGTH
P. Lantos and C. E. Alissandrakis (Athens Univ., Greece.) *In* NASA. Goddard Space Flight Center Coronal and Prominence Plasmas Dec. 1986 p 257-261 (For primary document see N87-20871 13-92)
Avail: NTIS HC A19/MF A01 CSCL 03B

The Mark III Nancay Radioheliograph is used to observe the Sun at 169 MHz with a time resolution of 25 East-West and North-South images per second. When the brightness distribution of the Sun is stable during the eight hours of daily observation, a two dimensional map can be produced using the technique of earth rotation synthesis. The best images are obtained during the period April to August, when the declination of the Sun is high to give a good coverage in the uv plane and a reasonable North-South resolution. The spatial resolution is 1.5' East-West and in summer, 3.5' North-South. The maps are calibrated using Cygnus A as a reference. Examples of the maps are given and discussed. Author

N87-20912*# Hawaii Univ., Honolulu. Inst. for Astronomy.
THE WHITE LIGHT CORONA AND PHOTOSPHERIC MAGNETIC FIELDS
Marie K. McCabe *In* NASA. Goddard Space Flight Center Coronal and Prominence Plasmas Dec. 1986 p 263-267 (For primary document see N87-20871 13-92)
(Grant NGL12-001-011)
Avail: NTIS HC A19/MF A01 CSCL 03B

Some results are presented from a continuing investigation of the coronal structure vs. the photospheric magnetic field relationship. Two approaches to the problem are considered. First, the individual coronal features recorded at each limb were located on a chart of the magnetic field measured with low spatial resolution, depicting the large scale or global field configuration. Second, the characteristics of neutral line segments, defined by the presence of H alpha line filament, with no associated coronal structure were investigated. Preliminary results are discussed. E.R.

N87-20913*# Middlebury Coll., Vt. Dept. of Physics.
QUASISTATIC EVOLUTION OF MAGNETOSTATIC CORONAL STRUCTURES
Richard Wolfson *In* NASA. Goddard Space Flight Center Coronal and Prominence Plasmas Dec. 1986 p 269-273 (For primary document see N87-20871 13-92)
(Grant NSF ATS-83-11338)
Avail: NTIS HC A19/MF A01 CSCL 03B

Four separate but related studies of coronal magnetostatic equilibria under a variety of boundary conditions and distributions of coronal current are reviewed. Physically, all four studies assume an axisymmetric corona whose radial magnetic field at the coronal base is dipolar. Electric currents in the model coronas are assumed to flow in the azimuthal direction, giving rise to Lorentz forces that must be balanced by pressure gradients and gravity. Mathematically, such coronas are described by the equation of magnetostatic force balance and Ampere's law. Although highly idealized, the axisymmetric magnetostatic models described provide insights into the behavior of a variety of coronal structures. The models show how more realistic current sheet boundary conditions and coronal density variations may be modeled. Author

N87-20914*# National Center for Atmospheric Research, Boulder, Colo. High Altitude Observatory.
THREE-DIMENSIONAL MAGNETOSTATIC MODELS OF THE LARGE-SCALE CORONA
T. J. Bogdan and B. C. Low *In* NASA. Goddard Space Flight Center Coronal and Prominence Plasmas Dec. 1986 p 275-278 Sponsored in part by NSF (For primary document see N87-20871 13-92)
Avail: NTIS HC A19/MF A01 CSCL 03B

A special class of magnetostatic equilibria is described, which are mathematically simple and yet sufficiently versatile so as to fit any arbitrary normal magnetic flux prescribed at the photosphere. With these solutions, the corona can be modeled with precisely the same mathematically simple procedure as has previously been done with potential fields. The magnetostatic model predicts, in addition to the coronal magnetic field, the three dimensional coronal density which can be compared with coronagraph observations. E.R.

N87-20915*# Tufts Univ., Medford, Mass. Dept. of Physics and Astronomy.
CORONAL DIAGNOSTICS.
Kenneth R. Lang *In* NASA. Goddard Space Flight Center Coronal and Prominence Plasmas Dec. 1986 p 279-289 (For primary document see N87-20871 13-92)
(Grant NAG5-501; Contract N0014-86-K-0068; Grant AF-AFOSR-0019-83)
Avail: NTIS HC A19/MF A01 CSCL 03B

This is an introduction to this part of the proceedings and an overview of coronal diagnostics. The current understanding of coronal loops is summarized. Included are observations from ground-based radio telescopes and from X ray telescopes lofted above the atmosphere, as well as theoretical interpretations of these observations. Also included in these introductory remarks is a discussion of the three dimensional structure of coronal loops. Alternative radiation mechanisms are then described within the context of both the radio and X ray emission. Various methods of determining the strength and structure of the coronal magnetic field are then described, followed by the coronae of nearby stars and future prospects for radio diagnostic of coronal loops. E.R.

N87-20916*# Maryland Univ., College Park. Astronomy Program.
THREE DIMENSIONAL STRUCTURES OF SOLAR ACTIVE REGIONS
M. R. Kundu *In* NASA. Goddard Space Flight Center Coronal and Prominence Plasmas Dec. 1986 p 291-295 (For primary document see N87-20871 13-92)
Avail: NTIS HC A19/MF A01 CSCL 03B

Three dimensional structure of an active region is determined from observations with the Very Large Array (VLA) at 2, 6, and 20 cm. This region exhibits a single magnetic loop of length approx. 10 to the 10th power cm. The 2 cm radiation is mostly thermal bremsstrahlung and originates from the footpoints of the loop. The 6 and 20 cm radiation is dominated by the low harmonic gyroresonance radiation and originates from the upper portion of the legs or the top of the loop. The loop broadens toward the apex. The top of the loop is not found to be the hottest point, but two temperature maxima on either side of the loop apex are observed, which is consistent with the model proposed for long loops. From 2 and 6 cm observations it can be concluded that the electron density and temperature cannot be uniform in a plane perpendicular to the axis of the loop; the density should decrease away from the axis of the loop. Author

N87-20917*# National Aeronautics and Space Administration. Goddard Space Flight Center, Greenbelt, Md.
HIGH-SPATIAL-RESOLUTION MICROWAVE AND RELATED OBSERVATIONS AS DIAGNOSTICS OF CORONAL LOOPS
Gordon D. Holman *In its* Coronal and Prominence Plasmas Dec. 1986 p 297-301 (For primary document see N87-20871 13-92)
Avail: NTIS HC A19/MF A01 CSCL 03B

High spatial resolution microwave observations of coronal loops, together with theoretical models for the loop emission, can provide detailed information about the temperature, density, and magnetic field within the loop, as well as the environment around the loop. The capability for studying magnetic fields is particularly important, since there is no comparable method for obtaining direct information about coronal magnetic fields. Knowledge of the magnetic field strength and structure in coronal loops is important for understanding both coronal heating and flares. With arc-second-resolution microwave observations from the Very Large Array (VLA), supplemental high-spectral-resolution microwave data from a facility such as the Owens Valley frequency-agile interferometer, and the ability to obtain second-of-arc resolution EUV aor soft X ray images, the capability already exists for obtaining much more detailed information about coronal plasma and magnetic structures than is presently available. This capability is discussed. Author

N87-20918*# National Aeronautics and Space Administration. Goddard Space Flight Center, Greenbelt, Md.
THEORETICAL MODELS OF FREE-FREE MICROWAVE EMISSION FROM SOLAR MAGNETIC LOOPS
Jeffrey W. Brosius and Gordon D. Holman *In its* Coronal and Prominence Plasmas Dec. 1986 p 303-307 (For primary document see N87-20871 13-92)
Avail: NTIS HC A19/MF A01 CSCL 03B

The free-free microwave emission is calculated from a series of model magnetic loops. The loops are surrounded by a cooler external plasma, as required by recent simultaneous X ray and microwave observations, and a narrow transition zone separating the loops from the external plasma. To be consistent with the observational results, upper limits on the density and temperature scale lengths in the transition zone are found to be 360 km and 250 km, respectively. The models which best produce agreement with X ray and microwave observations also yielded emission measure curves which agree well with observational emission measure curves for solar active regions. E.R.

N87-20919*# Tufts Univ., Medford, Mass. Dept. of Physics and Astronomy.
CORONAL PLASMAS ON THE SUN AND NEARBY STARS
Kenneth R. Lang *In its* Coronal and Prominence Plasmas Dec. 1986 p 303-317 (For primary document see N87-20871 13-92)
(Grant NAG5-501; Contract N0014-86-K-0068; Grant AF-AFOSR-0019-83)
Avail: NTIS HC A19/MF A01 CSCL 03B

The current understanding of the quiescent, or non-flaring, microwave emission from solar active regions is summarized. The thermal radiation mechanisms that account for most of the quiescent emission is reviewed, while it is also pointed out that current-amplified magnetic fields or non-thermal radiation may be required in some instances. The 20 cm radiation of coronal loops and the thermal cyclotron lines that accurately specify their

magnetic field strength are discussed. The 20 cm and X ray emission of the coronal plasma are then compared. The coronae of nearby stars is next discussed, where coherent radiation processes seem to prevail. Some thoughts toward directions for future exploration are given. E.R.

N87-20920*# California Inst. of Tech., Pasadena. Solar Astronomy.

MEASUREMENT OF CORONAL FIELDS USING SPATIALLY RESOLVED MICROWAVE SPECTROSCOPY

G. J. Hurford and D. E. Gary *In* NASA. Goddard Space Flight Center Coronal and Prominence Plasmas Dec. 1986 p 319-323 (For primary document see N87-20871 13-92)

(Contract F19628-84-K-0023; Grants NSF ATM-83-09955; NSF ATM-86-10330; NSF AST-83-15217)
Avail: NTIS HC A19/MF A01 CSCL 03B

The potential implications of observations which combine both high spatial and high spectral resolution are considered. In particular, interest is on the ability to measure the magnetic field at the base of the corona on a point by point basis, as in a true magnetograph. Model calculations are presented of the microwave brightness temperature spectrum along specific lines of sight near a sunspot. E.R.

N87-20921*# Iowa Univ., Iowa City. Dept. of Physics and Astronomy.

GUIDED MHD WAVES AS A CORONAL DIAGNOSTIC TOOL

B. Roberts *In* NASA. Goddard Space Flight Center Coronal and Prominence Plasmas Dec. 1986 p 325-327 (For primary document see N87-20871 13-92)

(Grant NGL-16-001-043)
Avail: NTIS HC A19/MF A01 CSCL 03B

A description is provided of how fast magnetoacoustic waves are ducted along regions of low Alfven velocity (high density) in the corona, exhibiting a distinctive wave signature which may be used as a diagnostic probe of in situ coronal conditions (magnetic field strength, density inhomogeneity, etc.). Some observational knowledge of the start time of the impulsive wave source, possibly a flare, the start and end times of the generated wave event, and the frequency of the pulsations in that event permits a seismological deduction of the physical properties of the coronal medium in which the wave propagated. With good observations the theory offers a new means of probing the coronal atmosphere. Author

N87-20922*# Emmanuel Coll., Boston, Mass.

SMALL-SCALE CORONAL STRUCTURE, PART 3

David F. Webb *In* NASA. Goddard Space Flight Center Coronal and Prominence Plasmas Dec. 1986 p 329-342 Prepared in cooperation with American Science and Engineering, Inc., Cambridge, Mass. (For primary document see N87-20871 13-92)

Avail: NTIS HC A19/MF A01 CSCL 03B

Recent observations and models pertaining specifically to solar coronal bright points (BPs) and generally to small-scale coronal structure are reviewed. Two questions were addressed: What is the degree of correspondence among various alleged signatures of BPs at different levels of atmosphere and what can PBs tell about the emerging flux spectrum of the sun? B.G.

N87-20923*# Harvard-Smithsonian Center for Astrophysics, Cambridge, Mass.

SIMULTANEOUS OBSERVATIONS OF CHANGES IN CORONAL BRIGHT POINT EMISSION AT THE 20 cm RADIO AND He LAMBDA 10830 WAVELENGTHS

Shadia R. Habbal and Karen L. Harvey (Solar Physics Research Corp., Tucson, Ariz.) *In* NASA. Goddard Space Flight Center Coronal and Prominence Plasmas Dec. 1986 p 343-347 (For primary document see N87-20871 13-92)

(Contract NAS5-28728; Grant NgR21-002-199)
Avail: NTIS HC A19/MF A01 CSCL 03B

Preliminary results of observations of solar coronal bright points acquired simultaneously from ground based observatories at the radio wavelength of 20 cm and in the He I wavelength 10830 line on September 8, 1985, are reported. The impetus for obtaining simultaneous radio and optical data is to identify correlations, if any, in changes of the low transition-coronal signatures of bright points with the evolution of the magnetic field, and to distinguish between intermittent heating and changes in the magnetic field topology. Although simultaneous observations of H alpha emission and the photospheric magnetic field at Big Bear were also made, as well as radio observations from Owen Valley Radio Interferometer and Solar Maximum Mission (SSM) (O VIII line), only the comparison between He 10830 and the Very Large Array (VLA) radio data are presented. B.G.

N87-20924*# Maryland Univ., College Park. Astronomy Program.

VLA OBSERVATIONS OF CORONAL BRIGHT POINTS AT 6 AND 20 cm WAVELENGTHS

M. R. Kundu *In* NASA. Goddard Space Flight Center Coronal and Prominence Plasmas Dec. 1986 p 349-351 (For primary document see N87-20871 13-92)

Avail: NTIS HC A19/MF A01 CSCL 03B

Prior to and during the Spacelab-2 operation, observations were made at 6 and 20 cm of solar coronal bright points, using the Very Large Array (VLA) in the C-configuration. The ultraviolet coverage ranged from 200 to 18,000 wavelengths. The maps were convolved with beams of 18 x 18 inches at 20 km and 4 x 4 inches at 6 cm. Only the preliminary results from July 15 and July 31, 1985 observations. B.G.

N87-20925*# Tufts Univ., Medford, Mass. Dept. of Physics and Astronomy.

COMPACT, VARIABLE, MOVING SOURCES OBSERVED ON THE SUN AT 2 CENTIMETERS WAVELENGTH

Kenneth R. Lang and Robert F. Willson *In* NASA. Goddard Space Flight Center Coronal and Prominence Plasmas Dec. 1986 p 353-357 (For primary document see N87-20871 13-92)

(Contract N0014-86-K-0068; Grant AF-AFOSR-0019-83)
Avail: NTIS HC A19/MF A01 CSCL 03B

The Very Large Array (VLA) was used to observe the active region AT 4508 in the C-configuration between 1530 and 2330 UT on June 4, 1984. The position of this region was N06 E57 at 1300 UT on this day. Followup observations were made between 1500 and 2300 UT on January 17, 1986 in the D-configuration. Observations were compared with Mt. Wilson magnetograms. Results are discussed. B.G.

N87-20926*# Solar Physics Research Corp., Tucson, Ariz.

THE ASSOCIATION OF CHROMOSPHERIC AND CORONAL PHENOMENA WITH THE EVOLUTION OF THE QUIET SUN MAGNETIC FIELDS

Karen L. Harvey, Frances Tang (California Inst. of Tech., Pasadena.), and Victor Gaizauskas (National Research Council of Canada, Ottawa, Ontario.) *In* NASA. Goddard Space Flight Center Coronal and Prominence Plasmas Dec. 1986 p 359-363 (For primary document see N87-20871 13-92)

(Contract NAS5-28728; NA84-RA-A06789)
(ESD-TR-84-611) Avail: NTIS HC A19/MF A01 CSCL 03B

Using daily full-disk magnetograms and He I 10830 spectroheliograms to study the count and surface distribution of ephemeral regions over the solar cycle, Harvey (1985) concluded that the small dark structures seen in 10830, thought to correspond to X-ray bright points, were more often associated with magnetic bipoles that appeared to result from an encounter of already existing opposite polarity magentic flux than with emerging small magnetic bipoles (ephemeral regions). Such encounters would be more likely to occur in areas of mixed polarity. The fractional area of the sun covered by mixed polarity fields varies anti-correlated with the solar cycle leading to a possible explanation for the 180 degrees out of phase solar cycle variation of X-ray bright points. To establish the validity of this suggestion, a detailed study of time-sequence magnetic field, He I wavelength 10830, Ha, C IV, and Si II observations of selected areas of the quiet sun was initiated about 2 years ago. The preliminary results of this study are reported. Author

N87-20927*# Smithsonian Astrophysical Observatory, Cambridge, Mass.
MAGNETOGRAM AND SOFT X-RAY COMPARISONS OF XBP AND ER
Leon Golub, Karen L. Harvey (Solar Physics Research Corp., Tucson, Ariz.), and David F. Webb (Air Force Geophysics Lab., Hanscom AFB, Mass.) *In* NASA. Goddard Space Flight Center Coronal and Prominence Plasmas Dec. 1986 p 365-367 (For primary document see N87-20871 13-92)
(Grant NAGw-112)
Avail: NTIS HC A19/MF A01 CSCL 03B

The potential importance of the smallest emerging flux regions on the sun was discussed in numerous publications. The association between the objects seen in ground-based data, such as high resolution magnetrons or H alpha and soft X-ray data has produced results which are often contradictory. In the hope of resolving the present impasse, as much simultaneous soft X-ray and magnetogram data as possible were assembled in order to clarify the situation. It was found that separation of magnetic features into chance encounters and emerging flux makes some difference in overlapp with X-ray bright points (XBPs), although the effect is not overwhelming. The difference in solar cycle dependence between XBP and ephemeral regions is not explainable in terms of the results. B.G.

N87-20928*# California Inst. of Tech., Pasadena. Infrared Processing and Analysis Center.
SMALL-SCALE ERUPTIVE FILAMENTS ON THE QUIET SUN
Linda M. Hermans and Sara F. Martin *In* NASA. Goddard Space Flight Center Coronal and Prominence Plasmas Dec. 1986 p 369-375 (For primary document see N87-20871 13-92)
(Grants NGL05-002-034; NSF ATM-82-11002; AF-AFOSR-00118-82; AF-AFOSR-0018-82)
Avail: NTIS HC A19/MF A01 CSCL 03B

A study of a little known class of eruptive events on the quiet sun was conducted. All of 61 small-scale eruptive filamentary structures were identified in a systematic survey of 32 days of H alpha time-lapse films of the quiet sun acquired at Big Bear Solar Observatory. When fully developed, these structures have an average length of 15 arc seconds before eruption. They appear to be the small-scale analog of large-scale eruptive filaments observed against the disk. At the observed rate of 1.9 small-scale eruptive features per field of view per average 7.0 hour day, the rate of occurence of these events on the sun were estimated to be greater than 600 per 24 hour day.. The average duration of the eruptive phase was 26 minutes while the average lifetime from formation through eruption was 70 minutes. A majority of the small-scale filamentary sturctures were spatially related to cancelling magnetic features in line-of-sight photospheric magnetograms. Similar to large-scale filaments, the small-scale filamentary structures sometimes divided opposite polarity cancelling fragments but often had one or both ends terminating at a cancellation site. Their high numbers appear to reflect the much greater flux on the quiet sun. From their characteristics, evolution, and relationship to photospheric magnetic flux, it was concluded that the structures described are small-scale eruptive filaments and are a subset of all filaments. Author

N87-20929*# Swarthmore Coll., Pa.
OBSERVATIONS OF THE Ca II K LINE IN HeI0830A DARK POINTS ON AUGUST 3, 1985
Rush D. Holt, Albert H. Park, Joseph C. Thompson, and D. M. Mullan (Delaware Univ., Newark.) *In* NASA. Goddard Space Flight Center Coronal and Prominence Plasmas Dec. 1986 p 377-381 Sponsored in part by Swarthmore College, Pa. (For primary document see N87-20871 13-92)
(Grant NSF ATM-82-10936)
Avail: NTIS HC A19/MF A01 CSCL 03B

Spectroheliograms taken in the light of He I 10830 A at the National Solar Observatory Vacuum Telescope on Kitt Peak were used to identify coronal holes and bright points (BPs). Target points were identified, coordinates calculated, and spectra recorded. For each spectrum, the difference in wavelength between the Ca II K minimum and the FeI reference line was calculated. It was noteworthy that the overall effect is a blueshift. It should be noted that if material of chromospheric density moves outward at this velocity, it could supply the mass flux of the solar wind if this chromospheric flow was concentrated in a few dozen sources, each of a diameter of a few arc seconds. B.G.

N87-20930*# National Aeronautics and Space Administration. Marshall Space Flight Center, Huntsville, Ala.
MAGNETIC LOCATION OF C IV EVENTS IN THE QUIET NETWORK
Jason G. Porter, Ed J. Reichmann, Ronald L. Moore, and Karen L. Harvey (Solar Physics Research Corp., Tucson, Ariz.) *In* NASA. Goddard Space Flight Center Coronal and Prominence Plasmas Dec. 1986 p 383-387 (For primary document see N87-20871 13-92)
Avail: NTIS HC A19/MF A01 CSCL 03B

Ultraviolet Spectrograph and Polarimeter (UVSP) observations of C IV intensity in the quiet sun were examined and compared to magnetograms and He I 10830 A spectroheliograms from Kitt Peak National Laboratory. The observations were made between 3 and 9 April, 1985. Spatially rastered UVSP intensity measurements were obtained at 11 wavelength positions in the 1548 A line of C IV. It was concluded that the stochastic process whereby convective shuffling of loop footprints leads to many topically dissipative events in active regions and the larger bipoles treated here continues to operate in regions of fewer, weaker flux loops, but the resulting events above threshold are less frequent. B.G.

N87-20931*# Naval Research Lab., Washington, D. C. Center for Space Research.
A NUMERICAL STUDY OF THE THERMAL STABILITY OF LOW-LYING CORONAL LOOPS
J. A. Klimchuk, S. K. Antiochos, and J. T. Mariska *In* NASA. Goddard Space Flight Center Coronal and Prominence Plasmas Dec. 1986 p 389-393 Sponsored in part by Navy (For primary document see N87-20871 13-92)
Avail: NTIS HC A19/MF A01 CSCL 03B

The nonlinear evolution of loops that are subjected to a variety of small but finite perturbations was studied. Only the low-lying loops are considered. The analysis was performed numerically using a one-dimensional hydrodynamical model developed at the Naval Research Laboratory. The computer codes solve the time-dependent equations for mass, momentum, and energy transport. The primary interest is the active region filaments, hence a geometry appropriate to those structures was considered. The static solutions were subjected to a moderate sized perturbation and allowed to evolve. The results suggest that both hot and cool loops of the geometry considered are thermally stable against amplitude perturbations of all kinds. B.G.

N87-20932*# Hawaii Univ., Honolulu. Inst. for Astronomy.
SMALL-SCALE STRUCTURES AND THE DENSITY IRREGULARITY OF THE INNER CORONA
F. Q. Orrall and G. J. Rottman (Colorado Univ., Boulder.) *In* NASA. Goddard Space Flight Center Coronal and Prominence Plasmas Dec. 1986 p 395-399 (For primary document see N87-20871 13-92)
(Grants NsG5-5178; NGL12-001-011)
Avail: NTIS HC A19/MF A01 CSCL 03B

The observational evidence is considered that the electron density irregularity factor is much greater than unity in the inner corona, in particular, evidence derived from the photometric comparison of the K-corona emission p Beta with the EUV emission from coronal ions. A simple mathematical model was developed for the irregularity having a minimum number of parameters. This model was used to explore some implications of the observations and to show that well-known resolved structures such as polar plumes and coronal loops as presently understood cannot alone explain the irregularity. Author

N87-20933*# National Aeronautics and Space Administration. Goddard Space Flight Center, Greenbelt, Md.

PHLEGETHON FLOW: A PROPOSED ORIGIN FOR SPICULES AND CORONAL HEATING

Kenneth H. Schatten and Hans G. Mayr *In its* Coronal and Prominence Plasmas Dec. 1986 p 401-405 (For primary document see N87-20871 13-92)

Avail: NTIS HC A19/MF A01 CSCL 03B

A model was develped for the mass, energy, and magnetic field transport into the corona. The focus is on the flow below the photosphere which allows the energy to pass into, and be dissipated within, the solar atmosphere. The high flow velocities observed in spicules are explained. A treatment following the work of Bailyn et al. (1985) is examined. It was concluded that within the framework of the model, energy may dissipate at a temperature comparable to the temperature where the waves originated, allowing for an equipartition solution of atmospheric flow, departing the sun at velocities approaching the maximum Alfven speed. B.G.

N87-20934*# National Aeronautics and Space Administration. Goddard Space Flight Center, Greenbelt, Md.

ENERGY CONVERSION IN THE CORONAL PLASMA

P. C. H. Martens *In its* Coronal and Prominence Plasmas Dec. 1986 p 407-417 (For primary document see N87-20871 13-92)

Avail: NTIS HC A19/MF A01 CSCL 03B

Solar and stellar X-ray emission are the observed waste products of the interplay between magnetic fields and the motion of stellar plasma. Theoretical understanding of the process of coronal heating is of utmost importance, since the high temperature is what defines the corona in the first place. Most of the research described deals with the aspects of the several rivalling theories for coronal heating. The rest of the papers deal with processes of energy conversion related to flares. B.G.

N87-20935*# Naval Research Lab., Washington, D. C. Center for Space Research.

TOPOLOGICAL CONSTRAINTS AND THE EXISTENCE OF FORCE-FREE FIELDS

S. K. Antiochos *In* NASA. Goddard Space Flight Center Coronal and Prominence Plasmas Dec. 1986 p 419-423 Sponsored by NASA (For primary document see N87-20871 13-92)

Avail: NTIS HC A19/MF A01 CSCL 03B

A fundamental problem in plasma theory is the question of the existence of MHD equilibria. The issue of topological constraints is of crucial importance for the problem of the existence of equilibria. Heuristic methods are used to discuss the coronal wrapping pattern. It is concluded that for a given set of footpoint positions the wrapping pattern in the corona is completely fixed. The topological constraints are included in the boundary conditions on the Euler potentials and impost no additional restrictions on possible equilibria. Although this does not prove that equilibria always exist, it does show that the force-free problem is not overdetermined and that existence of equilibria is still an open question. B.G.

N87-20936*# National Center for Atmospheric Research, Boulder, Colo. High Altitude Observatory.

THE TOPOLOGICAL DESCRIPTION OF CORONAL MAGNETIC FIELDS

Mitchell A. Berger *In* NASA. Goddard Space Flight Center Coronal and Prominence Plasmas Dec. 1986 p 425-429 Sponsored in part by NSF (For primary document see N87-20871 13-92)

Avail: NTIS HC A19/MF A01 CSCL 03B

Determining the structure and behavior of solar coronal magnetic fields is a central problem in solar physics. At the photosphere, the field is believed to be strongly localized into discrete flux tubes. After providing a rigorous definition of field topology, how the topology of a finite collection of flux tubes may be classified is discussed. B.G.

N87-20937*# National Aeronautics and Space Administration. Goddard Space Flight Center, Greenbelt, Md.

A COORDINATE FREE DESCRIPTION OF MAGNETOHYDROSTATIC EQUILIBRIA

P. C. H. Martens *In its* Coronal and Prominence Plasmas Dec. 1986 p 431-437 (For primary document see N87-20871 13-92)

Avail: NTIS HC A19/MF A01 CSCL 03B

The question what geometrical restrictions are imposed on static magnetic fields by the magnetohydrostatic (MHS) equation is addressed. The general mathematical problem is therefore to determine the solutions of the MHS equations in the corona subject to an arbitrary normal component of the magnetic field at the boundary and arbitrary connectivity. What constraints the MHS equations impose on the geometry of the solutions, expressed in metric tensors, will be determined. B.G.

N87-20938*# Harvard-Smithsonian Center for Astrophysics, Cambridge, Mass.

CASCADE MODEL OF CORONAL HEATING

A. A. vanBallegooijen *In* NASA. Goddard Space Flight Center Coronal and Prominence Dec. 1986 p 439-443 (For primary document see N87-20871 13-92)

Avail: NTIS HC A19/MF A01 CSCL 03B

It is suggested that the quasi-static evolution of coronal magnetic structures is characterized by a cascade of magnetic energy to smaller length scales. This cascade process takes place on a time scale t sub b determined entirely by the photospheric motions. The Ohmic heating rate E sub H in the statistically stationary state was estimated using observational data on the diffusivity of photospheric motions; E sub H turned out to be too small by a factor of 40 when compared with observed coronal energy losses. However, given the fact that the theoretical estimate is based on a rather uncertain extrapolation to the diffusive regime, current heating cannot be ruled out as a viable mechanism of coronal heating. B.G.

N87-20939*# National Aeronautics and Space Administration. Goddard Space Flight Center, Greenbelt, Md.

HEATING OF THE SOLAR CORONA BY THE RESONANT ABSORPTION OF ALFVEN WAVES

Joseph M. Davila *In its* Coronal and Prominence Plasmas Dec. 1986 p 445-449 (For primary document see N87-20871 13-92)

Avail: NTIS HC A19/MF A01 CSCL 03B

An improved method for calculating the resonance absorption heating rate is discussed and the results are compared with observations in the solar corona. The primary conclusion to be drawn from these calculations is that to the level of the approximation adopted, the observations of the heating rate and nonthermal line broadening in the solar corona are consistent with heating by the resonance absorption mechanism. B.G.

N87-20940*# National Center for Atmospheric Research, Boulder, Colo. High Altitude Observatory.

MAGNETIC HELICITY AS A CONSTRAINT ON CORONAL DISSIPATION

Arnab Rai Choudhuri *In* NASA. Goddard Space Flight Center Coronal and Prominence Plasmas Dec. 1986 p 451-456 (For primary document see N87-20871 13-92)

Avail: NTIS HC A19/MF A01 CSCL 03B

The Taylor hypothesis has provided a model for the relaxed magnetic configurations of not only laboratory plasmas, but also of astrophysical plasmas. However, energy dissipation is possible only for systems which depart from a strict Taylor state, and hence a parameter describing that departure must be introduced, when the Taylor hypothesis is used to estimate the dissipation. An application of the Taylor hypothesis to the problem of coronal heating provides an insight into this difficult problem. When particular sorts of footpoint motions put energy and helicity in the corona, the conservation of helicity puts a constraint on how much of the energy can be dissipated. However, on considering a random distribution of footpoint motions, this constraint gets washed away, and the Taylor hypothesis is probably not going to play any significant role in the actual calculation of relevant physical quantities in the coronal heating problem. B.G.

N87-20941*# Saint Andrew's Univ. (Scotland). Dept. of Applied Mathematics.

THE STABILITY OF CORONAL AND PROMINENCE MAGNETIC FIELDS

A. W. Hood *In* NASA. Goddard Space Flight Center Coronal and Prominence Plasmas Dec. 1986 p 457-460 (For primary document see N87-20871 13-92)
Avail: NTIS HC A19/MF A01 CSCL 03B

The significance of the localized instabilities is not yet fully understood. The nonlinear coupling of these modes may give rise to an explosive instability, with the modes coupling to longer wavelengths. On the other hand, if the modes saturate early, than the main effect of the instability may be an enhancement of transport coefficients. Nonetheless, the equation provides a simple test for the stability of cylindrical magnetic fields. B.G.

N87-20942*# Saint Andrew's Univ. (Scotland). Dept. of Applied Mathematics.
RESISTIVE BALLOONING MODES IN LINE-TIED CORONAL ARCADES
Marco Velli *In* NASA. Goddard Space Flight Center Coronal and Prominence Plasmas Dec. 1986 p 461-463 (For primary document see N87-20871 13-92)
Avail: NTIS HC A19/MF A01 CSCL 03B

The equations describing the linear evolution of resistive ballooning modes are obtained by using a modified WKB expansion in the short perpendicular wavelength, while variations of the perturbations along the field are described by a slowly varying amplitude, on which the tying boundary conditions are imposed. In general, given an equilibrium, there are certain ranges of magnetic surfaces for which the system predicts instability even without dissipation. The main conclusion is that within the resistive MHD approximation cylindrically symmetric arcades with pressure falling with radius are unstable to resistive localized modes; the growth rates, close to ideal marginal stability, are large, so that it would appear that energy could be released during 10 to 100 Alfven times. The wavelength of the modes is expected to be limited by the ion gyroradius, when stabilizing drift effects must be taken into account. The nonlinear evolution of resistive ballooning modes should be studied to assess their overall relevance to the violent and rapidly evolving phenomena observed on the sun. B.G.

N87-20943*# Scuola Normale Superiore, Pisa (Italy).
EFFECTS OF FLOWS ON VISCOUS AND RESISTIVE MHD STABILITY
Giorgio Einaudi *In* NASA. Goddard Space Flight Center Coronal and Prominence Plasmas Dec. 1986 p 465-468 (For primary document see N87-20871 13-92)
Avail: NTIS HC A19/MF A01 CSCL 03B

In many solar applications the viscosity appears to be more important than resistivity. In order to discuss the instabilities in solar conditions, an idealized configuration is considered in which the plasma is flowing in the z-direction along the magnetic field B sub 0 with a velocity V sub 0. As far as the velocity is concerned two different velocity profiles, with different hydrodynmaic stability properties are discussed. The results are summarized. B.G.

N87-20944*# Los Alamos National Lab., N. Mex.
LARGE-SCALE ELECTRIC FIELDS RESULTING FROM MAGNETIC RECONNECTION IN THE CORONA
R. A. Kopp and G. Poletto *In* NASA. Goddard Space Flight Center Coronal and Prominence Plasmas Dec. 1986 p 469-473 Previously announced as N87-13383 (For primary document see N87-20871 13-92)
Avail: NTIS HC A19/MF A01 CSCL 03B

The method of Forbes and Priest (2-D model) is applied to the large two-ribbon flare of July 29, 1973, for which both detailed H observations and magnetic data are available. For this flare the ribbons were long, nearly straight, and parallel to each other, and the 2-D model for the coronal field geometry may be adequate. The temporal profile E(t) is calculated and indicates that reconnection sets in at the beginning of the decay phase. From this time the electric field grows rapidly to a maximum value of about 2 V/cm within just a few minutes. Thereafter it decreases monotonically with time. DOE

N87-20945*# Texas Univ., Austin. Inst. for Fusion Studies
DYNAMIC EVOLUTION OF CORONAL MAGNETIC FIELDS
Richard S. Steinolfson *In* NASA. Goddard Space Flight Center Coronal and Prominence Plasmas Dec. 1986 p 475-479 (For primary document see N87-20871 13-92)
(Grant NAGw-846; Contract F19628-85-K-0006; Grant NSF ATM-85-06646)
Avail: NTIS HC A19/MF A01 CSCL 03B

The response of coronal magnetic fields to photospheric motion is investigated using a time-dependent, two-dimensional MHD simulation. Starting with an initially uniform field, a circular section of the loop base is slowly rotated to represent the photospheric motion. The field lines at the base move with this flow in a manner consistent with the generated electric fields. The subsequent evolution of the field and flow can be characterized as passing through several distinct configurations. In the earliest phase the kinetic energy is negligible, and the current and field are parallel throughout most of the cylinder. This is followed by a period in which the field rotation increases, the axial field at and near the axis increases, and the acial field decreases in two cylindrical regions away from the axis. When the field in an appreciable portion of the cylinder has undergone one complete rotation, a rapid change in field configuration occurs with a large portion of the field making several rotations at large radii and a corresponding large reduction in the axial field. Author

N87-20946# Maryland Univ., College Park.
THE PROPAGATION OF AN ELECTRON BEAM THROUGH THE SOLAR CORONA Ph.D. Thesis
Theodore Nicholas LaRosa 1986 141 p
Avail: Univ. Microfilms Order No. DA8628992

The propagation of nonthermal electron beams that produce type III solar radio bursts has been studied under several quantitatively different approximations. It is the purpose of this thesis to investigate a model, based on nonlinear theory, for the propagation of an electron beam that includes the spatial structure of the beam and the evolution of the particle distribution function. The premise of this thesis is that nonlinear theory can be used to establish a boundary condition for a quasi-linear analysis of the leading edge of the electron beam. The moving site where the wave energy first reaches the threshold for nonlinear instability is identified as the front of the beam. The wave and particle distributions ahead of the front are computed using quasi-linear theory as functions of velocity and distance in a frame that moves with the front. The computations are significant in that the particle distribution was found to maintain a narrow width, even in the presence of nonlinear wave energy levels. The electron energy losses were found to be self-limiting; beam electrons are diffused to lower velocities, fall behind the front and are prevented from generating further waves by the nonlinear processes. The velocity distribution of the overtaken particles is linear and does not resemble a plateau. This analysis suggests a new interpretation of coronal type III drift rates and may also have implications for interplanetary observations of type III beams. Dissert. Abstr.

N87-20947*# National Aeronautics and Space Administration. Marshall Space Flight Center, Huntsville, Ala.
STATISTICAL ASPECTS OF SOLAR FLARES
Robert M. Wilson Apr. 1987 41 p
(NASA-TP-2714; NAS 1.60:2714) Avail: NTIS HC A03/MF A01 CSCL 03B

A survey of the statistical properties of 850 H alpha solar flares during 1975 is presented. Comparison of the results found here with those reported elsewhere for different epochs is accomplished. Distributions of rise time, decay time, and duration are given, as are the mean, mode, median, and 90th percentile values. Proportions by selected groupings are also determined. For flares in general, mean values for rise time, decay time, and duration are 5.2 + or - 0.4 min, and 18.1 + or 1.1 min, respectively. Subflares, accounting for nearly 90 percent of the flares, had mean values lower than those found for flares of H alpha importance greater than 1, and the differences are statistically significant. Likewise, flares of bright and normal relative brightness have mean

values of decay time and duration that are significantly longer than those computed for faint flares, and mass-motion related flares are significantly longer than non-mass-motion related flares. Seventy-three percent of the mass-motion related flares are categorized as being a two-ribbon flare and/or being accompanied by a high-speed dark filament. Slow rise time flares (rise time greater than 5 min) have a mean value for duration that is significantly longer than that computed for fast rise time flares, and long-lived duration flares (duration greater than 18 min) have a mean value for rise time that is significantly longer than that computed for short-lived duration flares, suggesting a positive linear relationship between rise time and duration for flares. Monthly occurrence rates for flares in general and by group are found to be linearly related in a positive sense to monthly sunspot number. Statistical testing reveals the association between sunspot number and numbers of flares to be significant at the 95 percent level of confidence, and the t statistic for slope is significant at greater than 99 percent level of confidence. Dependent upon the specific fit, between 58 percent and 94 percent of the variation can be accounted for with the linear fits. A statistically significant Northern Hemisphere flare excess (P less than 1 percent) was found, as was a Western Hemisphere excess (P approx 3 percent). Subflares were more prolific within 45 deg of central meridian (P less than 1 percent), while flares of H alpha importance or = 1 were more prolific near the limbs greater than 45 deg from central meridian; P approx 2 percent). Two-ribbon flares were more frequent within 45 deg of central meridian (P less than 1 percent). Slow rise time flares occurred more frequently in the western hemisphere (P approx 2 percent), as did short-lived duration flares (P approx 9 percent), but fast rise time flares were not preferentially distributed (in terms of east-west or limb-disk). Long-lived duration flares occurred more often within 45 deg 0 central meridian (P approx 7 percent). Mean durations for subflares and flares of H alpha importance or + 1, found within 45 deg of central meridian, are 14 percent and 70 percent, respectively, longer than those found for flares closer to the limb. As compared to flares occurring near cycle maximum, the flares of 1975 (near solar minimum) have mean values of rise time, decay time, and duration that are significantly shorter. A flare near solar maximum, on average, is about 1.6 times longer than one occurring near solar minimum. Author

N87-20948# National Geophysical Data Center, Boulder, Colo.
SOLAR-GEOPHYSICAL DATA NUMBER 506, OCTOBER 1986. PART 1: (PROMPT REPORTS). DATA FOR SEPTEMBER 1986, AUGUST 1986 AND LATE DATA
Helen E. Coffey, ed. Oct. 1986 102 p
(Contract N00014-86-F-0049)
(PB87-126389; SGD-506-Pt-1; ISSN-0038-0911; LC-79-640375)
Avail: NTIS HC A06/MF A01 CSCL 03B

Information addressed include: detailed index for 1986; data for September 1986 (advance and worldwide IUWDS alert periods, solar activity indices, solar flares, solar radio emission, and Stanford mean solar magnetic field); data for August 1986 (solar active regions, sudden ionospheric disturbances, solar radio spectral observations, cosmic ray measurements by neutron monitor, geomagnetic indices, and radio propagation indices); and late data (solar radio emission August 1986, solar active regions July 1986, cosmic ray measurements by neutron monitor, calcium plage data December 1985 to February 1986). GRA

N87-20677*# National Oceanic and Atmospheric Administration, Boulder, Colo. Space Environment Lab.
FORECASTS OF SOLAR AND GEOMAGNETIC ACTIVITY
JoAnn Joselyn *In* NASA. Marshall Space Flight Center Upper and Middle Atmospheric Density Modeling Requirements for Spacecraft Design and Operations Feb. 1987 p 141-149 (For primary document see N87-20665 13-46)
Avail: NTIS HC A13/MF A01 CSCL 03B

N87-20678*# National Aeronautics and Space Administration. Marshall Space Flight Center, Huntsville, Ala.
NASA/MSFC PREDICTION TECHNIQUES
Robert E. Smith *In its* Upper and Middle Atmospheric Density Modeling Requirements for Spacecraft Design and Operations Feb. 1987 p 151-153 (For primary document see N87-20665 13-46)
Avail: NTIS HC A13/MF A01 CSCL 03B

93 SPACE RADIATION

Includes cosmic radiation; and inner and outer earth's radiation belts.

For biological effects of radiation see *52 Aerospace Medicine*. For theory see *73 Nuclear and High-Energy Physics*.

N87-20949 Wisconsin Univ., Madison.
H I STRUCTURE AND THE SOFT X-RAY BACKGROUND Ph.D. Thesis
Keith Jahoda 1986 255 p
Avail: Univ. Microfilms Order No. DA8615639

The observed anticorrelation between diffuse soft X-ray flux and H I column density has been explained as absorption of soft X-rays produced in a hot galactic halo, assuming that the neutral interstellar material is sufficiently clumped to reduce the soft X-ray absorption cross section by a factor of two to three. A 21 cm emission line study was made of H I column density variations at intermediate and high galactic latitudes at 21' and 10' spatial resolution. The results, in combination with other data, appear to rule out the hypothesis that clumping of neutral interstellar matter on any angular scale significantly reduces X-ray absorption cross sections in the 0.13 to 0.28 keV energy range. It is concluded therefore that the observed anticorrelation is not primarily a consequence of absorption of soft X-rays produced in a hot galactic halo. Dissert. Abstr.

N87-20950 Wisconsin Univ., Madison.
A SEARCH FOR VERY HIGH ENERGY GAMMA RAY EMISSION FROM CYGNUS X-3 Ph.D. Thesis
Andrew Harold Szentgyorgyi 1986 225 p
Avail: Univ. Microfilms Order No. DA8621934

The Haleakala Gamma Ray Telescope is designed to detect very high energy gamma rays by the atmospheric Cherenkov technique, with an energy threshold of approximately 300 GeV. During 1985, approximately 113 hours of observations were conducted on Cygnus X-3. These data were analyzed to search for pulsar-like periodicity and periodicity correlated with the 4.8 hour period seen in X-ray and infrared data. No periodic structure has been detected at any of the aforementioned timescales. Long-term averaging indicates gamma ray emission from Cygnus X-3 is present, and is 2.3% of the ambient cosmic ray background. Dissert. Abstr.

N87-20951*# Alabama Univ., Huntsville. Cosmic Ray Lab.
SPACE RADIATION STUDIES Annual Report, Nov. 1985 - Nov. 1986
J. C. Gregory [1986] 56 p
(Contract NAS8-35354)
(NASA-CR-179037; NAS 1.26:179037) Avail: NTIS HC A04/MF A01 CSCL 03B

Instrument design and data analysis expertise was provided in support of several space radiation monitoring programs. The Verification of Flight Instrumentation (VFI) program at NASA included both the Active Radiation Detector (ARD) and the Nuclear Radiation Monitor (NRM). Design, partial fabrication, calibration and partial data analysis capability to the ARD program was provided, as well as detector head design and fabrication, software development and partial data analysis capability to the NRM program. The ARD flew on Spacelab-1 in 1983, performed flawlessly and was returned to MSFC after flight with unchanged calibration factors. The NRM, flown on Spacelab-2 in 1985, also performed without fault, not only recording the ambient gamma ray background on the Spacelab, but also recording radiation events of astrophysical significance. Author

N87-20952# Academy of Sciences of the Armenian SSR, Erivan.
ULTRA-HIGH ENERGY GAMMA-RAYS AS THE CARRIERS OF COSMOLOGICAL INFORMATION
F. A. Agaronyan and A. M. Atoyan 1985 24 p
(DE87-700680; EFI-788(15)-85) Avail: NTIS (US Sales Only) HC A02/MF A01

A possibility of verifying a number of cosmological hypotheses by searching the cutoffs in spectra of ultrahigh energy gamma rays from extragalactic sources is discussed. DOE

N87-20953# Pennsylvania Univ., Philadelphia.
SEARCH FOR MAGNETIC MONOPOLES, NEUTRINO OSCILLATIONS, AND SUPERHIGH ENERGY PHYSICS Technical Progress Report
Oct. 1986 14 p
(Contract DE-AC02-81ER-40012)
(DE87-005774; DOE/ER-40012/2) Avail: NTIS HC A02/MF A01

This report describes the technical progress with the Homestake cosmic ray and monopole detector system, and recent results. There are three components in the Homestake detector: a deep underground 150 ton liquid scintillator array in the form of a hollow box 8m x 8m x 16m, an extensive air shower array (consisting of 27 liquid scintillation counters, each 3 sq m, located on the surface above the underground detector) and a 1.6 m diameter Cerenkov telescope that views cosmic ray primary interactions in the upper atmosphere. The full detector complex has been in operation since late 1985. In 1986 the transient recorder circuitry necessary for the recognition of magnetic monopoles and other massive, slow particles underground was added. The goals of the Homestake experimental program are to: (1) search for massive magnetic monopoles, (2) measure the flux of high energy neutrinos, search for sources of these neutrinos and look for neutrino oscillations, particularly resonant neutrino oscillations in the Earth, (3) measure the composition of very high energy cosmic rays, (4) investigate the nature of the emissions from Cyg X-3, and (5) look for neutrino bursts from collapsing stars. DOE

99 GENERAL

No abstracts in this category.

Typical Subject Index Listing

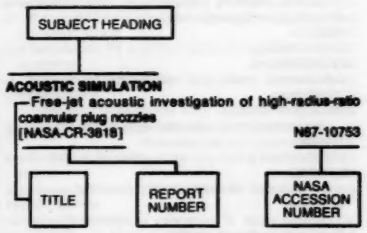

The subject heading is the key to the subject content of the document. Titles, report numbers, and accession numbers of pertinent documents are provided under each subject heading. When the title is insufficiently descriptive of the document content, a title extension has been added, separated from the title by three hyphens. The report number helps to indicate the type of document cited (e.g., NASA report, NASA translation, NASA contractor report). The NASA accession number is the number by which the document abstracts are arranged in this journal and by which the document is sold or requested. The titles, with title extensions if present, are arranged under each subject heading in ascending accession number order. The subject headings have been selected from the latest revision of the *NASA Thesaurus* (NASA SP-7053).

A

ABLATION
The acceleration and dissolution of stars moving through the blackbody radiation of a collapsing universe N87-20847

ABSORPTION
Solar power absorption in a glass tube [NASA-TM-89063] N87-20814

ABSORPTIVITY
Heating of the solar corona by the resonant absorption of Alfven waves N87-20939

ABSTRACTS
Summary of flat-plate solar array project documentation: Abstracts of published documents, 1975-1986, revision 1 [NASA-CR-180401-REV-1] N87-20845

ABUNDANCE
Carbon and nitrogen abundances along the evolutionary sequence of M57 N87-20848

AC GENERATORS
Resistojet control and power for high frequency ac buses [NASA-TM-89860] N87-20477

ACCELERATED LIFE TESTS
Composite repair of cocured J-stiffened panels: Design and test verification N87-20181

ACCELERATION (PHYSICS)
A rational approach to lifting surface theory with application to large angles of attack N87-20196
The digital processing of acceleration measurements for modal analysis N87-20439
The acceleration and dissolution of stars moving through the blackbody radiation of a collapsing universe N87-20847

ACCELEROMETERS
The pre-pulse in pyroshock measurement and analysis N87-20604
State-of-the-art accelerometer characteristics for pyrotechnic shock measurement N87-20608
Zero-shifted accelerometer outputs N87-20609
Questionable effects of shock data filtering N87-20610
Overview of shuttle data on density N87-20683

ACCRETION DISKS
Collisional dynamics of perturbed particle disks in the solar system [NASA-CR-180497] N87-20860

ACCUMULATORS
USC/AIAA student get away special project liquid droplet collector experiment N87-20316
Design, fabrication and performance of small, graphite electrode, multistage depressed collectors with 200-W, CW, 8- to 18-GHz traveling-wave tubes [NASA-TP-2693] N87-20474

ACOUSTIC EXCITATION
Supersonic flow induced cavity acoustics N87-20601

ACOUSTIC IMPEDANCE
Experimental validation of a two-dimensional shear-flow model for determining acoustic impedance [NASA-TP-2679] N87-20798

ACOUSTIC MEASUREMENT
A survey of achieved levels of airborne sound insulation in broadcasting studio centres [BBC-RD-1987/1] N87-20796
The 1985 small propeller-driven aircraft noise test program [AD-A175596] N87-20799

ACOUSTIC PROPERTIES
Biot theory and acoustical properties of high porosity fibrous materials and plastic foams [NASA-TM-88575] N87-20424
A survey of achieved levels of airborne sound insulation in broadcasting studio centres [BBC-RD-1987/1] N87-20796
The 1985 small propeller-driven aircraft noise test program [AD-A175596] N87-20799

ACOUSTIC SCATTERING
NORSTAR Project: Norfolk public schools student team for acoustical research N87-20309
Acoustic scattering from composite wind-wave surfaces II: Backscatter cross sections and Doppler effects at high frequencies and small angles for 'bubble-free' regimes [AD-A176081] N87-20715

ACOUSTIC SIMULATION
The Shock and Vibration Bulletin. Part 3: Invited Papers, Pyrotechnic Shock, Pyrotechnic Shock Workshop [AD-A175226] N87-20602
Aircraft noise synthesis system: Version 4 user instructions [NASA-TM-89089] N87-20797

ACOUSTIC VELOCITY
Physical, mechanical effect of velocity of sound in ocean sediments N87-20723

ACOUSTICS
Acoustic effects on the dynamic of lightweight structures N87-20372
USSR report: Physics and mathematics [JPRS-UPM-86-006] N87-20445
The acousto-ultrasonic approach [NASA-TM-89843] N87-20562

ACTIVATION ENERGY
Temperature shift considerations for damping materials N87-20593

ACTIVE CONTROL
Active structural controllers emulating structural elements by ICUs N87-20367
Air Force basic research in dynamics and control of large space structures N87-20577
Implementation of active force control for robots subject to dynamic loading N87-20586
An evaluation of active noise control in a cylindrical shell [NASA-TM-89090] N87-20794

ACTUATORS
Active structural controllers emulating structural elements by ICUs N87-20367
Multi-axis vibration tests on spacecraft using hydraulic exciters N87-20373

ADAPTIVE CONTROL
Adaptive mutual interference suppression method [AD-D012552] N87-20459
Adaptive control with a nonparametric model for the controlled system [ETN-87-99015] N87-20775

ADAPTIVE FILTERS
Modal parameter identification using adaptive digital filters N87-20583

ADAPTIVE OPTICS
Turbulence control on an airborne laser platform [NASA-CR-178249] N87-20503

ADDITION RESINS
Addition polymers from 1,4,5,8-tetrahydro-1,4;5,8-diepoxyanthracene and Bis-dienes: Processable resins for high temperature application [NASA-TM-89838] N87-20426

ADDITIVES
Operation of transversely excited N2O lasers [AD-D012583] N87-20543
Chemistry of glass-ceramic to metal bonding for header applications Part 2: Hydrogen bubble formation during glass-ceramic to metal sealing [DE87-004041] N87-20559
The effects of heavy doping on the electronic states in semiconductors [DE87-004421] N87-20824

ADHESION
Adhesion of a silicone based insulating material to rocket motors [FOA-C-20635-2.1] N87-20429

ADHESIVE BONDING
Development of field level repairs for composite structures N87-20177
Effect of adhesive bonding variables on the performance of bonded CFRP patch repairs of metallic structures N87-20182
Composite repair material and design development efforts N87-20188
British Airways experience with composite repairs N87-20192

ADHESIVES
Development of field level repairs for composite structures N87-20177

ADSORPTION
Moisture absorption in graphite/organic-matrix composites [DE87-004229] N87-20394
Effect of hemadsorption on rheological parameters of blood during seven-day antiorthostatic hypokinesia and in vitro studies N87-20740
Adsorption of atomic oxygen (N2O) on clean silicon surfaces and its influence on the surface state density; a comparison with O2 [B6868354] N87-20810

ADVECTION
Testing and comparison of several mixed-layer models [AD-A175959] N87-20712

AEROACOUSTICS
Documentation of the space station/aircraft acoustic apparatus [NASA-TM-89111] N87-20795

AEROASSIST
Aero-Assisted Orbital Transfer Vehicle (AOTV) N87-20682

AEROBRAKING
Aero-Assisted Orbital Transfer Vehicle (AOTV) N87-20682
Middle atmosphere density and models N87-20687

AERODYNAMIC BALANCE
Effect of dynamic stall and elastic parameters on the fundamental mechanisms of helicopter vibrations [AD-A175561] N87-20292
Visual display and alarm system for wind tunnel static and dynamic loads [NASA-TM-89455] N87-20298

AERODYNAMIC CHARACTERISTICS
The effect of heavy rain on an airfoil at high lift [NASA-CR-178248] N87-20232
Investigation of transonic region of high dynamic response encountered on an elastic supercritical wing [NASA-TM-89121] N87-20236

The aerodynamic effects of a serrated strip near the leading edge of an airfoil
[ETN-87-99480] N87-20248
Aerodynamic measurements and thermal tests of a strain-gage balance in a cryogenic wind tunnel
[NASA-TM-89039] N87-20517

AERODYNAMIC COEFFICIENTS
Comparison of finite difference calculations of a large region of recirculating flow near an airfoil trailing edge N87-20218
Calculations for a generic fighter at supersonic high-lift conditions N87-20226
Numerical simulation of the flow field around a complete aircraft N87-20231
Post-flight BET products for the 2nd discovery entry, STS-19 (51-A)
[NASA-CR-172572] N87-20344
Empirical modeling of the thermosphere: An overview N87-20675
Requirements for improved modeling of the orbital atmosphere N87-20676
Overview of shuttle data on density N87-20683
Shuttle derived atmosphere N87-20684

AERODYNAMIC CONFIGURATIONS
Applications of Computational Fluid Dynamics in Aeronautics
[AGARD-CP-412] N87-20199
New numerical techniques in the method of singularities for application to complex three-dimensional configurations N87-20205
Applications and developments of computational methods for the aerodynamic problems of complex configurations N87-20209
The integration of computational fluid dynamics into the military aircraft design process N87-20210
Application of the Navier-Stokes equations to solve aerodynamic problems N87-20225
Transonic Navier-Stokes wing solution using a zonal approach. Part 1: Solution methodology and code validation N87-20228
A multiple zone method for supersonic tactical missiles
[AD-A175938] N87-20244
An application of computational fluid dynamics to the design of optimum ramjet powered missile components N87-20338

AERODYNAMIC DRAG
Empirical modeling of the thermosphere: An overview N87-20675
Overview of shuttle data on density N87-20683
Shuttle derived atmosphere N87-20684

AERODYNAMIC INTERFERENCE
Integral method of wall interference correction in low-speed wind tunnels
[NASA-TT-20055] N87-20241
An investigation into the factors affecting the flow quality in a small suction wind tunnel
[BU-344] N87-20299

AERODYNAMIC LOADS
The prediction of transonic loading on advancing helicopter rotors N87-20206
Applications and developments of computational methods for the aerodynamic problems of complex configurations N87-20209

AERODYNAMIC STABILITY
Aeroelastic stability of bearingless rotors in forward flight N87-20260
Stability regions of relaxed static stability aircraft under control saturation constraints N87-20288

AERODYNAMIC STALLING
Effect of dynamic stall and elastic parameters on the fundamental mechanisms of helicopter vibrations
[AD-A175561] N87-20292

AERODYNAMICS
Utilization of Euler codes in nonlinear aerodynamics N87-20215
Unsteady transonic flow calculations for realistic aircraft configurations
[NASA-TM-89120] N87-20234
Surface pressure measurements on a double delta Wing/Body configuration at Mach 2 and Mach 3 (WTR 1396)
[AD-A175951] N87-20245
Activities report in computer science
[ETN-87-99377] N87-20758

AEROELASTICITY
Unsteady transonic flow calculations for realistic aircraft configurations
[NASA-TM-89120] N87-20234
Investigation of transonic region of high dynamic response encountered on an elastic supercritical wing
[NASA-TM-89121] N87-20236
Aeroelastic stability of bearingless rotors in forward flight N87-20260

AEROMANEUVERING
SAFE/DAE: Modal test in space N87-20584

AERONAUTICAL ENGINEERING
Aeronautical engineering: A continuing bibliography with indexes (supplement 212)
[NASA-SP-7037(212)] N87-20172

AERONAUTICS
Aeronautical engineering: A continuing bibliography with indexes (supplement 212)
[NASA-SP-7037(212)] N87-20172

AEROSOLS
Airborne lidar measurements of El Chichon stratospheric aerosols, January 1984
[NASA-RP-1175] N87-20663

AEROSPACE ENGINEERING
An advanced technology space station for the year 2025, study and concepts
[NASA-CR-178208] N87-20340
Activities report in computer science
[ETN-87-99377] N87-20758
Activities report in aerospace research
[ETN-87-99378] N87-20836

AEROSPACE ENVIRONMENTS
Manufacturing polymer thin films in a micro-gravity environment N87-20304
Phase partitioning, crystal growth, electrodeposition and cosmic ray experiments in microgravity N87-20305
Gas tungsten arc welding in a microgravity environment: Work done on GAS payload G-169 N87-20306
USC/AIAA student get away special project liquid droplet collector experiment N87-20316
Results of the joint utilization of laser integrated experiments flown on payload GAS-44v aboard Columbia mission 61-C N87-20317
The North Carolina A and T State University Student Space Shuttle Program N87-20318
Baking the first bread in space N87-20319
Multipurpose microcontroller design for PUGAS 2 N87-20321
Geotaxis baseline data for Drosophila N87-20322
Cal Poly Space Project G-279 N87-20324
The growth and harvesting of algae in a micro-gravity environment N87-20325
Recent results from MAUS payloads N87-20331
Microgravity effects on electrodeposition of metals and metal-cermet mixtures N87-20332
GAS-007: First step in a series of Explorer payloads N87-20333
In situ observation of mono-molecular growth steps on aqueous solution grown crystals and the transport of molecules to the crystals N87-20334
Liquid droplet radiator development status
[NASA-TM-89852] N87-20353
Baseline tensile tests of composite materials for LDEF (Long Duration Exposure Facility) exposure
[NASA-TM-89069] N87-20386
Analysis of 12 AH aerospace nickel-cadmium cells from the design variable program
[NASA-TM-87774] N87-20479
Initial investigations into the damping characteristics of wire rope vibration isolators
[NASA-CR-180698] N87-20569
Upper and Middle Atmospheric Density Modeling Requirements for Spacecraft Design and Operations
[NASA-CP-2480] N87-20665
Space radiation studies
[NASA-CR-179037] N87-20951

AEROSPACE INDUSTRY
Composites review
[NASA-TT-20008] N87-20388
Material characterization of superplastically formed titanium (Ti-6Al-2Sn-4Zr-2Mo) sheet
[NASA-TP-2674] N87-20407

AEROSPACE MEDICINE
USSR report: Space Biology and Aerospace Medicine, Volume 20, No. 3, May - June 1986
[JPRS-USB-86-005] N87-20731
Space biology and medicine on the twenty-fifth anniversary of the first spaceflight of Yuriy Alekseyevich Gagarin N87-20732
Stages of development of the problem of flight safety in aviation medicine N87-20733

AEROSPACE SYSTEMS
A survey of military aerospace systems technology developments in Western Europe and the Middle East
[AD-A175635] N87-20173
AGARD (Advisory Group for Aerospace Research and Development) engine disc material cooperative test
[AD-A175533] N87-20283

AEROSPACE VEHICLES
A survey of military aerospace systems technology developments in Western Europe and the Middle East
[AD-A175635] N87-20173
Application of the Navier-Stokes equations to solve aerodynamic problems N87-20225
Structures and Dynamics Division research and technology plans for FY 1987 and accomplishments for FY 1986
[NASA-TM-89141] N87-20570

AEROTHERMOCHEMISTRY
Theoretical study of the nonsteady combustion of composite fuel droplets
[ESA-TT-868] N87-20401

AFRICA
Real-time crop assessment using color theory and satellite data N87-20619

AFTERBODIES
Surface pressure measurements on a double delta Wing/Body configuration at Mach 2 and Mach 3 (WTR 1396)
[AD-A175951] N87-20245

AFTERBURNING
Numerical study of combustion processes in afterburners N87-20269

AGING (MATERIALS)
Risk evaluations of aging phenomena: The linear aging reliability model and its extensions
[DE87-002607] N87-20563

AILERONS
Development of field level repairs for composite structures N87-20177
Damage repair of in-service composite structures: Application to the Mirage 2000 N87-20184

AIR
Acoustic effects on the dynamic of lightweight structures N87-20372

AIR DEFENSE
On modern avionic and defense systems logistic support standardization and cost effectiveness N87-20761

AIR FLOW
Investigation of flow under the fuselage of a powered light aircraft model
[BU-351] N87-20247
The physics of fuel sprays. Volume 1: Experimental measurements
[AD-A175660] N87-20265

AIR LAND INTERACTIONS
Six reasons why thermospheric measurements and models disagree N87-20688

AIR MASSES
Numerical simulation of air mass modification over the East China Sea during the winter season N87-20660
The mesoscale organization, dynamics, and evolution of the marine planetary boundary layer during cold air outbreaks N87-20698

AIR POLLUTION
Characterization of the LTC catalyst: Performance against common air pollutants N87-20535
Airborne lidar measurements of El Chichon stratospheric aerosols, January 1984
[NASA-RP-1175] N87-20663

AIR PURIFICATION
Characterization of the LTC catalyst: Performance against common air pollutants N87-20535

AIR TRAFFIC CONTROL
Traffic scenario generation technique for piloted simulation studies
[NASA-TM-86397] N87-20254
NUSAT 1 methods for radar field strength measurement N87-20329

AIR WATER INTERACTIONS
Testing and comparison of several mixed-layer models
[AD-A175959] N87-20712
Wind-current relationships in the optoma domain off the Northern California Coast
[AD-A176019] N87-20714
Acoustic scattering from composite wind-wave surfaces II: Backscatter cross sections and Doppler effects at high frequencies and small angles for 'bubble-free' regimes
[AD-A176081] N87-20715

AIRBORNE EQUIPMENT
Airborne lidar measurements of El Chichon stratospheric aerosols, January 1984
[NASA-RP-1175] N87-20663
Definition and use of sensors for measuring electrical conductivity in thunderclouds
[ONERA-NT-1986-4] N87-20705
Lightning strikes on aircraft. Exploitation of Landes (France)-Front '84 campaign and complementary development of airborne electrical sensors
[ONERA-RF-91/7154-PY] N87-20706

AIRBORNE LASERS
Turbulence control on an airborne laser platform
[NASA-CR-178249] N87-20503

AIRBORNE/SPACEBORNE COMPUTERS
Bubble memory module for spacecraft application
[NASA-TM-86411] N87-20476

AIRCRAFT ACCIDENT INVESTIGATION
WSUH-1D: Review of damage following lightning strike 30 November 1981
[RAE-TRANS-2103] N87-20262

AIRCRAFT CARRIERS
The retinal image of the fresnel lens optical landing system
[AD-A176090] N87-20258
AIRCRAFT CONFIGURATIONS
Numerical grid generation around complete aircraft configurations N87-20202
Geometry definition and grid generation for a complete fighter aircraft N87-20203
An assessment of the use of low-order panel methods for the calculation of supersonic flows N87-20204
Matrics, transonic potential flow calculations about transport aircraft N87-20208
Euler solution for a complete fighter aircraft at sub- and supersonic speed N87-20216
Calculations for a generic fighter at supersonic high-lift conditions N87-20226
High speed viscous flow calculations about complex configurations N87-20227
Transonic Navier-Stokes wing solutions using a zonal approach. Part 2: High angle-of-attack simulation N87-20229
Numerical simulation of the flow field around a complete aircraft N87-20231
Unsteady transonic flow calculations for realistic aircraft configurations
[NASA-TM-89120] N87-20234
Analysis of NLR configurations using OCM for pilot modeling
[NASA-CR-180656] N87-20289
AIRCRAFT CONSTRUCTION MATERIALS
Design for repairability of helicopter composite blades N87-20176
Effect of adhesive bonding variables on the performance of bonded CFRP patch repairs of metallic structures N87-20182
AIRCRAFT CONTROL
Stability regions of relaxed static stability aircraft under control saturation constraints N87-20288
AIRCRAFT DESIGN
Applications and developments of computational methods for the aerodynamic problems of complex configurations N87-20209
The integration of computational fluid dynamics into the military aircraft design process N87-20210
Application of the Navier-Stokes equations to solve aerodynamic problems N87-20225
The design of composite structures: Aircraft design
[NASA-TT-20011] N87-20261
Materials selection and design study of a composite microlight wing structure
[BU-335] N87-20263
Wind and turbulence data for development of design criteria for unmanned high-altitude low-speed endurance aircraft
[NASA-CR-4065] N87-20699
AIRCRAFT ENGINES
Theory and design of flight-vehicle engines
[NASA-TM-88583] N87-20281
High temperature protective coatings for aero engine gas turbine components
[AD-A176001] N87-20286
Advanced composite combustor structural concepts program
[NASA-CR-174733] N87-20367
AIRCRAFT HAZARDS
WSUH-1D: Review of damage following lightning strike 30 November 1981
[RAE-TRANS-2103] N87-20262
AIRCRAFT INDUSTRY
A survey of military aerospace systems technology developments in Western Europe and the Middle East
[AD-A175635] N87-20173
AIRCRAFT INSTRUMENTS
Airspeed sensing pressure valve system
[AD-D012569] N87-20266
AIRCRAFT LANDING
The retinal image of the fresnel lens optical landing system
[AD-A176090] N87-20258
AIRCRAFT MAINTENANCE
The Repair of Aircraft Structures Involving Composite Materials
[AGARD-CP-402] N87-20174
Repair procedures for composite parts on the alpha jet N87-20175
Design for repairability of helicopter composite blades N87-20176
Development of field level repairs for composite structures N87-20177
A.T.R. 42 carbon fibre flap repair design and inspection N87-20178
Repair of helicopter composite structure techniques and substantiations N87-20179
Composite repair of cocured J-stiffened panels: Design and test verification N87-20181
Effect of adhesive bonding variables on the performance of bonded CFRP patch repairs of metallic structures N87-20182
Composite repair of cracked aluminum structure N87-20183
Damage repair of in-service composite structures: Application to the Mirage 2000 N87-20184
Composite structure repairs carried out according to aeronautical techniques N87-20185
Composite repair techniques for J-stiffened composite fuselage structures N87-20186
Fibre composite repair of cracked metallic aircraft components: Practical and basic aspects N87-20187
Composite repair material and design development efforts N87-20188
Battle damage repair of composite structures N87-20189
Unconventional approaches to field repair N87-20190
Patch repair of corroded aircraft skin areas N87-20191
British Airways experience with composite repairs N87-20192
AIRCRAFT MODELS
Investigation of flow under the fuselage of a powered light aircraft model
[BU-351] N87-20247
AIRCRAFT NOISE
Documentation of the space station/aircraft acoustic apparatus
[NASA-TM-89111] N87-20795
Aircraft noise synthesis system: Version 4 user instructions
[NASA-TM-89089] N87-20797
The 1985 small propeller-driven aircraft noise test program
[AD-A175596] N87-20799
Noise measurements on the helicopter BK 117 design. Weighted noise levels and influence of airspeed
[ESA-TT-748] N87-20800
AIRCRAFT PERFORMANCE
Development of a takeoff performance monitoring system
[NASA-CR-178255] N87-20264
Analysis of NLR configurations using OCM for pilot modeling
[NASA-CR-180656] N87-20289
AIRCRAFT PILOTS
Automated anthropometric data measurement system
[AD-D012575] N87-20748
AIRCRAFT SPIN
Spin-tunnel investigation of a 1/15-scale model of an Australian trainer airplane
[NASA-TM-89049] N87-20240
AIRCRAFT STABILITY
Stability regions of relaxed static stability aircraft under control saturation constraints N87-20288
AIRCRAFT STRUCTURES
The Repair of Aircraft Structures Involving Composite Materials
[AGARD-CP-402] N87-20174
Composite repair of cracked aluminum structure N87-20183
Damage repair of in-service composite structures: Application to the Mirage 2000 N87-20184
Composite structure repairs carried out according to aeronautical techniques N87-20185
Fibre composite repair of cracked metallic aircraft components: Practical and basic aspects N87-20187
Battle damage repair of composite structures N87-20189
The design of composite structures: Aircraft design
[NASA-TT-20011] N87-20261
Development of powder metallurgy 2XXX series Al alloy plate and sheet materials for high temperature aircraft structural applications, FY 1963/1964
[NASA-CR-172521] N87-20406
AIRFOIL PROFILES
The aerodynamic effects of a serrated strip near the leading edge of an airfoil
[ETN-87-99460] N87-20248
AIRFOILS
Computation of transonic flow over porous airfoils N87-20194
Numerical solutions of unsteady flow past rotor sections N87-20198
Flexible grid generation for complex geometries in two space dimensions based on variational principles N87-20200
Comparison of finite difference calculations of a large region of recirculating flow near an airfoil trailing edge N87-20218
Zonal solutions for airfoils using Euler boundary-layer and Navier-Stokes equations N87-20219
The effect of heavy rain on an airfoil at high lift
[NASA-CR-178248] N87-20232
Multigrid calculation of boundary-fitted orthogonal coordinates with applications to unsteady flows N87-20237
Lewis inverse design code (LINDES): Users manual
[NASA-TP-2676] N87-20238
AIRPORTS
Performance of recycled asphalt concrete airport pavement surfaces
[DOT/FAA-PM-86-12] N87-20432
Resilient modulus of freeze-thaw affected granular soils for pavement design and evaluation. Part 3: Laboratory tests on soils from Albany County Airport
[DOT/FAA-PM-84-16.3] N87-20433
AIRSPEED
Integration of altitude and airspeed information into a primary flight display via moving-tape formats
[NASA-TM-89064] N87-20265
Airspeed sensing pressure valve system
[AD-D012569] N87-20266
Design and verification by nonlinear simulation of a Mach/CAS control law for the NASA TCV B737 aircraft
[NASA-CR-178029] N87-20290
Noise measurements on the helicopter BK 117 design. Weighted noise levels and influence of airspeed
[ESA-TT-748] N87-20800
ALGAE
The growth and harvesting of algae in a micro-gravity environment N87-20325
Effect of light and development of photosynthetic cells
[DE87-005183] N87-20728
Microalgae culture collection, 1986-1987
[DE87-005578] N87-20729
ALGEBRA
MACSYMA usage at Langley, revision 1
[NASA-CR-172518] N87-20753
Algebra and topology for applications to physics
[NASA-TT-20056] N87-20784
ALGORITHMS
Using the boundary-layer equations in three-dimensional viscous flow simulation N87-20222
Transonic Navier-Stokes wing solution using a zonal approach. Part 1: Solution methodology and code validation N87-20228
A Navier-Stokes solver using the LU-SSOR TVD algorithm
[NASA-CR-179608] N87-20243
Turbulence control on an airborne laser platform
[NASA-CR-178249] N87-20503
The algorithm and application of a new multi-input-multi-output modal parameter identification method N87-20582
A technique to estimate the ocean surface energy flux using VAS multispectral data N87-20710
A system for routing arbitrary directed graphs on SIMD architectures
[NASA-CR-178265] N87-20764
Performance studies of the multigrid algorithms implemented on hypercube multiprocessor systems
[NASA-CR-178237] N87-20769
Parallel processing of networks
[AD-A175641] N87-20771
Estimability and regulability of linear systems
[NASA-TM-89427] N87-20790
A self critical approach to data analysis and model building
[AD-A175640] N87-20791
ALLOYS
Mechanisms of the oxidation of metals and alloys:
[DE87-003389] N87-20412
Effects of elastic anisotropy on the anomalous yield behavior of cubic ordered alloys
[DE87-005328] N87-20417
Dislocation reactions at grain boundaries in Li2 ordered alloys
[DE87-005713] N87-20827
ALPHA JET AIRCRAFT
Repair procedures for composite parts on the alpha jet N87-20175
ALTERNATING DIRECTION IMPLICIT METHODS
Numerical solutions of unsteady flow past rotor sections N87-20198
ALTITUDE
Integration of altitude and airspeed information into a primary flight display via moving-tape formats
[NASA-TM-89064] N87-20265
ALTITUDE SIMULATION
Detailed flow surveys of turning vanes designed for a 0.1-scale model of NASA Lewis Research Center's proposed altitude wind tunnel
[NASA-TP-2680] N87-20295
ALUMINUM
Composite repair of cracked aluminum structure N87-20183
The variation of subgrain misorientation in aluminum deformed to large steady-state creep strains
[DE87-003238] N87-20415

Superplasticity of metals with special reference to Ti-6Al-4V
[DE87-005795] N87-20419
Electroforming with nickel, iron, and aluminum
[DE87-005589] N87-20442
Shot peening for Ti-6Al-4V alloy compressor blades
[NASA-TP-2711] N87-20566
Studies of X-ray satellites in sodium, magnesium, aluminum, argon, and iron
[ETN-87-99364] N87-20612

ALUMINUM ALLOYS
Patch repair of corroded aircraft skin areas N87-20191
Consolidation processing parameters and alternative processing methods for powder metallurgy Al-Cu-Mg-X-X alloys
[NASA-CR-178227] N87-20404
Development of powder metallurgy 2XXX series Al alloy plate and sheet materials for high temperature aircraft structural applications, FY 1983/1984
[NASA-CR-172521] N87-20406
Ductility and fracture behavior of polycrystalline Ni3Al alloys
[DE87-005340] N87-20413

ALUMINUM OXIDES
Erosion and strength degradation in alumina
[DE87-003341] N87-20428
Alumina-supported Pd-Ag catalysts for low-temperature CO and methanol oxidation N87-20536

AMORPHOUS MATERIALS
Rapid thermal annealing of Amorphous Hydrogenated Carbon (a-C:H) films
[NASA-TM-89659] N87-20821

AMORPHOUS SILICON
Flat-plate solar array project. Volume 2: Silicon material
[NASA-CR-180659] N87-20647
Flat-plate solar array project. Volume 3: Silicon sheet: Wafers and ribbons
[NASA-CR-180661] N87-20648

ANAEROBES
Effect of light and development of photosynthetic cells
[DE87-005183] N87-20728

ANALOG SIMULATION
Numerical simulation of storm surges in the east China Sea N87-20718

ANALOG TO DIGITAL CONVERTERS
Satellite analog FDMA/FM to digital TDMA conversion
[NASA-CR-179605] N87-20467

ANALYSIS (MATHEMATICS)
Cumulative reports and publications through December 31, 1986
[NASA-CR-178257] N87-20754
Information-preserving models of physics and computation
[DE87-005354] N87-20793

ANCHORS (FASTENERS)
Arresting and recovery system for test missiles
[AD-D012574] N87-20337

ANEMOMETERS
Experimental evaluation of sub-cell turbulent models. Space-time correlations in a mixing layer
[ETN-87-99391] N87-20513

ANGLE OF ATTACK
A rational approach to lifting surface theory with application to large angles of attack N87-20196

ANGULAR MOMENTUM
Space station momentum management N87-20668
Self-consistent models of perfect triaxial galaxies N87-20859

ANGULAR VELOCITY
Force magnitude and angular velocity fluctuation reduction in a spring-restrained, flexibly-supported four-bar mechanical linkage N87-20589

ANISOTROPY
Effects of elastic anisotropy on the anomalous yield behavior of cubic ordered alloys
[DE87-005328] N87-20417
Material with anisotropic properties for magnetic shielding purposes
[AD-A175864] N87-20453

ANNEALING
Rapid thermal annealing of Amorphous Hydrogenated Carbon (a-C:H) films
[NASA-TM-89659] N87-20821

ANNUAL VARIATIONS
Mathematical model of steady-state circulation in the south China Sea N87-20719

ANNULAR SUSPENSION AND POINTING SYSTEM
Description of a magnetic bearing test fixture
[NASA-TM-89081] N87-20478

ANODES
Characterization of monolithic fuel cell components
[DE87-004929] N87-20655

ANOMALIES
Small-scale structures and the density irregularity of the inner corona N87-20932

ANTARCTIC REGIONS
Magnetotelluric measurements in Antarctica
[INPE-4056-PRE/1017] N87-20661

ANTENNA ARRAYS
Propagation of RF signals through structured ionization. Theory and antenna aperture effect applications
[AD-A175522] N87-20451
The in-situ calibration of a bilateral space-fed phased array antenna
[AD-A176069] N87-20456

ANTENNA COMPONENTS
The in-situ calibration of a bilateral space-fed phased array antenna
[AD-A176069] N87-20456

ANTENNA DESIGN
Expert systems for diagnostic purposes, prospected applications to the radar field N87-20760
Automatic graphics applied to antenna computer aided design N87-20763

ANTENNA RADIATION PATTERNS
NUSAT update N87-20312
Effects of space plasma discharge on the performance of large antenna structures in low Earth orbit
[NASA-TM-89118] N87-20339

ANTENNAS
Analysis of the receiving characteristics of the circular diffraction antenna with both a flush-mounted and a recessed center post
[DE87-003283] N87-20460
System architecture of MMIC-based large aperture arrays for space application
[NASA-TM-89840] N87-20468

ANTHROPOMETRY
Automated anthropometric data measurement system
[AD-D012575] N87-20748

APPLICATIONS PROGRAMS (COMPUTERS)
Traffic scenario generation technique for piloted simulation studies
[NASA-TM-86397] N87-20254
Strain energy release rates of composite interlaminar end-notch and mixed-mode fracture: A sublaminate/ply level analysis and a computer code
[NASA-TM-89827] N87-20389
HARPA: A versatile three-dimensional Hamiltonian ray-tracing program for acoustic waves in the atmosphere above irregular terrain
[PB87-132031] N87-20601

APPROXIMATION
Experiments and modeling of dilution jet flow fields N87-20276
Piecewise linear approximation for hereditary control problems
[NASA-CR-178260] N87-20778

ARC JET ENGINES
Arcjet component conditions through a multistart test
[NASA-TM-89857] N87-20382

ARCHITECTURE
System architecture of MMIC-based large aperture arrays for space application
[NASA-TM-89840] N87-20468

ARCHITECTURE (COMPUTERS)
Satellite analog FDMA/FM to digital TDMA conversion
[NASA-CR-179605] N87-20467
Bubble memory module for spacecraft application
[NASA-TM-86411] N87-20476
A dynamic multicomputer system for managing scientific and engineering databases
[DE87-002497] N87-20757
A system for routing arbitrary directed graphs on SIMD architectures
[NASA-CR-178265] N87-20764
The hypercluster: A parallel processing test-bed architecture for computational mechanics applications
[NASA-TM-89823] N87-20767

ARCTIC REGIONS
Comparison of 6.2L arctic and standard fuel injection pumps using JP-8 fuel
[AD-A175597] N87-20558

AREA
Experimental thrust performance of a high-area-ratio rocket nozzle
[NASA-TP-2720] N87-20381

ARGON
Studies of X-ray satellites in sodium, magnesium, aluminum, argon, and iron
[ETN-87-99364] N87-20812

ARGON ISOTOPES
Pre-compaction irradiation of meteorites N87-20850

ARMOR
Army research in shock mechanics N87-20576

ARRAYS
Injection-seeding studies of diode laser array behavior
[DE87-002051] N87-20546
Fly's eye sensor nonlinear signal processing
[AD-D012564] N87-20815

ARRESTING GEAR
Arresting and recovery system for test missiles
[AD-D012574] N87-20337

ARTIFICIAL SATELLITES
Satellite servicing mission preliminary cost estimation model
[NASA-CR-171978] N87-20335
Low frequency vibration testing on satellites N87-20364

ASTEROID MISSIONS
The concentration principle applied to spaceborne solar arrays. AGORA mission: Studies synthesis
[SNIAS-959-CA/CG] N87-20657

ASTROMETRY
An astrometric facility for planetary detection on the space station
[NASA-TM-89436] N87-20841
Fiducial reference for the HIPPARCOS reference system
[NASA-CR-180250] N87-20842

ASTRONAUTS
Radiation protection guidelines for space missions
[NASA-TM-89278] N87-20730

ASTRONOMICAL MODELS
The magnetic and turbulent evolution of the Taurus molecular cloud N87-20852

ASTRONOMICAL PHOTOGRAPHY
To catch a comet 2: Technical update on CAN-DO N87-20326
To catch a child's imagination 2: Educational update on CAN-DO N87-20327
Qualification of the faint object camera N87-20359

ASTRONOMICAL PHOTOMETRY
Abundances and kinematics of K giants in the galactic nuclear bulge N87-20856

ASTRONOMICAL SPECTROSCOPY
Abundances and kinematics of K giants in the galactic nuclear bulge N87-20856

ASYMMETRY
Attitude motion of torque-free asymmetric dual-spin spacecraft
[AD-A175531] N87-20354
Interlabyrinthine asymmetry, vestibular dysfunction and space motion sickness N87-20734
Link between asymmetry of optokinetic nystagmus, optovestibular and vestibulovegetative stability N87-20738

ASYMPTOTIC METHODS
Calculation of Rayleigh-Taylor flows using vortex blobs
[DE87-002551] N87-20507
An asymptotic analysis of supersonic reacting mixing layers
[NASA-CR-178266] N87-20756

ATLANTIC OCEAN
Moored current meter and temperature-pressure recorder measurements from the Western North Atlantic (high energy benthic boundary layer and abyssal circulation experiments 1983-1984), volume 39
[AD-A176014] N87-20713

ATLAS CENTAUR LAUNCH VEHICLE
The Shock and Vibration Bulletin. Part 3: Invited Papers, Pyrotechnic Shock, Pyrotechnic Shock Workshop
[AD-A175226] N87-20602

ATMOSPHERIC CIRCULATION
Numerical simulation of air mass modification over the East China Sea during the winter season N87-20660
Six reasons why thermospheric measurements and models disagree N87-20688
The mesoscale organization, dynamics, and evolution of the marine planetary boundary layer during cold air outbreaks N87-20696

ATMOSPHERIC DENSITY
Upper and Middle Atmospheric Density Modeling Requirements for Spacecraft Design and Operations
[NASA-CP-2460] N87-20665
Satellite lifetime prediction N87-20666
Density uncertainty effect on cost of space station reboost N87-20667
Space station momentum management N87-20668
NORAD satellite tracking N87-20671
NORAD/SPACECMD comments concerning the atmospheric density models N87-20672
Orbital atmospheric physics and dynamics N87-20673
Limitations to modeling the thermosphere and exosphere N87-20674
Empirical modeling of the thermosphere: An overview N87-20675
Requirements for improved modeling of the orbital atmosphere N87-20676
Forecasts of solar and geomagnetic activity N87-20677
Users of middle atmosphere models remarks N87-20679

Utilization of Global Reference Atmosphere Model (GRAM) for shuttle entry N87-20680
Use of the 4D-Global Reference Atmosphere Model (GRAM) for space shuttle descent design N87-20681
Aero-Assisted Orbital Transfer Vehicle (AOTV) N87-20682
Overview of shuttle data on density N87-20683
Shuttle derived atmosphere N87-20684
Gravity waves N87-20685
The GRAM-3 model N87-20686
Middle atmosphere density and models N87-20687

ATMOSPHERIC EFFECTS
Acoustic gravity waves: A computational approach [NASA-CR-178270] N87-20781

ATMOSPHERIC ELECTRICITY
Lightning strikes on aircraft. Exploitation of Landes (France)-Front '84 campaign and complementary development of airborne electrical sensors [ONERA-RF-91/7154-PY] N87-20706
Study of surface discharges [ONERA-RF-11/7236-PY] N87-20707

ATMOSPHERIC ENTRY
Post-flight BET products for the 2nd discovery entry, STS-19 (51-A) [NASA-CR-172572] N87-20344

ATMOSPHERIC MODELS
Upper and Middle Atmospheric Density Modeling Requirements for Spacecraft Design and Operations [NASA-CP-2460] N87-20685
Satellite lifetime prediction N87-20686
NORAD satellite tracking N87-20671
NORAD/SPACECMD comments concerning the atmospheric density models N87-20672
Orbital atmospheric physics and dynamics N87-20673
Limitations to modeling the thermosphere and exosphere N87-20674
Empirical modeling of the thermosphere: An overview N87-20675
Requirements for improved modeling of the orbital atmosphere N87-20676
Forecasts of solar and geomagnetic activity N87-20677
The GRAM-3 model N87-20686
Middle atmosphere density and models N87-20687
Six reasons why thermospheric measurements and models disagree N87-20688
LOWTRAN modeling of near-horizon infrared sky radiances in the presence of clouds [AD-A175861] N87-20691
Study of surface discharges [ONERA-RF-11/7236-PY] N87-20707
Wind-current relationships in the optoma domain off the Northern California Coast [AD-A176019] N87-20714
HARPA: A versatile three-dimensional Hamiltonian ray-tracing program for acoustic waves in the atmosphere above irregular terrain [PB87-132031] N87-20801

ATMOSPHERIC OPTICS
Atmospheric contrast transmittance monitor [AD-D012555] N87-20520

ATMOSPHERIC PHYSICS
Orbital atmospheric physics and dynamics N87-20673

ATMOSPHERIC SOUNDING
The use of visible data for improving VAS satellite soundings N87-20620
Report of the atmosphere panel N87-20633

ATMOSPHERIC STRATIFICATION
Shuttle derived atmosphere N87-20684

ATMOSPHERIC TEMPERATURE
Gravity waves N87-20685

ATMOSPHERIC TIDES
Gravity waves N87-20685

ATMOSPHERIC TURBULENCE
Wind and turbulence data for development of design criteria for unmanned high-altitude low-speed endurance aircraft [NASA-CR-4065] N87-20699

ATOMIC EXCITATIONS
Investigation of excited states of Li7 by means of thermal neutron capture N87-20805
Investigation of excited states of B11 and Li7 by means of thermal neutron capture on B10 nuclei N87-20806

ATOMIC SPECTRA
Studies of X-ray satellites in sodium, magnesium, aluminum, argon, and iron [ETN-87-99364] N87-20812

ATOMIZERS
Experimental and analytical investigation of the variation of spray characteristics along a radial distance downstream of a pressure-swirl atomizer N87-20271
Combustion research activities at the Gas Turbine Research Institute N87-20273

ATTENUATION
A normal incidence X-ray telescope [NASA-CR-180107] N87-20840

ATTITUDE (INCLINATION)
New book deals with spatial orientation N87-20746

ATTITUDE CONTROL
Propellant tank resupply system [AD-D012559] N87-20375

ATTITUDE INDICATORS
NUSAT 1 attitude determination N87-20328

ATTITUDE STABILITY
Dynamic and thermal effects in very large space structures N87-20347

AUDIO FREQUENCIES
The 1985 small propeller-driven aircraft noise test program [AD-A175596] N87-20799

AUGMENTATION
Range filtering for sequential GPS receivers with external sensor augmentation [NASA-TM-89419] N87-20257

AUSTRALIA
Spin-tunnel investigation of a 1/15-scale model of an Australian trainer airplane [NASA-TM-89049] N87-20240

AUTOMATIC CONTROL
Automation and robotics [INPE-4088-PRE/1033] N87-20581
Integrated digital control and man-machine interface for complex remote handling systems [DE87-003002] N87-20749

AUTOMOBILES
Composite structure repairs carried out according to aeronautical techniques N87-20185
Criteria and methodology for lightweight design of vehicle components [LBF-TB-176(1986)] N87-20550

AUXILIARY PROPULSION
Arcjet component conditions through a multistart test [NASA-TM-89857] N87-20382

AVALANCHE DIODES
Optically tuned millimeter-wave CW. IMPATT source [AD-A175838] N87-20482

AVIONICS
Rivista Tecnica Selenia, volume 10, number 1 [ETN-87-99091] N87-20759
On modern avionic and defense systems logistic support standardization and cost effectiveness N87-20761

AXES (REFERENCE LINES)
Multi-axis vibration tests on spacecraft using hydraulic exciters N87-20373

AXIAL FLOW
Application of a laser-induced breakdown time-of-flight technique in a flow diagnostic in a CO2 free-jet expansion [DE87-002890] N87-20506

AXISYMMETRIC FLOW
A holographic interferometry study of an axisymmetric shock-wave/boundary-layer strong interaction flow N87-20496
Numerical and optical experiments on the Weissenberg effect [ESA-TT-879] N87-20510

B

BACKGROUND RADIATION
H I structure and the soft X-ray background N87-20949

BACKSCATTERING
Radar scene generation for tactical decision aids [NASA-CR-180234] N87-20449
NASA/MSFC large stretch press study [NASA-CR-180376] N87-20554
Acoustic scattering from composite wind-wave surfaces II: Backscatter cross sections and Doppler effects at high frequencies and small angles for 'bubble-free' regimes [AD-A176081] N87-20715

BALLISTIC MISSILES
Arresting and recovery system for test missiles [AD-D012574] N87-20337

BALLISTICS
Requirements for improved modeling of the orbital atmosphere N87-20676

BALLOON-BORNE INSTRUMENTS
A gondola and pointing system for a gamma ray telescope [DE87-004561] N87-20843

BALLOONING MODES
Resistive ballooning modes in line-tied coronal arcades N87-20942

BALLOONS
A gondola and pointing system for a gamma ray telescope [DE87-004561] N87-20843

BARIUM
Statistical properties of barium stars N87-20857

BAROCLINIC INSTABILITY
Linear baroclinic instability in the presence of large scale topography [NASA-CR-4057] N87-20700

BATHYMETERS
Potential of laser remote sensing of oil below water surface [FOA-C-30435-3.1] N87-20659

BEAMS (SUPPORTS)
Inverse problems in the modeling of vibrations of flexible beams [NASA-CR-178259] N87-20777

BEARING (DIRECTION)
New book deals with spatial orientation N87-20746

BEARINGLESS ROTORS
Aeroelastic stability of bearingless rotors in forward flight N87-20260

BEARINGS
Flexibility effects on tooth contact location in spiral bevel gear transmissions [NASA-CR-4055] N87-20552

BELL AIRCRAFT
WSUH-1D: Review of damage following lightning strike 30 November 1981 [RAE-TRANS-2103] N87-20262

BEND TESTS
Structural degradation of impacted graphite/epoxy laminates N87-20586

BERYLLIUM ALLOYS
Proximity-induced Josephson effect and its application to heavy fermion superconductor UBe-13 [DE87-003049] N87-20485

BIBLIOGRAPHIES
Aeronautical engineering: A continuing bibliography with indexes (supplement 212) [NASA-SP-7037(212)] N87-20172
Hydrogen embrittlement of titanium and its alloys: A literature review [DE87-750405] N87-20410
Recent studies in plate vibrations: 1981-1985. Part 1: Classical theory N87-20437
Management: A bibliography for NASA managers [NASA-SP-7500(21)] N87-20833

BIG BANG COSMOLOGY
Thermal production of not so invisible axions in the early universe [DE87-005404] N87-20866

BINARY ALLOYS
Thermodynamic data of intermetallic compounds [DE87-701244] N87-20831

BINARY STARS
A systematic search for millisecond pulsars N87-20839

BIOCHEMISTRY
USSR report: Life sciences. Biomedical and behavioral sciences [JPRS-UBB-87-003] N87-20751

BIOCONVERSION
Effect of light and development of photosynthetic cells [DE87-005183] N87-20728

BIOELECTRIC POTENTIAL
Dynamics of bioelectric activity of human brain in a continuous waking state N87-20745
Investigation of microstructure of arbitrary motions of operator N87-20752

BIOMASS
Microalgae culture collection, 1986-1987 [DE87-005578] N87-20729

BIOSYNTHESIS
Microalgae culture collection, 1986-1987 [DE87-005578] N87-20729

BIOT METHOD
Biot theory and acoustical properties of high porosity fibrous materials and plastic foams [NASA-TM-88575] N87-20424

BIPOLAR TRANSISTORS
Deep ion implantation for bipolar silicon devices; investigations into the use of the third dimension [88672201] N87-20828

BIT ERROR RATE
Unique bit-error-rate measurement system for satellite communication systems [NASA-TP-2699] N87-20448
Flexible satellite communications systems simulator standard device groups [AD-A175944] N87-20454

BLACK BODY RADIATION
The acceleration and dissolution of stars moving through the blackbody radiation of a collapsing universe N87-20847

BLOOD
Blood lipids and incidence of lipemia in flight personnel N87-20737

Effect of hemadsorption on rheological parameters of blood during seven-day antiorthostatic hypokinesia and in vitro studies N87-20740

BLUFF BODIES

Numerical simulation of separated flows past bluff bodies N87-20499

BOATS

Composite structure repairs carried out according to aeronautical techniques N87-20185

BODY-WING CONFIGURATIONS

Prediction of wing-body-store aerodynamics using a small perturbation method and a grid embedding technique N87-20207

Simulation of transonic viscous wing and wing-fuselage flows using zonal methods
[NASA-TM-89421] N87-20242

Surface pressure measurements on a double delta Wing/Body configuration at Mach 2 and Mach 3 (WTR 1396)
[AD-A175951] N87-20245

BOLTS

Composite repair material and design development efforts N87-20188

BORN APPROXIMATION

Radar scene generation for tactical decision aids
[NASA-CR-180234] N87-20449

BORON FIBERS

Composite repair of cracked aluminum structure N87-20183

Damage repair of in-service composite structures: Application to the Mirage 2000 N87-20184

Fibre composite repair of cracked metallic aircraft components: Practical and basic aspects N87-20187

BORON ISOTOPES

Investigation of excited states of B11 and Li7 by means of thermal neutron capture on B10 nuclei N87-20606

BORON 10

Capture of thermal neutrons B10 and Li6: Applications in spectroscopy and in the study of weak nucleon interactions
[ECN-184] N87-20603

An investigation of the admixture of strong and weak interactions in the B10 (n, alpha) Li7 reaction with slow neutrons N87-20607

BOUNDARY INTEGRAL METHOD

Integral method of wall interference correction in low-speed wind tunnels
[NASA-TT-20055] N87-20241

BOUNDARY LAYER EQUATIONS

Zonal solutions for airfoils using Euler boundary-layer and Navier-Stokes equations N87-20219

Theoretical analysis of flows around helicopter fuselages: Application to design and development N87-20221

Using the boundary-layer equations in three-dimensional viscous flow simulation N87-20222

High speed viscous flow calculations about complex configurations N87-20227

Numerical simulation of separated flows past bluff bodies N87-20499

BOUNDARY LAYER SEPARATION

Theoretical analysis of flows around helicopter fuselages: Application to design and development N87-20221

Applications of RAE viscous flow methods near separation boundaries for three-dimensional wings in transonic flow N87-20224

Simulation of three-dimensional transonic flow with separation past a hemisphere cylinder configuration N87-20230

Acta mechanica sinica (selected articles)
[AD-A176240] N87-20246

Two-dimensional flow computation in straight blade arrays — turbine blades
[ONERA-RT-35/1621-RY-053-R] N87-20511

BOUNDARY LAYERS

The terminal area simulation system. Volume 1: Theoretical formulation
[NASA-CR-4046-VOL-1] N87-20255

The fully nonlinear development of Goertler vortices in growing boundary layers
[NASA-CR-178268] N87-20502

Moored current meter and temperature-pressure recorder measurements from the Western North Atlantic (high energy benthic boundary layer and abyssal circulation experiments 1963-1964), volume 39
[AD-A176014] N87-20713

BOUNDARY VALUE PROBLEMS

Numerical grid generation around complete aircraft configurations N87-20202

Strain energy release rates of composite interlaminar end-notch and mixed-mode fracture: A sublaminate/ply level analysis and a computer code
[NASA-TM-89827] N87-20389

Three-body calculations at Los Alamos
[DE87-001959] N87-20786

A numerical study of the thermal stability of low-lying coronal loops N87-20931

Magnetic helicity as a constraint on coronal dissipation N87-20940

Large-scale electric fields resulting from magnetic reconnection in the corona N87-20944

BRAIN

Effect of long-term spaceflight on rat brain polyamine content N87-20741

Dynamics of bioelectric activity of human brain in a continuous waking state N87-20745

BRAKES (FOR ARRESTING MOTION)

Repair procedures for composite parts on the alpha jet N87-20175

BRANCHING (MATHEMATICS)

Nonlinear dynamics of some condensed matter devices and materials
[ETN-87-99363] N87-20629

BREMSSTRAHLUNG

Theoretical models of free-free microwave emission from solar magnetic loops N87-20918

BRIGHTNESS

Non-LTE hydrogen-line formation in moving prominences N87-20895

Observations of the Ca II K line in Hel0830A dark points on August 3, 1985 N87-20929

BRIGHTNESS DISTRIBUTION

Synoptic study of the corona at meter wavelength N87-20911

The white light corona and photospheric magnetic fields N87-20912

BRIGHTNESS TEMPERATURE

VLA observations of slar filaments at 6 and 20 cm wavelengths N87-20888

Synoptic study of the corona at meter wavelength N87-20911

Three dimensional structures of solar active regions N87-20916

Measurement of coronal fields using spatially resolved microwave spectroscopy N87-20920

VLA observations of coronal bright points at 6 and 20 cm wavelengths N87-20924

Compact, variable, moving sources observed on the sun at 2 centimeters wavelength N87-20925

BROADCASTING

A survey of achieved levels of airborne sound insulation in broadcasting studio centres
[BBC-RD-1987/1] N87-20796

BUBBLE MEMORY DEVICES

Bubble memory module for spacecraft application
[NASA-TM-86411] N87-20476

BUBBLES

Chemistry of glass-ceramic to metal bonding for header applications Part 2: Hydrogen bubble formation during glass-ceramic to metal sealing
[DE87-004041] N87-20559

C

C-135 AIRCRAFT

Rapid melt/quench furnace using commercially available hardware
[NASA-TM-86500] N87-20431

CABLES (ROPES)

Initial investigations into the damping characteristics of wire rope vibration isolators
[NASA-CR-180698] N87-20569

CALCULUS OF VARIATIONS

Dynamical and thermodynamical characteristics of a squall-line determined from dual-Doppler data N87-20697

CALIBRATING

Design and verification by nonlinear simulation of a Mach/CAS control law for the NASA TCV B737 aircraft
[NASA-CR-178029] N87-20290

The in-situ calibration of a bilateral space-fed phased array antenna
[AD-A176069] N87-20456

Zero-shifted accelerometer outputs N87-20609

Panel report on new approaches to calibration and validation — Columbus polar platforms N87-20638

CAPACITANCE SWITCHES

Low pass PI section digital phase shifter apparatus
[AD-D012553] N87-20483

CAPILLARY FLOW

Investigation of thermal-fluid mechanical characteristics of the capillary pump and the pumped two-phase loop
[NASA-CR-180509] N87-20557

CARBON

Analysis of experimental determinations of the thermal conductivity of CBCF (Carbon-Bonded Carbon Fiber) insulation
[DE87-004025] N87-20393

Rapid thermal annealing of Amorphous Hydrogenated Carbon (a-C:H) films
[NASA-TM-89859] N87-20821

Carbon and nitrogen abundances along the evolutionary sequence of M67 N87-20848

CARBON DIOXIDE

High temperature CO2 study: Anti-Stokes coherent Raman diffusion and infrared spectroscopy
[ONERA-P-1986-2] N87-20402

CARBON DIOXIDE LASERS

Closed-Cycle, Frequency-Stable CO2 Laser Technology
[NASA-CP-2456] N87-20522

Review of the frequency stabilization of TEA CO2 laser oscillators N87-20523

Large mode radius resonators N87-20524

Wind velocity measurement accuracy with highly stable 12 mJ/pulse high repetition rate CO2 laser master oscillator power amplifier N87-20525

Analysis of intrapulse chirp in CO2 oscillators N87-20526

Frequency stabilization in injection controlled pulsed CO2 lasers N87-20527

High repetition rate sealed CO2 TEA lasers using heterogeneous catalysts N87-20529

Catalysts for long-life closed-cycle CO2 lasers N87-20532

Strong metal-support interactions N87-20533

Studies of long-life pulsed CO2 laser with Pt/SnO2 catalyst N87-20540

An overview of DREV's activities on pulsed CO2 laser transmitters: Frequency stability and lifetime aspects N87-20542

CARBON FIBER REINFORCED PLASTICS

A.T.R. 42 carbon fibre flap repair design and inspection N87-20178

Effect of adhesive bonding variables on the performance of bonded CFRP patch repairs of metallic structures N87-20182

Damage repair of in-service composite structures: Application to the Mirage 2000 N87-20184

Composite repair techniques for J-stiffened composite fuselage structures N87-20186

Damage in carbon-resin composites: Transversal cracking and peeling
[ONERA-RT-42/7086-M] N87-20398

CARBON FIBERS

British Airways experience with composite repairs N87-20192

Screening testing for composite prepregs
[DE87-004557] N87-20395

CARBON MONOXIDE

The oxidation of carbon monoxide using a tin oxide catalyst N87-20528

CO oxidation studies over supported noble metal catalysts and single crystals: A review N87-20530

Chemical engineering design of CO oxidation catalysts N87-20531

Reaction rate oscillations during catalytic CO oxidation: A brief overview N87-20534

Alumina-supported Pd-Ag catalysts for low-temperature CO and methanol oxidation N87-20536

Rare isotope studies involving catalytic oxidation of CO over platinum-tin oxide N87-20538

Studies of CO oxidation on Pt/SnO2 catalyst in a surrogate CO2 laser facility N87-20539

Characterization of Pt/SnO2 catalysts for CO oxidation N87-20541

Operation of transversely excited N2O lasers
[AD-D012583] N87-20543

Molecular clouds in the outer galaxy N87-20854

CARBON TETRAFLUORIDE

Computational analysis and preliminary redesign of the nozzle contour of the Langley hypersonic CF4 tunnel
[NASA-TM-89042] N87-20296

CARBON-CARBON COMPOSITES

Advanced composite combustor structural concepts program
[NASA-CR-174733] N87-20387

CARRIER DENSITY (SOLID STATE)

A study of III-V semiconductor processing employing high purity epitaxial gallium arsenide N87-20819

CARRIER MOBILITY

A study of III-V semiconductor processing employing high purity epitaxial gallium arsenide N87-20819

CASCADE FLOW

The high-speed cascade wind tunnel - still an important test facility for turbomachinery blade investigations
[ESA-TT-1012] N87-20300

CASCADE WIND TUNNELS

The high-speed cascade wind tunnel - still an important test facility for turbomachinery blade investigations
[ESA-TT-1012] N87-20300

CATALYSIS

Rare isotope studies involving catalytic oxidation of CO over platinum-tin oxide N87-20538

CATALYSTS
Catalysts for long-life closed-cycle CO2 lasers N87-20532
Characterization of the LTC catalyst: Performance against common air pollutants N87-20535
Alumina-supported Pd-Ag catalysts for low-temperature CO and methanol oxidation N87-20536
A review of tin oxide-based catalytic systems: Preparation, characterization and catalytic behavior N87-20537
Studies of CO oxidation on Pt/SnO2 catalyst in a surrogate CO2 laser facility N87-20539
Studies of long-life pulsed CO2 laser with Pt/SnO2 catalyst N87-20540
Characterization of Pt/SnO2 catalysts for CO oxidation N87-20541
CATALYTIC ACTIVITY
The oxidation of carbon monoxide using a tin oxide catalyst N87-20528
CO oxidation studies over supported noble metal catalysts and single crystals: A review N87-20530
Chemical engineering design of CO oxidation catalysts N87-20531
Reaction rate oscillations during catalytic CO oxidation: A brief overview N87-20534
A review of tin oxide-based catalytic systems: Preparation, characterization and catalytic behavior N87-20537
CATHODES
Characterization of monolithic fuel cell components [DE87-004929] N87-20655
CAVITATION CORROSION
Deformation and fracture of single-crystal and sintered polycrystalline silicon carbide produced by cavitation [NASA-TM-88961] N87-20422
CAVITATION FLOW
Supersonic flow induced cavity acoustics N87-20601
CAVITIES
Patch repair of corroded aircraft skin areas N87-20191
Supersonic flow induced cavity acoustics N87-20601
CAVITY RESONATORS
Factors limiting the operation of structures under high gradient — linear accelerators [DE87-005132] N87-20461
CELLS (BIOLOGY)
Microalgae culture collection, 1986-1987 [DE87-005578] N87-20729
CENTER OF GRAVITY
Space station control moment gyro control N87-20669
CENTER OF PRESSURE
Space station control moment gyro control N87-20669
CENTRIFUGAL COMPRESSORS
Experimental and theoretical investigation of the flow phenomena in return channels of radial compressor stages, especially those with small channel width [MITT-85-01] N87-20267
CERAMIC COATINGS
High temperature protective coatings for aero engine gas turbine components [AD-A176001] N87-20286
CERAMIC MATRIX COMPOSITES
Advanced composite combustor structural concepts program [NASA-CR-174733] N87-20387
CERAMICS
Chemistry of glass-ceramic to metal bonding for header applications Part 2: Hydrogen bubble formation during glass-ceramic to metal sealing [DE87-004041] N87-20559
CERENKOV RADIATION
A search for very high energy gamma ray emission from Cygnus X-3 N87-20950
CHANNEL FLOW
Experimental and theoretical investigation of the flow phenomena in return channels of radial compressor stages, especially those with small channel width [MITT-85-01] N87-20267
CHAOS
Nonlinear dynamics of some condensed matter devices and materials [ETN-87-99363] N87-20829
CHARACTERIZATION
Characterization of Pt/SnO2 catalysts for CO oxidation N87-20541
CHARPY IMPACT TEST
Impact energy relationships for directly rolled uranium strip [DE87-005789] N87-20418
CHEMICAL COMPOSITION
Measurements of iridium and the hypothesis of meteoritic impact as the end of the Cretaceous period [INPE-4070-TDL/248] N87-20661
CHEMICAL EFFECTS
Effect of long-term spaceflight on rat brain polyamine content N87-20741
CHEMICAL ELEMENTS
Thermodynamic data of intermetallic compounds [DE87-701244] N87-20831
CHEMICAL ENGINEERING
Chemical engineering design of CO oxidation catalysts N87-20531
CHEMICAL REACTIONS
Theoretical kinetic computations in complex reacting systems N87-20277
The chemical shock tube as a tool for studying high-temperature chemical kinetics N87-20279
Strong metal-support interactions N87-20533
An asymptotic analysis of supersonic reacting mixing layers [NASA-CR-178266] N87-20756
CHEMICAL REACTORS
Laser spectroscopy and gas-phase chemistry in CVD [DE86-007392] N87-20548
CHINA
USSR report: Physics and mathematics [JPRS-UPM-86-008] N87-20445
China report: Science and technology [JPRS-CST-86-025] N87-20708
Hydrologic features in cyclonic eddy region of northern east China Sea in cold seasons N87-20709
China report: Science and technology [JPRS-CST-87-005] N87-20717
CHINESE SPACECRAFT
Attitude motion of torque-free asymmetric dual-spin spacecraft [AD-A175531] N87-20354
CHIRP
Analysis of intrapulse chirp in CO2 oscillators N87-20526
CHLORIDES
Determination of the ternary viscosity diagram NaCl-KCl-LiCl by the flow method [INSA-IDTC1-8604] N87-20403
CHROMOSPHERE
Formation and support of prominence N87-20674
Formation of active region and quiescent prominence magnetic field configurations N87-20679
On the formation of active region prominences (H alpha filaments) N87-20684
The prominence-corona interface and its relationship to the chromosphere-corona transition N87-20891
Observations of the Ca II K line in Hel0830A dark points on August 3, 1985 N87-20929
CIRCULAR WAVEGUIDES
China report: Science and technology [JPRS-CST-87-005] N87-20717
CIVIL AVIATION
China report: Science and technology [JPRS-CST-87-005] N87-20717
CLINICAL MEDICINE
Blood lipids and incidence of lipemia in flight personnel N87-20737
USSR report: Life sciences. Biomedical and behavioral sciences [JPRS-UBB-87-003] N87-20751
CLOSED CYCLES
Closed-Cycle, Frequency-Stable CO2 Laser Technology [NASA-CP-2456] N87-20522
Catalysts for long-life closed-cycle CO2 lasers N87-20532
CLOSED ECOLOGICAL SYSTEMS
Phycomyces in space: A problem in bioengineering N87-20308
CLOUD HEIGHT INDICATORS
A bispectral method for the determination of the altitude of ice clouds [ESA-TT-993] N87-20704
CLOUD PHYSICS
Definition and use of sensors for measuring electrical conductivity in thunderclouds [ONERA-NT-1986-4] N87-20705
CLOUDS
LOWTRAN modeling of near-horizon infrared sky radiances in the presence of clouds [AD-A175661] N87-20691
CLOUDS (METEOROLOGY)
The terminal area simulation system. Volume 1: Theoretical formulation [NASA-CR-4046-VOL-1] N87-20255
A bispectral method for the determination of the altitude of ice clouds [ESA-TT-993] N87-20704
COASTAL WATER
Continental shelf processes affecting the oceanography of the South Atlantic Bight [DE87-005303] N87-20716
COCKPITS
Traffic scenario generation technique for piloted simulation studies [NASA-TM-86397] N87-20254
Integration of altitude and airspeed information into a primary flight display via moving-tape formats [NASA-TM-89064] N87-20265
CODING
Lewis inverse design code (LINDES): Users manual [NASA-TP-2676] N87-20238
COHERENT ELECTROMAGNETIC RADIATION
The laser strength of active elements made of Gadolinium-Scandium-Gallium garnet (GSGG) N87-20446
COLD CATHODES
Investigation of low-current-density nanosecond electron beam diode [IPPJ-T-36] N87-20818
COLD FRONTS
Numerical simulation of air mass modification over the East China Sea during the winter season N87-20660
COLD WEATHER TESTS
A freeze-thaw test to determine the frost susceptibility of soils [DOT/FAA-PM-85-20] N87-20434
COLLAPSE
The acceleration and dissolution of stars moving through the blackbody radiation of a collapsing universe N87-20847
COLLISION AVOIDANCE
The 3-D world modelling with updating capability based on combinatorial geometry [DE87-004257] N87-20643
COLLISIONAL PLASMAS
Spectral characteristics of interchange turbulence in the ionosphere [AD-A175975] N87-20692
COLLISIONS
The star-forming properties of violently interacting galaxies N87-20849
COLOR CODING
Evaluation of the performance of a geographically distributed data base management system using stochastic Petri nets [ENST-86C002] N87-20637
COLOR INFRARED PHOTOGRAPHY
Real-time crop assessment using color theory and satellite data N87-20619
COMBINATORIAL ANALYSIS
The 3-D world modelling with updating capability based on combinatorial geometry [DE87-004257] N87-20643
COMBUSTION
NASA-Chinese Aeronautical Establishment (CAE) Symposium [NASA-CP-2433] N87-20267
Remarks on the stability analysis of reactive flows [NASA-CR-178269] N87-20780
COMBUSTION CHAMBERS
Numerical calculations of turbulent reacting flow in a gas-turbine combustor [NASA-TM-89842] N87-20171
Modeling turbulent, reactig flow N87-20270
Effect of flame-tube head structure on combustion chamber performance N87-20275
Advanced composite combustor structural concepts program [NASA-CR-174733] N87-20387
Prediction of recirculation zones in isothermal coaxial jet flows relevant to combustors [NASA-CR-4064] N87-20501
COMBUSTION EFFICIENCY
Numerical calculations of turbulent reacting flow in a gas-turbine combustor [NASA-TM-89842] N87-20171
Performance and efficiency evaluation and heat release study of an outboard Marine Corporation Rotary Combustion Engine [NASA-TM-89833] N87-20262
COMBUSTION PHYSICS
Combustion research in the Internal Fluid Mechanics Division N87-20268
Combustion research activities at the Gas Turbine Research Institute N87-20273
Thermodynamics and combustion modeling N87-20274
Effect of flame-tube head structure on combustion chamber performance N87-20275
Theoretical study of the nonsteady combustion of composite fuel droplets [ESA-TT-868] N87-20401
COMBUSTION PRODUCTS
Thermodynamics and combustion modeling N87-20274

COMET HEADS
Encounter 86: An international rendezvous with Halley's comet
[ESA-BR-27] N87-20867
COMET NUCLEI
Encounter 86: An international rendezvous with Halley's comet
[ESA-BR-27] N87-20867
COMET TAILS
Encounter 86: An international rendezvous with Halley's comet
[ESA-BR-27] N87-20867
COMETARY ATMOSPHERES
MHD waves detected by ion at distances 28 x 10 km from Comet Halley: Cometary or solar wind origin
[DE87-005122] N87-20663
COMMERCE
Remote sensing applications: Commercial issues and opportunities for space station — SPOT N87-20626
COMMUNICATION NETWORKS
Unique bit-error-rate measurement system for satellite communication systems
[NASA-TP-2699] N87-20448
Propagation of RF signals through structured ionization. Theory and antenna aperture effect applications
[AD-A175522] N87-20451
COMMUNICATION SATELLITES
STS-61C, Columbia flight N87-20315
Dynamic analysis of direct television satellite TV-SAT/TDF.1 N87-20360
Modal testing of the Olympus development model stowed solar array N87-20366
COMMUNICATION THEORY
Research investigation directed toward extending the useful range of the electromagnetic spectrum
[AD-A175644] N87-20452
COMPILERS
The fault-tree compiler
[NASA-TM-89098] N87-20765
COMPOSITE FUNCTIONS
Composite grid and finite-volume LU implicit scheme for turbine flow analysis
[NASA-TM-89828] N87-20235
COMPOSITE MATERIALS
The Repair of Aircraft Structures Involving Composite Materials
[AGARD-CP-402] N87-20174
Design for repairability of helicopter composite blades N87-20176
TV-holography: A promising inspection tool for analysis of composite materials N87-20180
British Airways experience with composite repairs N87-20192
Use of lightweight composites for GAS payload structures N87-20307
Composite motor case nomenclature
[AD-A176418] N87-20384
Baseline tensile tests of composite materials for LDEF (Long Duration Exposure Facility) exposure
[NASA-TM-89069] N87-20386
Composites review
[NASA-TT-20008] N87-20388
High performance thermoplastics: A review of neat resin and composite properties
[NASA-TM-89104] N87-20390
Institute for Materials Science Engineering, Polymers: Technical activities 1986
[PB87-136693] N87-20420
Characterization of monolithic fuel cell components
[DE87-004929] N87-20655
COMPOSITE STRUCTURES
The Repair of Aircraft Structures Involving Composite Materials
[AGARD-CP-402] N87-20174
Development of field level repairs for composite structures N87-20177
A.T.R. 42 carbon fibre flap repair design and inspection N87-20178
Repair of helicopter composite structure techniques and substantiations N87-20179
Composite repair of cocured J-stiffened panels: Design and test verification N87-20181
Effect of adhesive bonding variables on the performance of bonded CFRP patch repairs of metallic structures N87-20182
Damage repair of in-service composite structures: Application to the Mirage 2000 N87-20184
Composite structure repairs carried out according to aeronautical techniques N87-20185
Composite repair techniques for J-stiffened composite fuselage structures N87-20186
Fibre composite repair of cracked metallic aircraft components: Practical and basic aspects N87-20187
Composite repair material and design development efforts N87-20188
Battle damage repair of composite structures N87-20189
The design of composite structures: Aircraft design
[NASA-TT-20011] N87-20261
Strain energy release rates of composite interlaminar end-notch and mixed-mode fracture: A sublaminate/ply level analysis and a computer code
[NASA-TM-89827] N87-20369
Residual effects in laminated, curved, composite panels
[DE87-005624] N87-20397
COMPRESSIBLE FLOW
Numerical solutions of unsteady flow past rotor sections N87-20198
Acta mechanica sinica (selected articles)
[AD-A176240] N87-20246
A holographic interferometry study of an axisymmetric shock-wave/boundary-layer strong interaction flow N87-20498
Remarks on the stability analysis of reactive flows
[NASA-CR-178269] N87-20780
COMPRESSOR BLADES
Shot peening for Ti-6Al-4V alloy compressor blades
[NASA-TP-2711] N87-20566
COMPUTATION
Theoretical kinetic computations in complex reacting systems N87-20277
Computations for the 16-foot transonic tunnel, NASA, Langley Research Center, revision 1
[NASA-TM-86319-REV-1] N87-20294
Computational analysis and preliminary redesign of the nozzle contour of the Langley hypersonic CF4 tunnel
[NASA-TM-89042] N87-20296
The pre-pulse in pyroshock measurement and analysis N87-20604
COMPUTATIONAL FLUID DYNAMICS
A numerical study of the Weis-Fogh mechanism N87-20197
Numerical solutions of unsteady flow past rotor sections N87-20198
Applications of Computational Fluid Dynamics in Aeronautics
[AGARD-CP-412] N87-20199
Flexible grid generation for complex geometries in two space dimensions based on variational principles N87-20200
New numerical techniques in the method of singularities for application to complex three-dimensional configurations N87-20205
The integration of computational fluid dynamics into the military aircraft design process N87-20210
Utilization of Euler codes in nonlinear aerodynamics N87-20215
Using the boundary-layer equations in three-dimensional viscous flow simulation N87-20222
Applications of RAE viscous flow methods near separation boundaries for three-dimensional wings in transonic flow N87-20224
Transonic Navier-Stokes wing solutions using a zonal approach. Part 2: High angle-of-attack simulation N87-20229
Integral method of wall interference correction in low-speed wind tunnels
[NASA-TT-20055] N87-20241
Simulation of transonic viscous wing and wing-fuselage flows using zonal methods
[NASA-TM-89421] N87-20242
Wing-nacelle interactions. Program 1985. Part two: Development of a finite element code for an isolated nacelle
[ONERA-RTS-21/3271-AY] N87-20250
Combustion research in the Internal Fluid Mechanics Division N87-20268
Modeling turbulent, reactig flow N87-20270
An application of computational fluid dynamics to the design of optimum ramjet powered missile components N87-20338
Development of a computational aero/fluids analysis system
[NASA-CR-179046] N87-20343
Numerical simulation of separated flows past bluff bodies N87-20499
A predictor-corrector method for calculation of incompressible fluid flow dynamics
[DE87-003804] N87-20508
Two-dimensional flow computation in straight blade arrays — turbine blades
[ONERA-RT-35/1621-RY-053-R] N87-20511
Activities report in computer science
[ETN-87-99377] N87-20758
Acoustic gravity waves: A computational approach
[NASA-CR-178270] N87-20781
COMPUTATIONAL GRIDS
Applications of Computational Fluid Dynamics in Aeronautics
[AGARD-CP-412] N87-20199
Flexible grid generation for complex geometries in two space dimensions based on variational principles N87-20200
A discussion on a mesh generation technique applicable to complex geometries N87-20201
Numerical grid generation around complete aircraft configurations N87-20202
Geometry definition and grid generation for a complete fighter aircraft N87-20203
New numerical techniques in the method of singularities for application to complex three-dimensional configurations N87-20205
Prediction of wing-body-store aerodynamics using a small perturbation method and a grid embedding technique N87-20207
A second order Godunov method for tactical missiles N87-20211
Analysis of the F-16 flow field by a block grid Euler approach N87-20217
Composite grid and finite-volume LU implicit scheme for turbine flow analysis
[NASA-TM-89828] N87-20235
Multigrid calculation of boundary-fitted orthogonal coordinates with applications to unsteady flows N87-20237
Simulation of transonic viscous wing and wing-fuselage flows using zonal methods
[NASA-TM-89421] N87-20242
Time-partitioning simulation models for calculation on parallel computers
[NASA-TM-89850] N87-20766
Performance studies of the multigrid algorithms implemented on hypercube multiprocessor systems
[NASA-CR-178237] N87-20769
COMPUTER AIDED DESIGN
Geometry definition and grid generation for a complete fighter aircraft N87-20203
An application of computational fluid dynamics to the design of optimum ramjet powered missile components N87-20338
Automatic graphics applied to antenna computer aided design N87-20763
COMPUTER AIDED MANUFACTURING
Geometry definition and grid generation for a complete fighter aircraft N87-20203
COMPUTER GRAPHICS
Applications of Computational Fluid Dynamics in Aeronautics
[AGARD-CP-412] N87-20199
Geometry definition and grid generation for a complete fighter aircraft N87-20203
Human-display interactions: Context-specific biases
[NASA-TM-89430] N87-20747
Rivista Tecnica Selenia, volume 10, number 1
[ETN-87-99091] N87-20759
Automatic graphics applied to antenna computer aided design N87-20763
COMPUTER INFORMATION SECURITY
Guide to sharing personal computer resources via local area networks, revised
[DE86-016088] N87-20772
COMPUTER NETWORKS
Activities report in computer science
[ETN-87-99377] N87-20758
COMPUTER PROGRAMMING
Conversion of ARO-1 to an implicit Navier-Stokes solver
[AD-A175967] N87-20505
A computer controlled signal preprocessor for laser fringe anemometer applications
[NASA-TM-88982] N87-20516
COMPUTER PROGRAMS
Simulation of an integrated fire and flight control system for air-to-air gunnery
[ETN-87-99479] N87-20293
Comparison of two procedures for predicting rocket engine nozzle performance
[NASA-TM-89814] N87-20379
Cryogenic regenerators
[DE87-701264] N87-20443
Nickel cadmium battery expert system
[NASA-CR-179031] N87-20471
Requirements specification for nickel cadmium battery expert system
[NASA-CR-179034] N87-20473
Modal test and analysis: Multiple tests concept for improved validation of large space structure mathematical models N87-20581
MACSYMA usage at Langley, revision 1
[NASA-CR-172518] N87-20753
A preliminary transient-fault experiment on the SIFT computer system
[NASA-TM-89058] N87-20770
Parallel processing of networks
[AD-A175641] N87-20771

COMPUTER STORAGE DEVICES
Bubble memory module for spacecraft application
[NASA-TM-86411] N87-20476
COMPUTER SYSTEMS DESIGN
A dynamic multicomputer system for managing scientific and engineering databases
[DE87-002497] N87-20757
COMPUTER SYSTEMS PERFORMANCE
A dynamic multicomputer system for managing scientific and engineering databases
[DE87-002497] N87-20757
COMPUTER SYSTEMS SIMULATION
A dynamic multicomputer system for managing scientific and engineering databases
[DE87-002497] N87-20757
COMPUTER TECHNIQUES
Conversion of ARO-1 to an implicit Navier-Stokes solver
[AD-A175967] N87-20505
Activities report in computer science
[ETN-87-99377] N87-20758
Searching the UVSP database and a list of experiments showing mass motions N87-20899
COMPUTER VISION
The 3-D world modelling with updating capability based on combinatorial geometry
[DE87-004257] N87-20643
COMPUTERIZED SIMULATION
Simulation of a jet deflection system with the aid of the Euler equations N87-20212
Numerical simulation of internal and external inviscid and viscous 3-D flow fields N87-20213
Application of the Navier-Stokes equations to solve aerodynamic problems N87-20225
Transonic Navier-Stokes wing solution using a zonal approach. Part 1: Solution methodology and code validation N87-20226
Simulation of three-dimensional transonic flow with separation past a hemisphere cylinder configuration N87-20230
Numerical simulation of the flow field around a complete aircraft N87-20231
The terminal area simulation system. Volume 2: Verification cases
[NASA-CR-4047-VOL-2] N87-20252
Traffic scenario generation technique for piloted simulation studies
[NASA-TM-86397] N87-20254
Performance and efficiency evaluation and heat release study of an outboard Marine Corporation Rotary Combustion Engine
[NASA-TM-89833] N87-20262
Multilevel representation and simulation for VLSI design
[AD-A175663] N87-20481
On the use of CORLIB subroutines for the solution of a model fluid flow problem
[DE87-005285] N87-20509
Force magnitude and angular velocity fluctuation reduction in a spring-restrained, flexibly-supported four-bar mechanical linkage N87-20589
Effectiveness of on-off damper in isolating dynamical systems N87-20594
Flat-plate solar array project. Volume 8: Project analysis and integration
[NASA-CR-180695] N87-20653
AFGWC's Advanced Weather Analysis and Prediction System (AWAPS)
[AD-A172801] N87-20702
China report: Science and technology
[JPRS-CST-87-005] N87-20717
A computer simulator for development of engineering system design methodologies
[NASA-TM-89109] N87-20755
Time-partitioning simulation models for calculation on parallel computers
[NASA-TM-89850] N87-20766
An investigation of transitional management problems for the NSTS
[NASA-CR-171979] N87-20834
A stochastic approach to project planning in an R and D environment
[DE87-005347] N87-20835
Computer simulation and analysis of spatial galaxy distributions N87-20851
A numerical study of some spherically-symmetric and axisymmetric cosmological models N87-20853
Double inflation: A possible resolution of the large-scale structure problem
[DE87-005403] N87-20865
COMPUTERS
Engineering thrust areas, 1987
[DE87-004443] N87-20441
Cumulative reports and publications through December 31, 1986
[NASA-CR-178257] N87-20754
Information-preserving models of physics and computation
[DE87-005354] N87-20793
CONCENTRATORS
The concentration principle applied to spaceborne solar arrays. AGORA mission: Studies synthesis
[SNIAS-959-CA/CG] N87-20657
CONDENSING
Can prominences form in current sheets N87-20876
CONDUCTIVE HEAT TRANSFER
Transient heat transfer to supercritical helium at low temperatures
[ETN-87-99321] N87-20832
The growth of radiative filamentation modes in sheared magnetic fields N87-20875
The prominence-corona interface and its relationship to the chromosphere-corona transition N87-20891
CONES
Optimization of hypersonic waveriders derived from cone flows including viscous effects N87-20193
CONFERENCES
The Repair of Aircraft Structures Involving Composite Materials
[AGARD-CP-402] N87-20174
The 1986 Get Away Special Experimenter's Symposium
[NASA-CP-2438] N87-20302
Mechanical Qualification of Large Flexible Spacecraft Structures
[AD-A175529] N87-20355
The Shock and Vibration Bulletin. Part 1: Welcome, Invited Papers, Shipboard Shock, Blast and Ground Shock, Shock Testing and Analysis
[AD-A175224] N87-20574
The Shock and Vibration Bulletin. Part 3: Invited Papers, Pyrotechnic Shock, Pyrotechnic Shock Workshop
[AD-A175228] N87-20602
Proceedings of the European Symposium on Polar platform Opportunities and Instrumentation for Remote-Sensing (ESPOIR)
[ESA-SP-266] N87-20621
Yosemite Conference on Ionospheric Plasma in the Magnetosphere: Sources, Mechanisms and Consequences, meeting report
[NASA-TM-86589] N87-20689
New book deals with spatial orientation N87-20746
The US Workshop on the Physics and Chemistry of Mercury Cadmium Telluride: Extended abstracts
[AD-A175593] N87-20822
Coronal and Prominence Plasmas
[NASA-CP-2442] N87-20871
CONGRESSIONAL REPORTS
Assured access to space: 1986
[GPO-60-627] N87-20838
CONNECTORS
Analysis of the receiving characteristics of the circular diffraction antenna with both a flush-mounted and a recessed center post
[DE87-003263] N87-20460
CONSTRUCTION
A self critical approach to data analysis and model building
[AD-A175640] N87-20791
CONTACT LOADS
Flexibility effects on tooth contact location in spiral bevel gear transmissions
[NASA-CR-4055] N87-20552
CONTAMINANTS
Shuttle/Spacelab contamination environment and effects handbook
[NASA-CR-4053] N87-20350
CONTINENTAL DRIFT
Wilson cycle studies
[NASA-CR-180503] N87-20664
CONTINENTAL SHELVES
Continental shelf processes affecting the oceanography of the South Atlantic Bight
[DE87-005303] N87-20716
CONTINGENCY
Contingency power for small turboshaft engines using water injection into turbine cooling air
[NASA-TM-89817] N87-20280
CONTOURS
Dynamic presentation of long term upper ocean study (LOTUS) data using videotape
[AD-A175535] N87-20711
CONTRAST
Atmospheric contrast transmittance monitor
[AD-D012555] N87-20520
CONTROL
Multipurpose microcontroller design for PUGAS 2 N87-20321
Turnaround control for mechanically scanned radar antennas
[AD-D012563] N87-20457
A computer controlled signal preprocessor for laser fringe anemometer applications
[NASA-TM-88982] N87-20516
CONTROL EQUIPMENT
Description of a magnetic bearing test fixture
[NASA-TM-89081] N87-20478
CONTROL MOMENT GYROSCOPES
Space station momentum management N87-20668
Space station control moment gyro control N87-20669
CONTROL SIMULATION
Simulation of an integrated fire and flight control system for air-to-air gunnery
[ETN-87-99479] N87-20293
CONTROL SYSTEMS DESIGN
Stability regions of relaxed static stability aircraft under control saturation constraints N87-20288
Sophisticated software systems for small self-contained space shuttle payload G285 N87-20313
Control aspects of the launch phase of a vertically-launched short-range surface-to-air missile
[ETN-87-99478] N87-20341
Benefits of passive damping as applied to active control of large space structures N87-20371
Multi-axis vibration tests on spacecraft using hydraulic exciters N87-20373
Characteristic decomposition and the multivariable generalization of predictive self-tuning control
[OUEL-1651/86] N87-20776
CONTROL THEORY
Benefits of passive damping as applied to active control of large space structures N87-20371
Air Force basic research in dynamics and control of large space structures N87-20577
Adaptive control with a nonparametric model for the controlled system
[ETN-87-99015] N87-20775
Piecewise linear approximation for hereditary control problems
[NASA-CR-178260] N87-20778
CONTROLLABILITY
Analysis of NLR configurations using OCM for pilot modeling
[NASA-CR-180656] N87-20289
Estimability and regulability of linear systems
[NASA-TM-89427] N87-20790
CONTROLLERS
Active structural controllers emulating structural elements by ICUs N87-20367
Multi-axis vibration tests on spacecraft using hydraulic exciters N87-20373
Integrated digital control and man-machine interface for complex remote handling systems
[DE87-003002] N87-20749
CONVECTION
The terminal area simulation system. Volume 1: Theoretical formulation
[NASA-CR-4046-VOL-1] N87-20255
Testing and comparison of several mixed-layer models
[AD-A175959] N87-20712
Numerical simulations of a siphon mechanism for quiescent prominence formation N87-20880
Magnetic location of C IV events in the quiet network N87-20930
CONVECTION CURRENTS
Numerical simulation of air mass modification over the East China Sea during the winter season N87-20660
CONVERGENCE
Modeling and control of flexible structures N87-20564
A new approach to least squares estimation, with applications
[CWI-MS-R8602] N87-20787
COORDINATE TRANSFORMATIONS
Flexible grid generation for complex geometries in two space dimensions based on variational principles N87-20200
COPLANARITY
Propagation characteristics of some novel coplanar waveguide transmission lines on GaAs at MM-wave frequencies
[NASA-TM-89839] N87-20469
CORONAL HOLES
Magnetic field re-arrangement after prominence eruption N87-20907
Large scale structure of the corona N87-20909
Large scale structure of the sun's radio corona N87-20910
Synoptic study of the corona at meter wavelength N87-20911
Coronal plasmas on the sun and nearby stars N87-20919
Observations of the Ca II K line in HeI0830A dark points on August 3, 1985 N87-20929

CORONAL LOOPS
Constraints on filament models deduced from dynamical analysis N87-20897
Filament disappearances N87-20903
Coronal diagnostics. N87-20915
Three dimensional structures of solar active regions N87-20916
High-spatial-resolution microwave and related observations as diagnostics of coronal loops N87-20917
Theoretical models of free-free microwave emission from solar magnetic loops N87-20918
Coronal plasmas on the sun and nearby stars N87-20919
Measurement of coronal fields using spatially resolved microwave spectroscopy N87-20920
A numerical study of the thermal stability of low-lying coronal loops N87-20931
Cascade model of coronal heating N87-20938
Dynamic evolution of coronal magnetic fields N87-20945

CORRELATION
Progress in the development of holographic scheme for pair correlation estimation
[AD-A175573] N87-20518
H I structure and the soft X-ray background N87-20949

CORROSION
Patch repair of corroded aircraft skin areas N87-20191
Apparatus for high temperature in situ laser Raman spectroelectrochemical studies of metal corrosion and passivation in aqueous environments
[DE87-004868] N87-20416

CORROSION RESISTANCE
High temperature protective coatings for aero engine gas turbine components
[AD-A176001] N87-20286
Galvanic corrosion resistance of welded dissimilar nickel-base alloys
[DE87-002656] N87-20409

COSMIC RAY SHOWERS
Search for magnetic monopoles, neutrino oscillations, and superhigh energy physics
[DE87-005774] N87-20953

COSMIC RAYS
Phase partitioning, crystal growth, electrodeposition and cosmic ray experiments in microgravity N87-20305
Solar-geophysical data number 506, October 1986. Part 1: (Prompt reports). Data for September 1986, August 1986 and late data
[PB87-126389] N87-20948
Ultra-high energy gamma-rays as the carriers of cosmological information
[DE87-700680] N87-20952

COSMOLOGY
On the de Sitter and Nariai space-times in a generalized theory of gravitation
[DE86-703483] N87-20830
Problems in quantum cosmology N87-20846
The acceleration and dissolution of stars moving through the blackbody radiation of a collapsing universe N87-20847
A numerical study of some spherically-symmetric and axisymmetric cosmological models N87-20853
Ultra-high energy gamma-rays as the carriers of cosmological information
[DE87-700680] N87-20952

COST ANALYSIS
Satellite servicing mission preliminary cost estimation model
[NASA-CR-171978] N87-20335
Density uncertainty effect on cost of space station reboost N87-20667

COST EFFECTIVENESS
On modern avionic and defense systems logistic support standardization and cost effectiveness N87-20761

CRACK INITIATION
Damage in carbon-resin composites: Transversal cracking and peeling
[ONERA-RT-42/7086-M] N87-20398

CRACK PROPAGATION
Effect of adhesive bonding variables on the performance of bonded CFRP patch repairs of metallic structures N87-20182
Composite repair of cracked aluminum structure N87-20183
Fibre composite repair of cracked metallic aircraft components: Practical and basic aspects N87-20187
Damage in carbon-resin composites: Transversal cracking and peeling
[ONERA-RT-42/7086-M] N87-20398
Load biaxiality and fracture: A two-sided history of complementing errors
[AD-A175972] N87-20573

CRACK TIPS
Inclined pileup of edge dislocations near the crack tip
[AD-A175610] N87-20571

CRACKING (FRACTURING)
Inclined pileup of edge dislocations near the crack tip
[AD-A175610] N87-20571

CRACKS
Fibre composite repair of cracked metallic aircraft components: Practical and basic aspects N87-20187
AGARD (Advisory Group for Aerospace Research and Development) engine disc material cooperative test
[AD-A175533] N87-20283
Inclined pileup of edge dislocations near the crack tip
[AD-A175610] N87-20571

CREEP PROPERTIES
Creep behavior of niobium alloy PWC-11
[NASA-TM-89834] N87-20405
The variation of subgrain misorientation in aluminum deformed to large steady-state creep strains
[DE87-003238] N87-20415
Numerical and optical experiments on the Weissenberg effect
[ESA-TT-879] N87-20510
Creep and Creep Fracture: Conference proceedings
[DE87-780056] N87-20615

CREEP RUPTURE STRENGTH
Creep behavior of niobium alloy PWC-11
[NASA-TM-89834] N87-20405

CRITICAL MASS
Linear nonadiabatic pulsations of homogeneous ZAMS stars
[DE87-003722] N87-20844

CROP IDENTIFICATION
Real-time crop assessment using color theory and satellite data N87-20619

CROP VIGOR
Real-time crop assessment using color theory and satellite data N87-20619

CROSS FLOW
Experiments and modeling of dilution jet flow fields N87-20276

CRYOGENIC EQUIPMENT
Cryogenic regenerators
[DE87-701264] N87-20443

CRYOGENIC WIND TUNNELS
Design study of advanced model support systems for the National Transonic Facility (NTF)
[NASA-CR-178214] N87-20297
Aerodynamic measurements and thermal tests of a strain-gage balance in a cryogenic wind tunnel
[NASA-TM-89039] N87-20517

CRYSTAL GROWTH
Phase partitioning, crystal growth, electrodeposition and cosmic ray experiments in microgravity N87-20305
In situ observation of mono-molecular growth steps on aqueous solution grown crystals and the transport of molecules to the crystals N87-20334
Liquid drop stability for protein crystal growth in microgravity
[NASA-TP-2724] N87-20727
Computational analyses of crystal growth
[NASA-CR-179027] N87-20820

CRYSTAL STRUCTURE
Deep ion implantation for bipolar silicon devices; investigations into the use of the third dimension
[B8672201] N87-20828

CRYSTALS
China report: Science and technology
[JPRS-CST-86-025] N87-20706

CURING
Composite repair material and design development efforts N87-20188
Residual effects in laminated, curved, composite panels
[DE87-005624] N87-20397

CURRENT DENSITY
Investigation of low-current-density nanosecond electron beam diode
[IPPJ-T-36] N87-20818

CURRENT SHEETS
Can prominences form in current sheets N87-20876
Static current-sheet models of quiescent prominences N87-20882
Quasistatic evolution of magnetostatic coronal structures N87-20913

CURVED PANELS
Residual effects in laminated, curved, composite panels
[DE87-005624] N87-20397

CYCLIC LOADS
Bithermal low-cycle fatigue behavior of a NiCoCrAlY-coated single crystal superalloy
[NASA-TM-89831] N87-20406
Fatigue and acoustics: Prediction of metal fatigue using Miner's rule N87-20596

CYCLONES
The effect of latent heat on kinetic energy conversions associated with South Pacific cyclones N87-20696

CYGNUS CONSTELLATION
A search for very high energy gamma ray emission from Cygnus X-3 N87-20950

CYLINDRICAL BODIES
Experimental and finite-element investigation of flow past single and multiple cylinders N87-20195

CYLINDRICAL PLASMAS
Condensation modes in magnetized plasmas N87-20877

CYLINDRICAL SHELLS
Structural dynamics: Buckling of ring-stiffened cylindrical shells with dynamic loads N87-20595
An evaluation of active noise control in a cylindrical shell
[NASA-TM-89090] N87-20794

D

DAMAGE
WSUH-1D: Review of damage following lightning strike 30 November 1981
[RAE-TRANS-2103] N87-20262
Effects of space shuttle launches STS-1 through STS-9 on terrestrial vegetation of John F. Kennedy Space Center, Florida
[NASA-TM-83103] N87-20658

DAMPING
An evaluation of active noise control in a cylindrical shell
[NASA-TM-89090] N87-20794

DARK MATTER
Double inflation: A possible resolution of the large-scale structure problem
[DE87-005403] N87-20865

DATA ACQUISITION
An automated two-dimensional laser velocimeter system
[DE87-005625] N87-20549
The mesoscale organization, dynamics, and evolution of the marine planetary boundary layer during cold air outbreaks N87-20698
Wind and turbulence data for development of design criteria for unmanned high-altitude low-speed endurance aircraft
[NASA-CR-4065] N87-20699
Solar-geophysical data number 506, October 1986. Part 1: (Prompt reports). Data for September 1986, August 1986 and late data
[PB87-126389] N87-20948

DATA BASE MANAGEMENT SYSTEMS
A vibroacoustic database management system and its application for a pyroshock database N87-20607
A dynamic multicomputer system for managing scientific and engineering databases
[DE87-002497] N87-20757
Evaluation of the performance of a geographically distributed data base management system using stochastic Petri nets
[ENST-86C002] N87-20837

DATA CORRELATION
State-of-the-art assessment of structural dynamic response analysis methods (DYNAS) N87-20578
Magnetogram and soft X-ray comparisons of XBP and ER N87-20927

DATA MANAGEMENT
Payload data management scheme planned for Earth observation sensors to be flown on the polar platforms in the framework of the space station/Columbus program N87-20630
Data management panel report --- Columbus polar platforms N87-20639

DATA PROCESSING
An automated two-dimensional laser velocimeter system
[DE87-005625] N87-20549
Magnetotelluric measurements in Antarctica
[INPE-4058-PRE/1017] N87-20661
A self critical approach to data analysis and model building
[AD-A175640] N87-20791

DATA REDUCTION
Computations for the 16-foot transonic tunnel, NASA, Langley Research Center, revision 1
[NASA-TM-86319-REV-1] N87-20294
A self critical approach to data analysis and model building
[AD-A175640] N87-20791

DATA RETRIEVAL
Searching the UVSP database and a list of experiments showing mass motions N87-20899

DATA SMOOTHING
NASA/MSFC prediction techniques N87-20678

DATA STRUCTURES
A vibroacoustic database management system and its application for a pyroshock database N87-20607
DATA SYSTEMS
Users manual for nickel cadmium battery expert system
[NASA-CR-179032] N87-20470
Nickel cadmium battery expert system
[NASA-CR-179031] N87-20471
Automated anthropometric data measurement system
[AD-D012575] N87-20748
DATA TRANSMISSION
Payload data management scheme planned for Earth observation sensors to be flown on the polar platforms in the framework of the space station/Columbus program N87-20630
Automated anthropometric data measurement system
[AD-D012575] N87-20748
DECAY
Thermal production of not so invisible axions in the early universe
[DE87-005404] N87-20666
DECISION MAKING
An investigation of transitional management problems for the NSTS
[NASA-CR-171979] N87-20634
DEFLECTION
Simulation of a jet deflection system with the aid of the Euler equations N87-20212
Flexibility effects on tooth contact location in spiral bevel gear transmissions
[NASA-CR-4055] N87-20552
DEFORMATION
Dynamic and thermal effects in very large space structures N87-20347
The variation of subgrain misorientation in aluminum deformed to large steady-state creep strains
[DE87-003236] N87-20415
Deformation and fracture of single-crystal and sintered polycrystalline silicon carbide produced by cavitation
[NASA-TM-88981] N87-20422
Inclined pileup of edge dislocations near the crack tip
[AD-A175610] N87-20571
Theoretical investigations of shear band formation in finite elasticity
[AD-A175657] N87-20572
Dislocation reactions at grain boundaries in Li2 ordered alloys
[DE87-005713] N87-20827
DEGRADATION
Future trends in spacecraft design and qualification N87-20356
Erosion and strength degradation in alumina
[DE87-003341] N87-20428
Structural degradation of impacted graphite/epoxy laminates N87-20586
DEGREES OF FREEDOM
Isolation and damping: A graphical method of determining the response of the cascaded two degree of freedom system N87-20592
DELAY LINES
Magnetostatic wave frequency analyzer apparatus
[AD-D012558] N87-20458
DELTA WINGS
Applications of Euler equations to sharp edge delta wings with leading edge vortices N87-20214
Investigation of leading-edge flap performance on delta and double-delta wings at supersonic speeds
[NASA-TP-2656] N87-20233
Surface pressure measurements on a double delta Wing/Body configuration at Mach 2 and Mach 3 (WTR 1396)
[AD-A175951] N87-20245
DEMOGRAPHY
Automated anthropometric data measurement system
[AD-D012575] N87-20748
DEOXYRIBONUCLEIC ACID
Effect of hypoxia on DNA synthesis and collagent content of regenerating skin N87-20742
DESCENT TRAJECTORIES
Users of middle atmosphere models remarks N87-20679
Utilization of Global Reference Atmosphere Model (GRAM) for shuttle entry N87-20680
Use of the 4D-Global Reference Atmosphere Model (GRAM) for space shuttle descent design N87-20681
Shuttle derived atmosphere N87-20684
DESCRIPTIVE GEOMETRY
Applications and developments of computational methods for the aerodynamic problems of complex configurations N87-20209
DESIGN ANALYSIS
Lewis inverse design code (LINDES): Users manual
[NASA-TP-2676] N87-20238
Design and analysis of advanced flight planning concepts
[NASA-CR-4063] N87-20253
Design, fabrication and performance of small, graphite electrode, multistage depressed collectors with 200-W, CW, 8- to 18-GHz traveling-wave tubes
[NASA-TP-2693] N87-20474
Analysis of 12 AH aerospace nickel-cadmium cells from the design variable program
[NASA-TM-87774] N87-20479
Chemical engineering design of CO oxidation catalysts N87-20531
Structural dynamic reanalysis using Ritz vectors N87-20597
A computer simulator for development of engineering system design methodologies
[NASA-TM-89109] N87-20755
DETECTION
Research investigation directed toward extending the useful range of the electromagnetic spectrum
[AD-A175644] N87-20452
DETONATORS
Feasibility study of a Semiconductor Bridge (SCB) for initiating pyrotechnics and explosives
[DE87-004444] N87-20430
DIAGNOSIS
Application of CARS to scramjet combustion
[NASA-CR-178245] N87-20400
DIAMINES
Composite repair material and design development efforts N87-20188
DIELECTRICS
A theoretical and experimental study of cylindrical dielectric resonators and their applications to microwave oscillators
[FOA-C-30434-3.2] N87-20495
Development of optical thin film technology for lasers and synchrotron radiation
[DE87-701254] N87-20817
DIESEL ENGINES
Comparison of 6.2L arctic and standard fuel injection pumps using JP-8 fuel
[AD-A175597] N87-20558
DIFFERENCE EQUATIONS
Numerical investigations of geometrically nonlinear shell kinetics
[ETN-87-99019] N87-20616
DIFFERENTIAL EQUATIONS
A multiple zone method for supersonic tactical missiles
[AD-A175938] N87-20244
Eigensystem analysis of classical relaxation techniques with applications to multigrid analysis
[NASA-TM-88377] N87-20785
DIFFRACTION
Analysis of the receiving characteristics of the circular diffraction antenna with both a flush-mounted and a recessed center post
[DE87-003283] N87-20460
Diffraction diffusion screen with holographically suppressed zero-order beam
[AD-D012565] N87-20519
DIFFUSERS
Combustion research activities at the Gas Turbine Research Institute N87-20273
DIFFUSION
Diffraction diffusion screen with holographically suppressed zero-order beam
[AD-D012565] N87-20519
DIGITAL FILTERS
Modal parameter identification using adaptive digital filters N87-20583
DIGITAL SIMULATION
Numerical simulation of air mass modification over the East China Sea during the winter season N87-20660
DIGITAL TECHNIQUES
The digital processing of acceleration measurements for modal analysis N87-20439
DIMENSIONAL STABILITY
Dynamic and thermal effects in very large space structures N87-20347
DIODES
Low pass Pi section digital phase shifter apparatus
[AD-D012553] N87-20483
Injection-seeding studies of diode laser array behavior
[DE87-002051] N87-20548
Investigation of low-current-density nanosecond electron beam diode
[IPPJ-T-36] N87-20618
DIPOLE ANTENNAS
Analysis of the receiving characteristics of the circular diffraction antenna with both a flush-mounted and a recessed center post
[DE87-003283] N87-20460
DISCONTINUITY
A practical assessment of spectral accuracy for hyperbolic problems with discontinuities
[NASA-CR-178226] N87-20779
DISCOVERY (ORBITER)
Post-flight BET products for the 2nd discovery entry, STS-19 (51-A)
[NASA-CR-172572] N87-20344
DISCRETE FUNCTIONS
Galerkin/Runge-Kutta discretizations for semilinear parabolic equations
[NASA-CR-178264] N87-20783
DISK GALAXIES
The star-forming properties of violently interacting galaxies N87-20849
DISPLAY DEVICES
Traffic scenario generation technique for piloted simulation studies
[NASA-TM-86397] N87-20254
The retinal image of the fresnel lens optical landing system
[AD-A176090] N87-20258
Integration of altitude and airspeed information into a primary flight display via moving-tape formats
[NASA-TM-89064] N87-20265
Human-display interactions: Context-specific biases
[NASA-TM-89430] N87-20747
DOPPLER EFFECT
Acoustic scattering from composite wind-wave surfaces II: Backscatter cross sections and Doppler effects at high frequencies and small angles for 'bubble-free' regimes
[AD-A176081] N87-20715
Non-LTE hydrogen-line formation in moving prominences N87-20895
C IV Doppler shifts observed in active region filaments N87-20896
DRAG CHUTES
A preliminary study into the constant drag parachute for aircrew escape systems
[BU-345] N87-20256
DRAG DEVICES
The effects of large-eddy manipulator devices on the turbulent spot and the turbulent boundary layer N87-20497
DRAG REDUCTION
The integration of computational fluid dynamics into the military aircraft design process N87-20210
DROPS (LIQUIDS)
The physics of fuel sprays. Volume 1: Experimental measurements
[AD-A175660] N87-20285
USC/AIAA student get away special project liquid droplet collector experiment N87-20316
Liquid droplet radiator development status
[NASA-TM-89852] N87-20353
Theoretical study of the nonsteady combustion of composite fuel droplets
[ESA-TT-868] N87-20401
Liquid drop stability for protein crystal growth in microgravity
[NASA-TP-2724] N87-20727
DUCTED FLOW
Experiments and modeling of dilution jet flow fields N87-20276
DUCTILITY
Ductility and fracture behavior of polycrystalline Ni3Al alloys
[DE87-005340] N87-20413
DUCTS
Decoupled bellmouth: An alternate method of measuring thrust in the sea level test cell
[AD-A175616] N87-20284
DWARF STARS
The acceleration and dissolution of stars moving through the blackbody radiation of a collapsing universe N87-20847
DYNAMIC CHARACTERISTICS
Flexibility effects on tooth contact location in spiral bevel gear transmissions
[NASA-CR-4055] N87-20552
Dynamic presentation of long term upper ocean study (LOTUS) data using videotape
[AD-A175535] N87-20711
DYNAMIC LOADS
Experimental and analytical evaluation of dynamic load and vibration of a 2240-kW (300-hp) rotorcraft transmission
[NASA-TM-88975] N87-20556
Implementation of active force control for robots subject to dynamic loading N87-20588
Structural dynamics: Buckling of ring-stiffened cylindrical shells with dynamic loads N87-20595
Evaluation of vibration specifications for static and dynamic material allowables N87-20600

DYNAMIC RESPONSE
Investigation of transonic region of high dynamic response encountered on an elastic supercritical wing [NASA-TM-89121] N87-20236
Use of a video-photogrammetry system for the measurement of the dynamic response of the shuttle remote manipulator arm N87-20370
Acoustic effects on the dynamic of lightweight structures N87-20372
Stable response of damped linear systems, part 3 N87-20440
State-of-the-art assessment of structural dynamic response analysis methods (DYNAS) N87-20578
The Shock and Vibration Bulletin. Part 2: Modal Test and Analysis, Testing Techniques, Machinery Dynamics, Isolation and Damping, Structural Dynamics [AD-A175225] N87-20580
The algorithm and application of a new multi-input-multi-output modal parameter identification method N87-20582
SAFE/DAE: Modal test in space N87-20584
Testing techniques. Random variation of modal frequencies: Experiments and analysis N87-20585
Machinery dynamics: Prediction of natural frequencies of flexible shaft-disc system N87-20587
Implementation of active force control for robots subject to dynamic loading N87-20588
A new approach for gearbox modelling in finite element analyses of torsional vibration of gear-branched propulsion systems N87-20591
Isolation and damping: A graphical method of determining the response of the cascaded two degree of freedom system N87-20592
Temperature shift considerations for damping materials N87-20593
Structural dynamics: Buckling of ring-stiffened cylindrical shells with dynamic loads N87-20595
Forced vibrations of stringer stiffened damped sandwich panel N87-20596
The Shock and Vibration Bulletin. Part 3: Invited Papers, Pyrotechnic Shock, Pyrotechnic Shock Workshop [AD-A175226] N87-20602
Super*Zip (linear separation) shock characteristics N87-20605
Numerical simulation of Atlas-Centaur stage-separation shaped charge firing and structural response N87-20606
Comparison of response from different resonant plate simulation techniques N87-20611
Multi-axis transient shock simulation using mechanical pulse generators N87-20613

DYNAMIC STABILITY
Aeroelastic stability of bearingless rotors in forward flight N87-20260

DYNAMIC STRUCTURAL ANALYSIS
Dynamic and thermal effects in very large space structures N87-20347
Studies in nonlinear structural dynamics: Chaotic behavior and poynting effect N87-20348
Mechanical Qualification of Large Flexible Spacecraft Structures [AD-A175529] N87-20355
Recent developments and future trends in structural dynamic design verification and qualification of large flexible spacecraft N87-20357
Dynamic analysis of direct television satellite TV-SAT/TDF.1 N87-20360
Structural qualification of large spacecraft N87-20361
Dynamic qualification of spacecraft by means of modal synthesis N87-20363
Modal-survey testing for system identification and dynamic qualification of spacecraft structures N87-20365
Modal testing of the Olympus development model stowed solar array N87-20366
Modeling of joints for the dynamic analysis of truss structures [NASA-TP-2661] N87-20567
Space station structures and dynamics test program [NASA-TP-2710] N87-20568
Structures and Dynamics Division research and technology plans for FY 1987 and accomplishments for FY 1986 [NASA-TM-89141] N87-20570
The Shock and Vibration Bulletin. Part 1: Welcome, Invited Papers, Shipboard Shock, Blast and Ground Shock, Shock Testing and Analysis [AD-A175224] N87-20574
State-of-the-art assessment of structural dynamic response analysis methods (DYNAS) N87-20578
The DYNAS survey. Part 2: A participant's view N87-20579
The Shock and Vibration Bulletin. Part 2: Modal Test and Analysis, Testing Techniques, Machinery Dynamics, Isolation and Damping, Structural Dynamics [AD-A175225] N87-20580
Modal test and analysis: Multiple tests concept for improved validation of large space structure mathematical models N87-20581
The algorithm and application of a new multi-input-multi-output modal parameter identification method N87-20582
Modal parameter identification using adaptive digital filters N87-20583
SAFE/DAE: Modal test in space N87-20584
Testing techniques. Random variation of modal frequencies: Experiments and analysis N87-20585
Structural dynamics: Buckling of ring-stiffened cylindrical shells with dynamic loads N87-20595
Structural dynamic reanalysis using Ritz vectors N87-20597
An application of Rayleigh's method to the fast calculation of the first vibration frequency of a missile launcher cell N87-20762

DYNAMIC TESTS
Space station structures and dynamics test program [NASA-TP-2710] N87-20568

DYNAMICAL SYSTEMS
Air Force basic research in dynamics and control of large space structures N87-20577
The interpretation of crustal dynamics data in terms of plate interactions and active tectonics of the Anatolian Plate and surrounding regions in the Middle East [NASA-CR-180501] N87-20662
Estimability and regulability of linear systems [NASA-TM-89427] N87-20790
Information-preserving models of physics and computation [DE87-005354] N87-20793
Collisional dynamics of perturbed particle disks in the solar system [NASA-CR-180497] N87-20860

E

E REGION
Amplification of an electron density perturbation in the polar E layer, induced by strong HF waves [ETN-87-99014] N87-20695

EARTH ATMOSPHERE
Nuclear geophysics in space and atmospheric research at INPE/BRAZIL [DE87-700426] N87-20693

EARTH CRUST
The interpretation of crustal dynamics data in terms of plate interactions and active tectonics of the Anatolian Plate and surrounding regions in the Middle East [NASA-CR-180501] N87-20662
Wilson cycle studies [NASA-CR-180503] N87-20664
Crustal dynamics project data analysis, 1986. Volume 1: Fixed station VLBI geodetic results [NASA-TM-87806] N87-20690

EARTH IONOSPHERE
Yosemite Conference on Ionospheric Plasma in the Magnetosphere: Sources, Mechanisms and Consequences, meeting report [NASA-TM-86589] N87-20689
Spectral characteristics of interchange turbulence in the ionosphere [AD-A175975] N87-20692

EARTH OBSERVATIONS (FROM SPACE)
Proceedings of the European Symposium on Polar platform Opportunities and Instrumentation for Remote-Sensing (ESPOIR) [ESA-SP-268] N87-20621
The Earth observation activities of the European Space Agency and the use of the polar platform of the International Space Station N87-20622
Working group on Earth observation requirements for the Polar Orbiting Platform Elements of the International Space Station (the POPE Working Group) N87-20625
Orbit configurations — space station polar platform N87-20629
Payload data management scheme planned for Earth observation sensors to be flown on the polar platforms in the framework of the space station/Columbus program N87-20630
Cooperation of the International Space Station partners in the preparation of the use of space station elements for Earth observation (platform and payload aspects) N87-20631
Report of the atmosphere panel N87-20633
Land panel report — International Space Station N87-20634
Ocean-ice panel report — International Space Station N87-20635
Solid Earth panel report — Columbus program N87-20636
Panel report on multidisciplinary instrumentation: New possibilities — Columbus space station N87-20637
Data management panel report — Columbus polar platforms N87-20639
The orbit configuration panel report — Columbus polar platforms N87-20640

EARTH ORBITAL ENVIRONMENTS
Effects of space plasma discharge on the performance of large antenna structures in low Earth orbit [NASA-TM-89118] N87-20339

EARTH RESOURCES
Land panel report — International Space Station N87-20634

EARTH ROTATION
Crustal dynamics project data analysis, 1986. Volume 1: Fixed station VLBI geodetic results [NASA-TM-87806] N87-20690

ECONOMIC ANALYSIS
Flat-plate solar array project. Volume 2: Silicon material [NASA-CR-180659] N87-20647
Flat-plate solar array project. Volume 8: Project analysis and integration [NASA-CR-180695] N87-20653

EDGE DISLOCATIONS
Inclined pileup of edge dislocations near the crack tip [AD-A175610] N87-20571

EIGENVALUES
A Lanczos eigenvalue method on a parallel computer [NASA-TM-89097] N87-20768

EIGENVECTORS
Eigensystem analysis of classical relaxation techniques with applications to multigrid analysis [NASA-TM-88377] N87-20785

EJECTION SEATS
A preliminary study into the constant drag parachute for aircrew escape systems [BU-345] N87-20256
Airspeed sensing pressure valve system [AD-D012789] N87-20266

EL NINO
A technique to estimate the ocean surface energy flux using VAS multispectral data N87-20710

ELASTIC ANISOTROPY
Effects of elastic anisotropy on the anomalous yield behavior of cubic ordered alloys [DE87-005328] N87-20417

ELASTIC BUCKLING
Structural dynamics: Buckling of ring-stiffened cylindrical shells with dynamic loads N87-20595

ELASTIC PROPERTIES
Theoretical investigations of shear band formation in finite elasticity [AD-A175657] N87-20572
Load biaxiality and fracture: A two-sided history of complementing errors [AD A175972] N87-20573

ELASTODYNAMICS
Dynamic qualification of spacecraft by means of modal synthesis N87-20363
Modal-survey testing for system identification and dynamic qualification of spacecraft structures N87-20365

ELASTOMERS
Energy absorption of polyurethane based polymer alloys [AD-A175542] N87-20427

ELECTRIC ARCS
WSUH-1D: Review of damage following lightning strike 30 November 1981 [RAE-TRANS-2103] N87-20262
Operation of transversely excited N2O lasers [AD-D012583] N87-20543

ELECTRIC AUTOMOBILES
Temperature effects on nickel/iron battery characteristics [DE87-004930] N87-20489

ELECTRIC BATTERIES
Safety characteristics of non-lithium battery systems, revision 1 [AD-A174577] N87-20480
Batteries for hybrid vehicles or other high-power applications [DE87-004928] N87-20488
Temperature effects on nickel/iron battery characteristics [DE87-004930] N87-20489
Fuel cells in transportation [DE87-003746] N87-20654

ELECTRIC CHARGE
Three-body calculations at Los Alamos [DE87-001959] N87-20786

ELECTRIC CURRENT
Static current-sheet models of quiescent prominences N87-20882
ELECTRIC DISCHARGES
Safety characteristics of non-lithium battery systems, revision 1
[AD-A174577] N87-20480
ELECTRIC FIELDS
Large-scale electric fields resulting from magnetic reconnection in the corona N87-20944
Dynamic evolution of coronal magnetic fields N87-20945
ELECTRIC GENERATORS
Conceptual design of a solar electric advanced Stirling power system
[DE87-005036] N87-20656
ELECTRIC HYBRID VEHICLES
Batteries for hybrid vehicles or other high-power applications
[DE87-004928] N87-20488
ELECTRIC POWER SUPPLIES
A research program to assess the impact of the electromagnetic pulse on electric power systems
[DE87-002415] N87-20486
ELECTRIC PROPULSION
Arcjet component conditions through a multistart test
[NASA-TM-89857] N87-20382
ELECTRICAL CONDUCTIVITY METERS
Definition and use of sensors for measuring electrical conductivity in thunderclouds
[ONERA-NT-1986-4] N87-20705
ELECTRICAL FAULTS
Requirements specification for nickel cadmium battery expert system
[NASA-CR-179034] N87-20473
ELECTRICAL MEASUREMENT
Lightning strikes on aircraft. Exploitation of Landes (France)-Front '84 campaign and complementary development of airborne electrical sensors
[ONERA-RF-91/7154-PY] N87-20706
ELECTRO-OPTICS
Atmospheric contrast transmittance monitor
[AD-D012555] N87-20520
ELECTROCARDIOGRAPHY
Interpretation of right heart kinetocardiogram N87-20744
ELECTROCHEMICAL CELLS
Analysis of 12 AH aerospace nickel-cadmium cells from the design variable program
[NASA-TM-87774] N87-20479
Sodium sulfur battery: An overview
[DE87-004920] N87-20491
ELECTROCHEMICAL CORROSION
Galvanic corrosion resistance of welded dissimilar nickel-base alloys
[DE87-002656] N87-20409
ELECTROCHEMISTRY
Characterization of monolithic fuel cell components
[DE87-004929] N87-20655
ELECTRODEPOSITION
Phase partitioning, crystal growth, electrodeposition and cosmic ray experiments in microgravity N87-20305
Microgravity effects on electrodeposition of metals and metal-cermet mixtures N87-20332
Electroforming with nickel, iron, and aluminum
[DE87-005589] N87-20442
ELECTRODES
Design, fabrication and performance of small, graphite electrode, multistage depressed collectors with 200-W, CW, 8- to 18-GHz traveling-wave tubes
[NASA-TP-2693] N87-20474
Morphological changes in the sulfur electrode of lifecycle-tested Na/S cells
[DE87-004961] N87-20493
ELECTROFORMING
Electroforming with nickel, iron, and aluminum
[DE87-005589] N87-20442
ELECTROLYTES
Characterization of monolithic fuel cell components
[DE87-004929] N87-20655
ELECTROMAGNETIC FIELDS
Factors limiting the operation of structures under high gradient — linear accelerators
[DE87-005132] N87-20461
ELECTROMAGNETIC INTERFERENCE
Effects of space plasma discharge on the performance of large antenna structures in low Earth orbit
[NASA-TM-89118] N87-20339
Adaptive mutual interference suppression method
[AD-D012552] N87-20459
Analysis of intrapulse chirp in CO2 oscillators N87-20526
ELECTROMAGNETIC PULSES
A research program to assess the impact of the electromagnetic pulse on electric power systems
[DE87-002415] N87-20486
ELECTROMAGNETIC SPECTRA
Research investigation directed toward extending the useful range of the electromagnetic spectrum
[AD-A175644] N87-20452
ELECTROMAGNETIC WAVE FILTERS
A comparison of nonlinear filters for orbit determination and estimation N87-20336
ELECTROMAGNETS
Blade damping measurements in a spin rig with nozzle passing excitation simulated by electromagnets N87-20590
ELECTRON BEAMS
The propagation of an electron beam through the solar corona N87-20946
ELECTRON DENSITY (CONCENTRATION)
Magnetic field vector and electron density diagnostics from linear polarization measurements in 14 solar prominences N87-20902
Three dimensional structures of solar active regions N87-20916
Small-scale structures and the density irregularity of the inner corona N87-20932
ELECTRON ENERGY
The density and thickness of quiescent prominences N87-20893
Three dimensional structures of solar active regions N87-20916
ELECTRON MICROSCOPY
Physical, mechanical effect of velocity of sound in ocean sediments N87-20723
ELECTRON PLASMA
Amplification of an electron density perturbation in the polar E layer, induced by strong HF waves
[ETN-87-99014] N87-20695
ELECTRON STATES
The effects of heavy doping on the electronic states in semiconductors
[DE87-004421] N87-20624
ELECTRON TRANSITIONS
Studies of X-ray satellites in sodium, magnesium, aluminum, argon, and iron
[ETN-87-99364] N87-20612
ELECTRON TUNNELING
Electron tunneling studies of Mo/(sub)1-xRe/(sup)x/: Enhancement of superconductivity by a resonance mode
[DE87-003048] N87-20484
ELECTRONIC TRANSDUCERS
Definition and use of sensors for measuring electrical conductivity in thunderclouds
[ONERA-NT-1986-4] N87-20705
ELECTRONICS
China report: Science and technology
[JPRS-CST-87-005] N87-20717
ELECTROPHYSICS
The US Workshop on the Physics and Chemistry of Mercury Cadmium Telluride: Extended abstracts
[AD-A175593] N87-20822
ELECTROPLATING
Cal Poly Space Project G-279 N87-20324
Electroforming with nickel, iron, and aluminum
[DE87-005589] N87-20442
ELECTROTHERMAL ENGINES
Experimental study of low Reynolds number nozzles
[NASA-TM-89858] N87-20383
ELEMENTARY PARTICLE INTERACTIONS
The fifth force — fundamental interactions
[DE87-004612] N87-20694
ELEMENTARY PARTICLES
Thermal production of not so invisible axions in the early universe
[DE87-005404] N87-20866
ELLIPSOMETERS
Investigation of PTFE transfer films by infrared emission spectroscopy and phase-locked ellipsometry
[NASA-TM-89844] N87-20421
ELLIPTIC DIFFERENTIAL EQUATIONS
Numerical grid generation around complete aircraft configurations N87-20202
ELLIPTICAL GALAXIES
Self-consistent models of perfect triaxial galaxies N87-20859
EMISSION
Non-LTE hydrogen-line formation in moving prominences N87-20895
EMISSION SPECTRA
A bispectral method for the determination of the altitude of ice clouds
[ESA-TT-993] N87-20704
Interpretation of the prominence differential emissions measure for 3 geometries N87-20890
A search for very high energy gamma ray emission from Cygnus X-3 N87-20950
ENCAPSULATING
Flat-plate solar array project. Volume 7: Module encapsulation
[NASA-CR-180665] N87-20652
ENERGY ABSORPTION
Energy absorption of polyurethane based polymer alloys
[AD-A175542] N87-20427
ENERGY CONVERSION
Energy conversion in the coronal plasma N87-20934
ENERGY CONVERSION EFFICIENCY
Monolithic fuel cell development
[DE87-004926] N87-20492
A ring-cavity for a quadrupled Nd-YAG laser
[DE87-004175] N87-20547
Flat-plate solar array project. Volume 1: Executive summary
[NASA-CR-180658] N87-20646
Flat-plate solar array project. Volume 4: High-efficiency solar cells
[NASA-CR-180662] N87-20649
Investigation of low-current-density nanosecond electron beam diode
[IPPJ-T-36] N87-20618
ENERGY DISTRIBUTION
A dynamic model of filament eruptions and two ribbon flares N87-20908
ENERGY LEVELS
Research investigation directed toward extending the useful range of the electromagnetic spectrum
[AD-A175644] N87-20452
ENERGY METHODS
An application of Rayleigh's method to the fast calculation of the first vibration frequency of a missile launcher cell N87-20762
ENERGY TRANSFER
Small-scale coronal structure, part 3 N87-20922
A numerical study of the thermal stability of low-lying coronal loops N87-20931
Phlegethon flow: A proposed origin for spicules and coronal heating N87-20933
Cascade model of coronal heating N87-20938
ENGINE COOLANTS
Contingency power for small turboshaft engines using water injection into turbine cooling air
[NASA-TM-89817] N87-20280
ENGINE DESIGN
Numerical calculations of turbulent reacting flow in a gas-turbine combustor
[NASA-TM-88842] N87-20171
Theory and design of flight-vehicle engines
[NASA-TM-88583] N87-20281
ENGINE INLETS
Decoupled bellmouth: An alternate method of measuring thrust in the sea level test cell
[AD-A175616] N87-20284
An application of computational fluid dynamics to the design of optimum ramjet powered missile components N87-20338
ENGINE PARTS
High temperature protective coatings for aero engine gas turbine components
[AD-A176001] N87-20286
Advanced composite combustor structural concepts program
[NASA-CR-174733] N87-20367
ENGINE TESTS
Contingency power for small turboshaft engines using water injection into turbine cooling air
[NASA-TM-89817] N87-20280
Theory and design of flight-vehicle engines
[NASA-TM-88583] N87-20281
AGARD (Advisory Group for Aerospace Research and Development) engine disc material cooperative test
[AD-A175533] N87-20283
Pretest uncertainty analysis for chemical rocket engine tests
[NASA-TM-89819] N87-20515
ENGINEERING MANAGEMENT
Stages of development of the problem of flight safety in aviation medicine N87-20733
ENVIRONMENT POLLUTION
Continental shelf processes affecting the oceanography of the South Atlantic Bight
[DE87-005303] N87-20716
EPIDEMIOLOGY
USSR report: Life sciences. Biomedical and behavioral sciences
[JPRS-UBB-87-003] N87-20751
EPOXY RESINS
Composite repair of cracked aluminum structure N87-20183
Composite repair material and design development efforts N87-20188
Unconventional approaches to field repair N87-20190
Mechanical and thermal characterization of unidirectional aramid/epoxy
[CCMS-86-08] N87-20385

EQUATIONS OF MOTION
Attitude motion of torque-free asymmetric dual-spin spacecraft
[AD-A175531] N87-20354
EQUILIBRIUM EQUATIONS
A new approach for gearbox modelling in finite element analyses of torsional vibration of gear-branched propulsion systems N87-20591
Quasistatic evolution of magnetostatic coronal structures N87-20913
Three-dimensional magnetostatic models of the large-scale corona N87-20914
The topological description of coronal magnetic fields N87-20936
EQUIPMENT SPECIFICATIONS
A freeze-thaw test to determine the frost susceptibility of soils
[DOT/FAA-PM-85-20] N87-20434
EQUIVALENCE
An investigation of the strong principle of equivalence through the use of freely falling geocentric coordinates N87-20862
EROSION
High temperature protective coatings for aero engine gas turbine components
[AD-A176001] N87-20286
Erosion and strength degradation in alumina
[DE87-003341] N87-20428
Army research in shock mechanics N87-20576
ERROR ANALYSIS
Mean-square error bounds for reduced-error linear state estimators
[NASA-TM-89441] N87-20291
Pretest uncertainty analysis for chemical rocket engine tests
[NASA-TM-89819] N87-20515
ERRORS
Load biaxiality and fracture: A two-sided history of complementing errors
[AD-A175972] N87-20573
The pre-pulse in pyroshock measurement and analysis N87-20604
Simulation of wind gradient errors in NROSS (Navy Remote Ocean Sensing System) radar scatterometer data in a simplified geometry
[AD-A175754] N87-20642
Dynamical and thermodynamical characteristics of a squall-line determined from dual-Doppler data N87-20697
ETCHING
Etching of LiNbO3 by laser-driven fusion of salts
[DE87-003033] N87-20544
Noble-gas ion bombardment on clean silicon surfaces studied using ellipsometry and desorption
[B8672200] N87-20609
EULER EQUATIONS OF MOTION
Numerical solutions of unsteady flow past rotor sections N87-20198
Flexible grid generation for complex geometries in two space dimensions based on variational principles N87-20200
A discussion on a mesh generation technique applicable to complex geometries N87-20201
Simulation of a jet deflection system with the aid of the Euler equations N87-20212
Numerical simulation of internal and external inviscid and viscous 3-D flow fields N87-20213
Applications of Euler equations to sharp edge delta wings with leading edge vortices N87-20214
Utilization of Euler codes in nonlinear aerodynamics N87-20215
Euler solution for a complete fighter aircraft at sub- and supersonic speed N87-20216
Analysis of the F-16 flow field by a block grid Euler approach N87-20217
Zonal solutions for airfoils using Euler boundary-layer and Navier-Stokes equations N87-20219
Topological constraints and the existence of force-free fields N87-20935
EULER-LAGRANGE EQUATION
Numerical simulation of separated flows past bluff bodies N87-20499
EUROPE
Land mobile satellite communication system. Volume 1: Executive summary
[ITS-TR-043/86-VOL1] N87-20464
Land mobile satellite communication system. Volume 2: Traffic analysis and market demand for the land mobile communications system in the European scenario
[ITS-TR-043/86-VOL-2] N87-20465
Monthly mean pressure reconstructions for Europe (back to 1780) and North America (to 1958)
[DE87-005556] N87-20703
EUROPEAN AIRBUS
The design of composite structures: Aircraft design
[NASA-TT-20011] N87-20261
EUROPEAN SPACE AGENCY
The Earth observation activities of the European Space Agency and the use of the polar platform of the International Space Station N87-20622
EUROPEAN SPACE PROGRAMS
The Earth observation activities of the European Space Agency and the use of the polar platform of the International Space Station N87-20622
The Columbus program: An overview N87-20623
European utilization aspects studies — space stations N87-20624
ESA Columbus polar platform design concept N87-20627
Servicing of the polar platform — Columbus space station N87-20628
USA-Europe coordination and cooperation activities: Announcements of Opportunity — polar platforms N87-20632
EVALUATION
Resilient modulus of freeze-thaw affected granular soils for pavement design and evaluation. Part 3: Laboratory tests on soils from Albany County Airport
[DOT/FAA-PM-84-16.3] N87-20433
Experimental and analytical evaluation of dynamic load and vibration of a 2240-kW (300-hp) rotorcraft transmission
[NASA-TM-88975] N87-20556
The acousto-ultrasonic approach
[NASA-TM-89843] N87-20562
Risk evaluations of aging phenomena: The linear aging reliability model and its extensions
[DE87-002607] N87-20563
Evaluation of physical work capacity of cosmonauts aboard Salyut-6 station N87-20735
EVAPORATION RATE
The physics of fuel sprays. Volume 1: Experimental measurements
[AD-A175660] N87-20285
EVOLUTION (DEVELOPMENT)
The magnetic and turbulent evolution of the Taurus molecular cloud N87-20852
EXCITATION
Studies of X-ray satellites in sodium, magnesium, aluminum, argon, and iron
[ETN-87-99364] N87-20812
EXHAUST GASES
Theoretical kinetic computations in complex reacting systems N87-20277
EXHAUST NOZZLES
An application of computational fluid dynamics to the design of optimum ramjet powered missile components N87-20338
EXOBIOLOGY
USSR report: Space Biology and Aerospace Medicine, Volume 20, No. 3, May - June 1986
[JPRS-USB-86-005] N87-20731
Space biology and medicine on the twenty-fifth anniversary of the first spaceflight of Yuriy Alekseyevich Gagarin N87-20732
EXOSPHERE
Limitations to modeling the thermosphere and exosphere N87-20674
EXPERIMENT DESIGN
Investigation of leading-edge flap performance on delta and double-delta wings at supersonic speeds
[NASA-TP-2656] N87-20233
NORSTAR Project: Norfolk public schools student team for acoustical research N87-20309
A systems-level performance history of get away specials after 25 space shuttle missions N87-20314
Shuttle/Spacelab contamination environment and effects handbook
[NASA-CR-4053] N87-20350
EXPERIMENTATION
Experimental and finite-element investigation of flow past single and multiple cylinders N87-20195
EXPERT SYSTEMS
Users manual for nickel cadmium battery expert system
[NASA-CR-179032] N87-20470
Nickel cadmium battery expert system
[NASA-CR-179031] N87-20471
Program maintenance manual for nickel cadmium battery expert system, version 1
[NASA-CR-179033] N87-20472
Requirements specification for nickel cadmium battery expert system
[NASA-CR-179034] N87-20473
Automation and robotics
[INPE-4088-PRE/1033] N87-20551
Rivista Tecnica Selenia, volume 10, number 1
[ETN-87-99091] N87-20759
Expert systems for diagnostic purposes, prospected applications to the radar field N87-20760
The Oak Ridge National Laboratory's Robotics and Intelligent Systems Program
[DE87-004627] N87-20774
EXPLOSIVES
Feasibility study of a Semiconductor Bridge (SCB) for initiating pyrotechnics and explosives
[DE87-004444] N87-20430
EXTERNAL STORE SEPARATION
Applications and developments of computational methods for the aerodynamic problems of complex configurations N87-20209
EXTERNAL STORES
Helicopter external load operations
[CAP-426] N87-20259
EXTINCTION
Measurements of iridium and the hypothesis of meteoritic impact as the end of the Cretaceous period
[INPE-4070-TDL/248] N87-20861
EXTRAGALACTIC RADIO SOURCES
Fiducial reference for the HIPPARCOS reference system
[NASA-CR-180250] N87-20842
EXTRATERRESTRIAL RADIATION
Nuclear geophysics in space and atmospheric research at INPE/BRAZIL
[DE87-700426] N87-20693
Space radiation studies
[NASA-CR-179037] N87-20951
EXTRAVEHICULAR ACTIVITY
Advanced EVA system design requirements study: EVAS/space station system interface requirements
[NASA-CR-171981] N87-20351
EXTREME ULTRAVIOLET RADIATION
Interpretation of the prominence differential emissions measure for 3 geometries N87-20890

F

FABRICATION
NORSTAR Project: Norfolk public schools student team for acoustical research N87-20309
Residual effects in laminated, curved, composite panels
[DE87-005624] N87-20397
Design, fabrication and performance of small, graphite electrode, multistage depressed collectors with 200-W, CW, 8- to 18-GHz traveling-wave tubes
[NASA-TP-2693] N87-20474
Monolithic fuel cell development
[DE87-004926] N87-20492
FABRICS
A.T.R. 42 carbon fibre flap repair design and inspection N87-20178
Damage repair of in-service composite structures: Application to the Mirage 2000 N87-20184
FACULAE
VLA observations of coronal bright points at 6 and 20 cm wavelengths N87-20924
FAILURE
Safety characteristics of non-lithium battery systems, revision 1
[AD-A174577] N87-20480
FAILURE ANALYSIS
A systems-level performance history of get away specials after 25 space shuttle missions N87-20314
Study of the nature of fracture failure in composite materials
[AD-A175554] N87-20391
Damage in carbon-resin composites: Transversal cracking and peeling
[ONERA-RT-42/7086-M] N87-20398
Nickel cadmium battery expert system
[NASA-CR-179031] N87-20471
Requirements specification for nickel cadmium battery expert system
[NASA-CR-179034] N87-20473
Numerical simulation of Atlas-Centaur stage-separation shaped charge firing and structural response N87-20606
A model for the degradation of composite structures
[ONERA-RT-30/3043-RY-057-R] N87-20617
FAILURE MODES
Strain energy release rates of composite interlaminar end-notch and mixed-mode fracture: A subliminate/ply level analysis and a computer code
[NASA-TM-89827] N87-20389
FAINT OBJECT CAMERA
Qualification of the faint object camera N87-20359
FAR INFRARED RADIATION
Molecular clouds in the outer galaxy N87-20854
FASTENERS
Patch repair of corroded aircraft skin areas N87-20191

FATIGUE (BIOLOGY)
Dynamics of bioelectric activity of human brain in a continuous waking state N87-20745
FATIGUE (MATERIALS)
AGARD (Advisory Group for Aerospace Research and Development) engine disc material cooperative test [AD-A175533] N87-20283
High temperature protective coatings for aero engine gas turbine components [AD-A176001] N87-20286
Study of the nature of fracture failure in composite materials [AD-A175554] N87-20391
Erosion and strength degradation in alumina [DE87-003341] N87-20428
Optimization of aerospace structures subjected to random vibration and fatigue constraints N87-20599
Evaluation of vibration specifications for static and dynamic material allowables N87-20600
FATIGUE LIFE
Advanced composite combustor structural concepts program [NASA-CR-174733] N87-20387
Bithermal low-cycle fatigue behavior of a NiCoCrAlY-coated single crystal superalloy [NASA-TM-89831] N87-20408
Calculation of thermomechanical fatigue life based on isothermal behavior [NASA-TM-88864] N87-20565
Fatigue and acoustics: Prediction of metal fatigue using Miner's rule N87-20596
Optimization of aerospace structures subjected to random vibration and fatigue constraints N87-20599
FATIGUE TESTS
Composite repair of cocured J-stiffened panels: Design and test verification N87-20181
Advanced composite combustor structural concepts program [NASA-CR-174733] N87-20387
FAULT TOLERANCE
The fault-tree compiler [NASA-TM-89098] N87-20765
A preliminary transient-fault experiment on the SIFT computer system [NASA-TM-89058] N87-20770
FAULT TREES
The fault-tree compiler [NASA-TM-89098] N87-20765
FEASIBILITY ANALYSIS
Feasibility of a phosphoric acid fuel cell basic technology program [DE87-001045] N87-20490
FEEDBACK
Research investigation directed toward extending the useful range of the electromagnetic spectrum [AD-A175644] N87-20452
FEEDBACK CONTROL
Modeling and control of flexible structures N87-20564
Characteristic decomposition and the multivariable generalization of predictive self-tuning control [OUEL-1651/86] N87-20776
Estimability and regulability of linear systems [NASA-TM-89427] N87-20790
FEMALES
Radiation protection guidelines for space missions [NASA-TM-89278] N87-20730
FERMAT PRINCIPLE
HARPA: A versatile three-dimensional Hamiltonian ray-tracing program for acoustic waves in the atmosphere above irregular terrain [PB87-132031] N87-20801
FIBER COMPOSITES
Screening testing for composite prepregs [DE87-004557] N87-20395
FIBER OPTICS
Unconventional approaches to field repair N87-20190
Referencing in fiber optic sensing systems [NASA-TM-89822] N87-20475
Integrated optical devices for high speed diagnostics [DE87-003160] N87-20816
FIBER REINFORCED COMPOSITES
Unconventional approaches to field repair N87-20190
Patch repair of corroded aircraft skin areas N87-20191
Advanced composite combustor structural concepts program [NASA-CR-174733] N87-20387
Study of the nature of fracture failure in composite materials [AD-A175554] N87-20391
FIBERS
Analysis of experimental determinations of the thermal conductivity of CBCF (Carbon-Bonded Carbon Fiber) insulation [DE87-004025] N87-20393
Biot theory and acoustical properties of high porosity fibrous materials and plastic foams [NASA-TM-88575] N87-20424
FIELD EFFECT TRANSISTORS
Linearization of GaAs field effect transistor power amplifiers in hyperfrequences [ENST-86E007] N87-20496
FIELD STRENGTH
High-spatial-resolution microwave and related observations as diagnostics of coronal loops N87-20917
Measurement of coronal fields using spatially resolved microwave spectroscopy N87-20920
Guided MHD waves as a coronal diagnostic tool N87-20921
FIELD THEORY (PHYSICS)
The fifth force — fundamental interactions [DE87-004612] N87-20684
On the de Sitter and Nariai space-times in a generalized theory of gravitation [DE86-703483] N87-20830
FIGHTER AIRCRAFT
A survey of military aerospace systems technology developments in Western Europe and the Middle East [AD-A175635] N87-20173
Geometry definition and grid generation for a complete fighter aircraft N87-20203
Euler solution for a complete fighter aircraft at sub- and supersonic speed N87-20216
Calculations for a generic fighter at supersonic high-lift conditions N87-20226
FILAMENT WINDING
Characterizing thermal/mechanical properties of filament wound composites [AD-A176238] N87-20392
FILLERS
Energy absorption of polyurethane based polymer alloys [AD-A175542] N87-20427
FINE STRUCTURE
Interpretation of the prominence differential emissions measure for 3 geometries N87-20890
Thermal stability analysis of the fine structure of solar prominences N87-20892
FINITE DIFFERENCE THEORY
Comparison of finite difference calculations of a large region of recirculating flow near an airfoil trailing edge N87-20218
Numerical investigation of the laminar boundary layer on a 3-D body started impulsively from rest N87-20220
Transonic Navier-Stokes wing solutions using a zonal approach. Part 2: High angle-of-attack simulation N87-20229
A finite difference scheme for three-dimensional steady laminar incompressible flow [NASA-TM-89851] N87-20504
Study of the development of a compressible turbulent boundary layer on a porous and rough wall [ETN-87-99390] N87-20512
Experimental evaluation of sub-cell turbulent models. Space-time correlations in a mixing layer [ETN-87-99391] N87-20513
Army research in shock mechanics N87-20576
Eigensystem analysis of classical relaxation techniques with applications to multigrid analysis [NASA-TM-88377] N87-20785
FINITE ELEMENT METHOD
Experimental and finite-element investigation of flow past single and multiple cylinders N87-20195
Wing-nacelle interactions. Program 1985. Part two: Development of a finite element code for an isolated nacelle [ONERA-RTS-21/3271-AY] N87-20250
Aeroelastic stability of bearingless rotors in forward flight N87-20260
Structural design of an in-line bolted joint for the space shuttle solid rocket motor case segments [NASA-TM-89027] N87-20349
Modal-survey testing for system identification and dynamic qualification of spacecraft structures N87-20365
Characterizing thermal/mechanical properties of filament wound composites [AD-A176238] N87-20392
Modeling and control of flexible structures N87-20564
The DYNAS survey. Part 2: A participant's view N87-20579
A new approach for gearbox modelling in finite element analyses of torsional vibration of gear-branched propulsion systems N87-20591
FINITE VOLUME METHOD
A second order Godunov method for tactical missiles N87-20211
Composite grid and finite-volume LU implicit scheme for turbine flow analysis [NASA-TM-89828] N87-20235
FINNED BODIES
A multiple zone method for supersonic tactical missiles [AD-A175938] N87-20244
FIRE CONTROL
Simulation of an integrated fire and flight control system for air-to-air gunnery [ETN-87-99479] N87-20293
FIRE PREVENTION
Fire safety concerns in space operations [NASA-TM-89648] N87-20342
FLAME HOLDERS
Experimental investigation of piloted flameholders N87-20278
FLAME PROPAGATION
Experimental investigation of piloted flameholders N87-20278
FLAME STABILITY
Experimental investigation of piloted flameholders N87-20278
FLAMES
Effect of flame-tube head structure on combustion chamber performance N87-20275
FLAPS (CONTROL SURFACES)
A.T.R. 42 carbon fibre flap repair design and inspection N87-20178
FLAT PLATES
Flat-plate solar array project of the US Department of Energy's National Photovoltaics Program: Ten years of progress [NASA-CR-180507] N87-20644
FLEXIBILITY
Machinery dynamics: Prediction of natural frequencies of flexible shaft-disc system N87-20587
FLEXIBLE BODIES
Dynamic and thermal effects in very large space structures N87-20347
Studies in nonlinear structural dynamics: Chaotic behavior and poynting effect N87-20348
Modeling and control of flexible structures N87-20564
Air Force basic research in dynamics and control of large space structures N87-20577
Inverse problems in the modeling of vibrations of flexible beams [NASA-CR-178259] N87-20777
FLEXIBLE SPACECRAFT
Mechanical Qualification of Large Flexible Spacecraft Structures [AD-A175529] N87-20355
Future trends in spacecraft design and qualification N87-20356
Recent developments and future trends in structural dynamic design verification and qualification of large flexible spacecraft N87-20357
Dynamic modeling and optimal control design for large flexible space structures N87-20358
Structural qualification of large spacecraft N87-20361
Spacecraft qualification using advanced vibration and modal testing techniques N87-20368
FLIGHT CONTROL
Development of a takeoff performance monitoring system [NASA-CR-178255] N87-20264
Design and verification by nonlinear simulation of a Mach/CAS control law for the NASA TCV B737 aircraft [NASA-CR-178029] N87-20290
Simulation of an integrated fire and flight control system for air-to-air gunnery [ETN-87-99479] N87-20293
FLIGHT CREWS
Blood lipids and incidence of lipemia in flight personnel N87-20737
Interpretation of right heart kinetocardiogram N87-20744
FLIGHT HAZARDS
Lightning strikes on aircraft. Exploitation of Landes (France)-Front '84 campaign and complementary development of airborne electrical sensors [ONERA-RF-91/7154-PY] N87-20706
FLIGHT MANAGEMENT SYSTEMS
Design and analysis of advanced flight planning concepts [NASA-CR-4063] N87-20253
Design and verification by nonlinear simulation of a Mach/CAS control law for the NASA TCV B737 aircraft [NASA-CR-178029] N87-20290

FLIGHT OPERATIONS
Helicopter external load operations
[CAP-426] N87-20259
FLIGHT PLANS
Design and analysis of advanced flight planning concepts
[NASA-CR-4063] N87-20253
FLIGHT SAFETY
Stages of development of the problem of flight safety in aviation medicine N87-20733
FLIGHT SIMULATION
Traffic scenario generation technique for piloted simulation studies
[NASA-TM-86397] N87-20254
Simulation of an integrated fire and flight control system for air-to-air gunnery
[ETN-87-99479] N87-20293
Aircraft noise synthesis system: Version 4 user instructions
[NASA-TM-89089] N87-20797
FLIGHT SIMULATORS
Documentation of the space station/aircraft acoustic apparatus
[NASA-TM-89111] N87-20795
FLIGHT TESTS
Liquid droplet radiator development status
[NASA-TM-89852] N87-20353
Use of a video-photogrammetry system for the measurement of the dynamic response of the shuttle remote manipulator arm N87-20370
SAFE/DAE: Modal test in space N87-20584
The 1985 small propeller-driven aircraft noise test program
[AD-A175596] N87-20799
FLIGHT VEHICLES
Theory and design of flight-vehicle engines
[NASA-TM-88583] N87-20281
FLOW CHARACTERISTICS
Investigation of flow under the fuselage of a powered light aircraft model
[BU-351] N87-20247
An investigation into the factors affecting the flow quality in a small suction wind tunnel
[BU-344] N87-20299
FLOW DISTRIBUTION
Applications of Computational Fluid Dynamics in Aeronautics
[AGARD-CP-412] N87-20199
A discussion on a mesh generation technique applicable to complex geometries N87-20201
Geometry definition and grid generation for a complete fighter aircraft N87-20203
An assessment of the use of low-order panel methods for the calculation of supersonic flows N87-20204
Prediction of wing-body-store aerodynamics using a small perturbation method and a grid embedding technique N87-20207
Matrics, transonic potential flow calculations about transport aircraft N87-20208
Applications and developments of computational methods for the aerodynamic problems of complex configurations N87-20209
The integration of computational fluid dynamics into the military aircraft design process N87-20210
Numerical simulation of internal and external inviscid and viscous 3-D flow fields N87-20213
Applications of Euler equations to sharp edge delta wings with leading edge vortices N87-20214
Analysis of the F-16 flow field by a block grid Euler approach N87-20217
Zonal solutions for airfoils using Euler boundary-layer and Navier-Stokes equations N87-20219
Numerical investigation of the laminar boundary layer on a 3-D body started impulsively from rest N87-20220
Computation of three-dimensional flows by viscous-inviscid interation using the MZM method N87-20223
Calculations for a generic fighter at supersonic high-lift conditions N87-20226
High speed viscous flow calculations about complex configurations N87-20227
Numerical simulation of the flow field around a complete aircraft N87-20231
Simulation of transonic viscous wing and wing-fuselage flows using zonal methods
[NASA-TM-89421] N87-20242
A multiple zone method for supersonic tactical missiles
[AD-A175936] N87-20244
Wing-nacelle interactions. Program 1985. Part two: Development of a finite element code for an isolated nacelle
[ONERA-RTS-21/3271-AY] N87-20250
Experiments and modeling of dilution jet flow fields N87-20276
Detailed flow surveys of turning vanes designed for a 0.1-scale model of NASA Lewis Research Center's proposed altitude wind tunnel
[NASA-TP-2680] N87-20295
A holographic interferometry study of an axisymmetric shock-wave/boundary-layer strong interaction flow N87-20498
Continental shelf processes affecting the oceanography of the South Atlantic Bight
[DE87-005303] N87-20716
Existence seen of cyclonic eddy in northern east China Sea N87-20721
FLOW EQUATIONS
A numerical study of the Weis-Fogh mechanism N87-20197
A discussion on a mesh generation technique applicable to complex geometries N87-20201
Acta mechanica sinica (selected articles)
[AD-A176240] N87-20246
Numerical simulation of separated flows past bluff bodies N87-20499
FLOW GEOMETRY
A discussion on a mesh generation technique applicable to complex geometries N87-20201
New numerical techniques in the method of singularities for application to complex three-dimensional configurations N87-20205
FLOW MEASUREMENT
Composite grid and finite-volume LU implicit scheme for turbine flow analysis
[NASA-TM-89828] N87-20235
Acta mechanica sinica (selected articles)
[AD-A176240] N87-20246
Experimental and theoretical investigation of the flow phenomena in return channels of radial compressor stages, especially those with small channel width
[MITT-85-01] N87-20287
Application of a laser-induced breakdown time-of-flight technique in a flow diagnostic in a CO2 free-jet expansion
[DE87-002890] N87-20506
An automated two-dimensional laser velocimeter system
[DE87-005625] N87-20549
FLOW STABILITY
Turbulence control on an airborne laser platform
[NASA-CR-178249] N87-20503
FLOW THEORY
Experimental and theoretical investigation of the flow phenomena in return channels of radial compressor stages, especially those with small channel width
[MITT-85-01] N87-20287
FLOW VELOCITY
Acta mechanica sinica (selected articles)
[AD-A176240] N87-20246
Application of a laser-induced breakdown time-of-flight technique in a flow diagnostic in a CO2 free-jet expansion
[DE87-002890] N87-20506
An automated two-dimensional laser velocimeter system
[DE87-005625] N87-20549
Observations of the Ca II K line in Hel0830A dark points on August 3, 1985 N87-20929
FLOW VISUALIZATION
Experimental and finite-element investigation of flow past single and multiple cylinders N87-20195
FLUID DYNAMICS
NASA-Chinese Aeronautical Establishment (CAE) Symposium
[NASA-CP-2433] N87-20267
USSR report: Physics and mathematics
[JPRS-UPM-86-008] N87-20445
FLUID FLOW
Experimental and finite-element investigation of flow past single and multiple cylinders N87-20195
A predictor-corrector method for calculation of incompressible fluid flow dynamics
[DE87-003804] N87-20508
On the use of CORLIB subroutines for the solution of a model fluid flow problem
[DE87-005285] N87-20509
An automated two-dimensional laser velocimeter system
[DE87-005625] N87-20549
Acoustic gravity waves: A computational approach
[NASA-CR-178270] N87-20781
Eigensystem analysis of classical relaxation techniques with applications to multigrid analysis
[NASA-TM-88377] N87-20785
Computational analyses of crystal growth
[NASA-CR-179027] N87-20820
Effects of flows on viscous and resistive MHD stability N87-20943
FLUID MECHANICS
Numerical and optical experiments on the Weissenberg effect
[ESA-TT-879] N87-20510
FLUX (RATE)
A coordinate free description of magnetohydrostatic equilibria N87-20937
FLUX DENSITY
A technique to estimate the ocean surface energy flux using VAS multispectral data N87-20710
FLYBY MISSIONS
Encounter 86: An international rendezvous with Halley's comet
[ESA-BR-27] N87-20867
FOAMS
Biot theory and acoustical properties of high porosity fibrous materials and plastic foams
[NASA-TM-88575] N87-20424
Energy absorption of polyurethane based polymer alloys
[AD-A175542] N87-20427
FOLDING STRUCTURES
Acoustic effects on the dynamic of lightweight structures N87-20372
Development of precision structural joints for large space structures N87-20374
FOOD PRODUCTION (IN SPACE)
Baking the first bread in space N87-20319
The growth and harvesting of algae in a micro-gravity environment N87-20325
FORCE DISTRIBUTION
A rational approach to lifting surface theory with application to large angles of attack N87-20196
A dynamic model of filament eruptions and two ribbon flares N87-20906
FORCED VIBRATION
Forced vibrations of stringer stiffened damped sandwich panel N87-20596
FOREBODIES
An application of computational fluid dynamics to the design of optimum ramjet powered missile components N87-20338
FORGING
AGARD (Advisory Group for Aerospace Research and Development) engine disc material cooperative test
[AD-A175533] N87-20283
FOURIER TRANSFORMATION
Propagation of RF signals through structured ionization. Theory and antenna aperture effect applications
[AD-A175522] N87-20451
FRACTURE MECHANICS
AGARD (Advisory Group for Aerospace Research and Development) engine disc material cooperative test
[AD-A175533] N87-20283
Strain energy release rates of composite interlaminar end-notch and mixed-mode fracture: A sublaminate/ply level analysis and a computer code
[NASA-TM-89827] N87-20389
Study of the nature of fracture failure in composite materials
[AD-A175554] N87-20391
Ductility and fracture behavior of polycrystalline Ni3Al alloys
[DE87-005340] N87-20413
Load biaxiality and fracture: A two-sided history of complementing errors
[AD-A175972] N87-20573
Solid mechanics program at ONR N87-20575
Creep and Creep Fracture: Conference proceedings
[DE87-780056] N87-20615
FRACTURE STRENGTH
High performance thermoplastics: A review of neat resin and composite properties
[NASA-TM-89104] N87-20390
Hot corrosion attack and strength degradation of SiC and Si(sub)3N(sub)4
[NASA-TM-89820] N87-20425
FRACTURES (MATERIALS)
Creep and Creep Fracture: Conference proceedings
[DE87-780056] N87-20615
FRACTURING
Deformation and fracture of single-crystal and sintered polycrystalline silicon carbide produced by cavitation
[NASA-TM-88961] N87-20422
Load biaxiality and fracture: A two-sided history of complementing errors
[AD-A175972] N87-20573
FREE FALL
An investigation of the strong principle of equivalence through the use of freely falling geocentric coordinates N87-20862
FREE FLOW
Applications of Euler equations to sharp edge delta wings with leading edge vortices N87-20214

Study of compressibility effects on supersonic free flow
[ETN-87-99392] N87-20251

FREE JETS
Application of a laser-induced breakdown time-of-flight technique in a flow diagnostic in a CO2 free-jet expansion
[DE87-002690] N87-20506

FREE VIBRATION
A Lanczos eigenvalue method on a parallel computer
[NASA-TM-89097] N87-20768

FREEZING
Resilient modulus of freeze-thaw affected granular soils for pavement design and evaluation. Part 3: Laboratory tests on soils from Albany County Airport
[DOT/FAA-PM-84-16.3] N87-20433
A freeze-thaw test to determine the frost susceptibility of soils
[DOT/FAA-PM-85-20] N87-20434

FREQUENCY ANALYZERS
Magnetostatic wave frequency analyzer apparatus
[AD-D012558] N87-20458

FREQUENCY CONTROL
Optically tuned millimeter-wave CW. IMPATT source
[AD-A175838] N87-20482

FREQUENCY DISTRIBUTION
Partial redistribution effects in the formation of hydrogen lines in quiescent prominences N87-20894

FREQUENCY DIVISION MULTIPLE ACCESS
Satellite analog FDMA/FM to digital TDMA conversion
[NASA-CR-179605] N87-20467

FREQUENCY MODULATION
A study of the effect of group delay distortion on an SMSK satellite communications channel
[NASA-TM-89835] N87-20450

FREQUENCY SHIFT KEYING
A study of the effect of group delay distortion on an SMSK satellite communications channel
[NASA-TM-89835] N87-20450

FREQUENCY STABILITY
Closed-Cycle, Frequency-Stable CO2 Laser Technology
[NASA-CP-2456] N87-20522
Review of the frequency stabilization of TEA CO2 laser oscillators N87-20523
Frequency stabilization in injection controlled pulsed CO2 lasers N87-20527
An overview of DREV's activities on pulsed CO2 laser transmitters: Frequency stability and lifetime aspects N87-20542

FREQUENCY SYNCHRONIZATION
NAVSAT time synchronization simulation study
[ESA-CR(P)-2305] N87-20376

FRESNEL LENSES
The retinal image of the fresnel lens optical landing system
[AD-A176090] N87-20258

FROST
A freeze-thaw test to determine the frost susceptibility of soils
[DOT/FAA-PM-85-20] N87-20434

FUEL CELL POWER PLANTS
Monolithic fuel cell development
[DE87-004926] N87-20492

FUEL CELLS
High-temperature fuel cells
[DE87-004870] N87-20487
Monolithic fuel cell development
[DE87-004926] N87-20492
Fuel cells in transportation
[DE87-003746] N87-20654
Characterization of monolithic fuel cell components
[DE87-004929] N87-20655

FUEL COMBUSTION
Numerical study of combustion processes in afterburners N87-20269
Combustion research activities at the Gas Turbine Research Institute N87-20273
Thermodynamics and combustion modeling N87-20274
Effect of flame-tube head structure on combustion chamber performance N87-20275
Theoretical kinetic computations in complex reacting systems N87-20277
Experimental investigation of piloted flameholders N87-20278
The chemical shock tube as a tool for studying high-temperature chemical kinetics N87-20279
Theoretical study of the nonsteady combustion of composite fuel droplets
[ESA-TT-868] N87-20401

FUEL INJECTION
Combustion research activities at the Gas Turbine Research Institute N87-20273
Comparison of 6.2L arctic and standard fuel injection pumps using JP-8 fuel
[AD-A175597] N87-20558

FUEL PUMPS
Comparison of 6.2L arctic and standard fuel injection pumps using JP-8 fuel
[AD-A175597] N87-20558

FUEL SPRAYS
Numerical study of combustion processes in afterburners N87-20269
Experimental and analytical investigation of the variation of spray characteristics along a radial distance downstream of a pressure-swirl atomizer N87-20271
Two-phase flow N87-20272
Effect of flame-tube head structure on combustion chamber performance N87-20275
The physics of fuel sprays. Volume 1: Experimental measurements
[AD-A175660] N87-20285

FUEL SYSTEMS
Comparison of 6.2L arctic and standard fuel injection pumps using JP-8 fuel
[AD-A175597] N87-20558

FUNCTIONAL DESIGN SPECIFICATIONS
Working group on Earth observation requirements for the Polar Orbiting Platform Elements of the International Space Station (the POPE Working Group) N87-20625

FUSELAGES
Repair of helicopter composite structure techniques and substantiations N87-20179
Composite repair of cocured J-stiffened panels: Design and test verification N87-20181
Composite repair techniques for J-stiffened composite fuselage structures N87-20186
Theoretical analysis of flows around helicopter fuselages: Application to design and development N87-20221
Investigation of flow under the fuselage of a powered light aircraft model
[BU-351] N87-20247

G

GADOLINIUM
The laser strength of active elements made of Gadolinium-Scandium-Gallium garnet (GSGG) N87-20446

GALACTIC COSMIC RAYS
Pre-compaction irradiation of meteorites N87-20650

GALACTIC EVOLUTION
Carbon and nitrogen abundances along the evolutionary sequence of M67 N87-20848
Computer simulation and analysis of spatial galaxy distributions N87-20851

GALACTIC NUCLEI
The star-forming properties of violently interacting galaxies N87-20849
Abundances and kinematics of K giants in the galactic nuclear bulge N87-20856

GALACTIC STRUCTURE
Computer simulation and analysis of spatial galaxy distributions N87-20851

GALERKIN METHOD
Galerkin/Runge-Kutta discretizations for semilinear parabolic equations
[NASA-CR-178264] N87-20783

GALLIUM ARSENIDES
Propagation characteristics of some novel coplanar waveguide transmission lines on GaAs at MM-wave frequencies
[NASA-TM-89839] N87-20469
Fabrication of microwave devices on ultrathin active GaAs substrates
[FOA-C-30431-3.2] N87-20494
Linearization of GaAs field effect transistor power amplifiers in hyperfrequences
[ENST-86E007] N87-20496
A study of III-V semiconductor processing employing high purity epitaxial gallium arsenide N87-20819

GALLIUM COMPOUNDS
The laser strength of active elements made of Gadolinium-Scandium-Gallium garnet (GSGG) N87-20446

GALVANIC SKIN RESPONSE
Electrodermal conductivity in man and monkeys N87-20743

GAMMA RAY SPECTRA
Ultra-high energy gamma-rays as the carriers of cosmological information
[DE87-700680] N87-20952

GAMMA RAY TELESCOPES
A gondola and pointing system for a gamma ray telescope
[DE87-004561] N87-20843

GAMMA RAYS
A search for very high energy gamma ray emission from Cygnus X-3 N87-20950

GARNETS
The laser strength of active elements made of Gadolinium-Scandium-Gallium garnet (GSGG) N87-20446

GAS ANALYSIS
Laser spectroscopy and gas-phase chemistry in CVD
[DE86-007392] N87-20548

GAS DENSITY
Spectral characteristics of interchange turbulence in the ionosphere
[AD-A175975] N87-20692

GAS DETECTORS
A simplified method for determining heat of combustion of natural gas
[NASA-TP-2682] N87-20514

GAS DISCHARGES
Study of surface discharges
[ONERA-RF-11/7236-PY] N87-20707

GAS DYNAMICS
USSR report: Physics and mathematics
[JPRS-UPM-86-008] N87-20445

GAS FLOW
Acta mechanica sinica (selected articles)
[AD-A176240] N87-20246
Kinetic model for the vibrational energy exchange in flowing molecular gas mixtures
[NASA-TM-88500] N87-20802

GAS MIXTURES
Experimental investigation of piloted flameholders N87-20278
Kinetic model for the vibrational energy exchange in flowing molecular gas mixtures
[NASA-TM-88500] N87-20802

GAS TUNGSTEN ARC WELDING
Gas tungsten arc welding in a microgravity environment: Work done on GAS payload G-169 N87-20306

GAS TURBINE ENGINES
Combustion research in the Internal Fluid Mechanics Division N87-20268
Combustion research activities at the Gas Turbine Research Institute N87-20273
Advanced composite combustor structural concepts program
[NASA-CR-174733] N87-20387

GAS TURBINES
Numerical calculations of turbulent reacting flow in a gas-turbine combustor
[NASA-TM-89842] N87-20171
The physics of fuel sprays. Volume 1: Experimental measurements
[AD-A175660] N87-20285
High temperature protective coatings for aero engine gas turbine components
[AD-A176001] N87-20286

GEAR TEETH
Flexibility effects on tooth contact location in spiral bevel gear transmissions
[NASA-CR-4055] N87-20552

GEARS
A new approach for gearbox modelling in finite element analyses of torsional vibration of gear-branched propulsion systems N87-20591

GEOCENTRIC COORDINATES
An investigation of the strong principle of equivalence through the use of freely falling geocentric coordinates N87-20862

GEODESY
Report on the Special Program 78 satellite geodesy of the Technical University of Munich
[ASTRON-GEODAET-ARB-48] N87-20618

GEODETIC COORDINATES
Report on the Special Program 78 satellite geodesy of the Technical University of Munich
[ASTRON-GEODAET-ARB-48] N87-20618

GEOLOGY
Solid Earth panel report --- Columbus program N87-20636

GEOMAGNETISM
Satellite lifetime prediction N87-20666
Hubble Space Telescope N87-20670
NORAD satellite tracking N87-20671
NORAD/SPACECMD comments concerning the atmospheric density models N87-20672
Limitations to modeling the thermosphere and exosphere N87-20674
Forecasts of solar and geomagnetic activity N87-20677
Amplification of an electron density perturbation in the polar E layer, induced by strong HF waves
[ETN-87-99014] N87-20695

GEOMETRY
The 3-D world modelling with updating capability based on combinatorial geometry
[DE87-004257] N87-20643
Computational analyses of crystal growth
[NASA-CR-179027] N87-20820
GEOPHYSICS
Magnetotelluric measurements in Antarctica
[INPE-4058-PRE/1017] N87-20661
Nuclear geophysics in space and atmospheric research at INPE/BRAZIL
[DE87-700426] N87-20693
The fifth force --- fundamental interactions
[DE87-004612] N87-20694
Solar-geophysical data number 506, October 1986. Part 1: (Prompt reports). Data for September 1986, August 1986 and late data
[PB87-126389] N87-20948
GET AWAY SPECIALS (STS)
The 1986 Get Away Special Experimenter's Symposium
[NASA-CP-2436] N87-20302
Tracking the GLOMR satellite N87-20303
Manufacturing polymer thin films in a micro-gravity environment N87-20304
Phase partitioning, crystal growth, electrodeposition and cosmic ray experiments in microgravity N87-20305
Gas tungsten arc welding in a microgravity environment: Work done on GAS payload G-169 N87-20306
Use of lightweight composites for GAS payload structures N87-20307
Phycomyces in space: A problem in bioengineering N87-20308
NORSTAR Project: Norfolk public schools student team for acoustical research N87-20309
Towards a better mirror N87-20310
Progress on the Ohio State University Get Away Special G-0318: DEAP N87-20311
NUSAT update N87-20312
Sophisticated software systems for small self-contained space shuttle payload G285 N87-20313
A systems-level performance history of get away specials after 25 space shuttle missions N87-20314
STS-61C, Columbia flight N87-20315
USC/AIAA student get away special project liquid droplet collector experiment N87-20316
Results of the joint utilization of laser integrated experiments flown on payload GAS-449 aboard Columbia mission 61-C N87-20317
The North Carolina A and T State University Student Space Shuttle Program N87-20318
Baking the first bread in space N87-20319
Hitchhiker-G: A new carrier system for attached shuttle payloads N87-20320
Multipurpose microcontroller design for PUGAS 2 N87-20321
Geotaxis baseline data for Drosophila N87-20322
Marshall Amateur Radio Club experiment (MARCE) post flight data analysis N87-20323
Cal Poly Space Project G-279 N87-20324
The growth and harvesting of algae in a micro-gravity environment N87-20325
To catch a comet 2: Technical update on CAN-DO N87-20326
To catch a child's imagination 2: Educational update on CAN-DO N87-20327
NUSAT 1 attitude determination N87-20328
NUSAT 1 methods for radar field strength measurement N87-20329
Recent results from MAUS payloads N87-20331
Microgravity effects on electrodepoeition of metals and metal-cermet mixtures N87-20332
GAS-007: First step in a series of Explorer payloads N87-20333
In situ observation of mono-molecular growth steps on aqueous solution grown crystals and the transport of molecules to the crystals N87-20334
GIACOBINI-ZINNER COMET
Steepened magnetosonic waves in the high Beta plasma surrounding Comet-Giacobini-Zinner
[NASA-CR-180614] N87-20868
GIANT STARS
Abundances and kinematics of K giants in the galactic nuclear bulge N87-20656
Statistical properties of barium stars N87-20657
GIBBS PHENOMENON
Uniqueness of Gibbs measures and absorption probabilities
[CWI-MS-R8610] N87-20789
GLASS
Chemistry of glass-ceramic to metal bonding for header applications Part 2: Hydrogen bubble formation during glass-ceramic to metal sealing
[DE87-004041] N87-20559
Solar power absorption in a glass tube
[NASA-TM-89063] N87-20814
GLASS FIBER REINFORCED PLASTICS
Materials selection and design study of a composite microlight wing structure
[BU-335] N87-20263
GLASS FIBERS
Characterizing thermal/mechanical properties of filament wound composites
[AD-A176238] N87-20392
GLIDE PATHS
The retinal image of the fresnel lens optical landing system
[AD-A176090] N87-20258
GLOBAL POSITIONING SYSTEM
Range filtering for sequential GPS receivers with external sensor augmentation
[NASA-TM-89418] N87-20257
GOALS
An investigation of transitional management problems for the NSTS
[NASA-CR-171979] N87-20834
GOERTLER INSTABILITY
The fully nonlinear development of Goertler vortices in growing boundary layers
[NASA-CR-178266] N87-20502
GOLD
Measurements of iridium and the hypothesis of meteoritic impact as the end of the Cretaceous period
[INPE-4070-TDL/248] N87-20661
GONDOLAS
A gondola and pointing system for a gamma ray telescope
[DE87-004561] N87-20643
GOVERNMENT/INDUSTRY RELATIONS
The 1986 Get Away Special Experimenter's Symposium
[NASA-CP-2436] N87-20302
GRAIN BOUNDARIES
Ductility and fracture behavior of polycrystalline Ni3Al alloys
[DE87-005340] N87-20413
The variation of subgrain misorientation in aluminum deformed to large steady-state creep strains
[DE87-003238] N87-20415
Dislocation reactions at grain boundaries in Li2 ordered alloys
[DE87-005713] N87-20827
GRANULAR MATERIALS
Resilient modulus of freeze-thaw affected granular soils for pavement design and evaluation. Part 3: Laboratory tests on soils from Albany County Airport
[DOT/FAA-PM-84-16.3] N87-20433
GRAPH THEORY
A system for routing arbitrary directed graphs on SIMD architectures
[NASA-CR-178265] N87-20764
GRAPHITE
Unconventional approaches to field repair N87-20190
GRAPHITE-EPOXY COMPOSITES
Fibre composite repair of cracked metallic aircraft components: Practical and basic aspects N87-20187
Characterizing thermal/mechanical properties of filament wound composites
[AD-A176238] N87-20392
Moisture absorption in graphite/organic-matrix composites
[DE87-004229] N87-20394
Studies of stress wave propagation in composites
[DE87-001433] N87-20396
Structural degradation of impacted graphite/epoxy laminates N87-20586
GRATINGS (SPECTRA)
Injection-seeding studies of diode laser array behavior
[DE87-002051] N87-20546
GRAVITATION
On the de Sitter and Nariai space-times in a generalized theory of gravitation
[DE86-703483] N87-20830
GRAVITATION THEORY
Gravitational collapse in relativistic theory of gravitation
[DE87-700730] N87-20792
GRAVITATIONAL COLLAPSE
Gravitational collapse in relativistic theory of gravitation
[DE87-700730] N87-20792
GRAVITATIONAL EFFECTS
Cal Poly Space Project G-279 N87-20324
Dynamic and thermal effects in very large space structures N87-20347
Space station momentum management N87-20668
GRAVITY WAVES
Gravity waves N87-20685
Acoustic gravity waves: A computational approach
[NASA-CR-178270] N87-20781
GREEN'S FUNCTIONS
Calculation of Rayleigh-Taylor flows using vortex blobs
[DE87-002551] N87-20507
GROUND STATE
Ground-state proton radioactivity in the domain of neutron-poor nuclei heavier than tin
[ETN-87-99342] N87-20811
GROUND TESTS
The 1985 small propeller-driven aircraft noise test program
[AD-A175596] N87-20799
GROWTH
The growth and harvesting of algae in a micro-gravity environment N87-20325
GUIDE VANES
Detailed flow surveys of turning vanes designed for a 0.1-scale model of NASA Lewis Research Center's proposed altitude wind tunnel
[NASA-TP-2680] N87-20295
GULFS
Spectral analysis of waves in Gulf of Tonkin described N87-20722
GUNN DIODES
Fabrication of microwave devices on ultrathin active GaAs substrates
[FOA-C-30431-3.2] N87-20494

H

H ALPHA LINE
The star-forming properties of violently interacting galaxies N87-20849
On the existence of oscillations in solar filaments observed in H alpha and C IV lines N87-20900
Filament disappearances N87-20903
H LINES
Partial redistribution effects in the formation of hydrogen lines in quiescent prominences N87-20894
H I structure and the soft X-ray background N87-20949
HAILSTORMS
The terminal area simulation system. Volume 2: Verification cases
[NASA-CR-4047-VOL-2] N87-20252
HALLEY'S COMET
To catch a comet 2: Technical update on CAN-DO N87-20326
To catch a child's imagination 2: Educational update on CAN-DO N87-20327
MHD waves detected by ion at distances 28 x 10 km from Comet Halley: Cometary or solar wind origin
[DE87-005122] N87-20863
Encounter 86: An international rendezvous with Halley's comet
[ESA-BR-27] N87-20867
HAMILTONIAN FUNCTIONS
HARPA: A versatile three-dimensional Hamiltonian ray-tracing program for acoustic waves in the atmosphere above irregular terrain
[PB87-132031] N87-20801
HAMMERS
The controlled response of resonating fixtures used to simulate pyroshock environments N87-20612
HANDBOOKS
Shuttle/Spacelab contamination environment and effects handbook
[NASA-CR-4053] N87-20350
HARMONIC EXCITATION
Structural dynamics: Buckling of ring-stiffened cylindrical shells with dynamic loads N87-20595
HARMONIC MOTION
Investigation of microstructure of arbitrary motions of operator N87-20752
HAZARDS
Safety characteristics of non-lithium battery systems, revision 1
[AD-A174577] N87-20480
HEART FUNCTION
Interpretation of right heart kinetocardiogram N87-20744
HEAT FLUX
A technique to estimate the ocean surface energy flux using VAS multispectral data N87-20710
HEAT OF COMBUSTION
A simplified method for determining heat of combustion of natural gas
[NASA-TP-2682] N87-20514
HEAT RESISTANT ALLOYS
High temperature protective coatings for aero engine gas turbine components
[AD-A176001] N87-20286
Advanced composite combustor structural concepts program
[NASA-CR-174733] N87-20387

Bithermal low-cycle fatigue behavior of a NiCoCrAlY-coated single crystal superalloy [NASA-TM-89631] N87-20408

HEAT TRANSFER
Performance and efficiency evaluation and heat release study of an outboard Marine Corporation Rotary Combustion Engine [NASA-TM-89833] N87-20282
A numerical heat transfer model for an advanced solar thermal propulsion system N87-20377

HEAT TRANSFER COEFFICIENTS
Cryogenic regenerators [DE87-701264] N87-20443

HEAT TREATMENT
A study of III-V semiconductor processing employing high purity epitaxial gallium arsenide N87-20819

HEATING
Heating of the stellar corona N87-20873
Small-scale coronal structure, part 3 N87-20922
Simultaneous observations of changes in coronal bright point emission at the 20 cm radio and He Lambda 10830 wavelengths N87-20923
Magnetic location of C IV events in the quiet network N87-20930
Phlegethon flow: A proposed origin for spicules and coronal heating N87-20933
Energy conversion in the coronal plasma N87-20934
Cascade model of coronal heating N87-20936
Heating of the solar corona by the resonant absorption of Alfven waves N87-20939
Magnetic helicity as a constraint on coronal dissipation N87-20940

HEATING EQUIPMENT
Laboratory investigation of lightweight heater tape for shuttle propellant tank [AD-A175997] N87-20345

HEAVY NUCLEI
Ground-state proton radioactivity in the domain of neutron-poor nuclei heavier than tin [ETN-87-99342] N87-20611

HELICOPTER DESIGN
Theoretical analysis of flows around helicopter fuselages: Application to design and development N87-20221

HELICOPTER TAIL ROTORS
Design for repairability of helicopter composite blades N87-20176

HELICOPTER WAKES
The prediction of transonic loading on advancing helicopter rotors N87-20206
Theoretical analysis of flows around helicopter fuselages: Application to design and development N87-20221

HELICOPTERS
Design for repairability of helicopter composite blades N87-20176
Repair of helicopter composite structure techniques and substantiations N87-20179
Helicopter external load operations [CAP-426] N87-20259
WSUH-1D: Review of damage following lightning strike 30 November 1981 [RAE-TRANS-2103] N87-20262
Effect of dynamic stall and elastic parameters on the fundamental mechanisms of helicopter vibrations [AD-A175561] N87-20292
Vibration characteristics of OH-58A helicopter main rotor transmission [NASA-TP-2705] N87-20555
Noise measurements on the helicopter BK 117 design. Weighted noise levels and influence of airspeed [ESA-TT-748] N87-20600

HEMATOLOGY
Effect of hemadsorption on rheological parameters of blood during seven-day antiorthostatic hypokinesia and in vitro studies N87-20740

HEURISTIC METHODS
Topological constraints and the existence of force-free fields N87-20935

HIGH ENERGY ELECTRONS
Ultra-high energy gamma-rays as the carriers of cosmological information [DE87-700680] N87-20952

HIGH FREQUENCIES
Stochastic effects on oblique HF (High Frequencies) propagation [AD-A176015] N87-20455

HIGH LEVEL LANGUAGES
MACSYMA usage at Langley, revision 1 [NASA-CR-172518] N87-20753

HIGH PASS FILTERS
Questionable effects of shock data filtering N87-20610

HIGH PRESSURE
The physics of fuel sprays. Volume 1: Experimental measurements [AD-A175660] N87-20285

HIGH RESOLUTION
AFGWC's Advanced Weather Analysis and Prediction System (AWAPS) [AD-A172801] N87-20702
The microwave structure of quiescent solar filaments at high resolution N87-20889

HIGH TEMPERATURE
The physics of fuel sprays. Volume 1: Experimental measurements [AD-A175660] N87-20285
Development of powder metallurgy 2XXX series Al alloy plate and sheet materials for high temperature aircraft structural applications, FY 1983/1984 [NASA-CR-172521] N87-20406
Addition polymers from 1,4,5,8-tetrahydro-1,4;5,8-diepoxyanthracene and Bis-dienes: Processable resins for high temperature application [NASA-TM-89838] N87-20426
High-temperature fuel cells [DE87-004870] N87-20487

HIGH TEMPERATURE ENVIRONMENTS
Apparatus for high temperature in situ laser Raman spectroelectrochemical studies of metal corrosion and passivation in aqueous environments [DE87-004868] N87-20416

HIGH TEMPERATURE GASES
The chemical shock tube as a tool for studying high-temperature chemical kinetics N87-20279
High temperature protective coatings for aero engine gas turbine components [AD-A176001] N87-20286
Theoretical and experimental investigations of ignition, combustion and expansion processes of hypergolic liquid fuel combinations at gas temperatures up to 3000 deg K [NASA-TM-88527] N87-20399
High temperature CO2 study: Anti-Stokes coherent Raman diffusion and infrared spectroscopy [ONERA-P-1986-2] N87-20402

HILBERT TRANSFORMATION
Magnetotelluric measurements in Antarctica [INPE-4058-PRE/1017] N87-20661

HIPPARCOS SATELLITE
Fiducial reference for the HIPPARCOS reference system [NASA-CR-180250] N87-20842

HISTORIES
Load biaxiality and fracture: A two-sided history of complementing errors [AD-A175972] N87-20573

HODOGRAPHS
Lewis inverse design code (LINDES): Users manual [NASA-TP-2676] N87-20238

HOLOGRAPHIC INTERFEROMETRY
TV-holography: A promising inspection tool for analysis of composite materials N87-20180
A holographic interferometry study of an axisymmetric shock-wave/boundary-layer strong interaction flow N87-20498
Numerical and optical experiments on the Weissenberg effect [ESA-TT-879] N87-20510

HOLOGRAPHY
Organic photochromic material for recording waveguide holograms N87-20447
Progress in the development of holographic scheme for pair correlation estimation [AD-A175573] N87-20518
Diffraction diffusion screen with holographically suppressed zero-order beam [AD-D012565] N87-20519

HOMOTOPY THEORY
Algebra and topology for applications to physics [NASA-TT-20056] N87-20784

HONEYCOMB STRUCTURES
Composite structure repairs carried out according to aeronautical techniques N87-20185
Battle damage repair of composite structures N87-20189
British Airways experience with composite repairs N87-20192

HORIZON
LOWTRAN modeling of near-horizon infrared sky radiances in the presence of clouds [AD-A175661] N87-20691

HORSEPOWER
Contingency power for small turboshaft engines using water injection into turbine cooling air [NASA-TM-89817] N87-20280

HOT CORROSION
High temperature protective coatings for aero engine gas turbine components [AD-A176001] N87-20286
Hot corrosion attack and strength degradation of SiC and Si(sub)3N(sub)4 [NASA-TM-89820] N87-20425

HOUSINGS
Hybrid methods for rotordynamic analysis [NASA-CR-179035] N87-20553

HUBBLE SPACE TELESCOPE
Qualification of the faint object camera N87-20359
Hubble Space Telescope N87-20670
Fiducial reference for the HIPPARCOS reference system [NASA-CR-180250] N87-20842

HUMAN FACTORS ENGINEERING
Stages of development of the problem of flight safety in aviation medicine N87-20733

HUMAN PATHOLOGY
Electrodermal conductivity in man and monkeys N87-20743

HUMAN PERFORMANCE
Effects of force reflection on servomanipulator task performance [DE87-003008] N87-20580

HYDRAULIC EQUIPMENT
Multi-axis vibration tests on spacecraft using hydraulic exciters N87-20373

HYDROCARBON FUELS
The chemical shock tube as a tool for studying high-temperature chemical kinetics N87-20279

HYDROGEN
Hydrogen degradation of pipeline steels [DE87-005585] N87-20414
Operation of transversely excited N2O lasers [AD-D012583] N87-20543
Non-LTE hydrogen-line formation in moving prominences N87-20695

HYDROGEN EMBRITTLEMENT
Hydrogen embrittlement of titanium and its alloys: A literature review [DE87-750405] N87-20410
Hydrogen degradation of pipeline steels [DE87-005585] N87-20414

HYDROGENATION
Rapid thermal annealing of Amorphous Hydrogenated Carbon (a-C:H) films [NASA-TM-89859] N87-20821

HYDROLOGY
China report: Science and technology [JPRS-CST-86-025] N87-20708
Hydrologic features in cyclonic eddy region of northern east China Sea in cold seasons N87-20709

HYPERBOLIC DIFFERENTIAL EQUATIONS
A practical assessment of spectral accuracy for hyperbolic problems with discontinuities [NASA-CR-178226] N87-20779

HYPERGEOMETRIC FUNCTIONS
A virtual-time operating-system shell for a hypercube in robotics applications [DE87-004256] N87-20773

HYPERGOLIC ROCKET PROPELLANTS
Theoretical and experimental investigations of ignition, combustion and expansion processes of hypergolic liquid fuel combinations at gas temperatures up to 3000 deg K [NASA-TM-88527] N87-20399

HYPERSONIC AIRCRAFT
Optimization of hypersonic waveriders derived from cone flows including viscous effects N87-20193

HYPERSONIC FLIGHT
Optimization of hypersonic waveriders derived from cone flows including viscous effects N87-20193

HYPERSONIC WIND TUNNELS
Computational analysis and preliminary redesign of the nozzle contour of the Langley hypersonic CF4 tunnel [NASA-TM-89042] N87-20296

HYPOKINESIA
Operator work capacity in tracking system when submitted to antiorthostatic hypokinesia N87-20736
Effect of hemadsorption on rheological parameters of blood during seven-day antiorthostatic hypokinesia and in vitro studies N87-20740

HYPOXIA
Effect of hypoxia on DNA synthesis and collagent content of regenerating skin N87-20742

I

IBM COMPUTERS
Guide to sharing personal computer resources via local area networks, revised [DE86-016088] N87-20772

ICE
A biospectral method for the determination of the altitude of ice clouds
[ESA-TT-903] N87-20704
MHD waves detected by ice at distances 28 x 10 km from Comet Halley: Cometary or solar wind origin
[DE87-005122] N87-20863
ICE FORMATION
Two-phase flow N87-20272
Laboratory investigation of lightweight heater tape for shuttle propellant tank
[AD-A175997] N87-20345
ICE PREVENTION
Laboratory investigation of lightweight heater tape for shuttle propellant tank
[AD-A175997] N87-20345
ICE REPORTING
Ocean-ice panel report — International Space Station N87-20635
IGNITION
Theoretical and experimental investigations of ignition, combustion and expansion processes of hypergolic liquid fuel combinations at gas temperatures up to 3000 deg K
[NASA-TM-88527] N87-20399
Feasibility study of a Semiconductor Bridge (SCB) for initiating pyrotechnics and explosives
[DE87-004444] N87-20430
IMAGE PROCESSING
Engineering thrust areas, 1987
[DE87-004443] N87-20441
Diffraction diffusion screen with holographically suppressed zero-order beam
[AD-D012565] N87-20519
Fly's eye sensor nonlinear signal processing
[AD-D012564] N87-20815
IMAGE TRANSDUCERS
Fly's eye sensor nonlinear signal processing
[AD-D012564] N87-20815
IMAGING TECHNIQUES
NASA/MSFC large stretch press study
[NASA-CR-180376] N87-20554
IMPACT DAMAGE
Erosion and strength degradation in alumina
[DE87-003341] N87-20428
Army research in shock mechanics N87-20576
Structural degradation of impacted graphite/epoxy laminates N87-20586
IMPACT TESTS
Structural degradation of impacted graphite/epoxy laminates N87-20586
INCOMPRESSIBLE FLOW
A finite difference scheme for three-dimensional steady laminar incompressible flow
[NASA-TM-89851] N87-20504
INCOMPRESSIBLE FLUIDS
A predictor-corrector method for calculation of incompressible fluid flow dynamics
[DE87-003804] N87-20508
INCONEL (TRADEMARK)
Chemistry of glass-ceramic to metal bonding for header applications Part 2: Hydrogen bubble formation during glass-ceramic to metal sealing
[DE87-004041] N87-20559
INDUCTION HEATING
On the thermal durability of solar prominences, or how to evaporate a prominence N87-20905
INERTIAL COORDINATES
An investigation of the strong principle of equivalence through the use of freely falling geocentric coordinates N87-20862
INFORMATION RETRIEVAL
A self critical approach to data analysis and model building
[AD-A175640] N87-20791
INFRARED IMAGERY
LOWTRAN modeling of near-horizon infrared sky radiances in the presence of clouds
[AD-A175661] N87-20691
INFRARED RADIATION
LOWTRAN modeling of near-horizon infrared sky radiances in the presence of clouds
[AD-A175661] N87-20691
INFRARED SPECTRA
Statistical properties of barium stars N87-20857
INFRARED SPECTROMETERS
Investigation of PTFE transfer films by infrared emission spectroscopy and phase-locked ellipsometry
[NASA-TM-89844] N87-20421
INFRARED SPECTROSCOPY
High temperature CO2 study: Anti-Stokes coherent Raman diffusion and infrared spectroscopy
[ONERA-P-1986-2] N87-20402
INJECTION
Formation of active region and quiescent prominence magnetic field configurations N87-20879
INJECTION LOCKING
Frequency stabilization in injection controlled pulsed CO2 lasers N87-20527
INSPECTION
A.T.R. 42 carbon fibre flap repair design and inspection N87-20178
TV-holography: A promising inspection tool for analysis of composite materials N87-20160
INSULATION
Laboratory investigation of lightweight heater tape for shuttle propellant tank
[AD-A175997] N87-20345
A survey of achieved levels of airborne sound insulation in broadcasting studio centres
[BBC-RD-1987/1] N87-20796
INTEGRAL EQUATIONS
On the use of CORLIB subroutines for the solution of a model fluid flow problem
[DE87-005285] N87-20509
INTEGRATED CIRCUITS
System architecture of MMIC-based large aperture arrays for space application
[NASA-TM-89840] N87-20468
Multilevel representation and simulation for VLSI design
[AD-A175663] N87-20481
Fly's eye sensor nonlinear signal processing
[AD-D012564] N87-20815
Integrated optical devices for high speed diagnostics
[DE87-003160] N87-20816
INTERACTIONAL AERODYNAMICS
Computation of three-dimensional flows by viscous-inviscid interation using the MZM method N87-20223
INTERFACES
Strong metal-support interactions N87-20533
The prominence-corona interface and its relationship to the chromosphere-corona transition N87-20891
INTERGALACTIC MEDIA
Ultra-high energy gamma-rays as the carriers of cosmological information
[DE87-700680] N87-20952
INTERMETALLICS
Effects of elastic anisotropy on the anomalous yield behavior of cubic ordered alloys
[DE87-005328] N87-20417
Thermodynamic data of intermetallic compounds
[DE87-701244] N87-20831
INTERNAL COMBUSTION ENGINES
Thermodynamics and combustion modeling N87-20274
INTERNATIONAL COOPERATION
International system of units (SI)
[PB86-244159] N87-20444
Proceedings of the European Symposium on Polar platform Opportunities and Instrumentation for Remote-Sensing (ESPOIR)
[ESA-SP-266] N87-20621
Cooperation of the International Space Station partners in the preparation of the use of space station elements for Earth observation (platform and payload aspects) N87-20631
USA-Europe coordination and cooperation activities: Announcements of Opportunity — polar platforms N87-20632
Encounter 86: An international rendezvous with Halley's comet
[ESA-BR-27] N87-20867
INTERNATIONAL SYSTEM OF UNITS
International system of units (SI)
[PB86-244159] N87-20444
INTERPOLATION
Simulation of wind gradient errors in NROSS (Navy Remote Ocean Sensing System) radar scatterometer data in a simplified geometry
[AD-A175754] N87-20642
INVERSIONS
Lewis inverse design code (LINDES): Users manual
[NASA-TP-2676] N87-20238
INVISCID FLOW
Numerical simulation of internal and external inviscid and viscous 3-D flow fields N87-20213
Computation of three-dimensional flows by viscous-inviscid interation using the MZM method N87-20223
ION BEAMS
Microstructure of metastable metallic alloy films produced by laser breakdown chemical vapor depoeition and ion implantation
[DE87-002914] N87-20411
Noble-gas ion bombardment on clean silicon surfaces studied using ellipsometry and desorption
[B8672200] N87-20809
ION IMPLANTATION
Microstructure of metastable metallic alloy films produced by laser breakdown chemical vapor deposition and ion implantation
[DE87-002914] N87-20411
Deep ion implantation for bipolar silicon devices; investigations into the use of the third dimension
[B8672201] N87-20828
IONIZATION
Stochastic effects on oblique HF (High Frequencies) propagation
[AD-A176015] N87-20455
IONOSPHERIC DISTURBANCES
Spectral characteristics of interchange turbulence in the ionosphere
[AD-A175975] N87-20692
IONOSPHERIC DRIFT
Propagation of RF signals through structured ionization. Theory and antenna aperture effect applications
[AD-A175522] N87-20451
IONOSPHERIC ELECTRON DENSITY
Amplification of an electron density perturbation in the polar E layer, induced by strong HF waves
[ETN-87-99014] N87-20695
IONOSPHERIC PROPAGATION
Stochastic effects on oblique HF (High Frequencies) propagation
[AD-A176015] N87-20455
IONS
Observations of sunward and tailward ion streaming in the magnetotail of Jupiter with Voyager 2 N87-20869
IRIDIUM
Measurements of iridium and the hypothesis of meteoritic impact as the end of the Cretaceous period
[INPE-4070-TDL/248] N87-20861
IRON
Electroforming with nickel, iron, and aluminum
[DE87-005589] N87-20442
Studies of X-ray satellites in sodium, magnesium, aluminum, argon, and iron
[ETN-87-99364] N87-20812
IRRADIATION
Pre-compaction irradiation of meteorites N87-20850
ISLAND ARCS
Wilson cycle studies
[NASA-CR-180503] N87-20664
ISOTHERMAL FLOW
Prediction of recirculation zones in isothermal coaxial jet flows relevant to combustors
[NASA-CR-4064] N87-20501
ISOTHERMAL PROCESSES
Calculation of thermomechanical fatigue life based on isothermal behavior
[NASA-TM-88864] N87-20565

J

JET CONTROL
Simulation of a jet deflection system with the aid of the Euler equations N87-20212
JET ENGINES
Theoretical kinetic computations in complex reacting systems N87-20277
JET FLOW
Experiments and modeling of dilution jet flow fields N87-20276
JOINTS (JUNCTIONS)
Structural design of an in-line bolted joint for the space shuttle solid rocket motor case segments
[NASA-TM-89027] N87-20349
Development of precision structural joints for large space structures N87-20374
Modeling of joints for the dynamic analysis of truss structures
[NASA-TP-2661] N87-20567
JP-8 JET FUEL
Comparison of 6.2L arctic and standard fuel injection pumps using JP-8 fuel
[AD-A175597] N87-20558
JUPITER (PLANET)
Observations of sunward and tailward ion streaming in the magnetotail of Jupiter with Voyager 2 N87-20869

K

KALMAN FILTERS
Range filtering for sequential GPS receivers with external sensor augmentation
[NASA-TM-89418] N87-20257
Estimability and regulability of linear systems
[NASA-TM-89427] N87-20790
KAONS
The fifth force — fundamental interactions
[DE87-004612] N87-20694

KINEMATICS
Abundances and kinematics of K giants in the galactic nuclear bulge N87-20656
KINETIC ENERGY
The effect of latent heat on kinetic energy conversions associated with South Pacific cyclones N87-20696
Dynamic presentation of long term upper ocean study (LOTUS) data using videotape [AD-A175535] N87-20711
KINETIC EQUATIONS
Numerical investigations of geometrically nonlinear shell kinetics [ETN-87-99019] N87-20616
KINETIC THEORY
Kinetic model for the vibrational energy exchange in flowing molecular gas mixtures [NASA-TM-88500] N87-20602
KINETICS
Theoretical kinetic computations in complex reacting systems N87-20277
Link between asymmetry of optokinetic nystagmus, optovestibular and vestibulovegetative stability N87-20738

L

L-1011 AIRCRAFT
Development of field level repairs for composite structures N87-20177
LABYRINTH
Interlabyrinthine asymmetry, vestibular dysfunction and space motion sickness N87-20734
LAMINAR BOUNDARY LAYER
Numerical investigation of the laminar boundary layer on a 3-D body started impulsively from rest N87-20220
LAMINAR FLOW
Simulation of three-dimensional transonic flow with separation past a hemisphere cylinder configuration N87-20230
A finite difference scheme for three-dimensional steady laminar incompressible flow [NASA-TM-89851] N87-20504
LAMINAR MIXING
An asymptotic analysis of supersonic reacting mixing layers [NASA-CR-178266] N87-20756
LAMINATES
Repair procedures for composite parts on the alpha jet N87-20175
Mechanical and thermal characterization of unidirectional aramid/epoxy [CCMS-86-08] N87-20385
Characterizing thermal/mechanical properties of filament wound composites [AD-A176238] N87-20392
Studies of stress wave propagation in composites [DE87-001433] N87-20396
Residual effects in laminated, curved, composite panels [DE87-005624] N87-20397
Structural degradation of impacted graphite/epoxy laminates N87-20586
A model for the degradation of composite structures [ONERA-RT-30/3043-RY-057-R] N87-20617
LAND MOBILE SATELLITE SERVICE
Land mobile communications satellite mission (LAMOCOSAMIS) Task 1: Market study [ESA-CR(P)-2302-VOL-1] N87-20462
Land mobile communications satellite missions (LAMOCOSAMIS), executive summary [ESA-CR(P)-2302-VOL-6] N87-20463
Land mobile satellite communication system. Volume 1: Executive summary [ITS-TR-043/86-VOL1] N87-20464
Land mobile satellite communication system. Volume 2: Traffic analysis and market demand for the land mobile communications system in the European scenario [ITS-TR-043/86-VOL-2] N87-20465
LANDING AIDS
The retinal image of the fresnel lens optical landing system [AD-A176090] N87-20258
LARGE SPACE STRUCTURES
Effects of space plasma discharge on the performance of large antenna structures in low Earth orbit [NASA-TM-89118] N87-20339
Dynamic and thermal effects in very large space structures N87-20347
Studies in nonlinear structural dynamics: Chaotic behavior and poynting effect N87-20348
Large space antennas: A systems analysis case history [NASA-TM-89072] N87-20352
Mechanical Qualification of Large Flexible Spacecraft Structures [AD-A175529] N87-20355
Future trends in spacecraft design and qualification N87-20356
Recent developments and future trends in structural dynamic design verification and qualification of large flexible spacecraft N87-20357
Dynamic modeling and optimal control design for large flexible space structures N87-20358
Structural qualification of large spacecraft N87-20361
Effect of modal damping in modal synthesis of spacecraft structures N87-20362
Active structural controllers emulating structural elements by ICUs N87-20367
Spacecraft qualification using advanced vibration and modal testing techniques N87-20368
Influence co-efficient testing as a substitute for modal survey testing of large space structures N87-20369
Benefits of passive damping as applied to active control of large space structures N87-20371
Development of precision structural joints for large space structures N87-20374
Solar array flight experiment/dynamic augmentation experiment [NASA-TP-2690] N87-20380
System architecture of MMIC-based large aperture arrays for space application [NASA-TM-89840] N87-20488
Modeling of joints for the dynamic analysis of truss structures [NASA-TP-2661] N87-20567
Space station structures and dynamics test program [NASA-TP-2710] N87-20568
The Shock and Vibration Bulletin. Part 1: Welcome, Invited Papers, Shipboard Shock, Blast and Ground Shock, Shock Testing and Analysis [AD-A175224] N87-20574
Air Force basic research in dynamics and control of large space structures N87-20577
Modal test and analysis: Multiple tests concept for improved validation of large space structure mathematical models N87-20581
LASER ANEMOMETERS
A computer controlled signal preprocessor for laser fringe anemometer applications [NASA-TM-88962] N87-20516
LASER APPLICATIONS
TV-holography: A promising inspection tool for analysis of composite materials N87-20180
Experimental and analytical investigation of the variation of spray characteristics along a radial distance downstream of a pressure-swirl atomizer N87-20271
Application of a laser-induced breakdown time-of-flight technique in a flow diagnostic in a CO2 free-jet expansion [DE87-002890] N87-20506
Potential of laser remote sensing of oil below water surface [FOA-C-30435-3.1] N87-20659
Development of optical thin film technology for lasers and synchrotron radiation [DE87-701254] N87-20817
LASER DOPPLER VELOCIMETERS
Experimental and finite-element investigation of flow past single and multiple cylinders N87-20195
An automated two-dimensional laser velocimeter system [DE87-005625] N87-20549
LASER GYROSCOPES
Preliminary examination of the construction of laser gyroscopes with reduced lock-in threshold [ETN-87-99016] N87-20521
LASER INDUCED FLUORESCENCE
Potential of laser remote sensing of oil below water surface [FOA-C-30435-3.1] N87-20659
LASER MODE LOCKING
Preliminary examination of the construction of laser gyroscopes with reduced lock-in threshold [ETN-87-99016] N87-20521
LASER OUTPUTS
Etching of LiNbO3 by laser-driven fusion of salts [DE87-003033] N87-20544
LASER PUMPING
The laser strength of active elements made of Gadolinium-Scandium-Gallium garnet (GSGG) N87-20446
Investigation of low-current-density nanosecond electron beam diode [IPPJ-T-36] N87-20618
LASER RANGE FINDERS
Report on the Special Program 78 satellite geodesy of the Technical University of Munich [ASTRON-GEODAET-ARB-48] N87-20618
LASER SPECTROSCOPY
Laser spectroscopy and gas-phase chemistry in CVD [DE86-007392] N87-20548
LASER STABILITY
Preliminary examination of the construction of laser gyroscopes with reduced lock-in threshold [ETN-87-99016] N87-20521
LASERS
Microstructure of metastable metallic alloy films produced by laser breakdown chemical vapor deposition and ion implantation [DE87-002914] N87-20411
LATE STARS
Abundances and kinematics of K giants in the galactic nuclear bulge N87-20656
LATENT HEAT
The effect of latent heat on kinetic energy conversions associated with South Pacific cyclones N87-20696
LAUNCHING PADS
Effects of space shuttle launches STS-1 through STS-9 on terrestrial vegetation of John F. Kennedy Space Center, Florida [NASA-TM-83103] N87-20658
LEAD SULFIDES
High field properties of SnMo6S8 and PbMo6S8 ribbons prepared using a vapor transport technique [DE87-004707] N87-20828
LEADING EDGE FLAPS
Investigation of leading-edge flap performance on delta and double-delta wings at supersonic speeds [NASA-TP-2656] N87-20233
LEADING EDGES
The aerodynamic effects of a serrated strip near the leading edge of an airfoil [ETN-87-99480] N87-20248
LEAST SQUARES METHOD
A new approach to least squares estimation, with applications [CWI-MS-R8602] N87-20787
LIFE (DURABILITY)
Morphological changes in the sulfur electrode of lifecycle-tested Na/S cells [DE87-004961] N87-20493
Studies of long-life pulsed CO2 laser with Pt/SnO2 catalyst N87-20540
An overview of DREV's activities on pulsed CO2 laser transmitters: Frequency stability and lifetime aspects N87-20542
LIFE SCIENCES
China report: Science and technology [JPRS-CST-86-025] N87-20708
LIFE SUPPORT SYSTEMS
Phycomyces in space: A problem in bioengineering N87-20306
LIFT
A rational approach to lifting surface theory with application to large angles of attack N87-20196
Calculations for a generic fighter at supersonic high-lift conditions N87-20226
Numerical simulation of the flow field around a complete aircraft N87-20231
LIFT DEVICES
Effect of dynamic stall and elastic parameters on the fundamental mechanisms of helicopter vibrations [AD-A175561] N87-20292
LIFT DRAG RATIO
Optimization of hypersonic waveriders derived from cone flows including viscous effects N87-20193
The effect of heavy rain on an airfoil at high lift [NASA-CR-178248] N87-20232
LIGHT (VISIBLE RADIATION)
Research investigation directed toward extending the useful range of the electromagnetic spectrum [AD-A175644] N87-20452
The use of visible data for improving VAS satellite soundings N87-20620
LIGHT SCATTERING
Experimental and analytical investigation of the variation of spray characteristics along a radial distance downstream of a pressure-swirl atomizer N87-20271
LOWTRAN modeling of near-horizon infrared sky radiances in the presence of clouds [AD-A175661] N87-20691
LIGHT TRANSMISSION
Diffraction diffusion screen with holographically suppressed zero-order beam [AD-D012565] N87-20519
LIGHTNING
WSUH-1D: Review of damage following lightning strike 30 November 1981 [RAE-TRANS-2103] N87-20262
Lightning strikes on aircraft. Exploitation of Landes (France)-Front '84 campaign and complementary development of airborne electrical sensors [ONERA-RF-91/7154-PY] N87-20706

LIMBS (ANATOMY)
Electrodermal conductivity in man and monkeys N87-20743
LINE SPECTRA
Acta mechanica sinica (selected articles) [AD-A176240] N87-20246
Molecular clouds in the outer galaxy N87-20854
Ring galaxies: An investigation of the physical conditions in closely interacting systems N87-20858
C IV Doppler shifts observed in active region filaments N87-20896
Measurements of magnetic fields in solar prominences N87-20901
Magnetic field vector and electron density diagnostics from linear polarization measurements in 14 solar prominences N87-20902
The heating of filaments as a disappearance process N87-20904
LINEAR ACCELERATORS
Factors limiting the operation of structures under high gradient — linear accelerators [DE87-005132] N87-20461
LINEAR EQUATIONS
Galerkin/Runge-Kutta discretizations for semilinear parabolic equations [NASA-CR-178264] N87-20783
LINEAR POLARIZATION
Magnetic field vector and electron density diagnostics from linear polarization measurements in 14 solar prominences N87-20902
LINEAR PREDICTION
NASA/MSFC prediction techniques N87-20678
LINEAR SYSTEMS
Mean-square error bounds for reduced-error linear state estimators [NASA-TM-89441] N87-20291
Stable response of damped linear systems, part 3 N87-20440
Risk evaluations of aging phenomena: The linear aging reliability model and its extensions [DE87-002607] N87-20563
Linear baroclinic instability in the presence of large scale topography [NASA-CR-4057] N87-20700
Piecewise linear approximation for hereditary control problems [NASA-CR-178260] N87-20776
Structural properties of linear periodic systems [REPT-86-004-REV] N87-20788
LININGS
Advanced composite combustor structural concepts program [NASA-CR-174733] N87-20387
LINKAGES
Force magnitude and angular velocity fluctuation reduction in a spring-restrained, flexibly-supported four-bar mechanical linkage N87-20589
LIPID METABOLISM
Blood lipids and incidence of lipemia in flight personnel N87-20737
LIPSCHITZ CONDITION
On Lipschitz continuity of nonlinear differential operators [NASA-CR-178263] N87-20782
LIQUID ATOMIZATION
The physics of fuel sprays. Volume 1: Experimental measurements [AD-A175660] N87-20285
LIQUID HELIUM
Transient heat transfer to supercritical helium at low temperatures [ETN-87-99321] N87-20632
LIQUID PHASE EPITAXY
A study of III-V semiconductor processing employing high purity epitaxial gallium arsenide N87-20819
Liquid Phase Epitaxy (LPE) of silicon carbide [AD-D012571] N87-20823
LIQUID-SOLID INTERFACES
Solid mechanics program at ONR N87-20575
LITERATURE
Underwater acoustic modeling techniques N87-20436
LITHIUM COMPOUNDS
Etching of LiNbO3 by laser-driven fusion of salts [DE87-003033] N87-20544
LITHIUM ISOTOPES
Capture of thermal neutrons B10 and Li6: Applications in spectroscopy and in the study of weak nucleon interactions [ECN-164] N87-20803
Investigation of excited states of Li7 by means of thermal neutron capture N87-20805
An investigation of the admixture of strong and weak interactions in the B10 (n, alpha) Li7 reaction with slow neutrons N87-20807
LOAD TESTS
Evaluation of vibration specifications for static and dynamic material allowables N87-20600
LOADS (FORCES)
Structural qualification of large spacecraft N87-20361
LOCAL AREA NETWORKS
Guide to sharing personal computer resources via local area networks, revised [DE86-016068] N87-20772
LOGISTICS
On modern avionic and defense systems logistic support standardization and cost effectiveness N87-20761
LONG DURATION EXPOSURE FACILITY
Baseline tensile tests of composite materials for LDEF (Long Duration Exposure Facility) exposure [NASA-TM-89069] N87-20386
LONG DURATION SPACE FLIGHT
Manned Mars missions: A working group report [NASA-TM-89214] N87-20301
Effect of long-term spaceflight on rat brain polyamine content N87-20741
LOOPS
Investigation of thermal-fluid mechanical characteristics of the capillary pump and the pumped two-phase loop [NASA-CR-180509] N87-20557
LORENTZ FORCE
Static current-sheet models of quiescent prominences N87-20882
LOW ALTITUDE
A preliminary study into the constant drag parachute for aircrew escape systems [BU-345] N87-20256
LOW FREQUENCIES
Low frequency vibration testing on satellites N87-20364
An evaluation of active noise control in a cylindrical shell [NASA-TM-89090] N87-20794
LOW REYNOLDS NUMBER
Experimental study of low Reynolds number nozzles [NASA-TM-89858] N87-20383
LOW SPEED WIND TUNNELS
Integral method of wall interference correction in low-speed wind tunnels [NASA-TT-20055] N87-20241
LOW TEMPERATURE
Characterization of the LTC catalyst: Performance against common air pollutants N87-20535
Alumina-supported Pd-Ag catalysts for low-temperature CO and methanol oxidation N87-20536
LUMINOSITY
Thermal production of not so invisible axions in the early universe [DE87-005404] N87-20866
LYMAN SPECTRA
Interpretation of the prominence differential emissions measure for 3 geometries N87-20890

M

MACHINING
Implementation of active force control for robots subject to dynamic loading N87-20588
MAGNESIUM
Studies of X-ray satellites in sodium, magnesium, aluminum, argon, and iron [ETN-87-99364] N87-20612
MAGNETIC BEARINGS
Description of a magnetic bearing test fixture [NASA-TM-89081] N87-20478
MAGNETIC CONTROL
Hubble Space Telescope N87-20670
MAGNETIC FIELD CONFIGURATIONS
Coronal and Prominence Plasmas [NASA-CP-2442] N87-20871
Some crucial corona and prominence observations N87-20872
Heating of the stellar corona N87-20873
Formation and support of prominence N87-20874
Condensation modes in magnetized plasmas N87-20877
Filament formation due to photospheric shear N87-20878
Formation of active region and quiescent prominence magnetic field configurations N87-20879
Static current-sheet models of quiescent prominences N87-20882
Recent observations of the formation of filaments N87-20883
Magnetic helicity as a constraint on coronal dissipation N87-20940
Dynamic evolution of coronal magnetic fields N87-20945
MAGNETIC FIELDS
Orbital atmospheric physics and dynamics N87-20673
High field properties of SnMo6S8 and PbMo6S8 ribbons prepared using a vapor transport technique [DE87-004707] N87-20826
The magnetic and turbulent evolution of the Taurus molecular cloud N87-20852
Small-scale coronal structure, part 3 N87-20922
Phlegethon flow: A proposed origin for spicules and coronal heating N87-20933
The topological description of coronal magnetic fields N87-20936
A coordinate free description of magnetohydrostatic equilibria N87-20937
Cascade model of coronal heating N87-20938
The stability of coronal and prominence magnetic fields N87-20941
Resistive ballooning modes in line-tied coronal arcades N87-20942
MAGNETIC FLUX
The association of chromospheric and coronal phenomena with the evolution of the quiet sun magnetic fields [ESD-TR-84-611] N87-20926
Magnetogram and soft X-ray comparisons of XBP and ER N87-20927
Small-scale eruptive filaments on the quiet sun N87-20928
MAGNETIC MATERIALS
Material with anisotropic properties for magnetic shielding purposes [AD-A175864] N87-20453
MAGNETIC MONOPOLES
Search for magnetic monopoles, neutrino oscillations, and superhigh energy physics [DE87-005774] N87-20953
MAGNETIC PERMEABILITY
Material with anisotropic properties for magnetic shielding purposes [AD-A175864] N87-20453
MAGNETIC PROPERTIES
Material with anisotropic properties for magnetic shielding purposes [AD-A175864] N87-20453
Highlights from the physics in metallic superlattices [DE87-004657] N87-20825
MAGNETIC SHIELDING
Material with anisotropic properties for magnetic shielding purposes [AD-A175864] N87-20453
MAGNETIC SIGNATURES
Guided MHD waves as a coronal diagnostic tool N87-20921
MAGNETIC SURVEYS
Magnetotelluric measurements in Antarctica [INPE-4058-PRE/1017] N87-20661
MAGNETOACOUSTIC WAVES
Steepened magnetosonic waves in the high Beta plasma surrounding Comet-Giacobini-Zinner [NASA-CR-180614] N87-20868
Guided MHD waves as a coronal diagnostic tool N87-20921
MAGNETOHYDRODYNAMIC STABILITY
Coronal and Prominence Plasmas [NASA-CP-2442] N87-20871
Condensation modes in magnetized plasmas N87-20877
The stability of coronal and prominence magnetic fields N87-20941
Resistive ballooning modes in line-tied coronal arcades N87-20942
Effects of flows on viscous and resistive MHD stability N87-20943
MAGNETOHYDRODYNAMIC WAVES
MHD waves detected by ice at distances 28 x 10 km from Comet Halley: Cometary or solar wind origin [DE87-005122] N87-20863
Heating of the stellar corona N87-20873
Can prominences form in current sheets N87-20876
Alfven-wave dissipation: A support mechanism for quiescent prominences N87-20881
Guided MHD waves as a coronal diagnostic tool N87-20921
Heating of the solar corona by the resonant absorption of Alfven waves N87-20939
MAGNETOHYDRODYNAMICS
Filament formation due to photospheric shear N87-20878
Formation of active region and quiescent prominence magnetic field configurations N87-20879
Topological constraints and the existence of force-free fields N87-20935
Large-scale electric fields resulting from magnetic reconnection in the corona N87-20944

MAGNETOHYDROSTATICS
A coordinate free description of magnetohydrostatic equilibria N87-20937
MAGNETOSPHERE
Yosemite Conference on Ionospheric Plasma in the Magnetosphere: Sources, Mechanisms and Consequences, meeting report [NASA-TM-86589] N87-20689
Observations of sunward and tailward ion streaming in the magnetotail of Jupiter with Voyager 2 N87-20869
MAGNETOSTATIC FIELDS
Quasistatic evolution of magnetostatic coronal structures N87-20913
Three-dimensional magnetostatic models of the large-scale corona N87-20914
MAGNETOSTATICS
Magnetostatic wave frequency analyzer apparatus [AD-D012558] N87-20458
Coronal and Prominence Plasmas [NASA-CP-2442] N87-20871
MAIN SEQUENCE STARS
Linear nonadiabatic pulsations of homogeneous ZAMS stars [DE87-003722] N87-20844
MAINTENANCE
Advanced EVA system design requirements study: EVAS/space station system interface requirements [NASA-CR-171981] N87-20351
Program maintenance manual for nickel cadmium battery expert system, version 1 [NASA-CR-179033] N87-20472
Integrated digital control and man-machine interface for complex remote handling systems [DE87-003002] N87-20749
Advanced remote handling for future applications: The advanced integrated maintenance system [DE87-003004] N87-20750
Expert systems for diagnostic purposes, prospected applications to the radar field N87-20760
MALES
Radiation protection guidelines for space missions [NASA-TM-89278] N87-20730
MAN-COMPUTER INTERFACE
Human-display interactions: Context-specific biases [NASA-TM-89430] N87-20747
MANAGEMENT
Management: A bibliography for NASA managers [NASA-SP-7500(21)] N87-20833
MANAGEMENT METHODS
Management: A bibliography for NASA managers [NASA-SP-7500(21)] N87-20833
An investigation of transitional management problems for the NSTS [NASA-CR-171979] N87-20834
MANAGEMENT PLANNING
Management: A bibliography for NASA managers [NASA-SP-7500(21)] N87-20833
MANIPULATORS
Effects of force reflection on servomanipulator task performance [DE87-003008] N87-20560
Integrated digital control and man-machine interface for complex remote handling systems [DE87-003002] N87-20749
Advanced remote handling for future applications: The advanced integrated maintenance system [DE87-003004] N87-20750
MANNED ORBITAL RESEARCH LABORATORIES
The Columbus program: An overview N87-20623
MANNED SPACE FLIGHT
Manned Mars missions: A working group report [NASA-TM-89214] N87-20301
Space biology and medicine on the twenty-fifth anniversary of the first spaceflight of Yuriy Alekseyevich Gagarin N87-20732
MANUFACTURING
Manufacturing polymer thin films in a micro-gravity environment N87-20304
Safety characteristics of non-lithium battery systems, revision 1 [AD-A174577] N87-20480
State-of-the-art accelerometer characteristics for pyrotechnic shock measurement N87-20608
MANY BODY PROBLEM
Three-body calculations at Los Alamos [DE87-001959] N87-20786
MAPPING
The topological description of coronal magnetic fields N87-20936
MARINE METEOROLOGY
Numerical simulation of air mass modification over the East China Sea during the winter season N87-20660
Wind-current relationships in the optoma domain off the Northern California Coast [AD-A176019] N87-20714
MARKET RESEARCH
Land mobile communications satellite mission (LAMOCOSAMIS) Task 1: Market study [ESA-CR(P)-2302-VOL-1] N87-20462
Land mobile satellite communication system. Volume 1: Executive summary [ITS-TR-043/86-VOL1] N87-20464
Land mobile satellite communication system. Volume 2: Traffic analysis and market demand for the land mobile communications system in the European scenario [ITS-TR-043/86-VOL-2] N87-20465
MARKOV CHAINS
Uniqueness of Gibbs measures and absorption probabilities [CWI-MS-R8610] N87-20789
MARS (PLANET)
Manned Mars missions: A working group report [NASA-TM-89214] N87-20301
MASS
The large-scale peculiar velocity field in flat models of the universe [DE87-005402] N87-20864
MASS FLOW
On the formation of active region prominences (H alpha filaments) N87-20884
Vertical motions in the quiescent prominences observed in the He I Lambda10830Angstrom line N87-20896
MASS TRANSFER
Study of the development of a compressible turbulent boundary layer on a porous and rough wall [ETN-87-99390] N87-20512
Phlegethon flow: A proposed origin for apicules and coronal heating N87-20933
MATERIAL ABSORPTION
Biot theory and acoustical properties of high porosity fibrous materials and plastic foams [NASA-TM-88575] N87-20424
MATERIALS HANDLING
Hydrogen degradation of pipeline steels [DE87-005585] N87-20414
Theoretical investigations of shear band formation in finite elasticity [AD-A175657] N87-20572
MATHEMATICAL MODELS
Numerical calculations of turbulent reacting flow in a gas-turbine combustor [NASA-TM-89842] N87-20171
The terminal area simulation system. Volume 2: Verification cases [NASA-CR-4047-VOL-2] N87-20252
The terminal area simulation system. Volume 1: Theoretical formulation [NASA-CR-4046-VOL-1] N87-20255
Aeroelastic stability of bearingless rotors in forward flight N87-20260
Dynamic and thermal effects in very large space structures N87-20347
Structural design of an in-line bolted joint for the space shuttle solid rocket motor case segments [NASA-TM-89027] N87-20349
Spacecraft qualification using advanced vibration and modal testing techniques N87-20368
A numerical heat transfer model for an advanced solar thermal propulsion system N87-20377
Hybrid methods for rotordynamic analysis [NASA-CR-179035] N87-20553
Modeling and control of flexible structures N87-20564
The DYNAS survey. Part 2: A participant's view N87-20579
Modal test and analysis: Multiple tests concept for improved validation of large space structure mathematical models N87-20581
Numerical simulation of Atlas-Centaur stage-separation shaped charge firing and structural response N87-20606
A model for the degradation of composite structures [ONERA-RT-30/3043-RY-057-R] N87-20617
AFGWC's Advanced Weather Analysis and Prediction System (AWAPS) [AD-A172801] N87-20702
Mathematical model of steady-state circulation in the south China Sea N87-20719
Comparison of deepwater wind-wave prediction models N87-20724
Phase speed of wind-wave component studied N87-20726
Adaptive control with a nonparametric model for the controlled system [ETN-87-99015] N87-20775
Inverse problems in the modeling of vibrations of flexible beams [NASA-CR-178259] N87-20777
Remarks on the stability analysis of reactive flows [NASA-CR-178269] N87-20780
A self critical approach to data analysis and model building [AD-A175640] N87-20791
Computational analyses of crystal growth [NASA-CR-179027] N87-20820
A numerical study of some spherically-symmetric and axisymmetric cosmological models N87-20853
Small-scale structures and the density irregularity of the inner corona N87-20932
The stability of coronal and prominence magnetic fields N87-20941
Resistive ballooning modes in line-tied coronal arcades N87-20942
Effects of flows on viscous and resistive MHD stability N87-20943
Dynamic evolution of coronal magnetic fields N87-20945
MATRICES (MATHEMATICS)
A new approach for gearbox modelling in finite element analyses of torsional vibration of gear-branched propulsion systems N87-20591
Eigensystem analysis of classical relaxation techniques with applications to multigrid analysis [NASA-TM-88377] N87-20785
MATRIX MATERIALS
Unconventional approaches to field repair N87-20190
MATRIX METHODS
Forced vibrations of stringer stiffened damped sandwich panel N87-20596
MAXIMUM ENTROPY METHOD
Methods of frequency spectrum estimation of sea water compared N87-20725
MEAN
Monthly mean pressure reconstructions for Europe (back to 1780) and North America (to 1958) [DE87-005556] N87-20703
MEAN SQUARE VALUES
Mean-square error bounds for reduced-error linear state estimators [NASA-TM-89441] N87-20291
MEASURING INSTRUMENTS
Aerodynamic measurements and thermal tests of a strain-gage balance in a cryogenic wind tunnel [NASA-TM-89039] N87-20517
On requirements for a satellite mission to measure tropical rainfall [NASA-RP-1163] N87-20701
MECHANICAL PROPERTIES
High performance thermoplastics: A review of neat resin and composite properties [NASA-TM-89104] N87-20390
Investigation of thermal-fluid mechanical characteristics of the capillary pump and the pumped two-phase loop [NASA-CR-180509] N87-20557
MECHANICAL SHOCK
The Shock and Vibration Digest, Volume 19, No. 2 N87-20435
The Shock and Vibration Digest, Volume 18, No. 10 [AD-A175726] N87-20438
The Shock and Vibration Bulletin. Part 2: Modal Test and Analysis, Testing Techniques, Machinery Dynamics, Isolation and Damping, Structural Dynamics [AD-A175225] N87-20580
MEDITERRANEAN SEA
The interpretation of crustal dynamics data in terms of plate interactions and active tectonics of the Anatolian Plate and surrounding regions in the Middle East [NASA-CR-180501] N87-20662
MELTING
Resilient modulus of freeze-thaw affected granular soils for pavement design and evaluation. Part 3: Laboratory tests on soils from Albany County Airport [DOT/FAA-PM-84-16.3] N87-20433
A freeze-thaw test to determine the frost susceptibility of soils [DOT/FAA-PM-85-20] N87-20434
MELTS (CRYSTAL GROWTH)
Computational analyses of crystal growth [NASA-CR-179027] N87-20820
MERCURY CADMIUM TELLURIDES
Computational analyses of crystal growth [NASA-CR-179027] N87-20820
The US Workshop on the Physics and Chemistry of Mercury Cadmium Telluride: Extended abstracts [AD-A175593] N87-20822
MESH
Diffraction diffusion screen with holographically suppressed zero-order beam [AD-D012585] N87-20519
MESOSCALE PHENOMENA
The mesoscale organization, dynamics, and evolution of the marine planetary boundary layer during cold air outbreaks N87-20696

Linear baroclinic instability in the presence of large scale topography
[NASA-CR-4057] N87-20700

METAL BONDING
Chemistry of glass-ceramic to metal bonding for header applications Part 2: Hydrogen bubble formation during glass-ceramic to metal sealing
[DE87-004041] N87-20559

METAL FATIGUE
Fatigue and acoustics: Prediction of metal fatigue using Miner's rule N87-20598

METAL FILMS
Microstructure of metastable metallic alloy films produced by laser breakdown chemical vapor deposition and ion implantation
[DE87-002914] N87-20411

METAL MATRIX COMPOSITES
Advanced composite combustor structural concepts program
[NASA-CR-174733] N87-20387
Study of the nature of fracture failure in composite materials
[AD-A175554] N87-20391

METAL POWDER
Consolidation processing parameters and alternative processing methods for powder metallurgy Al-Cu-Mg-X-X alloys
[NASA-CR-178227] N87-20404

METAL SHEETS
Effect of adhesive bonding variables on the performance of bonded CFRP patch repairs of metallic structures N87-20182
Patch repair of corroded aircraft skin areas N87-20191
Flat-plate solar array project. Volume 3: Silicon sheet: Wafers and ribbons
[NASA-CR-180661] N87-20648

METAL STRIPS
Impact energy relationships for directly rolled uranium strip
[DE87-005789] N87-20418

METAL WORKING
Impact energy relationships for directly rolled uranium strip
[DE87-005789] N87-20418

METALS
Cal Poly Space Project G-279 N87-20324
Mechanisms of the oxidation of metals and alloys:
[DE87-003389] N87-20412
Strong metal-support interactions N87-20533
Calculation of thermomechanical fatigue life based on isothermal behavior
[NASA-TM-88864] N87-20565
Highlights from the physics in metallic superlattices
[DE87-004657] N87-20625

METEORITE COLLISIONS
Measurements of iridium and the hypothesis of meteoritic impact as the end of the Cretaceous period
[INPE-4070-TDL/248] N87-20661

METEORITES
Pre-compaction irradiation of meteorites N87-20650

METEOROLOGICAL FLIGHT
Definition and use of sensors for measuring electrical conductivity in thunderclouds
[ONERA-NT-1986-4] N87-20705
Lightning strikes on aircraft. Exploitation of Landes (France)-Front '84 campaign and complementary development of airborne electrical sensors
[ONERA-RF-91/7154-PY] N87-20706

METEOROLOGICAL SATELLITES
On requirements for a satellite mission to measure tropical rainfall
[NASA-RP-1183] N87-20701

METHYL ALCOHOL
Alumina-supported Pd-Ag catalysts for low-temperature CO and methanol oxidation N87-20536

MICROBIOLOGY
USSR report: Life sciences. Biomedical and behavioral sciences
[JPRS-UBB-87-003] N87-20751

MICROBURSTS
The terminal area simulation system. Volume 2: Verification cases
[NASA-CR-4047-VOL-2] N87-20252

MICROCOMPUTERS
Automated anthropometric data measurement system
[AD-D012575] N87-20748

MICROELECTRONICS
Engineering thrust areas, 1987
[DE87-004443] N87-20441

MICROGRAVITY APPLICATIONS
G-300: The first French Getaway Special microgravity measurements of fluid thermal conductivity N87-20330
Microgravity effects on electrodeposition of metals and metal-cermet mixtures N87-20332
GAS-007: First step in a series of Explorer payloads N87-20333
In situ observation of mono-molecular growth steps on aqueous solution grown crystals and the transport of molecules to the crystals N87-20334
Rapid melt/quench furnace using commercially available hardware
[NASA-TM-86590] N87-20431
Liquid drop stability for protein crystal growth in microgravity
[NASA-TP-2724] N87-20727

MICROPHONES
The 1985 small propeller-driven aircraft noise test program
[AD-A175596] N87-20799

MICROPROCESSORS
Sophisticated software systems for small self-contained space shuttle payload G285 N87-20313
Multipurpose microcontroller design for PUGAS 2 N87-20321

MICROSTRUCTURE
Microstructure of metastable metallic alloy films produced by laser breakdown chemical vapor deposition and ion implantation
[DE87-002914] N87-20411

MICROWAVE AMPLIFIERS
Linearization of GaAs field effect transistor power amplifiers in hyperfrequences
[ENST-86E007] N87-20496

MICROWAVE EMISSION
Theoretical models of free-free microwave emission from solar magnetic loops N87-20918
Coronal plasmas on the sun and nearby stars N87-20919
Measurement of coronal fields using spatially resolved microwave spectroscopy N87-20920

MICROWAVE OSCILLATORS
A theoretical and experimental study of cylindrical dielectric resonators and their applications to microwave oscillators
[FOA-C-30434-3.2] N87-20495

MICROWAVE SENSORS
Range filtering for sequential GPS receivers with external sensor augmentation
[NASA-TM-89418] N87-20257

MICROWAVE SPECTRA
Measurement of coronal fields using spatially resolved microwave spectroscopy N87-20920

MICROWAVE TRANSMISSION
Propagation characteristics of some novel coplanar waveguide transmission lines on GaAs at MM-wave frequencies
[NASA-TM-89639] N87-20469

MICROWAVES
The microwave structure of quiescent solar filaments at high resolution N87-20689

MIDDLE ATMOSPHERE
Users of middle atmosphere models remarks N87-20679
Utilization of Global Reference Atmosphere Model (GRAM) for shuttle entry N87-20680
Gravity waves N87-20685
The GRAM-3 model N87-20686
Middle atmosphere density and models N87-20687

MILITARY HELICOPTERS
A survey of military aerospace systems technology developments in Western Europe and the Middle East
[AD-A175635] N87-20173

MILITARY TECHNOLOGY
Theoretical investigations of shear band formation in finite elasticity
[AD-A175657] N87-20572

MILKY WAY GALAXY
Molecular clouds in the outer galaxy N87-20854
Abundances and kinematics of K giants in the galactic nuclear bulge N87-20856

MILLIMETER WAVES
System architecture of MMIC-based large aperture arrays for space application
[NASA-TM-89840] N87-20468
Propagation characteristics of some novel coplanar waveguide transmission lines on GaAs at MM-wave frequencies
[NASA-TM-89639] N87-20469

MIMD (COMPUTERS)
Parallel processing of networks
[AD-A175841] N87-20771

MINICOMPUTERS
China report: Science and technology
[JPRS-CST-86-025] N87-20708

MINKOWSKI SPACE
Gravitational collapse in relativistic theory of gravitation
[DE87-700730] N87-20792

MIRRORS
Towards a better mirror N87-20310

MISSILE COMPONENTS
An application of computational fluid dynamics to the design of optimum ramjet powered missile components N87-20338

MISSILE CONFIGURATIONS
A second order Godunov method for tactical missiles N87-20211
Simulation of a jet deflection system with the aid of the Euler equations N87-20212
A multiple zone method for supersonic tactical missiles
[AD-A175938] N87-20244
An application of computational fluid dynamics to the design of optimum ramjet powered missile components N87-20338

MISSILE CONTROL
Control aspects of the launch phase of a vertically-launched short-range surface-to-air missile
[ETN-87-99478] N87-20341
A study of the methods used to carry out RF telemetry testing of surface-to-air missiles
[ETN-87-99481] N87-20346

MISSILE DESIGN
An application of computational fluid dynamics to the design of optimum ramjet powered missile components N87-20338

MISSILE VIBRATION
Rivista Tecnica Selenia, volume 10, number 1
[ETN-87-99091] N87-20759
An application of Rayleigh's method to the fast calculation of the first vibration frequency of a missile launcher cell N87-20762

MISSION PLANNING
Manned Mars missions: A working group report
[NASA-TM-89214] N87-20301
Satellite servicing mission preliminary cost estimation model
[NASA-CR-171978] N87-20335
An advanced technology space station for the year 2025, study and concepts
[NASA-CR-178208] N87-20340

MIXING
Experiments and modeling of dilution jet flow fields N87-20276
Testing and comparison of several mixed-layer models
[AD-A175959] N87-20712

MODAL RESPONSE
Dynamic qualification of spacecraft by means of modal synthesis N87-20363
The digital processing of acceleration measurements for modal analysis N87-20439
Stable response of damped linear systems, part 3 N87-20440
The algorithm and application of a new multi-input-multi-output modal parameter identification method N87-20582
Modal parameter identification using adaptive digital filters N87-20583
Testing techniques. Random variation of modal frequencies: Experiments and analysis N87-20585
Blade damping measurements in a spin rig with nozzle passing excitation simulated by electromagnets N87-20590

MODELS
Underwater acoustic modeling techniques N87-20436
Risk evaluations of aging phenomena: The linear aging reliability model and its extensions
[DE87-002607] N87-20563
Modeling of joints for the dynamic analysis of truss structures
[NASA-TP-2661] N87-20567
Experimental validation of a two-dimensional shear-flow model for determining acoustic impedance
[NASA-TM-2679] N87-20798
Computer simulation and analysis of spatial galaxy distributions N87-20851
The large-scale peculiar velocity field in flat models of the universe
[DE87-005402] N87-20864
Double inflation: A possible resolution of the large-scale structure problem
[DE87-005403] N87-20865

MODES
Large mode radius resonators N87-20524

MODULES
Conceptual design and integration of a space station resistojet propulsion assembly
[NASA-TM-89847] N87-20378

MODULUS OF ELASTICITY
Design study of advanced model support systems for the National Transonic Facility (NTF)
[NASA-CR-178214] N87-20297

MOIRE INTERFEROMETRY
Studies of stress wave propagation in composites
[DE87-001433] N87-20396

MOISTURE
Moisture absorption in graphite/organic-matrix composites
[DE87-004229] N87-20394
MOLECULAR BEAM EPITAXY
Fabrication of microwave devices on ultrathin active GaAs substrates
[FOA-C-30431-3.2] N87-20494
A study of III-V semiconductor processing employing high purity epitaxial gallium arsenide N87-20619
MOLECULAR CLOUDS
The magnetic and turbulent evolution of the Taurus molecular cloud N87-20652
Molecular clouds in the outer galaxy N87-20654
MOLECULAR GASES
Kinetic model for the vibrational energy exchange in flowing molecular gas mixtures
[NASA-TM-88500] N87-20802
MOLECULES
Microgravity crystallization of macromolecules: An interim report and proposal for continued research
[NASA-TP-2671] N87-20423
MOLTEN SALTS
Determination of the ternary viscosity diagram NaCl-KCl-LiCl by the flow method
[INSA-IDTC1-8604] N87-20403
High-temperature fuel cells
[DE87-004870] N87-20487
Etching of LiNbO3 by laser-driven fusion of salts
[DE87-003033] N87-20544
MOLYBDENUM ALLOYS
Electron tunneling studies of Mo/(sub)1-xRe/(sup)x/: Enhancement of superconductivity by a resonance mode
[DE87-003048] N87-20484
MONITORS
Development of a takeoff performance monitoring system
[NASA-CR-178255] N87-20264
Atmospheric contrast transmittance monitor
[AD-D012555] N87-20520
MONKEYS
Electrodermal conductivity in man and monkeys N87-20743
MONTE CARLO METHOD
A model and computer code for the Monte Carlo simulation of relativistic electron and positron penetration through matter
[USIP-86-11] N87-20808
Computer simulation and analysis of spatial galaxy distributions N87-20851
MOORING
Moored current meter and temperature-pressure recorder measurements from the Western North Atlantic (high energy benthic boundary layer and abyssal circulation experiments 1983-1984), volume 39
[AD-A176014] N87-20713
MORPHOLOGY
Morphological changes in the sulfur electrode of lifecycle-tested Na/S cells
[DE87-004961] N87-20493
MOTION SICKNESS
Interlabyrinthine asymmetry, vestibular dysfunction and space motion sickness N87-20734
MOTOR VEHICLES
Fuel cells in transportation
[DE87-003746] N87-20654
MULTILAYER INSULATION
Material with anisotropic properties for magnetic shielding purposes
[AD-A175864] N87-20453
MULTIPROCESSING (COMPUTERS)
Performance studies of the multigrid algorithms implemented on hypercube multiprocessor systems
[NASA-CR-178237] N87-20769
A virtual-time operating-system shell for a hypercube in robotics applications
[DE87-004256] N87-20773
MYLAR (TRADEMARK)
Laboratory investigation of lightweight heater tape for shuttle propellant tank
[AD-A175997] N87-20345

N

NACELLES
Wing-nacelle interactions. Program 1985. Part two: Development of a finite element code for an isolated nacelle
[ONERA-RTS-21/3271-AY] N87-20250
NASA PROGRAMS
USA-Europe coordination and cooperation activities: Announcements of Opportunity — polar platforms N87-20632
Management: A bibliography for NASA managers
[NASA-SP-7500(21)] N87-20633
NATURAL GAS
A simplified method for determining heat of combustion of natural gas
[NASA-TP-2682] N87-20514
NAVIER-STOKES EQUATION
Numerical solutions of unsteady flow past rotor sections N87-20196
Zonal solutions for airfoils using Euler boundary-layer and Navier-Stokes equations N87-20219
Using the boundary-layer equations in three-dimensional viscous flow simulation N87-20222
Application of the Navier-Stokes equations to solve aerodynamic problems N87-20225
Calculations for a generic fighter at supersonic high-lift conditions N87-20226
High speed viscous flow calculations about complex configurations N87-20227
Transonic Navier-Stokes wing solution using a zonal approach. Part 1: Solution methodology and code validation N87-20228
Transonic Navier-Stokes wing solutions using a zonal approach. Part 2: High angle-of-attack simulation N87-20229
Numerical simulation of the flow field around a complete aircraft N87-20231
Simulation of transonic viscous wing and wing-fuselage flows using zonal methods
[NASA-TM-89421] N87-20242
A Navier-Stokes solver using the LU-SSOR TVD algorithm
[NASA-CR-179608] N87-20243
A finite difference scheme for three-dimensional steady laminar incompressible flow
[NASA-TM-89851] N87-20504
Conversion of ARO-1 to an implicit Navier-Stokes solver
[AD-A175967] N87-20505
A predictor-corrector method for calculation of incompressible fluid flow dynamics
[DE87-003804] N87-20508
NAVIGATION SATELLITES
NAVSAT time synchronization simulation study
[ESA-CR(P)-2305] N87-20376
NEAR ULTRAVIOLET RADIATION
UBVRI-photometry of the antiflare stars V586 Ori and IU Ori
[DE87-700760] N87-20845
NEODYMIUM LASERS
USSR report: Physics and mathematics
[JPRS-UPM-86-008] N87-20445
The laser strength of active elements made of Gadolinium-Scandium-Gallium garnet (GSGG) N87-20446
A ring-cavity for a quadrupled Nd-YAG laser
[DE87-004175] N87-20547
NEPHELOMETERS
Atmospheric contrast transmittance monitor
[AD-D012555] N87-20520
NEUTRAL ATMOSPHERES
NORAD/SPACECMD comments concerning the atmospheric density models N87-20672
NEUTRAL GASES
Spectral characteristics of interchange turbulence in the ionosphere
[AD-A175975] N87-20692
NEUTRAL SHEETS
Observations of sunward and tailward ion streaming in the magnetotail of Jupiter with Voyager 2 N87-20869
NEUTRINOS
Search for magnetic monopoles, neutrino oscillations, and superhigh energy physics
[DE87-005774] N87-20953
NEUTRON ACTIVATION ANALYSIS
Measurements of iridium and the hypothesis of meteoritic impact as the end of the Cretaceous period
[INPE-4070-TDL/248] N87-20861
NEUTRON BEAMS
Capture of thermal neutrons B10 and Li6: Applications in spectroscopy and in the study of weak nucleon interactions
[ECN-184] N87-20803
General introduction to capture of thermal neutrons in B10 and Li6: Applications in spectroscopy and in the study of weak nucleon interactions N87-20804
NEUTRON STARS
The acceleration and dissolution of stars moving through the blackbody radiation of a collapsing universe N87-20847
NICKEL
Electroforming with nickel, iron, and aluminum
[DE87-005589] N87-20442
NICKEL ALLOYS
Bithermal low-cycle fatigue behavior of a NiCoCrAlY-coated single crystal superalloy
[NASA-TM-89631] N87-20408
Galvanic corrosion resistance of welded dissimilar nickel-base alloys
[DE87-002656] N87-20409
Ductility and fracture behavior of polycrystalline Ni3Al alloys
[DE87-005340] N87-20413
NICKEL CADMIUM BATTERIES
Users manual for nickel cadmium battery expert system
[NASA-CR-179032] N87-20470
Nickel cadmium battery expert system
[NASA-CR-179031] N87-20471
Program maintenance manual for nickel cadmium battery expert system, version 1
[NASA-CR-179033] N87-20472
Requirements specification for nickel cadmium battery expert system
[NASA-CR-179034] N87-20473
Analysis of 12 AH aerospace nickel-cadmium cells from the design variable program
[NASA-TM-87774] N87-20479
NIOBATES
Etching of LiNbO3 by laser-driven fusion of salts
[DE87-003033] N87-20544
NIOBIUM ALLOYS
Creep behavior of niobium alloy PWC-11
[NASA-TM-89834] N87-20405
NITROGEN
Carbon and nitrogen abundances along the evolutionary sequence of M67 N87-20848
NITROUS OXIDES
Adsorption of atomic oxygen (N2O) on clean silicon surfaces and its influence on the surface state density; a comparison with O2
[B6668354] N87-20810
NOBLE METALS
CO oxidation studies over supported noble metal catalysts and single crystals: A review N87-20530
NOISE (SOUND)
The 1985 small propeller-driven aircraft noise test program
[AD-A175596] N87-20799
NOISE REDUCTION
An evaluation of active noise control in a cylindrical shell
[NASA-TM-89090] N87-20794
A survey of achieved levels of airborne sound insulation in broadcasting studio centres
[BBC-RD-1987/1] N87-20796
NOMENCLATURES
Composite motor case nomenclature
[AD-A176418] N87-20384
NONADIABATIC CONDITIONS
Linear nonadiabatic pulsations of homogeneous ZAMS stars
[DE87-003722] N87-20844
NONDESTRUCTIVE TESTS
Damage in carbon-resin composites: Transversal cracking and peeling
[ONERA-RT-42/7066-M] N87-20396
Application of CARS to scramjet combustion
[NASA-CR-178245] N87-20400
The acousto-ultrasonic approach
[NASA-TM-89843] N87-20562
NONLINEAR EQUATIONS
On Lipschitz continuity of nonlinear differential operators
[NASA-CR-178263] N87-20782
NONLINEAR FILTERS
A comparison of nonlinear filters for orbit determination and estimation N87-20336
NONLINEAR SYSTEMS
Utilization of Euler codes in nonlinear aerodynamics N87-20215
Design and verification by nonlinear simulation of a Mach/CAS control law for the NASA TCV B737 aircraft
[NASA-CR-178029] N87-20290
Linearization of GaAs field effect transistor power amplifiers in hyperfrequences
[ENST-86E007] N87-20496
The fully nonlinear development of Goertler vortices in growing boundary layers
[NASA-CR-178268] N87-20502
Hybrid methods for rotordynamic analysis
[NASA-CR-179035] N87-20553
Numerical investigations of geometrically nonlinear shell kinetics
[ETN-87-99019] N87-20616
Fly's eye sensor nonlinear signal processing
[AD-D012564] N87-20815
Nonlinear dynamics of some condensed matter devices and materials
[ETN-87-99363] N87-20829
The propagation of an electron beam through the solar corona N87-20946

NONLINEARITY
Studies in nonlinear structural dynamics: Chaotic behavior and poynting effect N87-20348
Mechanical and thermal characterization of unidirectional aramid/epoxy [CCMS-86-06] N87-20385

NONPARAMETRIC STATISTICS
Adaptive control with a nonparametric model for the controlled system [ETN-87-99015] N87-20775

NORTH AMERICA
Monthly mean pressure reconstructions for Europe (back to 1780) and North America (to 1958) [DE87-005556] N87-20703

NOZZLE DESIGN
An application of computational fluid dynamics to the design of optimum ramjet powered missile components N87-20338

NOZZLE FLOW
Simulation of a jet deflection system with the aid of the Euler equations N87-20212
Conversion of ARO-1 to an implicit Navier-Stokes solver [AD-A175967] N87-20505

NOZZLE GEOMETRY
Computational analysis and preliminary redesign of the nozzle contour of the Langley hypersonic CF4 tunnel [NASA-TM-89042] N87-20296
Experimental thrust performance of a high-area-ratio rocket nozzle [NASA-TP-2720] N87-20381
Experimental study of low Reynolds number nozzles [NASA-TM-89858] N87-20383

NUCLEAR CAPTURE
Capture of thermal neutrons B10 and Li6: Applications in spectroscopy and in the study of weak nucleon interactions [ECN-184] N87-20803
General introduction to capture of thermal neutrons in B10 and Li6: Applications in spectroscopy and in the study of weak nucleon interactions N87-20804
Investigation of excited states of Li7 by means of thermal neutron capture N87-20805
Investigation of excited states of B11 and Li7 by means of thermal neutron capture on B10 nuclei N87-20806

NUCLEAR CHEMISTRY
Capture of thermal neutrons B10 and Li6: Applications in spectroscopy and in the study of weak nucleon interactions [ECN-184] N87-20803
Investigation of excited states of Li7 by means of thermal neutron capture N87-20805
Investigation of excited states of B11 and Li7 by means of thermal neutron capture on B10 nuclei N87-20806
An investigation of the admixture of strong and weak interactions in the B10 (n, alpha) Li7 reaction with slow neutrons N87-20807

NUCLEAR EXPLOSION EFFECT
A research program to assess the impact of the electromagnetic pulse on electric power systems [DE87-002415] N87-20486

NUCLEAR EXPLOSIONS
Propagation of RF signals through structured ionization. Theory and antenna aperture effect applications [AD-A175522] N87-20451
A research program to assess the impact of the electromagnetic pulse on electric power systems [DE87-002415] N87-20486

NUCLEAR FUEL REPROCESSING
Integrated digital control and man-machine interface for complex remote handling systems [DE87-003002] N87-20749
Advanced remote handling for future applications: The advanced integrated maintenance system [DE87-003004] N87-20750

NUCLEAR PARTICLES
Nuclear geophysics in space and atmospheric research at INPE/BRAZIL [DE87-700426] N87-20693

NUCLEAR PHYSICS
USSR report: Physics and mathematics [JPRS-UPM-86-008] N87-20445

NUCLEAR RADIATION
Space radiation studies [NASA-CR-179037] N87-20951

NUCLEAR RADIATION SPECTROSCOPY
General introduction to capture of thermal neutrons in B10 and Li6: Applications in spectroscopy and in the study of weak nucleon interactions N87-20804

NUCLEI (NUCLEAR PHYSICS)
Statistical analysis of secondary particle distributions in relativistic nucleus-nucleus collisions [NASA-CR-4054] N87-20813

NUCLEONS
Capture of thermal neutrons B10 and Li6: Applications in spectroscopy and in the study of weak nucleon interactions [ECN-184] N87-20803
General introduction to capture of thermal neutrons in B10 and Li6: Applications in spectroscopy and in the study of weak nucleon interactions N87-20804
An investigation of the admixture of strong and weak interactions in the B10 (n, alpha) Li7 reaction with slow neutrons N87-20807

NUMERICAL ANALYSIS
Computation of transonic flow over porous airfoils N87-20194
A numerical study of the Weis-Fogh mechanism N87-20197
Multigrid calculation of boundary-fitted orthogonal coordinates with applications to unsteady flows N87-20237
A Navier-Stokes solver using the LU-SSOR TVD algorithm [NASA-CR-179608] N87-20243
A multiple zone method for supersonic tactical missiles [AD-A175938] N87-20244
Numerical study of combustion processes in afterburners N87-20269
Computations for the 16-foot transonic tunnel, NASA, Langley Research Center, revision 1 [NASA-TM-86319-REV-1] N87-20294
Cumulative reports and publications through December 31, 1986 [NASA-CR-178257] N87-20754
Acoustic gravity waves: A computational approach [NASA-CR-178270] N87-20781
Theory and simulation of the evolution of the large-scale solar magnetic field N87-20870

NYSTAGMUS
Link between asymmetry of optokinetic nystagmus, optovestibular and vestibulovegetative stability N87-20738

O

O RING SEALS
Structural design of an in-line bolted joint for the space shuttle solid rocket motor case segments [NASA-TM-89027] N87-20349

OCEAN BOTTOM
Moored current meter and temperature-pressure recorder measurements from the Western North Atlantic (high energy benthic boundary layer and abyssal circulation experiments 1983-1984), volume 39 [AD-A176014] N87-20713
Physical, mechanical effect of velocity of sound in ocean sediments N87-20723

OCEAN CURRENTS
China report: Science and technology [JPRS-CST-86-025] N87-20708
Hydrologic features in cyclonic eddy region of northern east China Sea in cold seasons N87-20709
Moored current meter and temperature-pressure recorder measurements from the Western North Atlantic (high energy benthic boundary layer and abyssal circulation experiments 1983-1984), volume 39 [AD-A176014] N87-20713
Wind-current relationships in the optoma domain off the Northern California Coast [AD-A176019] N87-20714
China Report: Science and technology [JPRS-CST-86-031] N87-20720
Existence seen of cyclonic eddy in northern east China Sea N87-20721

OCEAN DATA ACQUISITIONS SYSTEMS
Ocean-ice panel report — International Space Station N87-20635
Simulation of wind gradient errors in NROSS (Navy Remote Ocean Sensing System) radar scatterometer data in a simplified geometry [AD-A175754] N87-20642

OCEAN MODELS
Testing and comparison of several mixed-layer models [AD-A175959] N87-20712

OCEAN SURFACE
A technique to estimate the ocean surface energy flux using VAS multispectral data N87-20710
Acoustic scattering from composite wind-wave surfaces II: Backscatter cross sections and Doppler effects at high frequencies and small angles for 'bubble-free' regimes [AD-A176081] N87-20715

OCEAN TEMPERATURE
Moored current meter and temperature-pressure recorder measurements from the Western North Atlantic (high energy benthic boundary layer and abyssal circulation experiments 1983-1984), volume 39 [AD-A176014] N87-20713

OCEANOGRAPHIC PARAMETERS
Dynamic presentation of long term upper ocean study (LOTUS) data using videotape [AD-A175535] N87-20711

OCEANOGRAPHY
Testing and comparison of several mixed-layer models [AD-A175959] N87-20712
Continental shelf processes affecting the oceanography of the South Atlantic Bight [DE87-005303] N87-20716
China report: Science and technology [JPRS-CST-87-005] N87-20717

OCEANS
Dynamic presentation of long term upper ocean study (LOTUS) data using videotape [AD-A175535] N87-20711
Testing and comparison of several mixed-layer models [AD-A175959] N87-20712

OFF-ON CONTROL
Effectiveness of on-off damper in isolating dynamical systems N87-20594

OHMIC DISSIPATION
On the thermal durability of solar prominences, or how to evaporate a prominence N87-20905

OIL POLLUTION
Potential of laser remote sensing of oil below water surface [FOA-C-30435-3.1] N87-20659

OILS
Multi-axis vibration tests on spacecraft using hydraulic exciters N87-20373

ONBOARD EQUIPMENT
Laboratory investigation of lightweight heater tape for shuttle propellant tank [AD-A175997] N87-20345

ONE DIMENSIONAL FLOW
Thermodynamics and combustion modeling N87-20274

OPERATOR PERFORMANCE
Human-display interactions: Context-specific biases [NASA-TM-89430] N87-20747
Investigation of microstructure of arbitrary motions of operator N87-20752

OPERATORS (MATHEMATICS)
On Lipschitz continuity of nonlinear differential operators [NASA-CR-178263] N87-20782

OPERATORS (PERSONNEL)
Effects of force reflection on servomanipulator task performance [DE87-003008] N87-20560

OPTICAL COMMUNICATION
Optically tuned millimeter-wave CW. IMPATT source [AD-A175838] N87-20482

OPTICAL DEPOLARIZATION
Magnetic field vector and electron density diagnostics from linear polarization measurements in 14 solar prominences N87-20902

OPTICAL EQUIPMENT
Referencing in fiber optic sensing systems [NASA-TM-89822] N87-20475
Integrated optical devices for high speed diagnostics [DE87-003160] N87-20816

OPTICAL MEASUREMENT
Link between asymmetry of optokinetic nystagmus, optovestibular and vestibulovegetative stability N87-20738

OPTICAL MEMORY (DATA STORAGE)
Organic photochromic material for recording waveguide holograms N87-20447

OPTICAL PROPERTIES
LOWTRAN modeling of near-horizon infrared sky radiances in the presence of clouds [AD-A175661] N87-20691

OPTICAL RADAR
Airborne lidar measurements of El Chichon stratospheric aerosols, January 1984 [NASA-RP-1175] N87-20663

OPTICAL WAVEGUIDES
Organic photochromic material for recording waveguide holograms N87-20447

OPTICS
Solar power absorption in a glass tube [NASA-TM-89063] N87-20814

OPTIMAL CONTROL
Analysis of NLR configurations using OCM for pilot modeling [NASA-CR-180656] N87-20289
Dynamic modeling and optimal control design for large flexible space structures N87-20358

OPTIMIZATION
Optimization of hypersonic waveriders derived from cone flows including viscous effects N87-20193
An application of computational fluid dynamics to the design of optimum ramjet powered missile components N87-20338
Optimization of aerospace structures subjected to random vibration and fatigue constraints N87-20599

ORBIT CALCULATION
A comparison of nonlinear filters for orbit determination and estimation N87-20336
NORAD satellite tracking N87-20671

ORBIT PERTURBATION
Dynamic and thermal effects in very large space structures N87-20347

ORBIT TRANSFER VEHICLES
Aero-Assisted Orbital Transfer Vehicle (AOTV) N87-20682

ORBITAL MANEUVERS
Conceptual design and integration of a space station resistojet propulsion assembly [NASA-TM-89647] N87-20378
Hubble Space Telescope N87-20670

ORBITAL MECHANICS
Tracking the GLOMR satellite N87-20303
The orbit configuration panel report --- Columbus polar platforms N87-20640

ORBITAL SERVICING
Progress on the Ohio State University Get Away Special G-0318: DEAP N87-20311
Satellite servicing mission preliminary cost estimation model [NASA-CR-171978] N87-20335
Servicing of the polar platform --- Columbus space station N87-20628
Panel report on the polar platform servicing approach and its implications --- Columbus space station N87-20641

ORBITAL SPACE STATIONS
Advanced EVA system design requirements study: EVAS/space station system interface requirements [NASA-CR-171961] N87-20351
Proceedings of the European Symposium on Polar platform Opportunities and Instrumentation for Remote-Sensing (ESPOIR) [ESA-SP-266] N87-20621
The Earth observation activities of the European Space Agency and the use of the polar platform of the International Space Station N87-20622
The Columbus program: An overview N87-20623
European utilization aspects studies --- space stations N87-20624
ESA Columbus polar platform design concept N87-20627
Servicing of the polar platform --- Columbus space station N87-20628
Orbit configurations --- space station polar platform N87-20629
Payload data management scheme planned for Earth observation sensors to be flown on the polar platforms in the framework of the space station/Columbus program N87-20630
Cooperation of the International Space Station partners in the preparation of the use of space station elements for Earth observation (platform and payload aspects) N87-20631
USA-Europe coordination and cooperation activities: Announcements of Opportunity --- polar platforms N87-20632
Land panel report --- International Space Station N87-20634
Ocean-ice panel report --- International Space Station N87-20635
Solid Earth panel report --- Columbus program N87-20636
Panel report on multidisciplinary instrumentation: New possibilities --- Columbus space station N87-20637
Panel report on new approaches to calibration and validation --- Columbus polar platforms N87-20638
Data management panel report --- Columbus polar platforms N87-20639
The orbit configuration panel report --- Columbus polar platforms N87-20640
Panel report on the polar platform servicing approach and its implications --- Columbus space station N87-20641
Density uncertainty effect on cost of space station reboost N87-20667
An astrometric facility for planetary detection on the space station [NASA-TM-89436] N87-20841

ORDER-DISORDER TRANSFORMATIONS
Dislocation reactions at grain boundaries in Li2 ordered alloys [DE87-005713] N87-20627

ORIFICE FLOW
Experiments and modeling of dilution jet flow fields N87-20276

ORION NEBULA
UBVRI-photometry of the antiflare stars V586 Ori and IU Ori [DE87-700760] N87-20845

ORTHOGONAL FUNCTIONS
Multigrid calculation of boundary-fitted orthogonal coordinates with applications to unsteady flows N87-20237

ORTHOSTATIC TOLERANCE
Operator work capacity in tracking system when submitted to antiorthostatic hypokinesia N87-20736
Effect of hemadsorption on rheological parameters of blood during seven-day antiorthostatic hypokinesia and in vitro studies N87-20740

OSCILLATIONS
Reaction rate oscillations during catalytic CO oxidation: A brief overview N87-20534
Search for magnetic monopoles, neutrino oscillations, and superhigh energy physics [DE87-005774] N87-20953

OSCILLATORS
Optically tuned millimeter-wave CW. IMPATT source [AD-A175838] N87-20482
Review of the frequency stabilization of TEA CO2 laser oscillators N87-20523
Wind velocity measurement accuracy with highly stable 12 mJ/pulse high repetition rate CO2 laser master oscillator power amplifier N87-20525
Analysis of intrapulse chirp in CO2 oscillators N87-20526
Injection-seeding studies of diode laser array behavior [DE87-002051] N87-20546

OTOLITH ORGANS
Interlabyrinthine asymmetry, vestibular dysfunction and space motion sickness N87-20734

OXIDATION
Mechanisms of the oxidation of metals and alloys: [DE87-003389] N87-20412
The oxidation of carbon monoxide using a tin oxide catalyst N87-20528
CO oxidation studies over supported noble metal catalysts and single crystals: A review N87-20530
Chemical engineering design of CO oxidation catalysts N87-20531
Reaction rate oscillations during catalytic CO oxidation: A brief overview N87-20534
Alumina-supported Pd-Ag catalysts for low-temperature CO and methanol oxidation N87-20536
Rare isotope studies involving catalytic oxidation of CO over platinum-tin oxide N87-20538
Studies of CO oxidation on Pt/SnO2 catalyst in a surrogate CO2 laser facility N87-20539
Characterization of Pt/SnO2 catalysts for CO oxidation N87-20541

OXIDATION RESISTANCE
High temperature protective coatings for aero engine gas turbine components [AD-A176001] N87-20286

OXIDES
High-temperature fuel cells [DE87-004870] N87-20487

OXYGEN
Adsorption of atomic oxygen (N2O) on clean silicon surfaces and its influence on the surface state density; a comparison with O2 [B8668354] N87-20810

OXYGEN SUPPLY EQUIPMENT
A simplified method for determining heat of combustion of natural gas [NASA-TP-2682] N87-20514

P

PACIFIC OCEAN
The effect of latent heat on kinetic energy conversions associated with South Pacific cyclones N87-20696

PALMGREN-MINER RULE
Fatigue and acoustics: Prediction of metal fatigue using Miner's rule N87-20598

PANEL METHOD (FLUID DYNAMICS)
An assessment of the use of low-order panel methods for the calculation of supersonic flows N87-20204

PANELS
Composite repair of cocured J-stiffened panels: Design and test verification N87-20181
Composite repair of cracked aluminum structure N87-20183
Fibre composite repair of cracked metallic aircraft components: Practical and basic aspects N87-20187

PARABOLIC DIFFERENTIAL EQUATIONS
Galerkin/Runge-Kutta discretizations for semilinear parabolic equations [NASA-CR-178264] N87-20763

PARABOLIC FLIGHT
Rapid melt/quench furnace using commercially available hardware [NASA-TM-88590] N87-20431

PARACHUTES
Airspeed sensing pressure valve system [AD-D012569] N87-20266

PARALLEL COMPUTERS
Time-partitioning simulation models for calculation on parallel computers [NASA-TM-89850] N87-20766
A Lanczos eigenvalue method on a parallel computer [NASA-TM-89097] N87-20768

PARALLEL PROCESSING (COMPUTERS)
A system for routing arbitrary directed graphs on SIMD architectures [NASA-CR-178265] N87-20764
Time-partitioning simulation models for calculation on parallel computers [NASA-TM-89850] N87-20766
The hypercluster: A parallel processing test-bed architecture for computational mechanics applications [NASA-TM-89823] N87-20767
Parallel processing of networks [AD-A175641] N87-20771

PARAMETER IDENTIFICATION
Computations for the 16-foot transonic tunnel, NASA, Langley Research Center, revision 1 [NASA-TM-86319-REV-1] N87-20294
The algorithm and application of a new multi-input-multi-output modal parameter identification method N87-20582
Modal parameter identification using adaptive digital filters N87-20583
Testing techniques. Random variation of modal frequencies: Experiments and analysis N87-20585

PARAMETERIZATION
Six reasons why thermospheric measurements and models disagree N87-20688

PARTIAL DIFFERENTIAL EQUATIONS
Studies in nonlinear structural dynamics: Chaotic behavior and poynting effect N87-20348
On the use of CORLIB subroutines for the solution of a model fluid flow problem [DE87-005285] N87-20509

PARTICLE ACCELERATION
Observations of sunward and tailward ion streaming in the magnetotail of Jupiter with Voyager 2 N87-20869

PARTICLE COLLISIONS
Statistical analysis of secondary particle distributions in relativistic nucleus-nucleus collisions [NASA-CR-4054] N87-20813
Collisional dynamics of perturbed particle disks in the solar system [NASA-CR-180497] N87-20660

PARTICLE ENERGY
Pre-compaction irradiation of meteorites N87-20650

PARTICLE INTERACTIONS
Statistical analysis of secondary particle distributions in relativistic nucleus-nucleus collisions [NASA-CR-4054] N87-20813

PARTICLE SIZE DISTRIBUTION
The physics of fuel sprays. Volume 1: Experimental measurements [AD-A175660] N87-20285
LOWTRAN modeling of near-horizon infrared sky radiance in the presence of clouds [AD-A175861] N87-20691

PARTITIONS (MATHEMATICS)
Time-partitioning simulation models for calculation on parallel computers [NASA-TM-89850] N87-20766

PARTITIONS (STRUCTURES)
A survey of achieved levels of airborne sound insulation in broadcasting studio centres [BBC-RD-1987/1] N87-20796

PASSIVITY
Apparatus for high temperature in situ laser Raman spectroelectrochemical studies of metal corrosion and passivation in aqueous environments [DE87-004868] N87-20416

PAVEMENTS
Performance of recycled asphalt concrete airport pavement surfaces [DOT/FAA-PM-86-12] N87-20432
Resilient modulus of freeze-thaw affected granular soils for pavement design and evaluation. Part 3: Laboratory tests on soils from Albany County Airport [DOT/FAA-PM-84-16.3] N87-20433

PAYLOADS
Helicopter external load operations [CAP-426] N87-20259

Modal testing of the Olympus development model stowed solar array N87-20366
An astrometric facility for planetary detection on the space station
[NASA-TM-89436] N87-20841

PCM TELEMETRY
A study of the methods used to carry out RF telemetry testing of surface-to-air missiles
[ETN-87-99481] N87-20346

PEELING
Damage in carbon-resin composites: Transversal cracking and peeling
[ONERA-RT-42/7086-M] N87-20398

PERFORMANCE PREDICTION
The prediction of transonic loading on advancing helicopter rotors N87-20205
Prediction of wing-body-store aerodynamics using a small perturbation method and a grid embedding technique N87-20207
Development of a takeoff performance monitoring system
[NASA-CR-178255] N87-20264
Performance and efficiency evaluation and heat release study of an outboard Marine Corporation Rotary Combustion Engine
[NASA-TM-89833] N87-20282
Comparison of two procedures for predicting rocket engine nozzle performance
[NASA-TM-89614] N87-20379
Hybrid methods for rotordynamic analysis
[NASA-CR-179035] N87-20553
Satellite lifetime prediction N87-20666
Performance studies of the multigrid algorithms implemented on hypercube multiprocessor systems
[NASA-CR-178237] N87-20769

PERFORMANCE TESTS
Performance and efficiency evaluation and heat release study of an outboard Marine Corporation Rotary Combustion Engine
[NASA-TM-89833] N87-20282
Arcjet component conditions through a multistart test
[NASA-TM-89857] N87-20382
Mechanical and thermal characterization of unidirectional aramid/epoxy
[CCMS-86-06] N87-20385
Analysis of 12 AH aerospace nickel-cadmium cells from the design variable program
[NASA-TM-87774] N87-20479
Safety characteristics of non-lithium battery systems, revision 1
[AD-A174577] N87-20480
Comparison of response from different resonant plate simulation techniques N87-20611

PERIODIC VARIATIONS
Structural properties of linear periodic systems
[REPT-86-004-REV] N87-20788

PERMITTIVITY
Radar scene generation for tactical decision aids
[NASA-CR-180234] N87-20449
NASA/MSFC large stretch press study
[NASA-CR-180376] N87-20554

PERSONAL COMPUTERS
Guide to sharing personal computer resources via local area networks, revised
[DE86-016088] N87-20772

PERTURBATION
Amplification of an electron density perturbation in the polar E layer, induced by strong HF waves
[ETN-87-99014] N87-20695
A numerical study of the thermal stability of low-lying coronal loops N87-20931

PERTURBATION THEORY
Prediction of wing-body-store aerodynamics using a small perturbation method and a grid embedding technique N87-20207

PETRI NETS
Evaluation of the performance of a geographically distributed data base management system using stochastic Petri nets
[ENST-86C002] N87-20837

PHARMACOLOGY
USSR report: Life sciences. Biomedical and behavioral sciences
[JPRS-UBB-87-003] N87-20751

PHASE SHIFT
The in-situ calibration of a bilateral space-fed phased array antenna
[AD-A176069] N87-20456

PHASE SHIFT CIRCUITS
Low pass PI section digital phase shifter apparatus
[AD-D012553] N87-20483

PHASE TRANSFORMATIONS
Phase partitioning, crystal growth, electrodeposition and cosmic ray experiments in microgravity N87-20305

PHASE VELOCITY
The physics of fuel sprays. Volume 1: Experimental measurements
[AD-A175660] N87-20285
Numerical simulation of storm surges in the east China Sea N87-20718
Phase speed of wind-wave component studied N87-20726

PHASED ARRAYS
The in-situ calibration of a bilateral space-fed phased array antenna
[AD-A176069] N87-20456

PHOSPHORESCENCE
Opportunities and problems in wavelength tunable lasers based on vacancy defects in refractory oxides
[DE87-002406] N87-20545

PHOSPHORIC ACID FUEL CELLS
Feasibility of a phosphoric acid fuel cell basic technology program
[DE87-001045] N87-20490

PHOTOCHROMISM
Organic photochromic material for recording waveguide holograms N87-20447

PHOTOGRAMMETRY
Use of a video-photogrammetry system for the measurement of the dynamic response of the shuttle remote manipulator arm N87-20370

PHOTOOXIDATION
Effect of light and development of photosynthetic cells
[DE87-005183] N87-20728

PHOTOSPHERE
Filament formation due to photospheric shear N87-20878
C IV Doppler shifts observed in active region filaments N87-20898
Filament eruption connected to protospheric activity N87-20906
The white light corona and photospheric magnetic fields N87-20912
Three-dimensional magnetostatic models of the large-scale corona N87-20914
Small-scale coronal structure, part 3 N87-20922
Compact, variable, moving sources observed on the sun at 2 centimeters wavelength N87-20925
Small-scale eruptive filaments on the quiet sun N87-20928
A coordinate free description of magnetohydrostatic equilibria N87-20937
Cascade model of coronal heating N87-20938
Magnetic helicity as a constraint on coronal dissipation N87-20940
Dynamic evolution of coronal magnetic fields N87-20945

PHOTOSYNTHESIS
Effect of light and development of photosynthetic cells
[DE87-005183] N87-20728

PHOTOVOLTAIC CELLS
Flat-plate solar array project of the US Department of Energy's National Photovoltaics Program: Ten years of progress
[NASA-CR-180507] N87-20644
Summary of flat-plate solar array project documentation: Abstracts of published documents, 1975-1986, revision 1
[NASA-CR-180401-REV-1] N87-20645
Flat-plate solar array project. Volume 1: Executive summary
[NASA-CR-180658] N87-20646
Flat-plate solar array project. Volume 2: Silicon material
[NASA-CR-180659] N87-20647
Flat-plate solar array project. Volume 3: Silicon sheet: Wafers and ribbons
[NASA-CR-180661] N87-20648
Flat-plate solar array project. Volume 4: High-efficiency solar cells
[NASA-CR-180662] N87-20649
Flat-plate solar array project. Volume 5: Process development
[NASA-CR-180663] N87-20650
Flat-plate solar array project. Volume 6: Engineering sciences and reliability
[NASA-CR-180664] N87-20651
Flat-plate solar array project. Volume 7: Module encapsulation
[NASA-CR-180665] N87-20652
Flat-plate solar array project. Volume 8: Project analysis and integration
[NASA-CR-180695] N87-20653

PILOT PERFORMANCE
Analysis of NLR configurations using OCM for pilot modeling
[NASA-CR-180656] N87-20289

PIPELINES
Hydrogen degradation of pipeline steels
[DE87-005585] N87-20414

PIPES (TUBES)
Effect of flame-tube head structure on combustion chamber performance N87-20275
Rapid melt/quench furnace using commercially available hardware
[NASA-TM-86590] N87-20431
Solar power absorption in a glass tube
[NASA-TM-89063] N87-20814

PITTING
Hot corrosion attack and strength degradation of SiC and Si(sub)3N(sub)4
[NASA-TM-89820] N87-20425

PLANETARY BOUNDARY LAYER
The mesoscale organization, dynamics, and evolution of the marine planetary boundary layer during cold air outbreaks N87-20698

PLANETARY RINGS
Collisional dynamics of perturbed particle disks in the solar system
[NASA-CR-180497] N87-20860

PLASMA DENSITY
Filament formation due to photospheric shear N87-20878

PLASMA EQUILIBRIUM
Topological constraints and the existence of force-free fields N87-20935

PLASMA HEATING
On the thermal durability of solar prominences, or how to evaporate a prominence N87-20905

PLASMA JETS
Effects of space plasma discharge on the performance of large antenna structures in low Earth orbit
[NASA-TM-89118] N87-20339

PLASMA PHYSICS
USSR report: Physics and mathematics
[JPRS-UPM-86-006] N87-20445

PLASMA SPECTRA
Spectral characteristics of interchange turbulence in the ionosphere
[AD-A175975] N87-20692

PLASMA TEMPERATURE
Can prominences form in current sheets N87-20876

PLASMA WAVES
Steepened magnetoeonic waves in the high Beta plasma surrounding Comet-Giacobini-Zinner
[NASA-CR-180614] N87-20868

PLASMAS (PHYSICS)
Yosemite Conference on Ionospheric Plasma in the Magnetosphere: Sources, Mechanisms and Consequences, meeting report
[NASA-TM-86589] N87-20689
Coronal and Prominence Plasmas
[NASA-CP-2442] N87-20871
Some crucial corona and prominence observations N87-20872
The growth of radiative filamentation modes in sheared magnetic fields N87-20875
Can prominences form in current sheets N87-20876
Filament formation due to photospheric shear N87-20878
Formation of active region and quiescent prominence magnetic field configurations N87-20879
Static current-sheet models of quiescent prominences N87-20882
The microwave structure of quiescent solar filaments at high resolution N87-20889
The prominence-corona interface and its relationship to the chromosphere-corona transition N87-20891
Non-LTE hydrogen-line formation in moving prominences N87-20895
Energy conversion in the coronal plasma N87-20934
Effects of flows on viscous and resistive MHD stability N87-20943
Large-scale electric fields resulting from magnetic reconnection in the corona N87-20944

PLASMASPHERE
Yosemite Conference on Ionospheric Plasma in the Magnetosphere: Sources, Mechanisms and Consequences, meeting report
[NASA-TM-86589] N87-20689

PLASTIC PROPERTIES
Inclined pileup of edge dislocations near the crack tip
[AD-A175610] N87-20571
Theoretical investigations of shear band formation in finite elasticity
[AD-A175657] N87-20572

PLASTICIZERS
Energy absorption of polyurethane based polymer alloys
[AD-A175542] N87-20427

PLATES
Development of powder metallurgy 2XXX series Al alloy plate and sheet materials for high temperature aircraft structural applications, FY 1983/1984
[NASA-CR-172521] N87-20406

PLATES (STRUCTURAL MEMBERS)
Recent studies in plate vibrations: 1981-1985. Part 1: Classical theory N87-20437
Comparison of response from different resonant plate simulation techniques N87-20611
PLATES (TECTONICS)
The interpretation of crustal dynamics data in terms of plate interactions and active tectonics of the Anatolian Plate and surrounding regions in the Middle East [NASA-CR-180501] N87-20662
Crustal dynamics project data analysis, 1986. Volume 1: Fixed station VLBI geodetic results [NASA-TM-87806] N87-20690
PLATFORMS
Turbulence control on an airborne laser platform [NASA-CR-178249] N87-20503
PLATINUM
Rare isotope studies involving catalytic oxidation of CO over platinum-tin oxide N87-20538
Studies of CO oxidation on Pt/SnO2 catalyst in a surrogate CO2 laser facility N87-20539
Studies of long-life pulsed CO2 laser with Pt/SnO2 catalyst N87-20540
Characterization of Pt/SnO2 catalysts for CO oxidation N87-20541
POINTING CONTROL SYSTEMS
A gondola and pointing system for a gamma ray telescope [DE87-004561] N87-20843
POLAR ORBITS
Proceedings of the European Symposium on Polar platform Opportunities and Instrumentation for Remote-Sensing (ESPOIR) [ESA-SP-266] N87-20621
Working group on Earth observation requirements for the Polar Orbiting Platform Elements of the International Space Station (the POPE Working Group) N87-20625
ESA Columbus polar platform design concept N87-20627
Servicing of the polar platform — Columbus space station N87-20628
Orbit configurations — space station polar platform N87-20629
Payload data management scheme planned for Earth observation sensors to be flown on the polar platforms in the framework of the space station/Columbus program N87-20630
USA-Europe coordination and cooperation activities: Announcements of Opportunity — polar platforms N87-20632
Report of the atmosphere panel N87-20633
Land panel report — International Space Station N87-20634
Ocean-ice panel report — International Space Station N87-20635
Solid Earth panel report — Columbus program N87-20636
Panel report on multidisciplinary instrumentation: New possibilities — Columbus space station N87-20637
Panel report on new approaches to calibration and validation — Columbus polar platforms N87-20638
Data management panel report — Columbus polar platforms N87-20639
The orbit configuration panel report — Columbus polar platforms N87-20640
Panel report on the polar platform servicing approach and its implications — Columbus space station N87-20641
POLAR REGIONS
Amplification of an electron density perturbation in the polar E layer, induced by strong HF waves [ETN-87-99014] N87-20695
POLARIZATION (WAVES)
Radar scene generation for tactical decision aids [NASA-CR-180234] N87-20449
NASA/MSFC large stretch press study [NASA-CR-180376] N87-20554
POLLUTION TRANSPORT
Airborne lidar measurements of El Chichon stratospheric aerosols, January 1984 [NASA-RP-1175] N87-20663
Continental shelf processes affecting the oceanography of the South Atlantic Bight [DE87-005303] N87-20716
POLYCRYSTALS
Ductility and fracture behavior of polycrystalline Ni3Al alloys [DE87-005340] N87-20413
Deformation and fracture of single-crystal and sintered polycrystalline silicon carbide produced by cavitation [NASA-TM-88981] N87-20422
POLYMER CHEMISTRY
Microgravity crystallization of macromolecules: An interim report and proposal for continued research [NASA-TP-2671] N87-20423
POLYMER MATRIX COMPOSITES
Addition polymers from 1,4,5,8-tetrahydro-1,4:5,8-diepoxyanthracene and Bis-dienes: Processable resins for high temperature application [NASA-TM-89838] N87-20426
POLYMERIC FILMS
Manufacturing polymer thin films in a micro-gravity environment N87-20304
POLYMERIZATION
Institute for Materials Science Engineering, Polymers: Technical activities 1986 [PB87-136693] N87-20420
POLYTETRAFLUOROETHYLENE
Investigation of PTFE transfer films by infrared emission spectroscopy and phase-locked ellipsometry [NASA-TM-89844] N87-20421
POLYURETHANE RESINS
Energy absorption of polyurethane based polymer alloys [AD-A175542] N87-20427
POROSITY
Computation of transonic flow over porous airfoils N87-20194
POROUS WALLS
Study of the development of a compressible turbulent boundary layer on a porous and rough wall [ETN-87-99390] N87-20512
POSITIONING
New book deals with spatial orientation N87-20748
POSITRONS
A model and computer code for the Monte Carlo simulation of relativistic electron and positron penetration through matter [USIP-86-11] N87-20608
POSTFLIGHT ANALYSIS
Microgravity effects on electrodeposition of metals and metal-cermet mixtures N87-20332
Post-flight BET products for the 2nd discovery entry, STS-19 (51-A) [NASA-CR-172572] N87-20344
A normal incidence X-ray telescope [NASA-CR-180107] N87-20840
POTENTIAL FLOW
Matrics, transonic potential flow calculations about transport aircraft N87-20208
Theoretical analysis of flows around helicopter fuselages: Application to design and development N87-20221
POWDER METALLURGY
Consolidation processing parameters and alternative processing methods for powder metallurgy Al-Cu-Mg-X-X alloys [NASA-CR-178227] N87-20404
Development of powder metallurgy 20XX series Al alloy plate and sheet materials for high temperature aircraft structural applications, FY 1983/1984 [NASA-CR-172521] N87-20406
POWER AMPLIFIERS
Wind velocity measurement accuracy with highly stable 12 mJ/pulse high repetition rate CO2 laser master oscillator power amplifier N87-20525
POWER FACTOR CONTROLLERS
Resistojet control and power for high frequency ac buses [NASA-TM-89860] N87-20477
POWER SPECTRA
Methods of frequency spectrum estimation of sea water compared N87-20725
POYNTING THEOREM
Studies in nonlinear structural dynamics: Chaotic behavior and poynting effect N87-20346
PREDICTION ANALYSIS TECHNIQUES
Using the boundary-layer equations in three-dimensional viscous flow simulation N87-20222
Development of a rotor wake/vortex model. Volume 2: User's manual for computer program [NASA-CR-174850-VOL-2] N87-20239
A multiple zone method for supersonic tactical missiles [AD-A175938] N87-20244
A predictor-corrector method for calculation of incompressible fluid flow dynamics [DE87-003604] N87-20508
The DYNAS survey. Part 2: A participant's view N87-20579
Super*Zip (linear separation) shock characteristics N87-20605
China Report: Science and technology [JPRS-CST-86-031] N87-20720
Comparison of deepwater wind-wave prediction models N87-20724
PREDICTIONS
Prediction of recirculation zones in isothermal coaxial jet flows relevant to combustors [NASA-CR-4064] N87-20501
Calculation of thermomechanical fatigue life based on isothermal behavior [NASA-TM-88964] N87-20565
The mesoscale organization, dynamics, and evolution of the marine planetary boundary layer during cold air outbreaks N87-20696
Characteristic decomposition and the multivariable generalization of predictive self-tuning control [OUEL-1651/86] N87-20776
PREFLIGHT OPERATIONS
A normal incidence X-ray telescope [NASA-CR-180107] N87-20840
PREPREGS
Screening testing for composite prepregs [DE87-004557] N87-20395
PREPROCESSING
A computer controlled signal preprocessor for laser fringe anemometer applications [NASA-TM-88962] N87-20516
PRESSURE
Airspeed sensing pressure valve system [AD-D012589] N87-20266
Monthly mean pressure reconstructions for Europe (back to 1780) and North America (to 1958) [DE87-005556] N87-20703
PRESSURE DISTRIBUTION
An assessment of the use of low-order panel methods for the calculation of supersonic flows N87-20204
Comparison of finite difference calculations of a large region of recirculating flow near an airfoil trailing edge N87-20218
Calculations for a generic fighter at supersonic high-lift conditions N87-20226
Study of the unsteady pressure field on the RA16SC1 profile in vibrating condition [ONERA-RTS-17/3423-AY] N87-20249
Supersonic flow induced cavity acoustics N87-20601
PRESSURE MEASUREMENT
Decoupled bellmouth: An alternate method of measuring thrust in the sea level test cell [AD-A175616] N87-20284
Moored current meter and temperature-pressure recorder measurements from the Western North Atlantic (high energy benthic boundary layer and abyssal circulation experiments 1983-1984), volume 39 [AD-A176014] N87-20713
PRESSURE RECORDERS
Moored current meter and temperature-pressure recorder measurements from the Western North Atlantic (high energy benthic boundary layer and abyssal circulation experiments 1983-1984), volume 39 [AD-A176014] N87-20713
PRETREATMENT
Effect of adhesive bonding variables on the performance of bonded CFRP patch repairs of metallic structures N87-20182
PROBLEM SOLVING
Utilization of Euler codes in nonlinear aerodynamics N87-20215
A Navier-Stokes solver using the LU-SSOR TVD algorithm [NASA-CR-179608] N87-20243
The fault-tree compiler [NASA-TM-89098] N87-20765
PROCESS CONTROL (INDUSTRY)
Consolidation processing parameters and alternative processing methods for powder metallurgy Al-Cu-Mg-X-X alloys [NASA-CR-178227] N87-20404
PRODUCT DEVELOPMENT
Composites review [NASA-TT-20008] N87-20368
Preliminary examination of the construction of laser gyroscopes with reduced lock-in threshold [ETN-87-99016] N87-20521
PRODUCTION ENGINEERING
Fabrication of microwave devices on ultrathin active GaAs substrates [FOA-C-30431-3.2] N87-20494
PRODUCTION MANAGEMENT
Flat-plate solar array project. Volume 5: Process development [NASA-CR-180663] N87-20650
PROFILES
Design and verification by nonlinear simulation of a Mach/CAS control law for the NASA TCV B737 aircraft [NASA-CR-178029] N87-20290
PROJECT MANAGEMENT
USA-Europe coordination and cooperation activities: Announcements of Opportunity — polar platforms N87-20632
A stochastic approach to project planning in an R and D environment [DE87-005347] N87-20835

PROJECT PLANNING
Flat-plate solar array project. Volume 8: Project analysis and integration
[NASA-CR-180695] N87-20653
A stochastic approach to project planning in an R and D environment
[DE87-005347] N87-20835
PROJECTILES
Army research in shock mechanics N87-20576
PROMINENCES
Small-scale eruptive filaments on the quiet sun N87-20928
The stability of coronal and prominence magnetic fields N87-20941
PROPAGATION VELOCITY
The propagation of an electron beam through the solar corona N87-20946
PROPELLANT COMBUSTION
Theoretical and experimental investigations of ignition, combustion and expansion processes of hypergolic liquid fuel combinations at gas temperatures up to 3000 deg K
[NASA-TM-88527] N87-20399
PROPELLANT TANKS
Laboratory investigation of lightweight heater tape for shuttle propellant tank
[AD-A175997] N87-20345
Propellant tank resupply system
[AD-D012559] N87-20375
PROPELLER SLIPSTREAMS
Investigation of flow under the fuselage of a powered light aircraft model
[BU-351] N87-20247
PROPELLERS
The 1985 small propeller-driven aircraft noise test program
[AD-A175596] N87-20799
PROPRIOCEPTION
Physiological mechanisms limiting external resistance to respiration N87-20739
PROPULSIVE EFFICIENCY
Density uncertainty effect on cost of space station reboost N87-20667
PROTECTIVE COATINGS
High temperature protective coatings for aero engine gas turbine components
[AD-A176001] N87-20286
Bithermal low-cycle fatigue behavior of a NiCoCrAlY-coated single crystal superalloy
[NASA-TM-89831] N87-20408
PROTEIN SYNTHESIS
Liquid drop stability for protein crystal growth in microgravity
[NASA-TP-2724] N87-20727
PROTON IRRADIATION
Ground-state proton radioactivity in the domain of neutron-poor nuclei heavier than tin
[ETN-87-99342] N87-20811
PROTONS
Ground-state proton radioactivity in the domain of neutron-poor nuclei heavier than tin
[ETN-87-99342] N87-20811
PROVING
Composite repair of cocured J-stiffened panels: Design and test verification N87-20181
Panel report on new approaches to calibration and validation — Columbus polar platforms N87-20638
PSYCHOLOGY
USSR report: Life sciences. Biomedical and behavioral sciences
[JPRS-UBB-87-003] N87-20751
PUBLIC HEALTH
USSR report: Life sciences. Biomedical and behavioral sciences
[JPRS-UBB-87-003] N87-20751
PULLEYS
Arresting and recovery system for test missiles
[AD-D012574] N87-20337
PULSARS
A systematic search for millisecond pulsars N87-20839
Timing millisecond pulsars N87-20855
PULSE AMPLITUDE MODULATION
Propagation of RF signals through structured ionization. Theory and antenna aperture effect applications
[AD-A175522] N87-20451
PULSE DOPPLER RADAR
Adaptive mutual interference suppression method
[AD-D012552] N87-20459
PULSE GENERATORS
Multi-axis transient shock simulation using mechanical pulse generators N87-20613
PULSE RATE
A systematic search for millisecond pulsars N87-20839
PULSE REPETITION RATE
Adaptive mutual interference suppression method
[AD-D012552] N87-20459
Wind velocity measurement accuracy with highly stable 12 mJ/pulse high repetition rate CO2 laser master oscillator power amplifier N87-20525
High repetition rate sealed CO2 TEA lasers using heterogeneous catalysts N87-20529
PULSED LASERS
Frequency stabilization in injection controlled pulsed CO2 lasers N87-20527
Studies of long-life pulsed CO2 laser with Pt/SnO2 catalyst N87-20540
An overview of DREV's activities on pulsed CO2 laser transmitters: Frequency stability and lifetime aspects N87-20542
PUMPS
Investigation of thermal-fluid mechanical characteristics of the capillary pump and the pumped two-phase loop
[NASA-CR-180509] N87-20557
PYROLYTIC GRAPHITE
Design, fabrication and performance of small, graphite electrode, multistage depressed collectors with 200-W, CW, 8- to 18-GHz traveling-wave tubes
[NASA-TP-2683] N87-20474
PYROTECHNICS
The Shock and Vibration Bulletin. Part 3: Invited Papers, Pyrotechnic Shock, Pyrotechnic Shock Workshop
[AD-A175226] N87-20602
Views of the world of pyrotechnic shock N87-20603
Super*Zip (linear separation) shock characteristics N87-20605
A vibroacoustic database management system and its application for a pyroshock database N87-20607
State-of-the-art accelerometer characteristics for pyrotechnic shock measurement N87-20608
The controlled response of resonating fixtures used to simulate pyroshock environments N87-20612
Multi-axis transient shock simulation using mechanical pulse generators N87-20613
Summary of testing techniques N87-20614

Q

QUALIFICATIONS
Mechanical Qualification of Large Flexible Spacecraft Structures
[AD-A175529] N87-20355
Future trends in spacecraft design and qualification N87-20356
Recent developments and future trends in structural dynamic design verification and qualification of large flexible spacecraft N87-20357
Qualification of the faint object camera N87-20359
Dynamic analysis of direct television satellite TV-SAT/TDF.1 N87-20360
Structural qualification of large spacecraft N87-20361
Dynamic qualification of spacecraft by means of modal synthesis N87-20363
Low frequency vibration testing on satellites N87-20364
Modal-survey testing for system identification and dynamic qualification of spacecraft structures N87-20365
QUANTUM THEORY
Problems in quantum cosmology N87-20646

R

RADAR
Analysis of the receiving characteristics of the circular diffraction antenna with both a flush-mounted and a recessed center post
[DE87-003283] N87-20460
RADAR ANTENNAS
NUSAT update N87-20312
Turnaround control for mechanically scanned radar antennas
[AD-D012563] N87-20457
Expert systems for diagnostic purposes, prospected applications to the radar field N87-20760
RADAR DATA
Simulation of wind gradient errors in NROSS (Navy Remote Ocean Sensing System) radar scatterometer data in a simplified geometry
[AD-A175754] N87-20642
RADAR IMAGERY
Radar scene generation for tactical decision aids
[NASA-CR-180234] N87-20449
NASA/MSFC large stretch press study
[NASA-CR-180376] N87-20554
RADAR NAVIGATION
NUSAT 1 methods for radar field strength measurement N87-20329
RADAR SCANNING
Turnaround control for mechanically scanned radar antennas
[AD-D012563] N87-20457
RADAR TRACKING
A comparison of nonlinear filters for orbit determination and estimation N87-20336
RADIANCE
LOWTRAN modeling of near-horizon infrared sky radiances in the presence of clouds
[AD-A175661] N87-20691
RADIANT FLUX DENSITY
Organic photochromic material for recording waveguide holograms N87-20447
Space radiation studies
[NASA-CR-179037] N87-20951
RADIATION COUNTERS
A model and computer code for the Monte Carlo simulation of relativistic electron and positron penetration through matter
[USIP-86-11] N87-20808
RADIATION DETECTORS
Space radiation studies
[NASA-CR-179037] N87-20951
RADIATION DOSAGE
Radiation protection guidelines for space missions
[NASA-TM-89278] N87-20730
RADIATION MEASURING INSTRUMENTS
Atmospheric contrast transmittance monitor
[AD-D012555] N87-20520
RADIATION PRESSURE
Dynamic and thermal effects in very large space structures N87-20347
RADIATION PROTECTION
Radiation protection guidelines for space missions
[NASA-TM-89278] N87-20730
RADIATION SPECTRA
Space radiation studies
[NASA-CR-179037] N87-20951
RADIATIVE HEAT TRANSFER
Modeling turbulent, reactig flow N87-20270
RADII
Large mode radius resonators N87-20524
RADIO ASTRONOMY
Timing millisecond pulsars N87-20855
Coronal and Prominence Plasmas
[NASA-CP-2442] N87-20871
Diagnostics and structure N87-20885
VLA observations of slar filaments at 6 and 20 cm wavelengths N87-20888
The microwave structure of quiescent solar filaments at high resolution N87-20889
Constraints on filament models deduced from dynamical analysis N87-20897
Simultaneous observations of changes in coronal bright point emission at the 20 cm radio and He Lambda 10830 wavelengths N87-20923
Compact, variable, moving sources observed on the sun at 2 centimeters wavelength N87-20925
Observations of the Ca II K line in HeI0830A dark points on August 3, 1985 N87-20929
RADIO COMMUNICATION
Marshall Amateur Radio Club experiment (MARCE) post flight data analysis N87-20323
Propagation of RF signals through structured ionization. Theory and antenna aperture effect applications
[AD-A175522] N87-20451
RADIO EMISSION
Molecular clouds in the outer galaxy N87-20854
Ring galaxies: An investigation of the physical conditions in closely interacting systems N87-20858
Coronal diagnostics. N87-20915
RADIO FREQUENCIES
Propagation of RF signals through structured ionization. Theory and antenna aperture effect applications
[AD-A175522] N87-20451
The in-situ calibration of a bilateral space-fed phased array antenna
[AD-A176069] N87-20456
Low pass PI section digital phase shifter apparatus
[AD-D012553] N87-20483
RADIO INTERFEROMETERS
Lightning strikes on aircraft. Exploitation of Landes (France)-Front '84 campaign and complementary development of airborne electrical sensors
[ONERA-RF-91/7154-PY] N87-20706
RADIO TELEMETRY
A study of the methods used to carry out RF telemetry testing of surface-to-air missiles
[ETN-87-99481] N87-20346
RADIO TELESCOPES
Dark filaments observed at 8.3mm and 3.1mm wavelength N87-20887

RADIOACTIVE DECAY
Ground-state proton radioactivity in the domain of neutron-poor nuclei heavier than tin
[ETN-87-99342] N87-20811
RADIOACTIVITY
Ground-state proton radioactivity in the domain of neutron-poor nuclei heavier than tin
[ETN-87-99342] N87-20811
RAIN
The effect of heavy rain on an airfoil at high lift
[NASA-CR-178248] N87-20232
RAIN GAGES
On requirements for a satellite mission to measure tropical rainfall
[NASA-RP-1183] N87-20701
RAMAN SPECTRA
Apparatus for high temperature in situ laser Raman spectroelectrochemical studies of metal corrosion and passivation in aqueous environments
[DE87-004868] N87-20416
RAMAN SPECTROSCOPY
Application of CARS to scramjet combustion
[NASA-CR-178245] N87-20400
High temperature CO2 study: Anti-Stokes coherent Raman diffusion and infrared spectroscopy
[ONERA-P-1986-2] N87-20402
RAMJET MISSILES
An application of computational fluid dynamics to the design of optimum ramjet powered missile components N87-20336
RANDOM VIBRATION
Optimization of aerospace structures subjected to random vibration and fatigue constraints N87-20599
Evaluation of vibration specifications for static and dynamic material allowables N87-20600
RAPID QUENCHING (METALLURGY)
Rapid melt/quench furnace using commercially available hardware
[NASA-TM-86590] N87-20431
RARE GASES
Noble-gas ion bombardment on clean silicon surfaces studied using ellipsometry and desorption
[B8672200] N87-20609
RATS
Effect of long-term spaceflight on rat brain polyamine content N87-20741
RAY TRACING
HARPA: A versatile three-dimensional Hamiltonian ray-tracing program for acoustic waves in the atmosphere above irregular terrain
[PB87-132031] N87-20601
RAYLEIGH NUMBER
The mesoscale organization, dynamics, and evolution of the marine planetary boundary layer during cold air outbreaks N87-20698
REACTION KINETICS
Numerical calculations of turbulent reacting flow in a gas-turbine combustor
[NASA-TM-89842] N87-20171
The chemical shock tube as a tool for studying high-temperature chemical kinetics N87-20279
Theoretical study of the nonsteady combustion of composite fuel droplets
[ESA-TT-868] N87-20401
Reaction rate oscillations during catalytic CO oxidation: A brief overview N87-20534
Remarks on the stability analysis of reactive flows
[NASA-CR-178269] N87-20780
Kinetic model for the vibrational energy exchange in flowing molecular gas mixtures
[NASA-TM-88500] N87-20802
READ-ONLY MEMORY DEVICES
Bubble memory module for spacecraft application
[NASA-TM-86411] N87-20476
REAL TIME OPERATION
TV-holography: A promising inspection tool for analysis of composite materials N87-20180
Development of a takeoff performance monitoring system
[NASA-CR-178255] N87-20264
Flexible satellite communications systems simulator standard device groups
[AD-A175944] N87-20454
Real-time crop assessment using color theory and satellite data N87-20619
RECEIVERS
Range filtering for sequential GPS receivers with external sensor augmentation
[NASA-TM-89418] N87-20257
RECIRCULATIVE FLUID FLOW
Comparison of finite difference calculations of a large region of recirculating flow near an airfoil trailing edge N87-20218
Prediction of recirculation zones in isothermal coaxial jet flows relevant to combustors
[NASA-CR-4064] N87-20501
RECONSTRUCTION
Performance of recycled asphalt concrete airport pavement surfaces
[DOT/FAA-PM-86-12] N87-20432
RECOVERABILITY
Arresting and recovery system for test missiles
[AD-D012574] N87-20337
RECRYSTALLIZATION
Microgravity crystallization of macromolecules: An interim report and proposal for continued research
[NASA-TP-2671] N87-20423
RECYCLING
Performance of recycled asphalt concrete airport pavement surfaces
[DOT/FAA-PM-86-12] N87-20432
RED SHIFT
Vertical motions in the quiescent prominences observed in the He I Lambda10830Angstrom line N87-20696
C IV Doppler shifts observed in active region filaments N87-20698
REDUCED GRAVITY
Manufacturing polymer thin films in a micro-gravity environment N87-20304
Phase partitioning, crystal growth, electrodeposition and cosmic ray experiments in microgravity N87-20305
Gas tungsten arc welding in a microgravity environment: Work done on GAS payload G-169 N87-20306
Cal Poly Space Project G-279 N87-20324
Liquid droplet radiator development status
[NASA-TM-89852] N87-20353
Microgravity crystallization of macromolecules: An interim report and proposal for continued research
[NASA-TP-2671] N87-20423
Initial investigations into the damping characteristics of wire rope vibration isolators
[NASA-CR-180698] N87-20569
REDUCED ORDER FILTERS
Mean-square error bounds for reduced-error linear state estimators
[NASA-TM-89441] N87-20291
REENTRY EFFECTS
Users of middle atmosphere models remarks N87-20679
REFERENCE ATMOSPHERES
Users of middle atmosphere models remarks N87-20679
Utilization of Global Reference Atmosphere Model (GRAM) for shuttle entry N87-20680
Use of the 4D-Global Reference Atmosphere Model (GRAM) for space shuttle descent design N87-20681
Overview of shuttle data on density N87-20683
REFILLING
Propellant tank resupply system
[AD-D012559] N87-20375
REFLECTANCE
A normal incidence X-ray telescope
[NASA-CR-180107] N87-20640
REFRIGERATORS
Cryogenic regenerators
[DE87-701264] N87-20443
REFUELING
Propellant tank resupply system
[AD-D012559] N87-20375
REGENERATION (PHYSIOLOGY)
Effect of hypoxia on DNA synthesis and collagent content of regenerating skin N87-20742
REGENERATORS
Cryogenic regenerators
[DE87-701264] N87-20443
REGRESSION ANALYSIS
NASA/MSFC prediction techniques N87-20678
A technique to estimate the ocean surface energy flux using VAS multispectral data N87-20710
A new approach to least squares estimation, with applications
[CWI-MS-R8602] N87-20787
RELATIVISTIC EFFECTS
Statistical analysis of secondary particle distributions in relativistic nucleus-nucleus collisions
[NASA-CR-4054] N87-20813
RELATIVISTIC ELECTRON BEAMS
A model and computer code for the Monte Carlo simulation of relativistic electron and positron penetration through matter
[USIP-86-11] N87-20808
RELATIVISTIC THEORY
Gravitational collapse in relativistic theory of gravitation
[DE87-700730] N87-20792
RELATIVITY
A numerical study of some spherically-symmetric and axisymmetric cosmological models N87-20653
RELAXATION (MECHANICS)
Effectiveness of on-off damper in isolating dynamical systems N87-20594
RELAXATION METHOD (MATHEMATICS)
Eigensystem analysis of classical relaxation techniques with applications to multigrid analysis
[NASA-TM-88377] N87-20785
RELIABILITY
Institute for Materials Science Engineering, Polymers: Technical activities 1986
[PB87-136693] N87-20420
RELIABILITY ANALYSIS
Arcjet component conditions through a multistart test
[NASA-TM-89857] N87-20382
Risk evaluations of aging phenomena: The linear aging reliability model and its extensions
[DE87-002607] N87-20583
Flat-plate solar array project. Volume 5: Process development
[NASA-CR-180663] N87-20650
Flat-plate solar array project. Volume 6: Engineering sciences and reliability
[NASA-CR-180664] N87-20651
Flat-plate solar array project. Volume 7: Module encapsulation
[NASA-CR-180665] N87-20652
The fault-tree compiler
[NASA-TM-89098] N87-20765
REMOTE HANDLING
Integrated digital control and man-machine interface for complex remote handling systems
[DE87-003002] N87-20749
Advanced remote handling for future applications: The advanced integrated maintenance system
[DE87-003004] N87-20750
REMOTE MANIPULATOR SYSTEM
Use of a video-photogrammetry system for the measurement of the dynamic response of the shuttle remote manipulator arm N87-20370
REMOTE SENSING
Engineering thrust areas, 1987
[DE87-004443] N87-20441
Radar scene generation for tactical decision aids
[NASA-CR-180234] N87-20449
NASA/MSFC large stretch press study
[NASA-CR-180376] N87-20554
SAFE/DAE: Modal test in space N87-20584
Real-time crop assessment using color theory and satellite data N87-20619
Proceedings of the European Symposium on Polar platform Opportunities and Instrumentation for Remote-Sensing (ESPOIR)
[ESA-SP-266] N87-20621
Remote sensing applications: Commercial issues and opportunities for space station — SPOT N87-20626
Land panel report — International Space Station N87-20634
Potential of laser remote sensing of oil below water surface
[FOA-C-30435-3.1] N87-20659
REMOTE SENSORS
Payload data management scheme planned for Earth observation sensors to be flown on the polar platforms in the framework of the space station/Columbus program N87-20630
RENDEZVOUS SPACECRAFT
The concentration principle applied to spaceborne solar arrays. AGORA mission: Studies synthesis
[SNIAS-959-CA/CG] N87-20657
REPORTS
The Shock and Vibration Digest, Volume 19, No. 2 N87-20435
REQUIREMENTS
Development of a computational aero/fluids analysis system
[NASA-CR-179046] N87-20343
RESEARCH AND DEVELOPMENT
Activities report of the Department of Systems and Communications
[ENST-86D002] N87-20466
An investigation of transitional management problems for the NSTS
[NASA-CR-171979] N87-20634
A stochastic approach to project planning in an R and D environment
[DE87-005347] N87-20835
RESEARCH MANAGEMENT
Activities report of the Department of Systems and Communications
[ENST-86D002] N87-20466
Closed-Cycle, Frequency-Stable CO2 Laser Technology
[NASA-CP-2456] N87-20522
Structures and Dynamics Division research and technology plans for FY 1987 and accomplishments for FY 1986
[NASA-TM-89141] N87-20570

Flat-plate solar array project of the US Department of Energy's National Photovoltaics Program: Ten years of progress
[NASA-CR-180507] N87-20644
Activities report in aerospace research
[ETN-87-99378] N87-20636
RESIDUAL STRESS
Characterizing thermal/mechanical properties of filament wound composites
[AD-A176238] N87-20392
RESISTOJET ENGINES
Conceptual design and integration of a space station resistojet propulsion assembly
[NASA-TM-89947] N87-20378
Resistojet control and power for high frequency ac buses
[NASA-TM-89860] N87-20477
RESONANCE
Electron tunneling studies of Mo/(sub)1-xRe/(sup)x/: Enhancement of superconductivity by a resonance mode
[DE87-003048] N87-20484
Heating of the solar corona by the resonant absorption of Alfven waves N87-20939
RESONANT FREQUENCIES
A theoretical and experimental study of cylindrical dielectric resonators and their applications to microwave oscillators
[FOA-C-30434-3.2] N87-20495
Testing techniques. Random variation of modal frequencies: Experiments and analysis N87-20585
Machinery dynamics: Prediction of natural frequencies of flexible shaft-disc system N87-20587
Isolation and damping: A graphical method of determining the response of the cascaded two degree of freedom system N87-20592
Supersonic flow induced cavity acoustics N87-20601
The controlled response of resonating fixtures used to simulate pyroshock environments N87-20612
RESONANT VIBRATION
Comparison of response from different resonant plate simulation techniques N87-20611
RESONATORS
A theoretical and experimental study of cylindrical dielectric resonators and their applications to microwave oscillators
[FOA-C-30434-3.2] N87-20495
Large mode radius resonators N87-20524
RESPIRATORY IMPEDANCE
Physiological mechanisms limiting external resistance to respiration N87-20739
RESPIRATORY PHYSIOLOGY
Physiological mechanisms limiting external resistance to respiration N87-20739
RETINAL IMAGES
The retinal image of the fresnel lens optical landing system
[AD-A176090] N87-20258
REVIEWING
Underwater acoustic modeling techniques N87-20436
RHEOLOGY
Screening testing for composite prepregs
[DE87-004557] N87-20395
Effect of hemadsorption on rheological parameters of blood during seven-day antiorthostatic hypokinesia and in vitro studies N87-20740
RIBBONS
Flat-plate solar array project. Volume 3: Silicon sheet: Wafers and ribbons
[NASA-CR-180661] N87-20648
High field properties of SnMo6S8 and PbMo6S8 ribbons prepared using a vapor transport technique
[DE87-004707] N87-20826
RING LASERS
Preliminary examination of the construction of laser gyroscopes with reduced lock-in threshold
[ETN-87-99016] N87-20521
RISK
Risk evaluations of aging phenomena: The linear aging reliability model and its extensions
[DE87-002607] N87-20563
An investigation of transitional management problems for the NSTS
[NASA-CR-171979] N87-20634
RITZ AVERAGING METHOD
Structural dynamic reanalysis using Ritz vectors N87-20597
ROBOTICS
Automation and robotics
[INPE-4088-PRE/1033] N87-20551
Implementation of active force control for robots subject to dynamic loading N87-20588
A virtual-time operating-system shell for a hypercube in robotics applications
[DE87-004256] N87-20773
The Oak Ridge National Laboratory's Robotics and Intelligent Systems Program
[DE87-004627] N87-20774
ROBOTS
Automation and robotics
[INPE-4088-PRE/1033] N87-20551
The 3-D world modelling with updating capability based on combinatorial geometry
[DE87-004257] N87-20643
ROCKET ENGINE CASES
Composite motor case nomenclature
[AD-A176418] N87-20384
Adhesion of a silicone based insulating material to rocket motors
[FOA-C-20635-2.1] N87-20429
ROCKET ENGINES
Theory and design of flight-vehicle engines
[NASA-TM-88583] N87-20261
Comparison of two procedures for predicting rocket engine nozzle performance
[NASA-TM-89614] N87-20379
Pretest uncertainty analysis for chemical rocket engine tests
[NASA-TM-89619] N87-20515
ROCKET NOZZLES
Theoretical kinetic computations in complex reacting systems N87-20277
Comparison of two procedures for predicting rocket engine nozzle performance
[NASA-TM-89614] N87-20379
Experimental thrust performance of a high-area-ratio rocket nozzle
[NASA-TP-2720] N87-20381
ROCKET THRUST
A numerical heat transfer model for an advanced solar thermal propulsion system N87-20377
Experimental thrust performance of a high-area-ratio rocket nozzle
[NASA-TP-2720] N87-20381
ROLL FORMING
Impact energy relationships for directly rolled uranium strip
[DE87-005789] N87-20418
ROOMS
A survey of achieved levels of airborne sound insulation in broadcasting studio centres
[BBC-RD-1987/1] N87-20798
ROTARY ENGINES
Performance and efficiency evaluation and heat release study of an outboard Marine Corporation Rotary Combustion Engine
[NASA-TM-89833] N87-20282
ROTARY WING AIRCRAFT
Contingency power for small turboshaft engines using water injection into turbine cooling air
[NASA-TM-89817] N87-20280
Experimental and analytical evaluation of dynamic load and vibration of a 2240-kW (300-hp) rotorcraft transmission
[NASA-TM-88975] N87-20556
ROTARY WINGS
The prediction of transonic loading on advancing helicopter rotors N87-20206
Aeroelastic stability of bearingless rotors in forward flight N87-20260
Effect of dynamic stall and elastic parameters on the fundamental mechanisms of helicopter vibrations
[AD-A175561] N87-20292
ROTATING DISKS
Machinery dynamics: Prediction of natural frequencies of flexible shaft-disc system N87-20587
ROTATING SHAFTS
Machinery dynamics: Prediction of natural frequencies of flexible shaft-disc system N87-20587
Force magnitude and angular velocity fluctuation reduction in a spring-restrained, flexibly-supported four-bar mechanical linkage N87-20589
ROTOR AERODYNAMICS
Numerical solutions of unsteady flow past rotor sections N87-20198
Vibration characteristics of OH-58A helicopter main rotor transmission
[NASA-TP-2705] N87-20555
ROTOR BLADES
Repair of helicopter composite structure techniques and substantiations N87-20179
ROTOR BLADES (TURBOMACHINERY)
Development of a rotor wake/vortex model. Volume 2: User's manual for computer program
[NASA-CR-174850-VOL-2] N87-20239
The high-speed cascade wind tunnel - still an important test facility for turbomachinery blade investigations
[ESA-TT-1012] N87-20300
ROTORS
Hybrid methods for rotordynamic analysis
[NASA-CR-179035] N87-20553
Machinery dynamics: Prediction of natural frequencies of flexible shaft-disc system N87-20587
RUNGE-KUTTA METHOD
Calculation of Rayleigh-Taylor flows using vortex blobs
[DE87-002551] N87-20507
Galerkin/Runge-Kutta discretizations for semilinear parabolic equations
[NASA-CR-178264] N87-20783
RUNWAY CONDITIONS
Performance of recycled asphalt concrete airport pavement surfaces
[DOT/FAA-PM-86-12] N87-20432

S

SADDLE POINTS
Stability regions of relaxed static stability aircraft under control saturation constraints N87-20268
SAFETY MANAGEMENT
Fire safety concerns in space operations
[NASA-TM-89848] N87-20342
SALINITY
Hydrologic features in cyclonic eddy region of northern east China Sea in cold seasons N87-20709
Continental shelf processes affecting the oceanography of the South Atlantic Bight
[DE87-005303] N87-20716
SALYUT SPACE STATION
Evaluation of physical work capacity of cosmonauts aboard Salyut-6 station N87-20735
SANDWICH STRUCTURES
Repair procedures for composite parts on the alpha jet N87-20175
Forced vibrations of stringer stiffened damped sandwich panel N87-20596
SATELLITE COMMUNICATION
Unique bit-error-rate measurement system for satellite communication systems
[NASA-TP-2699] N87-20448
A study of the effect of group delay distortion on an SMSK satellite communications channel
[NASA-TM-89835] N87-20450
Flexible satellite communications systems simulator standard device groups
[AD-A175944] N87-20454
SATELLITE DESIGN
Satellite analog FDMA/FM to digital TDMA conversion
[NASA-CR-179805] N87-20467
Working group on Earth observation requirements for the Polar Orbiting Platform Elements of the International Space Station (the POPE Working Group) N87-20625
ESA Columbus polar platform design concept N87-20627
SATELLITE LIFETIME
Satellite lifetime prediction N87-20666
SATELLITE OBSERVATION
Report on the Special Program 78 satellite geodesy of the Technical University of Munich
[ASTRON-GEODAET-ARB-48] N87-20618
SATELLITE ORBITS
Orbital atmospheric physics and dynamics N87-20673
Requirements for improved modeling of the orbital atmosphere N87-20676
SATELLITE PERTURBATION
NORAD satellite tracking N87-20671
SATELLITE SOUNDING
The use of visible data for improving VAS satellite soundings N87-20620
SATELLITE TRACKING
Tracking the GLOMR satellite N87-20303
NORAD satellite tracking N87-20671
SATELLITE-BORNE INSTRUMENTS
Panel report on multidisciplinary instrumentation: New possibilities — Columbus space station N87-20637
SCANDIUM COMPOUNDS
The laser strength of active elements made of Gadolinium-Scandium-Gallium garnet (GSGG) N87-20446
SCATTER PROPAGATION
Propagation of RF signals through structured ionization. Theory and antenna aperture effect applications
[AD-A175522] N87-20451
SCATTERING CROSS SECTIONS
NORSTAR Project: Norfolk public schools student team for acoustical research N87-20309
SCATTEROMETERS
Simulation of wind gradient errors in NROSS (Navy Remote Ocean Sensing System) radar scatterometer data in a simplified geometry
[AD-A175754] N87-20642
SCENE ANALYSIS
The 3-D world modelling with updating capability based on combinatorial geometry
[DE87-004257] N87-20643

SCHEDULES
Assured access to space: 1986
[GPO-60-627] N87-20838
SEA WATER
Methods of frequency spectrum estimation of sea water compared N87-20725
Phase speed of wind-wave component studied N87-20726
SEALING
Development of field level repairs for composite structures N87-20177
High repetition rate sealed CO2 TEA lasers using heterogeneous catalysts N87-20529
Chemistry of glass-ceramic to metal bonding for header applications Part 2: Hydrogen bubble formation during glass-ceramic to metal sealing
[DE87-004041] N87-20559
SEARCH PROFILES
Searching the UVSP database and a list of experiments showing mass motions N87-20899
SECONDARY EMISSION
Statistical analysis of secondary particle distributions in relativistic nucleus-nucleus collisions
[NASA-CR-4054] N87-20813
SEDIMENTS
China Report: Science and technology
[JPRS-CST-86-031] N87-20720
Physical, mechanical effect of velocity of sound in ocean sediments N87-20723
SEMICONDUCTOR DEVICES
Feasibility study of a Semiconductor Bridge (SCB) for initiating pyrotechnics and explosives
[DE87-004444] N87-20430
A study of III-V semiconductor processing employing high purity epitaxial gallium arsenide N87-20819
SEMICONDUCTOR JUNCTIONS
Liquid Phase Epitaxy (LPE) of silicon carbide
[AD-D012571] N87-20823
SEMICONDUCTORS (MATERIALS)
Feasibility study of a Semiconductor Bridge (SCB) for initiating pyrotechnics and explosives
[DE87-004444] N87-20430
A study of III-V semiconductor processing employing high purity epitaxial gallium arsenide N87-20819
The effects of heavy doping on the electronic states in semiconductors
[DE87-004421] N87-20824
SENSITIVITY
A self critical approach to data analysis and model building
[AD-A175640] N87-20791
SENSORS
Referencing in fiber optic sensing systems
[NASA-TM-89822] N87-20475
SEPARATED FLOW
Using the boundary-layer equations in three-dimensional viscous flow simulation N87-20222
Numerical simulation of separated flows past bluff bodies N87-20499
SEQUENCING
Range filtering for sequential GPS receivers with external sensor augmentation
[NASA-TM-89418] N87-20257
SERVICE LIFE
Catalysts for long-life closed-cycle CO2 lasers N87-20532
Criteria and methodology for lightweight design of vehicle components
[LBF-TB-176(1986)] N87-20550
Flat-plate solar array project. Volume 7: Module encapsulation
[NASA-CR-180665] N87-20652
SERVOMECHANISMS
Effects of force reflection on servomanipulator task performance
[DE87-003008] N87-20560
Implementation of active force control for robots subject to dynamic loading N87-20588
Advanced remote handling for future applications: The advanced integrated maintenance system
[DE87-003004] N87-20750
SET THEORY
Algebra and topology for applications to physics
[NASA-TT-20056] N87-20784
SHAKERS
Spacecraft qualification using advanced vibration and modal testing techniques N87-20388
SHAPE CONTROL
Dynamic modeling and optimal control design for large flexible space structures N87-20358
SHAPED CHARGES
Numerical simulation of Atlas-Centaur stage-separation shaped charge firing and structural response N87-20606
SHARP LEADING EDGES
Applications of Euler equations to sharp edge delta wings with leading edge vortices N87-20214
SHEAR FLOW
Experimental validation of a two-dimensional shear-flow model for determining acoustic impedance
[NASA-TP-2679] N87-20798
SHEAR PROPERTIES
Theoretical investigations of shear band formation in finite elasticity
[AD-A175657] N87-20572
SHEETS
Development of powder metallurgy 2XXX series Al alloy plate and sheet materials for high temperature aircraft structural applications, FY 1983/1984
[NASA-CR-172521] N87-20406
SHELL THEORY
Numerical investigations of geometrically nonlinear shell kinetics
[ETN-87-99019] N87-20616
SHELLS (STRUCTURAL FORMS)
Numerical investigations of geometrically nonlinear shell kinetics
[ETN-87-99019] N87-20616
SHOCK
Multi-axis transient shock simulation using mechanical pulse generators N87-20613
SHOCK MEASURING INSTRUMENTS
The digital processing of acceleration measurements for modal analysis N87-20439
SHOCK SPECTRA
The pre-pulse in pyroshock measurement and analysis N87-20604
Zero-shifted accelerometer outputs N87-20609
Questionable effects of shock data filtering N87-20610
Comparison of response from different resonant plate simulation techniques N87-20611
The controlled response of resonating fixtures used to simulate pyroshock environments N87-20612
Summary of testing techniques N87-20614
SHOCK TESTS
The Shock and Vibration Bulletin. Part 1: Welcome, Invited Papers, Shipboard Shock, Blast and Ground Shock, Shock Testing and Analysis
[AD-A175224] N87-20574
Super^Zip (linear separation) shock characteristics N87-20605
SHOCK TUBES
The chemical shock tube as a tool for studying high-temperature chemical kinetics N87-20279
SHOCK WAVE INTERACTION
Study of the unsteady pressure field on the RA16SC1 profile in vibrating condition
[ONERA-RTS-17/3423-AY] N87-20249
A holographic interferometry study of an axisymmetric shock-wave/boundary-layer strong interaction flow N87-20498
SHOCK WAVES
The Shock and Vibration Digest, Volume 19, No. 2 N87-20435
The Shock and Vibration Digest, Volume 18, No. 10
[AD-A175726] N87-20438
SHORELINES
Mathematical model of steady-state circulation in the south China Sea N87-20719
SHORT CIRCUITS
Low pass Pi section digital phase shifter apparatus
[AD-D012553] N87-20483
SHORT WAVE RADIO TRANSMISSION
Stochastic effects on oblique HF (High Frequencies) propagation
[AD-A176015] N87-20455
SHOT PEENING
Shot peening for Ti-6Al-4V alloy compressor blades
[NASA-TP-2711] N87-20566
SIGNAL ANALYSIS
Engineering thrust areas, 1987
[DE87-004443] N87-20441
SIGNAL DISTORTION
A study of the effect of group delay distortion on an SMSK satellite communications channel
[NASA-TM-89835] N87-20450
SIGNAL MEASUREMENT
Automated anthropometric data measurement system
[AD-D012575] N87-20748
SIGNAL PROCESSING
A computer controlled signal preprocessor for laser fringe anemometer applications
[NASA-TM-88982] N87-20518
Progress in the development of holographic scheme for pair correlation estimation
[AD-A175573] N87-20518
Questionable effects of shock data filtering N87-20610
Fly's eye sensor nonlinear signal processing
[AD-D012564] N87-20815
SILANES
Laser spectroscopy and gas-phase chemistry in CVD
[DE86-007392] N87-20548
SILICON
Noble-gas ion bombardment on clean silicon surfaces studied using ellipsometry and desorption
[B8672200] N87-20609
Adsorption of atomic oxygen (N2O) on clean silicon surfaces and its influence on the surface state density; a comparison with O2
[B8668354] N87-20610
Deep ion implantation for bipolar silicon devices; investigations into the use of the third dimension
[B8672201] N87-20828
SILICON CARBIDES
Deformation and fracture of single-crystal and sintered polycrystalline silicon carbide produced by cavitation
[NASA-TM-88981] N87-20422
Hot corrosion attack and strength degradation of SiC and Si(sub)3N(sub)4
[NASA-TM-89820] N87-20425
Liquid Phase Epitaxy (LPE) of silicon carbide
[AD-D012571] N87-20823
SILICON COMPOUNDS
Adhesion of a silicone based insulating material to rocket motors
[FOA-C-20635-2.1] N87-20429
SILICON NITRIDES
Hot corrosion attack and strength degradation of SiC and Si(sub)3N(sub)4
[NASA-TM-89820] N87-20425
SIMD (COMPUTERS)
A system for routing arbitrary directed graphs on SIMD architectures
[NASA-CR-178265] N87-20764
SIMULATION
Design and verification by nonlinear simulation of a Mach/CAS control law for the NASA TCV B737 aircraft
[NASA-CR-178029] N87-20290
Air Force basic research in dynamics and control of large space structures N87-20577
Summary of testing techniques N87-20614
Simulation of wind gradient errors in NROSS (Navy Remote Ocean Sensing System) radar scatterometer data in a simplified geometry
[AD-A175754] N87-20642
Filament formation due to photospheric shear N87-20678
SIMULATORS
Flexible satellite communications systems simulator standard device groups
[AD-A175944] N87-20454
SINGLE CRYSTALS
Bithermal low-cycle fatigue behavior of a NiCoCrAlY-coated single crystal superalloy
[NASA-TM-89831] N87-20408
Deformation and fracture of single-crystal and sintered polycrystalline silicon carbide produced by cavitation
[NASA-TM-88981] N87-20422
CO oxidation studies over supported noble metal catalysts and single crystals: A review N87-20530
SINGULARITY (MATHEMATICS)
New numerical techniques in the method of singularities for application to complex three-dimensional configurations N87-20205
Stability regions of relaxed static stability aircraft under control saturation constraints N87-20288
SINTERING
Deformation and fracture of single-crystal and sintered polycrystalline silicon carbide produced by cavitation
[NASA-TM-88981] N87-20422
SKIN (ANATOMY)
Effect of hypoxia on DNA synthesis and collagent content of regenerating skin N87-20742
Electrodermal conductivity in man and monkeys N87-20743
SKIN (STRUCTURAL MEMBER)
Composite repair of cocured J-stiffened panels: Design and test verification N87-20181
Composite repair techniques for J-stiffened composite fuselage structures N87-20186
Battle damage repair of composite structures N87-20189
Patch repair of corroded aircraft skin areas N87-20191
SKY
LOWTRAN modeling of near-horizon infrared sky radiances in the presence of clouds
[AD-A175661] N87-20691
SLEEP DEPRIVATION
Dynamics of bioelectric activity of human brain in a continuous waking state N87-20745

SMOOTHING
Calculation of Rayleigh-Taylor flows using vortex blobs
[DE87-002551] N87-20507
SODIUM
Studies of X-ray satellites in sodium, magnesium, aluminum, argon, and iron
[ETN-87-99364] N87-20812
SODIUM SULFUR BATTERIES
Sodium sulfur battery: An overview
[DE87-004920] N87-20491
Morphological changes in the sulfur electrode of lifecycle-tested Na/S cells
[DE87-004961] N87-20493
SOFTWARE ENGINEERING
A vibroacoustic database management system and its application for a pyroshock database N87-20607
The fault-tree compiler
[NASA-TM-89099] N87-20765
Guide to sharing personal computer resources via local area networks, revised
[DE86-016086] N87-20772
SOFTWARE TOOLS
Sophisticated software systems for small self-contained space shuttle payload G285 N87-20313
The hypercluster: A parallel processing test-bed architecture for computational mechanics applications
[NASA-TM-89823] N87-20767
SOIL MECHANICS
Resilient modulus of freeze-thaw affected granular soils for pavement design and evaluation. Part 3: Laboratory tests on soils from Albany County Airport
[DOT/FAA-PM-84-16.3] N87-20433
SOILS
A freeze-thaw test to determine the frost susceptibility of soils
[DOT/FAA-PM-85-20] N87-20434
SOLAR ACTIVITY
Satellite lifetime prediction N87-20666
NORAD satellite tracking N87-20671
NORAD/SPACECMD comments concerning the atmospheric density models N87-20672
Forecasts of solar and geomagnetic activity N87-20677
NASA/MSFC prediction techniques N87-20678
Three dimensional structures of solar active regions N87-20916
Coronal plasmas on the sun and nearby stars N87-20919
The association of chromospheric and coronal phenomena with the evolution of the quiet sun magnetic fields
[ESD-TR-84-611] N87-20926
Small-scale eruptive filaments on the quiet sun N87-20928
Magnetic location of C IV events in the quiet network N87-20930
Solar-geophysical data number 506, October 1986. Part 1: (Prompt reports). Data for September 1986, August 1986 and late data
[PB87-126389] N87-20948
SOLAR ARRAYS
Modal testing of the Olympus development model stowed solar array N87-20366
Acoustic effects on the dynamic of lightweight structures N87-20372
Solar array flight experiment/dynamic augmentation experiment
[NASA-TP-2690] N87-20380
SAFE/DAE: Modal test in space N87-20584
Flat-plate solar array project of the US Department of Energy's National Photovoltaics Program: Ten years of progress
[NASA-CR-180507] N87-20644
Summary of flat-plate solar array project documentation: Abstracts of published documents, 1975-1986, revision 1
[NASA-CR-180401-REV-1] N87-20645
Flat-plate solar array project. Volume 1: Executive summary
[NASA-CR-180658] N87-20646
Flat-plate solar array project. Volume 2: Silicon material
[NASA-CR-180659] N87-20647
Flat-plate solar array project. Volume 3: Silicon sheet: Wafers and ribbons
[NASA-CR-180661] N87-20648
Flat-plate solar array project. Volume 4: High-efficiency solar cells
[NASA-CR-180662] N87-20649
Flat-plate solar array project. Volume 5: Process development
[NASA-CR-180663] N87-20650
Flat-plate solar array project. Volume 6: Engineering sciences and reliability
[NASA-CR-180664] N87-20651
Flat-plate solar array project. Volume 7: Module encapsulation
[NASA-CR-180665] N87-20652
Flat-plate solar array project. Volume 8: Project analysis and integration
[NASA-CR-180695] N87-20653
The concentration principle applied to spaceborne solar arrays. AGORA mission: Studies synthesis
[SNIAS-959-CA/CG] N87-20657
SOLAR ATMOSPHERE
Coronal and Prominence Plasmas
[NASA-CP-2442] N87-20671
Heating of the stellar corona N87-20673
Formation and support of prominence N87-20674
Filament formation due to photospheric shear N87-20678
Numerical simulations of a siphon mechanism for quiescent prominence formation N87-20680
Recent observations of the formation of filaments N87-20683
On the formation of active region prominences (H alpha filaments) N87-20684
Partial redistribution effects in the formation of hydrogen lines in quiescent prominences N87-20694
Guided MHD waves as a coronal diagnostic tool N87-20921
SOLAR CELLS
Flat-plate solar array project of the US Department of Energy's National Photovoltaics Program: Ten years of progress
[NASA-CR-180507] N87-20644
Summary of flat-plate solar array project documentation: Abstracts of published documents, 1975-1986, revision 1
[NASA-CR-180401-REV-1] N87-20645
Flat-plate solar array project. Volume 1: Executive summary
[NASA-CR-180658] N87-20646
Flat-plate solar array project. Volume 2: Silicon material
[NASA-CR-180659] N87-20647
Flat-plate solar array project. Volume 3: Silicon sheet: Wafers and ribbons
[NASA-CR-180661] N87-20648
Flat-plate solar array project. Volume 4: High-efficiency solar cells
[NASA-CR-180662] N87-20649
Flat-plate solar array project. Volume 5: Process development
[NASA-CR-180663] N87-20650
Flat-plate solar array project. Volume 6: Engineering sciences and reliability
[NASA-CR-180664] N87-20651
Flat-plate solar array project. Volume 7: Module encapsulation
[NASA-CR-180665] N87-20652
Flat-plate solar array project. Volume 8: Project analysis and integration
[NASA-CR-180695] N87-20653
SOLAR CORONA
Coronal and Prominence Plasmas
[NASA-CP-2442] N87-20671
Some crucial corona and prominence observations N87-20672
Heating of the stellar corona N87-20673
The growth of radiative filamentation modes in sheared magnetic fields N87-20675
Can prominences form in current sheets N87-20676
Condensation modes in magnetized plasmas N87-20677
Formation of active region and quiescent prominence magnetic field configurations N87-20679
Numerical simulations of a siphon mechanism for quiescent prominence formation N87-20680
Diagnostics and structure N87-20685
VLA observations of slar filaments at 6 and 20 cm wavelengths N87-20688
The microwave structure of quiescent solar filaments at high resolution N87-20689
Interpretation of the prominence differential emissions measure for 3 geometries N87-20690
The prominence-corona interface and its relationship to the chromosphere-corona transition N87-20691
The density and thickness of quiescent prominences N87-20693
Non-LTE hydrogen-line formation in moving prominences N87-20695
On the existence of oscillations in solar filaments observed in H alpha and C IV lines N87-20900
The heating of filaments as a disappearance process N87-20904
On the thermal durability of solar prominences, or how to evaporate a prominence N87-20905
Magnetic field re-arrangement after prominence eruption N87-20907
Large scale structure of the corona N87-20909
Large scale structure of the sun's radio corona N87-20910
Synoptic study of the corona at meter wavelength N87-20911
The white light corona and photospheric magnetic fields N87-20912
Quasistatic evolution of magnetostatic coronal structures N87-20913
Three-dimensional magnetostatic models of the large-scale corona N87-20914
Guided MHD waves as a coronal diagnostic tool N87-20921
Small-scale coronal structure, part 3 N87-20922
Simultaneous observations of changes in coronal bright point emission at the 20 cm radio and He Lambda 10830 wavelengths N87-20923
VLA observations of coronal bright points at 6 and 20 cm wavelengths N87-20924
Magnetogram and soft X-ray comparisons of XBP and ER N87-20927
Magnetic location of C IV events in the quiet network N87-20930
Small-scale structures and the density irregularity of the inner corona N87-20932
Phlegethon flow: A proposed origin for spicules and coronal heating N87-20933
Energy conversion in the coronal plasma N87-20934
Topological constraints and the existence of force-free fields N87-20935
The topological description of coronal magnetic fields N87-20936
A coordinate free description of magnetohydrostatic equilibria N87-20937
Cascade model of coronal heating N87-20938
Heating of the solar corona by the resonant absorption of Alfven waves N87-20939
Magnetic helicity as a constraint on coronal dissipation N87-20940
The stability of coronal and prominence magnetic fields N87-20941
Resistive ballooning modes in line-tied coronal arcades N87-20942
Effects of flows on viscous and resistive MHD stability N87-20943
Large-scale electric fields resulting from magnetic reconnection in the corona N87-20944
Dynamic evolution of coronal magnetic fields N87-20945
The propagation of an electron beam through the solar corona N87-20946
SOLAR CORPUSCULAR RADIATION
Pre-compaction irradiation of meteorites N87-20850
Large scale structure of the sun's radio corona N87-20910
SOLAR CYCLES
Forecasts of solar and geomagnetic activity N87-20677
NASA/MSFC prediction techniques N87-20678
The association of chromospheric and coronal phenomena with the evolution of the quiet sun magnetic fields
[ESD-TR-84-611] N87-20926
Magnetogram and soft X-ray comparisons of XBP and ER N87-20927
Small-scale eruptive filaments on the quiet sun N87-20928
SOLAR DYNAMIC POWER SYSTEMS
Solar array flight experiment/dynamic augmentation experiment
[NASA-TP-2690] N87-20380
Conceptual design of a solar electric advanced Stirling power system
[DE87-005036] N87-20656
SOLAR ENERGY CONVERSION
Summary of flat-plate solar array project documentation: Abstracts of published documents, 1975-1986, revision 1
[NASA-CR-180401-REV-1] N87-20645
Flat-plate solar array project. Volume 1: Executive summary
[NASA-CR-180658] N87-20646
Flat-plate solar array project. Volume 4: High-efficiency solar cells
[NASA-CR-180662] N87-20649
Solar power absorption in a glass tube
[NASA-TM-89083] N87-20814
SOLAR FLARES
Filament eruption connected to protospheric activity N87-20906
Magnetic field re-arrangement after prominence eruption N87-20907
A dynamic model of filament eruptions and two ribbon flares N87-20908
High-spatial-resolution microwave and related observations as diagnostics of coronal loops N87-20917

Small-scale eruptive filaments on the quiet sun N87-20928
Large-scale electric fields resulting from magnetic reconnection in the corona N87-20944
Statistical aspects of solar flares [NASA-TP-2714] N87-20947
Solar-geophysical data number 506, October 1986. Part 1: (Prompt reports). Data for September 1986, August 1986 and late data [PB87-126389] N87-20948

SOLAR FLUX
NORAD satellite tracking N87-20671
NORAD/SPACECMD comments concerning the atmospheric density models N87-20672
Limitations to modeling the thermosphere and exosphere N87-20674
Filament eruption connected to protospheric activity N87-20906
A dynamic model of filament eruptions and two ribbon flares N87-20908

SOLAR FLUX DENSITY
Quasistatic evolution of magnetostatic coronal structures N87-20913
Three-dimensional magnetostatic models of the large-scale corona N87-20914
High-spatial-resolution microwave and related observations as diagnostics of coronal loops N87-20917

SOLAR GRANULATION
Formation and support of prominence N87-20874
Small-scale coronal structure, part 3 N87-20922
Simultaneous observations of changes in coronal bright point emission at the 20 cm radio and He Lambda 10830 wavelengths N87-20923
VLA observations of coronal bright points at 6 and 20 cm wavelengths N87-20924
The association of chromospheric and coronal phenomena with the evolution of the quiet sun magnetic fields [ESD-TR-84-611] N87-20926
Magnetogram and soft X-ray comparisons of XBP and ER N87-20927
Magnetic location of C IV events in the quiet network N87-20930

SOLAR GRAVITATION
Numerical simulations of a siphon mechanism for quiescent prominence formation N87-20880

SOLAR HEATING
The heating of filaments as a disappearance process N87-20904
High-spatial-resolution microwave and related observations as diagnostics of coronal loops N87-20917

SOLAR LIMB
The white light corona and photospheric magnetic fields N87-20912

SOLAR MAGNETIC FIELD
Theory and simulation of the evolution of the large-scale solar magnetic field N87-20870
Coronal and Prominence Plasmas [NASA-CP-2442] N87-20871
Some crucial corona and prominence observations N87-20872
Formation and support of prominence N87-20874
The growth of radiative filamentation modes in sheared magnetic fields N87-20875
Condensation modes in magnetized plasmas N87-20877
Filament formation due to photospheric shear N87-20878
Formation of active region and quiescent prominence magnetic field configurations N87-20879
Numerical simulations of a siphon mechanism for quiescent prominence formation N87-20880
Alfven-wave dissipation: A support mechanism for quiescent prominences N87-20881
Static current-sheet models of quiescent prominences N87-20882
Recent observations of the formation of filaments N87-20883
On the formation of active region prominences (H alpha filaments) N87-20884
The prominence-corona interface and its relationship to the chromosphere-corona transition N87-20891
C IV Doppler shifts observed in active region filaments N87-20898
On the existence of oscillations in solar filaments observed in H alpha and C IV lines N87-20900
Measurements of magnetic fields in solar prominences N87-20901
Magnetic field vector and electron density diagnostics from linear polarization measurements in 14 solar prominences N87-20902
Filament disappearances N87-20903
Filament eruption connected to protospheric activity N87-20906
Magnetic field re-arrangement after prominence eruption N87-20907
A dynamic model of filament eruptions and two ribbon flares N87-20908
The white light corona and photospheric magnetic fields N87-20912
Coronal diagnostics. N87-20915
High-spatial-resolution microwave and related observations as diagnostics of coronal loops N87-20917
Theoretical models of free-free microwave emission from solar magnetic loops N87-20918
Measurement of coronal fields using spatially resolved microwave spectroscopy N87-20920
Energy conversion in the coronal plasma N87-20934

SOLAR MAXIMUM MISSION
Searching the UVSP database and a list of experiments showing mass motions N87-20899

SOLAR OSCILLATIONS
On the existence of oscillations in solar filaments observed in H alpha and C IV lines N87-20900

SOLAR PHYSICS
Coronal and Prominence Plasmas [NASA-CP-2442] N87-20871
The growth of radiative filamentation modes in sheared magnetic fields N87-20875
Can prominences form in current sheets N87-20876
Condensation modes in magnetized plasmas N87-20877
Filament formation due to photospheric shear N87-20878
Formation of active region and quiescent prominence magnetic field configurations N87-20879
Numerical simulations of a siphon mechanism for quiescent prominence formation N87-20880
Alfven-wave dissipation: A support mechanism for quiescent prominences N87-20881
Recent observations of the formation of filaments N87-20883
On the formation of active region prominences (H alpha filaments) N87-20884
Diagnostics and structure N87-20885
Dark filaments observed at 8.3mm and 3.1mm wavelength N87-20887
The prominence-corona interface and its relationship to the chromosphere-corona transition N87-20891
Thermal stability analysis of the fine structure of solar prominences N87-20892
The density and thickness of quiescent prominences N87-20893

SOLAR PROMINENCES
Coronal and Prominence Plasmas [NASA-CP-2442] N87-20871
Some crucial corona and prominence observations N87-20872
Formation and support of prominence N87-20874
The growth of radiative filamentation modes in sheared magnetic fields N87-20875
Can prominences form in current sheets N87-20876
Condensation modes in magnetized plasmas N87-20877
Filament formation due to photospheric shear N87-20878
Formation of active region and quiescent prominence magnetic field configurations N87-20879
Numerical simulations of a siphon mechanism for quiescent prominence formation N87-20880
Alfven-wave dissipation: A support mechanism for quiescent prominences N87-20881
Static current-sheet models of quiescent prominences N87-20882
Recent observations of the formation of filaments N87-20883
On the formation of active region prominences (H alpha filaments) N87-20884
Diagnostics and structure N87-20885
Temperatures of quiescent prominences measured from hydrogen Paschen and CaII IR lines N87-20886
Dark filaments observed at 8.3mm and 3.1mm wavelength N87-20887
VLA observations of slar filaments at 6 and 20 cm wavelengths N87-20888
Interpretation of the prominence differential emissions measure for 3 geometries N87-20890
The prominence-corona interface and its relationship to the chromosphere-corona transition N87-20891
Thermal stability analysis of the fine structure of solar prominences N87-20892
The density and thickness of quiescent prominences N87-20893
Partial redistribution effects in the formation of hydrogen lines in quiescent prominences N87-20894
Non-LTE hydrogen-line formation in moving prominences N87-20895
Vertical motions in the quiescent prominences observed in the He I Lambda10830Angstrom line N87-20896
Constraints on filament models deduced from dynamical analysis N87-20897
C IV Doppler shifts observed in active region filaments N87-20898
On the existence of oscillations in solar filaments observed in H alpha and C IV lines N87-20900
Measurements of magnetic fields in solar prominences N87-20901
Magnetic field vector and electron density diagnostics from linear polarization measurements in 14 solar prominences N87-20902
Filament disappearances N87-20903
The heating of filaments as a disappearance process N87-20904
On the thermal durability of solar prominences, or how to evaporate a prominence N87-20905
Filament eruption connected to protospheric activity N87-20906
Magnetic field re-arrangement after prominence eruption N87-20907
A dynamic model of filament eruptions and two ribbon flares N87-20908
Statistical aspects of solar flares [NASA-TP-2714] N87-20947

SOLAR RADIATION
Partial redistribution effects in the formation of hydrogen lines in quiescent prominences N87-20894
Three dimensional structures of solar active regions N87-20916

SOLAR RADIO EMISSION
Large scale structure of the sun's radio corona N87-20910

SOLAR SPECTRA
Temperatures of quiescent prominences measured from hydrogen Paschen and CaII IR lines N87-20886
Interpretation of the prominence differential emissions measure for 3 geometries N87-20890
Partial redistribution effects in the formation of hydrogen lines in quiescent prominences N87-20894

SOLAR SYSTEM
Collisional dynamics of perturbed particle disks in the solar system [NASA-CR-180497] N87-20860

SOLAR TEMPERATURE
Heating of the stellar corona N87-20873
Filament formation due to photospheric shear N87-20878
Temperatures of quiescent prominences measured from hydrogen Paschen and CaII IR lines N87-20886
VLA observations of slar filaments at 6 and 20 cm wavelengths N87-20888
Thermal stability analysis of the fine structure of solar prominences N87-20892
High-spatial-resolution microwave and related observations as diagnostics of coronal loops N87-20917

SOLAR THERMAL PROPULSION
A numerical heat transfer model for an advanced solar thermal propulsion system N87-20377

SOLAR WIND
MHD waves detected by ice at distances 28 x 10 km from Comet Halley: Cometary or solar wind origin [DE87-005122] N87-20863
Constraints on filament models deduced from dynamical analysis N87-20897
Measurements of magnetic fields in solar prominences N87-20901
The heating of filaments as a disappearance process N87-20904
Quasistatic evolution of magnetostatic coronal structures N87-20913
Theoretical models of free-free microwave emission from solar magnetic loops N87-20918
Coronal plasmas on the sun and nearby stars N87-20919

SOLAR X-RAYS
Coronal diagnostics. N87-20915

SOLID ELECTROLYTES
High-temperature fuel cells [DE87-004870] N87-20487
Sodium sulfur battery: An overview [DE87-004920] N87-20491

SOLID LUBRICANTS
Investigation of PTFE transfer films by infrared emission spectroscopy and phase-locked ellipsometry [NASA-TM-88844] N87-20421

SOLID MECHANICS
Studies in nonlinear structural dynamics: Chaotic behavior and poynting effect N87-20348
Solid mechanics program at ONR N87-20575
Army research in shock mechanics N87-20576

SOLID PROPELLANT ROCKET ENGINES
Composite motor case nomenclature [AD-A176418] N87-20364

SOLID STATE LASERS
Injection-seeding studies of diode laser array behavior
[DE87-002051] N87-20546
SOLUBILITY
Cal Poly Space Project G-279 N87-20324
SOUND WAVES
Biot theory and acoustical properties of high porosity fibrous materials and plastic foams
[NASA-TM-88575] N87-20424
Physical, mechanical effect of velocity of sound in ocean sediments N87-20723
Acoustic gravity waves: A computational approach
[NASA-CR-178270] N87-20781
SPACE COMMERCIALIZATION
Assured access to space: 1986
[GPO-60-627] N87-20838
SPACE ERECTABLE STRUCTURES
Large space antennas: A systems analysis case history
[NASA-TM-89072] N87-20352
Solar array flight experiment/dynamic augmentation experiment
[NASA-TP-2690] N87-20380
SPACE FLIGHT STRESS
Evaluation of physical work capacity of cosmonauts aboard Salyut-6 station N87-20735
SPACE MAINTENANCE
Servicing of the polar platform — Columbus space station N87-20628
SPACE MANUFACTURING
Towards a better mirror N87-20310
Progress on the Ohio State University Get Away Special G-0318: DEAP N87-20311
SPACE MISSIONS
Radiation protection guidelines for space missions
[NASA-TM-89278] N87-20730
SPACE OBSERVATIONS (FROM EARTH)
A systematic search for millisecond pulsars N87-20839
SPACE PERCEPTION
New book deals with spatial orientation N87-20746
SPACE PLASMAS
Effects of space plasma discharge on the performance of large antenna structures in low Earth orbit
[NASA-TM-89118] N87-20339
Steepened magnetosonic waves in the high Beta plasma surrounding Comet-Giacobini-Zinner
[NASA-CR-180614] N87-20868
SPACE PLATFORMS
Proceedings of the European Symposium on Polar platform Opportunities and Instrumentation for Remote-Sensing (ESPOIR)
[ESA-SP-266] N87-20621
The Earth observation activities of the European Space Agency and the use of the polar platform of the International Space Station N87-20622
Working group on Earth observation requirements for the Polar Orbiting Platform Elements of the International Space Station (the POPE Working Group) N87-20625
ESA Columbus polar platform design concept N87-20627
Servicing of the polar platform — Columbus space station N87-20628
Orbit configurations — space station polar platform N87-20629
Payload data management scheme planned for Earth observation sensors to be flown on the polar platforms in the framework of the space station/Columbus program N87-20630
Cooperation of the International Space Station partners in the preparation of the use of space station elements for Earth observation (platform and payload aspects) N87-20631
USA-Europe coordination and cooperation activities: Announcements of Opportunity — polar platforms N87-20632
Report of the atmosphere panel N87-20633
Land panel report — International Space Station N87-20634
Ocean-ice panel report — International Space Station N87-20635
Solid Earth panel report — Columbus program N87-20636
Panel report on multidisciplinary instrumentation: New possibilities — Columbus space station N87-20637
Data management panel report — Columbus polar platforms N87-20639
The orbit configuration panel report — Columbus polar platforms N87-20640
Panel report on the polar platform servicing approach and its implications — Columbus space station N87-20641
SPACE SHUTTLE BOOSTERS
Structural design of an in-line bolted joint for the space shuttle solid rocket motor case segments
[NASA-TM-89027] N87-20349
SPACE SHUTTLE MAIN ENGINE
Development of a computational aero/fluids analysis system
[NASA-CR-179046] N87-20343
Hybrid methods for rotordynamic analysis
[NASA-CR-179035] N87-20553
SPACE SHUTTLE MISSION 51-A
Post-flight BET products for the 2nd discovery entry, STS-19 (51-A)
[NASA-CR-172572] N87-20344
SPACE SHUTTLE MISSION 51-B
NUSAT update N87-20312
SPACE SHUTTLE MISSION 51-G
Recent results from MAUS payloads N87-20331
SPACE SHUTTLE MISSION 61-C
STS-61C, Columbia flight N87-20315
Marshall Amateur Radio Club experiment (MARCE) post flight data analysis N87-20323
SPACE SHUTTLE PAYLOADS
The 1985 Get Away Special Experimenter's Symposium
[NASA-CP-2438] N87-20302
Gas tungsten arc welding in a microgravity environment: Work done on GAS payload G-169 N87-20306
Use of lightweight composites for GAS payload structures N87-20307
Phycomyces in space: A problem in bioengineering N87-20308
NORSTAR Project: Norfolk public schools student team for acoustical research N87-20309
Towards a better mirror N87-20310
Progress on the Ohio State University Get Away Special G-0318: DEAP N87-20311
NUSAT update N87-20312
Sophisticated software systems for small self-contained space shuttle payload G285 N87-20313
A systems-level performance history of get away specials after 25 space shuttle missions N87-20314
STS-61C, Columbia flight N87-20315
USC/AIAA student get away special project liquid droplet collector experiment N87-20316
Results of the joint utilization of laser integrated experiments flown on payload GAS-449 aboard Columbia mission 61-C N87-20317
The North Carolina A and T State University Student Space Shuttle Program N87-20318
Baking the first bread in space N87-20319
Hitchhiker-G: A new carrier system for attached shuttle payloads N87-20320
Multipurpose microcontroller design for PUGAS 2 N87-20321
Geotaxis baseline data for Drosophila N87-20322
Marshall Amateur Radio Club experiment (MARCE) post flight data analysis N87-20323
Cal Poly Space Project G-279 N87-20324
The growth and harvesting of algae in a micro-gravity environment N87-20325
To catch a comet 2: Technical update on CAN-DO N87-20326
To catch a child's imagination 2: Educational update on CAN-DO N87-20327
NUSAT 1 attitude determination N87-20328
NUSAT 1 methods for radar field strength measurement N87-20329
Recent results from MAUS payloads N87-20331
Microgravity effects on electrodeposition of metals and metal-cermet mixtures N87-20332
GAS-007: First step in a series of Explorer payloads N87-20333
In situ observation of mono-molecular growth steps on aqueous solution grown crystals and the transport of molecules to the crystals N87-20334
Satellite servicing mission preliminary cost estimation model
[NASA-CR-171978] N87-20335
Liquid droplet radiator development status
[NASA-TM-89852] N87-20353
Influence co-efficient testing as a substitute for modal survey testing of large space structures N87-20369
Solar array flight experiment/dynamic augmentation experiment
[NASA-TP-2690] N87-20380
Assured access to space: 1986
[GPO-60-627] N87-20838
SPACE SHUTTLES
Laboratory investigation of lightweight heater tape for shuttle propellant tank
[AD-A175997] N87-20345
Influence co-efficient testing as a substitute for modal survey testing of large space structures N87-20369
Servicing of the polar platform — Columbus space station N87-20628
Effects of space shuttle launches STS-1 through STS-9 on terrestrial vegetation of John F. Kennedy Space Center, Florida
[NASA-TM-83103] N87-20658
SPACE STATION PROPULSION
Conceptual design and integration of a space station resistojet propulsion assembly
[NASA-TM-89847] N87-20378
Density uncertainty effect on cost of space station reboost N87-20667
Space station momentum management N87-20668
Space station control moment gyro control N87-20669
SPACE STATIONS
An advanced technology space station for the year 2025, study and concepts
[NASA-CR-178208] N87-20340
Fire safety concerns in space operations
[NASA-TM-89848] N87-20342
Liquid droplet radiator development status
[NASA-TM-89852] N87-20353
Resistojet control and power for high frequency ac buses
[NASA-TM-89860] N87-20477
Space station structures and dynamics test program
[NASA-TP-2710] N87-20568
Documentation of the space station/aircraft acoustic apparatus
[NASA-TM-89111] N87-20795
SPACE TRANSPORTATION SYSTEM
Shuttle/Spacelab contamination environment and effects handbook
[NASA-CR-4053] N87-20350
Assured access to space: 1986
[GPO-60-627] N87-20838
SPACE TRANSPORTATION SYSTEM FLIGHTS
Utilization of Global Reference Atmosphere Model (GRAM) for shuttle entry N87-20680
SPACE-TIME FUNCTIONS
On the de Sitter and Nariai space-times in a generalized theory of gravitation
[DE86-703483] N87-20830
A numerical study of some spherically-symmetric and axisymmetric cosmological models N87-20853
SPACEBORNE EXPERIMENTS
G-300: The first French Getaway Special microgravity measurements of fluid thermal conductivity N87-20330
SPACEBORNE TELESCOPES
An astrometric facility for planetary detection on the space station
[NASA-TM-89436] N87-20841
SPACECRAFT ANTENNAS
Large space antennas: A systems analysis case history
[NASA-TM-89072] N87-20352
System architecture of MMIC-based large aperture arrays for space application
[NASA-TM-89840] N87-20468
SPACECRAFT CONFIGURATIONS
Modal testing of the Olympus development model stowed solar array N87-20366
SPACECRAFT CONSTRUCTION MATERIALS
Future trends in spacecraft design and qualification N87-20356
SPACECRAFT CONTROL
Propellant tank resupply system
[AD-D012559] N87-20375
Space station momentum management N87-20668
Space station control moment gyro control N87-20669
Use of the 4D-Global Reference Atmosphere Model (GRAM) for space shuttle descent design N87-20681
Aero-Assisted Orbital Transfer Vehicle (AOTV) N87-20682
SPACECRAFT DESIGN
Future trends in spacecraft design and qualification N87-20356
Recent developments and future trends in structural dynamic design verification and qualification of large flexible spacecraft N87-20357
Dynamic modeling and optimal control design for large flexible space structures N87-20358
Effect of modal damping in modal synthesis of spacecraft structures N87-20362
Benefits of passive damping as applied to active control of large space structures N87-20371
Upper and Middle Atmospheric Density Modeling Requirements for Spacecraft Design and Operations
[NASA-CP-2460] N87-20665
SPACECRAFT ELECTRONIC EQUIPMENT
Bubble memory module for spacecraft application
[NASA-TM-86411] N87-20476
SPACECRAFT LANDING
Post-flight BET products for the 2nd discovery entry, STS-19 (51-A)
[NASA-CR-172572] N87-20344
Users of middle atmosphere models remarks N87-20679

SPACECRAFT LAUNCHING
Super*Zip (linear separation) shock characteristics N87-20605
Effects of space shuttle launches STS-1 through STS-9 on terrestrial vegetation of John F. Kennedy Space Center, Florida
[NASA-TM-83103] N87-20656
SPACECRAFT MODELS
Influence co-efficient testing as a substitute for modal survey testing of large space structures N87-20369
SPACECRAFT MOTION
Attitude motion of torque-free asymmetric dual-spin spacecraft
[AD-A175531] N87-20354
SPACECRAFT PERFORMANCE
An investigation of transitional management problems for the NSTS
[NASA-CR-171979] N87-20634
SPACECRAFT POWER SUPPLIES
Use of lightweight composites for GAS payload structures N87-20307
Liquid droplet radiator development status
[NASA-TM-89852] N87-20353
Requirements specification for nickel cadmium battery expert system
[NASA-CR-179034] N87-20473
Resistojet control and power for high frequency ac buses
[NASA-TM-89860] N87-20477
The concentration principle applied to spaceborne solar arrays. AGORA mission: Studies synthesis
[SNIAS-959-CA/CG] N87-20657
SPACECRAFT PROPULSION
Propellant tank resupply system
[AD-D012559] N87-20375
A numerical heat transfer model for an advanced solar thermal propulsion system N87-20377
SPACECRAFT RADIATORS
USC/AIAA student get away special project liquid droplet collector experiment N87-20316
Liquid droplet radiator development status
[NASA-TM-89852] N87-20353
SPACECRAFT REENTRY
Post-flight BET products for the 2nd discovery entry, STS-19 (51-A)
[NASA-CR-172572] N87-20344
Utilization of Global Reference Atmosphere Model (GRAM) for shuttle entry N87-20630
Shuttle derived atmosphere N87-20634
SPACECRAFT RELIABILITY
Recent developments and future trends in structural dynamic design verification and qualification of large flexible spacecraft N87-20357
SPACECRAFT STRUCTURES
Mechanical Qualification of Large Flexible Spacecraft Structures
[AD-A175529] N87-20355
Future trends in spacecraft design and qualification N87-20356
Dynamic analysis of direct television satellite TV-SAT/TDF.1 N87-20360
Structural qualification of large spacecraft N87-20361
Effect of modal damping in modal synthesis of spacecraft structures N87-20362
Dynamic qualification of spacecraft by means of modal synthesis N87-20363
Low frequency vibration testing on satellites N87-20364
Modal-survey testing for system identification and dynamic qualification of spacecraft structures N87-20365
Active structural controllers emulating structural elements by ICUs N87-20367
Spacecraft qualification using advanced vibration and modal testing techniques N87-20368
Influence co-efficient testing as a substitute for modal survey testing of large space structures N87-20369
Acoustic effects on the dynamic of lightweight structures N87-20372
Multi-axis vibration tests on spacecraft using hydraulic exciters N87-20373
Optimization of aerospace structures subjected to random vibration and fatigue constraints N87-20599
SPACECRAFT SURVIVABILITY
Results of the joint utilization of laser integrated experiments flown on payload GAS-449 aboard Columbia mission 61-C N87-20317
SPACECRAFT TEMPERATURE
Use of the 4D-Global Reference Atmosphere Model (GRAM) for space shuttle descent design N87-20681
SPACECRAFT TRAJECTORIES
Post-flight BET products for the 2nd discovery entry, STS-19 (51-A)
[NASA-CR-172572] N87-20344
SPACECREWS
Radiation protection guidelines for space missions
[NASA-TM-89278] N87-20730
Evaluation of physical work capacity of cosmonauts aboard Salyut-6 station N87-20735
Operator work capacity in tracking system when submitted to antiorthostatic hypokinesia N87-20736
SPACELAB
Shuttle/Spacelab contamination environment and effects handbook
[NASA-CR-4053] N87-20350
SPATIAL DISTRIBUTION
Hydrologic features in cyclonic eddy region of northern east China Sea in cold seasons N87-20709
Computer simulation and analysis of spatial galaxy distributions N87-20851
SPATIAL MARCHING
Computation of three-dimensional flows by viscous-inviscid interation using the MZM method N87-20223
SPATIAL RESOLUTION
Dark filaments observed at 8.3mm and 3.1mm wavelength N87-20887
SPECIFICATIONS
Batteries for hybrid vehicles or other high-power applications
[DE87-004928] N87-20486
SPECTRAL ENERGY DISTRIBUTION
Spectral analysis of waves in Gulf of Tonkin described N87-20722
SPECTRAL METHODS
A practical assessment of spectral accuracy for hyperbolic problems with discontinuities
[NASA-CR-178226] N87-20779
SPECTROHELIOGRAPHS
VLA observations of star filaments at 6 and 20 cm wavelengths N87-20888
Large scale structure of the corona N87-20909
Large scale structure of the sun's radio corona N87-20910
SPECTROPHOTOMETRY
UBVRI-photometry of the antiflare stars V586 Ori and IU Ori
[DE87-700760] N87-20845
SPECTROSCOPY
Diagnostics and structure N87-20885
Vertical motions in the quiescent prominences observed in the He I Lambda10830Angstrom line N87-20896
SPECTRUM ANALYSIS
China Report: Science and technology
[JPRS-CST-86-031] N87-20720
Spectral analysis of waves in Gulf of Tonkin described N87-20722
SPEED INDICATORS
Airspeed sensing pressure valve system
[AD-D012569] N87-20266
SPHERES
NORSTAR Project: Norfolk public schools student team for acoustical research N87-20309
SPICULES
Phlegethon flow: A proposed origin for spicules and coronal heating N87-20933
SPIN DYNAMICS
Attitude motion of torque-free asymmetric dual-spin spacecraft
[AD-A175531] N87-20354
SPIN TESTS
Spin-tunnel investigation of a 1/15-scale model of an Australian trainer airplane
[NASA-TM-89049] N87-20240
SPIRAL GALAXIES
Ring galaxies: An investigation of the physical conditions in closely interacting systems N87-20858
SPLINE FUNCTIONS
Three-body calculations at Los Alamos
[DE87-001959] N87-20786
SPOT (FRENCH SATELLITE)
Remote sensing applications: Commercial issues and opportunities for space station --- SPOT N87-20626
SPRAY NOZZLES
Two-phase flow N87-20272
Effect of flame-tube head structure on combustion chamber performance N87-20275
SPRAYERS
The physics of fuel sprays. Volume 1: Experimental measurements
[AD-A175660] N87-20285
SPRINGS (ELASTIC)
Force magnitude and angular velocity fluctuation reduction in a spring-restrained, flexibly-supported four-bar mechanical linkage N87-20589
STABILITY
Stable response of damped linear systems, part 3 N87-20440
Stability, transition and turbulence
[NASA-CR-178258] N87-20500
Liquid drop stability for protein crystal growth in microgravity
[NASA-TP-2724] N87-20727
Remarks on the stability analysis of reactive flows
[NASA-CR-178269] N87-20780
STAGE SEPARATION
The Shock and Vibration Bulletin. Part 3: Invited Papers, Pyrotechnic Shock, Pyrotechnic Shock Workshop
[AD-A175226] N87-20602
Super*Zip (linear separation) shock characteristics N87-20605
Numerical simulation of Atlas-Centaur stage-separation shaped charge firing and structural response N87-20606
Summary of testing techniques N87-20614
STANDARDIZATION
On modern avionic and defense systems logistic support standardization and cost effectiveness N87-20761
STANDARDS
Institute for Materials Science Engineering, Polymers: Technical activities 1986
[PB87-136693] N87-20420
International system of units (SI)
[PB86-244159] N87-20444
Views of the world of pyrotechnic shock N87-20603
STAR CLUSTERS
Carbon and nitrogen abundances along the evolutionary sequence of M67 N87-20848
STAR FORMATION
The star-forming properties of violently interacting galaxies N87-20849
Molecular clouds in the outer galaxy N87-20854
STATE ESTIMATION
Mean-square error bounds for reduced-error linear state estimators
[NASA-TM-89441] N87-20291
Estimability and regulability of linear systems
[NASA-TM-89427] N87-20790
STATE VECTORS
Estimability and regulability of linear systems
[NASA-TM-89427] N87-20790
STATIC LOADS
Influence co-efficient testing as a substitute for modal survey testing of large space structures N87-20369
Structural dynamics: Buckling of ring-stiffened cylindrical shells with dynamic loads N87-20595
Evaluation of vibration specifications for static and dynamic material allowables N87-20600
STATIC STABILITY
Stability regions of relaxed static stability aircraft under control saturation constraints N87-20288
STATIONKEEPING
Wind and turbulence data for development of design criteria for unmanned high-altitude low-speed endurance aircraft
[NASA-CR-4065] N87-20699
STATISTICAL ANALYSIS
Spectral analysis of waves in Gulf of Tonkin described N87-20722
Statistical analysis of secondary particle distributions in relativistic nucleus-nucleus collisions
[NASA-CR-4054] N87-20813
Statistical aspects of solar flares
[NASA-TP-2714] N87-20947
STATISTICAL CORRELATION
Experimental evaluation of sub-cell turbulent models. Space-time correlations in a mixing layer
[ETN-87-99391] N87-20513
STATISTICAL DISTRIBUTIONS
Statistical properties of barium stars N87-20857
STATORS
Development of a rotor wake/vortex model. Volume 2: User's manual for computer program
[NASA-CR-174850-VOL-2] N87-20239
STEADY FLOW
A second order Godunov method for tactical missiles N87-20211
STEADY STATE
The variation of subgrain misorientation in aluminum deformed to large steady-state creep strains
[DE87-003238] N87-20415
A finite difference scheme for three-dimensional steady laminar incompressible flow
[NASA-TM-89851] N87-20504
Mathematical model of steady-state circulation in the south China Sea N87-20719
STELLAR ATMOSPHERES
Coronal diagnostics. N87-20915
STELLAR COMPOSITION
Abundances and kinematics of K giants in the galactic nuclear bulge N87-20856
STELLAR EVOLUTION
Linear nonadiabatic pulsations of homogeneous ZAMS stars
[DE87-003722] N87-20844

Carbon and nitrogen abundances along the evolutionary sequence of M67 N87-20848
STELLAR LUMINOSITY
UBVRI-photometry of the antiflare stars V586 Ori and IU Ori
[DE87-700760] N87-20845
STELLAR MASS
Linear nonadiabatic pulsations of homogeneous ZAMS stars
[DE87-003722] N87-20844
The acceleration and dissolution of stars moving through the blackbody radiation of a collapsing universe N87-20847
Self-consistent models of perfect triaxial galaxies N87-20859
STELLAR MASS EJECTION
Some crucial corona and prominence observations N87-20872
STELLAR MODELS
Self-consistent models of perfect triaxial galaxies N87-20859
STELLAR MOTIONS
Fiducial reference for the HIPPARCOS reference system
[NASA-CR-180250] N87-20842
The acceleration and dissolution of stars moving through the blackbody radiation of a collapsing universe N87-20847
STELLAR RADIATION
UBVRI-photometry of the antiflare stars V586 Ori and IU Ori
[DE87-700760] N87-20845
STELLAR SPECTRA
Ring galaxies: An investigation of the physical conditions in closely interacting systems N87-20858
STIFFENING
Composite repair techniques for J-stiffened composite fuselage structures N87-20186
STIRLING ENGINES
Conceptual design of a solar electric advanced Stirling power system
[DE87-005036] N87-20656
STOCHASTIC PROCESSES
Stochastic effects on oblique HF (High Frequencies) propagation
[AD-A176015] N87-20455
Modal parameter identification using adaptive digital filters N87-20583
A stochastic approach to project planning in an R and D environment
[DE87-005347] N87-20835
Evaluation of the performance of a geographically distributed data base management system using stochastic Petri nets
[ENST-86C002] N87-20837
Magnetic location of C IV events in the quiet network N87-20930
STORAGE BATTERIES
Use of lightweight composites for GAS payload structures N87-20307
STORAGE RINGS (PARTICLE ACCELERATORS)
A ring-cavity for a quadrupled Nd-YAG laser
[DE87-004175] N87-20547
STORM SURGES
Numerical simulation of storm surges in the east China Sea N87-20718
STORMS
The effect of heavy rain on an airfoil at high lift
[NASA-CR-178248] N87-20232
STORMS (METEOROLOGY)
The terminal area simulation system. Volume 1: Theoretical formulation
[NASA-CR-4046-VOL-1] N87-20255
Dynamical and thermodynamical characteristics of a squall-line determined from dual-Doppler data N87-20697
STRAIN ENERGY RELEASE RATE
Strain energy release rates of composite interlaminar end-notch and mixed-mode fracture: A sublaminate/ply level analysis and a computer code
[NASA-TM-89627] N87-20389
STRAIN GAGE BALANCES
Aerodynamic measurements and thermal tests of a strain-gage balance in a cryogenic wind tunnel
[NASA-TM-89039] N87-20517
STRATOSPHERE
Airborne lidar measurements of El Chichon stratospheric aerosols, January 1984
[NASA-RP-1175] N87-20663
STRESS (PHYSIOLOGY)
Effect of hypoxia on DNA synthesis and collagent content of regenerating skin N87-20742
STRESS ANALYSIS
Evaluation of vibration specifications for static and dynamic material allowables N87-20600
STRESS CONCENTRATION
Theoretical investigations of shear band formation in finite elasticity
[AD-A175657] N87-20572
STRESS WAVES
Studies of stress wave propagation in composites
[DE87-001493] N87-20396
STRESS-STRAIN RELATIONSHIPS
Theoretical investigations of shear band formation in finite elasticity
[AD-A175657] N87-20572
STRESSES
Strain energy release rates of composite interlaminar end-notch and mixed-mode fracture: A sublaminate/ply level analysis and a computer code
[NASA-TM-89627] N87-20389
STRONG INTERACTIONS (FIELD THEORY)
An investigation of the admixture of strong and weak interactions in the B10 (n, alpha) Li7 reaction with slow neutrons N87-20807
STRUCTURAL ANALYSIS
Dynamic modeling and optimal control design for large flexible space structures N87-20358
Solid mechanics program at ONR N87-20575
The Shock and Vibration Bulletin. Part 3: Invited Papers, Pyrotechnic Shock, Pyrotechnic Shock Workshop
[AD-A175226] N87-20602
STRUCTURAL DESIGN
Structural design of an in-line bolted joint for the space shuttle solid rocket motor case segments
[NASA-TM-89027] N87-20349
STRUCTURAL DESIGN CRITERIA
Advanced EVA system design requirements study: EVAS/space station system interface requirements
[NASA-CR-171981] N87-20351
Criteria and methodology for lightweight design of vehicle components
[LBF-TB-176(1986)] N87-20550
A model for the degradation of composite structures
[ONERA-RT-30/3043-RY-057-R] N87-20617
Wind and turbulence data for development of design criteria for unmanned high-altitude low-speed endurance aircraft
[NASA-CR-4065] N87-20699
STRUCTURAL PROPERTIES (GEOLOGY)
Wilson cycle studies
[NASA-CR-180503] N87-20664
STRUCTURAL STABILITY
Dynamic and thermal effects in very large space structures N87-20347
STRUCTURAL VIBRATION
Dynamic analysis of direct television satellite TV-SAT/TDF.1 N87-20360
Dynamic qualification of spacecraft by means of modal synthesis N87-20363
Low frequency vibration testing on satellites N87-20364
Benefits of passive damping as applied to active control of large space structures N87-20371
Multi-axis vibration tests on spacecraft using hydraulic exciters N87-20373
The pre-pulse in pyroshock measurement and analysis N87-20604
SUBROUTINES
On the use of CORLIB subroutines for the solution of a model fluid flow problem
[DE87-005285] N87-20509
A model and computer code for the Monte Carlo simulation of relativistic electron and positron penetration through matter
[USIP-86-11] N87-20808
SUBSONIC FLOW
Euler solution for a complete fighter aircraft at sub- and supersonic speed N87-20216
SUBSTRATES
Fabrication of microwave devices on ultrathin active GaAs substrates
[FOA-C-30431-3.2] N87-20494
CO oxidation studies over supported noble metal catalysts and single crystals: A review N87-20530
Rare isotope studies involving catalytic oxidation of CO over platinum-tin oxide N87-20538
Studies of CO oxidation on Pt/SnO2 catalyst in a surrogate CO2 laser facility N87-20539
SUDDEN IONOSPHERIC DISTURBANCES
Solar-geophysical data number 506, October 1986. Part 1: (Prompt reports). Data for September 1986, August 1986 and late data
[PB87-126389] N87-20948
SUN
Theory and simulation of the evolution of the large-scale solar magnetic field N87-20670
Coronal and Prominence Plasmas
[NASA-CP-2442] N87-20671
Some crucial corona and prominence observations N87-20872
Heating of the stellar corona N87-20873
Formation and support of prominence N87-20874
Can prominences form in current sheets N87-20876
Condensation modes in magnetized plasmas N87-20877
Filament formation due to photospheric shear N87-20878
Formation of active region and quiescent prominence magnetic field configurations N87-20879
Numerical simulations of a siphon mechanism for quiescent prominence formation N87-20880
Alfven-wave dissipation: A support mechanism for quiescent prominences N87-20881
Static current-sheet models of quiescent prominences N87-20882
Recent observations of the formation of filaments N87-20883
On the formation of active region prominences (H alpha filaments) N87-20884
Diagnostics and structure N87-20885
Temperatures of quiescent prominences measured from hydrogen Paschen and CaII IR lines N87-20886
Dark filaments observed at 8.3mm and 3.1mm wavelength N87-20887
VLA observations of slar filaments at 6 and 20 cm wavelengths N87-20888
The microwave structure of quiescent solar filaments at high resolution N87-20889
The prominence-corona interface and its relationship to the chromosphere-corona transition N87-20891
Thermal stability analysis of the fine structure of solar prominences N87-20892
The density and thickness of quiescent prominences N87-20893
Partial redistribution effects in the formation of hydrogen lines in quiescent prominences N87-20894
Non-LTE hydrogen-line formation in moving prominences N87-20895
Vertical motions in the quiescent prominences observed in the He I Lambda10830Angstrom line N87-20896
Small-scale coronal structure, part 3 N87-20922
Compact, variable, moving sources observed on the sun at 2 centimeters wavelength N87-20925
The association of chromospheric and coronal phenomena with the evolution of the quiet sun magnetic fields
[ESD-TR-84-611] N87-20926
SUNSPOT CYCLE
Filament disappearances N87-20903
SUNSPOTS
Theory and simulation of the evolution of the large-scale solar magnetic field N87-20670
On the formation of active region prominences (H alpha filaments) N87-20884
Filament eruption connected to protospheric activity N87-20906
SUPERCONDUCTIVITY
Electron tunneling studies of Mo/(sub)1-xRe/(sup)x/: Enhancement of superconductivity by a resonance mode
[DE87-003048] N87-20484
Proximity-induced Josephson effect and its application to heavy fermion superconductor UBe-13
[DE87-003049] N87-20485
Highlights from the physics in metallic superlattices
[DE87-004657] N87-20625
High field properties of SnMo6S8 and PbMo6S8 ribbons prepared using a vapor transport technique
[DE87-004707] N87-20626
Transient heat transfer to supercritical helium at low temperatures
[ETN-87-99321] N87-20632
SUPERCONDUCTORS
Proximity-induced Josephson effect and its application to heavy fermion superconductor UBe-13
[DE87-003049] N87-20485
SUPERCRITICAL FLOW
Transient heat transfer to supercritical helium at low temperatures
[ETN-87-99321] N87-20632
SUPERCRITICAL WINGS
Investigation of transonic region of high dynamic response encountered on an elastic supercritical wing
[NASA-TM-89121] N87-20236
SUPERLATTICES
Highlights from the physics in metallic superlattices
[DE87-004657] N87-20625
SUPERPLASTICITY
Material characterization of superplastically formed titanium (Ti-6Al-2Sn-4Zr-2Mo) sheet
[NASA-TP-2674] N87-20407
Superplasticity of metals with special reference to Ti-6Al-4V
[DE87-005795] N87-20419
SUPERSONIC COMBUSTION RAMJET ENGINES
Application of CARS to scramjet combustion
[NASA-CR-178245] N87-20400

SUPERSONIC FLOW
An assessment of the use of low-order panel methods for the calculation of supersonic flows N87-20204
The integration of computational fluid dynamics into the military aircraft design process N87-20210
A second order Godunov method for tactical missiles N87-20211
Euler solution for a complete fighter aircraft at sub- and supersonic speed N87-20216
A multiple zone method for supersonic tactical missiles
[AD-A175938] N87-20244
Surface pressure measurements on a double delta Wing/Body configuration at Mach 2 and Mach 3 (WTR 1396)
[AD-A175951] N87-20245
Acta mechanica sinica (selected articles)
[AD-A176240] N87-20246
Study of compressibility effects on supersonic free flow
[ETN-87-99392] N87-20251
An application of computational fluid dynamics to the design of optimum ramjet powered missile components N87-20338
Supersonic flow induced cavity acoustics N87-20601
An asymptotic analysis of supersonic reacting mixing layers
[NASA-CR-178266] N87-20756

SUPERSONIC SPEED
Investigation of leading-edge flap performance on delta and double-delta wings at supersonic speeds
[NASA-TP-2656] N87-20233

SUPERSONIC WIND TUNNELS
Surface pressure measurements on a double delta Wing/Body configuration at Mach 2 and Mach 3 (WTR 1396)
[AD-A175951] N87-20245

SUPPORTS
Design study of advanced model support systems for the National Transonic Facility (NTF)
[NASA-CR-178214] N87-20297

SUPPRESSORS
Operation of transversely excited N2O lasers
[AD-D012583] N87-20543

SURFACE COOLING
Laboratory investigation of lightweight heater tape for shuttle propellant tank
[AD-A175997] N87-20345

SURFACE IONIZATION
Study of surface discharges
[ONERA-RF-11/7236-PY] N87-20707

SURFACE ROUGHNESS EFFECTS
The aerodynamic effects of a serrated strip near the leading edge of an airfoil
[ETN-87-99480] N87-20248

SURFACE TEMPERATURE
Experimental measurement of thin plate SS 304 GTAW weld pool surface temperatures
[DE87-004545] N87-20561

SURFACE TO AIR MISSILES
Control aspects of the launch phase of a vertically-launched short-range surface-to-air missile
[ETN-87-99478] N87-20341
A study of the methods used to carry out RF telemetry testing of surface-to-air missiles
[ETN-87-99481] N87-20346

SURFACE WAVES
Acoustic scattering from composite wind-wave surfaces II: Backscatter cross sections and Doppler effects at high frequencies and small angles for 'bubble-free' regimes
[AD-A176081] N87-20715
Methods of frequency spectrum estimation of sea water compared N87-20725
Phase speed of wind-wave component studied N87-20726

SURVIVAL
A preliminary study into the constant drag parachute for aircrew escape systems
[BU-345] N87-20256

SWITCHING
Low pass PI section digital phase shifter apparatus
[AD-D012553] N87-20483

SYMMETRY
A numerical study of some spherically-symmetric and axisymmetric cosmological models N87-20653

SYNCHRONISM
Adaptive mutual interference suppression method
[AD-D012552] N87-20459

SYNCHRONOUS PLATFORMS
Working group on Earth observation requirements for the Polar Orbiting Platform Elements of the International Space Station (the POPE Working Group) N87-20625
Panel report on new approaches to calibration and validation — Columbus polar platforms N87-20638

SYNCHRONOUS SATELLITES
The use of visible data for improving VAS satellite soundings N87-20620

SYNCHROTRON RADIATION
Development of optical thin film technology for lasers and synchrotron radiation
[DE87-701254] N87-20817

SYNOPTIC MEASUREMENT
Large scale structure of the corona N87-20909
Synoptic study of the corona at meter wavelength N87-20911

SYNTHESIS (CHEMISTRY)
Effect of hypoxia on DNA synthesis and collagent content of regenerating skin N87-20742

SYSTEM IDENTIFICATION
Modal-survey testing for system identification and dynamic qualification of spacecraft structures N87-20365

SYSTEMS ANALYSIS
Design and analysis of advanced flight planning concepts
[NASA-CR-4063] N87-20253
A systems-level performance history of get away specials after 25 space shuttle missions N87-20314
Large space antennas: A systems analysis case history
[NASA-TM-89072] N87-20352
Unique bit-error-rate measurement system for satellite communication systems
[NASA-TP-2699] N87-20448
Space station structures and dynamics test program
[NASA-TP-2710] N87-20568
A computer simulator for development of engineering system design methodologies
[NASA-TM-89109] N87-20755
Structural properties of linear periodic systems
[REPT-86-004-REV] N87-20788
Information-preserving models of physics and computation
[DE87-005354] N87-20793
An astrometric facility for planetary detection on the space station
[NASA-TM-89436] N87-20841

SYSTEMS ENGINEERING
Dynamic analysis of direct television satellite TV-SAT/TDF.1 N87-20360
Engineering thrust areas, 1987
[DE87-004443] N87-20441
Activities report of the Department of Systems and Communications
[ENST-86D002] N87-20466
System architecture of MMIC-based large aperture arrays for space application
[NASA-TM-89840] N87-20468
Flat-plate solar array project. Volume 6: Engineering sciences and reliability
[NASA-CR-180664] N87-20651
A computer simulator for development of engineering system design methodologies
[NASA-TM-89109] N87-20755

SYSTEMS INTEGRATION
Simulation of an integrated fire and flight control system for air-to-air gunnery
[ETN-87-99479] N87-20293
Advanced EVA system design requirements study: EVAS/space station system interface requirements
[NASA-CR-171981] N87-20351
Qualification of the faint object camera N87-20359

SYSTEMS SIMULATION
A model and computer code for the Monte Carlo simulation of relativistic electron and positron penetration through matter
[USIP-86-11] N87-20808

T

TAIL ASSEMBLIES
Battle damage repair of composite structures N87-20189

TAKEOFF
Development of a takeoff performance monitoring system
[NASA-CR-178255] N87-20264

TASKS
Investigation of microstructure of arbitrary motions of operator N87-20752

TAYLOR INSTABILITY
Calculation of Rayleigh-Taylor flows using vortex blobs
[DE87-002551] N87-20507

TEA LASERS
Review of the frequency stabilization of TEA CO2 laser oscillators N87-20523
High repetition rate sealed CO2 TEA lasers using heterogeneous catalysts N87-20529
Operation of transversely excited N2O lasers
[AD-D012583] N87-20543

TECHNOLOGY ASSESSMENT
An advanced technology space station for the year 2025, study and concepts
[NASA-CR-178208] N87-20340
Development of a computational aero/fluids analysis system
[NASA-CR-179046] N87-20343
Land mobile communications satellite missions (LAMOCOSAMIS), executive summary
[ESA-CR(P)-2302-VOL-6] N87-20463
Land mobile satellite communication system. Volume 1: Executive summary
[ITS-TR-043/86-VOL1] N87-20464
Feasibility of a phosphoric acid fuel cell basic technology program
[DE87-001045] N87-20490
Structures and Dynamics Division research and technology plans for FY 1987 and accomplishments for FY 1986
[NASA-TM-89141] N87-20570
State-of-the-art assessment of structural dynamic response analysis methods (DYNAS) N87-20578
The Shock and Vibration Bulletin. Part 3: Invited Papers, Pyrotechnic Shock, Pyrotechnic Shock Workshop
[AD-A175228] N87-20602
Views of the world of pyrotechnic shock N87-20603
State-of-the-art accelerometer characteristics for pyrotechnic shock measurement N87-20606
Multi-axis transient shock simulation using mechanical pulse generators N87-20613
Flat-plate solar array project of the US Department of Energy's National Photovoltaics Program: Ten years of progress
[NASA-CR-180507] N87-20644
The concentration principle applied to spaceborne solar arrays. AGORA mission: Studies synthesis
[SNIAS-959-CA/CG] N87-20657

TECHNOLOGY TRANSFER
The Shock and Vibration Digest, Volume 19, No. 2 N87-20435
The Oak Ridge National Laboratory's Robotics and Intelligent Systems Program
[DE87-004627] N87-20774

TECHNOLOGY UTILIZATION
Composites review
[NASA-TT-20008] N87-20388
European utilization aspects studies — space stations N87-20624

TELECOMMUNICATION
Flexible satellite communications systems simulator standard device groups
[AD-A175944] N87-20454
Activities report of the Department of Systems and Communications
[ENST-86D002] N87-20466

TELEPHONY
Land mobile communications satellite mission (LAMOCOSAMIS) Task 1: Market study
[ESA-CR(P)-2302-VOL-1] N87-20462
Land mobile communications satellite missions (LAMOCOSAMIS), executive summary
[ESA-CR(P)-2302-VOL-6] N87-20463

TEMPERATURE DISTRIBUTION
Continental shelf processes affecting the oceanography of the South Atlantic Bight
[DE87-005303] N87-20716

TEMPERATURE EFFECTS
Temperature effects on nickel/iron battery characteristics
[DE87-004930] N87-20489

TEMPERATURE GRADIENTS
Temperature shift considerations for damping materials N87-20593

TEMPERATURE MEASUREMENT
Experimental measurement of thin plate SS 304 GTAW weld pool surface temperatures
[DE87-004545] N87-20561
Hydrologic features in cyclonic eddy region of northern east China Sea in cold seasons N87-20709
Moored current meter and temperature-pressure recorder measurements from the Western North Atlantic (high energy benthic boundary layer and abyssal circulation experiments 1983-1984), volume 39
[AD-A176014] N87-20713
Existence seen of cyclonic eddy in northern east China Sea N87-20721
Diagnostics and structure N87-20685

TENSILE CREEP
Material characterization of superplastically formed titanium (Ti-6Al-2Sn-4Zr-2Mo) sheet
[NASA-TP-2674] N87-20407

TENSILE STRENGTH
Design study of advanced model support systems for the National Transonic Facility (NTF)
[NASA-CR-178214] N87-20297
TENSILE TESTS
Baseline tensile tests of composite materials for LDEF (Long Duration Exposure Facility) exposure
[NASA-TM-89069] N87-20386
TERNARY SYSTEMS
Determination of the ternary viscosity diagram NaCl-KCl-LiCl by the flow method
[INSA-IDTC1-8604] N87-20403
TEST EQUIPMENT
The hypercluster: A parallel processing test-bed architecture for computational mechanics applications
[NASA-TM-89823] N87-20767
TEST FACILITIES
Structures and Dynamics Division research and technology plans for FY 1987 and accomplishments for FY 1986
[NASA-TM-89141] N87-20570
Conceptual design of a solar electric advanced Stirling power system
[DE87-005036] N87-20656
THEORETICAL PHYSICS
The fifth force — fundamental interactions
[DE87-004612] N87-20694
Algebra and topology for applications to physics
[NASA-TT-20056] N87-20784
Information-preserving models of physics and computation
[DE87-005354] N87-20793
THERMAL ANALYSIS
Aerodynamic measurements and thermal tests of a strain-gage balance in a cryogenic wind tunnel
[NASA-TM-89039] N87-20517
Computational analyses of crystal growth
[NASA-CR-179027] N87-20820
THERMAL CONDUCTIVITY
G-300: The first French Getaway Special microgravity measurements of fluid thermal conductivity N87-20330
Analysis of experimental determinations of the thermal conductivity of CBCF (Carbon-Bonded Carbon Fiber) insulation
[DE87-004025] N87-20393
On the thermal durability of solar prominences, or how to evaporate a prominence N87-20905
THERMAL CYCLING TESTS
Advanced composite combustor structural concepts program
[NASA-CR-174733] N87-20387
THERMAL EXPANSION
Characterizing thermal/mechanical properties of filament wound composites
[AD-A176238] N87-20392
THERMAL INSULATION
Analysis of experimental determinations of the thermal conductivity of CBCF (Carbon-Bonded Carbon Fiber) insulation
[DE87-004025] N87-20393
Adhesion of a silicone based insulating material to rocket motors
[FOA-C-20635-2.1] N87-20429
THERMAL NEUTRONS
Capture of thermal neutrons B10 and Li6: Applications in spectroscopy and in the study of weak nucleon interactions
[ECN-184] N87-20803
General introduction to capture of thermal neutrons in B10 and Li6: Applications in spectroscopy and in the study of weak nucleon interactions N87-20804
Investigation of excited states of Li7 by means of thermal neutron capture N87-20805
Investigation of excited states of B11 and Li7 by means of thermal neutron capture on B10 nuclei N87-20806
An investigation of the admixture of strong and weak interactions in the B10 (n, alpha) Li7 reaction with slow neutrons N87-20807
THERMAL PLASMAS
VLA observations of coronal bright points at 6 and 20 cm wavelengths N87-20924
THERMAL SHOCK
Views of the world of pyrotechnic shock N87-20603
THERMAL STABILITY
Thermal stability analysis of the fine structure of solar prominences N87-20892
A numerical study of the thermal stability of low-lying coronal loops N87-20931
THERMAL STRESSES
Dynamic and thermal effects in very large space structures N87-20347
THERMODYNAMIC PROPERTIES
Thermodynamics and combustion modeling N87-20274
Investigation of thermal-fluid mechanical characteristics of the capillary pump and the pumped two-phase loop
[NASA-CR-180509] N87-20557
Dynamical and thermodynamical characteristics of a squall-line determined from dual-Doppler data N87-20697
THERMODYNAMICS
NASA-Chinese Aeronautical Establishment (CAE) Symposium
[NASA-CP-2433] N87-20267
Thermodynamics and combustion modeling N87-20274
Theoretical kinetic computations in complex reacting systems N87-20277
Calculation of thermomechanical fatigue life based on isothermal behavior
[NASA-TM-88864] N87-20565
Thermodynamic data of intermetallic compounds
[DE87-701244] N87-20831
Can prominences form in current sheets N87-20876
THERMOPLASTIC RESINS
High performance thermoplastics: A review of neat resin and composite properties
[NASA-TM-89104] N87-20390
Moisture absorption in graphite/organic-matrix composites
[DE87-004229] N87-20394
THERMOSETTING RESINS
Moisture absorption in graphite/organic-matrix composites
[DE87-004229] N87-20394
THERMOSPHERE
Upper and Middle Atmospheric Density Modeling Requirements for Spacecraft Design and Operations
[NASA-CP-2460] N87-20665
Limitations to modeling the thermosphere and exosphere N87-20674
Empirical modeling of the thermosphere: An overview N87-20675
Forecasts of solar and geomagnetic activity N87-20677
Six reasons why thermospheric measurements and models disagree N87-20688
THICKNESS
The density and thickness of quiescent prominences N87-20893
THIN FILMS
Manufacturing polymer thin films in a micro-gravity environment N87-20304
USC/AIAA student get away special project liquid droplet collector experiment N87-20316
Microstructure of metastable metallic alloy films produced by laser breakdown chemical vapor deposition and ion implantation
[DE87-002914] N87-20411
Investigation of PTFE transfer films by infrared emission spectroscopy and phase-locked ellipsometry
[NASA-TM-89844] N87-20421
Development of optical thin film technology for lasers and synchrotron radiation
[DE87-701254] N87-20617
Rapid thermal annealing of Amorphous Hydrogenated Carbon (a-C:H) films
[NASA-TM-89859] N87-20821
THIN PLATES
Experimental measurement of thin plate SS 304 GTAW weld pool surface temperatures
[DE87-004545] N87-20561
THOMSON SCATTERING
Three-dimensional magnetostatic models of the large-scale corona N87-20914
THREE DIMENSIONAL BODIES
Numerical grid generation around complete aircraft configurations N87-20202
Numerical investigation of the laminar boundary layer on a 3-D body started impulsively from rest N87-20220
Applications of RAE viscous flow methods near separation boundaries for three-dimensional wings in transonic flow N87-20224
THREE DIMENSIONAL FLOW
A discussion on a mesh generation technique applicable to complex geometries N87-20201
New numerical techniques in the method of singularities for application to complex three-dimensional configurations N87-20205
Numerical simulation of internal and external inviscid and viscous 3-D flow fields N87-20213
Using the boundary-layer equations in three-dimensional viscous flow simulation N87-20222
Computation of three-dimensional flows by viscous-inviscid interation using the MZM method N87-20223
Application of the Navier-Stokes equations to solve aerodynamic problems N87-20225
Simulation of three-dimensional transonic flow with separation past a hemisphere cylinder configuration N87-20230
Wing-nacelle interactions. Program 1985. Part two: Development of a finite element code for an isolated nacelle
[ONERA-RTS-21/3271-AY] N87-20250
Experiments and modeling of dilution jet flow fields N87-20276
A finite difference scheme for three-dimensional steady laminar incompressible flow
[NASA-TM-89851] N87-20504
Conversion of ARC-1 to an implicit Navier-Stokes solver
[AD-A175967] N87-20505
THRUST MEASUREMENT
Decoupled bellmouth: An alternate method of measuring thrust in the sea level test cell
[AD-A175616] N87-20284
THRUST VECTOR CONTROL
Control aspects of the launch phase of a vertically-launched short-range surface-to-air missile
[ETN-87-99478] N87-20341
Conceptual design and integration of a space station resistojet propulsion assembly
[NASA-TM-89847] N87-20378
THUNDERSTORMS
The terminal area simulation system. Volume 2: Verification cases
[NASA-CR-4047-VOL-2] N87-20252
Definition and use of sensors for measuring electrical conductivity in thunderclouds
[ONERA-NT-1986-4] N87-20705
Lightning strikes on aircraft. Exploitation of Landes (France)-Front '84 campaign and complementary development of airborne electrical sensors
[ONERA-RF-91/7154-PY] N87-20706
TIME
Time-partitioning simulation models for calculation on parallel computers
[NASA-TM-89850] N87-20766
TIME DEPENDENCE
A numerical study of the Weis-Fogh mechanism N87-20197
TIME DIVISION MULTIPLE ACCESS
Satellite analog FDMA/FM to digital TDMA conversion
[NASA-CR-179605] N87-20467
TIME MARCHING
Computation of three-dimensional flows by viscous-inviscid interation using the MZM method N87-20223
TIME MEASUREMENT
Timing millisecond pulsars N87-20855
TIME SIGNALS
NAVSAT time synchronization simulation study
[ESA-CR(P)-2305] N87-20376
TIN
Ground-state proton radioactivity in the domain of neutron-poor nuclei heavier than tin
[ETN-87-99342] N87-20811
TIN OXIDES
The oxidation of carbon monoxide using a tin oxide catalyst N87-20528
A review of tin oxide-based catalytic systems: Preparation, characterization and catalytic behavior N87-20537
Rare isotope studies involving catalytic oxidation of CO over platinum-tin oxide N87-20538
Studies of CO oxidation on Pt/SnO2 catalyst in a surrogate CO2 laser facility N87-20539
Studies of long-life pulsed CO2 laser with Pt/SnO2 catalyst N87-20540
Characterization of Pt/SnO2 catalysts for CO oxidation N87-20541
TITANIUM
Hydrogen embrittlement of titanium and its alloys: A literature review
[DE87-750405] N87-20410
TITANIUM ALLOYS
AGARD (Advisory Group for Aerospace Research and Development) engine disc material cooperative test
[AD-A175533] N87-20283
Material characterization of superplastically formed titanium (Ti-6Al-2Sn-4Zr-2Mo) sheet
[NASA-TP-2674] N87-20407
Hydrogen embrittlement of titanium and its alloys: A literature review
[DE87-750405] N87-20410
Superplasticity of metals with special reference to Ti-6Al-4V
[DE87-005795] N87-20419
Shot peening for Ti-6Al-4V alloy compressor blades
[NASA-TP-2711] N87-20566

TOPOGRAPHY
Linear baroclinic instability in the presence of large scale topography
[NASA-CR-4057] N87-20700
TOPOLOGY
Algebra and topology for applications to physics
[NASA-TT-20056] N87-20784
The topological description of coronal magnetic fields N87-20936
TORNADOES
The terminal area simulation system. Volume 2: Verification cases
[NASA-CR-4047-VOL-2] N87-20252
TORQUE
Attitude motion of torque-free asymmetric dual-spin spacecraft
[AD-A175531] N87-20354
Hubble Space Telescope N87-20670
TORSIONAL VIBRATION
A new approach for gearbox modelling in finite element analyses of torsional vibration of gear-branched propulsion systems N87-20591
TOXICOLOGY
USSR report: Life sciences. Biomedical and behavioral sciences
[JPRS-UBB-87-003] N87-20751
TRACKING (POSITION)
Operator work capacity in tracking system when submitted to antiorthostatic hypokinesia N87-20736
Investigation of microstructure of arbitrary motions of operator N87-20752
TRACKING RADAR
Turnaround control for mechanically scanned radar antennas
[AD-D012563] N87-20457
TRAILING EDGES
Comparison of finite difference calculations of a large region of recirculating flow near an airfoil trailing edge N87-20218
TRAINING AIRCRAFT
Spin-tunnel investigation of a 1/15-scale model of an Australian trainer airplane
[NASA-TM-89049] N87-20240
TRAJECTORY ANALYSIS
The GRAM-3 model N87-20686
TRANSFERRING
Hydrogen degradation of pipeline steels
[DE87-005585] N87-20414
Investigation of PTFE transfer films by infrared emission spectroscopy and phase-locked ellipsometry
[NASA-TM-89844] N87-20421
TRANSIENT LOADS
Influence co-efficient testing as a substitute for modal survey testing of large space structures N87-20369
TRANSIENT RESPONSE
Hybrid methods for rotordynamic analysis
[NASA-CR-179035] N87-20553
Blade damping measurements in a spin rig with nozzle passing excitation simulated by electromagnets N87-20590
A preliminary transient-fault experiment on the SIFT computer system
[NASA-TM-89058] N87-20770
TRANSITION
Stability, transition and turbulence
[NASA-CR-178258] N87-20500
TRANSMISSION LINES
Propagation characteristics of some novel coplanar waveguide transmission lines on GaAs at MM-wave frequencies
[NASA-TM-89839] N87-20469
TRANSMISSIONS (MACHINE ELEMENTS)
Flexibility effects on tooth contact location in spiral bevel gear transmissions
[NASA-CR-4055] N87-20552
Vibration characteristics of OH-58A helicopter main rotor transmission
[NASA-TP-2705] N87-20555
Experimental and analytical evaluation of dynamic load and vibration of a 2240-kW (300-hp) rotorcraft transmission
[NASA-TM-88975] N87-20556
TRANSMITTANCE
Atmospheric contrast transmittance monitor
[AD-D012555] N87-20520
TRANSMITTERS
Frequency stabilization in injection controlled pulsed CO2 lasers N87-20527
An overview of DREV's activities on pulsed CO2 laser transmitters: Frequency stability and lifetime aspects N87-20542
TRANSONIC FLOW
Computation of transonic flow over porous airfoils N87-20194
The prediction of transonic loading on advancing helicopter rotors N87-20206
Prediction of wing-body-store aerodynamics using a small perturbation method and a grid embedding technique N87-20207
Matrics, transonic potential flow calculations about transport aircraft N87-20208
Analysis of the F-16 flow field by a block grid Euler approach N87-20217
Applications of RAE viscous flow methods near separation boundaries for three-dimensional wings in transonic flow N87-20224
Transonic Navier-Stokes wing solution using a zonal approach. Part 1: Solution methodology and code validation N87-20228
Transonic Navier-Stokes wing solutions using a zonal approach. Part 2: High angle-of-attack simulation N87-20229
Simulation of three-dimensional transonic flow with separation past a hemisphere cylinder configuration N87-20230
Unsteady transonic flow calculations for realistic aircraft configurations
[NASA-TM-89120] N87-20234
Study of the unsteady pressure field on the RA16SC1 profile in vibrating condition
[ONERA-RTS-17/3423-AY] N87-20249
TRANSONIC WIND TUNNELS
Computations for the 16-foot transonic tunnel, NASA, Langley Research Center, revision 1
[NASA-TM-88319-REV-1] N87-20294
Design study of advanced model support systems for the National Transonic Facility (NTF)
[NASA-CR-178214] N87-20297
TRANSPORT AIRCRAFT
Matrics, transonic potential flow calculations about transport aircraft N87-20208
TRANSPORT PROPERTIES
High field properties of SnMo6S8 and PbMo6S8 ribbons prepared using a vapor transport technique
[DE87-004707] N87-20826
TRANSPORT THEORY
Theory and simulation of the evolution of the large-scale solar magnetic field N87-20870
TRANSPORTATION ENERGY
Fuel cells in transportation
[DE87-003746] N87-20654
TRAVELING WAVE TUBES
Design, fabrication and performance of small, graphite electrode, multistage depressed collectors with 200-W, CW, 8- to 18-GHz traveling-wave tubes
[NASA-TP-2693] N87-20474
TREMORS
Investigation of microstructure of arbitrary motions of operator N87-20752
TRENDS
Composites review
[NASA-TT-20008] N87-20388
TROPICAL METEOROLOGY
On requirements for a satellite mission to measure tropical rainfall
[NASA-RP-1183] N87-20701
TROPICAL STORMS
On requirements for a satellite mission to measure tropical rainfall
[NASA-RP-1183] N87-20701
TRUSSES
Modeling of joints for the dynamic analysis of truss structures
[NASA-TP-2661] N87-20567
TUNABLE LASERS
Opportunities and problems in wavelength tunable lasers based on vacancy defects in refractory oxides
[DE87-002406] N87-20545
TUNING
The in-situ calibration of a bilateral space-fed phased array antenna
[AD-A176069] N87-20456
Characteristic decomposition and the multivariable generalization of predictive self-tuning control
[OUEL-1651/86] N87-20776
TURBINE BLADES
Lewis inverse design code (LINDES): Users manual
[NASA-TP-2676] N87-20238
Two-dimensional flow computation in straight blade arrays — turbine blades
[ONERA-RT-35/1621-RY-053-R] N87-20511
Blade damping measurements in a spin rig with nozzle passing excitation simulated by electromagnets N87-20590
TURBOFAN ENGINES
Numerical study of combustion processes in afterburners N87-20269
Experimental investigation of piloted flameholders N87-20278
Decoupled bellmouth: An alternate method of measuring thrust in the sea level test cell
[AD-A175616] N87-20284
TURBOMACHINERY
Composite grid and finite-volume LU implicit scheme for turbine flow analysis
[NASA-TM-89828] N87-20235
TURBOSHAFTS
Contingency power for small turboshaft engines using water injection into turbine cooling air
[NASA-TM-89817] N87-20280
TURBULENCE
Stability, transition and turbulence
[NASA-CR-178258] N87-20500
TURBULENT BOUNDARY LAYER
The effects of large-eddy manipulator devices on the turbulent spot and the turbulent boundary layer N87-20497
A holographic interferometry study of an axisymmetric shock-wave/boundary-layer strong interaction flow N87-20498
Study of the development of a compressible turbulent boundary layer on a porous and rough wall
[ETN-87-99390] N87-20512
TURBULENT FLOW
Study of compressibility effects on supersonic free flow
[ETN-87-99392] N87-20251
Modeling turbulent, reactig flow N87-20270
Experimental evaluation of sub-cell turbulent models. Space-time correlations in a mixing layer
[ETN-87-99391] N87-20513
TURBULENT JETS
Prediction of recirculation zones in isothermal coaxial jet flows relevant to combustors
[NASA-CR-4064] N87-20501
TWO DIMENSIONAL FLOW
Numerical solutions of unsteady flow past rotor sections N87-20198
Multigrid calculation of boundary-fitted orthogonal coordinates with applications to unsteady flows N87-20237
Numerical simulation of separated flows past bluff bodies N87-20499
Two-dimensional flow computation in straight blade arrays — turbine blades
[ONERA-RT-35/1621-RY-053-R] N87-20511
Experimental validation of a two-dimensional shear-flow model for determining acoustic impedance
[NASA-TP-2679] N87-20798
TWO PHASE FLOW
Two-phase flow N87-20272
Investigation of thermal-fluid mechanical characteristics of the capillary pump and the pumped two-phase loop
[NASA-CR-180509] N87-20557
TYPE 3 BURSTS
The propagation of an electron beam through the solar corona N87-20946
TYPHOONS
Numerical simulation of storm surges in the east China Sea N87-20718

U

U.S.S.R. SPACE PROGRAM
USSR report: Space Biology and Aerospace Medicine, Volume 20, No. 3, May - June 1986
[JPRS-USB-86-005] N87-20731
Space biology and medicine on the twenty-fifth anniversary of the first spaceflight of Yuriy Alekseyevich Gagarin N87-20732
ULTRAHIGH FREQUENCIES
NUSAT update N87-20312
Timing millisecond pulsars N87-20855
ULTRALIGHT AIRCRAFT
Materials selection and design study of a composite microlight wing structure
[BU-335] N87-20263
ULTRASONIC TESTS
Interpretation of right heart kinetocardiogram N87-20744
ULTRASONICS
The acousto-ultrasonic approach
[NASA-TM-89843] N87-20562
ULTRAVIOLET SPECTRA
Constraints on filament models deduced from dynamical analysis N87-20897
Searching the UVSP database and a list of experiments showing mass motions N87-20899
UNDERWATER ACOUSTICS
Underwater acoustic modeling techniques N87-20436
Acoustic scattering from composite wind-wave surfaces II: Backscatter cross sections and Doppler effects at high frequencies and small angles for 'bubble-free' regimes
[AD-A176081] N87-20715

UNIQUENESS
Uniqueness of Gibbs measures and absorption probabilities
[CWI-MS-R8610] N87-20789
UNIVERSE
Problems in quantum cosmology N87-20846
The acceleration and dissolution of stars moving through the blackbody radiation of a collapsing universe N87-20847
Computer simulation and analysis of spatial galaxy distributions N87-20851
A numerical study of some spherically-symmetric and axisymmetric cosmological models N87-20853
The large-scale peculiar velocity field in flat models of the universe
[DE87-005402] N87-20864
Double inflation: A possible resolution of the large-scale structure problem
[DE87-005403] N87-20865
Thermal production of not so invisible axions in the early universe
[DE87-005404] N87-20866
UNIVERSITIES
The 1986 Get Away Special Experimenter's Symposium
[NASA-CP-2438] N87-20302
UNSTEADY FLOW
Numerical solutions of unsteady flow past rotor sections N87-20196
Numerical investigation of the laminar boundary layer on a 3-D body started impulsively from rest N87-20220
Simulation of three-dimensional transonic flow with separation past a hemisphere cylinder configuration N87-20230
Unsteady transonic flow calculations for realistic aircraft configurations
[NASA-TM-89120] N87-20234
Multigrid calculation of boundary-fitted orthogonal coordinates with applications to unsteady flows N87-20237
Study of the unsteady pressure field on the RA16SC1 profile in vibrating condition
[ONERA-RTS-17/3423-AY] N87-20249
URANIUM
Impact energy relationships for directly rolled uranium strip
[DE87-005789] N87-20418
USER MANUALS (COMPUTER PROGRAMS)
Lewis inverse design code (LINDES): Users manual
[NASA-TP-2676] N87-20238
Development of a rotor wake/vortex model. Volume 2: User's manual for computer program
[NASA-CR-174850-VOL-2] N87-20239
Users manual for nickel cadmium battery expert system
[NASA-CR-179032] N87-20470
Program maintenance manual for nickel cadmium battery expert system, version 1
[NASA-CR-179033] N87-20472
USER REQUIREMENTS
Hitchhiker-G: A new carrier system for attached shuttle payloads N87-20320
Advanced EVA system design requirements study: EVAS/space station system interface requirements
[NASA-CR-171981] N87-20351
Land mobile communications satellite missions (LAMOCOSAMIS), executive summary
[ESA-CR(P)-2302-VOL-6] N87-20463
Land mobile satellite communication system. Volume 2: Traffic analysis and market demand for the land mobile communications system in the European scenario
[ITS-TR-043/86-VOL-2] N87-20485
European utilization aspects studies — space stations N87-20624
Guide to sharing personal computer resources via local area networks, revised
[DE86-016066] N87-20772

V

VACANCIES (CRYSTAL DEFECTS)
Opportunities and problems in wavelength tunable lasers based on vacancy defects in refractory oxides
[DE87-002406] N87-20545
VACUUM DEPOSITION
Development of optical thin film technology for lasers and synchrotron radiation
[DE87-701254] N87-20817
VALVES
Airspeed sensing pressure valve system
[AD-D012569] N87-20266
VANADIUM
Superplasticity of metals with special reference to Ti-6Al-4V
[DE87-005795] N87-20419
Shot peening for Ti-6Al-4V alloy compressor blades
[NASA-TP-2711] N87-20566
VAPOR DEPOSITION
Microstructure of metastable metallic alloy films produced by laser breakdown chemical vapor deposition and ion implantation
[DE87-002914] N87-20411
Laser spectroscopy and gas-phase chemistry in CVD
[DE86-007392] N87-20548
Liquid Phase Epitaxy (LPE) of silicon carbide
[AD-D012571] N87-20823
VAPORS
High field properties of SnMo6S8 and PbMo6S8 ribbons prepared using a vapor transport technique
[DE87-004707] N87-20826
VARIABLE STARS
UBVRI-photometry of the antiflare stars V586 Ori and IU Ori
[DE87-700760] N87-20845
VECTOR ANALYSIS
Structural dynamic reanalysis using Ritz vectors N87-20597
VEGETATION
Effects of space shuttle launches STS-1 through STS-9 on terrestrial vegetation of John F. Kennedy Space Center, Florida
[NASA-TM-83103] N87-20658
VEGETATION GROWTH
Microalgae culture collection, 1986-1987
[DE87-005578] N87-20729
VELOCITY DISTRIBUTION
The large-scale peculiar velocity field in flat models of the universe
[DE87-005402] N87-20864
VERY LARGE SCALE INTEGRATION
Multilevel representation and simulation for VLSI design
[AD-A175663] N87-20481
VERY LONG BASE INTERFEROMETRY
Crustal dynamics project data analysis, 1986. Volume 1: Fixed station VLBI geodetic results
[NASA-TM-87806] N87-20690
VESTIBULAR NYSTAGMUS
Interlabyrinthine asymmetry, vestibular dysfunction and space motion sickness N87-20734
VESTIBULAR TESTS
Link between asymmetry of optokinetic nystagmus, optovestibular and vestibulovegetative stability N87-20738
VIBRATION
Effect of dynamic stall and elastic parameters on the fundamental mechanisms of helicopter vibrations
[AD-A175561] N87-20292
The Shock and Vibration Digest, Volume 19, No. 2 N87-20435
Recent studies in plate vibrations: 1981-1985. Part 1: Classical theory N87-20437
The Shock and Vibration Digest, Volume 18, No. 10
[AD-A175726] N87-20438
The Shock and Vibration Bulletin. Part 1: Welcome, Invited Papers, Shipboard Shock, Blast and Ground Shock, Shock Testing and Analysis
[AD-A175224] N87-20574
State-of-the-art assessment of structural dynamic response analysis methods (DYNAS) N87-20578
Summary of testing techniques N87-20614
VIBRATION DAMPING
Effect of modal damping in modal synthesis of spacecraft structures N87-20362
Modal-survey testing for system identification and dynamic qualification of spacecraft structures N87-20365
Benefits of passive damping as applied to active control of large space structures N87-20371
Stable response of damped linear systems, part 3 N87-20440
Modeling and control of flexible structures N87-20564
Initial investigations into the damping characteristics of wire rope vibration isolators
[NASA-CR-180698] N87-20569
The Shock and Vibration Bulletin. Part 2: Modal Test and Analysis, Testing Techniques, Machinery Dynamics, Isolation and Damping, Structural Dynamics
[AD-A175225] N87-20580
Blade damping measurements in a spin rig with nozzle passing excitation simulated by electromagnets N87-20590
Temperature shift considerations for damping materials N87-20593
Effectiveness of on-off damper in isolating dynamical systems N87-20594
Forced vibrations of stringer stiffened damped sandwich panel N87-20596
Inverse problems in the modeling of vibrations of flexible beams
[NASA-CR-178259] N87-20777
VIBRATION ISOLATORS
Initial investigations into the damping characteristics of wire rope vibration isolators
[NASA-CR-180698] N87-20569
The Shock and Vibration Bulletin. Part 2: Modal Test and Analysis, Testing Techniques, Machinery Dynamics, Isolation and Damping, Structural Dynamics
[AD-A175225] N87-20580
Force magnitude and angular velocity fluctuation reduction in a spring-restrained, flexibly-supported four-bar mechanical linkage N87-20589
Effectiveness of on-off damper in isolating dynamical systems N87-20594
VIBRATION MEASUREMENT
Vibration characteristics of OH-58A helicopter main rotor transmission
[NASA-TP-2705] N87-20555
Experimental and analytical evaluation of dynamic load and vibration of a 2240-kW (300-hp) rotorcraft transmission
[NASA-TM-88975] N87-20556
Views of the world of pyrotechnic shock N87-20803
A Lanczos eigenvalue method on a parallel computer
[NASA-TM-89097] N87-20768
VIBRATION MODE
Effect of modal damping in modal synthesis of spacecraft structures N87-20362
The digital processing of acceleration measurements for modal analysis N87-20439
VIBRATION TESTS
Low frequency vibration testing on satellites N87-20364
Spacecraft qualification using advanced vibration and modal testing techniques N87-20368
Multi-axis vibration tests on spacecraft using hydraulic exciters N87-20373
VIBRATORY LOADS
Isolation and damping: A graphical method of determining the response of the cascaded two degree of freedom system N87-20592
VIDEO DATA
Dynamic presentation of long term upper ocean study (LOTUS) data using videotape
[AD-A175535] N87-20711
VIDEO EQUIPMENT
TV-holography: A promising inspection tool for analysis of composite materials N87-20180
Use of a video-photogrammetry system for the measurement of the dynamic response of the shuttle remote manipulator arm N87-20370
VIDEO SIGNALS
Use of a video-photogrammetry system for the measurement of the dynamic response of the shuttle remote manipulator arm N87-20370
VISCOELASTIC DAMPING
Temperature shift considerations for damping materials N87-20593
Forced vibrations of stringer stiffened damped sandwich panel N87-20596
VISCOELASTICITY
Two-dimensional flow computation in straight blade arrays — turbine blades
[ONERA-RT-35/1621-RY-053-R] N87-20511
VISCOMETERS
Determination of the ternary viscosity diagram NaCl-KCl-LiCl by the flow method
[INSA-IDTC1-8604] N87-20403
VISCOSITY
Determination of the ternary viscosity diagram NaCl-KCl-LiCl by the flow method
[INSA-IDTC1-8604] N87-20403
Effects of flows on viscous and resistive MHD stability N87-20943
VISCOUS DAMPING
Dynamic qualification of spacecraft by means of modal synthesis N87-20363
Benefits of passive damping as applied to active control of large space structures N87-20371
VISCOUS DRAG
Optimization of hypersonic waveriders derived from cone flows including viscous effects N87-20193
VISCOUS FLOW
A numerical study of the Weis-Fogh mechanism N87-20197
Numerical simulation of internal and external inviscid and viscous 3-D flow fields N87-20213
Zonal solutions for airfoils using Euler boundary-layer and Navier-Stokes equations N87-20219
Computation of three-dimensional flows by viscous-inviscid interation using the MZM method N87-20223

Applications of RAE viscous flow methods near separation boundaries for three-dimensional wings in transonic flow N87-20224
High speed viscous flow calculations about complex configurations N87-20227
Acta mechanica sinica (selected articles) [AD-A176240] N87-20246

VISUAL PERCEPTION
Human-display interactions: Context-specific biases [NASA-TM-89430] N87-20747

VOLCANOES
Airborne lidar measurements of El Chichon stratospheric aerosols, January 1984 [NASA-RP-1175] N87-20663

VORTEX FILAMENTS
Wind-current relationships in the optoma domain off the Northern California Coast [AD-A176019] N87-20714

VORTICES
Numerical solutions of unsteady flow past rotor sections N87-20198
Applications of Euler equations to sharp edge delta wings with leading edge vortices N87-20214
Theoretical analysis of flows around helicopter fuselages: Application to design and development N87-20221
Development of a rotor wake/vortex model. Volume 2: User's manual for computer program [NASA-CR-174850-VOL-2] N87-20239
Acta mechanica sinica (selected articles) [AD-A176240] N87-20246
The effects of large-eddy manipulator devices on the turbulent spot and the turbulent boundary layer N87-20497
The fully nonlinear development of Goertler vortices in growing boundary layers [NASA-CR-178268] N87-20502
Calculation of Rayleigh-Taylor flows using vortex blobs [DE87-002551] N87-20507
Existence seen of cyclonic eddy in northern east China Sea N87-20721

VORTICITY
A numerical study of the Weis-Fogh mechanism N87-20197
Numerical simulation of separated flows past bluff bodies N87-20499

W

WAFERS
Flat-plate solar array project. Volume 3: Silicon sheet: Wafers and ribbons [NASA-CR-180661] N87-20648

WAKES
The effects of large-eddy manipulator devices on the turbulent spot and the turbulent boundary layer N87-20497

WALL FLOW
Integral method of wall interference correction in low-speed wind tunnels [NASA-TT-20055] N87-20241

WARNING SYSTEMS
Visual display and alarm system for wind tunnel static and dynamic loads [NASA-TM-89455] N87-20298

WATER CIRCULATION
Mathematical model of steady-state circulation in the south China Sea N87-20719

WATER DEPTH
Numerical simulation of storm surges in the east China Sea N87-20718
Mathematical model of steady-state circulation in the south China Sea N87-20719

WATER INJECTION
Contingency power for small turboshaft engines using water injection into turbine cooling air [NASA-TM-89817] N87-20280

WATER WAVES
Numerical simulation of storm surges in the east China Sea N87-20718
Spectral analysis of waves in Gulf of Tonkin described N87-20722
Comparison of deepwater wind-wave prediction models N87-20724

WAVE PROPAGATION
Studies of stress wave propagation in composites [DE87-001433] N87-20396
Biot theory and acoustical properties of high porosity fibrous materials and plastic foams [NASA-TM-88575] N87-20424
Stochastic effects on oblique HF (High Frequencies) propagation [AD-A176015] N87-20455
Propagation characteristics of some novel coplanar waveguide transmission lines on GaAs at MM-wave frequencies [NASA-TM-89639] N87-20469
Physical, mechanical effect of velocity of sound in ocean sediments N87-20723
Steepened magnetosonic waves in the high Beta plasma surrounding Comet-Giacobini-Zinner [NASA-CR-180614] N87-20668
Alfven-wave dissipation: A support mechanism for quiescent prominences N87-20681

WAVEGUIDES
Propagation characteristics of some novel coplanar waveguide transmission lines on GaAs at MM-wave frequencies [NASA-TM-89639] N87-20469
Integrated optical devices for high speed diagnostics [DE87-003160] N87-20816

WEAK INTERACTIONS (FIELD THEORY)
General introduction to capture of thermal neutrons in B10 and Li6: Applications in spectroscopy and in the study of weak nucleon interactions N87-20604

WEAPONS
A survey of military aerospace systems technology developments in Western Europe and the Middle East [AD-A175635] N87-20173

WEATHER FORECASTING
AFGWC's Advanced Weather Analysis and Prediction System (AWAPS) [AD-A172801] N87-20702

WEIGHT INDICATORS
Visual display and alarm system for wind tunnel static and dynamic loads [NASA-TM-89455] N87-20298

WEIGHT REDUCTION
The design of composite structures: Aircraft design [NASA-TT-20011] N87-20261
Use of lightweight composites for GAS payload structures N87-20307
Criteria and methodology for lightweight design of vehicle components [LBF-TB-176(1986)] N87-20550

WEIGHTING FUNCTIONS
Flexible grid generation for complex geometries in two space dimensions based on variational principles N87-20200
Noise measurements on the helicopter BK 117 design. Weighted noise levels and influence of airspeed [ESA-TT-748] N87-20800

WEIGHTLESSNESS
Towards a better mirror N87-20310

WELDED JOINTS
Galvanic corrosion resistance of welded dissimilar nickel-base alloys [DE87-002656] N87-20409

WELDING
Rapid melt/quench furnace using commercially available hardware [NASA-TM-86590] N87-20431
Experimental measurement of thin plate SS 304 GTAW weld pool surface temperatures [DE87-004545] N87-20561

WHITE DWARF STARS
The acceleration and dissolution of stars moving through the blackbody radiation of a collapsing universe N87-20847

WHITE LIGHT HOLOGRAPHY
The white light corona and photospheric magnetic fields N87-20912

WIND (METEOROLOGY)
Dynamical and thermodynamical characteristics of a squall-line determined from dual-Doppler data N87-20697
Wind and turbulence data for development of design criteria for unmanned high-altitude low-speed endurance aircraft [NASA-CR-4065] N87-20699
Testing and comparison of several mixed-layer models [AD-A175959] N87-20712
Wind-current relationships in the optoma domain off the Northern California Coast [AD-A176019] N87-20714
Acoustic scattering from composite wind-wave surfaces II: Backscatter cross sections and Doppler effects at high frequencies and small angles for "bubble-free" regimes [AD-A176081] N87-20715
Comparison of deepwater wind-wave prediction models N87-20724

WIND EFFECTS
China Report: Science and technology [JPRS-CST-86-031] N87-20720

WIND MEASUREMENT
Simulation of wind gradient errors in NROSS (Navy Remote Ocean Sensing System) radar scatterometer data in a simplified geometry [AD-A175754] N87-20642

WIND SHEAR
The effect of heavy rain on an airfoil at high lift [NASA-CR-178248] N87-20232
The terminal area simulation system. Volume 1: Theoretical formulation [NASA-CR-4046-VOL-1] N87-20255

WIND TUNNEL APPARATUS
Detailed flow surveys of turning vanes designed for a 0.1-scale model of NASA Lewis Research Center's proposed altitude wind tunnel [NASA-TP-2680] N87-20295
Visual display and alarm system for wind tunnel static and dynamic loads [NASA-TM-89455] N87-20298

WIND TUNNEL DRIVES
Detailed flow surveys of turning vanes designed for a 0.1-scale model of NASA Lewis Research Center's proposed altitude wind tunnel [NASA-TP-2680] N87-20295

WIND TUNNEL MODELS
Design study of advanced model support systems for the National Transonic Facility (NTF) [NASA-CR-178214] N87-20297

WIND TUNNEL NOZZLES
Computational analysis and preliminary redesign of the nozzle contour of the Langley hypersonic CF4 tunnel [NASA-TM-89042] N87-20296

WIND TUNNEL TESTS
Spin-tunnel investigation of a 1/15-scale model of an Australian trainer airplane [NASA-TM-89049] N87-20240
Study of the unsteady pressure field on the RA16SC1 profile in vibrating condition [ONERA-RTS-17/3423-AY] N87-20249
Study of compressibility effects on supersonic free flow [ETN-87-99392] N87-20251
A preliminary study into the constant drag parachute for aircrew escape systems [BU-345] N87-20256
Visual display and alarm system for wind tunnel static and dynamic loads [NASA-TM-89455] N87-20298
An investigation into the factors affecting the flow quality in a small suction wind tunnel [BU-344] N87-20299
The high-speed cascade wind tunnel - still an important test facility for turbomachinery blade investigations [ESA-TT-1012] N87-20300

WIND TUNNEL WALLS
Integral method of wall interference correction in low-speed wind tunnels [NASA-TT-20055] N87-20241

WIND TUNNELS
An investigation into the factors affecting the flow quality in a small suction wind tunnel [BU-344] N87-20299

WIND VELOCITY
Phase speed of wind-wave component studied N87-20726

WIND VELOCITY MEASUREMENT
Wind velocity measurement accuracy with highly stable 12 mJ/pulse high repetition rate CO2 laser master oscillator power amplifier N87-20525

WING LOADING
A rational approach to lifting surface theory with application to large angles of attack N87-20196

WING PANELS
Applications and developments of computational methods for the aerodynamic problems of complex configurations N87-20209

WING PROFILES
Materials selection and design study of a composite microlight wing structure [BU-335] N87-20263

WING TIP VORTICES
The prediction of transonic loading on advancing helicopter rotors N87-20206

WING-FUSELAGE STORES
Prediction of wing-body-store aerodynamics using a small perturbation method and a grid embedding technique N87-20207

WINGS
Composite repair of cocured J-stiffened panels: Design and test verification N87-20181
Battle damage repair of composite structures N87-20189
A numerical study of the Weis-Fogh mechanism N87-20197
Transonic Navier-Stokes wing solution using a zonal approach. Part 1: Solution methodology and code validation N87-20228
Transonic Navier-Stokes wing solutions using a zonal approach. Part 2: High angle-of-attack simulation N87-20229

Acta mechanica sinica (selected articles)
[AD-A176240] N87-20246
WINTER
Numerical simulation of air mass modification over the East China Sea during the winter season N87-20660
WIRE
Initial investigations into the damping characteristics of wire rope vibration isolators
[NASA-CR-180698] N87-20569
WORK CAPACITY
Operator work capacity in tracking system when submitted to antiorthostatic hypokinesia N87-20736
Dynamics of bioelectric activity of human brain in a continuous waking state N87-20745
WORKLOADS (PSYCHOPHYSIOLOGY)
Evaluation of physical work capacity of cosmonauts aboard Salyut-6 station N87-20735
WOUND HEALING
Effect of hypoxia on DNA synthesis and collagent content of regenerating skin N87-20742

X

X RAY ANALYSIS
Studies of X-ray satellites in sodium, magnesium, aluminum, argon, and iron
[ETN-87-99364] N87-20812
X RAY ASTRONOMY
Heating of the stellar corona N87-20673
X RAY SPECTRA
H I structure and the soft X-ray background N87-20949
X RAY TELESCOPES
A normal incidence X-ray telescope
[NASA-CR-180107] N87-20640

Y

YAG LASERS
A ring-cavity for a quadrupled Nd-YAG laser
[DE87-004175] N87-20547
YEAST
Baking the first bread in space N87-20319

Z

ZEEMAN EFFECT
Measurements of magnetic fields in solar prominences N87-20901

Typical Personal Author Index Listing

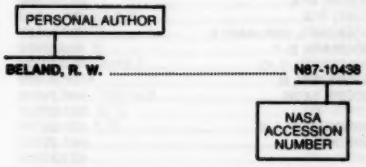

Listings in this index are arranged alphabetically by personal author. The NASA accession number denotes the number by which the citation is identified.

A

ABBOTT, TERENCE S. N87-20265
ABDALLAH, M. N87-20396
ABEYARATNE, R. N87-20572
ABHYANKAR, HANDAKISHOR SADASHIV N87-20348
ABLER, S. B. N87-20794
ABRAHAMS, K. N87-20805
N87-20806
N87-20807
ADAMOVSKY, GRIGORY N87-20475
ADDAMIANO, ARRIGO N87-20823
ADDY, H. E. N87-20282
ADELFANG, STANLEY I. N87-20699
AGARONYAN, F. A. N87-20952
AHO-MANTILA, IRINA N87-20410
AHRENS, S. T. N87-20318
AKNINE, A. N87-20424
ALEXANDER, P. N87-20650
ALEXANDROU, ANDREAS NEOPHYTOU N87-20499
ALISSANDRAKIS, C. E. N87-20911
ALLAN, T. D. N87-20635
ALLARD, J. N87-20424
ALTEROVITZ, SAMUEL A. N87-20821
ALTIDIS, P. C. N87-20552
AMADIEU, PATRICE N87-20359
AMBROZIAK, RUSSELL ANDREW N87-20619
AMOS, ANTHONY K. N87-20577
AMSTERDAMSKI, PIOTR N87-20846
AN, C.-H. N87-20879
AN, CHANG-HYUK N87-20877
ANCELLET, GERARD M. N87-20527
ANDERS, KLAUS P. N87-20800
ANDERSSON, THORWALD N87-20494
ANTCLIFF, R. R. N87-20400
ANTIOCHOS, S. K. N87-20931
N87-20935
ARGON, ALICE L. N87-20847
ARMSTRONG, K. B. N87-20192
ARONSON, S. H. N87-20694
ARTAMONOV, N. N. N87-20737
ASHBY, CAROL I. H. N87-20544
ASNANI, N. T. N87-20596
ASOM, MOSES TERLUMUN N87-20819
ASYAMOLOVA, N. M. N87-20739
ATKINSON, L. P. N87-20716
ATOYAN, A. M. N87-20952
AUSHERMAN, DONALD W. N87-20245
AYOUB, PETER N87-20266

B

BABCOCK, C. D. N87-20595
BAITINGER, KARL N87-20616
BAKER, A. A. N87-20187
BAKER, W. E. N87-20595
BALES, KAY S. N87-20570
BALLESTEROS, C. N87-20545
BALLOUKI, EL HASSAN N87-20403
BANKS, H. T. N87-20777
BAO, J. J. N87-20879
BARACHEVSKIY, V. A. N87-20447
BARAM, Y. N87-20291
BARAM, YORAM N87-20790
BARBOSA, M. J. F. N87-20661
BARCLAY, W. N87-20729
BAREISS, L. E. N87-20350
BARHEN, J. N87-20773
BARKER, R. A. N87-20248
BARNES, P. R. N87-20486
BARTHOLOMEW, JAMES C. N87-20748
BASSO, G. L. N87-20370
BATES, JOHN JOSEPH N87-20710
BATINA, JOHN T. N87-20234
BATTEN, C. E. N87-20541
BATTEN, CARMEN E. N87-20522
N87-20532
N87-20539
BATTRICK, B. N87-20621
BELEDA, R. V. N87-20737
BELKANIYA, G. S. N87-20743
BELL, R. J. N87-20444
BELVIN, W. KEITH N87-20567
BENGELSDORF, I. N87-20649
BENNETT, R. J. N87-20457
BENNETT, ROBERT M. N87-20234
BENNIGHOF, JEFFREY KENT N87-20564
BENOIT, B. N87-20249
BENTLEY, D. L. N87-20433
BERBEE, H. C. P. N87-20789
BERGER, BRETT N87-20260
BERGER, MITCHELL A. N87-20936
BERGER, RUSSELL G. N87-20526
BERRIER, BOBBY L. N87-20294
BERTRAM, A. N87-20363
BHARGAVA, R. N87-20322
BHASIN, K. B. N87-20468
BHAT, R. B. N87-20599
BHATIA, S. P. N87-20600
BIAGI, MASSIMO N87-20763
BICKES, R. W., JR. N87-20430
BIESIADNY, THOMAS J. N87-20280
BILBRO, JAMES W. N87-20525
BINGQIU, LIN N87-20246
BIS, RICHARD F. N87-20480
BITTANTI, SERGIO N87-20788
BITTKER, DAVID A. N87-20277
BIWER, R. L. N87-20489
BLACKBURN, P. E. N87-20492
BLANCHARD, ROBERT N87-20683
BLAND, SAMUEL R. N87-20234
BLECH, RICHARD A. N87-20766
N87-20767
BLOEM, WILLEM BEREND N87-20832
BLOM, G. N87-20226
BLUME, HANS-JUERGEN C. N87-20339
BODECHTEL, J. N87-20634
BODEN, DARYL GENE N87-20336
BOECKER, DIRK N87-20530
BOGDAN, T. J. N87-20914
BOGDAN, THOMAS N87-20884
BOLDMAN, DONALD R. N87-20295
BOMMIER, V. N87-20902
BOND, T. H. N87-20282
BONDIOU, A. N87-20706
BONNET, J. P. N87-20251
N87-20513
BONSALL, CHARLES A. N87-20312
BORDANO, ALDO N87-20669
BORODAKIY, YU. V. N87-20447
BOSTIC, SUSAN W. N87-20768
BOTT, JERRY F. N87-20345
BOWCUTT, KEVIN GERALD N87-20193
BOWMAN, JAMES S., JR. N87-20240
BOYDEN, RICHMOND P. N87-20517
BRABBS, THEODORE A. N87-20279
BRACHET, G. N87-20626
BRANNON, P. J. N87-20544
BRANSTETTER, LINDA J. N87-20585
BREDIF, M. N87-20212
BREILAND, W. G. N87-20548
BREININGER, D. N87-20658
BREITBACH, E. N87-20357
BREMAND, P. N87-20587
BREWE, D. L. N87-20626
BRIFFA, K. R. N87-20703
BRIGLIO, A. N87-20648
BRINCA, A. L. N87-20863
BROOM, BETH H. N87-20727
BROSIUS, JEFFREY W. N87-20918
BROWN, A. T. N87-20656
BROWN, D. W. N87-20454
BROWN, DALE CALVIN N87-20869
BROWN, JEFFERY ALLAN N87-20848
BROWN, K. G. N87-20541
BROWN, KENNETH G. N87-20532
BRUCE, KEVIN R. N87-20290
BRUNET, A. N87-20707
BRUNT, S. N87-20482
BRUZZI, S. N87-20638
BRYANOV, I. I. N87-20734
BRYNILDSEN, NILS N87-20866
BUCKALEW, V. N87-20668
BUCKLEY, DONALD H. N87-20422
BUGROV, S. A. N87-20737
BUNTING, BRUCE G. N87-20421
BUONTEMPO, VINCENZO N87-20761
BURCH, J. L. N87-20689
BURGER, D. N87-20649
N87-20650
BURGESS, J. L. N87-20454
BURKHARDT, ROBERT N87-20313
BURNEY, LEWIS G. N87-20532
BUSCA, O. N87-20376
BUSCH, D. E. N87-20492
BUSH, HAROLD G. N87-20349
BUSHOUSE, HOWARD ALAN N87-20849
BUSS, W. D. N87-20554
BUTLER, RICKY W. N87-20765
N87-20770
BUTLER, T. A. N87-20595
BUTTERFIELD, A. J. N87-20340
BYKOVSKIY, YU. A. N87-20447

C

CAFFEE, MARC WILLIAM N87-20850
CAGLE, CLIFFORD M. N87-20748
CAHN, J. H. N87-20844
CALLAGHAN, W. N87-20646
CAPONE, D. W., II N87-20826
CAPONE, FRANCIS J. N87-20294
CAPONE, R. N87-20464
N87-20465
CAREK, GERALD A. N87-20568
CAREY, D. A. N87-20395
CARNEBIANCA, C. N87-20464
N87-20465
CASTELLANI, ANTONIO N87-20362
CHADERJIAN, NEAL M. N87-20229
CHAMBERLAIN, EDWIN J. N87-20434
CHAMIS, C. C. N87-20389
CHAMPION, K. N87-20687
CHANG, KURNG Y. N87-20605
CHAO, PIUS N87-20606
CHATTOT, J. J. N87-20212
CHAUMETTE, DANIEL N87-20184
CHAUSSEE, DENNY S. N87-20227
CHEGINI, HOSHANG N87-20514
CHEKIRDA, I. F. N87-20752
CHELF, P. N87-20729
CHELLMAN, D. J. N87-20406
CHEN, CHUNG-LUNG N87-20194
CHEN, Y. N87-20545
CHENG, L. N87-20649
CHERN, MAO-JIN N87-20519
CHERNYAYEV, A. N. N87-20742
CHIMA, RODRICK V. N87-20766
CHIN, J. S. N87-20271
CHOATE, M. W. N87-20554
CHOKSHI, ARATI N87-20851
CHOO, YUNG K. N87-20235
CHOUDHURI, ARNAB RAI N87-20940
CHOY, FRED K. N87-20556
CHRETIEN, P. N87-20330
CHRISTENSEN, E. N87-20649

CHRISTENSEN, ELMER N87-20644
CHRISTIANSON, C. C. N87-20488
N87-20489
CHUN, K. S. N87-20282
CIALONE, H. J. N87-20414
CIVINSKAS, KESTUTIS C. N87-20235
CLAAR, T. D. N87-20492
CLARK, DAVID A. N87-20280
CLAUS, RUSSELL W. N87-20270
CLER, A. N87-20221
CLEVENSON, SHERMAN A. N87-20795
CLINE, G. D. N87-20432
CLOUD, D. J. N87-20776
COBLE, H. DWAIN N87-20332
COBURN, L. L. N87-20173
COCHRAN, J. E., JR. N87-20569
COCHRAN, R. C. N87-20188
COFFEY, HELEN E. N87-20948
COLE, D. M. N87-20433
COLLINGS, E. W. N87-20414
COLLINS, MARCIA F. N87-20535
COLTRIN, M. E. N87-20548
CONRAD, P. N87-20363
CORBETT, R. A. N87-20409
COULBERT, C. N87-20652
COVELL, PETER F. N87-20233
COX, A. N. N87-20844
COY, JOHN J. N87-20555
CRAVEN, S. M. N87-20559
CREMA, LUIGI BALIS N87-20362
CROOP, HAROLD C. N87-20374
CRUICKSHANK, JAMES N87-20542
CUDDIHY, E. N87-20652
CUDDIHY, W. F. N87-20340
CURRAN, FRANK M. N87-20382
CUTCHINS, M. A. N87-20569

D

DAHLGREN, ULF N87-20494
DAKHOUL, YOUSSEF M. N87-20620
DALLMANN, U. N87-20230
DANA, ROGER A. N87-20451
DANIEL, RON N87-20727
DANILOVTSEV, V. V. N87-20752
DAUD, T. N87-20649
DAVIDIAN, KENNETH J. N87-20379
N87-20515
DAVIE, NEIL T. N87-20612
DAVILA, JOSEPH M. N87-20939
DAVIS, M. H. N87-20665
DAVIS, S. F. N87-20211
DAVISON, DAVID N87-20606
DAVYDKIN, A. F. N87-20740
DEASON, V. A. N87-20396
DECKARD, TODD W. N87-20321
DEES, D. W. N87-20492
N87-20655
DEGLINNOCENTI, EGIDIO LANDI N87-20901
DEGTYAREV, V. A. N87-20744
DEHAAS, J. B. M. N87-20806
DEINEKA, ROMAN N87-20284
DELANNOY, A. N87-20706
DELOATCH, SANDRA JEAN N87-20753
DELUCA, W. H. N87-20489
DELVILLE, J. N87-20513
DEMOULIN, P. N87-20897
DEMOULIN, PASCAL N87-20892
DEO, NARSINGH N87-20771
DESAUSSURE, G. N87-20643
DESILVA, C. W. N87-20439
DEVILLIERS, D. N87-20640
DEVILLIERS, N. N87-20625
N87-20629
DEVINCENTI, PAOLO N87-20763
DEVORE, CARL RICHARD N87-20870
DHAUBHADEL, MANORANJAN N87-20195
DHONDT, G. D. N87-20571
DING, ZONGXIN N87-20709
DIRECTOR, S. W. N87-20481
DODGE, LEE G. N87-20285
DONALDSON, COLEMAN DUP. N87-20232
DONNELLAN, T. M. N87-20188
DORSEY, JOHN T. N87-20349
DOWDICAN, M. C. N87-20843
DOWNING, DAVID R. N87-20264
DRAISEY, S. N87-20366
DRAJESKE, M. H. N87-20289
DRAPER, J. V. N87-20560
DRAUGLIS, E. J. N87-20414
DRESS, DAVID A. N87-20517
DRIGGERS, T. N87-20467
DUCHOSSOIS, G. N87-20632
N87-20637
DUKE, MICHAEL B. N87-20301
DULL, ANDREW LYNNE N87-20260
DUMAS, K. N87-20648
DUNAGAN, STEPHEN EMIL N87-20498
DUNCOMBE, R. L. N87-20842
DUPOIRIEUX, FRANCIS N87-20401
DURELL, G. D. N87-20433
DUSEK, J. N87-20492
DUTT, P. K. N87-20781

E

EASLER, T. E. N87-20492
EATHERLY, W. P. N87-20393
EBERLE, ALBRECHT N87-20216
EBIHARA, BEN T. N87-20474
ECKSTROM, CLINTON V. N87-20236
EDWARDS, THOMAS A. N87-20203
EFTIS, JOHN N87-20573
EINAUDI, GIORGIO N87-20943
EINSTEIN, J. R. N87-20773
EITELBERG, GEORG N87-20510
ELKS, CARL R. N87-20770
ELLINGSON, W. A. N87-20492
ELZEKI, M. N87-20366
ENGVOLD, ODDBJORN N87-20886
N87-20896
EPSTEIN, J. S. N87-20396
ERINGEN, A. C. N87-20571
ERMAKOV, O. N. N87-20807
ETTER, P. C. N87-20436
EWINS, D. J. N87-20578

F

FANCONI, B. M. N87-20420
FARLEY, DAVID R. N87-20324
FAURE, F. N87-20707
FAVRE, J. P. N87-20398
FEE, D. C. N87-20492
FERRARIS, G. N87-20587
FERRIS, ALICE T. N87-20517
FILIPPI, RICCARDO N87-20760
FINDLAY, J. T. N87-20344
FINDLAY, JOHN N87-20684
FINES, N. R. N87-20456
FINK, BRUCE K. N87-20392
FINZI, AMALIA ERCOLI N87-20367
FIRMIN, M. C. P. N87-20224
FISCHBACH, E. N87-20694
FISCHER, H. N87-20633
FITZ-COY, N. G. N87-20589
FITZPATRICK, P. N87-20588
FLANDERMEYER, B. K. N87-20492
FLORES, J. N87-20228
FLORES, JOLEN N87-20242
FLOYD, ROBERT E. N87-20458
FLYNN, GEORGE W. N87-20452
FOGARTY, JAMES T. N87-20298
FOLEY, S. N87-20588
FORBES, T. G. N87-20874
N87-20876
N87-20905
FORSEY, C. R. N87-20201
FORTUNATO, RONALD C. N87-20309
FOUSEK, R. J. N87-20492
FOX, DENNIS S. N87-20425
FRIAR, J. L. N87-20786
FRIEDMAN, ROBERT N87-20342
FRISCH, KURT C. N87-20427
FRITTS, DAVID N87-20685
FRITZ, WILLY N87-20202
FROMME, GEORG N87-20775
FRY, R. J. M. N87-20730
FULTON, ROBERT E. N87-20768
FUNTOVA, I. I. N87-20735

G

GABB, T. P. N87-20408
GAD-EL-HAK, MOHAMED N87-20503
GAIZAUSKAS, VICTOR N87-20926
GALEF, A. E. N87-20604
GALEF, ARNOLD N87-20609
GALLAGHER, B. N87-20650
GALLAGHER, D. L. N87-20689
GALLUS, H. E. N87-20287
GAMBLE, JOE N87-20679
GAO, XINSHENG N87-20725
GAREM, H. N87-20513
GARN, P. A. N87-20340
GARNIER, C. N87-20330
GARNIER, CH. N87-20358
GARY, D. E. N87-20920
GARY, DALE E. N87-20869
GAUERT, ROLF N87-20521
GAYDA, J. N87-20408
GAZENKO, O. G. N87-20731
N87-20732
GEHLING, R. N. N87-20371
GELDER, THOMAS F. N87-20295
GEORGES, T. M. N87-20601
GESZTELYI, L. N87-20906
GIBBS, M. N87-20728
GIBSON, JOHN W. N87-20190
GILLITZER, ALBRECHT N87-20811
GIRARD, A. N87-20364
GIRARD, R. N87-20617
GIVENS, JOHN J. N87-20841
GLASER, R. J. N87-20581
GLIEBE, P. R. N87-20239
GOBL, T. A. N87-20262
GOLDBERG, BENJAMIN E. N87-20423
GOLDMAN, D. T. N87-20444
GOLDSMITH, T. C. N87-20320
GOLDSTEIN, M. N87-20643
GOLUB, LEON N87-20840
N87-20927
GONCHAROV, I. B. N87-20740
GONDOT, P. N87-20705
N87-20706
GONZALEZ, R. N87-20545
GONZALEZ, RICHARD D. N87-20530
GORDON, JIM N87-20606
GORGILADZE, G. I. N87-20734
GOSLING, J. T. N87-20863
N87-20868
GOUTTEBROZE, P. N87-20894
GRANDLE, ROBERT E. N87-20797
GRAYSTON, ALAN M. N87-20294
GREGORY, DANNY L. N87-20585
GREGORY, J. C. N87-20951
GRIGOROVA, V. K. N87-20738
GRISNIK, STANLEY P. N87-20383
GROBSTEIN, T. L. N87-20405
GROOM, NELSON J. N87-20478
GROSSFIELD, J. N87-20322
GRUBER, ROBERT P. N87-20477
GRUBISIC, V. N87-20550
GU, MINQQI N87-20275
GUDDE, NICHOLAS J. N87-20528
GUENTHER, GEORG N87-20181
GUILE, R. N87-20586
GULCAT, U. N87-20220
GUNDY, K. N87-20228
GUO, C. F. N87-20278
GUPTA, A. N87-20652
GUPTA, K. N87-20590
GURDAL, ZAFER N87-20385
GUROVSKIY, N. N. N87-20732
GYURDZHIAN, A. A. N87-20732
N87-20746

H

HAAG, THOMAS W. N87-20382
HABBAL, SHADIA R. N87-20923
HADLEY, G. R. N87-20546
HAENNINEN, HANNU N87-20410
HAHN, H. N87-20373
HAHN, M. N87-20176
HAIXING, YANG N87-20354
HAKKILA, JON ERIC N87-20857
HALFORD, G. R. N87-20408
HALFORD, GARY R. N87-20565
HALL, PHILIP N87-20502
HALL, W. N87-20692
HAMMETTER, J. R. N87-20418
HAMMOND, R. B. N87-20549
HAN, S. N87-20485
HANCOCK, STEVEN N87-20606
HANKEY, W. L. N87-20225
HANKS, BRANTLEY R. N87-20356
HANLY, RICHARD D. N87-20298
HARA, HIROSHI N87-20543
HARCROW, H. W. N87-20371
HARIHARAN, S. I. N87-20781
HARRIES, J. E. N87-20633
HARRIS, MICHAEL R. N87-20524
HARVEY, KAREN L. N87-20923
N87-20926
N87-20927
N87-20930
HASSAM, A. B. N87-20692
HATTORI, SHUJI N87-20422
HAYES, P. J. N87-20476
HECK, M. L. N87-20344
HEDIN, A. N87-20675
HEINZEL, P. N87-20894
N87-20895

HELLARD, G. N87-20261
HELLARD, GUY N87-20178
HEMEON-HEYER, MARK C. N87-20652
HENRICKS, W. N87-20607
HENRIOT, FRANCOISE N87-20184
HENRY, P. N87-20653
HERAKOVICH, CARL T. N87-20385
HERCZFELD, P. R. N87-20468
HERGENROTHER, PAUL M. N87-20390
HERMANS, LINDA M. N87-20928
HERNDON, J. N. N87-20560
N87-20750
HERZ, RICHARD K. N87-20531
HESS, ROBERT V. N87-20532
N87-20538
HIDDE, JEFFREY S. N87-20385
HIEBER, GEORGE M. N87-20592
HIEL, E. N87-20887
HILL, ACQUILLA S. N87-20517
HILL, OLIVER N87-20682
HINKLE, C. R. N87-20658
HINKLE, THOMAS V. N87-20189
HINKS, D. G. N87-20826
HIRAYAMA, TADASHI N87-20893
HIRONAKA, M. C. N87-20432
HIRSCHEL, E. H. N87-20219
HO, P. N87-20548
HOF, D. E. N87-20506
HOFFER, DAVID N87-20310
HOFLUND, GAR B. N87-20537
HOHEISEL, HEINZ N87-20300
HOHIMER, J. P. N87-20546
HOLBROOK, J. H. N87-20414
HOLCOMB, KATHERINE ANN N87-20853
HOLDEMAN, JAMES D. N87-20276
HOLLOWELL, R. N87-20588
HOLMAN, GORDON D. N87-20917
N87-20918
HOLST, T. L. N87-20228
HOLT, RUSH D. N87-20929
HOLTSLAG, ANTONIUS HENDRICUS MARIA
N87-20809
HONG, SEUNG HO N87-20589
HOOD, A. W. N87-20941
HOOKER, F. D. N87-20318
HOPKINS, MIRIAM N87-20668
HORDONNEAU, A. N87-20388
HORGAN, C. O. N87-20572
HORNSTRA, F. N87-20489
HORNUNG, E. N87-20357
HOUTHAAN, ANTONI JOHAN N87-20828
HOYT, RONALD F. N87-20532
N87-20538
HSU, WU-RON N87-20660
HUBA, J. D. N87-20692
HUENERS, H. N87-20365
HUFF, J. R. N87-20654
HUGHES, H. G. N87-20691
HUGHES, ROBERT E. N87-20748
HUISKAMP, W. J. N87-20805
N87-20806
N87-20807
HUIZING, G. H. N87-20200
HUNG, E. K. N87-20456
HUNSUCKER, JOHN L. N87-20834
HURFORD, G. J. N87-20920
HUSSAINI, M. Y. N87-20500
N87-20756
HUYNH, HUNG T. N87-20504
HWANG, DANNY P. N87-20504

I

IBRAHIM, B. B. N87-20549
IMMARIGEON, J.-P. N87-20286
IMREGUN, M. N87-20578
IPAVICH, F. M. N87-20663
ISHIGURO, M. N87-20887
ISMAIL, M. N87-20908
IVANCHIKOV, A. P. N87-20737
IVANOV, A. P. N87-20740
IVEY, EDWARD W. N87-20568

J

JACKSON, R. J. N87-20418
JACKSON, T. L. N87-20756
JACOBSON, NATHAN S. N87-20425
JAHODA, KEITH N87-20949
JAKUS, K. N87-20428
JAY, G. C. N87-20554
JEFFERSON, D. N87-20773
JENSEN, EBERHART N87-20881
JERVIS, T. R. N87-20411
JESKE, NORBERT ALAN N87-20858
JHA, V. K. N87-20599
JIANG, DECAI N87-20725
JOHANSEN, J. N87-20729
JOHNSON, D. L. N87-20665
JOHNSON, RICHARD W. N87-20520
JOHNSON, STEVEN C. N87-20525
JOHNSON, T. C. N87-20433
JOHNSON, WILLIAM G., JR. N87-20517
JOHNSTON, NORMAN J. N87-20390
JOLLES, MITCHELL I. N87-20573
JONES, A. S. N87-20366
JONES, KENNETH E. N87-20799
JONES, MICHAEL G. N87-20796
JONES, P. D. N87-20703
JONES, R. M. N87-20801
JONES, WILLIAM R., JR. N87-20421
JOOSTEN, KENT N87-20680
JOSELYN, JOANN N87-20677
JOUAN, JEAN-ALAIN N87-20185
JUSTUS, C. G. N87-20686
JUSZKIEWICZ, R. N87-20865

K

KACYNSKI, KENNETH J. N87-20381
KAFYEKE, FASSI N87-20207
KAILATH, THOMAS N87-20790
KAISER, MARY KISTER N87-20747
KALIT, G. N87-20291
KAM, M. N87-20468
KANDA, HIROSHI N87-20582
KANILEYKO, YU. K. N87-20446
KANN, DEIRDRE MARY N87-20696
KARMAN, STEVE L., JR. N87-20217
KARPIKHIN, J. L. N87-20807
KASHIWA, B. A. N87-20508
KASSNER, M. E. N87-20415
KAVI, N. N87-20596
KAYNAK, UNVER N87-20228
KEAFER, LLOYD S. N87-20352
KEATES, T. F. N87-20369
KEATON, PAUL W. N87-20301
KEELING, STEPHEN L. N87-20782
N87-20783
KEIL, STEPHEN L. N87-20896
KEIM, ENRICO GEORGE N87-20810
KELLEY, P. B. N87-20343
KELLY, G. M. N87-20344
KELLY, LARRY G. N87-20183
KENNEDY, ROBERT E. N87-20337
KERCZEWSKI, ROBERT J. N87-20450
KERN, DENNIS L. N87-20605
KERR, R. M. N87-20507
KESKINEN, M. J. N87-20692
KHACHATURYANTS, L. S. N87-20736
KHOMULLO, G. V. N87-20742
KHVINGIYA, M. V. N87-20752
KILLEEN, TIMOTHY N87-20673
KING, A. H. N87-20827
KING, C. B. N87-20340
KIPER, ALI M. N87-20557
KIRILLOVA, Z. A. N87-20744
KISELEV, R. K. N87-20737
KISIELEWSKI, KEITH M. N87-20217
KITCHENS, PHILIP H. N87-20333
KITIS, L. N87-20597
KLANN, GARY A. N87-20260
KLEIN, LEONARD H. N87-20822
KLEMPNER, DANIEL N87-20427
KLIMCHUK, J. A. N87-20880
N87-20898
N87-20931
KLUMPAR, D. M. N87-20689
KNEILE, KARL R. N87-20505
KNOTT, W. M., III N87-20658
KOECK, C. N87-20212
KOK, P. J. J. N87-20803
N87-20804
N87-20805
N87-20806
N87-20807
KOLAVENNU, V. N87-20467
KOLKAILAH, FAYSAL A. N87-20306
KOLLER, A. M., JR. N87-20658
KONG, J. A. N87-20449
KOPP, R. A. N87-20907
N87-20944
KOPRIVA, DAVID A. N87-20779
KORDULLA, W. N87-20230
KORMER, A. YA. N87-20744
KOSUGI, T. N87-20887
KOUVARITAKIS, B. N87-20776
KOVALCHUK, G. U. N87-20845
KOVALEV, V. YU. N87-20741
KOZENKOV, V. M. N87-20447
KRAMER, D. P. N87-20559
KRAUS, H. G. N87-20561
KRING, C. T. N87-20750
KRUPCHITSKY, P. A. N87-20807
KUBOTA, YUSUKE N87-20618
KUDRYASHOVA, ZH. M. N87-20740
KUIN, N. PAUL M. N87-20908
KULCHYSKI, R. B. N87-20370
KUMAR, K. N87-20589
KUNATH, R. R. N87-20468
KUNDU, M. R. N87-20888
N87-20909
N87-20910
N87-20916
N87-20924
KUO, C-P. N87-20581
KURZINER, R. I. N87-20281
KUSHNER, ALAN S. N87-20575

L

LAGET, R. N87-20657
LAIZET, J. C. N87-20398
LAKIN, WILLIAM D. N87-20502
LAKNER, J. F. N87-20442
LANDGREBE, A. L. N87-20491
LANG, KENNETH R. N87-20915
N87-20919
N87-20925
LANTOS, P. N87-20911
LANZ, MASSIMILIANO N87-20367
LANZL, F. N87-20634
LAPRADE, N. N87-20468
LAPTEV, V. V. N87-20446
LARIGALDIE, S. N87-20707
LAROCHE, P. N87-20706
LAROSA, THEODORE NICHOLAS N87-20946
LAUER, JAMES L. N87-20421
LAW, JAPHET S. N87-20834
LAWSON, S. E. B. N87-20299
LAZAREFF, M. N87-20223
LE, T. H. N87-20205
LEBALLEUR, J. C. N87-20223
LEBEN, ROBERT R. N87-20237
LEBLANC, R. N87-20512
LECAUDE, N. N87-20330
LECOURTDEBERU, H. N87-20707
LEDWA, K. N87-20186
LEE, C. M. N87-20282
LEE, EUN U. N87-20283
LEE, J. N87-20488
LEE, Y. ALBERT N87-20607
LEICHER, STEFAN N87-20213
LEIPHOLZ, H. H. E. N87-20598
LEIPOLD, M. N87-20648
N87-20649
LEISSA, A. W. N87-20437
LELANNE, M. N87-20587
LEMKE, P. N87-20729
LEMMER, LUDWIG N87-20181
LESTER, H. C. N87-20794
LEVESQUE, RAYMOND J., II N87-20316
LEVY, ELLEN N87-20713
LEWICKI, DAVID G. N87-20555
LI, W. M. N87-20271
LIANG, R. N87-20652
LIANG, YUANBO N87-20723
LILJEQUIST, D. N87-20808
LIN, CHIN-SHUN N87-20171
LIN, JEN-HONG (JEFF) N87-20697
LINGMI, ZHANG N87-20582
LIU, C. T. N87-20413
LIU, DAHSIN N87-20586
LIU, QIN-RONG N87-20620
LIU, JOSEPH J. F. N87-20671
N87-20672
LOBOV, G. A. N87-20607
LOEMBE, ANDRE N87-20496
LOGUNOV, A. A. N87-20792
LOHMANN, R. P. N87-20387
LOKBERG, OLE J. N87-20180
LOMAX, HARVARD N87-20785
LONGDON, NORMAN N87-20857
LOONEY, K. T. N87-20476
LOTOVA, V. I. N87-20742
LOVELACE, U. M. N87-20352
LOW, B. C. N87-20882
N87-20914
LU, BO N87-20723
LUTWACK, R. N87-20647

M

MA, C. N87-20690
MAJJIGI, R. K. N87-20239
MAKSYMUK, CATHERINE N87-20785
MALHERBE, J. M. N87-20876
N87-20897
N87-20900
N87-20905
MALHERBE, JEAN-MARIE N87-20892
MALL, GERALD H. N87-20514
MALLA, RAMESH-BABU N87-20347
MALMO, JAN T. N87-20180
MALVERN, L. E. N87-20586
MAMODE, A. N87-20364
MANTEGAZZA, PAOLO N87-20367
MARAIS, X. N87-20398
MARCHBANK, W. R. N87-20210
MARCOS, FRANK A. N87-20676
MARECHAL, J. N87-20250
MARELLI, L. N87-20630
N87-20639
MARINHO, E. V. A. N87-20693
MARISKA, J. T. N87-20680
N87-20931
MARKS, G. N87-20366
MARQUE, J. P. N87-20707
MARSHALL, P. D. N87-20256
MARTENS, P. C. H. N87-20934
N87-20937
MARTENS, PIET C. H. N87-20908
MARTENSEN, ANNA L. N87-20765
MARTIN, PAUL J. N87-20712
MARTIN, SARA F. N87-20883
N87-20928
MARTRES, M. J. N87-20904
MARZI, ADRIANA N87-20759
MATHIEU, PIERRE N87-20542
MATONE, G. N87-20547
MATSUMOTO, H. N87-20868
MAYBEE, GEORGE W. N87-20332
MAYR, HANS G. N87-20933
MCCABE, MARIE K. N87-20912
MCCABE, R. W. N87-20536
MCCARTY, S. M. N87-20681
MCCONNELL, B. W. N87-20486
MCCONNELL, J. G. N87-20344
MCCORMICK, M. PATRICK N87-20663
MCCURDY, DAVID A. N87-20797
MCDONALD, M. M. N87-20419
MCDONALD, R. N87-20646
MCGUIRE, P. N87-20653
MCGUIRE, STEPHEN C. N87-20613
MCLAUCHLAN, ROBERT A. N87-20589
MCMAHON, J. J. N87-20416
MCMAHON, M. E. N87-20415
MCWRIGHT, G. M. N87-20816
MEACHAM, S. A. N87-20774
MEAD, KATHRYN N. N87-20854
MEADOR, MARY ANN B. N87-20426
MEARES, D. J. N87-20796
MEELKER, J. H. N87-20208
MEIN, N N87-20906
MEIN, P. N87-20900
MEISL, CLAUS N87-20667
MELENDRES, C. A. N87-20416
MENON, S. K. N87-20411
MENZIES, ROBERT T. N87-20527
MERCER, CHARLES E. N87-20294
MERCIER, F. N87-20364
MESCALL, JOHN F. N87-20576
MIDDLETON, DAVID N87-20715
MIKKOLA, ESKO N87-20612
MILLER, DAVID PAUL N87-20377
MILLER, DAVID S. N87-20233
MILLER, I. M. N87-20541
MILLER, IRVIN M. N87-20522
N87-20532
N87-20539
MILLER, J. F. N87-20488
MILNER, EDWARD J. N87-20766
MINAYEV, YU. P. N87-20446
MINER, R. V. N87-20408
MISEGADES, KENT N87-20216
MIYAHARA, AKIRA N87-20818
MIYOSHI, KAZUHISA N87-20422
MODDEMAN, W. E. N87-20559
MOE, KENNETH N87-20688
MOENING, CHARLES N87-20603
MOKASHI, A. N87-20549
MONACO, WILLIAM A. N87-20258
MONTEMAYOR, ALAN F. N87-20558
MONTGOMERY, ELLYN T. N87-20711
MOODY, STEPHEN E. N87-20526
MOORE, CARLETON J. N87-20568
MOORE, RONALD L. N87-20930
MOORE, ROYCE D. N87-20295
MOORE, T. E. N87-20689
MOORE, T. J. N87-20405
MOORE, W. E. N87-20560
MORCHOISNE, Y. N87-20205
MOREL, A. N87-20635
MORONEY, WILLIAM F. N87-20748
MOROSOW, G. N87-20371
MORRISON, A. N87-20648
MORRISON, W. S. N87-20409
MORROW, GEORGE N87-20479
MORSE, ROBERT E. N87-20611
MORTCHELEWICZ, G. D. N87-20511
MORTENSEN, A. J. N87-20311
MOSIER, FRANCES L. N87-20302
MOURADIAN, Z. N87-20904
MRAZEK, F. C. N87-20655
MUCKERHEIDE, M. C. N87-20317
MUEHLBAUER, K. N87-20368
MUELLER, JAMES L. N87-20642
MUIR, ARTHUR H., JR. N87-20306
MULARZ, EDWARD J. N87-20268
MULLAN, D. M. N87-20929
MUNI, BHAVESH N87-20427
MURMAN, EARLL M. N87-20214
MURPHY, A. J. N87-20263
MURPHY, ROBERT M. N87-20480
MURRAY, D. C. N87-20263
MURRAY, H. S. N87-20654
MURRY, J. N87-20649
MUSTARDE, R. B. N87-20256

N

NACHTWEY, D. S. N87-20730
NAGLE-ESHLEMAN, JUDITH N87-20435
N87-20438
NAGLE, N. N87-20729
NAIK, VIJAY K. N87-20769
NALLASAMY, M. N87-20501
NARIAI, HIDEKAZU N87-20830
NASTASI, M. N87-20411
NEALSON, W. P. N87-20554
NEBORSKIY, A. T. N87-20743
NECHAYEV, A. P. N87-20745
NEEF, JAMES D. N87-20337
NESMAN, T. E. N87-20584
NGUYEN, H. L. N87-20282
NGUYEN, T. N87-20467
NICHOLS, C. D. N87-20476
NICHOLSON, D. W. N87-20440
NICHOLSON, JAMES H. N87-20327
NICKISCH, L. J. N87-20455
NIEDBAL, H. N87-20365
NIKOLAYEV, V. N. N87-20446
NISHIOKA, KENJI N87-20841
NOAH, SHERIF T. N87-20553
NORDEMANN, D. J. R. N87-20693
NURRE, G. N87-20670

O

OBERLE, LAWRENCE G. N87-20516
OBRIEN, THOMAS J. N87-20326
ODEGARD, B. C., JR. N87-20394
ODONNELL, BERNARD N. N87-20459
OERY, H. N87-20357
OFFENHAEUSER, F. N87-20802
OKADA, TSUNENORI N87-20422
ONEIL, JASON C. N87-20303
ORERA, V. M. N87-20545
ORRALL, F. Q. N87-20890
N87-20932
ORTON, GEORGE F. N87-20375
OSBORN, M. T. N87-20663
OSGOOD, RICHARD M., JR. N87-20452
OSKAM, B. N87-20200
OSSA, WILLIAM A. N87-20407
OSTLIE, D. A. N87-20844
OSWALD, FRED B. N87-20556
OTTO, G. H. N87-20331
OWEN, ROBERT B. N87-20727
OWENS, EDWIN C. N87-20558
OWYOUNG, A. N87-20546

P

PACE, PAUL N87-20542
PACK, HOMER C., JR. N87-20380
PADILHA, A. L. N87-20661
PADULA, S. L. N87-20755
PAEZ, THOMAS L. N87-20585
PAIELLI, RUSSELL N87-20257
PAPAZIAN, H. A. N87-20350
PAPINEAU, NICOLE N87-20402
PAQUET, P. N87-20636
PARK, ALBERT H. N87-20929
PARKER, E. N. N87-20873
PARROTT, TONY L. N87-20798
PASSERON, L. N87-20358
PATNAIK, P. C. N87-20266
PAULIN, P. A. N87-20541
PAULIN, PATRICIA A. N87-20532
N87-20539
PAULSON, A. S. N87-20791
PAVESI, B. N87-20464
N87-20465
PAVLI, ALBERT J. N87-20381
PAWEL, R. E. N87-20393
PAYTON, R. M. N87-20350
PEREIRA, E. B. N87-20693
PEREPLITSA, V. F. N87-20807
PERRIER, PIERRE N87-20215
PERRON, J. C. N87-20330
PERUZZI, ARMANDO N87-20762
PETERS, DAVID A. N87-20292
PETRIE, J. A. H. N87-20209
PFEIFFER, B. N87-20622
N87-20631
N87-20641
PHILLIPS, M. J. N87-20645
PIERCE, R. D. N87-20487
PILKEY, W. D. N87-20597
PIN, F. G. N87-20643
PINDERA, MAREK-JERZY N87-20385
PINSON, LARRY D. N87-20356
PLAKHATNYUK, V. I. N87-20737
PLISSONNEAU, BERNARD N87-20179
PLUMAT, Y. N87-20360
POLAND, A. I. N87-20860
N87-20897
POLAND, ARTHUR I. N87-20871
POLETTO, G. N87-20907
N87-20944
POLLINGER, WERNER N87-20704
PONOMARENKO, V. A. N87-20733
POOLE, P. N87-20162
POOLE, WILLIAM L. N87-20478
POORMAN, RICHARD M. N87-20431
PORTER, JASON G. N87-20930
POSTMA, H. N87-20805
N87-20806
N87-20807
POUCH, JOHN J. N87-20821
POWERS, DAN N87-20614
POWERS, R. K. N87-20777
PRICE, H. T. N87-20529
PRIOLO, F. J. N87-20244
PRITCHARD, A. R. N87-20348
PROCTOR, F. H. N87-20252
N87-20255
PRODONOFF, V. N87-20591
PROFFITT, DENNIS R. N87-20747
PROFST, GEORG N87-20778

Q

QUEIJO, M. J. N87-20340

R

RAADU, MICKAEL A. N87-20892
RAASCH, W. N87-20373
RABIN, DOUGLAS N87-20891
RAGOZIN, V. N. N87-20744
RAKHEJA, S. N87-20594
RAMINS, PETER N87-20474
RAMSEY, CHARLES L. N87-20189
RAO, J. S. N87-20590
RAO, R. N. N87-20391
RAWLEY, LLOYD ALEXANDER N87-20855
RAZA, IRFAN N87-20427
REED, D. K. N87-20584
REICHMANN, ED J. N87-20930
REIS, L. N87-20218
REISS, KEITH W. N87-20303
REUTER, R. C., JR. N87-20397
REYNOLDS, NATHANIEL DUNTON N87-20700
RICH, ROBERT MICHAEL N87-20856
RICHARD, P. N87-20706
RIDENOURE, REX W. N87-20314
RILEY, CLYDE N87-20332
RILEY, D. J. N87-20480
RILEY, J. P. N87-20801
RIOSNETO, ATAIR N87-20551
RITALA, R. K. N87-20829
RITTER, J. E. N87-20428

RIZZI, ARTHUR N87-20214
ROBBINS, J. M. N87-20393
ROBERTS, B. N87-20921
ROBERTS, W. W. N87-20660
ROBERTSON, ANDREW R. N87-20374
ROBLE, RAYMOND N87-20673
ROESSLER, P. N87-20729
ROGERS, LYNN N87-20593
ROGOV, V. A. N87-20744
ROLFE, E. J. N87-20621
ROMPOLT, B. N87-20895
ROMPOLT, BOGDAN N87-20884
ROSE, K. E. N87-20201
ROSEN, I. G. N87-20777
ROSENFELD, L. N87-20428
ROSENZWEIG, E. L. N87-20188
ROSS, R. G., JR. N87-20651
ROTHERMEL, JEFFRY N87-20525
ROTHSTEIN, E. N87-20287
ROTTMAN, G. J. N87-20932
ROWE, J. C. N87-20749
N87-20750
ROYSTER, DICK M. N87-20407
ROZHKOV, S. S. N87-20784
RUDNER, STAFFAN N87-20494
RUPP, CHARLES C. N87-20323
RUTHER, W. N87-20416
RYAN, J. N87-20205
RYAN, J. W. N87-20690
RYDEN, EVA N87-20429

S

SAFFORD, F. B. N87-20613
SALTSMAN, JAMES F. N87-20565
SALTZ, LARRY E. N87-20383
SAMARIN, G. I. N87-20734
SAMPSON, CHRISTOPHER F. N87-20526
SANDFORD, MAYNARD C. N87-20236
SANE, R. C. N87-20534
SANKA, S. N87-20594
SANKAR, T. S. N87-20599
SANKARAN, K. K. N87-20404
SANZ, JOSE M. N87-20238
SARIGUL, NESRIN N87-20311
SATTAR, M. A. N87-20387
SAVAGE, M. N87-20552
SAYERS, A. D. N87-20643
SCARF, F. L. N87-20663
SCARGLE, JEFFREY D. N87-20841
SCHATTEN, KENNETH H. N87-20933
SCHERR, S. J. N87-20231
SCHEURER, B. N87-20780
SCHILDT, U. N87-20368
SCHLUDE, F. N87-20624
SCHMAHL, E. J. N87-20890
SCHMALZER, P. A. N87-20658
SCHMATZ, M. A. N87-20219
SCHMID, H. N87-20453
SCHMIDT, J. H. N87-20800
SCHMIEDER, B. N87-20897
N87-20900
N87-20906
SCHMIEDER, BRIGITTE N87-20892
SCHNEBEL, E. M. N87-20322
SCHNEIDER, MANFRED N87-20618
SCHNEIDER, RICHARD T. N87-20815
SCHNERINGER, JULIE A. N87-20308
SCHRIBER, S. O. N87-20461
SCHRYER, D. R. N87-20541
SCHRYER, DAVID R. N87-20532
SCHRYER, J. N87-20541
SCHRYER, JACQUELINE N87-20539
SCHULLER, I. K. N87-20825
SCHULZ, HARRY N87-20399
SCHWARZ, A. C. N87-20430
SCHWEICKERT, THOMAS F. N87-20375
SCOTT, PETER D. N87-20518
SEDGHI, BIJAN N87-20427
SEEDS, A. J. N87-20482
SEGELSTEIN, DAVID J. N87-20839
SEIDEL, DAVID A. N87-20234
N87-20236
SEN, R. K. N87-20491
SENNETT, MICHAEL S. N87-20190
SERNELIUS, B. E. N87-20824
SEVENNEC, B. N87-20358
SEYEDGHASEMIPOUR, S. J. N87-20835
SHANG, J. S. N87-20225
N87-20231
SHAO, ZHONGPU N87-20273
SHAPLAND, D. J. N87-20623
SHAW, DAVID T. N87-20518
SHAW, J. A. N87-20201
SHAW, LEONARD L. N87-20601
SHAW, S. R. N87-20529
SHCHERBAKOV, I. A. N87-20446
SHCHERBAKOV, YE. YU. N87-20744
SHEA, RICHARD N87-20576
SHERMAN, C. D. N87-20294
SHIBASAKI, K. N87-20867
SHIPKOV, YU. YU. N87-20746
SHRIVASTAVA, PRAKASH CHANDRA N87-20286
SHULEV, YU. V. N87-20447
SHUM, D. P.C. N87-20484
SHYNE, RICKEY J. N87-20295
SIDNEY, B. D. N87-20541
SIDNEY, BARRY D. N87-20532
N87-20540
SIDORIN, A. V. N87-20446
SIGETY, P. N87-20398
SILCOX, R. J. N87-20794
SILK, J. N87-20865
SIMON, G. N87-20897
N87-20906
SIMONS, RAINEE N. N87-20469
SINCLAIR, P. M. N87-20209
SINGH, JAG J. N87-20514
SINGLETON, J. F. N87-20432
SIRCILLINETO, F. N87-20693
SIRCILLINETO, FRANCISCO N87-20861
SLOWEY, JOHN N87-20674
SMAGA, J. A. N87-20493
SMIALEK, JAMES L. N87-20425
SMIRNOV, V. L. N87-20447
SMITH, D. R. N87-20293
SMITH, E. J. N87-20863
N87-20868
SMITH, J. S. N87-20204
SMITH, L. E. N87-20420
SMITH, R. E. N87-20665
SMITH, ROBERT E. N87-20678
SMITH, RONALD T. N87-20519
SMITH, S. A. N87-20247
SMITH, TAMARA A. N87-20381
N87-20383
SMOKLER, M. I. N87-20651
SNYDER, R. J. N87-20409
SNYDER, ROBERT S. N87-20727
SOBIESZCZANSKI-SOBIESKI, J. N87-20755
SOEDERBERG, DENNIS N87-20494
SOHN, MYONGHAN N87-20197
SOLOMON, J. M. N87-20244
SOMERS, MARK DOUGLAS N87-20862
SORENSEN, JOHN A. N87-20253
SORU-ESCAUT, I. N87-20904
SPENCER, DONALD J. N87-20345
SPENCER, MARK B. N87-20307
SPIEGEL, KARL-HEINZ N87-20800
SPILLE, R. F. N87-20749
SPLETTSTOESSER, WOLF R. N87-20800
SRIVATSAN, RAGHAVACHARI N87-20264
STANIEK, S. N87-20331
STASSINOPOULOS, A. N87-20512
STATLER, THOMAS STUART N87-20859
STECHER-RASMUSSEN, F. N87-20807
STECKER, JOHANNES N87-20695
STEGER, JOSEPH L. N87-20222
STEIN, PETER A. N87-20349
STEINBRENNER, JOHN P. N87-20217
STEINMETZ, GEORGE G. N87-20265
STEINOLFSON, RICHARD S. N87-20945
STEINVALL, OVE N87-20659
STEPANTSOV, V. I. N87-20735
STEWART, A. P. R. N87-20299
STEWART, G. R. N87-20860
STLUKA, EDWARD F. N87-20315
STOBIE, JAMES G. N87-20702
STONE, M. H. N87-20182
STONE, ROBERT H. N87-20177
STRAND, ARVID N87-20180
STRAUSS, PAUL R. N87-20610
STRAWN, R. C. N87-20206
SU, S. Y. W. N87-20757
SUDARSKY, D. N87-20694
SULLIVAN, BRENDA M. N87-20797
SULLIVAN, ROGER D. N87-20232
SUMMERS, STEVEN J. N87-20714
SUN, C. T. N87-20566
SURGET, J. N87-20707
SUTTON, G. R. N87-20182
SUTTON, KENNETH N87-20296
SVEDIN, JAN N87-20495
SZAFER, A. N87-20694
SZENTGYORGYI, ANDREW HAROLD N87-20950

T

TAASAN, SHLOMO N87-20769
TACINA, ROBERT R. N87-20272
N87-20378
TALAGA, PAUL N87-20328
N87-20329
TALMADGE, C. N87-20694
TANDBERG-HANSSEN, E. N87-20900
TANDBERG-HANSSEN, E. A. N87-20872
TANG, FRANCES N87-20926
TANG, WEI N87-20198
TARBELL, SUSAN A. N87-20713
TAVARES, H. F. N87-20591
TAYLOR, STEPHEN N87-20497
TEMME, LEONARD A. N87-20258
THART, W. G. J. N87-20191
THAYER, WILLIAM J., III N87-20526
THIELE, OTTO W. N87-20701
THIELE, TH. N87-20175
THOMAS, D. E. N87-20481
THOMAS, LAWRENCE R. N87-20302
THOMAS, S. D. N87-20228
THOMPSON, B. E. N87-20218
THOMPSON, JOSEPH C. N87-20929
THOMPSON, R. A. N87-20296
THOMPSON, S. N87-20509
THOMPSON, WILLIAM N87-20899
THORNE, R. M. N87-20863
N87-20868
TIGRANYAN, R. A. N87-20741
TIKHONOV, M. A. N87-20739
TINKER, M. L. N87-20569
TISHLER, V. A. N87-20735
TITRAN, R. H. N87-20405
TOKSOZ, M. NAFI N87-20662
TOLPEKIN, V. YE. N87-20744
TOMBOULIAN, SHERRYL N87-20764
TOROPKIN, G. N. N87-20446
TORRES, MANUEL N87-20179
TOWNSEND, DENNIS P. N87-20556
TOWNSEND, JOHN S. N87-20568
TRABOCCO, R. E. N87-20186
TRIVEDI, N. B. N87-20661
TROUTMAN, P. A. N87-20344
TSOTSIS, T. T. N87-20534
TSUKAMOTO, KATSUO N87-20334
TSULAYA, G. G. N87-20752
TSURUTANI, B. T. N87-20863
N87-20868
TSYGANOK, V. A. N87-20737
TSYGANOV, L. P. N87-20744
TUMMILLO, A. F. N87-20489
TUNG, C. N87-20206
TUOZZI, A. N87-20464
N87-20465
TURNER, M. S. N87-20864
N87-20865
N87-20866
TURNER, R. M. N87-20456
TYCHINA, V. P. N87-20745

U

UNTERBERG, WALTER N87-20667
UPCHURCH, B. T. N87-20541
UPCHURCH, BILLY T. N87-20538

V

VALENTINY, G. N87-20628
VALISETTY, R. R. N87-20369
VANBALLEGOOIJEN, A. A. N87-20936
VANDALSEM, WILLIAM R. N87-20222
VANDEGEER, SARA A. N87-20787
VANDERVOOREN, J. N87-20208
VANDERWEES, A. J. N87-20208
VANDIVER, T. L. N87-20384
VANES, JACK N87-20189
VANHOVEN, GERARD N87-20875
VANNICE, M. ALBERT N87-20533
VANNIEKERK, BECKER N87-20196
VANWIE, DAVID MICHAEL N87-20338
VARY, ALEX N87-20562
VASANTH, KUNIGAHALLI L. N87-20479
VELLI, MARCO N87-20942
VENARUCCI, GIAN FABRIZIO N87-20762
VENNERI, SAMUEL L. N87-20356
VERA, IVAN N87-20304
VESELY, W. E. N87-20563
VEYRAT, D. N87-20767
VIAL, J. C. N87-20885
N87-20894
VILLUMSEN, J. V. N87-20865
VINOGRADOV, I. N. N87-20742
VISTE, NORM N87-20606
VITTORIO, N. N87-20864
N87-20865
VLASOV, A. A. N87-20792

VOLLMERS, H. N87-20230
VYAS, N. N87-20590

W

WADA, B. K. N87-20581
WADA, BEN K. N87-20361
WAGNER, WILLIAM J. N87-20903
WAI, J. C. N87-20226
WAITE, J. H., JR. N87-20689
WALTER, BERNARD A., JR. N87-20698
WANG, BINGXIANG N87-20724
WANG, JIA N87-20719
WANG, JINGYONG N87-20718
WANG, NAIYAN N87-20818
WANG, WENZHI N87-20722
WANG, X. F. N87-20271
WANHILL, R. J. H. N87-20191
WANTUCK, P. J. N87-20506
WARDLAW, A. B. N87-20244
WARDLAW, A. B., JR. N87-20211
WARNER, JOSEPH D. N87-20921
WATERS, L. A. N87-20344
WATSON, WILLIE R. N87-20796
WEATHERILL, N. P. N87-20201
WEBB, DAVID F. N87-20922
N87-20927
WEBER, DAVID M. N87-20321
WEBER, JACK N87-20606
WEIL, B. S. N87-20560
WEISSIN, C. R. N87-20643
WELCHER, BLAKE A. N87-20306
WELLS, DOUGLAS C. N87-20254
WENDLER, B. H. N87-20583
WENDLING, PETER N87-20704
WENTWORTH, STANLEY E. N87-20190
WERLE, P. N87-20212
WESSLING, FRANCIS C. N87-20305
WEST, S. P. N87-20341
WESTIN, JOHAN N87-20494
WHIPPLE, RAYMOND D. N87-20240
WHITE, K. ALAN, III N87-20353
WHITE, M. A. N87-20656
WHITE, WILLIAM L. N87-20240
WHITNEY, WAYNE T. N87-20543
WHITTIER, JAMES S. N87-20345
WIGLEY, T. M. L. N87-20703
WIJKER, J. J. N87-20372
WILLETTS, DAVID V. N87-20522
N87-20523
WILLIAMS, DAVID H. N87-20254
WILLIAMS, MICHAEL D. N87-20614
WILLIAMS, R. J. N87-20247
WILLSON, ROBERT F. N87-20925
WILSON, JON N87-20608
WILSON, R. H. N87-20182
WILSON, ROBERT M. N87-20947
WILTBERGER, NANCY L. N87-20325
WINDELL, R. W. N87-20579
WINDMILLER, MARY JO N87-20448
WINKLER, L. N87-20772
WITTE, WILLIAM G. N87-20386
WITTENSTEIN, GERALD N87-20666
WOLF, P. N87-20627
WOLFSON, RICHARD N87-20913
WOOD, G. M. N87-20541
WOOD, GEORGE M. N87-20532
WOOD, GEORGE M., JR. N87-20522
N87-20538
WOOD, RICHARD M. N87-20233
WOODS, T. G. N87-20351
WOODWARD, D. S. N87-20204
WU, F. N87-20882
WU, GUIQIU N87-20724
WU, S. T. N87-20678
N87-20679

X

XIAO, Y. C. N87-20678
XIE, Q. M. N87-20278
XU, DELUN N87-20726

Y

YARMAN, BINBOGA S. N87-20483
YEPISHKIN, A. K. N87-20736
YEREMIN, A. V. N87-20735
YOO, M. H. N87-20417
N87-20827
YOON, SEOKKWAN N87-20235
N87-20243
YOSHIHARA, H. N87-20226
YOUNG, LEIGHTON E. N87-20380
YUREK, G. J. N87-20412

Z

ZAHO, BAOREN N87-20721
ZELEZNIK, FRANK J. N87-20274
ZENIE, ALEXANDRE N87-20837
ZHANG, JIUZI N87-20724
ZHANG, XIAOCHUN N87-20269
ZHANG, Y. H. N87-20278
ZHARIKOV, YE. V. N87-20446
ZHDANOV, V. T. N87-20281
ZHI, GAO N87-20246
ZHOU, CHANGHAI N87-20241
ZHOU, XIAOQING N87-20269
ZIMMERMANN, S. D. N87-20749

Typical Corporate Source Index Listing

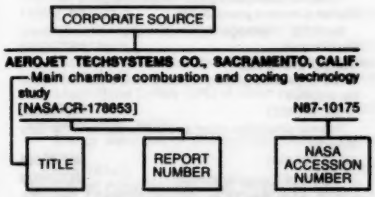

Listings in this index are arranged alphabetically by corporate source. The title of the document provides the user with a brief description of the subject matter. The report number helps to indicate the type of document cited (e.g., NASA report, translation, NASA contractor report). The NASA accession number denotes the number by which the citation is identified. The titles are arranged under each corporate source in ascending accession number order.

A

ACADEMY OF SCIENCES OF THE ARMENIAN SSR, ERIVAN.
Ultra-high energy gamma-rays as the carriers of cosmological information
[DE87-700680] N87-20952

ACADEMY OF SCIENCES OF THE UKRAINIAN SSR, KIEV.
UBVRI-photometry of the antiflare stars V586 Ori and IU Ori
[DE87-700760] N87-20845

ADMIRALTY RESEARCH ESTABLISHMENT, PORTLAND (ENGLAND).
The DYNAS survey. Part 2: A participant's view N87-20579

ADVANCED BATTERY GROUP, LANCASTER, N.Y.
Safety characteristics of non-lithium battery systems, revision 1
[AD-A174577] N87-20480

ADVISORY GROUP FOR AEROSPACE RESEARCH AND DEVELOPMENT, NEUILLY-SUR-SEINE (FRANCE).
The Repair of Aircraft Structures Involving Composite Materials
[AGARD-CP-402] N87-20174
Patch repair of corroded aircraft skin areas N87-20191
Applications of Computational Fluid Dynamics in Aeronautics
[AGARD-CP-412] N87-20199
Mechanical Qualification of Large Flexible Spacecraft Structures
[AD-A175529] N87-20355

AERONAUTICAL RESEARCH LABS., MELBOURNE (AUSTRALIA).
Fibre composite repair of cracked metallic aircraft components: Practical and basic aspects N87-20187

AEROSPACE CORP., EL SEGUNDO, CALIF.
Laboratory investigation of lightweight heater tape for shuttle propellant tank
[AD-A175997] N87-20345

AEROSPACE CORP., LOS ANGELES, CALIF.
Views of the world of pyrotechnic shock N87-20603

AGBABIAN ASSOCIATES, EL SEGUNDO, CALIF.
Multi-axis transient shock simulation using mechanical pulse generators N87-20613

AIR COMMAND AND STAFF COLL., MAXWELL AFB, ALA.
AFGWC's Advanced Weather Analysis and Prediction System (AWAPS)
[AD-A172801] N87-20702

AIR FORCE ACADEMY, COLO.
Recent studies in plate vibrations: 1981-1985. Part 1: Classical theory N87-20437

AIR FORCE FLIGHT DYNAMICS LAB., WRIGHT-PATTERSON AFB, OHIO.
Development of precision structural joints for large space structures N87-20374

AIR FORCE GEOPHYSICS LAB., HANSCOM AFB, MASS.
Requirements for improved modeling of the orbital atmosphere N87-20676
Middle atmosphere density and models N87-20687

AIR FORCE OFFICE OF SCIENTIFIC RESEARCH, BOLLING AFB, WASHINGTON, D.C.
Air Force basic research in dynamics and control of large space structures N87-20577

AIR FORCE SYSTEMS COMMAND, WRIGHT-PATTERSON AFB, OHIO.
Acta mechanica sinica (selected articles)
[AD-A176240] N87-20246
Attitude motion of torque-free asymmetric dual-spin spacecraft
[AD-A175531] N87-20354
Material with anisotropic properties for magnetic shielding purposes
[AD-A175864] N87-20453
Supersonic flow induced cavity acoustics N87-20601

AIR FORCE WRIGHT AERONAUTICAL LABS., WRIGHT-PATTERSON AFB, OHIO.
Composite repair of cracked aluminum structure N87-20183
Application of the Navier-Stokes equations to solve aerodynamic problems N87-20225
Numerical simulation of the flow field around a complete aircraft N87-20231
Temperature shift considerations for damping materials N87-20593

AIR/OCEAN REMOTE SENSING CO., SAN DIEGO, CALIF.
Simulation of wind gradient errors in NROSS (Navy Remote Ocean Sensing System) radar scatterometer data in a simplified geometry
[AD-A175754] N87-20642

AIRCRAFT RESEARCH ASSOCIATION LTD., BEDFORD (ENGLAND).
A discussion on a mesh generation technique applicable to complex geometries N87-20201

AKRON UNIV., OHIO.
Flexibility effects on tooth contact location in spiral bevel gear transmissions
[NASA-CR-4055] N87-20552

ALABAMA A & M UNIV., NORMAL.
Statistical analysis of secondary particle distributions in relativistic nucleus-nucleus collisions
[NASA-CR-4054] N87-20813

ALABAMA UNIV., HUNTSVILLE.
Phase partitioning, crystal growth, electrodeposition and cosmic ray experiments in microgravity N87-20305
Filament formation due to photospheric shear N87-20878
Space radiation studies
[NASA-CR-179037] N87-20951

ALASKA UNIV., FAIRBANKS.
Gravity waves N87-20685

ALLIED BENDIX CORP., KANSAS CITY, MO.
Screening testing for composite preprgs
[DE87-004557] N87-20395

ALUMINUM CO. OF AMERICA, ALCOA CENTER, PA.
Mechanical and thermal characterization of unidirectional aramid/epoxy
[CCMS-86-08] N87-20385

AMERICAN SCIENCE AND ENGINEERING, INC., CAMBRIDGE, MASS.
Small-scale coronal structure, part 3 N87-20922

AMES LAB., IOWA.
Electron tunneling studies of Mo/(sub)1-xRe/(sup)x/: Enhancement of superconductivity by a resonance mode
[DE87-003048] N87-20484
Proximity-induced Josephson effect and its application to heavy fermion superconductor UBe-13
[DE87-003049] N87-20485

ANALYTICAL MECHANICS ASSOCIATES, INC., HAMPTON, VA.
Post-flight BET products for the 2nd discovery entry, STS-19 (51-A)
[NASA-CR-172572] N87-20344

ANALYTICAL MECHANICS ASSOCIATES, INC., MOUNTAIN VIEW, CALIF.
Design and analysis of advanced flight planning concepts
[NASA-CR-4063] N87-20253

APPLIED RESEARCH CORP., LANDOVER, MD.
Searching the UVSP database and a list of experiments showing mass motions N87-20699

ARGONNE NATIONAL LAB., ILL.
Apparatus for high temperature in situ laser Raman spectroelectrochemical studies of metal corrosion and passivation in aqueous environments
[DE87-004868] N87-20416
High-temperature fuel cells
[DE87-004870] N87-20487
Batteries for hybrid vehicles or other high-power applications
[DE87-004928] N87-20488
Temperature effects on nickel/iron battery characteristics
[DE87-004930] N87-20489
Monolithic fuel cell development
[DE87-004926] N87-20492
Morphological changes in the sulfur electrode of lifecycle-tested Na/S cells
[DE87-004961] N87-20493
Characterization of monolithic fuel cell components
[DE87-004929] N87-20655
Guide to sharing personal computer resources via local area networks, revised
[DE86-016088] N87-20772
Highlights from the physics in metallic superlattices
[DE87-004857] N87-20825
High field properties of SnMo6S8 and PbMo6S8 ribbons prepared using a vapor transport technique
[DE87-004707] N87-20826

ARMY AVIATION RESEARCH AND DEVELOPMENT COMMAND, CLEVELAND, OHIO.
Vibration characteristics of OH-58A helicopter main rotor transmission
[NASA-TP-2705] N87-20555

ARMY COLD REGIONS RESEARCH AND ENGINEERING LAB., HANOVER, N. H.
Resilient modulus of freeze-thaw affected granular soils for pavement design and evaluation. Part 3: Laboratory tests on soils from Albany County Airport
[DOT/FAA-PM-84-16.3] N87-20433
A freeze-thaw test to determine the frost susceptibility of soils
[DOT/FAA-PM-85-20] N87-20434

ARMY MATERIALS TECHNOLOGY LAB., WATERTOWN, MASS.
Unconventional approaches to field repair N87-20190
Army research in shock mechanics N87-20576

ARMY MILITARY PERSONNEL CENTER, ALEXANDRIA, VA.
Characterizing thermal/mechanical properties of filament wound composites
[AD-A176238] N87-20392

AUBURN UNIV., ALA.
Initial investigations into the damping characteristics of wire rope vibration isolators
[NASA-CR-180698] N87-20569

AVIONS MARCEL DASSAULT, SAINT-CLOUD (FRANCE).
Utilization of Euler codes in nonlinear aerodynamics N87-20215

AVIONS MARCEL DASSAULT-BREGUET AVIATION, SAINT-CLOUD (FRANCE).
Damage repair of in-service composite structures: Application to the Mirage 2000 N87-20184

B

BATTELLE COLUMBUS LABS., OHIO.
Hydrogen degradation of pipeline steels
[DE87-005585] N87-20414
BAYERISCHE AKADEMIE DER WISSENSCHAFTEN, MUNICH (WEST GERMANY).
Report on the Special Program 78 satellite geodesy of the Technical University of Munich
[ASTRON-GEODAET-ARB-48] N87-20618
BEIJING INST. OF AERONAUTICS AND ASTRONAUTICS (CHINA).
Experimental and analytical investigation of the variation of spray characteristics along a radial distance downstream of a pressure-swirl atomizer N87-20271
BELGIAN ROYAL OBSERVATORY, BRUSSELS.
Solid Earth panel report N87-20636
BETTIS ATOMIC POWER LAB., WEST MIFFLIN, PA.
An automated two-dimensional laser velocimeter system
[DE87-005625] N87-20549
BHABHA ATOMIC RESEARCH CENTRE, BOMBAY (INDIA).
Cryogenic regenerators
[DE87-701264] N87-20443
Development of optical thin film technology for lasers and synchrotron radiation
[DE87-701254] N87-20817
Thermodynamic data of intermetallic compounds
[DE87-701244] N87-20831
BIONETICS CORP., COCOA BEACH, FLA.
Effects of space shuttle launches STS-1 through STS-9 on terrestrial vegetation of John F. Kennedy Space Center, Florida
[NASA-TM-83103] N87-20658
BIONETICS CORP., HAMPTON, VA.
An advanced technology space station for the year 2025, study and concepts
[NASA-CR-178208] N87-20340
BOEING AEROSPACE CO., SEATTLE, WASH.
NASA/MSFC large stretch press study
[NASA-CR-180376] N87-20554
BOEING COMMERCIAL AIRPLANE CO., SEATTLE, WASH.
Design and verification by nonlinear simulation of a Mach/CAS control law for the NASA TCV B737 aircraft
[NASA-CR-178029] N87-20290
BOEING MILITARY AIRPLANE DEVELOPMENT, SEATTLE, WASH.
Calculations for a generic fighter at supersonic high-lift conditions N87-20226
BRANDEIS UNIV., WALTHAM, MASS.
Effect of light and development of photosynthetic cells
[DE87-005183] N87-20728
BRISTOL UNIV. (ENGLAND).
Investigation of flow under the fuselage of a powered light aircraft model
[BU-351] N87-20247
A preliminary study into the constant drag parachute for aircrew escape systems
[BU-345] N87-20256
Materials selection and design study of a composite microlight wing structure
[BU-335] N87-20263
An investigation into the factors affecting the flow quality in a small suction wind tunnel
[BU-344] N87-20299
BRITISH AEROSPACE AIRCRAFT GROUP, WARTON (ENGLAND).
Applications and developments of computational methods for the aerodynamic problems of complex configurations N87-20209
The integration of computational fluid dynamics into the military aircraft design process N87-20210
BRITISH AEROSPACE PUBLIC LTD. CO., STEVENAGE (ENGLAND).
Influence co-efficient testing as a substitute for modal survey testing of large space structures N87-20369
BRITISH AIRWAYS, MIDDLESEX (ENGLAND).
British Airways experience with composite repairs N87-20192
BRITISH BROADCASTING CORP., LONDON (ENGLAND).
A survey of achieved levels of airborne sound insulation in broadcasting studio centres
[BBC-RD-1987/1] N87-20796
BROOKHAVEN NATIONAL LAB., UPTON, N. Y.
Hydrogen degradation of pipeline steels
[DE87-005585] N87-20414
A ring-cavity for a quadrupled Nd-YAG laser
[DE87-004175] N87-20547
The fifth force
[DE87-004612] N87-20694

C

CALIFORNIA INST. OF TECH., PASADENA.
The effects of large-eddy manipulator devices on the turbulent spot and the turbulent boundary layer N87-20497
Abundances and kinematics of K giants in the galactic nuclear bulge N87-20656
Double inflation: A possible resolution of the large-scale structure problem
[DE87-005403] N87-20865
Recent observations of the formation of filaments N87-20883
The microwave structure of quiescent solar filaments at high resolution N87-20889
Measurement of coronal fields using spatially resolved microwave spectroscopy N87-20920
Small-scale eruptive filaments on the quiet sun N87-20928
CALIFORNIA POLYTECHNIC STATE UNIV., SAN LUIS OBISPO.
Cal Poly Space Project G-279 N87-20324
CALIFORNIA UNIV., BERKELEY.
Ring galaxies: An investigation of the physical conditions in closely interacting systems N87-20658
The large-scale peculiar velocity field in flat models of the universe
[DE87-005402] N87-20864
Double inflation: A possible resolution of the large-scale structure problem
[DE87-005403] N87-20865
CALIFORNIA UNIV., FULLERTON.
Six reasons why thermospheric measurements and models disagree N87-20688
CALIFORNIA UNIV., IRVINE.
The growth of radiative filamentation modes in sheared magnetic fields N87-20875
CALIFORNIA UNIV., LOS ANGELES.
A virtual-time operating-system shell for a hypercube in robotics applications
[DE87-004256] N87-20773
Computer simulation and analysis of spatial galaxy distributions N87-20851
MHD waves detected by ice at distances 28 x 10 km from Comet Halley: Cometary or solar wind origin
[DE87-005122] N87-20863
Steepened magnetosonic waves in the high Beta plasma surrounding Comet-Giacobini-Zinner
[NASA-CR-180614] N87-20868
CALIFORNIA UNIV., SAN DIEGO, LA JOLLA.
Chemical engineering design of CO oxidation catalysts N87-20531
CALIFORNIA UNIV., SANTA BARBARA.
Problems in quantum cosmology N87-20846
CANADAIR LTD., MONTREAL (QUEBEC).
Prediction of wing-body-store aerodynamics using a small perturbation method and a grid embedding technique N87-20207
CARNEGIE-MELLON UNIV., PITTSBURGH, PA.
The digital processing of acceleration measurements for modal analysis N87-20439
Multilevel representation and simulation for VLSI design
[AD-A175663] N87-20481
CENTER FOR INNOVATIVE TECHNOLOGY, HERNDON, VA.
Mechanical and thermal characterization of unidirectional aramid/epoxy
[CCMS-86-08] N87-20385
CENTER FOR MATHEMATICS AND COMPUTER SCIENCE, AMSTERDAM (NETHERLANDS).
A new approach to least squares estimation, with applications
[CWI-MS-R8602] N87-20787
Uniqueness of Gibbs measures and absorption probabilities
[CWI-MS-R8610] N87-20789
CENTRE D'ETUDES AERODYNAMIQUES ET THERMIQUES, POITIERS (FRANCE).
Study of compressibility effects on supersonic free flow
[ETN-87-99392] N87-20251
Study of the development of a compressible turbulent boundary layer on a porous and rough wall
[ETN-87-99390] N87-20512
Experimental evaluation of sub-cell turbulent models. Space-time correlations in a mixing layer
[ETN-87-99391] N87-20513
CENTRE NATIONAL D'ETUDES SPATIALES, TOULOUSE (FRANCE).
Low frequency vibration testing on satellites N87-20364
Remote sensing applications: Commercial issues and opportunities for space station N87-20626
CENTRE NATIONAL DE LA RECHERCHE SCIENTIFIQUE, VERRIERES-LE BUISSON (FRANCE).
Diagnostics and structure N87-20865
CEPSTRUM ENGEHARIA LTDA., SAO PAULO (BRAZIL).
A new approach for gearbox modelling in finite element analyses of torsional vibration of gear-branched propulsion systems N87-20591
CESKOSLOVENSKA AKADEMIE VED, BRNO.
Creep and Creep Fracture: Conference proceedings
[DE87-780056] N87-20615
CESKOSLOVENSKA AKADEMIE VED, ONDREJOV.
Partial redistribution effects in the formation of hydrogen lines in quiescent prominences N87-20894
Non-LTE hydrogen-line formation in moving prominences N87-20895
CHICAGO UNIV., ILL.
The large-scale peculiar velocity field in flat models of the universe
[DE87-005402] N87-20864
Thermal production of not so invisible axions in the early universe
[DE87-005404] N87-20866
Heating of the stellar corona N87-20873
CHINESE AERONAUTICAL ESTABLISHMENT, BEIJING.
Numerical study of combustion processes in afterburners N87-20269
CITY COLL. OF THE CITY UNIV. OF NEW YORK.
Geotaxis baseline data for Drosophila N87-20322
CIVIL AVIATION AUTHORITY, LONDON (ENGLAND).
Helicopter external load operations
[CAP-426] N87-20259
COLORADO UNIV., BOULDER.
Computation of transonic flow over porous airfoils N87-20194
Multigrid calculation of boundary-fitted orthogonal coordinates with applications to unsteady flows N87-20237
Phycomyces in space: A problem in bioengineering N87-20308
Sophisticated software systems for small self-contained space shuttle payload G285 N87-20313
The growth and harvesting of algae in a micro-gravity environment N87-20325
COLUMBIA UNIV., NEW YORK.
Research investigation directed toward extending the useful range of the electromagnetic spectrum
[AD-A175644] N87-20452
COMMITTEE ON SCIENCE AND TECHNOLOGY (U. S. HOUSE).
Assured access to space: 1986
[GPO-60-627] N87-20838
COMMUNICATIONS RESEARCH CENTRE, OTTAWA (ONTARIO).
The in-situ calibration of a bilateral space-fed phased array antenna
[AD-A176069] N87-20456
COMPUTER SCIENCES CORP., FALLS CHURCH, VA.
Flexible satellite communications systems simulator standard device groups
[AD-A175944] N87-20454
CONCORDIA UNIV., MONTREAL (QUEBEC).
Effectiveness of on-off damper in isolating dynamical systems N87-20594
CONTINUUM, INC., HUNTSVILLE, ALA.
Computational analyses of crystal growth
[NASA-CR-179027] N87-20820

D

DEFENCE RESEARCH ESTABLISHMENT VALCARTIER (QUEBEC).
An overview of DREV's activities on pulsed CO2 laser transmitters: Frequency stability and lifetime aspects N87-20542
DEFENSE SYSTEMS, INC., MCLEAN, VA.
Tracking the GLOMR satellite N87-20303
DELAWARE UNIV., NEWARK.
Real-time crop assessment using color theory and satellite data N87-20619
DEPARTMENT OF ENERGY, MORGANTOWN, W. VA.
Feasibility of a phosphoric acid fuel cell basic technology program
[DE87-001045] N87-20490
DEPARTMENT OF THE AIR FORCE, WASHINGTON, D.C.
Propellant tank resupply system
[AD-D012559] N87-20375
Turnaround control for mechanically scanned radar antennas
[AD-D012563] N87-20457
Magnetostatic wave frequency analyzer apparatus
[AD-D012558] N87-20458
Adaptive mutual interference suppression method
[AD-D012552] N87-20459

Low pass Pi section digital phase shifter apparatus
[AD-D012553] N87-20483
Diffraction diffusion screen with holographically suppressed zero-order beam
[AD-D012565] N87-20519
Atmospheric contrast transmittance monitor
[AD-D012555] N87-20520
Fly's eye sensor nonlinear signal processing
[AD-D012564] N87-20815

DEPARTMENT OF THE NAVY, WASHINGTON, D. C.
Airspeed sensing pressure valve system
[AD-D012569] N87-20266
Arresting and recovery system for test missiles
[AD-D012574] N87-20337
Operation of transversely excited N2O lasers
[AD-D012583] N87-20543
Automated anthropometric data measurement system
[AD-D012575] N87-20748
Liquid Phase Epitaxy (LPE) of silicon carbide
[AD-D012571] N87-20823

DETROIT UNIV., MICH.
Energy absorption of polyurethane based polymer alloys
[AD-A175542] N87-20427

DEUTSCHE FORSCHUNGS- UND VERSUCHSANSTALT FUER LUFT- UND RAUMFAHRT, COLOGNE (WEST GERMANY).
Recent results from MAUS payloads N87-20331

DEUTSCHE FORSCHUNGS- UND VERSUCHSANSTALT FUER LUFT- UND RAUMFAHRT, GOETTINGEN (WEST GERMANY).
Simulation of three-dimensional transonic flow with separation past a hemisphere cylinder configuration N87-20230
Dynamic qualification of spacecraft by means of modal synthesis N87-20363
Modal-survey testing for system identification and dynamic qualification of spacecraft structures N87-20365

DEUTSCHE FORSCHUNGS- UND VERSUCHSANSTALT FUER LUFT- UND RAUMFAHRT, OBERPFAFFENHOFEN (WEST GERMANY).
European utilization aspects studies N87-20624
Land panel report N87-20634

DORNIER-WERKE G.M.B.H., FRIEDRICHSHAFEN (WEST GERMANY).
Repair procedures for composite parts on the alpha jet N87-20175
Numerical grid generation around complete aircraft configurations N87-20202
Numerical simulation of internal and external inviscid and viscous 3-D flow fields N87-20213

DU PONT DE NEMOURS (E. I.) AND CO., AIKEN, S.C.
Galvanic corrosion resistance of welded dissimilar nickel-base alloys
[DE87-002656] N87-20409

E

EAST ANGLIA UNIV., NORWICH (ENGLAND).
Monthly mean pressure reconstructions for Europe (back to 1780) and North America (to 1958)
[DE87-005556] N87-20703

EAST CAROLINA UNIV., GREENVILLE, N.C.
A stochastic approach to project planning in an R and D environment
[DE87-005347] N87-20835

ECOLE NATIONALE SUPERIEURE DES TELECOMMUNICATIONS, PARIS (FRANCE).
Activities report of the Department of Systems and Communications
[ENST-86D002] N87-20486
Linearization of GaAs field effect transistor power amplifiers in hyperfrequences
[ENST-86E007] N87-20496
Evaluation of the performance of a geographically distributed data base management system using stochastic Petri nets
[ENST-86C002] N87-20837

ECOLE SUPERIEURE D'ELECTRICITE, GIF-SUR-YVETTE (FRANCE).
G-300: The first French Getaway Special microgravity measurements of fluid thermal conductivity N87-20330

EDGERTON, GERMESHAUSEN AND GRIER, INC., IDAHO FALLS, IDAHO.
Studies of stress wave propagation in composites
[DE87-001433] N87-20396
Experimental measurement of thin plate SS 304 GTAW weld pool surface temperatures
[DE87-004545] N87-20561
Risk evaluations of aging phenomena: The linear aging reliability model and its extensions
[DE87-002607] N87-20563

EMBASSY OF INDIA, WASHINGTON, D.C.
Blade damping measurements in a spin rig with nozzle passing excitation simulated by electromagnets N87-20590

EMMANUEL COLL., BOSTON, MASS.
Small-scale coronal structure, part 3 N87-20922

EUROPEAN ORGANIZATION FOR NUCLEAR RESEARCH, GENEVA (SWITZERLAND).
The fifth force
[DE87-004612] N87-20694

EUROPEAN SPACE AGENCY, PARIS (FRANCE).
The high-speed cascade wind tunnel - still an important test facility for turbomachinary blade investigations
[ESA-TT-1012] N87-20300
Theoretical study of the nonsteady combustion of composite fuel droplets
[ESA-TT-868] N87-20401
Numerical and optical experiments on the Weissenberg effect
[ESA-TT-879] N87-20510
Proceedings of the European Symposium on Polar platform Opportunities and Instrumentation for Remote-Sensing (ESPOIR)
[ESA-SP-266] N87-20621
The Columbus program: An overview N87-20623
Servicing of the polar platform N87-20628
USA-Europe coordination and cooperation activities: Announcements of Opportunity N87-20632
Panel report on multidisciplinary instrumentation: New possibilities N87-20637
Panel report on new approaches to calibration and validation N87-20638
A bispectral method for the determination of the altitude of ice clouds
[ESA-TT-993] N87-20704
Noise measurements on the helicopter BK 117 design. Weighted noise levels and influence of airspeed
[ESA-TT-748] N87-20800
Encounter 86: An international rendezvous with Halley's comet
[ESA-BR-27] N87-20867

EUROPEAN SPACE AGENCY. ESRIN, FRASCATI (ITALY).
Payload data management scheme planned for Earth observation sensors to be flown on the polar platforms in the framework of the space station/Columbus program N87-20630
Data management panel report N87-20639

EUROPEAN SPACE AGENCY. EUROPEAN SPACE RESEARCH AND TECHNOLOGY CENTER, ESTEC, NOORDWIJK (NETHERLANDS).
The Earth observation activities of the European Space Agency and the use of the polar platform of the International Space Station N87-20622
Working group on Earth observation requirements for the Polar Orbiting Platform Elements of the International Space Station (the POPE Working Group) N87-20625
ESA Columbus polar platform design concept N87-20627
Orbit configurations N87-20629
Cooperation of the International Space Station partners in the preparation of the use of space station elements for Earth observation (platform and payload aspects) N87-20631
The orbit configuration panel report N87-20640
Panel report on the polar platform servicing approach and its implications N87-20641

F

FEDERAL AVIATION ADMINISTRATION, WASHINGTON, D.C.
The 1985 small propeller-driven aircraft noise test program
[AD-A175596] N87-20799

FERMI NATIONAL ACCELERATOR LAB., BATAVIA, ILL.
The large-scale peculiar velocity field in flat models of the universe
[DE87-005402] N87-20684
Double inflation: A possible resolution of the large-scale structure problem
[DE87-005403] N87-20865
Thermal production of not so invisible axions in the early universe
[DE87-005404] N87-20866

FLIGHT MECHANICS AND CONTROL, INC., HAMPTON, VA.
Shuttle derived atmosphere N87-20684

FLORENCE UNIV. (ITALY).
Measurements of magnetic fields in solar prominences N87-20901

FLORIDA UNIV., GAINESVILLE.
A review of tin oxide-based catalytic systems: Preparation, characterization and catalytic behavior N87-20537

A dynamic multicomputer system for managing scientific and engineering databases
[DE87-002497] N87-20757

FLOW RESEARCH, INC., KENT, WASH.
Turbulence control on an airborne laser platform
[NASA-CR-178249] N87-20503

FORD AEROSPACE AND COMMUNICATIONS CORP., PALO ALTO, CALIF.
Satellite analog FDMA/FM to digital TDMA conversion
[NASA-CR-179605] N87-20467

FRAUNHOFER-INST. FUER BETRIEBSFESTIGKEIT, DARMSTADT (WEST GERMANY).
Criteria and methodology for lightweight design of vehicle components
[LBF-TB-176(1986)] N87-20550

G

GAS TURBINE RESEARCH INST., JIANGYOU (CHINA).
Combustion research activities at the Gas Turbine Research Institute N87-20273
Experimental investigation of piloted flameholders N87-20278

GENERAL DYNAMICS/CONVAIR, SAN DIEGO, CALIF.
Design study of advanced model support systems for the National Transonic Facility (NTF)
[NASA-CR-178214] N87-20297

GENERAL DYNAMICS CORP., FORT WORTH, TEX.
Analysis of the F-16 flow field by a block grid Euler approach N87-20217

GENERAL ELECTRIC CO., CINCINNATI, OHIO.
Development of a rotor wake/vortex model. Volume 2: User's manual for computer program
[NASA-CR-174850-VOL-2] N87-20239

GENERAL MOTORS RESEARCH LABS., WARREN, MICH.
Alumina-supported Pd-Ag catalysts for low-temperature CO and methanol oxidation N87-20536

GEO-CENTERS, INC., SUITLAND, MD.
Load biaxiality and fracture: A two-sided history of complementing errors
[AD-A175972] N87-20573

GEORGE WASHINGTON UNIV., WASHINGTON, D.C.
Investigation of thermal-fluid mechanical characteristics of the capillary pump and the pumped two-phase loop
[NASA-CR-180509] N87-20557

GEORGIA INST. OF TECH., ATLANTA.
A numerical study of the Weis-Fogh mechanism N87-20197
Numerical solutions of unsteady flow past rotor sections N87-20198
Effect of dynamic stall and elastic parameters on the fundamental mechanisms of helicopter vibrations
[AD-A175561] N87-20292
Studies in nonlinear structural dynamics: Chaotic behavior and poynting effect N87-20348
The GRAM-3 model N87-20686

GOETTINGEN UNIV. (WEST GERMANY).
Amplification of an electron density perturbation in the polar E layer, induced by strong HF waves
[ETN-87-99014] N87-20695

GOSUDARSTVENNYI KOMITET PO ISPOLZOVANIYU ATOMNOI ENERGII, SERPUKHOV (USSR).
Gravitational collapse in relativistic theory of gravitation
[DE87-700730] N87-20792

H

HARVARD-SMITHSONIAN CENTER FOR ASTROPHYSICS, CAMBRIDGE, MASS.
Simultaneous observations of changes in coronal bright point emission at the 20 cm radio and He Lambda 10830 wavelengths N87-20923
Cascade model of coronal heating N87-20938

HAWAII UNIV., HONOLULU.
The white light corona and photospheric magnetic fields N87-20912
Small-scale structures and the density irregularity of the inner corona N87-20932

HELSINKI UNIV. OF TECHNOLOGY, ESPOO (FINLAND).
Studies of X-ray satellites in sodium, magnesium, aluminum, argon, and iron
[ETN-87-99364] N87-20812
Nonlinear dynamics of some condensed matter devices and materials
[ETN-87-99363] N87-20829

HIEBER ENGINEERING, WATCHING, N.J.
Isolation and damping: A graphical method of determining the response of the cascaded two degree of freedom system N87-20592

HIROSHIMA UNIV., TAKEHARA (JAPAN).
On the de Sitter and Narlai space-times in a generalized theory of gravitation
[DE86-703483] N87-20830
HOUSTON UNIV., TEX.
An investigation of transitional management problems for the NSTS
[NASA-CR-171979] N87-20834
HOWARD UNIV., WASHINGTON, D. C.
A study of III-V semiconductor processing employing high purity epitaxial gallium arsenide N87-20819

I

ILLINOIS UNIV., CHICAGO.
CO oxidation studies over supported noble metal catalysts and single crystals: A review N87-20530
ILLINOIS UNIV., URBANA-CHAMPAIGN.
A comparison of nonlinear filters for orbit determination and estimation N87-20336
The star-forming properties of violently interacting galaxies N87-20849
IMPERIAL COLL. OF SCIENCE AND TECHNOLOGY, LONDON (ENGLAND).
Comparison of finite difference calculations of a large region of recirculating flow near an airfoil trailing edge N87-20218
State-of-the-art assessment of structural dynamic response analysis methods (DYNAS) N87-20578
INDIAN INST. OF TECH., NEW DELHI.
Forced vibrations of stringer stiffened damped sandwich panel N87-20596
INDUSTRIEANLAGEN-BETRIEBSGESELLSCHAFT M.B.H., OTTOBRUNN (WEST GERMANY).
Spacecraft qualification using advanced vibration and modal testing techniques N87-20388
Multi-axis vibration tests on spacecraft using hydraulic exciters N87-20373
INSTITUT NATIONAL DES SCIENCES APPLIQUEES DE LYON, VILLEURBANNE (FRANCE).
Machinery dynamics: Prediction of natural frequencies of flexible shaft-disc system N87-20587
INSTITUT NATIONAL DES SCIENCES APPLIQUEES, LYON (FRANCE).
Determination of the ternary viscosity diagram NaCl-KCl-LiCl by the flow method
[INSA-IDTC1-8604] N87-20403
INSTITUTO DE PESQUISAS ESPACIAIS, SAO JOSE DOS CAMPOS (BRAZIL).
Automation and robotics
[INPE-4088-PRE/1033] N87-20551
Magnetotelluric measurements in Antarctica
[INPE-4058-PRE/1017] N87-20661
Nuclear geophysics in space and atmospheric research at INPE/BRAZIL
[DE87-700426] N87-20693
Measurements of iridium and the hypothesis of meteoritic impact as the end of the Cretaceous period
[INPE-4070-TDL/248] N87-20861
IOWA UNIV., IOWA CITY.
Guided MHD waves as a coronal diagnostic tool N87-20921
ISTANBUL UNIV. (TURKEY).
Numerical investigation of the laminar boundary layer on a 3-D body started impulsively from rest N87-20220
ITALSPAZIO, ROME (ITALY).
Land mobile satellite communication system. Volume 1: Executive summary
[ITS-TR-043/86-VOL1] N87-20464
Land mobile satellite communication system. Volume 2: Traffic analysis and market demand for the land mobile communications system in the European scenario
[ITS-TR-043/86-VOL-2] N87-20465

J

JET PROPULSION LAB., CALIFORNIA INST. OF TECH., PASADENA.
Structural qualification of large spacecraft N87-20361
Frequency stabilization in injection controlled pulsed CO2 lasers N87-20527
Modal test and analysis: Multiple tests concept for improved validation of large space structure mathematical models N87-20581
Super*Zip (linear separation) shock characteristics N87-20605
Flat-plate solar array project of the US Department of Energy's National Photovoltaics Program: Ten years of progress
[NASA-CR-180507] N87-20644
Summary of flat-plate solar array project documentation: Abstracts of published documents, 1975-1986, revision 1
[NASA-CR-180401-REV-1] N87-20645
Flat-plate solar array project. Volume 1: Executive summary
[NASA-CR-180658] N87-20646
Flat-plate solar array project. Volume 2: Silicon material
[NASA-CR-180659] N87-20647
Flat-plate solar array project. Volume 3: Silicon sheet: Wafers and ribbons
[NASA-CR-180661] N87-20648
Flat-plate solar array project. Volume 4: High-efficiency solar cells
[NASA-CR-180662] N87-20649
Flat-plate solar array project. Volume 5: Process development
[NASA-CR-180663] N87-20650
Flat-plate solar array project. Volume 6: Engineering sciences and reliability
[NASA-CR-180664] N87-20651
Flat-plate solar array project. Volume 7: Module encapsulation
[NASA-CR-180665] N87-20652
Flat-plate solar array project. Volume 8: Project analysis and integration
[NASA-CR-180695] N87-20653
MHD waves detected by ice at distances 28 x 10 km from Comet Halley: Cometary or solar wind origin
[DE87-005122] N87-20863
Steepened magnetosonic waves in the high Beta plasma surrounding Comet-Giacobini-Zinner
[NASA-CR-180614] N87-20868
JOHNS HOPKINS UNIV., SILVER SPRING, MD.
Composite motor case nomenclature
[AD-A176418] N87-20384
JOINT PUBLICATIONS RESEARCH SERVICE, ARLINGTON, VA.
USSR report: Physics and mathematics
[JPRS-UPM-86-008] N87-20445
The laser strength of active elements made of Gadolinium-Scandium-Gallium garnet (GSGG) N87-20446
Organic photochromic material for recording waveguide holograms N87-20447
China report: Science and technology
[JPRS-CST-86-025] N87-20708
Hydrologic features in cyclonic eddy region of northern east China Sea in cold seasons N87-20709
China report: Science and technology
[JPRS-CST-87-005] N87-20717
Numerical simulation of storm surges in the east China Sea N87-20718
Mathematical model of steady-state circulation in the south China Sea N87-20719
China Report: Science and technology
[JPRS-CST-86-031] N87-20720
Existence seen of cyclonic eddy in northern east China Sea N87-20721
Spectral analysis of waves in Gulf of Tonkin described N87-20722
Physical, mechanical effect of velocity of sound in ocean sediments N87-20723
Comparison of deepwater wind-wave prediction models N87-20724
Methods of frequency spectrum estimation of sea water compared N87-20725
Phase speed of wind-wave component studied N87-20726
USSR report: Space Biology and Aerospace Medicine, Volume 20, No. 3, May - June 1986
[JPRS-USB-86-005] N87-20731
Space biology and medicine on the twenty-fifth anniversary of the first spaceflight of Yuriy Alekseyevich Gagarin N87-20732
Stages of development of the problem of flight safety in aviation medicine N87-20733
Interlabyrinthine asymmetry, vestibular dysfunction and space motion sickness N87-20734
Evaluation of physical work capacity of cosmonauts aboard Salyut-6 station N87-20735
Operator work capacity in tracking system when submitted to antiorthostatic hypokinesia N87-20736
Blood lipids and incidence of lipemia in flight personnel N87-20737
Link between asymmetry of optokinetic nystagmus, optovestibular and vestibulovegetative stability N87-20738
Physiological mechanisms limiting external resistance to respiration N87-20739
Effect of hemadsorption on rheological parameters of blood during seven-day antiorthostatic hypokinesia and in vitro studies N87-20740
Effect of long-term spaceflight on rat brain polyamine content N87-20741
Effect of hypoxia on DNA synthesis and collagent content of regenerating skin N87-20742
Electrodermal conductivity in man and monkeys N87-20743
Interpretation of right heart kinetocardiogram N87-20744
Dynamics of bioelectric activity of human brain in a continuous waking state N87-20745
New book deals with spatial orientation N87-20746
USSR report: Life sciences. Biomedical and behavioral sciences
[JPRS-UBB-87-003] N87-20751
Investigation of microstructure of arbitrary motions of operator N87-20752

K

KANSAS UNIV. CENTER FOR RESEARCH, INC., LAWRENCE.
Development of a takeoff performance monitoring system
[NASA-CR-178255] N87-20264
KYOTO UNIV. (JAPAN).
Steepened magnetosonic waves in the high Beta plasma surrounding Comet-Giacobini-Zinner
[NASA-CR-180614] N87-20868

L

LAWRENCE LIVERMORE NATIONAL LAB., CALIF.
The variation of subgrain misorientation in aluminum deformed to large steady-state creep strains
[DE87-003236] N87-20415
Engineering thrust areas, 1987
[DE87-004443] N87-20441
Electroforming with nickel, iron, and aluminum
[DE87-005589] N87-20442
Calculation of Rayleigh-Taylor flows using vortex blobs
[DE87-002551] N87-20507
Integrated optical devices for high speed diagnostics
[DE87-003160] N87-20616
LOCKHEED-CALIFORNIA CO., BURBANK.
Development of field level repairs for composite structures N87-20177
Development of powder metallurgy 2XXX series Al alloy plate and sheet materials for high temperature aircraft structural applications, FY 1983/1984
[NASA-CR-172521] N87-20406
LOCKHEED MISSILES AND SPACE CO., HUNTSVILLE, ALA.
Development of a computational aero/fluids analysis system
[NASA-CR-179046] N87-20343
LOCKHEED MISSILES AND SPACE CO., SUNNYVALE, CALIF.
A vibroacoustic database management system and its application for a pyroshock database N87-20607
LOS ALAMOS NATIONAL LAB., N. MEX.
Microstructure of metastable metallic alloy films produced by laser breakdown chemical vapor deposition and ion implantation
[DE87-002914] N87-20411
Factors limiting the operation of structures under high gradient
[DE87-005132] N87-20461
Application of a laser-induced breakdown time-of-flight technique in a flow diagnostic in a CO2 free-jet expansion
[DE87-002890] N87-20506
A predictor-corrector method for calculation of incompressible fluid flow dynamics
[DE87-003804] N87-20508
Structural dynamics: Buckling of ring-stiffened cylindrical shells with dynamic loads N87-20595
Fuel cells in transportation
[DE87-003746] N87-20654
Three-body calculations at Los Alamos
[DE87-001959] N87-20786
Linear nonadiabatic pulsations of homogeneous ZAMS stars
[DE87-003722] N87-20844
MHD waves detected by ice at distances 28 x 10 km from Comet Halley: Cometary or solar wind origin
[DE87-005122] N87-20863
Steepened magnetosonic waves in the high Beta plasma surrounding Comet-Giacobini-Zinner
[NASA-CR-180614] N87-20868
Magnetic field re-arrangement after prominence eruption N87-20907
Large-scale electric fields resulting from magnetic reconnection in the corona N87-20944
LUNAR AND PLANETARY INST., HOUSTON, TEX.
Wilson cycle studies
[NASA-CR-180503] N87-20664

M

MAPLE LEAF MILLS, OTTAWA (ONTARIO).
Baking the first bread in space N87-20319
MARCONI AVIONICS LTD., BOREHAMWOOD (ENGLAND).
High repetition rate sealed CO2 TEA lasers using heterogeneous catalysts N87-20529
MARCONI ELECTRONIC DEVICES LTD., LINCOLN (ENGLAND).
Optically tuned millimeter-wave CW. IMPATT source [AD-A175836] N87-20482
MARTIN MARIETTA AEROSPACE, DENVER, COLO.
Shuttle/Spacelab contamination environment and effects handbook [NASA-CR-4053] N87-20350
Benefits of passive damping as applied to active control of large space structures N87-20371
Users manual for nickel cadmium battery expert system [NASA-CR-179032] N87-20470
Nickel cadmium battery expert system [NASA-CR-179031] N87-20471
Program maintenance manual for nickel cadmium battery expert system, version 1 [NASA-CR-179033] N87-20472
Requirements specification for nickel cadmium battery expert system [NASA-CR-179034] N87-20473
MARYLAND UNIV., COLLEGE PARK.
Optimization of hypersonic waveriders derived from cone flows including viscous effects N87-20193
Aeroelastic stability of bearingless rotors in forward flight N87-20260
An application of computational fluid dynamics to the design of optimum ramjet powered missile components N87-20338
An investigation of the strong principle of equivalence through the use of freely falling geocentric coordinates N87-20862
MHD waves detected by ice at distances 26 x 10 km from Comet Halley: Cometary or solar wind origin [DE87-005122] N87-20863
Observations of sunward and tailward ion streaming in the magnetotail of Jupiter with Voyager 2 N87-20869
VLA observations of slar filaments at 6 and 20 cm wavelengths N87-20888
Interpretation of the prominence differential emissions measure for 3 geometries N87-20890
Large scale structure of the corona N87-20909
Large scale structure of the sun's radio corona N87-20910
Three dimensional structures of solar active regions N87-20916
VLA observations of coronal bright points at 6 and 20 cm wavelengths N87-20924
The propagation of an electron beam through the solar corona N87-20946
MASSACHUSETTS INST. OF TECH., CAMBRIDGE.
Applications of Euler equations to sharp edge delta wings with leading edge vortices N87-20214
Mechanisms of the oxidation of metals and alloys: [DE87-003389] N87-20412
Radar scene generation for tactical decision aids [NASA-CR-180234] N87-20449
The interpretation of crustal dynamics data in terms of plate interactions and active tectonics of the Anatolian Plate and surrounding regions in the Middle East [NASA-CR-180501] N87-20662
Information-preserving models of physics and computation [DE87-005354] N87-20793
MASSACHUSETTS UNIV., AMHERST.
Dynamic and thermal effects in very large space structures N87-20347
Erosion and strength degradation in alumina [DE87-003341] N87-20428
The acceleration and dissolution of stars moving through the blackbody radiation of a collapsing universe N87-20847
The magnetic and turbulent evolution of the Taurus molecular cloud N87-20852
MATRA ESPACE, TOULOUSE (FRANCE).
Qualification of the faint object camera N87-20359
MATRA SERVICE AERODYNAMIQUE, VELIZY-VILLACOUBLAY (FRANCE).
Simulation of a jet deflection system with the aid of the Euler equations N87-20212
MCDONNELL AIRCRAFT CO., ST. LOUIS, MO.
Battle damage repair of composite structures N87-20189
MCDONNELL-DOUGLAS ASTRONAUTICS CO., HUNTSVILLE, ALA.
Microgravity effects on electrodeposition of metals and metal-cermet mixtures N87-20332
MCDONNELL-DOUGLAS ASTRONAUTICS CO., ST. LOUIS, MO.
Advanced EVA system design requirements study: EVAS/space station system interface requirements [NASA-CR-171981] N87-20351
Consolidation processing parameters and alternative processing methods for powder metallurgy Al-Cu-Mg-X-X alloys [NASA-CR-178227] N87-20404
MCDONNELL-DOUGLAS CORP., HUNTINGTON BEACH, CALIF.
Summary of testing techniques N87-20614
MCDONNELL-DOUGLAS CORP., ST. LOUIS, MO.
Use of the 4D-Global Reference Atmosphere Model (GRAM) for space shuttle descent design N87-20681
MECHANICAL TECHNOLOGY, INC., LATHAM, N. Y.
Conceptual design of a solar electric advanced Stirling power system [DE87-005036] N87-20656
MEDICAL UNIV. OF SOUTH CAROLINA, CHARLESTON.
To catch a comet 2: Technical update on CAN-DO N87-20326
To catch a child's imagination 2: Educational update on CAN-DO N87-20327
MESOSCALE ENVIRONMENTAL SIMULATIONS, INC., HAMPTON, VA.
The terminal area simulation system. Volume 2: Verification cases [NASA-CR-4047-VOL-2] N87-20252
The terminal area simulation system. Volume 1: Theoretical formulation [NASA-CR-4046-VOL-1] N87-20255
MESSERSCHMITT-BOELKOW-BLOHM/ENTWICKLUNG SPRING NORD, BREMEN (WEST GERMANY).
Recent developments and future trends in structural dynamic design verification and qualification of large flexible spacecraft N87-20357
MESSERSCHMITT-BOELKOW-BLOHM G.M.B.H., MUNICH (WEST GERMANY).
Design for repairability of helicopter composite blades N87-20176
Composite repair of cocured J-stiffened panels: Design and test verification N87-20181
Composite repair techniques for J-stiffened composite fuselage structures N87-20186
Euler solution for a complete fighter aircraft at sub- and supersonic speed N87-20216
Zonal solutions for airfoils using Euler boundary-layer and Navier-Stokes equations N87-20219
METEOROLOGICAL OFFICE, BRACKNELL (ENGLAND).
Ocean-ice panel report N87-20635
MICHIGAN STATE UNIV., EAST LANSING.
Theoretical investigations of shear band formation in finite elasticity [AD-A175657] N87-20572
Structural degradation of impacted graphite/epoxy laminates N87-20586
MICHIGAN UNIV., ANN ARBOR.
Numerical simulation of separated flows past bluff bodies N87-20439
MIDDLEBURY COLL., VT.
Quasistatic evolution of magnetostatic coronal structures N87-20913
MIDWEST RESEARCH INST., GOLDEN, COLO.
Microalgae culture collection, 1986-1987 [DE87-005578] N87-20729
MISSION RESEARCH CORP., SANTA BARBARA, CALIF.
Propagation of RF signals through structured ionization. Theory and antenna aperture effect applications [AD-A175522] N87-20451
Stochastic effects on oblique HF (High Frequencies) propagation [AD-A176015] N87-20455
MISSOURI UNIV., COLUMBIA.
A holographic interferometry study of an axisymmetric shock-wave/boundary-layer strong interaction flow N87-20498
MOUND LAB., MIAMISBURG, OHIO.
Chemistry of glass-ceramic to metal bonding for header applications Part 2: Hydrogen bubble formation during glass-ceramic to metal sealing [DE87-004041] N87-20559

N

NAGOYA UNIV. (JAPAN).
Investigation of low-current-density nanosecond electron beam diode [IPPJ-T-36] N87-20818
NANJING AERONAUTICAL INST. (CHINA).
The algorithm and application of a new multi-input-multi-output modal parameter identification method N87-20582
NATIONAL AERONAUTICAL ESTABLISHMENT, OTTAWA (ONTARIO).
High temperature protective coatings for aero engine gas turbine components [AD-A176001] N87-20286
Use of a video-photogrammetry system for the measurement of the dynamic response of the shuttle remote manipulator arm N87-20370
NATIONAL AERONAUTICS AND SPACE ADMINISTRATION, WASHINGTON, D.C.
Aeronautical engineering: A continuing bibliography with indexes (supplement 212) [NASA-SP-7037(212)] N87-20172
Integral method of wall interference correction in low-speed wind tunnels [NASA-TT-20055] N87-20241
The design of composite structures: Aircraft design [NASA-TT-20011] N87-20261
Theory and design of flight-vehicle engines [NASA-TM-88583] N87-20281
Future trends in spacecraft design and qualification N87-20356
Composites review [NASA-TT-20008] N87-20388
Theoretical and experimental investigations of ignition, combustion and expansion processes of hypergolic liquid fuel combinations at gas temperatures up to 3000 deg K [NASA-TM-88527] N87-20399
Biot theory and acoustical properties of high porosity fibrous materials and plastic foams [NASA-TM-88575] N87-20424
Algebra and topology for applications to physics [NASA-TT-20056] N87-20784
Kinetic model for the vibrational energy exchange in flowing molecular gas mixtures [NASA-TM-88500] N87-20802
Management: A bibliography for NASA managers [NASA-SP-7500(21)] N87-20833
NATIONAL AERONAUTICS AND SPACE ADMINISTRATION. AMES RESEARCH CENTER, MOFFETT FIELD, CALIF.
Geometry definition and grid generation for a complete fighter aircraft N87-20203
The prediction of transonic loading on advancing helicopter rotors N87-20206
Using the boundary-layer equations in three-dimensional viscous flow simulation N87-20222
High speed viscous flow calculations about complex configurations N87-20227
Transonic Navier-Stokes wing solution using a zonal approach. Part 1: Solution methodology and code validation N87-20228
Transonic Navier-Stokes wing solutions using a zonal approach. Part 2: High angle-of-attack simulation N87-20229
Simulation of transonic viscous wing and wing-fuselage flows using zonal methods [NASA-TM-89421] N87-20242
Range filtering for sequential GPS receivers with external sensor augmentation [NASA-TM-89418] N87-20257
Mean-square error bounds for reduced-error linear state estimators [NASA-TM-89441] N87-20291
Visual display and alarm system for wind tunnel static and dynamic loads [NASA-TM-89455] N87-20298
Human-display interactions: Context-specific biases [NASA-TM-89430] N87-20747
Eigensystem analysis of classical relaxation techniques with applications to multigrid analysis [NASA-TM-88377] N87-20785
Estimability and regulability of linear systems [NASA-TM-89427] N87-20790
An astrometric facility for planetary detection on the space station [NASA-TM-89436] N87-20841
NATIONAL AERONAUTICS AND SPACE ADMINISTRATION. GODDARD SPACE FLIGHT CENTER, GREENBELT, MD.
The 1986 Get Away Special Experimenter's Symposium [NASA-CP-2438] N87-20302
Gas tungsten arc welding in a microgravity environment: Work done on GAS payload G-169 N87-20306
STS-61C, Columbia flight N87-20315
USC/AIAA student get away special project liquid droplet collector experiment N87-20316
Hitchhiker-G: A new carrier system for attached shuttle payloads N87-20320
Analysis of 12 AH aerospace nickel-cadmium cells from the design variable program [NASA-TM-87774] N87-20479
Empirical modeling of the thermosphere: An overview N87-20675

Crustal dynamics project data analysis, 1986. Volume 1: Fixed station VLBI geodetic results
[NASA-TM-87806] N87-20690
On requirements for a satellite mission to measure tropical rainfall
[NASA-RP-1183] N87-20701
Coronal and Prominence Plasmas
[NASA-CP-2442] N87-20871
Numerical simulations of a siphon mechanism for quiescent prominence formation N87-20880
Constraints on filament models deduced from dynamical analysis N87-20897
The heating of filaments as a disappearance process N87-20904
A dynamic model of filament eruptions and two ribbon flares N87-20906
High-spatial-resolution microwave and related observations as diagnostics of coronal loops N87-20917
Theoretical models of free-free microwave emission from solar magnetic loops N87-20918
Phlegethon flow: A proposed origin for spicules and coronal heating N87-20933
Energy conversion in the coronal plasma N87-20934
A coordinate free description of magnetohydrostatic equilibria N87-20937
Heating of the solar corona by the resonant absorption of Alfven waves N87-20939

NATIONAL AERONAUTICS AND SPACE ADMINISTRATION. LYNDON B. JOHNSON SPACE CENTER, HOUSTON, TEX.

Manned Mars missions: A working group report
[NASA-TM-89214] N87-20301
Space station control moment gyro control N87-20669
Users of middle atmosphere models remarks N87-20679
Utilization of Global Reference Atmosphere Model (GRAM) for shuttle entry N87-20680
Aero-Assisted Orbital Transfer Vehicle (AOTV) N87-20682
Radiation protection guidelines for space missions
[NASA-TM-89276] N87-20730

NATIONAL AERONAUTICS AND SPACE ADMINISTRATION. LANGLEY RESEARCH CENTER, HAMPTON, VA.

Investigation of leading-edge flap performance on delta and double-delta wings at supersonic speeds
[NASA-TP-2656] N87-20233
Unsteady transonic flow calculations for realistic aircraft configurations
[NASA-TM-89120] N87-20234
Investigation of transonic region of high dynamic response encountered on an elastic supercritical wing
[NASA-TM-89121] N87-20236
Spin-tunnel investigation of a 1/15-scale model of an Australian trainer airplane
[NASA-TM-89049] N87-20240
Traffic scenario generation technique for piloted simulation studies
[NASA-TM-86397] N87-20254
Integration of altitude and airspeed information into a primary flight display via moving-tape formats
[NASA-TM-89064] N87-20265
Computations for the 16-foot transonic tunnel, NASA, Langley Research Center, revision 1
[NASA-TM-86319-REV-1] N87-20294
Computational analysis and preliminary redesign of the nozzle contour of the Langley hypersonic CF4 tunnel
[NASA-TM-89042] N87-20296
Effects of space plasma discharge on the performance of large antenna structures in low Earth orbit
[NASA-TM-89118] N87-20339
Structural design of an in-line bolted joint for the space shuttle solid rocket motor case segments
[NASA-TM-89027] N87-20349
Large space antennas: A systems analysis case history
[NASA-TM-89072] N87-20352
Baseline tensile tests of composite materials for LDEF (Long Duration Exposure Facility) exposure
[NASA-TM-89069] N87-20366
High performance thermoplastics: A review of neat resin and composite properties
[NASA-TM-89104] N87-20390
Material characterization of superplastically formed titanium (Ti-6Al-2Sn-4Zr-2Mo) sheet
[NASA-TP-2674] N87-20407
Bubble memory module for spacecraft application
[NASA-TM-86411] N87-20476
Description of a magnetic bearing test fixture
[NASA-TM-89061] N87-20478
Stability, transition and turbulence
[NASA-CR-178258] N87-20500
The fully nonlinear development of Goertler vortices in growing boundary layers
[NASA-CR-178268] N87-20502
A simplified method for determining heat of combustion of natural gas
[NASA-TP-2682] N87-20514
Aerodynamic measurements and thermal tests of a strain-gage balance in a cryogenic wind tunnel
[NASA-TM-89039] N87-20517
Closed-Cycle, Frequency-Stable CO2 Laser Technology
[NASA-CP-2456] N87-20522
Catalysts for long-life closed-cycle CO2 lasers N87-20532
Rare isotope studies involving catalytic oxidation of CO over platinum-tin oxide N87-20538
Studies of CO oxidation on Pt/SnO2 catalyst in a surrogate CO2 laser facility N87-20539
Studies of long-life pulsed CO2 laser with Pt/SnO2 catalyst N87-20540
Characterization of Pt/SnO2 catalysts for CO oxidation N87-20541
Modeling of joints for the dynamic analysis of truss structures
[NASA-TP-2661] N87-20567
Structures and Dynamics Division research and technology plans for FY 1987 and accomplishments for FY 1986
[NASA-TM-89141] N87-20570
Airborne lidar measurements of El Chichon stratospheric aerosols, January 1984
[NASA-RP-1175] N87-20663
Overview of shuttle data on density N87-20683
Cumulative reports and publications through December 31, 1986
[NASA-CR-178257] N87-20754
A computer simulator for development of engineering system design methodologies
[NASA-TM-89109] N87-20755
An asymptotic analysis of supersonic reacting mixing layers
[NASA-CR-178266] N87-20756
A system for routing arbitrary directed graphs on SIMD architectures
[NASA-CR-178265] N87-20764
The fault-tree compiler
[NASA-TM-89098] N87-20765
A Lanczos eigenvalue method on a parallel computer
[NASA-TM-89097] N87-20768
Performance studies of the multigrid algorithms implemented on hypercube multiprocessor systems
[NASA-CR-178237] N87-20769
A preliminary transient-fault experiment on the SIFT computer system
[NASA-TM-89058] N87-20770
Inverse problems in the modeling of vibrations of flexible beams
[NASA-CR-178259] N87-20777
Piecewise linear approximation for hereditary control problems
[NASA-CR-178260] N87-20778
A practical assessment of spectral accuracy for hyperbolic problems with discontinuities
[NASA-CR-178226] N87-20779
Remarks on the stability analysis of reactive flows
[NASA-CR-178269] N87-20780
Acoustic gravity waves: A computational approach
[NASA-CR-178270] N87-20781
On Lipschitz continuity of nonlinear differential operators
[NASA-CR-178263] N87-20782
Galerkin/Runge-Kutta discretizations for semilinear parabolic equations
[NASA-CR-178264] N87-20783
An evaluation of active noise control in a cylindrical shell
[NASA-TM-89090] N87-20794
Documentation of the space station/aircraft acoustic apparatus
[NASA-TM-89111] N87-20795
Aircraft noise synthesis system: Version 4 user instructions
[NASA-TM-89089] N87-20797
Experimental validation of a two-dimensional shear-flow model for determining acoustic impedance
[NASA-TP-2679] N87-20798
Solar power absorption in a glass tube
[NASA-TM-89063] N87-20814

NATIONAL AERONAUTICS AND SPACE ADMINISTRATION. LEWIS RESEARCH CENTER, CLEVELAND, OHIO.

Numerical calculations of turbulent reacting flow in a gas-turbine combustor
[NASA-TM-89842] N87-20171
Composite grid and finite-volume LU implicit scheme for turbine flow analysis
[NASA-TM-89828] N87-20235
Lewis inverse design code (LINDES): Users manual
[NASA-TP-2676] N87-20238
NASA-Chinese Aeronautical Establishment (CAE) Symposium
[NASA-CP-2433] N87-20267
Combustion research in the Internal Fluid Mechanics Division N87-20268
Modeling turbulent, reactig flow N87-20270
Two-phase flow N87-20272
Thermodynamics and combustion modeling N87-20274
Experiments and modeling of dilution jet flow fields N87-20276
Theoretical kinetic computations in complex reacting systems N87-20277
The chemical shock tube as a tool for studying high-temperature chemical kinetics N87-20279
Contingency power for small turboshaft engines using water injection into turbine cooling air
[NASA-TM-89817] N87-20280
Performance and efficiency evaluation and heat release study of an outboard Marine Corporation Rotary Combustion Engine
[NASA-TM-89833] N87-20282
Detailed flow surveys of turning vanes designed for a 0.1-scale model of NASA Lewis Research Center's proposed altitude wind tunnel
[NASA-TP-2680] N87-20295
Fire safety concerns in space operations
[NASA-TM-89848] N87-20342
Liquid droplet radiator development status
[NASA-TM-89852] N87-20353
Conceptual design and integration of a space station resistojet propulsion assembly
[NASA-TM-89847] N87-20378
Comparison of two procedures for predicting rocket engine nozzle performance
[NASA-TM-89814] N87-20379
Experimental thrust performance of a high-area-ratio rocket nozzle
[NASA-TP-2720] N87-20381
Arcjet component conditions through a multistart test
[NASA-TM-89857] N87-20382
Experimental study of low Reynolds number nozzles
[NASA-TM-89858] N87-20383
Strain energy release rates of composite interlaminar end-notch and mixed-mode fracture: A sublaminate/ply level analysis and a computer code
[NASA-TM-89827] N87-20389
Creep behavior of niobium alloy PWC-11
[NASA-TM-89834] N87-20405
Bithermal low-cycle fatigue behavior of a NiCoCrAlY-coated single crystal superalloy
[NASA-TM-89831] N87-20408
Investigation of PTFE transfer films by infrared emission spectroscopy and phase-locked ellipsometry
[NASA-TM-89844] N87-20421
Deformation and fracture of single-crystal and sintered polycrystalline silicon carbide produced by cavitation
[NASA-TM-88961] N87-20422
Hot corrosion attack and strength degradation of SiC and Si(sub)3N(sub)4
[NASA-TM-89820] N87-20425
Addition polymers from 1,4,5,8-tetrahydro-1,4;5,8-diepoxyanthracene and Bis-dienes: Processable resins for high temperature application
[NASA-TM-89838] N87-20426
Unique bit-error-rate measurement system for satellite communication systems
[NASA-TP-2699] N87-20448
A study of the effect of group delay distortion on an SMSK satellite communications channel
[NASA-TM-89835] N87-20450
System architecture of MMIC-based large aperture arrays for space application
[NASA-TM-89840] N87-20468
Propagation characteristics of some novel coplanar waveguide transmission lines on GaAs at MM-wave frequencies
[NASA-TM-89839] N87-20469
Design, fabrication and performance of small, graphite electrode, multistage depressed collectors with 200-W, CW, 8- to 18-GHz traveling-wave tubes
[NASA-TP-2693] N87-20474
Referencing in fiber optic sensing systems
[NASA-TM-89822] N87-20475
Resistojet control and power for high frequency ac buses
[NASA-TM-89860] N87-20477
A finite difference scheme for three-dimensional steady laminar incompressible flow
[NASA-TM-89851] N87-20504

Pretest uncertainty analysis for chemical rocket engine tests
[NASA-TM-89819] N87-20515
A computer controlled signal preprocessor for laser fringe anemometer applications
[NASA-TM-88982] N87-20516
Vibration characteristics of OH-58A helicopter main rotor transmission
[NASA-TP-2705] N87-20555
Experimental and analytical evaluation of dynamic load and vibration of a 2240-kW (300-hp) rotorcraft transmission
[NASA-TM-88975] N87-20556
The acousto-ultrasonic approach
[NASA-TM-89643] N87-20562
Calculation of thermomechanical fatigue life based on isothermal behavior
[NASA-TM-88864] N87-20565
Shot peening for Ti-6Al-4V alloy compressor blades
[NASA-TP-2711] N87-20566
Time-partitioning simulation models for calculation on parallel computers
[NASA-TM-89850] N87-20766
The hypercluster: A parallel processing test-bed architecture for computational mechanics applications
[NASA-TM-89623] N87-20767
Rapid thermal annealing of Amorphous Hydrogenated Carbon (a-C:H) films
[NASA-TM-89659] N87-20821

NATIONAL AERONAUTICS AND SPACE ADMINISTRATION. MARSHALL SPACE FLIGHT CENTER, HUNTSVILLE, ALA.
Solar array flight experiment/dynamic augmentation experiment
[NASA-TP-2690] N87-20380
Microgravity crystallization of macromolecules: An interim report and proposal for continued research
[NASA-TP-2671] N87-20423
Rapid melt/quench furnace using commercially available hardware
[NASA-TM-86590] N87-20431
Wind velocity measurement accuracy with highly stable 12 mJ/pulse high repetition rate CO2 laser master oscillator power amplifier N87-20525
Space station structures and dynamics test program
[NASA-TP-2710] N87-20568
SAFE/DAE: Modal test in space N87-20584
Upper and Middle Atmospheric Density Modeling Requirements for Spacecraft Design and Operations
[NASA-CP-2460] N87-20665
Satellite lifetime prediction N87-20666
Space station momentum management N87-20668
Hubble Space Telescope N87-20670
NASA/MSFC prediction techniques N87-20678
Yosemite Conference on Ionospheric Plasma in the Magnetosphere: Sources, Mechanisms and Consequences, meeting report
[NASA-TM-86589] N87-20689
Liquid drop stability for protein crystal growth in microgravity
[NASA-TP-2724] N87-20727
Some crucial corona and prominence observations N87-20872
Condensation modes in magnetized plasmas N87-20877
Formation of active region and quiescent prominence magnetic field configurations N87-20879
On the existence of oscillations in solar filaments observed in H alpha and C IV lines N87-20900
Magnetic location of C IV events in the quiet network N87-20930
Statistical aspects of solar flares
[NASA-TP-2714] N87-20947

NATIONAL AEROSPACE LAB., AMSTERDAM (NETHERLANDS).
Flexible grid generation for complex geometries in two space dimensions based on variational principles N87-20200
Matrics, transonic potential flow calculations about transport aircraft N87-20208

NATIONAL BUREAU OF STANDARDS, GAITHERSBURG, MD.
Institute for Materials Science Engineering, Polymers: Technical activities 1986
[PB87-136893] N87-20420
International system of units (SI)
[PB86-244159] N87-20444

NATIONAL CENTER FOR ATMOSPHERIC RESEARCH, BOULDER, COLO.
Orbital atmospheric physics and dynamics N87-20673
Static current-sheet models of quiescent prominences N87-20882
On the formation of active region prominences (H alpha filaments) N87-20884
Three-dimensional magnetostatic models of the large-scale corona N87-20914
The topological description of coronal magnetic fields N87-20938
Magnetic helicity as a constraint on coronal dissipation N87-20940

NATIONAL ELECTRIC CO. OF VENEZUELA, CARACAS.
Manufacturing polymer thin films in a micro-gravity environment N87-20304

NATIONAL GEOPHYSICAL DATA CENTER, BOULDER, COLO.
Solar-geophysical data number 506, October 1986. Part 1: (Prompt reports). Data for September 1986, August 1986 and late data
[PB87-126389] N87-20948

NATIONAL OCEANIC AND ATMOSPHERIC ADMINISTRATION, BOULDER, COLO.
Forecasts of solar and geomagnetic activity N87-20577
HARPA: A versatile three-dimensional Hamiltonian ray-tracing program for acoustic waves in the atmosphere above irregular terrain
[PB87-132031] N87-20601
Filament disappearances N87-20903

NATIONAL OPTICAL ASTRONOMY LAB. TUCSON, ARIZ.
The prominence-corona interface and its relationship to the chromosphere-corona transition N87-20891

NATIONAL PHYSICAL LAB., TEDDINGTON (ENGLAND).
International system of units (SI)
[PB86-244159] N87-20444

NAVAL AEROSPACE MEDICAL RESEARCH LAB., PENSACOLA, FLA.
The retinal image of the fresnel lens optical landing system
[AD-A176090] N87-20258

NAVAL AIR DEVELOPMENT CENTER, WARMINSTER, PA.
Composite repair material and design development efforts N87-20188
AGARD (Advisory Group for Aerospace Research and Development) engine disc material cooperative test
[AD-A175533] N87-20283

NAVAL AIR PROPULSION TEST CENTER, TRENTON, N.J.
Decoupled bellmouth: An alternate method of measuring thrust in the sea level test cell
[AD-A175616] N87-20284

NAVAL CIVIL ENGINEERING LAB., PORT HUENEME, CALIF.
Performance of recycled asphalt concrete airport pavement surfaces
[DOT/FAA-PM-86-12] N87-20432

NAVAL OCEAN RESEARCH AND DEVELOPMENT ACTIVITY, BAY ST. LOUIS, MISS.
Testing and comparison of several mixed-layer models
[AD-A175959] N87-20712

NAVAL OCEAN SYSTEMS CENTER, SAN DIEGO, CALIF.
LOWTRAN modeling of near-horizon infrared sky radiances in the presence of clouds
[AD-A175661] N87-20691

NAVAL POSTGRADUATE SCHOOL, MONTEREY, CALIF.
The variation of subgrain misorientation in aluminum deformed to large steady-state creep strains
[DE87-003238] N87-20415
Wind-current relationships in the optoma domain off the Northern California Coast
[AD-A176019] N87-20714

NAVAL RESEARCH LAB., WASHINGTON, D. C.
C IV Doppler shifts observed in active region filaments N87-20898
A numerical study of the thermal stability of low-lying coronal loops N87-20931
Topological constraints and the existence of force-free fields N87-20935

NAVAL SURFACE WEAPONS CENTER, SILVER SPRING, MD.
A second order Godunov method for tactical missiles N87-20211
A multiple zone method for supersonic tactical missiles
[AD-A175938] N87-20244
Surface pressure measurements on a double delta Wing/Body configuration at Mach 2 and Mach 3 (WTR 1396)
[AD-A175951] N87-20245

NAVAL UNDERWATER SYSTEMS CENTER, NEW LONDON, CONN.
Acoustic scattering from composite wind-wave surfaces II: Backscatter cross sections and Doppler effects at high frequencies and small angles for 'bubble-free' regimes
[AD-A176081] N87-20715

NETHERLANDS ENERGY RESEARCH FOUNDATION, PETTEN.
Capture of thermal neutrons B10 and Li6: Applications in spectroscopy and in the study of weak nucleon interactions
[ECN-184] N87-20803
General introduction to capture of thermal neutrons in B10 and Li6: Applications in spectroscopy and in the study of weak nucleon interactions N87-20804
Investigation of excited states of Li7 by means of thermal neutron capture N87-20805
Investigation of excited states of B11 and Li7 by means of thermal neutron capture on B10 nuclei N87-20806
An investigation of the admixture of strong and weak interactions in the B10 (n, alpha) Li7 reaction with slow neutrons N87-20807
Transient heat transfer to supercritical helium at low temperatures
[ETN-87-99321] N87-20832

NEW HAMPSHIRE UNIV., DURHAM.
Formation and support of prominence N87-20874

NEW MEXICO STATE UNIV., LAS CRUCES.
Statistical properties of barium stars N87-20857

NORFOLK STATE COLL., VA.
MACSYMA usage at Langley, revision 1
[NASA-CR-172518] N87-20753

NORFOLK TECHNICAL VOCATIONAL CENTER, VA.
NORSTAR Project: Norfolk public schools student team for acoustical research N87-20309

NORGES TEKNISKE HOEGSKOLE, TRONDHEIM.
TV-holography: A promising inspection tool for analysis of composite materials N87-20180

NORTH CAROLINA AGRICULTURAL AND TECHNICAL STATE UNIV., GREENSBORO.
The North Carolina A and T State University Student Space Shuttle Program N87-20318

NORTHROP CORP., HAWTHORNE, CALIF.
Evaluation of vibration specifications for static and dynamic material allowables N87-20600

O

OAK RIDGE NATIONAL LAB., TENN.
Analysis of experimental determinations of the thermal conductivity of CBCF (Carbon-Bonded Carbon Fiber) insulation
[DE87-004025] N87-20393
Ductility and fracture behavior of polycrystalline Ni3Al alloys
[DE87-005340] N87-20413
Effects of elastic anisotropy on the anomalous yield behavior of cubic ordered alloys
[DE87-005328] N87-20417
A research program to assess the impact of the electromagnetic pulse on electric power systems
[DE87-002415] N87-20486
On the use of CORLIB subroutines for the solution of a model fluid flow problem
[DE87-005285] N87-20509
Opportunities and problems in wavelength tunable lasers based on vacancy defects in refractory oxides
[DE87-002406] N87-20545
Effects of force reflection on servomanipulator task performance
[DE87-003008] N87-20560
The 3-D world modelling with updating capability based on combinatorial geometry
[DE87-004257] N87-20643
Integrated digital control and man-machine interface for complex remote handling systems
[DE87-003002] N87-20749
Advanced remote handling for future applications: The advanced integrated maintenance system
[DE87-003004] N87-20750
A virtual-time operating-system shell for a hypercube in robotics applications
[DE87-004256] N87-20773
The Oak Ridge National Laboratory's Robotics and Intelligent Systems Program
[DE87-004627] N87-20774
The effects of heavy doping on the electronic states in semiconductors
[DE87-004421] N87-20824
Dislocation reactions at grain boundaries in Li2 ordered alloys
[DE87-005713] N87-20827

OBSERVATOIRE DE PARIS-MEUDON (FRANCE).
Can prominences form in current sheets N87-20876
Thermal stability analysis of the fine structure of solar prominences N87-20892
Magnetic field vector and electron density diagnostics from linear polarization measurements in 14 solar prominences N87-20902
On the thermal durability of solar prominences, or how to evaporate a prominence N87-20905

Filament eruption connected to protospheric activity N87-20906
Synoptic study of the corona at meter wavelength N87-20911

OCEAN DATA SYSTEMS, INC., ROCKVILLE, MD.
Underwater acoustic modeling techniques N87-20436

OFFICE NATIONAL D'ETUDES ET DE RECHERCHES AERONAUTIQUES, PARIS (FRANCE).
Computation of three-dimensional flows by viscous-inviscid interation using the MZM method N87-20223

OFFICE NATIONAL D'ETUDES ET DE RECHERCHES AEROSPATIALES, PARIS (FRANCE).
New numerical techniques in the method of singularities for application to complex three-dimensional configurations N87-20205
Study of the unsteady pressure field on the RA16SC1 profile in vibrating condition [ONERA-RTS-17/3423-AY] N87-20249
Wing-nacelle interactions. Program 1985. Part two: Development of a finite element code for an isolated nacelle [ONERA-RTS-21/3271-AY] N87-20250
Damage in carbon-resin composites: Transversal cracking and peeling [ONERA-RT-42/7066-M] N87-20398
High temperature CO2 study: Anti-Stokes coherent Raman diffusion and infrared spectroscopy [ONERA-P-1986-2] N87-20402
Two-dimensional flow computation in straight blade arrays [ONERA-RT-35/1621-RY-053-R] N87-20511
A model for the degradation of composite structures [ONERA-RT-30/3043-RY-057-R] N87-20617
Definition and use of sensors for measuring electrical conductivity in thunderclouds [ONERA-NT-1986-4] N87-20705
Lightning strikes on aircraft. Exploitation of Landes (France)-Front '84 campaign and complementary development of airborne electrical sensors [ONERA-RF-91/7154-PY] N87-20706
Study of surface discharges [ONERA-RF-11/7236-PY] N87-20707
Activities report in computer science [ETN-87-99377] N87-20758
Activities report in aerospace research [ETN-87-99378] N87-20836

OFFICE OF NAVAL RESEARCH, ARLINGTON, VA.
Solid mechanics program at ONR N87-20575

OFFICE OF NAVAL RESEARCH, LONDON (ENGLAND).
A survey of military aerospace systems technology developments in Western Europe and the Middle East [AD-A175635] N87-20173

OHIO STATE UNIV., COLUMBUS.
Progress on the Ohio State University Get Away Special G-0318: DEAP N87-20311

OLD DOMINION UNIV., NORFOLK, VA.
Continental shelf processes affecting the oceanography of the South Atlantic Bight [DE87-005303] N87-20716

OSCILLOQUARTZ S.A., NEUCHATEL (SWITZERLAND).
NAVSAT time synchronization simulation study [ESA-CR(P)-2305] N87-20376

OSLO UNIV. (NORWAY).
Alfven-wave dissipation: A support mechanism for quiescent prominences N87-20881
Temperatures of quiescent prominences measured from hydrogen Paschen and Call IR lines N87-20886
Vertical motions in the quiescent prominences observed in the He I Lambda10830Angstrom line N87-20896

OXFORD UNIV. (ENGLAND).
Characteristic decomposition and the multivariable generalization of predictive self-tuning control [OUEL-1651/86] N87-20776

P

PACIFIC NORTHWEST LABS., RICHLAND, WASH.
Sodium sulfur battery: An overview [DE87-004920] N87-20491

PALISADES INST. FOR RESEARCH SERVICES, INC., N.Y.
The US Workshop on the Physics and Chemistry of Mercury Cadmium Telluride: Extended abstracts [AD-A175593] N87-20822

PENNSYLVANIA STATE UNIV., UNIVERSITY PARK.
Strong metal-support interactions N87-20533

PENNSYLVANIA UNIV., PHILADELPHIA.
Search for magnetic monopoles, neutrino oscillations, and superhigh energy physics [DE87-005774] N87-20953

PHYSICS INTERNATIONAL CORP., SAN LEANDRO, CALIF.
Numerical simulation of Atlas-Centaur stage-separation shaped charge firing and structural response N87-20606

POLITECNICO DI MILANO (ITALY).
Active structural controllers emulating structural elements by ICUs N87-20367
Structural properties of linear periodic systems [REPT-86-004-REV] N87-20788

PRAIRIE VIEW AGRICULTURAL AND MECHANICAL COLL., TEX.
Study of the nature of fracture failure in composite materials [AD-A175554] N87-20391

PRATT AND WHITNEY AIRCRAFT, EAST HARTFORD, CONN.
Advanced composite combustor structural concepts program [NASA-CR-174733] N87-20387

PRINCETON UNIV., N. J.
Stability regions of relaxed static stability aircraft under control saturation constraints N87-20288
Inclined pileup of edge dislocations near the crack tip [AD-A175610] N87-20571
A systematic search for millisecond pulsars N87-20839
Timing millisecond pulsars N87-20855
Self-consistent models of perfect triaxial galaxies N87-20859
Theory and simulation of the evolution of the large-scale solar magnetic field N87-20870

PURDUE UNIV., WEST LAFAYETTE, IND.
Analysis of NLR configurations using OCM for pilot modeling [NASA-CR-180656] N87-20289
Use of lightweight composites for GAS payload structures N87-20307
Multipurpose microcontroller design for PUGAS 2 N87-20321
A numerical heat transfer model for an advanced solar thermal propulsion system N87-20377
Numerical simulation of air mass modification over the East China Sea during the winter season N87-20660
The fifth force [DE87-004612] N87-20694
The effect of latent heat on kinetic energy conversions associated with South Pacific cyclones N87-20696

R

REDSTONE SCIENTIFIC INFORMATION CENTER, REDSTONE ARSENAL, ALA.
GAS-007: First step in a series of Explorer payloads N87-20333

RENSSELAER POLYTECHNIC INST., TROY, N.Y.
A self critical approach to data analysis and model building [AD-A175640] N87-20791
Molecular clouds in the outer galaxy N87-20854

RESEARCH INST. OF NATIONAL DEFENCE, LINKOEPING (SWEDEN).
Fabrication of microwave devices on ultrathin active GaAs substrates [FOA-C-30431-3.2] N87-20494
A theoretical and experimental study of cylindrical dielectric resonators and their applications to microwave oscillators [FOA-C-30434-3.2] N87-20495
Potential of laser remote sensing of oil below water surface [FOA-C-30435-3.1] N87-20659

RESEARCH INST. OF NATIONAL DEFENCE, STOCKHOLM (SWEDEN).
Adhesion of a silicone based insulating material to rocket motors [FOA-C-20635-2.1] N87-20429

ROCKWELL INTERNATIONAL CORP., CANOGA PARK, CALIF.
Questionable effects of shock data filtering N87-20610
Density uncertainty effect on cost of space station reboost N87-20667

ROCKWELL INTERNATIONAL CORP., GOLDEN, COLO.
Impact energy relationships for directly rolled uranium strip [DE87-005789] N87-20418
Superplasticity of metals with special reference to Ti-6Al-4V [DE87-005795] N87-20419

ROME UNIV. (ITALY).
Effect of modal damping in modal synthesis of spacecraft structures N87-20362
Double inflation: A possible resolution of the large-scale structure problem [DE87-005403] N87-20885

ROYAL AIR FORCE COLL., CRANWELL (ENGLAND).
The aerodynamic effects of a serrated strip near the leading edge of an airfoil [ETN-87-99480] N87-20248
Simulation of an integrated fire and flight control system for air-to-air gunnery [ETN-87-99479] N87-20293
Control aspects of the launch phase of a vertically-launched short-range surface-to-air missile [ETN-87-99478] N87-20341
A study of the methods used to carry out RF telemetry testing of surface-to-air missiles [ETN-87-99481] N87-20346

ROYAL AIRCRAFT ESTABLISHMENT, FARNBOROUGH (ENGLAND).
Effect of adhesive bonding variables on the performance of bonded CFRP patch repairs of metallic structures N87-20182
An assessment of the use of low-order panel methods for the calculation of supersonic flows N87-20204
Applications of RAE viscous flow methods near separation boundaries for three-dimensional wings in transonic flow N87-20224
WSUH-1D: Review of damage following lightning strike 30 November 1981 [RAE-TRANS-2103] N87-20262

ROYAL NETHERLANDS AIRCRAFT FACTORIES FOKKER, SCHIPHOL-OOST.
Acoustic effects on the dynamic of lightweight structures N87-20372

ROYAL SIGNALS AND RADAR ESTABLISHMENT, MALVERN (ENGLAND).
Review of the frequency stabilization of TEA CO2 laser oscillators N87-20523
Large mode radius resonators N87-20524

RUPP (CHARLES C.), HUNTSVILLE, ALA.
Marshall Amateur Radio Club experiment (MARCE) post flight data analysis N87-20323

S

SAINT ANDREW'S UNIV. (SCOTLAND).
The stability of coronal and prominence magnetic fields N87-20941
Resistive ballooning modes in line-tied coronal arcades N87-20942

SAINT LOUIS UNIV., MO.
Dynamical and thermodynamical characteristics of a squall-line determined from dual-Doppler data N87-20697

SAINT MARY'S HOSPITAL, MILWAUKEE, WIS.
Results of the joint utilization of laser integrated experiments flown on payload GAS-449 aboard Columbia mission 61-C N87-20317

SANDIA NATIONAL LABS., ALBUQUERQUE, N. MEX.
Moisture absorption in graphite/organic-matrix composites [DE87-004229] N87-20394
Residual effects in laminated, curved, composite panels [DE87-005624] N87-20397
Feasibility study of a Semiconductor Bridge (SCB) for initiating pyrotechnics and explosives [DE87-004444] N87-20430
Analysis of the receiving characteristics of the circular diffraction antenna with both a flush-mounted and a recessed center post [DE87-003283] N87-20460
Etching of LiNbO3 by laser-driven fusion of salts [DE87-003033] N87-20544
Injection-seeding studies of diode laser array behavior [DE87-002051] N87-20546
Laser spectroscopy and gas-phase chemistry in CVD [DE86-007392] N87-20548
Testing techniques. Random variation of modal frequencies: Experiments and analysis N87-20585
The controlled response of resonating fixtures used to simulate pyroshock environments N87-20612
A gondola and pointing system for a gamma ray telescope [DE87-004561] N87-20843

SASC TECHNOLOGIES, INC., HAMPTON, VA.
The terminal area simulation system. Volume 1: Theoretical formulation [NASA-CR-4046-VOL-1] N87-20255

SATEL CONSEIL, PARIS (FRANCE).
Land mobile communications satellite mission (LAMOCOSAMIS) Task 1: Market study [ESA-CR(P)-2302-VOL-1] N87-20462
Land mobile communications satellite missions (LAMOCOSAMIS), executive summary [ESA-CR(P)-2302-VOL-6] N87-20463

SCIENCE APPLICATIONS INTERNATIONAL CORP., MCLEAN, VA.
Spectral characteristics of interchange turbulence in the ionosphere
[AD-A175975] N87-20692
SCIENCE APPLICATIONS INTERNATIONAL CORP., SCHAUMBERG, ILL.
Satellite servicing mission preliminary cost estimation model
[NASA-CR-171978] N87-20335
SCIENCE RESEARCH COUNCIL, CHILTON (ENGLAND).
Report of the atmosphere panel N87-20633
SCUOLA NORMALE SUPERIORE, PISA (ITALY).
Effects of flows on viscous and resistive MHD stability N87-20943
SELENIA INDUSTRIE ELETTRONICHE ASSOCIATE S.P.A., POMEZIA (ITALY).
Rivista Tecnica Selenia, volume 10, number 1
[ETN-87-99091] N87-20759
Expert systems for diagnostic purposes, prospected applications to the radar field N87-20760
On modern avionic and defense systems logistic support standardization and cost effectiveness N87-20761
An application of Rayleigh's method to the fast calculation of the first vibration frequency of a missile launcher cell N87-20762
Automatic graphics applied to antenna computer aided design N87-20763
SHENYANG AEROENGINE RESEARCH INST. (CHINA).
Effect of flame-tube head structure on combustion chamber performance N87-20275
SHOCK AND VIBRATION INFORMATION CENTER (DEFENSE), WASHINGTON, D. C.
The Shock and Vibration Digest, Volume 18, No. 10
[AD-A175726] N87-20438
The Shock and Vibration Bulletin. Part 1: Welcome, Invited Papers, Shipboard Shock, Blast and Ground Shock, Shock Testing and Analysis
[AD-A175224] N87-20574
The Shock and Vibration Bulletin. Part 2: Modal Test and Analysis, Testing Techniques, Machinery Dynamics, Isolation and Damping, Structural Dynamics
[AD-A175225] N87-20580
The Shock and Vibration Bulletin. Part 3: Invited Papers, Pyrotechnic Shock, Pyrotechnic Shock Workshop
[AD-A175226] N87-20602
The pre-pulse in pyroshock measurement and analysis N87-20604
SMITHSONIAN ASTROPHYSICAL OBSERVATORY, CAMBRIDGE, MASS.
Limitations to modeling the thermosphere and exosphere N87-20674
A normal incidence X-ray telescope
[NASA-CR-180107] N87-20840
Magnetogram and soft X-ray comparisons of XBP and ER N87-20927
SOCIETE DE CONSTRUCTION DES AVIONS HUREL-DUBOIS, PARIS (FRANCE).
Composite structure repairs carried out according to aeronautical techniques N87-20185
SOCIETE NATIONALE INDUSTRIELLE AEROSPATIALE, CANNES (FRANCE).
Dynamic modeling and optimal control design for large flexible space structures N87-20358
Dynamic analysis of direct television satellite TV-SAT/TDF.1 N87-20360
The concentration principle applied to spaceborne solar arrays. AGORA mission: Studies synthesis
[SNIAS-959-CA/CG] N87-20657
SOCIETE NATIONALE INDUSTRIELLE AEROSPATIALE, MARIGNANE (FRANCE).
Repair of helicopter composite structure techniques and substantiations N87-20179
Theoretical analysis of flows around helicopter fuselages: Application to design and development N87-20221
SOCIETE NATIONALE INDUSTRIELLE AEROSPATIALE, TOULOUSE (FRANCE).
A.T.R. 42 carbon fibre flap repair design and inspection N87-20178
SOLAR PHYSICS RESEARCH CORP., TUCSON, ARIZ.
The association of chromospheric and coronal phenomena with the evolution of the quiet sun magnetic fields
[ESD-TR-84-611] N87-20926
SOUTHEASTERN CENTER FOR ELECTRICAL ENGINEERING EDUCATION, INC., ST. CLOUD, FLA.
Progress in the development of holographic scheme for pair correlation estimation
[AD-A175573] N87-20518
SOUTHWEST RESEARCH INST., SAN ANTONIO, TEX.
The physics of fuel sprays. Volume 1: Experimental measurements
[AD-A175660] N87-20285
Comparison of 6.2L arctic and standard fuel injection pumps using JP-8 fuel
[AD-A175597] N87-20558
SPACE COMMAND, PETERSON AFB, COLO.
NORAD satellite tracking N87-20671
NORAD/SPACECMD comments concerning the atmospheric density models N87-20672
SPAR AEROSPACE LTD., STE-ANNE-DE-BELLEVUE (QUEBEC).
Optimization of aerospace structures subjected to random vibration and fatigue constraints N87-20599
SPAR AEROSPACE LTD., TORONTO (ONTARIO).
Baking the first bread in space N87-20319
SPAR AEROSPACE LTD., WESTON (ONTARIO).
Modal testing of the Olympus development model stowed solar array N87-20366
SPECTRA TECHNOLOGY, INC., BELLEVUE, WASH.
Analysis of intrapulse chirp in CO2 oscillators N87-20526
STANFORD UNIV., CALIF.
A rational approach to lifting surface theory with application to large angles of attack N87-20196
STATE UNIV. OF NEW YORK, BUFFALO.
Progress in the development of holographic scheme for pair correlation estimation
[AD-A175573] N87-20518
STATE UNIV. OF NEW YORK, STONY BROOK.
Dislocation reactions at grain boundaries in Li2 ordered alloys
[DE87-005713] N87-20827
STEVENS INST. OF TECH., HOBOKEN, N. J.
Stable response of damped linear systems, part 3 N87-20440
STIRLING TECHNOLOGY CO., RICHLAND, WASH.
Conceptual design of a solar electric advanced Stirling power system
[DE87-005036] N87-20656
STOCKHOLM UNIV. (SWEDEN).
A model and computer code for the Monte Carlo simulation of relativistic electron and positron penetration through matter
[USIP-86-11] N87-20808
STUTTGART UNIV. (WEST GERMANY).
Numerical investigations of geometrically nonlinear shell kinetics
[ETN-87-99019] N87-20616
SVERDRUP TECHNOLOGY, INC., ARNOLD AIR FORCE STATION, TENN.
Conversion of ARO-1 to an implicit Navier-Stokes solver
[AD-A175967] N87-20505
SVERDRUP TECHNOLOGY, INC., CLEVELAND, OHIO.
A Navier-Stokes solver using the LU-SSOR TVD algorithm
[NASA-CR-179608] N87-20243
SWARTHMORE COLL., PA.
Observations of the Ca II K line in Hel0830A dark points on August 3, 1985 N87-20929
SYSTEMS RESEARCH LABS., INC., DAYTON, OHIO.
Application of CARS to scramjet combustion
[NASA-CR-178245] N87-20400

T

TECHNICAL RESEARCH CENTRE OF FINLAND, HELSINKI.
Hydrogen embrittlement of titanium and its alloys: A literature review
[DE87-750405] N87-20410
TECHNISCHE HOCHSCHULE, AACHEN (WEST GERMANY).
Experimental and theoretical investigation of the flow phenomena in return channels of radial compressor stages, especially those with small channel width
[MITT-85-01] N87-20287
TECHNISCHE HOGESCHOOL TWENTE, ENSCHEDE (NETHERLANDS).
Noble-gas ion bombardment on clean silicon surfaces studied using ellipsometry and desorption
[B8672200] N87-20809
Adsorption of atomic oxygen (N2O) on clean silicon surfaces and its influence on the surface state density; a comparison with O2
[B8668354] N87-20810
Deep ion implantation for bipolar silicon devices; investigations into the use of the third dimension
[B8672201] N87-20828
TECHNISCHE UNIV., BRUNSWICK (WEST GERMANY).
Preliminary examination of the construction of laser gyroscopes with reduced lock-in threshold
[ETN-87-99016] N87-20521
Adaptive control with a nonparametric model for the controlled system
[ETN-87-99015] N87-20775
TECHNISCHE UNIV., MUNICH (WEST GERMANY).
Ground-state proton radioactivity in the domain of neutron-poor nuclei heavier than tin
[ETN-87-99342] N87-20811
TELEDYNE WATER PIK, FORT COLLINS, COLO.
Characterization of the LTC catalyst: Performance against common air pollutants N87-20535
TELESAT CANADA, OTTAWA (ONTARIO).
Towards a better mirror N87-20310
Baking the first bread in space N87-20319
TENNESSEE UNIV., KNOXVILLE.
The effects of heavy doping on the electronic states in semiconductors
[DE87-004421] N87-20824
TEXAS A&I UNIV., KINGSVILLE.
Force magnitude and angular velocity fluctuation reduction in a spring-restrained, flexibly-supported four-bar mechanical linkage N87-20589
TEXAS A&M UNIV., COLLEGE STATION.
Hybrid methods for rotordynamic analysis
[NASA-CR-179035] N87-20553
TEXAS UNIV., AUSTIN.
Fiducial reference for the HIPPARCOS reference system
[NASA-CR-180250] N87-20842
Carbon and nitrogen abundances along the evolutionary sequence of M67 N87-20848
A numerical study of some spherically-symmetric and axisymmetric cosmological models N87-20853
Dynamic evolution of coronal magnetic fields N87-20945
THERMACORE, INC., LANCASTER, PA.
Conceptual design of a solar electric advanced Stirling power system
[DE87-005036] N87-20656
TITAN SYSTEMS, INC., PRINCETON, N.J.
The effect of heavy rain on an airfoil at high lift
[NASA-CR-178248] N87-20232
TOHOKU UNIV., SENDAI (JAPAN).
In situ observation of mono-molecular growth steps on aqueous solution grown crystals and the transport of molecules to the crystals N87-20334
TOKYO ASTRONOMICAL OBSERVATORY, MITAKA (JAPAN).
Dark filaments observed at 8.3mm and 3.1mm wavelength N87-20867
The density and thickness of quiescent prominences N87-20893
TRW ELECTRONICS AND DEFENSE SECTOR, REDONDO BEACH, CALIF.
Zero-shifted accelerometer outputs N87-20609
Comparison of response from different resonant plate simulation techniques N87-20611
TRW SPACE TECHNOLOGY LABS., REDONDO BEACH, CALIF.
Modal parameter identification using adaptive digital filters N87-20583
MHD waves detected by ice at distances 28 x 10 km from Comet Halley: Cometary or solar wind origin
[DE87-005122] N87-20863
TUFTS UNIV., MEDFORD, MASS.
Coronal diagnostics. N87-20915
Coronal plasmas on the sun and nearby stars N87-20919
Compact, variable, moving sources observed on the sun at 2 centimeters wavelength N87-20925

U

UNITED KINGDOM ATOMIC ENERGY AUTHORITY, HARWELL (ENGLAND).
The oxidation of carbon monoxide using a tin oxide catalyst N87-20528
UNITED TECHNOLOGIES RESEARCH CENTER, EAST HARTFORD, CONN.
Implementation of active force control for robots subject to dynamic loading N87-20588
UNIVERSITIES SPACE RESEARCH ASSOCIATION, BOULDER, COLO.
Prediction of recirculation zones in isothermal coaxial jet flows relevant to combustors
[NASA-CR-4064] N87-20501
Wind and turbulence data for development of design criteria for unmanned high-altitude low-speed endurance aircraft
[NASA-CR-4065] N87-20699
UNIVERSITIES SPACE RESEARCH ASSOCIATION, HUNTSVILLE, ALA.
Linear baroclinic instability in the presence of large scale topography
[NASA-CR-4057] N87-20700
UNIVERSITY OF CENTRAL FLORIDA, ORLANDO.
Structural dynamic reanalysis using Ritz vectors N87-20597

UNIVERSITY OF SOUTHERN CALIFORNIA, LOS ANGELES.
Reaction rate oscillations during catalytic CO oxidation: A brief overview N87-20534
UTAH STATE UNIV., LOGAN.
A systems-level performance history of get away special after 25 space shuttle missions N87-20314

V

VIBRATION INST., CLARENDON HILLS, ILL.
The Shock and Vibration Digest, Volume 19, No. 2 N87-20435
VIRGINIA POLYTECHNIC INST. AND STATE UNIV., BLACKSBURG.
Experimental and finite-element investigation of flow past single and multiple cylinders N87-20195
Mechanical and thermal characterization of unidirectional aramid/epoxy [CCMS-86-08] N87-20385
Modeling and control of flexible structures N87-20564
VIRGINIA UNIV., CHARLOTTESVILLE.
Collisional dynamics of perturbed particle disks in the solar system [NASA-CR-180497] N87-20860

W

WASHINGTON STATE UNIV., PULLMAN.
Parallel processing of networks [AD-A175641] N87-20771
WASHINGTON UNIV., SEATTLE.
The fifth force [DE87-004612] N87-20694
The mesoscale organization, dynamics, and evolution of the marine planetary boundary layer during cold air outbreaks N87-20696
Pre-compaction irradiation of meteorites N87-20850
WATERLOO UNIV. (ONTARIO).
Fatigue and acoustics: Prediction of metal fatigue using Miner's rule N87-20598
WEBER STATE COLL., OGDEN, UTAH.
NUSAT update N87-20312
NUSAT 1 attitude determination N87-20328
NUSAT 1 methods for radar field strength measurement N87-20329
WILSON (JON), SAN JUAN CAPISTRANO, CALIF.
State-of-the-art accelerometer characteristics for pyrotechnic shock measurement N87-20608
WISCONSIN UNIV., MADISON.
The use of visible data for improving VAS satellite soundings N87-20620
A technique to estimate the ocean surface energy flux using VAS multispectral data N87-20710
H I structure and the soft X-ray background N87-20949
A search for very high energy gamma ray emission from Cygnus X-3 N87-20950
WOODS HOLE OCEANOGRAPHIC INSTITUTION, MASS.
Dynamic presentation of long term upper ocean study (LOTUS) data using videotape [AD-A175535] N87-20711
Moored current meter and temperature-pressure recorder measurements from the Western North Atlantic (high energy benthic boundary layer and abyssal circulation experiments 1983-1984), volume 39 [AD-A176014] N87-20713

Typical Contract Number Index Listing

Listings in this index are arranged alphanumerically by contract number. Under each contract number the NASA accession numbers denoting documents that have been produced as a result of research done under that contract are arranged in ascending order. The NASA accession number denotes the number by which the citation is identified.

AF-AFOSR-0013-84 ..... N87-20452
AF-AFOSR-0018-82 ..... N87-20883
N87-20928
AF-AFOSR-0019-83 ..... N87-20915
N87-20919
N87-20925
AF-AFOSR-00118-82 ..... N87-20928
DA PROJ. 1L1-61102-AH-45 ..... N87-20552
DA PROJ. 1L2-63104-D-150 ..... N87-20558
DA-183/1-1/2 ..... N87-20230
DAAG29-81-K-0110 ..... N87-20791
DAAG29-82-K-0107 ..... N87-20771
DAAG29-83-K-0083 ..... N87-20481
DAAG29-83-K-0145 ..... N87-20572
DAAG29-84-K-0199 ..... N87-20518
DAAG29-85-G-0123 ..... N87-20391
DAAG29-85-K-0049 ..... N87-20452
DAAG29-85-K-0129 ..... N87-20427
DAAG29-85-K-0228 ..... N87-20292
DAAK70-85-C-0007 ..... N87-20558
DAAL03-86-G-0175 ..... N87-20822
DAAL03-86-K-0019 ..... N87-20571
DAJA45-84-C-0045 ..... N87-20482
DCA100-77-C-0020 ..... N87-20454
DE-AC02-76CH-00016 ..... N87-20414
N87-20547
N87-20694
DE-AC02-76CH-03000 ..... N87-20884
N87-20885
N87-20886
DE-AC02-76ER-03231 ..... N87-20726
DE-AC02-78ER-04940 ..... N87-20452
DE-AC02-81ER-10950 ..... N87-20428
DE-AC02-81ER-40012 ..... N87-20953
DE-AC02-83CH-10093 ..... N87-20729
DE-AC02-83ER-13082 ..... N87-20793
DE-AC04-76DP-00053 ..... N87-20559
DE-AC04-76DP-00613 ..... N87-20395
DE-AC04-76DP-00789 ..... N87-20397
N87-20430
N87-20460
N87-20544
N87-20548
N87-20548
N87-20843
DE-AC04-76DP-03533 ..... N87-20418
N87-20419
DE-AC04-76DR-00789 ..... N87-20394
DE-AC05-84OR-21400 ..... N87-20393
N87-20413
N87-20417
N87-20486
N87-20509
N87-20545
N87-20560
N87-20843
N87-20730
N87-20749
N87-20750
N87-20773
N87-20774
N87-20824
N87-20827
DE-AC06-76RL-01830 ..... N87-20491
DE-AC07-76ID-01570 ..... N87-20396
N87-20561
N87-20563
DE-AC09-76SR-00001 ..... N87-20409
DE-AC11-76PN-00014 ..... N87-20549
DE-AI03-86SF-16310 ..... N87-20405
DE-AI04-80AL-13137 ..... N87-20656
DE-AS19-84BC-10828 ..... N87-20635
DE-AT04-85AL-33408 ..... N87-20656
DE-A101-85-CE-89008 ..... N87-20646
DE-A101-85CE-89008 ..... N87-20647
N87-20649
N87-20650
N87-20651
N87-20652
N87-20653
DE-FG02-85ER-45179 ..... N87-20412
DE-FG02-86ER-60397 ..... N87-20703
DE-FG05-84ER-13265 ..... N87-20757
DE-FG05-85ER-60348 ..... N87-20716
DFG-GA-180/12-1 ..... N87-20287
DFG-180/12-2 ..... N87-20287
DFG-180/12-3 ..... N87-20287
DNA001-84-C-0253 ..... N87-20455
DNA001-85-C-0067 ..... N87-20451
DRET-84-057 ..... N87-20251
N87-20512
N87-20513
DRET-85-34-001 ..... N87-20511
N87-20617
DRET-85-34-001-BC-24 ..... N87-20398
DRET-85-001 ..... N87-20706
N87-20707
DTFA01-83-Y-30593 ..... N87-20432
ESA-5805/84-F-RD(SC) N87-20376
ESA-5978/84-NL-PB(SC) N87-20657
ESA-6023/84-F-RD(SC) N87-20462
N87-20463
ESA-6024/84-F-RD(SC) N87-20464
N87-20465
FHWA-8-3-0187 ..... N87-20434
F04701-85-0086 ..... N87-20345
F04704-84-C-0084 ..... N87-20604
F19628-83-K004 ..... N87-20910
F19628-84-K-0023 ..... N87-20920
F19628-85-K-0006 ..... N87-20945
F49620-84-K-0022 ..... N87-20452
F49620-85-C-0067 ..... N87-20452
MAT-86-018 ..... N87-20385
NAGW-9 ..... N87-20878
N87-20879
NAGW-76 ..... N87-20874
N87-20876
N87-20905
NAGW-112 ..... N87-20927
NAGW-233 ..... N87-20842
NAGW-397 ..... N87-20840
NAGW-846 ..... N87-20945
NAGW-929 ..... N87-20860
NAG1-358 ..... N87-20214
NAG1-624 ..... N87-20781
NAG3-55 ..... N87-20552
NAG4-1 ..... N87-20269
NAG5-501 ..... N87-20915
N87-20919
NAG5-511 ..... N87-20888
NAG5-585 ..... N87-20884
NAG5-752 ..... N87-20910
NAG5-753 ..... N87-20662
NAG5-766 ..... N87-20883
NAG5-769 ..... N87-20449
NAG5-834 ..... N87-20557
NAG8-027 ..... N87-20813
NAG8-053 ..... N87-20878
N87-20879
NAG8-532 ..... N87-20569
NASA ORDER C-99066-G N87-20171
NASA ORDER L-997258 ..... N87-20297
NASW-4004 ..... N87-20399
NASW-4005 ..... N87-20241
N87-20261
N87-20281
N87-20388
N87-20784
NASW-4006 ..... N87-20424
N87-20802
NAS1-14101 ..... N87-20754
NAS1-14472 ..... N87-20754
NAS1-14880 ..... N87-20290
NAS1-15810 ..... N87-20754
NAS1-16048 ..... N87-20406
NAS1-16394 ..... N87-20754
NAS1-16582 ..... N87-20400
NAS1-16921 ..... N87-20753
NAS1-16967 ..... N87-20404
NAS1-17070 ..... N87-20754
N87-20777
N87-20778
NAS1-17130 ..... N87-20754
NAS1-17345 ..... N87-20253
NAS1-17409 ..... N87-20252
N87-20255
NAS1-17707 ..... N87-20344
NAS1-18088 ..... N87-20232
NAS1-18107 ..... N87-20500
N87-20502
N87-20754
N87-20756
N87-20764
N87-20769
N87-20777
N87-20778
N87-20779
N87-20780
N87-20781
N87-20782
N87-20783
NAS1-18213 ..... N87-20503
NAS1-18267 ..... N87-20340
NAS3-23284 ..... N87-20387
NAS3-23681 ..... N87-20239
NAS3-24105 ..... N87-20243
NAS3-24890 ..... N87-20467
NAS5-28728 ..... N87-20923
N87-20926
NAS8-33526 ..... N87-20878
NAS8-34010 ..... N87-20699
NAS8-35354 ..... N87-20951
NAS8-35770 ..... N87-20350
NAS8-35774 ..... N87-20343
NAS8-35918 ..... N87-20501
NAS8-35922 ..... N87-20470
N87-20471
N87-20472
N87-20473
NAS8-35969 ..... N87-20554
NAS8-36182 ..... N87-20553
NAS8-36400 ..... N87-20665
NAS8-36474 ..... N87-20700
NAS8-36483 ..... N87-20820
NAS9-17207 ..... N87-20335
NAS9-17299 ..... N87-20351
NAS9-17315 ..... N87-20634
NAS10-10285 ..... N87-20658
NA84-RA-A06789 ..... N87-20926
NCC1-79 ..... N87-20264
NGL-05-002-034 ..... N87-20883
NGL-14-001-001 ..... N87-20873
NGL-16-001-043 ..... N87-20921
NGL05-002-034 ..... N87-20928
NGL12-001-011 ..... N87-20912
N87-20932
NGR21-002-199 ..... N87-20886
N87-20923
NSF AST-83-15217 ..... N87-20920
NSF ATM-82-10936 ..... N87-20929
NSF ATM-82-11002 ..... N87-20883
N87-20928
NSF ATM-83-09955 ..... N87-20889
N87-20920
NSF ATM-84-15388 ..... N87-20888
NSF ATM-85-06646 ..... N87-20945
NSF ATM-85-07035 ..... N87-20876

NSF ATM-86-10330	N87-20920
NSF ATS-83-11338	N87-20913
NSF CHE-80-23747	N87-20452
NSF CHE-82-11593	N87-20452
NSF CHE-85-17460	N87-20452
NSF DMS-86-04047	N87-20781
NSF ECS-82-17677	N87-20452
NSF OCE-82-14925	N87-20713
NSG5-5176	N87-20932
N0014-86-K-0068	N87-20915
	N87-20919
	N87-20925
N00014-78-C-0197	N87-20711
	N87-20713
N00014-78-C-0517	N87-20452
N00014-82-C-0019	N87-20713
N00014-84-C-0134	N87-20711
N00014-85-C-0841	N87-20285
N00014-86-F-0049	N87-20948
N00024-85-C-5301	N87-20384
N60921-84-C-0027	N87-20480
N62271-86-M-0235	N87-20642
PHWA-8-3-0187	N87-20433
STPA-85-95-009	N87-20249
	N87-20250
TC196810TC	N87-20385
W-31-109-ENG-38	N87-20416
	N87-20492
	N87-20493
	N87-20772
	N87-20825
	N87-20826
W-7405-ENG-36	N87-20411
	N87-20461
	N87-20506
	N87-20508
	N87-20654
	N87-20786
	N87-20844
	N87-20863
	N87-20868
W-7405-ENG-48	N87-20415
	N87-20441
	N87-20442
	N87-20507
	N87-20816
W-7405-ENG-82	N87-20484
	N87-20485
W-31109-ENG-38	N87-20487
	N87-20488
	N87-20489
	N87-20655
146-74-06-70	N87-20522
186-30-21	N87-20841
188-38-53-01	N87-20918
481-02-02	N87-20378
483-32-03-02	N87-20795
505-33-13-01	N87-20406
505-33-62	N87-20421
505-35-13-03	N87-20254
505-40-90	N87-20504
505-41-5A	N87-20353
505-43-43-06	N87-20407
505-45-13-01	N87-20232
505-60	N87-20785
505-60-01	N87-20242
505-60-31-04	N87-20503
505-61-01-02	N87-20517
505-61-01-07	N87-20297
505-61-11-02	N87-20798
505-61-41-01	N87-20240
505-61-71-01	N87-20233
505-61-91	N87-20298
505-62-01	N87-20475
505-62-11	N87-20282
505-62-21	N87-20171
	N87-20235
	N87-20238
	N87-20243
	N87-20257
	N87-20766
	N87-20767
505-62-51	N87-20556
505-62-71	N87-20280
505-62-91-01	N87-20294
505-63-01	N87-20408
	N87-20426
505-63-01-01	N87-20390
505-63-01-02	N87-20404
505-63-11	N87-20389
	N87-20565
505-63-11-01	N87-20755
505-63-11-07	N87-20570
505-63-21-01	N87-20234
	N87-20236
505-63-31-02	N87-20768
505-63-51	N87-20552
	N87-20555
505-63-81-02	N87-20514
505-66-11	N87-20291
	N87-20790
505-66-21-01	N87-20765
	N87-20770
505-66-41-05	N87-20264
505-66-51-00	N87-20257
505-66-91-01	N87-20478
505-67-01-02	N87-20265
505-67-41	N87-20252
	N87-20255
505-90-21-01	N87-20500
	N87-20502
	N87-20754
	N87-20756
	N87-20764
	N87-20769
	N87-20777
	N87-20778
	N87-20779
	N87-20780
	N87-20781
	N87-20782
	N87-20783
505-90-21-02	N87-20753
506-40-11-02	N87-20296
506-41-3B	N87-20405
506-41-41-02	N87-20814
506-42-21	N87-20379
	N87-20515
506-42-31	N87-20382
	N87-20383
	N87-20477
506-43-11	N87-20422
	N87-20562
506-43-21-04	N87-20386
506-43-41-02	N87-20349
506-43-51-02	N87-20567
506-43-51-04	N87-20339
506-44-2A	N87-20468
506-44-2C	N87-20821
506-44-21	N87-20469
	N87-20474
506-47-11	N87-20747
506-49-3B	N87-20342
506-49-21-01	N87-20352
506-49-31-01	N87-20340
506-51-13-06	N87-20344
506-58-13-03	N87-20476
533-04-11	N87-20516
533-05-11	N87-20425
535-03-11-03	N87-20794
	N87-20797
650-60-23	N87-20448
	N87-20450
650-60-26	N87-20467
672-21-14-70	N87-20663

Typical Report Number Index Listing

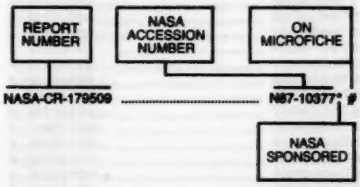

Listings in this index are arranged alphanumerically by report number. The NASA accession number denotes the number by which the citation is identified. An asterisk (*) indicates that the item is a NASA report. A pound sign (#) indicates that the item is available on microfiche.

A-86432 ..... N87-20785* #
A-87050 ..... N87-20257* #
A-87068 ..... N87-20242* #
A-87100 ..... N87-20790* #
A-87105 ..... N87-20298* #
A-87118 ..... N87-20747* #
A-87133 ..... N87-20841* #
A-87157 ..... N87-20291* #

ACSC-86-2405 ..... N87-20702 #

AD-A172801 ..... N87-20702 #
AD-A174577 ..... N87-20480 #
AD-A175224 ..... N87-20574 #
AD-A175225 ..... N87-20580 #
AD-A175226 ..... N87-20802 #
AD-A175522 ..... N87-20451 #
AD-A175529 ..... N87-20355 #
AD-A175531 ..... N87-20354 #
AD-A175533 ..... N87-20283 #
AD-A175535 ..... N87-20711 #
AD-A175542 ..... N87-20427 #
AD-A175554 ..... N87-20391 #
AD-A175561 ..... N87-20292 #
AD-A175573 ..... N87-20518 #
AD-A175593 ..... N87-20822 #
AD-A175596 ..... N87-20799 #
AD-A175597 ..... N87-20556 #
AD-A175610 ..... N87-20571 #
AD-A175616 ..... N87-20284 #
AD-A175635 ..... N87-20173 #
AD-A175640 ..... N87-20791 #
AD-A175641 ..... N87-20771 #
AD-A175644 ..... N87-20452 #
AD-A175657 ..... N87-20572 #
AD-A175660 ..... N87-20285 #
AD-A175661 ..... N87-20691 #
AD-A175663 ..... N87-20481 #
AD-A175726 ..... N87-20438 #
AD-A175754 ..... N87-20642 #
AD-A175836 ..... N87-20482 #
AD-A175864 ..... N87-20453 #
AD-A175938 ..... N87-20244 #
AD-A175944 ..... N87-20454 #
AD-A175951 ..... N87-20245 #
AD-A175959 ..... N87-20712 #
AD-A175967 ..... N87-20505 #
AD-A175972 ..... N87-20573 #
AD-A175975 ..... N87-20692 #
AD-A175997 ..... N87-20345 #
AD-A176001 ..... N87-20286 #
AD-A176014 ..... N87-20713 #
AD-A176015 ..... N87-20455 #
AD-A176019 ..... N87-20714 #
AD-A176069 ..... N87-20456 #
AD-A176081 ..... N87-20715 #
AD-A176090 ..... N87-20258 #
AD-A176238 ..... N87-20392 #
AD-A176240 ..... N87-20246 #
AD-A176418 ..... N87-20384 #

AD-D012552 ..... N87-20459
AD-D012553 ..... N87-20483
AD-D012555 ..... N87-20520
AD-D012558 ..... N87-20458
AD-D012559 ..... N87-20375
AD-D012563 ..... N87-20457
AD-D012564 ..... N87-20815
AD-D012565 ..... N87-20519
AD-D012569 ..... N87-20266
AD-D012571 ..... N87-20823
AD-D012574 ..... N87-20337
AD-D012575 ..... N87-20748
AD-D012583 ..... N87-20543

AEDC-TR-86-45 ..... N87-20505 #

AGARD-CP-397 ..... N87-20355 #
AGARD-CP-402 ..... N87-20174 #
AGARD-CP-412 ..... N87-20199 #

AIAA-87-0735-CP ..... N87-20236* #
AIAA-87-0850 ..... N87-20234* #
AIAA-87-0992 ..... N87-20383* #
AIAA-87-0994 ..... N87-20477* #
AIAA-87-1060 ..... N87-20382* #
AIAA-87-1906 ..... N87-20280* #

AMA-85-5 ..... N87-20344* #
AMA-85-09 ..... N87-20253* #

ANL/TM-438-REV ..... N87-20772 #

AO1-1(ST1) ..... N87-20642 #

ARAP-597 ..... N87-20232* #

ARO-18072.9-MA ..... N87-20791 #
ARO-18360.18-EL ..... N87-20771 #
ARO-19872.9-EG ..... N87-20572 #
ARO-20060.6-EL ..... N87-20481 #
ARO-21818.4-GS ..... N87-20518 #
ARO-22361.3-MS ..... N87-20427 #
ARO-22967.2-EG ..... N87-20571 #
ARO-23322.7-EG ..... N87-20292 #
ARO-23440.2-EG-H ..... N87-20391 #
ARO-23894.1-EL ..... N87-20822 #

ASTRON-GEODAET-ARB-48 ..... N87-20618

AVSCOM-TR-86-C-42 ..... N87-20555* #

AWS-TN-86/001 ..... N87-20702 #

BARC-1244 ..... N87-20631 #
BARC-1281 ..... N87-20617 #
BARC-1301 ..... N87-20443 #

BBC-RD-1987/1 ..... N87-20796

BDX-613-3642 ..... N87-20395 #

BFLRF-218 ..... N87-20558 #

BNL-39049 ..... N87-20547 #
BNL-39062 ..... N87-20694 #
BNL-52049 ..... N87-20414 #

BR101809 ..... N87-20262 #

BU-335 ..... N87-20283 #
BU-344 ..... N87-20299 #
BU-345 ..... N87-20258 #
BU-351 ..... N87-20247 #

B6668354 ..... N87-20610 #
B6672200 ..... N87-20609 #
B6672201 ..... N87-20628 #

CAP-426 ..... N87-20259

CCMS-86-06 ..... N87-20385 #

CI-FR-0102 ..... N87-20820* #

CONF-850415-5 ..... N87-20428 #
CONF-860629-68 ..... N87-20461 #
CONF-860701-70 ..... N87-20694 #
CONF-860914-33 ..... N87-20826 #
CONF-861008-5 ..... N87-20655 #
CONF-861008-6 ..... N87-20492 #
CONF-861038-1 ..... N87-20506 #
CONF-861044-5 ..... N87-20730* #
CONF-861068-14 ..... N87-20493 #
CONF-861068-17 ..... N87-20416 #
CONF-861186-1 ..... N87-20409 #
CONF-861207-12 ..... N87-20544 #
CONF-861207-15 ..... N87-20411 #
CONF-861207-54 ..... N87-20417 #
CONF-861207-58 ..... N87-20413 #
CONF-861207-68 ..... N87-20827 #
CONF-870111-2 ..... N87-20654 #
CONF-870134-1 ..... N87-20643 #
CONF-870144-1 ..... N87-20824 #
CONF-870148-1 ..... N87-20774 #
CONF-870220-3 ..... N87-20546 #
CONF-870235-2 ..... N87-20507 #
CONF-870301-4 ..... N87-20560 #
CONF-870301-5 ..... N87-20750 #
CONF-870301-7 ..... N87-20749 #
CONF-870304-1 ..... N87-20548 #
CONF-870305-2 ..... N87-20486 #
CONF-870372-1 ..... N87-20561 #
CONF-870447-1 ..... N87-20415 #
CONF-8510384-PT-2 ..... N87-20815 #
CONF-8604292-1 ..... N87-20816 #
CONF-8608130-10 ..... N87-20844 #
CONF-8609138-4 ..... N87-20545 #
CONF-8609160-2 ..... N87-20825 #
CONF-8609230-1 ..... N87-20487 #
CONF-8610122-12 ..... N87-20488 #
CONF-8610122-13 ..... N87-20489 #
CONF-8610135-11 ..... N87-20563 #
CONF-8610196-3 ..... N87-20786 #
CONF-8610207-6 ..... N87-20863 #
CONF-8610207-8 ..... N87-20868* #
CONF-8610215-2 ..... N87-20773 #
CONF-8610232-1 ..... N87-20491 #
CONF-8611110-1 ..... N87-20396 #

CPIA-PUB-454 ..... N87-20384 #

CRC-1370 ..... N87-20456 #

CRREL-87-2 ..... N87-20433 #

CWI-MS-R8602 ..... N87-20787 #
CWI-MS-R8610 ..... N87-20789 #

DE86-007392 ..... N87-20548 #
DE86-016088 ..... N87-20772 #
DE86-703483 ..... N87-20830 #
DE87-001045 ..... N87-20490 #
DE87-001433 ..... N87-20396 #
DE87-001959 ..... N87-20786 #
DE87-002051 ..... N87-20546 #
DE87-002406 ..... N87-20545 #
DE87-002415 ..... N87-20486 #
DE87-002497 ..... N87-20757 #
DE87-002551 ..... N87-20507 #
DE87-002607 ..... N87-20563 #
DE87-002656 ..... N87-20409 #
DE87-002815 ..... N87-20730* #
DE87-002890 ..... N87-20506 #
DE87-002914 ..... N87-20411 #
DE87-003002 ..... N87-20749 #
DE87-003004 ..... N87-20750 #
DE87-003008 ..... N87-20560 #
DE87-003033 ..... N87-20544 #
DE87-003048 ..... N87-20484 #
DE87-003049 ..... N87-20485 #
DE87-003160 ..... N87-20816 #
DE87-003238 ..... N87-20415 #
DE87-003263 ..... N87-20460 #
DE87-003341 ..... N87-20428 #
DE87-003389 ..... N87-20412 #
DE87-003722 ..... N87-20844 #
DE87-003746 ..... N87-20654 #

DE87-003804 ..... N87-20508 #
DE87-004025 ..... N87-20393 #
DE87-004041 ..... N87-20559 #
DE87-004175 ..... N87-20547 #
DE87-004229 ..... N87-20394 #
DE87-004256 ..... N87-20773 #
DE87-004257 ..... N87-20643 #
DE87-004421 ..... N87-20824 #
DE87-004443 ..... N87-20441 #
DE87-004444 ..... N87-20430 #
DE87-004545 ..... N87-20561 #
DE87-004557 ..... N87-20395 #
DE87-004561 ..... N87-20843 #
DE87-004612 ..... N87-20694 #
DE87-004627 ..... N87-20774 #
DE87-004657 ..... N87-20825 #
DE87-004707 ..... N87-20826 #
DE87-004868 ..... N87-20416 #
DE87-004870 ..... N87-20487 #
DE87-004920 ..... N87-20491 #
DE87-004926 ..... N87-20492 #
DE87-004928 ..... N87-20488 #
DE87-004929 ..... N87-20655 #
DE87-004930 ..... N87-20489 #
DE87-004961 ..... N87-20493 #
DE87-005036 ..... N87-20656 #
DE87-005122 ..... N87-20863 #
DE87-005123 ..... N87-20868* #
DE87-005132 ..... N87-20461 #
DE87-005183 ..... N87-20728 #
DE87-005265 ..... N87-20509 #
DE87-005303 ..... N87-20716 #
DE87-005328 ..... N87-20417 #
DE87-005340 ..... N87-20413 #
DE87-005347 ..... N87-20835 #
DE87-005354 ..... N87-20793 #
DE87-005402 ..... N87-20864 #
DE87-005403 ..... N87-20865 #
DE87-005404 ..... N87-20866 #
DE87-005556 ..... N87-20703 #
DE87-005578 ..... N87-20729 #
DE87-005585 ..... N87-20414 #
DE87-005589 ..... N87-20442 #
DE87-005624 ..... N87-20397 #
DE87-005625 ..... N87-20549 #
DE87-005713 ..... N87-20627 #
DE87-005774 ..... N87-20953 #
DE87-005789 ..... N87-20418 #
DE87-005795 ..... N87-20419 #
DE87-700426 ..... N87-20693 #
DE87-700680 ..... N87-20952 #
DE87-700730 ..... N87-20792 #
DE87-700760 ..... N87-20845 #
DE87-701244 ..... N87-20831 #
DE87-701254 ..... N87-20817 #
DE87-701264 ..... N87-20443 #
DE87-750405 ..... N87-20410 #
DE87-780056 ..... N87-20615 #

DFVLR-FB-84-04 ..... N87-20510 #
DFVLR-FB-86-03 ..... N87-20704 #

DFVLR-MITT-81-18 ..... N87-20800 #

DFVRL-MITT-86-11 ..... N87-20300 #

DNA-TR-86-74 ..... N87-20455 #
DNA-TR-86-158 ..... N87-20451 #

DOE/AL-33408/T3 ..... N87-20656 #

DOE/BC-10828/2 ..... N87-20635 #

DOE/ER-03231/10 ..... N87-20728 #
DOE/ER-13082/1 ..... N87-20793 #
DOE/ER-13285/T1 ..... N87-20757 #
DOE/ER-40012/2 ..... N87-20953 #
DOE/ER-45179/T1 ..... N87-20412 #
DOE/ER-60348/5 ..... N87-20716 #
DOE/ER-60397/H1 ..... N87-20703 #

DOE/JPL-1012-76-REV-1 ..... N87-20845* #
DOE/JPL-1012-125-VOL-1 ..... N87-20646* #
DOE/JPL-1012-125-VOL-2 ..... N87-20647* #
DOE/JPL-1012-125-VOL-3 ..... N87-20648* #
DOE/JPL-1012-125-VOL-4 ..... N87-20649* #
DOE/JPL-1012-125-VOL-5 ..... N87-20650* #
DOE/JPL-1012-125-VOL-6 ..... N87-20651* #
DOE/JPL-1012-125-VOL-7 ..... N87-20652* #
DOE/JPL-1012-125-VOL-8 ..... N87-20653* #

DOE/METC-87-6075 ..... N87-20490 #

DOE/NASA/16310-3 ..... N87-20405* #

DOT/FAA-PM-84-16.3 ..... N87-20433 #

DOT/FAA-PM-85-20 ..... N87-20434 #
DOT/FAA-PM-86-12 ..... N87-20432 #
DOT/FAA-PM-86/50-VOL-1 ..... N87-20255* #

DOT/FAA/EE-85-8 ..... N87-20799 #

DOT/FAA/PM-86/50-VOL-2 ..... N87-20252* #

DP-MS-86-111 ..... N87-20409 #

D180-27884-3 ..... N87-20554* #

E-2940 ..... N87-20565* #
E-3033 ..... N87-20267* #
E-3090 ..... N87-20474* #
E-3221 ..... N87-20238* #
E-3236-1 ..... N87-20381* #
E-3294 ..... N87-20295* #
E-3306 ..... N87-20405* #
E-3322 ..... N87-20448* #
E-3335 ..... N87-20469* #
E-3360 ..... N87-20552* #
E-3367 ..... N87-20422* #
E-3368 ..... N87-20555* #
E-3380 ..... N87-20556* #
E-3430 ..... N87-20566* #
E-3452 ..... N87-20516* #
E-3458 ..... N87-20379* #
E-3462 ..... N87-20280* #
E-3465 ..... N87-20515* #
E-3466 ..... N87-20425* #
E-3468 ..... N87-20475* #
E-3469 ..... N87-20767* #
E-3476 ..... N87-20389* #
E-3477 ..... N87-20235* #
E-3482 ..... N87-20468* #
E-3483 ..... N87-20378* #
E-3484 ..... N87-20408* #
E-3488 ..... N87-20282* #
E-3491 ..... N87-20450* #
E-3495 ..... N87-20426* #
E-3499 ..... N87-20243* #
E-3501 ..... N87-20171* #
E-3504 ..... N87-20562* #
E-3505 ..... N87-20421* #
E-3510 ..... N87-20353* #
E-3511 ..... N87-20342* #
E-3513 ..... N87-20504* #
E-3517 ..... N87-20766* #
E-3519 ..... N87-20621* #
E-3525 ..... N87-20382* #
E-3526 ..... N87-20383* #
E-3527 ..... N87-20477* #

ECN-184 ..... N87-20603 #

EFI-788(15)-85 ..... N87-20952 #

EGG-M-17586 ..... N87-20561 #
EGG-M-32786 ..... N87-20396 #
EGG-M-34086 ..... N87-20553 #

ENST-86C002 ..... N87-20637 #
ENST-86D002 ..... N87-20466 #
ENST-86E007 ..... N87-20496 #

ESA-BR-27 ..... N87-20867 #

ESA-CR(P)-2291-VOL-2 ..... N87-20657 #
ESA-CR(P)-2302-VOL-1 ..... N87-20462 #
ESA-CR(P)-2302-VOL-6 ..... N87-20463 #
ESA-CR(P)-2303-VOL-1 ..... N87-20464 #
ESA-CR(P)-2303-VOL-2 ..... N87-20465 #
ESA-CR(P)-2305 ..... N87-20376 #

ESA-SP-266 ..... N87-20621 #

ESA-TT-748 ..... N87-20800 #
ESA-TT-868 ..... N87-20401 #
ESA-TT-879 ..... N87-20510 #
ESA-TT-993 ..... N87-20704 #
ESA-TT-1012 ..... N87-20300 #

ESA-86-87170 ..... N87-20388* #

ESD-TR-84-611 ..... N87-20926* #

ETN-87-99974 ..... N87-20618
ETN-87-99014 ..... N87-20695 #
ETN-87-99015 ..... N87-20775 #
ETN-87-99016 ..... N87-20521 #
ETN-87-99019 ..... N87-20616 #
ETN-87-99091 ..... N87-20759 #
ETN-87-99105 ..... N87-20808 #
ETN-87-99196 ..... N87-20263 #
ETN-87-99206 ..... N87-20299 #
ETN-87-99207 ..... N87-20256 #
ETN-87-99212 ..... N87-20247 #
ETN-87-99216 ..... N87-20803 #
ETN-87-99244 ..... N87-20787 #
ETN-87-99318 ..... N87-20828 #
ETN-87-99319 ..... N87-20809 #
ETN-87-99320 ..... N87-20810 #
ETN-87-99321 ..... N87-20832 #
ETN-87-99332 ..... N87-20550
ETN-87-99336 ..... N87-20287 #
ETN-87-99342 ..... N87-20811 #
ETN-87-99355 ..... N87-20788 #
ETN-87-99363 ..... N87-20829 #
ETN-87-99364 ..... N87-20812 #
ETN-87-99377 ..... N87-20758 #
ETN-87-99378 ..... N87-20836 #
ETN-87-99380 ..... N87-20402 #
ETN-87-99381 ..... N87-20705 #
ETN-87-99382 ..... N87-20617 #
ETN-87-99383 ..... N87-20706 #
ETN-87-99384 ..... N87-20396 #
ETN-87-99385 ..... N87-20249 #
ETN-87-99386 ..... N87-20250 #
ETN-87-99387 ..... N87-20707 #
ETN-87-99388 ..... N87-20511 #
ETN-87-99390 ..... N87-20512 #
ETN-87-99391 ..... N87-20513 #
ETN-87-99392 ..... N87-20251 #
ETN-87-99399 ..... N87-20637 #
ETN-87-99400 ..... N87-20466 #
ETN-87-99401 ..... N87-20496 #
ETN-87-99405 ..... N87-20403 #
ETN-87-99423 ..... N87-20600 #
ETN-87-99424 ..... N87-20401 #
ETN-87-99425 ..... N87-20510 #
ETN-87-99428 ..... N87-20704 #
ETN-87-99430 ..... N87-20300 #
ETN-87-99432 ..... N87-20867 #
ETN-87-99434 ..... N87-20621 #
ETN-87-99438 ..... N87-20429 #
ETN-87-99439 ..... N87-20494 #
ETN-87-99440 ..... N87-20495 #
ETN-87-99441 ..... N87-20659 #
ETN-87-99459 ..... N87-20776 #
ETN-87-99478 ..... N87-20341 #
ETN-87-99479 ..... N87-20293 #
ETN-87-99480 ..... N87-20246 #
ETN-87-99481 ..... N87-20346 #
ETN-87-99483 ..... N87-20657 #
ETN-87-99484 ..... N87-20462 #
ETN-87-99489 ..... N87-20463 #
ETN-87-99490 ..... N87-20464 #
ETN-87-99491 ..... N87-20465 #
ETN-87-99495 ..... N87-20376 #
ETN-87-99496 ..... N87-20259
ETN-87-99530 ..... N87-20789 #

FNAL/PUB-86/79-A ..... N87-20864 #
FNAL/PUB-86/150-A ..... N87-20866 #
FNAL/PUB-86/158-A ..... N87-20865 #

FOA-C-20635-2.1 ..... N87-20429 #
FOA-C-30431-3.2 ..... N87-20494 #
FOA-C-30434-3.2 ..... N87-20495 #
FOA-C-30435-3.1 ..... N87-20659 #

FTD-ID(RS)T-1063-86 ..... N87-20354 #
FTD-ID(RS)T-1152-86 ..... N87-20246 #
FTD-ID(RS)T-1203-86 ..... N87-20453 #

GCO/GH/CL-442.026/85 ..... N87-20261* #

GPO-60-627 ..... N87-20638 #

ICASE-86-82 ..... N87-20779* #
ICASE-87-5 ..... N87-20769* #
ICASE-87-9 ..... N87-20500* #
ICASE-87-10 ..... N87-20777* #
ICASE-87-11 ..... N87-20778* #
ICASE-87-12 ..... N87-20782* #
ICASE-87-13 ..... N87-20783* #
ICASE-87-14 ..... N87-20764* #
ICASE-87-16 ..... N87-20502* #
ICASE-87-17 ..... N87-20756* #
ICASE-87-18 ..... N87-20780* #
ICASE-87-19 ..... N87-20781* #

ICOMP-87-2 ..... N87-20171* #

IFVE-OTF-85-167 ..... N87-20792 #

INIS-MF-10517 ..... N87-20615 #

INPE-3883 ..... N87-20693 #
INPE-4058-PRE/1017 ..... N87-20661 #
INPE-4070-TDL/248 ..... N87-20861 #

INPE-4088-PRE/1033 N87-20551 #

INSA-IDTC1-8604 N87-20403 #

IPPJ-T-36 N87-20618 #

IS-T-1244 N87-20485 #
IS-T-1246 N87-20484 #

ISBN-0-86039-287-2 N87-20259
ISBN-3-7696-9791-X N87-20618
ISBN-92-835-0396-1 N87-20355 #
ISBN-92-835-0400-3 N87-20174 #
ISBN-92-835-0402-X N87-20199 #

ISSN-0038-0911 N87-20948 #
ISSN-0078-379X N87-20402 #
ISSN-0078-3781 N87-20705 #
ISSN-0250-1589 N87-20667 #
ISSN-0340-7691 N87-20618
ISSN-0347-3694 N87-20429 #
ISSN-0347-3708 N87-20494 #
ISSN-0347-3708 N87-20495 #
ISSN-0347-3708 N87-20659 #
ISSN-0379-6566 N87-20621 #
ISSN-0721-5320 N87-20550
ISSN-0751-1337 N87-20637 #
ISSN-0751-1345 N87-20486 #
ISSN-0751-1353 N87-20496 #

ITF-86-29-R N87-20845 #

ITS-TR-043/86-VOL-2 N87-20465 #
ITS-TR-043/86-VOL1 N87-20464 #

JPL-PUB-82-79-REV-1 N87-20645* #
JPL-PUB-86-31-VOL-1 N87-20646* #
JPL-PUB-86-31-VOL-2 N87-20647* #
JPL-PUB-86-31-VOL-3 N87-20648* #
JPL-PUB-86-31-VOL-4 N87-20649* #
JPL-PUB-86-31-VOL-5 N87-20650* #
JPL-PUB-86-31-VOL-6 N87-20651* #
JPL-PUB-86-31-VOL-7 N87-20652* #
JPL-PUB-86-31-VOL-8 N87-20653* #

JPRS-CST-86-025 N87-20708 #
JPRS-CST-86-031 N87-20720 #
JPRS-CST-87-005 N87-20717 #

JPRS-UBB-87-003 N87-20751 #

JPRS-UPM-86-008 N87-20445 #

JPRS-USB-86-005 N87-20731 #

KU-FRL-629-1 N87-20264* #

L-16055 N87-20814* #
L-16115 N87-20407* #
L-16143 N87-20233* #
L-16163 N87-20567* #
L-16170 N87-20296* #
L-16191 N87-20240* #
L-16203 N87-20798* #
L-16208 N87-20517* #
L-16221 N87-20265* #
L-16234 N87-20683* #
L-16261 N87-20514* #
L-16271 N87-20522* #

LA-UR-86-3455 N87-20786 #
LA-UR-86-3643 N87-20461 #
LA-UR-86-3811 N87-20411 #
LA-UR-86-4052 N87-20506 #
LA-UR-86-4116 N87-20844 #
LA-UR-86-4296 N87-20654 #
LA-UR-87-38 N87-20868* #
LA-UR-87-39 N87-20863 #

LA-10854-MS N87-20508 #

LBF-TB-176(1986) N87-20550

LC-79-640375 N87-20948 #

LEGS-TN-15 N87-20547 #

LMSC-HEC-TR-D065566 N87-20343* #

LR-30775 N87-20406* #

M-548 N87-20665* #

MCR-85-583 N87-20350* #
MCR-85-641 N87-20471* #
MCR-86-673 N87-20470* #
MCR-86-674 N87-20473* #
MCR-86-675 N87-20472* #

MDC-W0070 N87-20351* #

MITT-85-01 N87-20287 #

MLM-3403 N87-20559 #

MRC-R-974 N87-20455 #
MRC-R-976 N87-20451 #

NADC-86045-60 N87-20283 #

NAE-AN-42 N87-20286 #

NAMRL-1323 N87-20258 #

NAPC-PE-155 N87-20284 #

NAS 1.15:83103 N87-20658* #
NAS 1.15:86319-REV-1 N87-20294* #
NAS 1.15:86397 N87-20254* #
NAS 1.15:86411 N87-20476* #
NAS 1.15:86589 N87-20689* #
NAS 1.15:86590 N87-20431* #
NAS 1.15:87774 N87-20479* #
NAS 1.15:87806 N87-20690* #
NAS 1.15:88377 N87-20785* #
NAS 1.15:88500 N87-20802* #
NAS 1.15:88527 N87-20399* #
NAS 1.15:88575 N87-20424* #
NAS 1.15:88583 N87-20281* #
NAS 1.15:88664 N87-20565* #
NAS 1.15:88975 N87-20556* #
NAS 1.15:88981 N87-20422* #
NAS 1.15:88982 N87-20516* #
NAS 1.15:89027 N87-20349* #
NAS 1.15:89039 N87-20517* #
NAS 1.15:89042 N87-20296* #
NAS 1.15:89049 N87-20240* #
NAS 1.15:89058 N87-20770* #
NAS 1.15:89063 N87-20814* #
NAS 1.15:89064 N87-20265* #
NAS 1.15:89069 N87-20386* #
NAS 1.15:89072 N87-20352* #
NAS 1.15:89081 N87-20478* #
NAS 1.15:89089 N87-20797* #
NAS 1.15:89090 N87-20794* #
NAS 1.15:89097 N87-20768* #
NAS 1.15:89098 N87-20785* #
NAS 1.15:89104 N87-20390* #
NAS 1.15:89109 N87-20755* #
NAS 1.15:89111 N87-20795* #
NAS 1.15:89118 N87-20339* #
NAS 1.15:89120 N87-20234* #
NAS 1.15:89121 N87-20236* #
NAS 1.15:89141 N87-20570* #
NAS 1.15:89214 N87-20301* #
NAS 1.15:89278 N87-20730* #
NAS 1.15:89418 N87-20257* #
NAS 1.15:89421 N87-20242* #
NAS 1.15:89427 N87-20790* #
NAS 1.15:89430 N87-20747* #
NAS 1.15:89436 N87-20841* #
NAS 1.15:89441 N87-20291* #
NAS 1.15:89455 N87-20298* #
NAS 1.15:89814 N87-20379* #
NAS 1.15:89817 N87-20280* #
NAS 1.15:89819 N87-20515* #
NAS 1.15:89820 N87-20425* #
NAS 1.15:89822 N87-20475* #
NAS 1.15:89823 N87-20767* #
NAS 1.15:89827 N87-20389* #
NAS 1.15:89828 N87-20235* #
NAS 1.15:89831 N87-20408* #
NAS 1.15:89833 N87-20282* #
NAS 1.15:89834 N87-20405* #
NAS 1.15:89835 N87-20450* #
NAS 1.15:89838 N87-20426* #
NAS 1.15:89839 N87-20469* #
NAS 1.15:89840 N87-20468* #
NAS 1.15:89842 N87-20171* #
NAS 1.15:89843 N87-20562* #
NAS 1.15:89844 N87-20421* #
NAS 1.15:89847 N87-20378* #
NAS 1.15:89848 N87-20342* #
NAS 1.15:89850 N87-20766* #
NAS 1.15:89851 N87-20504* #
NAS 1.15:89852 N87-20353* #
NAS 1.15:89857 N87-20382* #
NAS 1.15:89858 N87-20383* #
NAS 1.15:89859 N87-20821* #
NAS 1.15:89860 N87-20477* #
NAS 1.21:7037(212) N87-20172*
NAS 1.21:7500(21) N87-20633*
NAS 1.26:4046-VOL-1 N87-20255* #
NAS 1.26:4047-VOL-2 N87-20252* #
NAS 1.26:4053 N87-20350* #
NAS 1.26:4054 N87-20813* #
NAS 1.26:4055 N87-20552* #
NAS 1.26:4057 N87-20700* #
NAS 1.26:4063 N87-20253* #
NAS 1.26:4064 N87-20501* #
NAS 1.26:4065 N87-20699* #
NAS 1.26:171978 N87-20335* #
NAS 1.26:171979 N87-20634* #
NAS 1.26:171981 N87-20351* #
NAS 1.26:172518 N87-20753* #
NAS 1.26:172521 N87-20406* #
NAS 1.26:172572 N87-20344* #
NAS 1.26:174733 N87-20367* #
NAS 1.26:174850-VOL-2 N87-20239* #
NAS 1.26:178029 N87-20290* #
NAS 1.26:178208 N87-20340* #
NAS 1.26:178214 N87-20297* #
NAS 1.26:178226 N87-20779* #
NAS 1.26:178227 N87-20404* #
NAS 1.26:178237 N87-20769* #
NAS 1.26:178245 N87-20400* #
NAS 1.26:178248 N87-20232* #
NAS 1.26:178249 N87-20503* #
NAS 1.26:178255 N87-20264* #
NAS 1.26:178257 N87-20754* #
NAS 1.26:178258 N87-20500* #
NAS 1.26:178259 N87-20777* #
NAS 1.26:178260 N87-20778* #
NAS 1.26:178263 N87-20782* #
NAS 1.26:178264 N87-20783* #
NAS 1.26:178265 N87-20764* #
NAS 1.26:178266 N87-20756* #
NAS 1.26:178268 N87-20502* #
NAS 1.26:178269 N87-20780* #
NAS 1.26:178270 N87-20781* #
NAS 1.26:179027 N87-20820* #
NAS 1.26:179031 N87-20471* #
NAS 1.26:179032 N87-20470* #
NAS 1.26:179033 N87-20472* #
NAS 1.26:179034 N87-20473* #
NAS 1.26:179035 N87-20553* #
NAS 1.26:179037 N87-20951* #
NAS 1.26:179046 N87-20343* #
NAS 1.26:179605 N87-20467* #
NAS 1.26:179608 N87-20243* #
NAS 1.26:180107 N87-20840* #
NAS 1.26:180234 N87-20449* #
NAS 1.26:180250 N87-20842* #
NAS 1.26:180376 N87-20554* #
NAS 1.26:180401-REV-1 N87-20645* #
NAS 1.26:180497 N87-20660* #
NAS 1.26:180501 N87-20662* #
NAS 1.26:180503 N87-20664* #
NAS 1.26:180507 N87-20644* #
NAS 1.26:180509 N87-20557* #
NAS 1.26:180614 N87-20868* #
NAS 1.26:180656 N87-20289* #
NAS 1.26:180658 N87-20646* #
NAS 1.26:180659 N87-20647* #
NAS 1.26:180661 N87-20648* #
NAS 1.26:180662 N87-20649* #
NAS 1.26:180663 N87-20650* #
NAS 1.26:180664 N87-20651* #
NAS 1.26:180665 N87-20652* #
NAS 1.26:180695 N87-20653* #
NAS 1.26:180698 N87-20569* #
NAS 1.55:2433 N87-20267* #
NAS 1.55:2438 N87-20302* #
NAS 1.55:2442 N87-20871* #
NAS 1.55:2456 N87-20522* #
NAS 1.55:2460 N87-20665* #
NAS 1.60:2656 N87-20233* #
NAS 1.60:2661 N87-20567* #
NAS 1.60:2671 N87-20423* #
NAS 1.60:2674 N87-20407* #
NAS 1.60:2676 N87-20238* #
NAS 1.60:2679 N87-20798* #
NAS 1.60:2680 N87-20295* #
NAS 1.60:2682 N87-20514* #
NAS 1.60:2690 N87-20380* #
NAS 1.60:2693 N87-20474* #
NAS 1.60:2699 N87-20448* #
NAS 1.60:2705 N87-20555* #
NAS 1.60:2710 N87-20568* #
NAS 1.60:2711 N87-20566* #
NAS 1.60:2714 N87-20947* #
NAS 1.60:2720 N87-20381* #
NAS 1.60:2724 N87-20727* #
NAS 1.61:1175 N87-20663* #
NAS 1.61:1183 N87-20701* #
NAS 1.77:20008 N87-20388* #
NAS 1.77:20011 N87-20261* #
NAS 1.77:20055 N87-20241* #

NAS 1.77:20056 ..... N87-20784* #

NASA-CP-2433 ..... N87-20267* #
NASA-CP-2436 ..... N87-20302* #
NASA-CP-2442 ..... N87-20871* #
NASA-CP-2456 ..... N87-20522* #
NASA-CP-2460 ..... N87-20665* #

NASA-CR-4046-VOL-1 ..... N87-20255* #
NASA-CR-4047-VOL-2 ..... N87-20252* #
NASA-CR-4053 ..... N87-20350* #
NASA-CR-4054 ..... N87-20813* #
NASA-CR-4055 ..... N87-20552* #
NASA-CR-4057 ..... N87-20700* #
NASA-CR-4063 ..... N87-20253* #
NASA-CR-4064 ..... N87-20501* #
NASA-CR-4065 ..... N87-20699* #
NASA-CR-171978 ..... N87-20335* #
NASA-CR-171979 ..... N87-20634* #
NASA-CR-171981 ..... N87-20351* #
NASA-CR-172516 ..... N87-20753* #
NASA-CR-172521 ..... N87-20406* #
NASA-CR-172572 ..... N87-20344* #
NASA-CR-174733 ..... N87-20387* #
NASA-CR-174850-VOL-2 ..... N87-20239* #
NASA-CR-178029 ..... N87-20290* #
NASA-CR-178208 ..... N87-20340* #
NASA-CR-178214 ..... N87-20297* #
NASA-CR-178226 ..... N87-20779* #
NASA-CR-178227 ..... N87-20404* #
NASA-CR-178237 ..... N87-20769* #
NASA-CR-178245 ..... N87-20400* #
NASA-CR-178248 ..... N87-20232* #
NASA-CR-178249 ..... N87-20503* #
NASA-CR-178255 ..... N87-20264* #
NASA-CR-178257 ..... N87-20754* #
NASA-CR-178258 ..... N87-20500* #
NASA-CR-178259 ..... N87-20777* #
NASA-CR-178260 ..... N87-20778* #
NASA-CR-178263 ..... N87-20782* #
NASA-CR-178264 ..... N87-20783* #
NASA-CR-178265 ..... N87-20764* #
NASA-CR-178266 ..... N87-20756* #
NASA-CR-178268 ..... N87-20502* #
NASA-CR-178269 ..... N87-20780* #
NASA-CR-178270 ..... N87-20781* #
NASA-CR-179027 ..... N87-20620* #
NASA-CR-179031 ..... N87-20471* #
NASA-CR-179032 ..... N87-20470* #
NASA-CR-179033 ..... N87-20472* #
NASA-CR-179034 ..... N87-20473* #
NASA-CR-179035 ..... N87-20553* #
NASA-CR-179037 ..... N87-20951* #
NASA-CR-179046 ..... N87-20343* #
NASA-CR-179605 ..... N87-20467* #
NASA-CR-179606 ..... N87-20243* #
NASA-CR-180107 ..... N87-20840* #
NASA-CR-180234 ..... N87-20449* #
NASA-CR-180250 ..... N87-20842* #
NASA-CR-180376 ..... N87-20554* #
NASA-CR-180401-REV-1 ..... N87-20645* #
NASA-CR-180497 ..... N87-20860* #
NASA-CR-180501 ..... N87-20662* #
NASA-CR-180503 ..... N87-20664* #
NASA-CR-180507 ..... N87-20644* #
NASA-CR-180509 ..... N87-20557* #
NASA-CR-180614 ..... N87-20868* #
NASA-CR-180656 ..... N87-20289* #
NASA-CR-180658 ..... N87-20846* #
NASA-CR-180659 ..... N87-20647* #
NASA-CR-180661 ..... N87-20648* #
NASA-CR-180662 ..... N87-20649* #
NASA-CR-180663 ..... N87-20650* #
NASA-CR-180664 ..... N87-20651* #
NASA-CR-180665 ..... N87-20652* #
NASA-CR-180695 ..... N87-20653* #
NASA-CR-180698 ..... N87-20569* #

NASA-M001 ..... N87-20301* #

NASA-RP-1175 ..... N87-20663* #
NASA-RP-1183 ..... N87-20701* #

NASA-SP-7037(212) N87-20172*
NASA-SP-7500(21) N87-20833*

NASA-TM-83103 ..... N87-20656* #
NASA-TM-86319-REV-1 ..... N87-20294* #
NASA-TM-86397 ..... N87-20254* #
NASA-TM-86411 ..... N87-20476* #
NASA-TM-86589 ..... N87-20689* #
NASA-TM-86590 ..... N87-20431* #
NASA-TM-87774 ..... N87-20479* #
NASA-TM-87806 ..... N87-20690* #
NASA-TM-88377 ..... N87-20785* #
NASA-TM-88500 ..... N87-20802* #
NASA-TM-88527 ..... N87-20399* #
NASA-TM-88575 ..... N87-20424* #
NASA-TM-88583 ..... N87-20281* #
NASA-TM-88864 ..... N87-20565* #
NASA-TM-88975 ..... N87-20556* #
NASA-TM-88981 ..... N87-20422* #
NASA-TM-88982 ..... N87-20516* #
NASA-TM-89027 ..... N87-20349* #
NASA-TM-89039 ..... N87-20517* #
NASA-TM-89042 ..... N87-20296* #
NASA-TM-89049 ..... N87-20240* #
NASA-TM-89058 ..... N87-20770* #
NASA-TM-89063 ..... N87-20614* #
NASA-TM-89064 ..... N87-20265* #
NASA-TM-89069 ..... N87-20386* #
NASA-TM-89072 ..... N87-20352* #
NASA-TM-89081 ..... N87-20478* #
NASA-TM-89089 ..... N87-20797* #
NASA-TM-89090 ..... N87-20794* #
NASA-TM-89097 ..... N87-20768* #
NASA-TM-89098 ..... N87-20765* #
NASA-TM-89104 ..... N87-20390* #
NASA-TM-89109 ..... N87-20755* #
NASA-TM-89111 ..... N87-20795* #
NASA-TM-89118 ..... N87-20339* #
NASA-TM-89120 ..... N87-20234* #
NASA-TM-89121 ..... N87-20236* #
NASA-TM-89141 ..... N87-20570* #
NASA-TM-89214 ..... N87-20301* #
NASA-TM-89278 ..... N87-20730* #
NASA-TM-89418 ..... N87-20257* #
NASA-TM-89421 ..... N87-20242* #
NASA-TM-89427 ..... N87-20790* #
NASA-TM-89430 ..... N87-20747* #
NASA-TM-89436 ..... N87-20841* #
NASA-TM-89441 ..... N87-20291* #
NASA-TM-89455 ..... N87-20298* #
NASA-TM-89814 ..... N87-20379* #
NASA-TM-89817 ..... N87-20280* #
NASA-TM-89819 ..... N87-20515* #
NASA-TM-89820 ..... N87-20425* #
NASA-TM-89822 ..... N87-20475* #
NASA-TM-89823 ..... N87-20767* #
NASA-TM-89827 ..... N87-20389* #
NASA-TM-89828 ..... N87-20235* #
NASA-TM-89831 ..... N87-20408* #
NASA-TM-89833 ..... N87-20282* #
NASA-TM-89834 ..... N87-20405* #
NASA-TM-89835 ..... N87-20450* #
NASA-TM-89836 ..... N87-20426* #
NASA-TM-89839 ..... N87-20469* #
NASA-TM-89840 ..... N87-20468* #
NASA-TM-89842 ..... N87-20171* #
NASA-TM-89843 ..... N87-20562* #
NASA-TM-89844 ..... N87-20421* #
NASA-TM-89847 ..... N87-20378* #
NASA-TM-89848 ..... N87-20342* #
NASA-TM-89850 ..... N87-20766* #
NASA-TM-89851 ..... N87-20504* #
NASA-TM-89852 ..... N87-20353* #
NASA-TM-89857 ..... N87-20382* #
NASA-TM-89858 ..... N87-20383* #
NASA-TM-89859 ..... N87-20621* #
NASA-TM-89860 ..... N87-20477* #

NASA-TP-2656 ..... N87-20233* #
NASA-TP-2661 ..... N87-20567* #
NASA-TP-2671 ..... N87-20423* #
NASA-TP-2674 ..... N87-20407* #
NASA-TP-2676 ..... N87-20238* #
NASA-TP-2679 ..... N87-20798* #
NASA-TP-2680 ..... N87-20295* #
NASA-TP-2682 ..... N87-20514* #
NASA-TP-2690 ..... N87-20380* #
NASA-TP-2693 ..... N87-20474* #
NASA-TP-2699 ..... N87-20448* #
NASA-TP-2705 ..... N87-20555* #
NASA-TP-2710 ..... N87-20568* #
NASA-TP-2711 ..... N87-20566* #
NASA-TP-2714 ..... N87-20947* #
NASA-TP-2720 ..... N87-20381* #
NASA-TP-2724 ..... N87-20727* #

NASA-TT-20008 ..... N87-20388* #
NASA-TT-20011 ..... N87-20261* #
NASA-TT-20055 ..... N87-20241* #
NASA-TT-20056 ..... N87-20784* #

NBS/SP-330 ..... N87-20444 #

NBSIR-86/3437 ..... N87-20420 #

NEPRF-CR-86-05 ..... N87-20642 #

NOAA/SW/MT-87/001A ..... N87-20801 #

NORDA-143 ..... N87-20712 #

NOSC/TD-988 ..... N87-20691 #

NRC-26475 ..... N87-20286 #

NRL-MR-5793 ..... N87-20692 #
NRL-MR-5875 ..... N87-20573 #

NSWC-TR-84-302-REV-1 ..... N87-20480 #

NSWC/MP/86-240 ..... N87-20245 #

NSWC/TR-85-484 ..... N87-20244 #

NUSC-TR-7635 ..... N87-20715 #

ONERA-NT-1983-3 ..... N87-20401 #
ONERA-NT-1986-4 ..... N87-20705 #

ONERA-P-1986-2 ..... N87-20402 #

ONERA-RF-11/7236-PY ..... N87-20707 #
ONERA-RF-91/7154-PY ..... N87-20706 #

ONERA-RT-30/3043-RY-057-R ..... N87-20617 #
ONERA-RT-35/1621-RY-053-R ..... N87-20511 #
ONERA-RT-42/7086-M ..... N87-20396 #

ONERA-RTS-17/3423-AY ..... N87-20249 #
ONERA-RTS-21/3271-AY ..... N87-20250 #

ONRL-R-8-86 ..... N87-20173 #

ORNL-6302 ..... N87-20393 #

ORNL/TM-10038 ..... N87-20509 #

OUEL-1651/86 ..... N87-20776 #

PB86-244159 ..... N87-20444 #
PB87-126389 ..... N87-20948 #
PB87-132031 ..... N87-20801 #
PB87-136693 ..... N87-20420 #

PNL-SA-14579 ..... N87-20491 #

PR-36 ..... N87-20452 #

PWA-5890-24 ..... N87-20387* #

RAE-TRANS-2103 ..... N87-20262 #

REPT-86-004-REV ..... N87-20788 #
REPT-86BO186 ..... N87-20479* #
REPT-86BO536 ..... N87-20871* #
REPT-87B0118 ..... N87-20690* #
REPT-365 ..... N87-20503* #
REPT-5101-221-REV-1 ..... N87-20645* #
REPT-6657 ..... N87-20400* #

RFP-3862 ..... N87-20418 #
RFP-3909 ..... N87-20419 #

RRK-85-20 ..... N87-20830 #

SAIC-1-120-778-C14 ..... N87-20335* #
SAIC-87/1514 ..... N87-20335* #

SAND-86-0440C ..... N87-20548 #
SAND-86-0964 ..... N87-20843 #
SAND-86-1395C ..... N87-20544 #
SAND-86-2398 ..... N87-20460 #
SAND-86-2458C ..... N87-20546 #
SAND-86-2617 ..... N87-20430 #
SAND-86-2759 ..... N87-20397 #
SAND-86-8248 ..... N87-20394 #

SAPR-6 ..... N87-20840* #
SAPR-7 ..... N87-20840* #
SAPR-8 ..... N87-20840* #

SD-TR-86-88 ..... N87-20345 #

SERI/SP-232-3079 ..... N87-20729 #

SGD-506-PT-1 ..... N87-20948 #

SNIAS-861-111-103 ..... N87-20261* #
SNIAS-861-430-108 ..... N87-20388* #
SNIAS-959-CA/CG ..... N87-20657 #

SR-87-1 ..... N87-20434 #

SVIC-BULL-56-PT-1 ..... N87-20574 #
SVIC-BULL-56-PT-2 ..... N87-20580 #

SVIC-BULL-56-PT-3 ..... N87-20602 #

SWRI-8858/1-VOL-1 ..... N87-20285 #

TIR-29/81-BWB-ML ..... N87-20262 #

TN-N-1765 ..... N87-20432 #

TR-85 ..... N87-20482 #
TR-0086(6930-01)-11 ..... N87-20345 #

UCID-20366-87 ..... N87-20441 #

UCRL-53753 ..... N87-20442 #
UCRL-94402 ..... N87-20616 #
UCRL-94747 ..... N87-20415 #
UCRL-95629 ..... N87-20507 #

US-PATENT-APPL-SN-627-307 ..... N87-20266
US-PATENT-APPL-SN-610142 ..... N87-20520
US-PATENT-APPL-SN-622614 ..... N87-20457
US-PATENT-APPL-SN-624568 ..... N87-20459
US-PATENT-APPL-SN-627699 ..... N87-20458
US-PATENT-APPL-SN-637238 ..... N87-20337
US-PATENT-APPL-SN-640636 ..... N87-20375
US-PATENT-APPL-SN-651399 ..... N87-20543
US-PATENT-APPL-SN-667194 ..... N87-20519
US-PATENT-APPL-SN-741784 ..... N87-20823
US-PATENT-APPL-SN-767446 ..... N87-20483
US-PATENT-APPL-SN-788371 ..... N87-20748

US-PATENT-CLASS-33-512 ..... N87-20748
US-PATENT-CLASS-89-1.8 ..... N87-20337
US-PATENT-CLASS-244-122 ..... N87-20266
US-PATENT-CLASS-250-578 ..... N87-20815
US-PATENT-CLASS-333-133 ..... N87-20458
US-PATENT-CLASS-333-139 ..... N87-20483
US-PATENT-CLASS-343-17.1PF N87-20459
US-PATENT-CLASS-343-359 ..... N87-20457
US-PATENT-CLASS-350-37 ..... N87-20519
US-PATENT-CLASS-372-60 ..... N87-20543
US-PATENT-CLASS-427-249 ..... N87-20823

US-PATENT-4,603,486 ..... N87-20748
US-PATENT-4,603,823 ..... N87-20266
US-PATENT-4,604,938 ..... N87-20337
US-PATENT-4,609,169 ..... N87-20375
US-PATENT-4,610,499 ..... N87-20519
US-PATENT-4,611,124 ..... N87-20815
US-PATENT-4,611,210 ..... N87-20457
US-PATENT-4,612,642 ..... N87-20543
US-PATENT-4,613,862 ..... N87-20459
US-PATENT-4,614,429 ..... N87-20520
US-PATENT-4,614,672 ..... N87-20823
US-PATENT-4,614,919 ..... N87-20458
US-PATENT-4,614,921 ..... N87-20483

US-PATENT—APPL-SN-620211 ..... N87-20815

USAAVSCOM-TR-86-C-32 ..... N87-20260* #
USAAVSCOM-TR-87-C-5 ..... N87-20235* #

USIP-86-11 ..... N87-20808 #

UVA/528253/AM87/101 ..... N87-20860* #

VPI-86-29 ..... N87-20385 #

WAPD-TM-1616 ..... N87-20549 #

WDL-TR11068 ..... N87-20467* #

WHOI-86-14 ..... N87-20713 #
WHOI-86-33 ..... N87-20711 #

YJT-86-09 ..... N87-20410 #

FEDERAL DEPOSITORY LIBRARIES

ALABAMA

AUBURN UNIV. AT MONTGOMERY LIBRARY
Documents Department
Montgomery, AL 36193
(205) 279-9110, ext. 253

UNIV. OF ALABAMA LIBRARY
Documents Dept.-Box S
University, AL 35486
(205) 348-7369

ARIZONA

DEPT. OF LIBRARY, ARCHIVES AND PUBLIC RECORDS
Third Floor—State Cap.
1700 West Washington
Phoenix, AZ 85007
(602) 255-4121

UNIVERSITY OF ARIZONA LIB.
Government Documents Dept.
Tucson, AZ 85721
(602) 626-5233

ARKANSAS

ARKANSAS STATE LIBRARY
One Capitol Mall
Little Rock, AR 72201
(501) 371-2326

CALIFORNIA

CALIFORNIA STATE LIBRARY
Govt. Publications Section
P.O. Box 2037
Sacramento, CA 95809
(916) 322-4572

COLORADO

UNIV OF COLORADO LIB.
Government Pub. Division
Campus Box 184
Boulder, CO 80309
(303) 492-8834

DENVER PUBLIC LIBRARY
Govt. Pub. Department
1357 Broadway
Denver, CO 80203
(303) 571-2131

CONNECTICUT

CONNECTICUT STATE LIBRARY
Government Documents Unit
231 Capitol Avenue
Hartford, CT 06106
(203) 566-4971

FLORIDA

UNIV. OF FLORIDA LIBRARIES
Library West
Documents Department
Gainesville, FL 32611
(904) 392-0367

GEORGIA

UNIV. OF GEORGIA LIBRARIES
Government Reference Dept.
Athens, GA 30602
(404) 542-8951

HAWAII

UNIV. OF HAWAII LIBRARY
Govt. Documents Collection
2550 The Mall
Honolulu, HI 96822
(808) 948-8230

IDAHO

UNIV. OF IDAHO LIBRARY
Documents Section
Moscow, ID 83843
(208) 885-6344

ILLINOIS

ILLINOIS STATE LIBRARY
Information Services Branch
Centennial Building
Springfield, IL 62706
(217) 782-5185

INDIANA

INDIANA STATE LIBRARY
Serials Documents Section
140 North Senate Avenue
Indianapolis, IN 46204
(317) 232-3686

IOWA

UNIV. OF IOWA LIBRARIES
Govt. Documents Department
Iowa City, IA 52242
(319) 353-3318

KANSAS

UNIVERSITY OF KANSAS
Doc. Collect—Spencer Lib.
Lawrence, KS 66045
(913) 864-4662

KENTUCKY

UNIV. OF KENTUCKY LIBRARIES
Govt. Pub. Department
Lexington, KY 40506
(606) 257-3139

LOUISIANA

LOUISIANA STATE UNIVERSITY
Middleton Library
Govt. Docs. Dept.
Baton Rouge, LA 70803
(504) 388-2570

LOUISIANA TECHNICAL UNIV. LIBRARY
Documents Department
Ruston, LA 71272
(318) 257-4962

MAINE

UNIVERSITY OF MAINE
Raymond H. Fogler Library
Tri-State Regional Documents Depository
Orono, ME 04469
(207) 581-1680

MARYLAND

UNIVERSITY OF MARYLAND
McKeldin Lib.—Doc. Div.
College Park, MD 20742
(301) 454-3034

MASSACHUSETTS

BOSTON PUBLIC LIBRARY
Government Docs. Dept.
Boston, MA 02117
(617) 536-5400 ext.226

MICHIGAN

DETROIT PUBLIC LIBRARY
Sociology Department
5201 Woodard Avenue
Detroit, MI 48202
(313) 833-1409

MICHIGAN STATE LIBRARY
P.O. Box 30007
Lansing, MI 48909
(517) 373-0640

MINNESOTA

UNIVERSITY OF MINNESOTA
Government Pubs. Division
409 Wilson Library
309 19th Avenue South
Minneapolis, MN 55455
(612) 373-7813

MISSISSIPPI

UNIV. OF MISSISSIPPI LIB.
Documents Department
University, MS 38677
(601) 232-5857

MONTANA

UNIV. OF MONTANA
Mansfield Library
Documents Division
Missoula, MT 59812
(406) 243-6700

NEBRASKA

NEBRASKA LIBRARY COMM.
Federal Documents
1420 P Street
Lincoln, NE 68508
(402) 471-2045
In cooperation with University of Nebraska-Lincoln

NEVADA

UNIVERSITY OF NEVADA LIB.
Govt. Pub. Department
Reno, NV 89557
(702) 784-6579

NEW JERSEY

NEWARK PUBLIC LIBRARY
5 Washington Street
Newark, NJ 07101
(201) 733-7812

NEW MEXICO

UNIVERSITY OF NEW MEXICO
Zimmerman Library
Government Pub. Dept.
Albuquerque, NM 87131
(505) 277-5441

NEW MEXICO STATE LIBRARY
Reference Department
325 Don Gaspar Avenue
Santa Fe, NM 87501
(505) 827-2033, ext. 22

NEW YORK

NEW YORK STATE LIBRARY
Empire State Plaza
Albany, NY 12230
(518) 474-5563

NORTH CAROLINA

UNIVERSITY OF NORTH CAROLINA AT CHAPEL HILL
Wilson Library
BA/SS Documents Division
Chapel Hill, NC 27515
(919) 962-1321

NORTH DAKOTA

UNIVERSITY OF NORTH DAKOTA
Chester Fritz Library
Documents Department
Grand Forks, ND 58202
(701) 777-2617, ext. 27
In cooperation with North Dakota State Univ. Library

OHIO

STATE LIBRARY OF OHIO
Documents Department
65 South Front Street
Columbus, OH 43215
(614) 462-7051

OKLAHOMA

OKLAHOMA DEPT. OF LIB.
Government Documents
200 NE 18th Street
Oklahoma City, OK 73105
(405) 521-2502

OKLAHOMA STATE UNIV. LIB.
Documents Department
Stillwater, OK 74078
(405) 624-6546

OREGON

PORTLAND STATE UNIV. LIB.
Documents Department
P.O. Box 1151
Portland, OR 97207
(503) 229-3673

PENNSYLVANIA

STATE LIBRARY OF PENN.
Government Pub. Section
P.O. Box 1601
Harrisburg, PA 17105
(717) 787-3752

TEXAS

TEXAS STATE LIBRARY
Public Services Department
P.O. Box 12927—Cap. Sta.
Austin, TX 78753
(512) 471-2996

TEXAS TECH. UNIV. LIBRARY
Govt. Documents Department
Lubbock, TX 79409
(806) 742-2268

UTAH

UTAH STATE UNIVERSITY
Merrill Library, U.M.C. 30
Logan, UT 84322
(801) 750-2682

VIRGINIA

UNIVERSITY OF VIRGINIA
Alderman Lib.—Public Doc.
Charlottesville, VA 22901
(804) 924-3133

WASHINGTON

WASHINGTON STATE LIBRARY
Documents Section
Olympia, WA 98504
(206) 753-4027

WEST VIRGINIA

WEST VIRGINIA UNIV. LIB.
Documents Department
Morgantown, WV 26506
(304) 293-3640

WISCONSIN

MILWAUKEE PUBLIC LIBRARY
814 West Wisconsin Avenue
Milwaukee, WI 53233
(414) 278-3000

ST. HIST LIB. OF WISCONSIN
Government Pub. Section
816 State Street
Madison, WI 53706
(608) 262-4347

WYOMING

WYOMING STATE LIBRARY
Supreme Ct. & Library Bld.
Cheyenne, WY 82002
(307) 777-6344

National Aeronautics and
Space Administration
Code NTT-4
Washington, D.C.
20546

Official Business

Penalty for Private Use, $300

SPECIAL FOURTH-CLASS RATE
POSTAGE & FEES PAID
NASA
PERMIT No. G 27

NASA

POSTMASTER: If Undeliverable (Section 158
Postal Manual) Do Not Return

SEP 2 8 1989

ATE

58
um